ACTA CHIMICA

ACADEMIAE SCIENTIARUM HUNGARICAE

TOMUS 102 FASCICULUS 1

AKADÉMIAI KIADÓ, BUDAPEST

1979

ACTA CHIM. ACAD. SCI. HUNG. ACASA2 102 (1) 1–107 (1979)

ACTA CHIMICA

A MAGYAR TUDOMÁNYOS AKADÉMIA KÉMIAI TUDOMÁNYOK OSZTÁLYÁNAK IDEGEN NYELVŰ KÖZLEMÉNYEI

Acta Chimica is a journal for the publication of papers on all aspects of chemistry in English, German, French and Russian.

Acta Chimica is published in 4 volumes per year. Each volume consists of 4 issues of varying size.

Manuscripts should be sent to

Acta Chimica
Budapest, P.O. Box 67, H-1450, Hungary

Correspondence with the editors should be sent to the same address. Manuscripts are not returned to the authors.

Subscription: $36.00 per volume.

Hungarian subscribers should order from Akadémiai Kiadó, 1363 Budapest, P.O. Box 24. Account No. 215 11488.

Orders from other countries are to be sent to "Kultura" Foreign Trading Company (H-1389 Budapest 62, P.O. Box 149. Account No. 218 10990) or its representatives abroad.

ACTA CHIMICA

ACADEMIAE SCIENTIARUM HUNGARICAE

TOMUS 102

AKADÉMIAI KIADÓ, BUDAPEST

1979

ACTA CHIM. ACAD. SCI. HUNG.

ACTA CHIMICA

TOMUS 102

Fascilus 1

Fascilus 2

Fascilus 3

Fascilus 4

INDEX

Acta Chimica Academiae Scientiarum Hungaricae, Tomus 102 (1), pp. 1—10 (1979)

HYDRODECHLORINATION OF ALDRIN, DIELDRIN AND TOXAPHENE

R. B. LaPierre*, E. Biron, L. Guczi**, W. L. Kranich and A. H. Weiss***

(Department of Chemical Engineering, Worcester Polytechnic Institute Worcester, Mass. 01609 USA)

Received June 30, 1978

Accepted for publication October 3, 1978

The hydrodechlorination reactions of Aldrin, of its epoxide Dieldrin, and of Toxaphene were studied in C_2H_5OH—NaOH solution at 50 bar H_2, 130 °C, using 61% Ni on Kieselguhr catalyst. The stoichiometry of these heavy multifunctional species follows the rules established for simple low-molecular weight compounds. Concerted (*i.e.* multiple) reactions, in which intermediate species do not desorb, are typical:
For Aldrin:

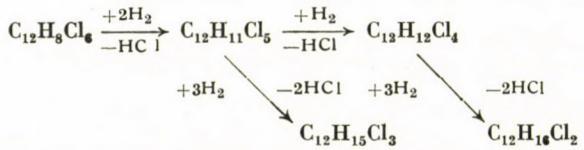

First, an olefinic group in a molecule hydrogenates (an epoxide is not affected at these conditions) in a step simultaneous with removal of a highly active geminal dichloride. The molecule then readsorbs to loose in one step its olefinic chlorine atoms and to hydrogenate that olefinic bond. The last highly unreactive chlorines to be removed are the aliphatic chlorines, and the consequence of their very low reactivity is that Dieldrin, Aldrin, and Toxaphene are not readily completely stripped to the corresponding hydrocarbon skeletons.

Introduction

We have recently reported on the catalytic hydrodechlorination of 1,1-Bis (*p*-chlorophenyl)-2,2-dichloroethylene (*p, p'* DDE) [1, 2], the corresponding ethane (*p p'* DDD) [1], and a typical polychlorinated biphenyl (PCB) mixture [3]. These studies were conducted in both the gas and liquid phase over supported Pd and Ni catalysts. Olefinic and aromatic chlorine were shown to be highly reactive, as these carbonchlorine bonds acquire a distinct double bond character when chlorine π-electron delocalization occurs on the catalytic site [4].

Hydrodechlorination of DDE olefinic chlorines is a concerted process, *i.e.*, a number of reactions occur without the need for intermediate species desorp-

* Present address: Mobil Research Corp., Princeton, N. J.

** Present and permanent address: Institute of Isotopes, Hungarian Academy of Sciences, Budapest, Hungary

*** To whom correspondence should be addressed.

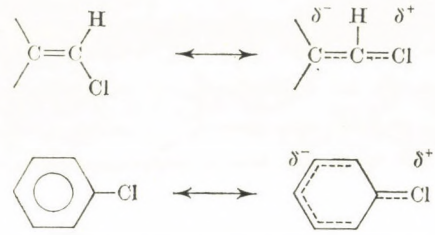

1

tion, for example, removal of both chlorines of DDE is followed by rapid hydrogenation of the dechlorinated olefin, all as one step without desorption of intermediates. Of course, reactions may or may not be stepwise on the surface. Aromatic hydrodechlorination [1—3] is on the other hand, a stepwise process, and has a lower hydrogen dependence than the olefinic reaction. WEISS and KRIEGER [5], in a study of the Pt catalyzed hydrodechlorination of 1,2-dichloroethylenes, vinyl chloride, and the corresponding chloroethanes showed that olefinic chlorine was much more reactive than aliphatic chlorine. Olefinic hydrodechlorination was, again, a precursor to hydrogenation of the olefin.

HORNER *et al.* [6], using Raney-Nickel in the liquid phase, established the following activity sequence for aliphatic hydrodechlorination:

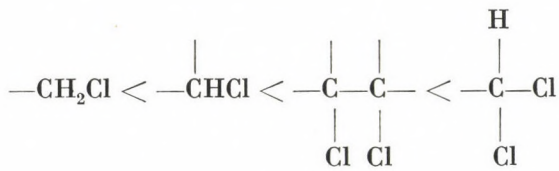

2

Both aliphatic chlorines in DDD [2] are removed in a concerted manner similar to that observed by WEISS *et al.* [7] in the concerted Pt-catalyzed hydrodechlorination of CCl_4 directly to methane.

Steric influences were observed to control the selectivity and relative rates of *ortho* to *(meta* plus *para)* PCB hydrodechlorination [3]. Chlorine substituted ortho to the ring juncture inhibits planarity of chlorinated biphenyl molecules and hence adsorption favorable for the hydrodechlorination reaction.

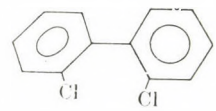

We now present the results of studies on the hydrodechlorination of the organochlorine pesticides Aldrin, Dieldrin, and Toxaphene which illustrate combined steric and substitutional effects and the resulting stoichiometry.

The structures of Aldrin and its corresponding epoxide Dieldrin are:

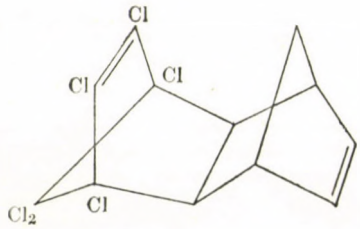

Aldrin

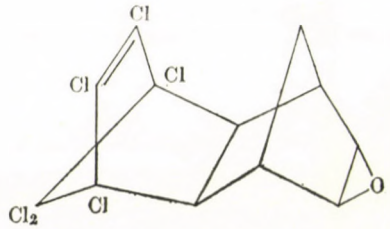

Dieldrin

Toxaphene is a complex mixture of polychlorinated hydrocarbons, typically 67—69% chlorine by weigth, prepared by the chlorination of camphene. The structure of camphene ($C_{10}H_{16}$) is:

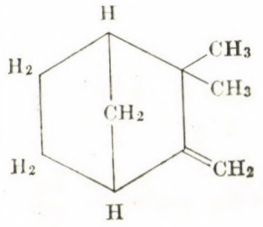

HOLMSTEAD *et al.* [8] have reported that over two thirds of the components of commercial toxaphene are $C_{10}H_{18-x}Cl_x$ compounds where the double bond has been saturated during chlorination. Isomerization also occurs during chlorination. A typical component which has been isolated from a representative toxaphene mixture [9] is a heptachlorobornane *i.e.*,

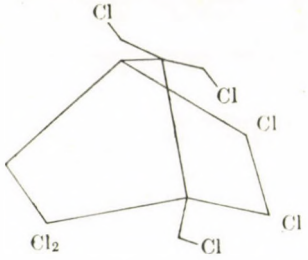

As a further example of the chemical complexity of toxaphene, SMITH [10] has calculated that the number of toxaphene isomers possible without stereo isomers, and assuming that the double bond has been chlorinated without rearrangement of the carbon skeleton, is 8640.

Experimental

Technical-grade chemicals were used in these studies. Samples of Aldrin and Dieldrin were donated by Shell Development Company, Modesto, California, and Toxaphene by Hercules Inc., Wilmington, Del. Experiments were carried out, using a teflon lined autoclave. The detailed description of this equipment and the experimental technique used are found elsewhere [2].

GC—MS techniques were used to characterize the reactants and products. The equipment used was a Perkin—Elmer 900 gas chromatograph interfaced with a DuPont 21—491 double focusing mass spectrometer. Separations were carried out on a 9′×1/2″ 3% OV-17 on 80—100 mesh Chromosorb W column and a 5′×1/8″ 3% OV-1 on 80—100 mesh Chromosorb W column.

The electron impact mass spectra of Aldrin and Dieldrin have been interpreted by SAFE and HUTZINGER [12]. The fragmentation patterns of both compounds are characterized by retro Diels-Alder (RDA) reactions accompanied by or preceded by expulsion of Cl or HCl. Similar spectra were obtained on Aldrin and Dieldrin reaction products. Fragments due to RDA reactions were much less intense from Aldrin products where the non-chlorinated olefin had been saturated. However, since the spectra were characterized by RDA reactions, no information could be obtained identifying which chlorine was removed during hydrodechlorination.

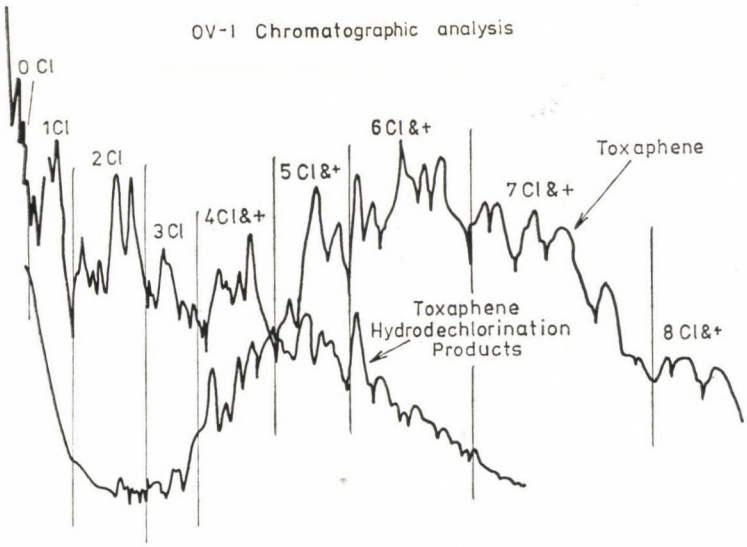

Fig. 1. Chromatograms of Toxaphene and its hydrodechlorination products (OV-1 column with MS partial identification of components)

Figure 1 shows OV-1 chromatograms of the Toxaphene reactant used and its typical reaction products, respectively. Better separation of products was obtained using the OV-17 column as indicated in Fig. 2. Compounds are partially identified by mass spectroscopy.

HOLMSTEAD *et al.* [8] have presented the mass spectra of two Toxaphene components, one a $C_{10}H_{11}Cl_7$ compound and the other a $C_{10}H_{10}Cl_8$ compound. Their results show that for both compounds no molecular ions are observed in both CI and EI spectra but rather $M-Cl^+$ ions are the heaviest species observed. This behavior is due to loss of one geminal chlorine atom from perchlorinated carbon atoms to form stabilized carbonium ions. As these chlorines are replaced by hydrogen during reaction, molecular ions should be observed. Therefore, at high conversion, chlorine number identification of Toxaphene products should be accurate, since geminal chlorines should be completely hydrodechlorinated, due to their reactivity. On the other hand, at low conversion, product analyses as well as the unreacted Toxaphene analyses will have serious distribution errors based on molecular weight mass determinations by mass spectrometer. The delineations for the higher chlorine numbers shown in Figs 1 and 2 are based on best judgment and contain some level of error. We indicate this by labeling the chlorine numbers 4 Cl & + for example.

Results

Comparative hydrodechlorination reactions of Aldrin and its corresponding epoxide Dieldrin are illustrated by data in Figs 3 and 4, respectively. These experiments were made, using a 61% Ni on Kieselguhr (Girdler G49) catalyst, which is an active catalyst for the hydrodechlorination of DDE and PCB's. In these experiments 100 g of 2 wt % solutions of the reactant in ethanol (containing NaOH 10% in excess of that needed to neutralize the HCl produced by removal of 6 atoms of chlorine) were reacted in the teflon autoclave over 50 mg catalyst at 130 °C and 50 bar H_2. Figures 3 and 4 show plots of relative

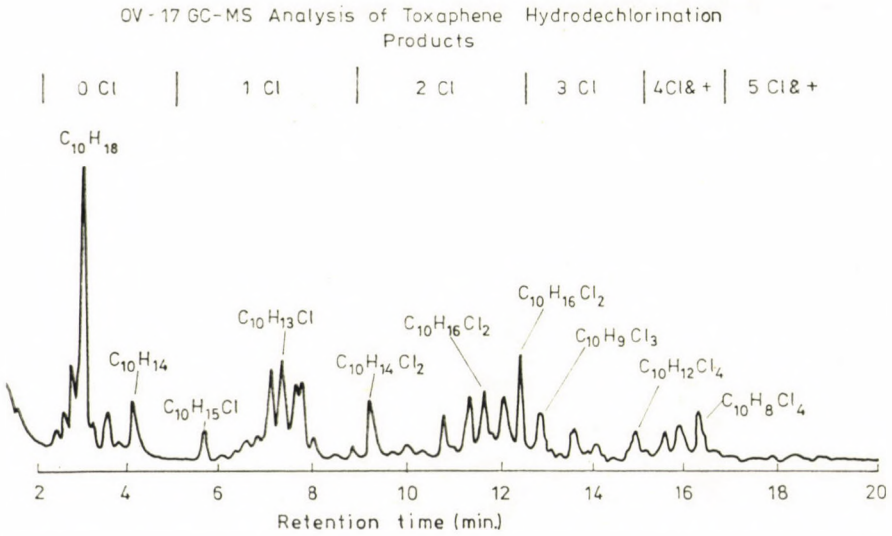

Fig. 2. Chromatogram of Toxaphene hydrodechlorination products (OV-17 column with MS partial identification of components)

mole fraction of the identified species *vs.* reaction time. Considering only the identified products, the apparent stoichiometry for the Aldrin experiment suggested by the results in Fig. 3 is

$$\underset{\text{ALDRIN}}{C_{12}H_8Cl_6} \xrightarrow[-HCl]{+2H_2} C_{12}H_{11}Cl_5 \xrightarrow[-HCl]{+H_2} C_{12}H_{12}Cl_4$$

$$C_{12}H_{11}Cl_5 \xrightarrow{-2HCl,\ +3H_2} C_{12}H_{15}Cl_3 \qquad C_{12}H_{12}Cl_4 \xrightarrow{-2HCl,\ +3H_2} C_{12}H_{16}Cl_2$$

Correspondingly for the Dieldrin experiment in Fig. 4

$$C_{12}H_8Cl_6O \xrightarrow[-HCl]{+H_2} C_{12}H_9Cl_5O \xrightarrow[-HCl]{+H_2} C_{12}H_{10}Cl_4O$$

This behavior can be explained as follows.

The fact that Aldrin initially hydrogenates and loses one chlorine, whereas Dieldrin initially only loses one chlorine indicates that the nonchlorinated olefin in Aldrin is hydrogenated in the initial step. We know from our work

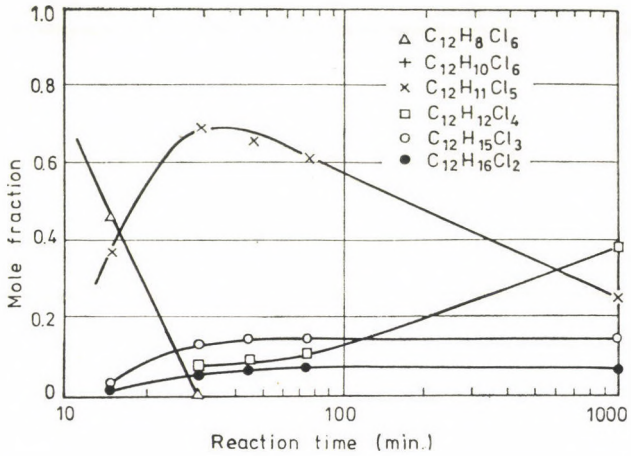

Fig. 3. **Distribution of hydrodechlorination products of Aldrin as a function of time**

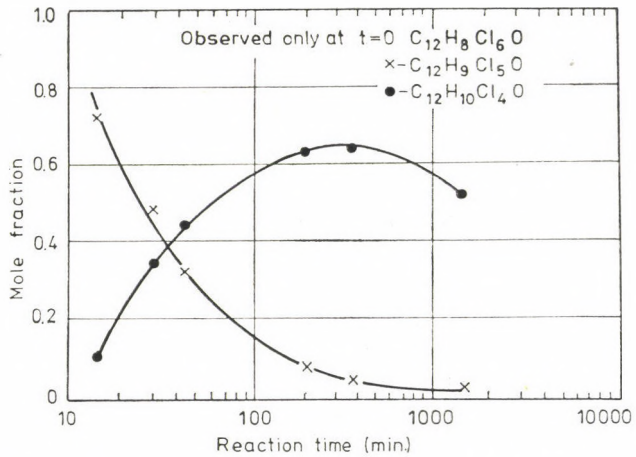

Fig. 4. **Distribution of hydrodechlorination products of Dieldrin as a function of time**

with 1,2 dichloroethylene [5] and DDE [1, 2] that hydrodechlorination at an olefinic bond precedes hydrogenation of an originally chlorinated olefinic bond, which is consistent with the results observed here. The first step is not hydrogenation of the dichloroethylene moiety but of the ethylene moiety along with removal of the geminal chlorine. Initial hydrogenation of the unchlorinated

olefin with the concerted removal of one chlorine suggests that Aldrin (**I**) is adsorbed mainly in the configuration shown below and that reaction proceeds at its points of contact*.

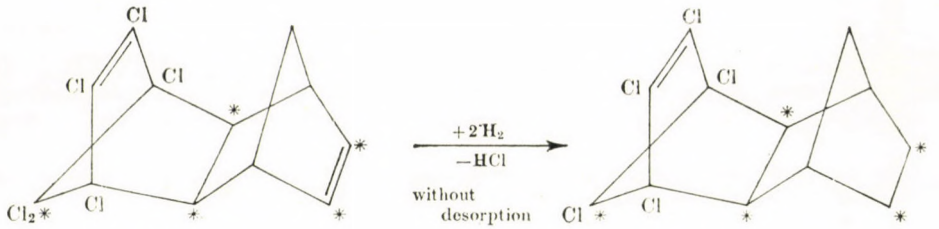

$C_{12}H_8Cl_6$ — **I**

$C_{12}H_{11}Cl_5$ — **II**

This configuration allows hydrodechlorination of one of the two geminal chlorines to proceed along with the hydrogenation reaction without desorption of intermediate, which is typical of the concerted behavior observed with hydrodechlorination systems. The resulting first step product (**II**) contains aliphatic chlorines (one secondary chlorine adsorbed) which are highly unreactive compared to the olefinic chlorines. However, the data show that this species

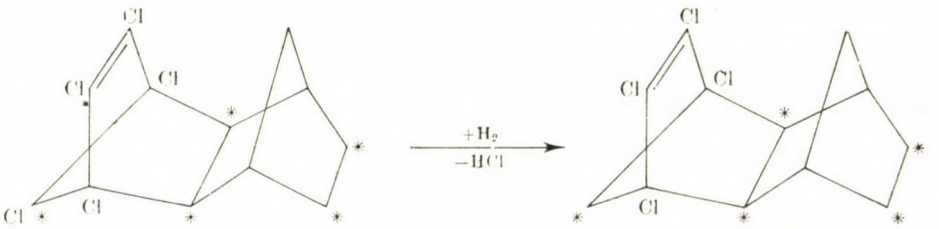

$C_{12}H_{11}Cl_5$ — **II**

$C_{12}H_{12}Cl_4$ — **III**

does react to a small extent, since $C_{12}H_{12}Cl_4$ (**III**) is formed in a single step. One can postulate that adsorption of **II** and **III** in an inverted position at the olefinic chlorine accounts for the production by concerted steps of $C_{12}H_{15}Cl_3$ (**IV**) and $C_{12}H_{16}Cl_2$ (**V**).

Subsequent removal of either an adsorbed or unadsorbed chlorine was not documented experimentally and this would be unfavored. Higher reaction severities would be needed to show significant quantities. Dieldrin, (**VI**) as noted, is not hydrogenated initially, but a broad spectrum of dechlorinated reaction products results. One pathway, analogous to Aldrin, accounts for the major products shown in Fig. 4 as shown below.

Removal of one olefinic chloride could also account for the large amounts of $C_{12}H_{10}Cl_4O$ (**VIIIa** and **VIIIb**) that are produced from $C_{12}H_9Cl_5O$ (**VII**).

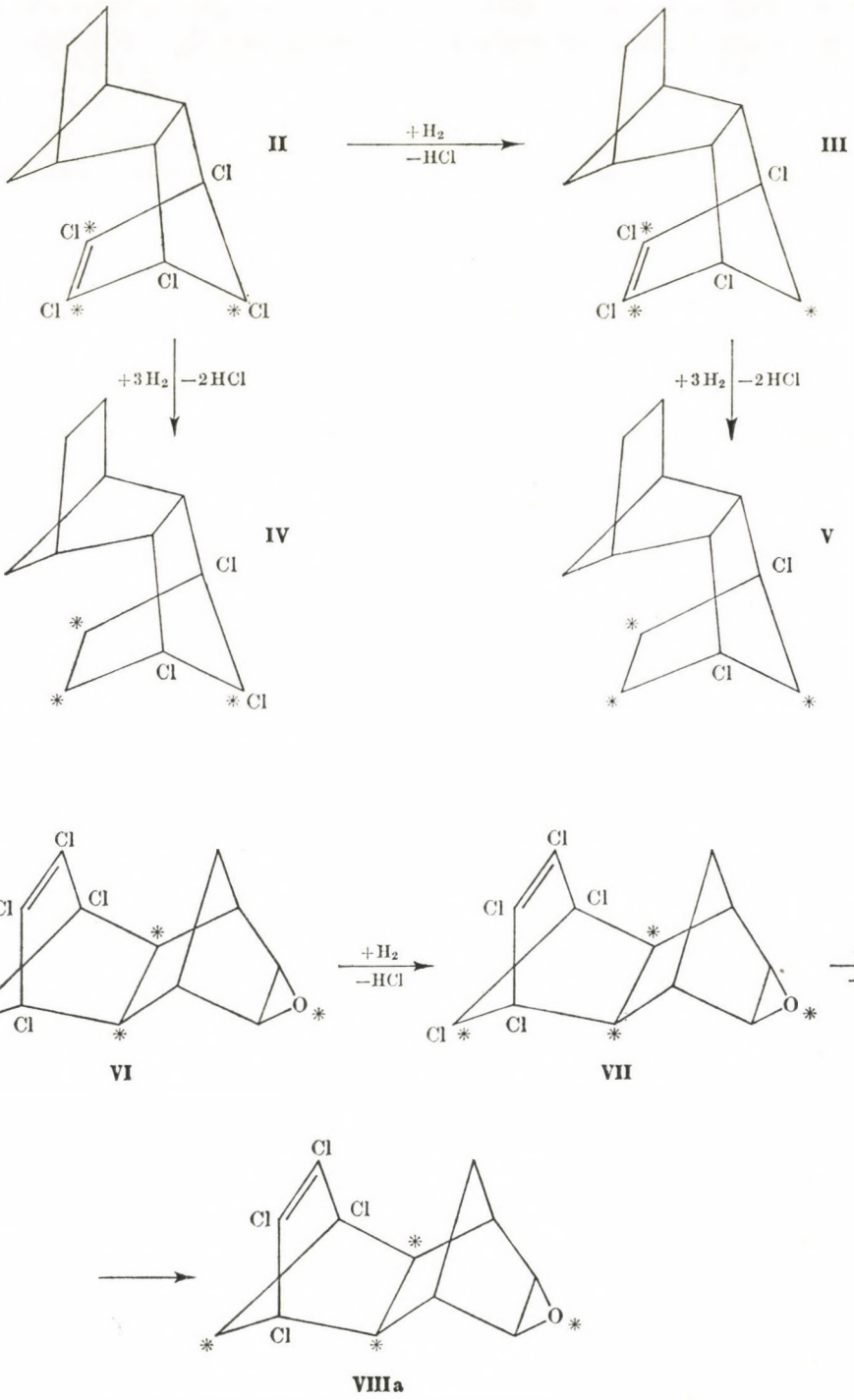
II
III
IV
V
VI
VII
VIIIa
+H2
−HCl
+3H2
−2HCl
Cl
O

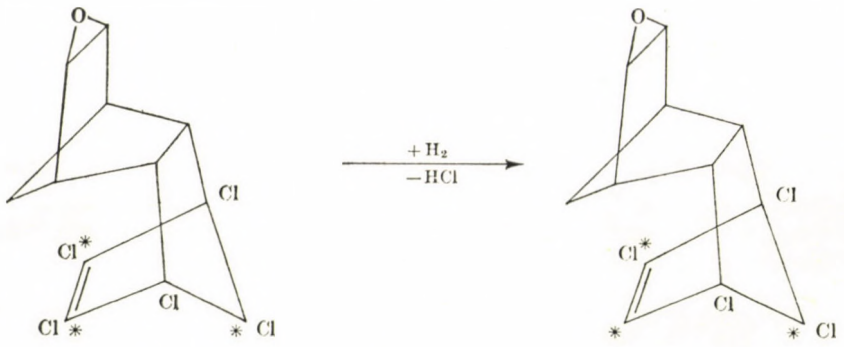

VII VIII b

Stepwise removal of olefinic chlorine atoms was observed by WEISS and KRIEGER for 1,2-dichloroethylene hydrodechlorination, where vinyl chloride was a measurable intermediate.

A similar set of experiments was carried out with Toxaphene. Experimental conditions and estimated product distribution are found in Table I.

Table I

Toxaphene hydrodechlorination at 100 °C 50 BAR
4—6 wt % Toxaphene in ethanol; 10 gm Toxaphene gm catalyst
(Ni on Kieselguhr)

Reaction time (hr)	2	4	19
Chlorine atoms/molecule	Distribution (%)		
0	16.5	32.4	37.2
1	21.4	29.0	25.8
2	29.9	20.3	24.2
3	9.4	2.8	1.2
4	8.5	11.6	10.5
5	5.5	2.0	1.1
6	6.1	1.9	
7	1.5		
8	1.2		

Based on its 68% (wt) chlorine, the original Toxaphene contained an average of 7.8 chlorine atoms per molecule

These results show that most of the chlorine was easily removed in the first two hours and then only minor changes were noted as time progressed. These results are consistent with an adsorbed configuration for the representative heptachlorobornane as follows.

With such configuration geminal chlorines and those linked directly to the surface can be easily removed but other aliphatic chlorines would be relatively inactive.

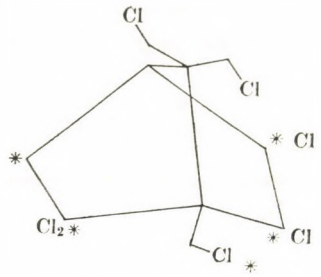

A similar pattern of successive hydrodechlorinations has been observed when other polychlorinated pesticides were exposed to the elements over a period of several years. CARLSON *et al.* [13] reported that Mirex, a polyring dodecachlorodecane, yields compounds in which hydrogen has replaced one or two chlorines (as well as oxygenated derivatives). Our catalyzed hydrodechlorination is analogous to this process of natural degradation.

*

The results presented here are part of a United States Environmental Protection Agency funded study "Catalytic Conversion of Hazardous and Toxic Chemicals", EPA Grant R 802-857-01. The work by Mr. LAPIERRE has been done in partial fulfillment of the requirements for the Ph. D. in Chemical Engineering at Worcester Polytechnic Institute.

REFERENCES

[1] LAPIERRE, R. B., WU, D., KRANICH, W. L., WEISS, A. H.: J. catal., **52,** 59 (1978
[2] LAPIERRE, R. B., BIRON, E., GUCZI, L., KRANICH, W. L., WEISS, A. H.: J. Catal., **52,** 218 (1978)
[3] *ibid.:* **52,** 230 (1978)
[4] COULSON, C. A., "Valence", 2nd. ed., pp. 356—365. Oxford University Press, London (1963)
[5] WEISS, A. H., KRIEGER, K. A., J. Catal., **6,** 167—185 (1966)
[6] HORNER, L., SCHLAFER, L., KAMMERER, H.: Chem. Ber., **92,** 1700 (1959)
[7] WEISS, A. H., GAMBHIR, B., LEON, R.: J. Catal., **22,** 245 (1971)
[8] HOLMSTEAD, R. L., KHALIFA, S., CASIDA, J. E.: J. Agr. Food Chem., **22,** No. 6 (1974)
[9] CASIDA, J. E., HOLMSTEAD, R. L., KHALIFA, L., KNOX, J. R., OHSAWA, T., PALMER, K. J., WONG, R. Y.: Science, **183,** 520 (1974)
[10] SMITH, D. H.: Anal. Chem., **47,** No. 7 (June 1975)
[11] LAPIERRE, R. B., BIRON, E., WU, D., GUCZI, L., KRANICH, W. L., WEISS, A. H.: "Handbook for Catalytic Hydrodechlorination of Polychlorinated Pesticides and Related Substances", Final Report EPA Grant R 802—857—01, (June 1976)
[12] SAFE, S., HUTZINGER, O.: "Mass Spectroscopy of Pesticides and Pollutants" CRC Press (1973)
[13] CARLSON, D. A., KONYHA, K. D., WHEELER, W. B., MARSHALL, G. P., ZAYLSKIE, R. G.: Science, **194,** 939 (1976)

René B. LAPIERRE — Mobil Research Corp., Princeton, N. J.
László GUCZI — H-1525 Budapest, P. O. Box 77.
Ehud BIRON, Wilmer L. KRANICH, Alvin H. WEISS — Worcester, Mass. 01609 USA

Acta Chimica Academiae Scientiarum Hungaricae, Tomus 102 (1), pp. 11—18 (1979)

SOURCES OF THE ERROR OF QUANTITATIVE DETERMINATION OF THE SOLID CRYSTALLINE MINERALS BY INFRARED SPECTROSCOPY

J. HLAVAY and J. INCZÉDY

(Institute of Analytical Chemistry, University of Chemical Engineering, Veszprém)

Received July 26, 1976
In revised form July 20, 1978

Accepted for publication October 18, 1978

Possibility of quantitative determination of four minerals of different origin with different physical characteristics [Zettlitz kaolin, Szegilong paper kaolin, Urkút quartz and Swedish feldspar (orthoclase)] was investigated by infrared spectroscopy and X-ray powder diffraction. Decrease of the particle size and change of the disorder of the crystalline state of the samples were carried out in a vibrating ball mill. Correlation functions between the average particle size of the samples and quantitative data derived from the infrared spectra and X-ray diffractograms, respectively, are presented.

Recently, considerable attention has been drawn to the detection and quantitative determination of the crystalline minerals by infrared spectroscopy and X-ray powder diffraction. Both methods have some advantages but both of them contain several sources of error. According to the experience, however, a little more qualitative and quantitative information could be in some special cases obtained by infrared spectroscopy than it is to be accomplished by X-ray powder diffraction. While characteristic O—H stretching vibrations of the clay minerals could be easily interpreted in the infrared spectra of the amorphous soil, no proper X-ray diffractograms could be obtained from the same sample [1]. Investigations of a hyalopilitic system could be also carried out by infrared spectroscopy, and the glazier phases of the material could be separated from the crystalline ones based on their absorption bands [2, 3].

Quantitative phase analysis of the minerals with X-ray powder diffraction was developed by ALEXANDER *et al.*, NÁRAY-SZABÓ and PÉTER, and CHUNG [4—10]. It was based on the evalution of the reflection peak of the internal standard samples.

The main problem of the quantitative determination of minerals with both infrared spectroscopy and X-ray powder diffraction is that the most important factors for the quantitative analysis (intensity of an absorption band and a peak in the diffractograms) are the function of the particle size and the crystalline state of the sample. In the infrared spectra of the crystalline minerals, due to the effect of crystalline state, some absorption bands become wider while others sharper, and occasionally some are split into several bands by the degenerate vibration.

Another serious problem is the particle size of the sample to be investigated by infrared spectroscopy. It is well-known that decreasing the particle size of a sample, an increase of the absorbance of the characteristic bands can be obtained. If the samples are ground by intensive vibration grinding to a so-called "amorphous state", the shape of the absorption bands will appear as a characteristic shape of the completely amorphous phase [11—13].

In the X-ray powder diffractograms the position of a reflection peak refers to the quality of the sample while the area of the peak related to any properly selected internal standard is a measure of the quantity of any minerals. The intensity of certain line depends on the particle size of an individual crystal unit of the solid sample in both the Debye-Scherrer and diffractometer techniques. Consequently, in the investigation of samples of the same origin but different crystalline states and particle sizes, the areas of the properly selected peaks may differ considerably. If the particle size is unknown and the crystalline states of the samples used for the calibration curve are different, 100% error may be easily accomplished in the quantitative determination.

In this work effects of the change of the particle size and crystalline state of some minerals on the infrared spectra and X-ray powder diffractograms are discussed in detail.

Experimental

The infrared spectra were taken on a Zeiss Model UR-10 spectrophotometer in KBr-pellet without compensation. Pellets were prepared under strictly identical conditions to allow for the comparison of the different spectra.

A dilution method was used to prepare the pellets and to minimize the error of weighing. One mg sample was imbedded in 800 mg potassium bromide. The X-ray powder diffractograms were taken on a Model 1051 Philips wide-angle powder diffractometer at 1.5405 Å wave length ($CuK_{\alpha average}$). All the diffractograms were recorded on 0.5 g samples The samples were subjected to intensive shaking for a long period to avoid the orientation effect.

100 g air-dry sample was ground in a l-liter vibration ball mill. The total grinding time was 10 days. Samples were taken daily and the infrared spectra and X-ray powder diffractograms were recorded. The particle size of the unground and samples ground for 10 days were determined by an automatic particle counter (Classimat Leitz, Wetzlar, GFR) and also from electron microscopic pictures.

Table I shows the characteristic wavenumbers in the infrared spectra and peaks in the X-ray powder diffractograms.

Table I

Sample	Infrared		X-ray Å
	wavenumber cm^{-1}	assignments	
Kaolins	3705, 3630	O—H stretching vibration	7.16
Quartz	800	Si—O symmetrical stretching vibration	3.346
	695	Si—O bending vibration	
Feldspar	—	—	6.463

No proper infrared absorption bands were found for feldspar

Results and discussion

VAN der MAREL and ZWIERS [14] pointed out that the infrared absorption band at 3705 cm^{-1} is the stretching vibration of O—H groups located between the octahedral and tetrahedral layers, and the absorption band at 3630 cm^{-1} is an O—H stretching vibration within the octahedral layers. These two different O—H groups can only be analysed by infrared spectroscopy.

Change of the absorbance at 3705 cm^{-1} as a function of the grinding time passes through a maximum [15—17]. The degree of disorder in the crystal lattice of the kaolins due to the grinding was characterized by intensity ratio of the two O—H stretching vibration bands. It was proved by X-ray powder diffractograms, electron microscopic pictures and thermal measurements that the ratio of the absorption bands is higher in a poorly ordered kaolin than in the well ordered original one.

The average particle size of the kaolins sampled daily was calculated by the semi-empirical exponential function of ALJAVDIN [21]. The correlation function for the Zettlitz kaolin was found to be the following:

$$y = 0.20 \frac{1}{d} + 0.48 \tag{1}$$

and for the Szegilong paper kaolin

$$y = 0.0225 \frac{1}{d} + 0.64 \tag{2}$$

where: y = absorbance ratio of two O—H stretching vibrations (calculated from the infrared spectra)

$$(y = A_{3630\ cm^{-1}}/A_{3705\ cm^{-1}})$$

d = average particle size of the samples.

The curves of the functions are shown in Figs 1 and 2.

It can be seen from the hyperbolic curves that below the 3 μm particle size limit there is a considerable change in the state of the crystalline structure. By comparing the two correlation functions and the shapes of the curves it can be established that a more pronounced decrease of the regularity of the well ordered crystal lattice of Zettlitz kaolin is obtained in an equal grinding period as in the originally poorly crystallized paper kaolin. In the quantitative determination of kaolins a much better accuracy and reproducibility can be achieved above a particle size of 3 μm and below this limit the determination will be rather uncertain.

The changes in crystallinity of a mineral by grinding can be most precisely followed by X-ray powder diffraction. According to experience the peak height

of a basal reflection changes with the decrease of the particle size and the peak area can be assumed to be constant. Therefore, the decrease of a selected peak area is caused by an increase of the structural lattice disorder. The degree of the order in crystallinity (x) was derived from the ratio of the peak areas of the

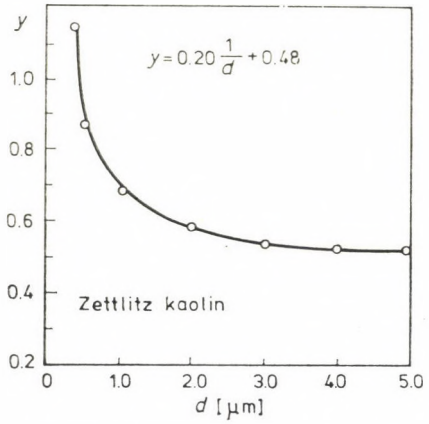

Fig. 1. Absorbance ratio (y) calculated from the IR spectra *vs.* average particle size (d) (Zettlitz kaolin)

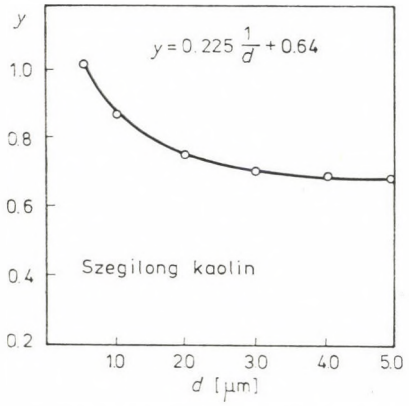

Fig. 2. Absorbance ratio (y) calculated from the IR spectra *vs.* average particle size (d) (Szegilong paper kaolin)

original and ground samples at a properly chosen basal reflection in the X-ray powder diffraction patterns (see Table I).

The correlation functions between the average particle size (d) and the order of the crystal lattice (x) are as follows: (Fig. 3)

$$x = 0.88\, d^{1/2} - 0.11 \qquad (3)$$

for Zettlitz kaolin, and

$$x = 0.128\, d^2 + 0.36 \tag{4}$$

for Szegilong paper kaolin,
where x = the degree of the order derived from the X-ray diffractogram.

It follows from Eqs 3 and 4 that below the 2 μm particle size limit there is a larger change in the basal reflection peak of Zettlitz kaolin while above this limit, due to the parabolic function, the order in the Szegilong paper kaolin decreases considerably. The explanation lies in the fact that the harder

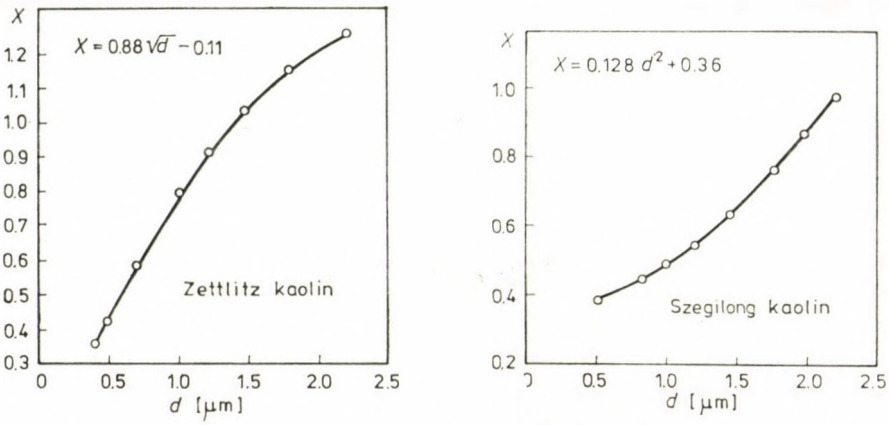

Fig. 3. Degree of order (x) calculated from the X-ray diffractograms *vs.* average particle size (d) (Zettlitz kaolin and Szegilong paper kaolin)

Zettlitz kaolin breaks into smaller pieces at first, but later the primary particles adhere to secondary agglomerates and a decrease in the disorder of the lattice is observed. These phenomena are well represented by the square root function, since the value of x does not change greatly at a larger particle size (> 3 μm).

This condition is reversed with the paper kaolin, which is originally poorly crystallized, because there is a considerable amount of amorphous material at the beginning of the grinding and the decrease of the order becomes slight in the smaller particle size range.

It was concluded from the results of both analytical methods (infrared spectroscopy and X-ray powder diffraction) that the degree of crystal lattice order essentially depended on the decrease of the particle size, especially below the 2 μm limit. By comparing the x *vs.* d and the y *vs.* d functions, it can be seen that the quantitative determination of the minerals by X-ray powder diffraction is more inaccurate than using the infrared method, due to the lack of "constant sections" in the curves. Therefore, samples of strictly identical particle size and crystalline states may be compared only.

It must be noted that each of the samples investigated by infrared and X-ray methods contained well crystallized and poorly crystallized fractions as well. The ratio of these fractions was shifted by grinding towards the poorly-crystallized state but the completely amorphous state has not been achieved yet. It was proved by investigating samples ground for 10 days that the position and intensity of the reflection peaks could be well measured.

Similar investigations were performed on the Urkút quartz and the Swedish feldspar (orthoclase). The determination of the well crystallized quartz in the presence of the amorphous one has been investigated by many scientists [2, 17, 22, 23]. The infrared spectroscopic determination is based on the ab-

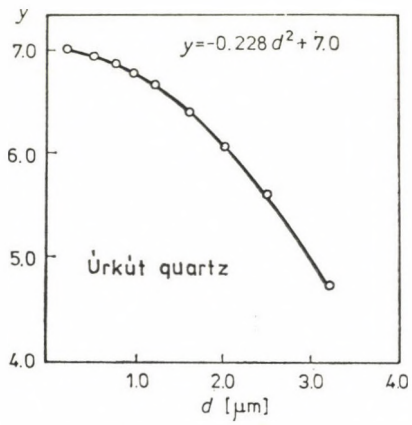

Fig. 4. Absorbance ratio (y) calculated from the IR spectra *vs.* average particle size (d) (Urkút quartz)

sorbance ratio at 802 cm^{-1} (Si—O symmetrical stretching vibration) and at 695 cm^{-1} (Si—O bending vibration) due to the fact that there is only one absorption band at 800 cm^{-1} in the amorphous quartz. Subsequently, if the sample contains amorphous fractions, the ratio of $A_{802\,cm^{-1}}/A_{695\,cm^{-1}}$ (y) is higher [2].

As a function of the average particle size y was found as follows: (Fig. 4)

$$y = -0.228\,d^2 + 7.0 \tag{5}$$

It can be seen from the shape of the curve that the decrease of crystallinity of Urkút quartz was continuous up to a value of $y = 7.0$ which was the assymptote of the function. The extent of the change was smaller at the smaller particles than at the larger ones.

Because of the possibility of the inaccuracy of the quantitative determination, due to the uncertain amorphous part of quartz, samples of identical particle size fractions and crystalline state can be only used for the measure-

ments [22, 23]. A linear function was found between the average particle size (d) and the order of the quartz (x) defined above as: (Fig. 5)

$$x = 0.20\, d + 0.37 \tag{6}$$

According to Eq. 6, it can be realized that there is no proper range for the quantitative determination of quartz due to the lack of a standard section in the curve. Consequently, the amount of quartz in a silicate or a soil sample

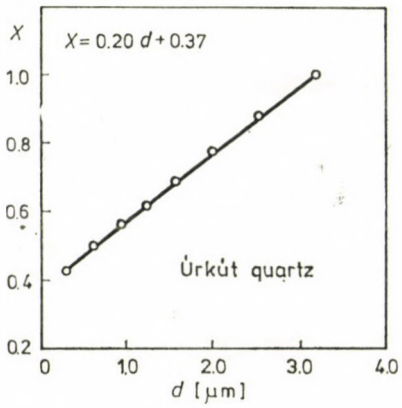

Fig. 5. Degree of order (x) calculated from the X-ray diffractograms *vs.* average particle size (d) (Urkút quartz)

can not be determined more accurately by X-ray powder diffraction than by infrared spectroscopy.

By investigating a properly selected infrared band of the Swedish feldspar, it could be established that during grinding of the mineral first a milling and later, due to the mechanochemical reactions, agglomeration takes place [15].

A closer look at the phenomenon of grinding of feldspar can be obtained by the X-ray powder diffractian pattern. A polynomial function was found between the average particle size (d) and the order (x) of the feldspar samples as follows (Fig. 6):

$$x = 0.03\, d^{2.5} + 0.22 \tag{7}$$

The shape of the curve in Fig. 6 shows that below the 2 μm particle size limit only small changes in the order of the crystalline state are obtained and this makes the quantitative determination by means of X-ray powder diffraction possible.

It can be concluded that the quantitative determination of minerals by infrared spectroscopy and X-ray powder diffraction can only be carried out on samples of strictly identical partical size and order of the structure. It is seen from the equations that valuable informations can be obtained from the

curves of absorbance ratio *vs.* grinding time for the original quality and state of the different minerals. The curves help us to choose the most suitable particle size range for quantitative determinations.

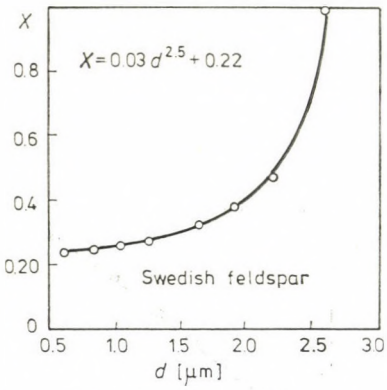

Fig. 6. Degree of order (x) calculated from the X-ray diffractograms *vs.* average particle size (d) (Swedish feldspar)

*

The authors greatly appreciate the help of Dr. K. JÓNÁS and Dr. S. ELEK for taking the infrared spectra and X-ray diffractograms.

REFERENCES

[1] WHITE, J. L.: Soil Science, **22,** 112 (1971)
[2] NEMECZ, E., BÉLAFINÉ: A Veszprémi Vegyipari Egyetem Közleményei, **5,** 287 (1961)
[3] TARTE, P.: Proceedings of the International Conference, Delft. July, 1964
[4] ALEXANDER, L., KLUG, P. H.: Anal. Chem., **20** (10), 886 (1948)
[5] ALEXANDER, L.: X-ray Diffraction Procedures, J. Wiley, New York, 1954
[6] ALEXANDER, L., KLUG, I. H., KUMMER, K.: J. Appl. Phys., **19,** 742 (1948)
[7] NÁRAY-SZABÓ, I., PÉTER, T.: Földtani Közlöny, **94,** 444 (1964)
[8] NÁRAY-SZABÓ, I., PÉTER, T.: Tschermaks mineralog. petrogr. Mitt., **10,** 120 (1965)
[9] CHUNG, H. F.: J. Appl. Cryst., **7,** 519 (1974a)
[10] *Ibid.* **8,** 17 (1975)
[11] JÓNÁS, K.: Thesis, 1976, Veszprém
[12] LARSEN, D. J., DOENHOFF, L. J., GRABLE, J. V.: J. Am. Ind. Hyg. Assoc., **6,** 367 (1972)
[13] SMALLWOOD, S. E., HART, P. B.: Spectrohim. Acta, **19,** 285 (1963)
[14] VAN der MAREL, H. W., ZWIERS, J. H. L.: Silicates Ind., **24,** 359 (1959)
[15] HLAVAY, J.: Thesis, 1975, Veszprém
[16] HLAVAY, J., ELEK, S., JÓNÁS, K., INCZÉDY, J.: Clays and Clay Minerals., **25,** 451 (1977)
[17] HLAVAY, J., ELEK, S., INCZÉDY, J.: Dunántúli Analitikai Konferencia (Transdanubian Analytical Chemistry Conference), Szekszárd, 1975
[18] PARKER, T. W.: Clay Minerals., **8,** 135 (1969)
[19] KEYSER, W. L., DE WOLLAST, R., LAET, L.: Proc. Int. Clay. Conf. Stockholm, 1963, **2** Oxford, Pergamon Press 1965
[20] CHUKROV, F. V., ZVYAGIN, B. B.: Proc. Int. Clay. Conf., **1,** Jerusalem, 1966
[21] BEKE, B.: Építőanyag, **4,** 121 (1974)
[22] LARSEN, D. J., DOENHOFF, L. J., CRABLE, J. V.: J. of Amer. Ind. Hyg. Assoc., **6,** 367 (1972)
[23] HLAVAY, J., ELEK, S., INCZÉDY J.: Hungarian Scientific Instruments HSI, **38,** 69 (1976)

József HLAVAY
János INCZÉDY
H-8201 Veszprém, P. O. Box 28.

Acta Chimica Academiae Scientiarum Hungaricae, Tomus 102 (1), pp. 19—26 (1979)

INVESTIGATION OF THE INTERFACIAL PROPERTIES OF PETROPORPHYRINS AT WATER/OIL INTERFACES

J. LAKATOS-SZABÓ

(Petroleum Engineering Research Laboratory of the Hungarian Academy of Sciences, Miskolc University City)

Received April 14, 1978

Accepted for publication October 18, 1978

The interfacial tension and film forming ability of hydrocarbon fractions containing porphyrins are studied in water/benzene systems. A correlation of these characteristics to porphyrin, nitrogen, and hetero element content, and C/H ratio is attempted. *Meso*-tetraphenyl-porphyrin, the vanadium- and the nickel complex are used as reference. It has been found that compounds with high hetero element content in natural hydrocarbon, mainly those with high oxygen content, decrease interfacial tension, while highly conjugated, unsaturated hydrocarbons decisively enhance film-formation. The possible role of porphyrins is depending not only on concentration but type too.

Introduction

In addition to their role in the settling of geochemical questions, the porphyrins are important because the origin of a number of problems in oil production and processing is just of what type and concentration they are present in crude oils.

LOTTERMOSER [1], MORREL [2], UREN [3] and their colleagues found, in the first third of this century, that the formation of some water-in-oil emulsions was caused by asphaltene-type components, among them by high-molecular weight compounds containing heteroelements. Subsequently, DENEKAS [4], DODD [5], DUNNING *et al.* [6] stated that vanadyl and nickel porphyrin complexes were the principal components of these natural surfactants. BAKER [7], then HODGSON, and HITCHON [8] suggested that, owing to their surfactant character, the porphyrin complexes, like other polar compounds, help the natural hydrocarbons to migrate in aqueous phase.

The film forming ability of crude oils was discussed first by DUNNING [6] and DENEKAS [4]. RIESBERG, and DOSCHER [9] found that displacement efficiency of oils greatly depends on the presence of rigid films which form at water/oil interface. Later DENEKAS *et al.* [10] proved that in the case of petroleum containing polar compounds in great concentration, the spontaneous imbitition rate of water by porous media is lower than it would be otherwise. It was DODD [11], however, who ultimately recognized that the cause of the phenomenon which adversely affects displacement efficiency is, on the one

hand, the great viscosity and the non-newtonian character of the rigid film formed at the water/oil interface, and on the other hand, the possibility that this film may plug the cross-section of free flow in hydrocarbon formations.

Results and discussion

The purpose of this study was to look for a correlation between the porphyrin content of various kinds of Hungarian crude oils or of various petroleum fractions and interfacial tension, and film-forming ability respectively. Therefore, the porphyrin content of the substances studied had to be determined, qualitatively as well as quantitatively, before everything else. Therefore, the porphyrins to be found in petroleum samples were concentrated, then the complexes were identified by means of standard spectrophotometric methods [12, 13].

The same types of petroleum were investigated as dealt with in the papers previously mentioned. In order to avoid repetition, the reader is referred also to Figure 1 in that communication; this figure can serve as a guide to the origin, and to the place of a given hydrocarbon fractions in the system of separation.

A certain measure of contradiction between data in the literature unescapably suggested that decrease of interfacial tension, and film-forming ability of the hydrocarbon fractions were due also to compounds other than porphyrins. Therefore, the hydrocarbon fractions obtained by separation were studied even if they contained only traces of porphyrins.

The pendent drop method [14] was used to measure the interfacial tension and film-forming ability of hydrocarbon fractions. Since the consistence of these hydrocarbon fractions precluded direct use of the water–hydrocarbon system, interfacial tension was determined on the basis of the specific properties of drops which were formed in the aqueous phase, from a solution in benzene. The hydrocarbon content of these solutions was 5 g dm^{-3} in every case.

The reference is the σ_0 of the pure benzene–water system. Results are presented as the change in time, of the difference $\Delta\sigma = \sigma_0 - \sigma_x$ between the interfacial tensions of the two systems. To attain the equilibrium value generally 40 minutes were needed.

In order to lay the preliminary data for our study, the interfacial tensions of the original petroleum samples in benzene were determined first; then the $\Delta\sigma$ values were measured for the extracts, for the fractions obtained by deasphaltation and, finally for the fractions eluated from silicagel columns [13].

As examples taken at random, the $\Delta\sigma$ curves for the original petroleum samples are shown in Fig. 1, while Figs 2 and 3 show such curves for the asphaltene-free fractions, and *iso*-octane asphaltenes respectively, which are separated

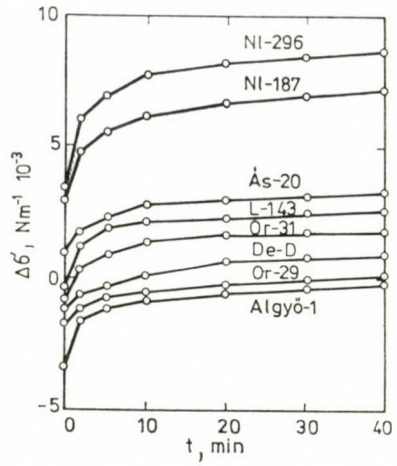

Fig. 1. $\Delta\sigma$ **of the petroleum samples studied, as a function of time**

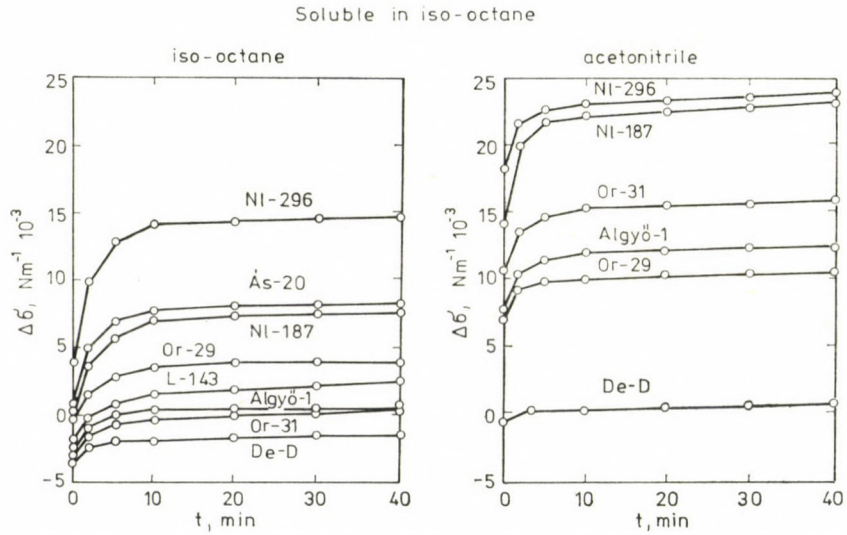

Fig. 2. $\Delta\sigma$ **of *iso*-octane soluble fractions of acetonitrile extracts as a function of time. The fractions were eluated from silica gel columns by *iso*-octane (a) and acetonitrile (b)**

by different solvents (*iso*-octane, cyclohexane and acetonitrile) on silicagel columns wetted with acetonitrile.

No statement valid for all the samples can be found upon the data obtained. The findings, which reveal a tendency, suggest specificity both according to the oil type and to the nature of the fraction (functional group or type of compound). General conclusions can be summarized as follows.

a) The interfacial tension of benzene/water system was decreased most by samples from Nagylengyel, which contain the greatest amount of porphyrin and of asphaltenes among the Hungarian crude oils.

b) The interfacial tension measured for the benzene/water system is hardly at all affected by the other petroleum samples which contain porphyrins in relatively low concentration.

c) The extracts obtained with acetonitrile appear in the sequence as shown for crude oils in Fig. 1.

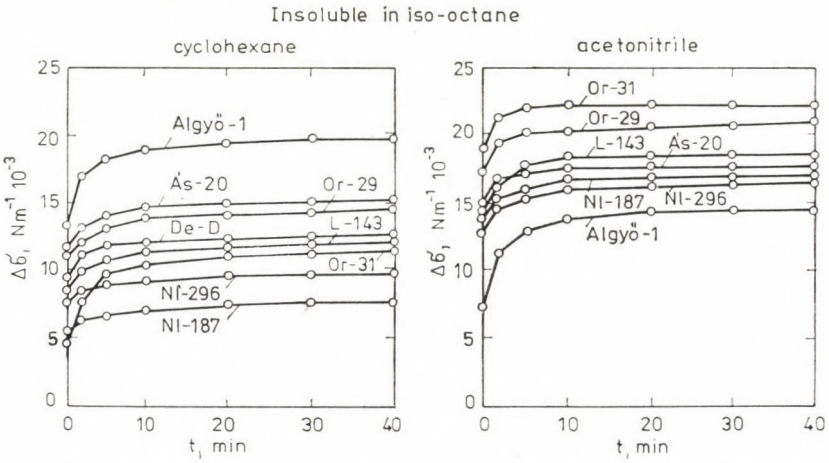

Fig. 3. $\Delta\sigma$ of *iso*-octane asphaltenes of acetonitrile extracts as a function of time. The fractions were eluated from silica gel columns by cyclohexane (a) and acetonitrile (b)

d) Subsequent to removal of asphaltene with *iso*-octane, the interfacial activity of asphaltenes is always greater than rest of the extracts soluble in *iso*-octane.

e) The chromatographic fractions eluated with acetonitrile are more active, as a rule, than the other ones.

After all, interfacial tension of a benzene/water system is decreased most, in every case, by hydrocarbon fractions which are enriched also in prophyrins.

The film-forming ability was observed visually. At retraction of the observed drop of solution into the capillary, at a certain dimension of the drop of a substance that tends towards film-formation, its surface scintillates and creases: a rigid film appears upon it. The specific character of the petroleum and the concentration of the film-forming substances determine [15] at which point during retraction this phenomenon is observable.

The statements that can be put forward concerning the film-forming ability of samples are the following.

a) Film-forming ability was observed at 35% of the hydrocarbon fractions tested.

b) Only one among the initial petroleum samples, *i.e.* the Hungarian petroleum marked L-143, and every fraction of it give a positive result.

c) With a few exceptions, a strong tendency to form a film is evident in the case of *iso*-octane asphaltenes and their column chromatographic fractions.

d) Constituents soluble in *iso*-octane, and their column chromatographic fractions, show a film-forming ability only in a few instances.

In the further course of these studies a correlation was sought, by means of mathematical statistics, of the equilibrium interfacial tension, of the fractions to porphyrin content as well as to the elementary composition of the fractions.

The evaluation, carried out by means of non-parametric statistical methods, subsumed the set of data obtained by cross checks on parameters measured for 45 hydrocarbon fractions. The dimension of the matrix constructed for this purpose was 45×7, the set of data was standardized for the sake of homogeneous derivation.

The non-parametric statistical method was resorted to partly because the relative paucity of samples: the rank correlation coefficients according to Spearman, and the so-called conformance factors according to Kendall, were determined.

The related data are collected in Table I, and shown in Figs 4 and 5. Dots in the figures mark substances which show also a film-forming ability.

Table I

Conformance factors according to the Kendall method

	$\Delta\sigma$	$c_{porphyrin}$
$c_{porphyrin}$	0.379	—
c_N	0.402	0.776
c_{S+O}	0.626	0.320
C/H	0.502	0.444

These data reflect the following general picture.

a) No correlation, expressible in numerical terms, of interfacial activity and film-formation to the porphyrin content of fractions, can be composed in the domain studied.

b) Tendency towards film-formation is due to the presence of highly conjugated, unsaturated hydrocarbons (C/H ratio 9.5—13) which contain also much nitrogen (0.8—3 per cent), occasionally much sulphur and oxygen.

c) **Compounds of high sulphur and oxygen contents in the natural hydrocarbons decrease the interfacial tension. Among these, certainly compounds of high oxygen content play a decisive and important role (Kendall coefficient 0.626).**

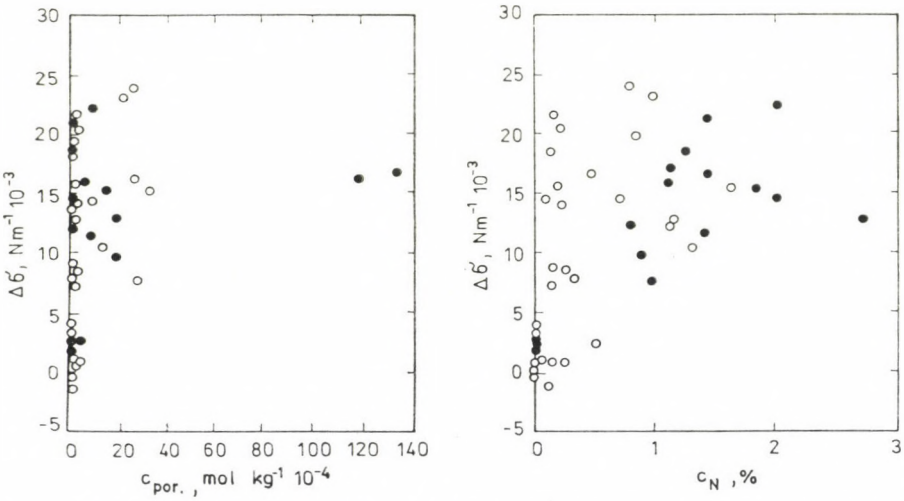

Fig. 4. $\Delta\sigma$ and film-forming tendency, as functions of porphyrin content (a), and of nitrogen content (b)

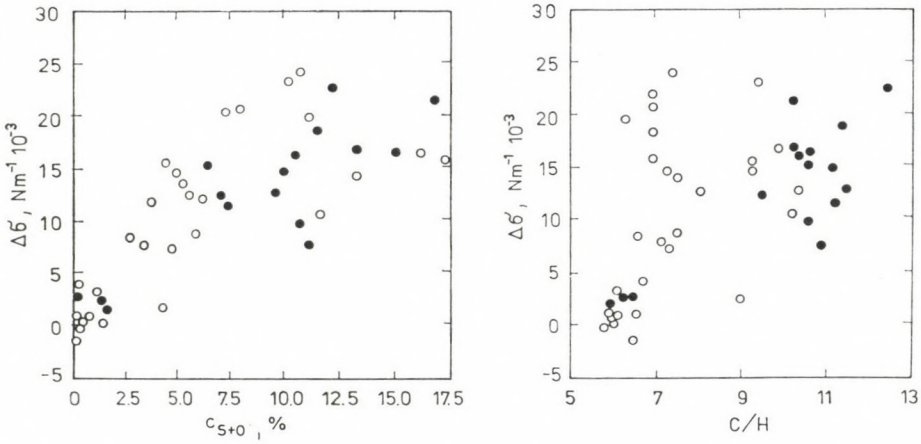

Fig. 5. $\Delta\sigma$ and film forming tendency, as functions of the sulphur, oxygen content of the fractions (a), and of the C/H ratio (b)

All the fractions studied contain porphyrin, but this porphyrin content varies within a relatively narrow range. This is the most likely cause why no definite numerical correlation of porphyrin content to interfacial activity can be found. Yet there manifested the tendency of hydrocarbon fraction within

one sort of petroleum enriched in porphyrins in the course of fractionation to decrease interfacial tension most, respectively the tendency, among the several petroleum samples (the one marked L-143 excepted), of fractions, with higher prophyrin and asphaltene content to be more active and more liable to form film.

In order to prove this, we measured the quilibrium interfacial tension of meso–tetraphenyl–porphyrin, and of its vanadyl- and nickel-complexes at up to 100 ppm solutions in benzene, against distilled water. These data are collected in Figure 6, and they unequivocally demonstrate that interfacial tension is not appreciably affected by porphyrins present at concentrations below 30—40 ppm.

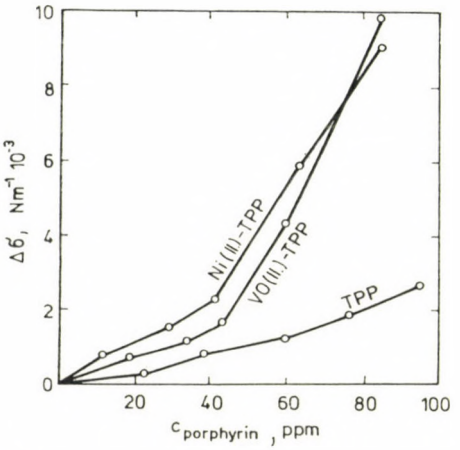

Fig. 6. $\Delta\sigma$ as a function of the concentration of *meso*-tetraphenyl-porphyrin and its complexes

Above this limit, however, their interfacial activity suddenly increases, especially that of metal complexes. As data obtained show, free porphyrins do not decrease considerably the interfacial tension.

If porphyrins at low concentrations ($<$ 30 ppm) do play some essential role in the decrease of interfacial tension, they cannot be but carboxylated pigments. Structural investigations in the fractions studied here do not show their presence (the products of the degradation of hemin during sediment accumulation and transformation are easily decarboxylated and stabilized as ethio-porphyrin [16]). It seems more probable that there is a relation between porphyrin content and film-formation ability. The porphyrin ring is highly conjugated, has a high content in a hetero element (nitrogen, 8—10 per cent), its configuration is planar with eight peripheral groups which are oriented prone on the water interface. It is very probable that the compression (diminution of the dimension of the drop) of the interfacial layer in the presence of such compounds is accompanied by an irreversible change: the formation of a

rigid film. The only fact contradictory to this supposition is found with petroleum from Lovászi. The porphyrin content in this sample is one of the lowest, yet the oil as well as its fractions have a strong tendency to form rigid films at water/oil interface. All in all, at one point the results of these tests divulge the contradiction when some authors consider the role played by porphyrins in interfacial phenomena to be decisive [4—6] and others deem this role to be negligible [17]. Obviously, this contradiction can be resolved by considering first the type, and second the concentration of porphyrins present in petroleum.

REFERENCES

[1] LOTTERMOSER, A., CALANTAR, N.: Kolloid Z., **48,** 362 (1929)
[2] MORREL, J. C., EGLOFF, G.: Colloidal Chemistry of Petroleum, in ALEXANDER, J.: Colloid Chemistry, Chemical Catalog Co., New York, 1931
[3] UREN, L. G.: Petroleum Production Engineering, Oil Field Exploration, McGraw-Hill, New York, 1939
[4] DENEKAS, M. O., CARLSON, F. T., MOORE, J. W., DODD, C. G.: Ind. Eng. Chem., **43,** 1165 (1951)
[5] DODD, C. G., MOORE, J. W., DENEKAS, M. O.: Ind. Eng. Chem., **44,** 2585 (1952)
[6] DUNNING, H. N., MOORE, J. W., DENEKAS, M. O.: Ind. Eng. Chem., **45,** 1759 (1953)
[7] BAKER, E. G.: B. AAPG, **46,** 76 (1962)
[8] HODGSON, G. W., HITCHON, B.: Proc. Comm. Mining Cong., 8th Publ., **5,** 9 (1966)
[9] RIESBERG, J., DOSCHER, T. M.: Producers Monthly, **21,** 43 (1965)
[10] DENEKAS, M. O., MATTAX, C., DAVIS, G. T.: Trans. AIME, **216,** 330 (1959)
[11] DODD, C. G.: J. Phys. Chem., **64,** 544 (1960)
[12] LAKATOS-SZABÓ, J.: Doctoral thesis, University of Chemical Engineering, Veszprém, 1975
[13] LAKATOS-SZABÓ J.; Acta Chim. Acad. Sci. Hung., **98,** 1 (1978)
[14] FORDHAM, S.: Proc. Roy. Soc. (London), **194 A**, 1 (1948)
[15] WAGNER, O.: MTA OBKL, **1,** 31 (1965) (in Hungarian)
[16] HODGSON, G. W., BAKER, B. L., PEAKE, E.: Geochemistry of Porphyrins, in NAGY, B., COLOMBO, U.: Fundamental Aspect of Petroleum Geochemistry. Elsevier, New York, 1967
[17] BURGOYNE, A. T., CAUDLE, B. H., KIMBLER, O. K.: Soc. Pet. Eng. J., **2,** 60 (1974)

Julianna LAKATOS-SZABÓ H-3515 Miskolc — Egyetemváros POB. 2.

Acta Chimica Academiae Scientiarum Hungaricae, Tomus 101 (1—2), pp. 27—37 (1979)

MÖSSBAUER SPECTROSCOPIC STUDY OF THE ELECTRON STRUCTURE OF IRON DIOXIME MIXED COMPLEXES

L. Korecz, A. A. Saghier, Cs. Várhelyi and K. Burger

(Department of Atomic Physics, and Institute of Inorganic and Analytical Chemistry, L. Eötvös University Budapest, Department of Chemistry, Babes—Bólyai University Cluj)

Received July 5, 1978

Accepted for publication October 18, 1978

The Mössbauer study of iron dioxime mixed complexes formed with monodentate nitrogen bases and molecular orbital calculations based upon experimental parameters was used for the determination of the effect of the ligand exchange on the electronic structure, *i.e.* upon the population of σ- and π-orbitals, and the effective charge of the iron central atom.

Introduction

Mössbauer spectroscopy is an adequate method to follow changes in the electron structure of iron complexes. Several papers [1, 2, 3] deal with the Mössbauer study of iron dimethyl glyoxime and its derivatives. Also some nioxime complexes of iron have been studied [4, 5] as well as a number of iron chelates in which the ligands of the chelate ring are bound *via* nitrogen to the iron [6, 9].

Our aim in this work was the Mössbauer spectroscopic study of the mixed iron complexes of dimethyl glyoxime, cyclo-hexanedione-dioxime (nioxime), cyclo-heptanedionedioxime (heptoxime), cyclo-octanedione-dioxime (octoxime), and *iso*-propyldione-dioxime (propoxime) with unidentate N-donor ligands (pyridine, picoline, aniline and their derivates) in order to define the effect of the various chelating agents and unidentate ligands exerted upon the electron structure of iron.

All the six coordination sites of iron are occupied by nitrogen donor atoms in the systems studied. Based on X-ray investigations of some iron complexes [12] and of the analogous copper, nickel and cobaltcomplexes [13] it can be assumed that in all the complexes studied, the nitrogen donor atoms of the dioxime ligands surround the iron in a close to square-planar geometry and the pyridine, picoline or aniline ligands occupy the axial positions. As an example, the structure of a nioxime complex [12] is shown in Fig. 1. In all of these complexes the dioxime ligands are held together, and stretched out in the plane, by O—H—O bridges.

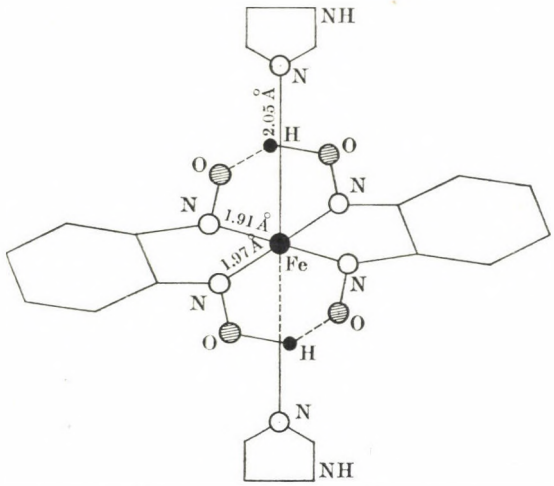

Fig. 1. The structure determined by X-ray diffraction [12] of the Fe(II) (niox. H)$_2$ (imidazole)$_2$ complex

Result and discussion

Mössbauer isomer shifts (δ) and quadrupole splittings (ΔE) of the complexes investigated are collected in Table I. Some data from the literature are also included. Our data agree well with those reported in the literature. The only exception is the lower quadrupole splitting of the bis (dimethyl-glyoximato)-iron-dipyridine complex than that given in the literature.

The quadrupole splittings of the iron(II) complexes are so high that they could be mistaken to belong to high-spin iron(II) or even low-spin iron(III) species. In order to distinguish between the possibilities the magnetic susceptibility of the mixed complexes was measured, and the results indicated that the mixed complexes of iron(II) were diamagnetic and thus the central atom was a low-spin iron(II). The isomer shift values are in agreement with this. This statement is supported by the fact that the isomer shifts of the two analogous mixed iron(III) complexes studied are smaller and their quadrupole splittings are significantly higher than those of the other complexes.

A comparison of Mössbauer data which reflect the effects of various ligands shows that the electron structure of mixed complexes containing pyridine or its derivates is not very sensitive to changes in the chelate or in the monofunctional ligand. The greatest change in isomer shift is 0.07 mm/s (accuracy of measurement is ± 0.015 mm/s), that of quadrupole splitting is more auspicious: 0.3 mm/s. This shows that the co-ordination of the nitrogen of various dioxime ligands to the iron is nearly equally strong. The substitution of an unidentate axial ligand exerts about the same effect upon the parameters

Table I

Mössbauer parameters of some iron-dioxime mixed complexes
Isomer shifts referred to the spectrum of iron recorded at room temperature

	300 K		80 K	
	δ	ΔE	δ	ΔE
Fe(II)(dmg)$_2$(py)$_2$ · 5 H$_2$O	0.24	1.54	0.32	1.52
	0.21*	1.67*	0.29*	1.69*
Fe(II)(dmg)$_2$(β-pic)$_2$	0.25	1.66	0.32	1.63
	0.23*	1.62*	0.33*	1.66*
Fe(II)(dmg)$_2$(γ-pic)$_2$ · H$_2$O	0.22	1.81	0.28	1.77
	0.24*	1.70*	0.29*	1.78*
Fe(II)(niox.H)$_2$(py)$_2$ · H$_2$O	0.18	1.76	0.26	1.75
	0.21**	1.79**	0.28**	1.79**
Fe(II)(niox.H)$_2$(β-pic)$_2$ · H$_2$O	0.20	1.80	0.25	1.80
			0.28**	1.74**
Fe(II)(niox.H)$_2$(γ-pic)$_2$ · H$_2$O	0.22	1.72	0.27	1.72
			0.28**	1.78**
Fe(II)(octox.H)$_2$(py)$_2$ · 1/2H$_2$O	0.20	1.67	0.29	1.67
Fe(II)(octox.H)$_2$(β-pic)$_2$ · H$_2$O	0.22	1.72	0.28	1.71
Fe(II)(octox.H)$_2$(γ-pic)$_2$ · H$_2$O	0.22	1.81	0.28	1.75
Fe(II)(heptox.H)$_2$(py)$_2$ · H$_2$O	0.22	1.63	0.29	1.59
Fe(II)(heptox.H)$_2$(β-pic)$_2$ · H$_2$O	0.22	1.80	0.29	1.76
Fe(II)(propox.H)$_2$(β-pic)$_2$	0.20	1.80	0.27	1.80
Fe(II)(propox.H)$_2$(γ-pic)$_2$	0.21	1.78	0.27	1.72
Fe(II)(octox.H)$_2$(aniline)$_2$	0.11	0.43	0.24	0.47
Fe(II)(octox.H)$_2$(CH$_3$-aniline)$_2$	0.16	0.44	0.23	0.46
Fe(II)(octox.H)$_2$(p-Cl-aniline)$_2$	0.23	0.21	0.31	0.28
Fe(II)(octox.H$_2$)(p-Br-aniline)$_2$	0.23	0.26	0.32	0.26
Fe(II)(octox.H)$_2$(p-I-aniline)$_2$	0.23	0.26	0.32	0.26
Fe(III)(dmg)$_2$(py)$_2$Br · 3 HBr	0.04	2.95	0.09	3.01
Fe(III)(dmg)$_2$(py)$_2$I · 2 HI	0.04	2.97	0.11	3.01

* Ref. [1]
** Ref. [4]

as the substitution of the dioxime ligand, though the latter forms a chelate ring of rather pronounced conjugation with the iron atom.

A linear correlation was found between the isomer shift and quadrupole splitting values (Fig. 2) in the case of pyridine mixed complexes with various dioximes. This reflected the following order in the π-acceptor strengths of the dioxime ligands: dimethyl-glyoxime $<$ heptoxime $<$ octoxime $<$ nioxime.

In the γ-picoline complexes, however, the isomer shift δ, and quadrupole splitting values ΔE are independent of the dioxime ligand. The greatest deviation in the isomer shift values is 0.01 mm/s and 0.09 mm/s in the quadrupole splittings. This phenomenon suggests that there exists a greater interaction of the two types of ligands, this interaction is reflected in the greater quadrupole splittings, too. This dual phenomenon can be interpreted as follows. Theoretical considerations [10] and experimental data [11] show that electron density on

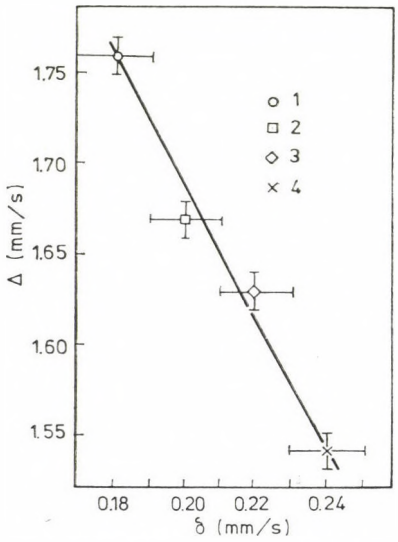

Fig. 2. Correlation of isomer shift and quadrupole splitting in mixed pyridine complexes of iron with various dioximes, at room temperature; 1 = nioxime, 2 = octoxime, 3 = heptoxime, 4 = dimethyl glyoxime

the heteronitrogen differs but very little in pyridine and in β-picoline complexes, while in γ-picoline complexes π-electron population is increased. According to NQR measurements [11] this change amounts to 0.04 electrons, while the σ-population remains unchanged. The π-acceptor ability of the nitrogen of the γ-picoline ring is diminished because of the increase of the population on the π-orbital, therefore an increase of back-coordination from d_{xz} and d_{yz} orbitals towards the equatorial dioxime ligands occurs. The latter effect can compensate the former one. Thus the *s* electrons are shielded in the same extent. This means that the isomer shift does not change the quadrupole splitting, however, gets a positive increment, thus becomes greater.

According to a molecular orbital scheme, the formers can be interpreted as follows. The coefficient of the *d* orbital of iron does not change in the linear combination of the appropriate orbitals while in the ligand orbital the significance of the planar ligand is increased at the expense of that of the axial one.

Considering energy levels, it can be said that owing to the changes in π-axial and π-planar levels the position of the π-level of the ligand is changed: the ligand π-orbital assumes the character of the planar ligand in a greater measure.

Comparing the data relevant to complexes in which only the axial ligands are substituted, the quadrupole splittings follow in the sequence

$$\text{py} < \beta\text{-pic} < \gamma\text{-pic},$$

in dimethyl-glyoxime, -heptoxime- and -octoxime mixed complexes. In the case of nioxime complexes a different sequence is evident, *viz.*

$$\gamma\text{-pic} < \text{py} < \beta\text{-pic},$$

and with propoxime complexes we found the following sequence:

$$\text{py} < \gamma\text{-pic} < \beta\text{-pic}.$$

It is to be supposed that these differences are due to steric reasons. The MO model calculations given in Table III lead to similar results. These data show that the character of σ-donor or π-acceptor ability of pyridine, β-picoline and γ-picoline depends on the nature of the equatorial ligand.

In the case of complexes with aniline or one of its derivatives as an axial ligand, low quadrupole splittings occur which deviate considerably from the former figures. ΔE decreased from 1.5—1.8 mm/s to 0.26—0.47 mm/s. Complexes with halogen substituents in the ligand have the lower values.

The extremely great decrease in quadrupole splittings reflects an increase in symmetry of charge distribution around iron(II). Low ΔE values point to a near octahedral charge distribution: the six nitrogens become very similar and their distance from iron nearly the same. The significantly higher quadrupole splittings of pyridine mixed complexes can be explained with distances much greater between pyridine nitrogens and iron than those between dioxime nitrogens and iron, the former being 2.05 Å, the latter 1.91—1.97 Å. This distortion is probably due to steric reasons. A slight deviation occurs also in the isomer shifts. This is smaller for the aniline- and *p*-methyl-aniline complexes, and greater for *p*-chloro-, *p*-bromo-, and *p*-iodoaniline complexes, than for those discussed above. This correlation suggests that electrophile halogen substituents favour π-interaction.

The changes in occupancy of π- and σ-orbitals due to substitution of ligands were calculated from the Mössbauer parameters, using a method partly obtained from the literature [1, 9] and modified in our earlier work [7, 8]. We assumed in these calculations, that the sign of the quadrupole splitting of the complexes is positive. This supposition was justified, since DALE *et al.* [5], by

having subjected $Fe(II)(niox)_2(py)_2$ to an external magnetic field, obtained positive sign for ΔE. Since the Mössbauer parameters of the other complexes are but slightly different from those of the complex mentioned, and since also their inner coordination sphere is similar, it is highly probable that also the sign of the splitting is the same. Based on the molecular orbital model mentioned above the positive sign turns up because the d_{xy} orbital is non-bonding and accommodates two electrons while the d_{xz} and d_{yz} are bonding orbitals partly belonging to the ligands. The latter two would only compensate for the positive sense of d_{xy} when completely filled and when belonging entirely to the iron atom.

The method of calculations is given later; the results are compiled in Tables II and III. The calculations aimed at the characterization of the changes brought about in the population of π- and σ-orbitals of the central iron atom, and in the effective charge by the substitution of a ligand in the separate systems. Accordingly, in Tables II and III, the $\Delta\alpha'$ figures give the variations in the populations of π-orbitals, the $\Delta\alpha$ figures those in that of σ-orbitals, and $\Delta\eta$ figures those in the effective charge, all compared to a reference complex. The reference complexes are selected so as to enable us to follow separately the effect of substitution of both monodentate (pyridine base) and chelating (dioxime) ligands on the σ- and the π-interactions. Correspondingly, Table II shows the effect of the substitution of a dioxime upon the electron structure of the central iron atom of mixed complexes with pyridine (compounds 1—4),

Table II

Changes of the population on the π-orbital ($\Delta\alpha'$), on the σ-orbital ($\Delta\alpha$) and of the effective charge ($\Delta\eta$) of the iron atom due to the dioxime ligand substitution

	Compound	$\Delta\alpha'$		$\Delta\alpha$		$\Delta\eta$	
		300 K	80 K	300 K	80 K	300 K	80 K
1	$Fe(II)(dmg)_2(py)_2 \cdot 5\,H_2O$	0	0	0	0	0	0
2	$Fe(II)(niox.H)_2(py)_2 \cdot H_2O$	−0.06	−0.06	−0.10	−0.11	+0.16	+0.17
3	$Fe(II)(octox.H)_2(py)_2 \cdot 1/2H_2O$	−0.04	−0.03	−0.04	−0.08	+0.08	+0.11
4	$Fe(II)(heptox.H)_2(py)_2 \cdot H_2O$	−0.02	−0.03	−0.05	−0.02	+0.07	+0.05
5	$Fe(II)(dmg)_2(\beta\text{-pic})_2$	0	0	0	0	0	0
6	$Fe(II)(niox.H)_2(\beta\text{-pic})_2 \cdot H_2O$	−0.05	−0.07	−0.04	−0.04	+0.09	+0.11
7	$Fe(II)(heptox.H)_2(\beta\text{-pic})_2 \cdot H_2O$	−0.03	−0.04	−0.01	−0.01	+0.04	+0.05
8	$Fe(II)(heptox.H)_2(\beta\text{-pic})_2 \cdot H_2O$	−0.03	−0.03	−0.07	−0.06	+0.10	+0.09
9	$Fe(II)(propox.H)_2(\beta\text{-pic})_2$	−0.05	−0.05	−0.04	−0.07	+0.09	+0.12
10	$Fe(II)(dmg)_2(\gamma\text{-pic})_2 \cdot H_2O$	0	0	0	0	0	0
11	$Fe(II)(niox.H)_2(\gamma\text{-pic})_2 \cdot H_2O$	0	−0.01	+0.07	+0.06	−0.07	−0.05
12	$Fe(II)(octox.H)_2(\gamma\text{-pic})_2 \cdot H_2O$	0	0	0	+0.02	0	−0.02
13	$Fe(II)(propox.H)_2(\gamma\text{-pic})_2$	−0.01	−0.01	+0.04	+0.06	−0.03	−0.05

Table III

Changes due to the substitution of the axial ligand, on the population of the π-orbital ($\Delta\alpha'$) of the σ-orbital ($\Delta\alpha$) and in the effective charge ($\Delta\eta$) of the iron atom

	Compound	$\Delta\alpha'$		$\Delta\alpha$		$\Delta\eta$	
		300 K	80 K	300 K	80 K	300 K	80 K
1	$Fe(II)(dmg)_2(py)_2 \cdot 5\ H_2O$	0	0	0	0	0	0
2	$Fe(II)(dmg)_2(\beta\text{-pic})_2$	+0.01	0	−0.12	−0.09	+0.11	+0.09
3	$Fe(II)(dmg)_2(\gamma\text{-pic})_2 \cdot H_2O$	−0.02	−0.04	−0.20	−0.15	+0.22	+0.19
4	$Fe(III)(dmg)_2(py)_2Br \cdot 3\ HBr$	−0.19	−0.22	−0.89	−0.91	+1.08	+1.13
5	$Fe(III)(dmg)_2(py)_2I \cdot 2\ HI$	−0.19	−0.20	−0.91	−0.94	+1.10	+1.14
6	$Fe(II)(niox.H)_2(py)_2 \cdot H_2O$	0	0	0	0	0	0
7	$Fe(II)(niox.H)_2(\beta\text{-pic})_2 \cdot H_2O$	+0.02	−0.01	−0.06	−0.03	+0.04	+0.04
8	$Fe(II)(niox.H)_2(\gamma\text{-pic})_2 \cdot H_2O$	+0.04	+0.01	−0.02	+0.01	−0.02	−0.02
9	$Fe(II)(octox.H)_2(py)_2 \cdot 1/2H_2O$	0	0	0	0	0	0
10	$Fe(II)(octox.H)_2(\beta\text{-pic})_2 \cdot H_2O$	+0.02	−0.01	−0.07	−0.02	+0.05	+0.03
11	$Fe(II)(octox.H)_2(\gamma\text{-pic})_2 \cdot H_2O$	+0.02	−0.01	−0.01	−0.05	−0.01	+0.06
12	$Fe(II)(heptox.H)_2(py)_2 \cdot H_2O$	0	0	0	0	0	0
13	$Fe(II)(heptox.H)_2(\beta\text{-pic})_2$	0	0	−0.14	−0.14	+0.14	+0.14

β-picoline (compounds 5—9), and γ-picoline (compounds 10—13). As discussed earlier, and reflected by the experimental Mössbauer parameters, the similar behaviour of pyridine and β-picoline complexes and the different behaviour of γ-picoline are more pronounced in the calculated data, indicating a stronger interaction of the two kinds of ligands in the latter systems.

Table III demonstrates the effect of monodentate ligands in systems with the same dioxime ligand. For each system the mixed complex with pyridine serves as a reference compound. It is to be seen that the effect on the electron structure of iron in the expected order py β-pic γ-pic is realized only in the dimethylglyoxime mixed complexes. In the systems stabilized by a hydrocarbon ring within the ligand, other, presumably steric, effects render connexions more involved.

It must be noted that parameters in Tables II and III are calculated from experimental Mössbauer parameters which show comparatively small deviations, thus a finer appreciation of weak interactions can not be expected on the basis of these either.

In Table III the data pertinent to the two iron(III) mixed complexes studied (compounds 4 and 5) are compared with those of the analogous iron(II) complexes. These data show that oxidation of the central iron atom brings about a significantly greater decrease of electron density on σ-orbitals than on π-orbitals. The result of the overall interaction is a one-electron change in the effective charge of the iron atom.

Table IV

Analysis data of the complexes

		Iron %		Nitrogen %	
		Calc.	Found	Calc.	Found
1	$Fe(II)(dmg)_2(py)_2 \cdot 5\ H_2O$	10.45	10.10	15.72	15.30
2	$Fe(II)(dmg)_2(\beta\text{-pic})_2$	11.82	11.30	17.80	17.20
3	$Fe(II)(dmg)_2(\gamma\text{-pic})_2 \cdot H_2O$	11.39	11.24	17.10	16.90
44	$Fe(III)(dmg)_2(py)_2Br \cdot 3\ HBr$	7.28	7.43	10.96	10.80
5	$Fe(III)(dmg)_2(py)_2I \cdot 2\ HI$	6.75	6.52	10.16	10.26
6	$Fe(II)(niox.H)_2(py)_2 \cdot H_2O$	10.90	10.35	16.34	16.10
7	$Fe(II)(niox.H)_2(\beta\text{-pic})_2 \cdot H_2O$	10.29	10.71	15.50	15.20
8	$Fe(II)(niox.H)_2(\gamma\text{-pic})_2 \cdot H_2O$	10.29	10.36	15.50	15.20
9	$Fe(II)(octox.H)_2(py)_2 \cdot 1/2H_2O$	9.64	9.50	14.50	14.66
10	$Fe(II)(octox.H)_2(\beta\text{-pic})_2 \cdot H_2O$	9.40	9.24	14.04	13.80
11	$Fe(II)(octox.H)_2(\gamma\text{-pic})_2 \cdot H_2O$	9.40	9.36	14.04	14.22
12	$Fe(II)(heptox.H)_2(py)_2 \cdot H_2O$	9.79	9.66	14.73	14.66
13	$Fe(II)(heptox.H)_2(\beta\text{-pic})_2 \cdot H_2O$	10.30	10.20	15.50	15.36
14	$Fe(II)(propox.H)_2(\gamma\text{-pic})_2$	10.57	10.33	15.90	15.77
15	$Fe(II)(propox.H)_2(\gamma\text{-pic})_2$	10.57	10.66	15.90	15.87

Experimental

Methods, published earlier [14—21] for the preparation of analogous cobalt complexes were applied for the preparation of the dioxime mixed complexes investigated. Iron(II) complexes were synthesized in an atmosphere of nitrogen gas free of oxygen. The complexes were analyzed for iron and nitrogen. The results, together with calculated figures, are collected in Table IV. The agreement between the two sets of figures is satisfactory, the deviations remain within the limits of error of measurement.

The recording of the Mössbauer spectra was carried out as described in a previous communication [8], at room temperature, and at the temperature of liquid nitrogen. The source was cobalt-57 diffused into copper (Amersham, England). A computer was used for the evaluation of the spectra. The isomer shift figures refer to the elementary iron at room temperature. Mössbauer parameters were reproducible within ± 0.015 mm/s.

The magnetic susceptibility of the complexes was measured by the Faraday method [22]. All the iron(II) complexes were found to be diamagnetic. The magnetic susceptibility of iron(III) compounds was not measured.

Methods of calculation

The changes caused by ligand substitution in the population of σ- and π-orbitals were calculated from Mössbauer parameters determined experimentally. For this purpose a simple MO-model [1, 7] was adopted in which the symmetry of the complexes was nearly octahedral. Then the σ-bonding molecular orbitals are the following:

$$\Psi_1(a_{1g}) = \alpha_1 s + \beta_1 \frac{1}{\sqrt{6}}(\sigma_1 + \sigma_4) + \gamma_1 \frac{1}{\sqrt{6}}(\sigma_2 + \sigma_3 + \sigma_5 + \sigma_6)$$

$$\Psi_2(a_{2u}) = \alpha_2 p_z + \beta_2 \frac{1}{\sqrt{2}}(\sigma_1 - \sigma_4)$$

$$\Psi_3(e_{1u}) = \alpha_3 p_x + \gamma_2 \frac{1}{\sqrt{2}}(\sigma_2 - \sigma_5)$$

$$\Psi_4(e_{1u}) = \alpha_3 p_y + \gamma_2 \frac{1}{\sqrt{2}}(\sigma_3 - \sigma_6)$$

$$\Psi_5(a_{1g}) = \alpha_4 d_z + \beta_3 \frac{1}{\sqrt{3}}(\sigma_1 + \sigma_4) + \gamma_3 \frac{1}{\sqrt{12}}(\sigma_2 + \sigma_3 + \sigma_5 + \sigma_6)$$

$$\Psi_6(b_{1g}) = \alpha_5 d_{x^2-y^2} + \gamma_4 \frac{1}{2}(\sigma_2 + \sigma_5 - \sigma_3 - \sigma_6)$$

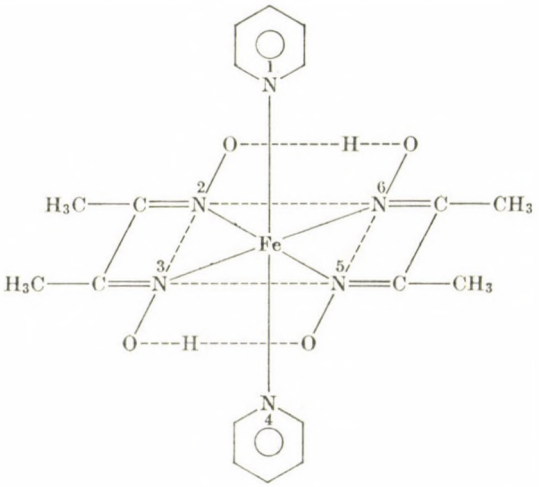

Fig. 3. Structural formula of Fe(II)(dimethyl-glyoxime.H)$_2$(pyridine)$_2$

where α represents the coefficients of the atomic orbitals of iron, β the orbitals of the axial (pyridine base) ligands, γ those of the planar (dioxime) ligands.

The numeration of the ligands is shown in Fig. 3. In a first approximation it may be supposed that substitution of axial ligands does not affect the orbitals of the planar ligands, *viz.* $\delta\gamma_1 = 0$, and *vice versa*: changing the ligands in the plane, $\delta\beta_i = 0$. With obvious suppositions concerning the changes of α and β and disregarding the overlaps, from normal conditions, it follows that the degrees of filling up of atomic orbitals can not change independently one from the other, but only in a definite ratio. For instance, owing to the effect of substitution of axial ligands the change of the charges on orbitals 4s, 4p$_z$ and 3d$_{z^2}$ will be in-the ratio

$$\Delta\alpha_1^2 : \Delta\alpha_2^2 : \Delta\alpha_4^2 = 1 : 3 : 2$$

If $\frac{\Delta\alpha_1^2}{2}$ is symbolized by Δx, then the overall change of the charge on σ-bonding iron orbitals can be written as $\Delta\alpha = 12\Delta x$, or. to express also the configuration $(3d^24s4p^3)^{2\Delta x}$.

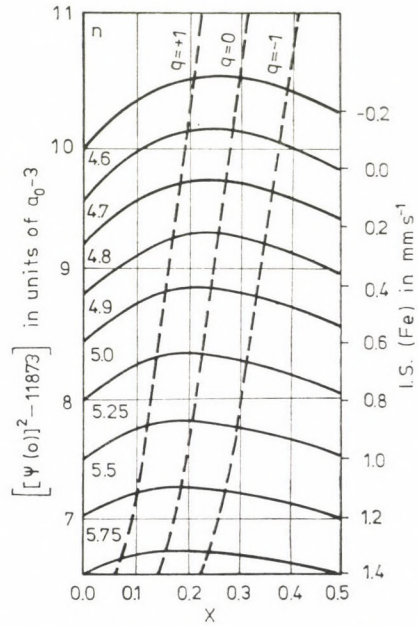

Fig. 4. Interpretationary diagram of Mössbauer isomer shifts of molecules with electron structure $3d^n(3d^24s4p^3)^{2X}$ where q is the effective charge of the iron atom. Left-hand ordinate = electron density at the nucleus of the iron atom (value diminished by 11 873, according to convention), in a_0^{-3} units, where a_0 = first Bohr radius of the hydrogen atom.

Back-coordination can be expected from π-bonding *i.e.* from $3d_{xz}$, $3d_{yz}$ and $3d_{xy}$ orbitals. Like the alteration of σ-bonding, also this can be characterized by one parameter, *viz.* $\Delta\alpha' = \Delta n$. Thus, in the case adduced as an example, the electron structre of the iron atom can be written in the form $3d^n(3d^24s4p^3)^{2x}$.

The two parameters of Mössbauer spectra, *i.e.* isomer shift and quadrupole splitting are functions of the electron structure. A given electron structure determines Mössbauer parameters, but inversely this is not so: a given set of parameters can account for many kinds of electron structures. Assignement can be rendered more specific by some assumption concerning electron structure, *e.g.* that the electron structure of the iron in these molecules is $3d^n(3d^24s4p^3)^{2x}$. The figures for n and x, respectively and the changes of these $\Delta\alpha$ and $\Delta\alpha'$ can be determined. Figure 4 shows the correlation of isomer shift with the parameters n and x based on the structure suggested. When it is supposed that the effective charge q of the iron atom in the complex is a small positive value $0 < q < 1$, then isomer shift reflects the change of back-coordi-

nation: represented by n, and is insensitive to that of the coordination represented by x (the tangents to the curves are between $q = 0$ and $q = 1$ nearly horizontal). The quadrupole splitting is, however, significantly affected by x. The change of isomer shift and of quadrupole splitting ($\delta - \delta_0$ and $\Delta E - \Delta E_0$) referred to an initial complex can be brought into correlation with the change of coordination and back-coordination (of $\Delta\alpha$ and $\Delta\alpha'$) as follows:

$$\delta - \delta_0 = 1.05\Delta\alpha' \text{ and}$$
$$\Delta E - \Delta E_0 = -1.2\Delta\alpha - 1.8\Delta\alpha'$$

For the latter equation the contribution of one electron to the quadrupole splitting is taken to be 3.6 mm/s. Similar considerations help us to find analogous correlations in the case of substitution of planar ligands. Results of such calculations are collected in Tables II and III.

REFERENCES

[1] Ablov, A. V., Goldanskii, V. I., Stukan, R. A., Makarov, E. F.: Dokl. Akad. Nauk SSSR, **170,** 128 (1966)
[2] Ablov, A. V., Goldanskii, V. I., Stukan, R. A., Turta, K. I., Zubarev, B. N.: Dokl. Akad. Nauk SSSR, **186,** 850 (1969)
[3] Burger, K., Korecz, L., Manuba, I. B. A., Mag, P.: J. Inorg. Nucl. Chem., **28,** 1973 (1966)
[4] Dale, B. W., Williams, R. J. P., Edwards, P. R., Johnson, C. E.: Trans. Faraday Soc., **64,** 620 (1968)
[5] Dale, B. W., Williams, R. J. P., Edwards, P. R., Johnson, C. E.: Trans. Faraday Soc., **64,** 3011 (1968)
[6] Turta, K. I.: Thesis, Kishinev, 1971
[7] Korecz, L.: Proc. Conf. Mössbauer spectroscopy, Bratislava 1973, Part I., p. 215
[8] Korecz, L., Abou, H., Ortaggi, G., Graziani, M., Belluco, U., Burger, K.: Inorg. Chim. Acta, **9,** 209 (1974)
[9] Safranskii, V. N., Zubarev, V. N., Stukan, R. A., Turta, K. I., Buburuz, D. D.: Izv. Akad. Nauk SSSR Ser. Himia 1976, no. **2,** 260; Stukan, R. A., Turta, K. I., Ablov, A. V., Zubarev, V. N., Goldman, A. M.: Zhurn. Neorg. Him., **21,** 286 (1976)
[10] Cartier, J. P., Sandorfy, C.: Canad. J. Chem., **41,** 2759 (1963)
[11] Lucken, E. A. C.: Nuclear Quadrupole Coupling Constants, Academic Press, London and New York, 1969, p. 242
[12] Prout, C. K., Wiseman, T. J.: J. Chem. Soc., **1964,** 497
[13] Godycki, L. E., Rundle, R. E.: Acta Cryst., **6,** 487 (1953) Frasson, E., Bardi, R., Bezzi, S.: Acta Cryst., **12,** 201 (1959)
[14] Cambi, L., Corriselli, S.: Gazz. Chim. Ital., **66,** 81 (1936)
[15] Feigl, F., Rubinstein, H.: Liebigs Ann., **433,** 183 (1923)
[16] Ablov, A. V.: Bull. Soc. Chim. France, **57,** 151 (1940)
[17] Finta, Z., Várhelyi, Cs.: Acta Chim. (Budapest) **83,** 281 (1974)
[18] Babko, A. K. Korotum, V.: Zh. Obshch. Chim. (J. Allg. Chem. UdSSR), **24,** 597 (1954)
[19] Ablov, A. V.: Dokl. Akad. Nauk SSSR (Ber. Akad. Wiss. UdSSR), **97,** 1019 (1954)
[20] Várhelyi, Cs., Ganescu, I., Szotyori, L.: Z. Anorg. Allg. Chem., **386,** 232 (1971)
[21] Várhelyi, Cs. Finta, Z., Bedő, A., Mihálycsa, Sz.: Acta Chim. (Budapest) **89,** 45 (1976)
[22] Vértes, A., Burger, K., Tarnóczy, T., Papp-Molnár, E., Egyed, C. L.: Acta Chim. Acad. Sci. Hung., **59,** 15 (1969)

László Korecz
Al-Hassan A. Shagier
Csaba Várhelyi
Kálmán Burger

H-1088 Budapest, Múzeum krt. 4/b.

Acta Chimica Academiae Scientiarum Hungaricae, Tomus 102 (1), pp. 39—50 (1979)

AMINOPHTHALAZINONE DERIVATIVES, V*

SYNTHESIS OF 4-HYDRAZINO-1-(2*H*)-PHTHALAZINONES, I

K. KÖRMENDY, K. Á. JUHÁSZ** and É. LEMBERKOVICS**

(Department of Organic Chemistry, Eötvös Loránd University, Budapest)

Received April 13, 1978

Accepted for publication October 20, 1978

3-Oxo-1-iminoisoindoline (**3**) yields with monosubstituted alkylhydrazines aminophthalazinone derivatives (**5**) substituted at the N(2) position whose structures have been also confirmed in a preparative way. Substitution at N(2) hinders the exchange of the amino group for hydrazino group, therefore the pathway **3** → **5** → **6** is unsuitable for an extension of the KÖHLER synthesis [1]. Compound **3** with *N,N*-disubstituted alkyl and cyclic alkylenehydrazines (*e.g.*, *N*-aminopiperidine) gives hydrazonoisoindolinones (**9**) in satisfactory yields; these can be converted with hydrazine hydrate and with methylhydrazine and 2-hydroxyethylhydrazine into the hydrazinophthalazinone derivatives having the structures **10** and **11**, respectively. 4-Aminophthalazinone (**4**) and the hydrazinophthalazinones (**10**) prepared can be methylated at N(2) by means of dimethyl sulfate.

Of the hydrazine derivatives of phthalazine, the hydrochlorides of 1-hydrazinophthalazine and 1,4-dihydrazinophthalazine are available commercially as important hypotensive agents (Apresolin and Nepresol, Ciba AG). According to KÖHLER [1] *et al.*, 4-hydrazino-1(2*H*)-phthalazinone (**1**) also possesses a marked hypotensive effect.

There are several possibilities described in the literature [1] for the synthesis of hydrazinophthalazinone (**1**). Of these, the syntheses starting from 4-chlorophthalazinone (**2** → **1**) and from 3-oxo-1-iminoisoindoline through aminophthalazinone (**3** → **4** → **1**) have preparative importance. 3-Oxo-1-iminoisoindoline (**3**) was allowed to react with hydrazine first by ELVIDGE [2]; the product was assumed to be phthalimidrazone (**9**; Q = NH_2). Correction of the structure was made by KÖHLER, showing that the product was 4-aminophthalazinone (**4**).

In our studies on the hydrazinolysis of 3-oxo-1-iminoisoindoline (**3**), it was established that the first step of the complex conversion, the formation of aminophthalazinone (**3** → **4**), was a rapid reaction, whereas the final step (**4** → **1**) was very slow and practically did not take place at room temperature. It can be concluded that the hydrazinolysis of 3-oxo-1-iminoisoindoline at room temperature (the yield being 64% according to FLITSCH [3]), or preferably the

* Part IV, Acta Chim. Acad. Sci. Hung. **99**, 81—95 (1979)

** Results of the diploma theses (Budapest, 1972 and 1976) are used.

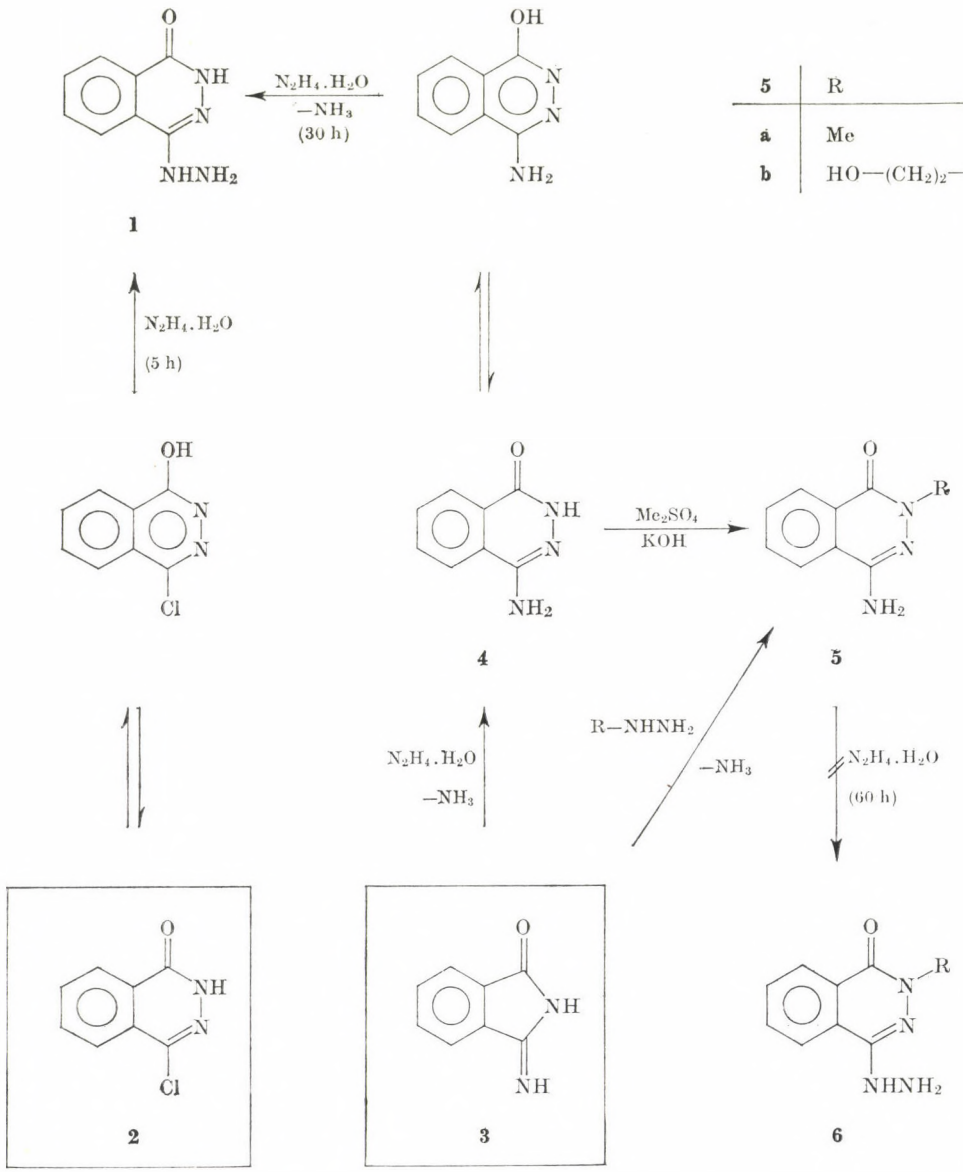

5	R
a	Me
b	HO—$(CH_2)_2$—

reaction suggested by us including a short refluxing (yield 85—90%), are the best syntheses for aminophthalazinone known today.

KÖHLER [1] regarded the conversion **4** → **1** with 100% hydrazine hydrate in 5 h as complete; however, our observations indicate that refluxing for about 25—30 h is necessary to achieve the formation of a uniform reaction product as shown by the IR spectra (complete development of the bands at 3300 and

990 cm^{-1}, characteristic of the hydrazino compound, requires about this period of time). Since hydrazinolysis of 4-chlorophthalazinone is practically complete in 5 h, this method (**2** → **1**) is the most suitable for the preparation of hydrazinophthalazinone.

3-Oxo-1-iminoisoindoline (**3**) yields with monosubstituted alkylhydrazines aminophthalazinones substituted at the N(2) position (**5**). In these compounds, in contrast with 4-aminophthalazinone (**4**), the exchange of the amino group by means of hydrazine hydrate (**5** → **6**) cannot be accomplished in the usual way [1]. The substitution reaction is hindered, probably owing to precluded aromatization due to the presence of the substituent at N(2). (To elucidate this assumption it may be mentioned that the *aromatic* 1.4-dichlorophthalazine is much more prone to participating in substitution reactions than 4-chlorophthalazinone is [3, 4]. In basic media, even if to a limited extent, the enolized, aromatic tautomeric forms of 4-chlorophthalazinone (**2**) and 4-aminophthalazinone (**4**) must be considered, and these, on the analogy of the above facts, must be more reactive than the acid amide forms. This may be responsible for the reactivity of **2** and **4** towards hydrazine hydrate.)

The monosubstituted hydrazine can be incorporated into the phthalazinone skeleton is two ways: substituent R may assume position N(2) or N(3). Earlier, the alkylation of 4-(2-hydroxyethylamino)-1(2*H*)-phthalazinone (the so-called β-spiroxazone) was studied in detail, and N(2) alkylation was confirmed by preparative [5], IR, NMR [6] and MS [7] evidence. The monomethyl derivative formed in the methylation of aminophthalazinone with dimethyl sulfate (**4** → **5a**) is entirely identical with the compound obtained from the **3** → **5a** reaction. This identity in itself substantiates the N(2) position of substituent R in compounds of type **5**, but decision between the two possible structural isomers, **5** and **5'**, was also made in a preparative way.

When fused with veratraldehyde, compounds **5a** and **5b** give readily crystallizing condensation products (**7**). The Schiff bases can be decomposed into the starting aminophthalazinones **5a** and **5b** by acid hydrolysis, which excludes any possibility of a **5** → **5'** transisomerization during the fusion process. Since only structure **5** containing a primary amino group is capable of condensation, group R is certainly in position N(2).

4-Aminophthalazinone (**4**) and its derivatives substituted at N(2) (**5a**, **5b**) react with phenyl isocyanate to give phthalazonylphenylurea derivatives (**8**). Compounds **4** and **5a** yield only the monophenylcarbamoyl derivatives even with a high excess of phenyl isocyanate, therefore the structure of the product can be only **8** or **8'**; the actual structure depends on the fact whether the aminophthalazinone reacts with the tautomeric form containing the endocyclic or exocyclic C = N group. Although the structural isomer **8'** cannot be definitely excluded on the basis of the present knowledge, still structure **8** seems to be more probable, since the tautomer containing the endocyclic

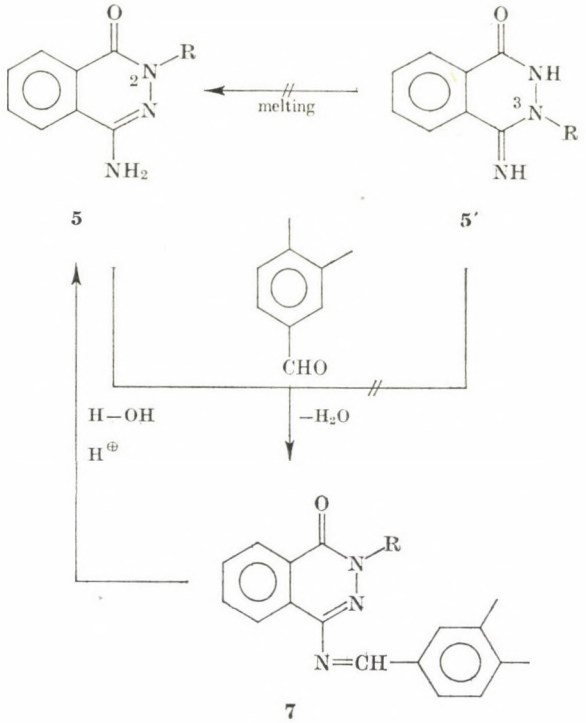

7

5, 7	R
a	Me
b	HO—$(CH_2)_2$—

C = N group was found to be the more stable form according to the literature [3] and our own observations [8, 9, 12].

In the reaction of *N*,*N*-disubstituted alkylhydrazines (*e.g.*, *N*,*N*-dimethylhydrazine) and cyclic alkylenehydrazines (*N*-aminopiperidine, *N*-aminohomopiperidine, *N*-aminomorpholine) with 3-oxo-1-iminoisoindoline (**3**), products of the phthalimidrazone type (**9**) are formed. Correctness of the structure is confirmed by the appearance of phthalimide on acid hydrolysis. When compounds **9** are refluxed with hydrazine, they transform into hydrazinophthalazinones of structure **10** with the elimination of ammonia. A small amount of aminophthalazinone (**4**; 5—25%) formed in the by-reaction hardly affects the excellent yield of the synthesis (70—93%). The main product of the hydrazinolysis effected with the more basic methylhydrazine is 4-amino-2-methyl-1(2*H*)-phthalazinone (**5a**), owing to an extensive transamination process; therefore the yield of derivatives **11** is significantly lower (31—42%). The simi-

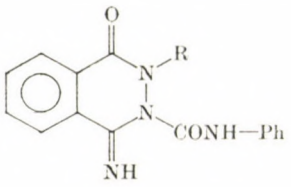

8'

or

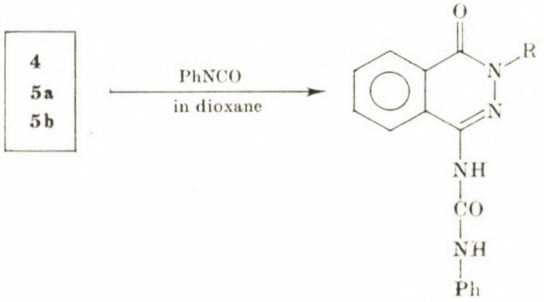

8	R
a	H
b	Me
c	Ph—NHOCO—$(CH_2)_2$—

8

lar solubility properties of **5a** and **11** present another preparative problems, making the separation difficult. Synthesis of compounds **11** can also be achieved through the methylation of **10**. A significant improvement in the yield was observed only in the case of **11d** (75% instead of 31%), yet methylation is to be considered the better method, as no by-product hard to eliminate interferes with the isolation.

In the literature [1], the melting point of hydrazinophthalazinone (**1**) is given erroneously. Compound **1** melts first at 235—240 °C with the evolution of gas, then becomes crystalline again and the second melting occurs at 268—269 °C. The thermally treated hydrazinophthalazinone proved to be aminophthalazinone according to the IR spectrum and elemental analysis. According to our experience, only the hydrazinophthalazinone is thermally unstable, the other hydrazine derivatives (**10**, **11**) were stable at the melting point.

Most of the hydrazinophthalazinones and their derivatives prepared in the course of the present work are regarded as possessing the tautomeric structure containing endocyclic C=N group (δNH 1540—1528 cm^{-1}). Exceptions are dimethylhydrazinophthalazinone (**10a**; δNH 1560 cm^{-1}) and (*N*-morpholinoamino)phthalazinone (**10d**; δNH 1552 cm^{-1}), in which the strikingly high δNH bands do not exclude the tautomeric exocyclic structure. The tautomerization of hydrazinophthalazinones will be discussed in a forthcoming part of this series of papers.

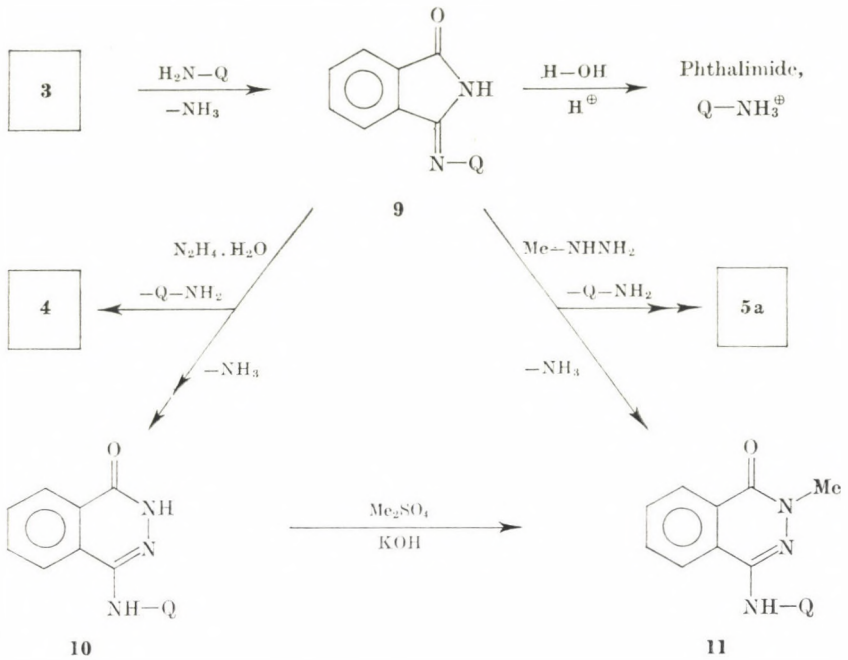

9, 10, 11	Q
a	—NMe$_2$
b	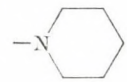
c	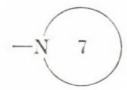
d	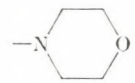

Experimental

M.p.'s were determined on a Boetius micro-hot-stage. The IR spectra were recorded in KBr pellets with a UR-10 (Zeiss, Jena) spectrophotometer.

o-Cyanobenzamide

It was prepared from phthalamide by BRAUN's method [10], using acetic anhydride for dehydration, in 40—50% yield; m.p. 188—189.5 °C (*lit.* m.p. 172—173 °C).

$C_8H_6N_2O$ (146.2). Calcd. N 19.2. Found N 19.2%.

IR: νNH_2 3360, 3177; νCN 2229; νCO_{amide} 1659; δNH_2 1622; 1,2-disubstituted Ar ring 761 cm^{-1}.

3-Oxo-1-iminoisoindoline (3)

Alkaline cyclization of *o*-cyanobenzamide [10] was advantageously replaced by a fusion process. In an open test tube, *o*-cyanobenzamide (15 g) was melted on a silicone oil bath at 220 °C (10—15 min). The slightly coloured melt crystallized on cooling, the yield of **3** being 100%; m.p. 203—204 °C (*lit.* [10] m.p. 203 °C).

$C_8H_6N_2O$ (146.2). Calcd. N 19.2. Found N 19.3%.

IR: νNH 3258, 3100—2000; νCO_{imide} and νC=N 1719, 1669; δNH 1525; 1,2-disubst. Ar ring 752 cm^{-1}.

4-Amino-1(2*H*)-phthalazinone (4)

(*a*) A mixture of 3-oxo-1-iminoisoindoline (**3**; 1.46 g; 0.01 mole), 100% hydrazine hydrate (1.5 ml) and ethanol (20 ml) was gently heated. The components dissolved rapidly, and soon colourless needles separated from the solution. After boiling for 5 min, the thick suspension was diluted with water and filtered (1.42 g; 88.2%). The crude product melted at 264—266 °C with sublimation. After sublimation in vacuum, the m.p. was 273—274 °C (*lit.* m.p.'s 266 °C, [3], 271—273 °C [11] and 274 °C [1]). According to the IR spectrum, the product was identical with the substance obtained by the ammonolysis of chlorophthalazinone [11].

(*b*) 4-Hydrazinophthalazinone (0.50 g) was fused in a bath of 270—280 °C until gas evolution ceased (10—15 min); the product was recrystallized from water, using decolourizing carbon, to obtain colourless needles (0.22 g), m.p. 267—269 °C; after sublimation in vacuum the substance had m.p. 273—274 °C. According to the IR spectrum, it was identical with the substance obtained according to (*a*).

(*c*) The same compound was obtained as a by-product from the hydrazinolysis of phthalimidrazones **9**, in 5—25% yield (see there).

$C_8H_7N_3O$ (161.2). Calcd. N 26.1. Found N 26.2%.

IR: νNH and νNH_2 3400—2800; νCO_{amide} 1645; δNH 1565; 1,2-disubst. Ar ring 760 cm^{-1}.

4-Amino-2-methyl-1(2*H*)-phthalazinone (5a)

(*a*) 3-Oxo-1-iminoisoindoline (1.46 g; 0.01 mole) was mixed with methylhydrazine (2 ml). A greenish yellow solution resulted with spontaneous warming and strong evolution of ammonia; cooling gave a deposit of crystals. After dilution with water (30 ml), the colourless product (1.26 g: 71.9%; m.p. 158—160 °C) was filtered off. It is well soluble in water and ethanol, moderately soluble in chlororom. Colourless needles were obtained from a small amount of ethanol, or big prisms from a mixture of chloroform and ether; m.p. 162—163 °C.

(*b*) Aminophthalazinone (16.1 g; 0.1 mole) was dissolved in 4% aqueous NaOH (1000 ml) with gentle heating, and dimethyl sulfate (37.8 g; 0.3 mole) was added dropwise, with mechanical stirring. Next day the crystals were filtered off. Further amounts of the product were obtained from the mother liquor after evaporation. Yield: 16.3 g (92.8%); m.p. 160—162 °C. Colourless prisms were obtained from a mixture of chloroform and ether, m.p. 162—163 °C. According to the IR spectrum, the product was identical with the substance prepared according to (*a*).

(*c*) The same compound was obtained in about 50% yield in the reaction of phthalimidrazones **9** with methylhydrazine (see there).

$C_9H_9N_3O$ (175.2). Calcd. N 24.0. Found N 24.1%.

IR: νNH_2 3376, 3310, 3200; νCO_{amide} 1619; νC=N 1570; δNH_2 1647; 1,2-disubst. Ar ring 785 cm^{-1}.

Reaction of 5a with hydrazine hydrate

The compound remained unchanged after refluxing with 100% hydrazine hydrate for 60 h.

Condensation of 5a with veratraldehyde (7a)

A mixture of **5a** (0.175 g; 1 mmole) and veratraldehyde (0.332 g; 2 mmoles) was fused, and the yellow melt was crystallized from ethanol to obtain yellow crystals, m.p. 171—173 °C.

$C_{18}H_{17}N_3O_3$ (323.4). Calcd. CH_3O 19.2. Found CH_3O 18.9%.

IR: $\nu CH_{methoxyl}$ 2832; $\nu C{=}N_{Schiff}$ 1648; νCO_{amide} 1617; νC=N 1574; $\nu C{-}O_{methoxyl}$ 1257, 1022; 1,2-disubstituted Ar ring 751 cm^{-1}.

Hydrolysis

The condensation product **7a** was boiled with 10% hydrochloric acid for a few minutes. The solution was then repeatedly evaporated to dryness with water. The evaporation residue was recrystallized from a mixture of chloroform and ether to give colourless prisms, m.p. 162—163 °C. According to the IR spectrum, the substance was compound **5a**.

4-Amino-2-(2-hydroxyethyl)-1(2*H*)-phthalazinone (5b)

A mixture of 3-oxo-1-iminoisoindoline (1.46 g; 0.01 mole) and 2-hydroxyethylhydrazine (3 ml) was heated on a water bath until the evolution of ammonia ceased (15 min). The yellowish syrup was dissolved in water (30 ml); crystals separated from the solution on standing. Yield: 1.43 g (69.7%), colourless needles or plates (from water), m.p. 205—206 °C.

$C_{10}H_{11}N_3O_2$ (205.2). Calcd. N 20.5. Found N 20.7%.

IR: νNH_2 and νOH 3386, 3330, 3228; νCO_{amide} 1627; $\nu C{=}N$ 1570; δNH_2 1652; $\nu C{-}O$ 1072; 1,2-disubst. Ar ring 735 cm^{-1}.

Condensation of 5b with veratraldehyde (7b)

A mixture of veratraldehyde (0.332 g; 2 mmoles) and **5b** (0.205 g; 1 mmole) was fused until the release of water was complete. Sulfur-yellow prisms were obtained from ethanol, m.p. 171—173 °C.

$C_{19}H_{19}N_3O_4$ (353.4) Calcd. CH_3O 17.6. Found CH_3O 17.8%.

IR: νOH 3438; $\nu CH_{methoxyl}$ 2837; $\nu C{=}H_{Schiff}$ 1639; νCO_{amide} and $\nu C{=}N$ 1620, 1574; $\nu C{-}O_{mehtoxyl}$ 1270, 1028; $\nu C{-}O_{alcohol}$ 1028; 1,2-disubst. Ar ring 743 or 755 cm^{-1}.

Hydrolysis

Compound **7b** decomposed into vertaraldehyde and compound **5b** when refluxed with dilute hydrochloric acid (m.p. 205—206 °C).

Phthalazonylphenylureas

4-Phenylureido-1(2*H*)-phthalazinone (8a)

4-Aminophthalazinone (**4**; 0.80 g; 5 mmoles) was refluxed with phenyl isocyanate (1.19 g; 0.01 mole) in dry dioxan (30 ml) for 8 h, with the careful exclusion of moisture. After dilution with water, a colourless powder separated which was filtered off, washed with water and cold ethanol (100 ml) to obtain 1.39 g (nearly 100%) of **8a**. The compound had no melting point; sublimation occurred at 300—310 °C.

$C_{15}H_{12}N_4O_2$ (280.3). Calcd. N 20.0. Found N 20.1%.

IR: νNH 3350—2700; $\nu CO_{amide,\ urea}$ 1662; δNH 1568, 1525; 1,2-disubst. Ar ring 755; monosubst. Ar ring 740, 689 cm^{-1}.

4-Phenylureido-2-methyl-1(2*H*)-phthalazinone (8b)

4-Amino-2-methyl-1(2*H*)-phthalazinone (**5a**; 0.88 g; 5 mmoles) was dissolved in hot anhydrous dioxan (30 ml) and allowed to react with phenyl isocyanate (1.19 g: 0.01 mole). After refluxing for about 30 min, the separation of colourless **8b** started from the yellowish solution. The reaction mixture was refluxed for 5 h, diluted with water (200 ml), the product was filtered off and washed with hot ethanol (50 ml). Yield: 1.14 g (77.6%), m.p. 276—278 °C; the melt rapidly crystallized into needles then underwent sublimation, leaving no residue, at 285—287 °C.

$C_{16}H_{14}N_4O_2$ (294.3). Calcd. N 19.0. Found N 18.9%.

IR: νNH 3340—2800; νCO_{urea} 1687; νCO_{amide} 1645; $\nu C{=}N$ 1588; δNH 1525 or 1561; 1,2-disubst. Ar ring 759; monosubst. Ar ring 750, 691 cm^{-1}.

4-Phenylureido-2-phenylurethano-1(2*H*)-phthalazinone (8c)

A mixture of phenyl isocyanate (0.60 g; 5 mmoles) and 4-amino-2-(2-hydroxyethyl)-1(2*H*)-phthalazinone (**5b**; 0.41 g; 2 mmoles) was refluxed in anhydrous dioxan (10 ml) for 2 h. Separation of the colourless reaction product from the yellow solution started from the beginning of refluxing. The mixture was diluted with water (100 ml), the crude product was filtered off, washed with water and ethanol to obtain 0.55 g, (62%), m.p. 220—221 °C (d.). After recrystallization from dioxan, the colourless needles had m.p. 223—225 °C (d.).

$C_{24}H_{21}N_5O_4$ (443.5). Calcd. N 15.8. Found N 16.0%.

IR: νNH 3270; $\nu CO_{urethane}$ 1732; νCO_{urea} 1685; νCO_{amide} 1653; νC=N 1588; δNH 1553; $\nu C-O_{ester}$ 1227, 1065; 1,2-disubst. Ar ring 755; monosubst. Ar ring 755, 693 cm^{-1}.

Phthalimidrazone derivatives (9)

3-Oxo-1-(2,2-dimethylhydrazono)isoindoline (9a)

3-Oxo-1-iminoisoindoline (2.92 g; 0.02 mole) was refluxed with *N,N*-dimethylhydrazine (2 ml) in ethanol (20 ml) for 2 h. After the addition of some water the yellow solution was evaporated to dryness in vacuum; yellow crystals were obtained on recrystallization from aqueous ethanol (3.11 g; 82.3%), m.p. 132—134 °C.

$C_{10}H_{11}N_3O$ (189.2). Calcd. N 22.2. Found N 22.4%.

IR: νNH 3300—2600; $\nu N-CH_3$ 2822, 2790, 2777; νCO_{imide} 1726; νC=N 1640; 1,2-disubst. Ar ring 775 cm^{-1}.

Hydrolysis

Compound **9a** was dissolved in 10% cold hydrochloric acid. The colourless crystalline substance (m.p. 233—235 °C, with sublimation) which deposited on short boiling was identical with phthalimide as shown by the IR spectrum.

3-Oxo-1-(*N*-piperidinoimino)isoindoline (9b)

A mixture of *N*-aminopiperidine (5.00 g; 0.05 mole), 3-oxo-1-iminoisoindoline (7.30 g; 0.05 mole) and ethanol (50 ml) was refluxed for 3 h. A yellow solution formed rapidly and strong evolution of ammonia was observed. The substance which separeted on dilution with water (300 ml) (10.65 g; 92.9%; m.p. 145—147 °C) was crystallized from aqueous ethanol to give yellow needles, m.p. 147—148 °C.

$C_{13}H_{15}N_3O$ (229.3). Calcd. N 18.3. Found N 18.4%.

IR: νNH 3190; $\nu N-CH_2$ 2822; νCO_{imide} 1721; νC=N 1648; 1,2-disubstituted Ar ring 779 cm^{-1}.

3-Oxo-1-(*N*-homopiperidinoimino)isoindoline (9c)

3-Oxo-1-iminoisoindoline (7.3 g; 0.05 mole) was refluxed with *N*-aminohomopiperidine (5.7 g; 0.05 mole) in ethanol (50 ml) until the evolution of ammonia had ceased (3 h). On the addition of water (300 ml), yellow crystals separated (10.95 g; 90.1%; m.p. 116—118 °C). Yellow needles were obtained from aqueous ethanol; m.p. 118—119 °C.

$C_{14}H_{17}N_3O$ (243.3). Calcd. N 17.3. Found N 17.4%.

IR: νNH 3170; $\nu N-CH_2$ 2818; νCO_{imide} 1709, νC=N 1640; 1,2-disubst. Ar ring 765 cm^{-1}.

3-Oxo-1-(*N*-morpholinoimino)isoindoline (9d)

A mixture of 3-oxo-1-iminoisoindoline (7.3 g; 0.05 mole) and *N*-aminomorpholine (5.1 g; 0.05 mole) was refluxed in ethanol (50 ml) until the evolution of ammonia had stopped (3 h). The solution turned rapidly yellow, and separation of the relatively poorly soluble **9d** started after boiling for about 30—60 min. After dilution with water (200 ml), the crude product was filtered off (10.60 g; 91.7%), m.p. 203—204 °C. Yellow needles were obtained on recrystallization from ethanol; m.p. 203—204 °C.

$C_{12}H_{13}N_3O_2$ (231.3). Calcd. N 18.2. Found N 18.2%.

IR: νNH 3182; $\nu N-CH_2$ 2838; νCO_{imide} 1722; νC=N 1642; νC—O 1112 or 1097 cm^{-1}.

4-Hydrazino-1(2*H*)-phthalazinone (1)

(*a*) Compound **1**, when prepared from 4-chlorophthalazinone with 100% hydrazine hydrate according to KÖHLER [1] (reflux for 5 h), was only contaminated with traces of chlorine. The reaction took place in a similarly satisfactory yield (about 90%) when more dilute (*e.g.*, 72%) hydrazine hydrate was used. After clarification with activated carbon, pale cream needles were obtained from water; m.p. 235—240 °C, (with the evolution of gas). When the temperature was slowly increased, the melt crystallized and melted again at 268—269 °C (*i.e.* at the m.p. of aminophthalazinone).

(*b*) A mixture of 4-aminophthalazinone (**4**, 1.6 g) and 100% hydrazine hydrate (20 ml) was refluxed in a flask equipped with a reflux condenser. The samples (1 ml each) taken from the solution in 5-h periods were diluted with water to tenfold volume. The IR spectrum of the crystalline product which separated varied in the different samples. Complete development of the bands at 3300 cm^{-1} and 990 cm^{-1}, characteristic of hydrazinophthalazinone, was observed only after refluxing for 25—30 h.

$C_8H_8N_4O$ (176.2). Calcd. N 31.8. Found N 31.9%.

IR: νNH and νNH_2 3400—2700; νCO_{amide} 1658; δNH_2 1625; δNH 1530; νC=N 1592; 1,2-disubst. Ar ring 778 cm^{-1}.

Hydrazinolysis of phthalimidrazone derivatives (9)

4-(2,2-Dimethylhydrazino)-1(2*H*)-phthalazinone (10a)

A mixture of 3-oxo-1-(2,2-dimethylhydrazono)isoindoline (**9a**; 3.78 g; 0.02 mole) and 72% hydrazine hydrate (4 ml) was refluxed in ethanol (40 ml) for 6 h in a flask equipped with a reflux condenser. The intensely yellow solution slowly became colourless with the evolution of ammonia. After the addition of water, the solvent and the excess hydrazine were evaporated in vacuum. The solid residue was suspended in some water, neutralized with hydrochloric acid and filtered off to obtain the product (3.78 g; 92.6%; m.p. 195—199 °C). It crystallized as long colourless needles from water, which disintegrated into a powder when heated slightly (*e.g.*, under a lamp); m.p. 199—201 °C.

$C_{10}H_{12}N_4O$ (204.2). Calcd. N 27.4. Found N 27.6%.

IR: νNH 3222, 3300—2700; $\nu N-CH_3$ 2818, 2773; νCO_{amide} 1640; νC=N 1588; δNH 1560; 1,2-disubst. Ar ring 753 cm^{-1}.

The combined mother liquors yielded 0.16 g (5%) of aminophthalazinone (m.p. 270—271 °C) on evaporation.

4-(*N*-Piperidinoamino)-1(2*H*)-phthalazinone (10b)

A mixture of 3-oxo-1-(*N*-piperidinoimino)isoindoline (**9b**; 2.29 g; 0.01 mole) and 72% hydrazine hydrate (2.5 ml) was refluxed in ethanol (25 ml) for 6 h. The solution which became colourless was diluted with water (300 ml) and neutralized with hydrochloric acid. The crude product was 1.95 g, m.p. 221—224 °C. Needles with fan-shaped arrangement were obtained from aqueous ethanol (2 : 1), plates from much water (1.72 g; 70.4%), m.p. 230—232 °C.

$C_{13}H_{16}N_4O$ (244.3). Calcd. N 22.9. Found N 23.0%.

IR: νNH 3250, 3192; νNH_{amide} 3450—2600; $\nu N-CH_2$ 2821, 2803; νCO_{amide} 1641; δNH 1534; δNH_{amide} 1563; νC=N 1590; 1,2-disubst. Ar ring 784 cm^{-1}.

The mother liquors yielded a by-product (0.40 g; 24.8%) which was identified as 4-aminophthalazinone (**4**) (m.p. 269—272 °C).

4-(*N*-Homopiperidinoamino)-1(2*H*)-phthalazinone (10c)

3-Oxo-1-(*N*-homopiperidinoimino)isoindoline (**9c**; 14.58 g; 0.06 mole) was refluxed with 72% hydrazine hydrate (15 ml) in ethanol (100 ml) for 6 h. The solution was then diluted with water (1000 ml), neutralized with hydrochloric acid and the crystalline product was filtered off (12.62 g; 81.5%). Colourless prisms were obtained from ethanol; m.p. 198—200 °C.

$C_{14}H_{18}N_4O$ (258.3). Calcd. N 21.7. Found N 21.6%.

IR: νNH 3270, 3210; νNH_{amide} 3380—2600; $\nu N-CH_2$ 2823; νCO_{amide} 1640; νC=N 1590; δNH 1528; δNH_{amide} 1560; 1,2-disubst. Ar ring 742 cm^{-1}.

4-Aminophthalazinone (1.38 g; 14.3% m.p. 269—272 °C) was isolated from the mother liquor.

4-(*N*-Morpholinoamino)-1(2*H*)-phthalazinone (10d)

A mixture of 3-oxo-1-(*N*-morpholinoimino)isoindoline (**9d**; 2.31 g; 0.01 mole) and 72% hydrazine hydrate (2.5 ml) was refluxed in ethanol (25 ml) for 6 h. Water was added to the almost completely colourless solution, and the solvent was evaporated in vacuum. An aqueous suspension of the solid residue was neutralized with hydrochloric acid and filtered off to obtain the crude product (2.23 g; m.p. 213—217 °C); colourless prisms after recrystallization from much ethanol (1.93 g; 78.4%), m.p. 225—227 °C.

$C_{12}H_{14}N_4O_2$ (246.3). Calcd. N 22.7. Found N 22.7%.

IR: νNH 3232; 3195; νNH_{amide} 3400—2700; $\nu N-CH_2$ 2834; νCO_{amide} 1649; δNH_{amide} 1572; δNH 1552; νC=N 1602; νC—O 1112; 1,2-disubst. Ar ring 786 cm^{-1}.

4-Aminophthalazinone (0.26 g; 16.2%, m.p. 269—273 °C) was obtained from the combined mother liquors.

4-(2,2-Dimethylhydrazino)-2-methyl-1(2*H*)-phthalazinone (11a)

(*a*) 3-Oxo-1(2,2-dimethylhydrazono)isoindoline (**9a**; 3.78 g; 0.02 mole) was refluxed with methylhydrazine (4 ml) in ethanol solution (30 ml) for 15 h. After evaporation in vacuum, the viscous residue was extracted with hot petroleum ether (b.p. 80—120 °C) to obtain 1.83 g (42.0%) colourless salt-like crystals, m.p. 111—112 °C. The component poorly soluble in petroleum ether was 4-amino-2-methyl-1(2*H*)-phthalazinone (**5a**; 1.71 g; 53.1%), m.p. 162—163 °C.

(*b*) Compound **10a** (2.04 g; 0.01 mole) was dissolved in cold methanolic (100 ml) potassium hydroxide (5.6 g) to give a solution with a reddish brown colour. Dimethyl sulfate (5 ml) was added dropwise under mechanical stirring, the mixture was allowed to stand for 1 h, then evaporated to dryness in vacuum. The red solid mass was extracted with dichloromethane at room temperature and the extract was evaporated. The strongly coloured evaporation residue gave the methylated product (1.05 g; 48.1%) as a pale yellow syrup after extraction with hot ether. Colourless crystals were obtained from petroleum ether; m.p. 111—113 °C. According to the mixed m.p. and IR spectra, the product was identical with the compound prepared according to (*a*).

$C_{11}H_{14}N_4O$ (218.3). Calcd. N 25.7. Found N 25.7%.

IR: νNH 3238; $\nu N-CH_3$ 2819, 2774; νCO_{amide} 1638; νC=N 1578; δNH 1535; 1,2-disubst. Ar ring 730 cm^{-1}.

4-(*N*-Piperidinoamino)-2-methyl-1(2*H*)-phthalazinone (11b)

(*a*) 3-Oxo-1-(*N*-piperidinoimino)isoindoline (**9b**, 4.58 g; 0.02 mole) was allowed to react with methylhydrazine (4 ml) in ethanol (30 ml). After refluxing for 15 h, the solution was evaporated in vacuum. The evaporation residue was extracted with hot petroleum ether (2×100 ml; b.p. 80—120 °C). The substance which separated from the solution and the insoluble residue of the extraction were 4-amino-2-methyl-1(2*H*)-phthalazinone (2.03 g; 58%; m.p. 162—163 °C). After filtration, the petroleum ether solution was evaporated to dryness and the solid residue crystallized from water, to obtain colourless needles. The hydrate had m.p. 59—62 °C. The substance became sticky when dried at room temperature over phosphorus pentoxide in vacuum. On drying first at 56 °C and then at 78 °C, a crystalline substance was obtained, m.p. 89—91 °C; yield: 1.90 g (36.8%).

(*b*) Compound **10b** (0.488 g; 2 mmoles) was dissolved in methanolic (20 ml) potassium hydroxide (1.2 g). Dimethyl sulfate (1.0 ml) was added to the yellow solution under stirring, then the methanol was evaporated in vacuum. The solid residue was extracted with cold dichloromethane. From the evaporation residue of the dichloromethane solution (about 0.5 g) the methylated product was extracted with hot petroleum ether (b.p. 80—120 °C) (0.228 g; 44.1%). Colourless needles were obtained on recrystallization from water; m.p. 89—90 °C (after drying).

$C_{14}H_{18}N_4O$ (258.3). Calcd. N 21.7. Found N 21.8%.

IR: νNH 3200; νCO_{amide} 1630; νC=N 1573; δNH 1535 cm^{-1}.

4-(*N*-Homopiperidinoamino)-2-methyl-1(2*H*)-phthalazinone (11c) hydrochloride

(*a*) A mixture of **9c** (4.86 g; 0.02 mole) and methylhydrazine (4 ml) was refluxed in ethanol (30 ml) for 15 h. The evaporation residue of the solution was extracted with hot petroleum ether to obtain a yellowish syrup (2.15 g; 39.5%), well soluble in hydrochloric acid; the compound could not be crystallized in the base form. The acid solution was evaporated to dryness

in vacuum to yield colourless crystals, which would be readily recrystallized from a mixture of ethanol and ether. The hydrochloride had m.p. 121—123 °C. The substance poorly soluble in gasoline was 4-amino-2-methyl-1(2*H*)-phthalazinone (1.90 g; 54.3%; m.p. 162—163 °C).

(*b*) Dimethyl sulfate (2.5 ml) was added dropwise, with stirring, to a solution of **10c** (1.20 g; 5 mmoles) in methanolic (50 ml) potassium hydroxide (2.8 g). After standing for 1 h, the solution with deepening colour was evaporated to dryness in vacuum, and the dry residue was extracted with cold dichloromethane. After the removal of the solvent the dark brownish-red resin was treated with hot ether to obtain a yellow honey-like material (0.50 g; 36.8%), which was converted into the hydrochloride as described in (*a*). Recrystallization from a mixture of ethanol and ether gave colourless crystals, m.p. 120—122 °C. This product was identical with the substance made according to (*a*).

$C_{15}H_{20}N_4O \cdot HCl$ (308.8). Calcd. Cl 11.5; N 18.1. Found Cl 11.8; N 18.0%.

IR: νNH 3200; νNH$^+$ 3100—2000; νCO_{amide} 1652; νC=N or δNH 1588; 1,2-disubst. Ar ring 775 cm^{-1}.

4-(*N*-Morpholinoamino)-2-methyl-1(2*H*)-phthalazinone (11d)

(*a*) A solution of **9d** (4.62 g; 0.02 mole) and methylhydrazine (4 ml) in ethanol (30 ml) was refluxed for 15 h. After evaporation to dryness in vacuum the residue was treated with hot petroleum ether (b.p. 80—120 °C) (2×150 ml) to obtain a crystalline product (1.61 g; 31.0%), m.p. 98—102 °C. Recrystallization from water gave colourless needles, m.p. 103—105 °C. After drying in vacuum over phosphorus pentoxide at 78 °C, the m.p. increased to 144—145.5 °C. The other product, poorly soluble in petroleum ether, was 4-amino-2-methyl-1(2*H*)-phthalazinone (2.15 g; 61.5%; m.p. 162—163 °C).

(*b*) Compound **10d** (0.492 g; 2 mmoles) was methylated with dimethyl sulfate (1.0 ml) in methanolic (20 ml) potassium hydroxide (1.2 g) solution. The reaction mixture was processed in the usual manner (extraction with dichloromethane, then with petroleum ether) to obtain the methyl derivative (0.390 g; 75.0%). Recrystallization from water gave colourless needles m.p. 144—145.5 °C (after drying at 78 °C in vacuum over phosphorus pentoxide). The substance was identical with that prepared according to (*a*).

$C_{13}H_{16}N_4O_2$ (260.3). Calcd. N 21.5. Found N 21.6%.

IR: νNH 3285, 3239, 3210; νCO_{amide} 1642; νC=N 1570; δNH 1535; νC—O 1105; 1,2-disubst. Ar ring 772 cm^{-1}.

*

The authors' thanks are due to Dr. F. RUFF for his help in recording and evaluating the IR spectra. Elemental analyses were made in the Microanalytical Laboratory of the Department (head: Dr. H. MEDZIHRADSZKY). The starting materials were supplied by the BRISTOL Laboratories, Syracuse, N.Y., USA; their help is gratefully acknowledged.

REFERENCES

[1] KÖHLER, W., BUBNER, M., ULBRICHT, G.: Chem. Ber., **100,** 1073 (1967)
[2] ELVIDGE, J. S., LINSTEAD, R. P.: J. Chem. Soc., **1952**, 5000
[3] FLITSCH, W., PETERS, H.: Chem. Ber., **102,** 1304 (1969)
[4] HAWORTH, R. D., ROBINSON, S.: J. Chem. Soc., **1948**, 777
[5] KÖRMENDY, K.: Amine, Amide and Hydrazine Addition of Cyclic Imino Ethers. Thesis (in Hungarian), Budapest, 1965
[6] SOHÁR, P., KÖRMENDY, K., PFISZTNER-FREUD, Á., RUFF, F.: Acta Chim. Acad. Sci. Hung., **60,** 273 (1969)
[7] BRUCK, P., TAMÁS, J., KÖRMENDY, K.: Org. Mass Spectrom., **9,** 335 (1974)
[8] KÖRMENDY, K.: Acta Chim. (Budapest) **88,** 129 (1976)
[9] KÖRMENDY, K.: Acta Chim. Acad. Sci. Hung. (In the press)
[10] BRAUN, A., TCHERNIAC, J.: Chem. Ber., **40,** 2709 (1907)
[11] STEPHENSON, E. F. M.: J. Chem. Soc., **1944,** 678
[12] KÖRMENDY, K.: Acta Chim. (Budapest) **94,** 373 (1977)

Károly KÖRMENDY
Katalin Ágnes JUHÁSZ
Éva LEMBERKOVICS
H-1088 Budapest, Múzeum krt. 4/b.

Acta Chimica Academiae Scientiarum Hungaricae, Tomus 102 (1), pp. 51—57 (1979)

SYNTHESES OF ISOFLAVAN-4-(1-PYRIDINIUM) SALTS*

V. SZABÓ, J. BORBÉLY and E. ANTAL

(Institute of Applied Chemistry, Kossuth Lajos University, Debrecen)

Received May 5, 1978

Accepted for publication October 20, 1978

Treatment of *trans*(α)- or *cis*(β)-4-hydroxyisoflavan (**Ia**, **Ib**) with tosyl chloride in pyridine gives, instead of the expected tosylates, the same isoflavan-4-(1-pyridinium) tosylate (**IVa**). The anion of **IVa** is exchangeable for other anions. Reductive methods convert **IVa** to isoflavan (**VII**) and 4-[1-(1,4-dihydropyridyl)]isoflavan (**VIII**); in alkaline medium it can be converted to isoflav-3-ene (**II**).

During the last decade syntheses of various C^4-substituted isoflavans of biological activity have been reported. CARNEY *et al.* [1] described contraceptives of the 3,4-diphenylchroman type. The preparation of such derivatives with similar bioactivity has also been reported by German [2, 3] and Indian [4—6] authors. These syntheses involved either coumarin derivatives, or the Grignard reaction of isoflavone with phenylmagnesium bromide. In the latter case the 4-phenyl-4-hydroxyisoflavans formed upon dehydration gave isoflav-3-ene derivatives. Catalytic hydrogenation completed the syntheses of the 4-phenylisoflavan derivatives.

In the present paper the syntheses and propertis of a heteroaryl analouge of these diphenylchromans is described.

Sodium borohydride reduction of isoflavanone gave a mixture of the 4-hydroxyisoflavan epimers. In our experiments — despite the claimed stereospecificity [7, 8] — about 30% of *trans*-4-hydroxyisoflavan (**Ia**) and 70% of the corresponding *cis* derivative (**Ib**) was obtained at room temperature. These compounds are separable in the form of their acetates by crystallization [9, 10].

4-Hydroxyisoflavans (**Ia**, **Ib** or their mixtures) in dichlormethane failed to react with an equimolar amount of tosyl chloride and triethylamine [11]. In triethylamine solution, however, the reaction resulted in the formation of isoflav-3-ene (**II**) almost exclusively.

Sodium alcoholates of **Ia** and **Ib** — in accordance with literature data [12] — also failed to give the tosylates or **II**. In further experiments, a mixture

* Presented in part at the Fourth Hungarian Bioflavonoid Symposium, "Topics in Flavonoid Chemistry and Biochemistry" (Eds L. FARKAS, M. GÁBOR and F. KÁLLAY), p. 139. Akadémiai Kiadó, Budapest and Elsevier, Amsterdam 1975.

Table I

Melting points of various isoflavan-4-(1-pyridinium) salts (**V**)

Compound	Anion (X^-)	Melting point [°C]
IVa	TsO^-	136—7
V	Cl^-	232—5
Vc	I^-	171—2
Vd	ClO_4^-	182
Ve	picrate	163

of **Ia** and **Ib** was treated with tosyl chloride in dry pyridine [13]. The reaction mixture contained some unchanged starting material as well as **II**, and a new compound. This new compound was shown by PMR and elemental analysis to be the pyridinium salt **IVa**. The tosylate anion of **IVa** could be readily exchanged for other anions, corroborating the structure. The melting points of these new salts are summarized in Table I.

4-Hydroxyisoflavans give neither **IVa** with pyridine, nor **II** with triethylamine. These products are formed only in the presence of tosyl chloride and the corresponding base, suggesting the transitory formation of the tosylate **III**. Triethylamine and pyridine converts **III** into **II** and **IVa**, respectively.

In order to obtain data concerning the mechanism of this "tosylation" reaction, **Ia** and **Ib** were treated separately under the above conditions; the reactions led to the formation of the same product, **IVa**. PMR and melting point

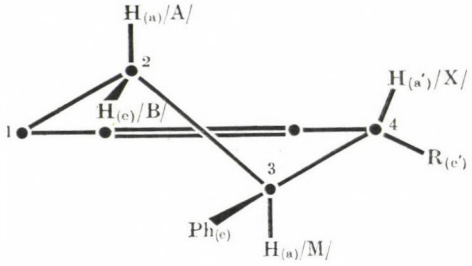

(**IVa**, **V**) R =

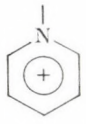

(**VIII**) R =

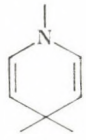

Fig. 1. Structure of the dihydropyran ring in **IVa, V** and **VIII**

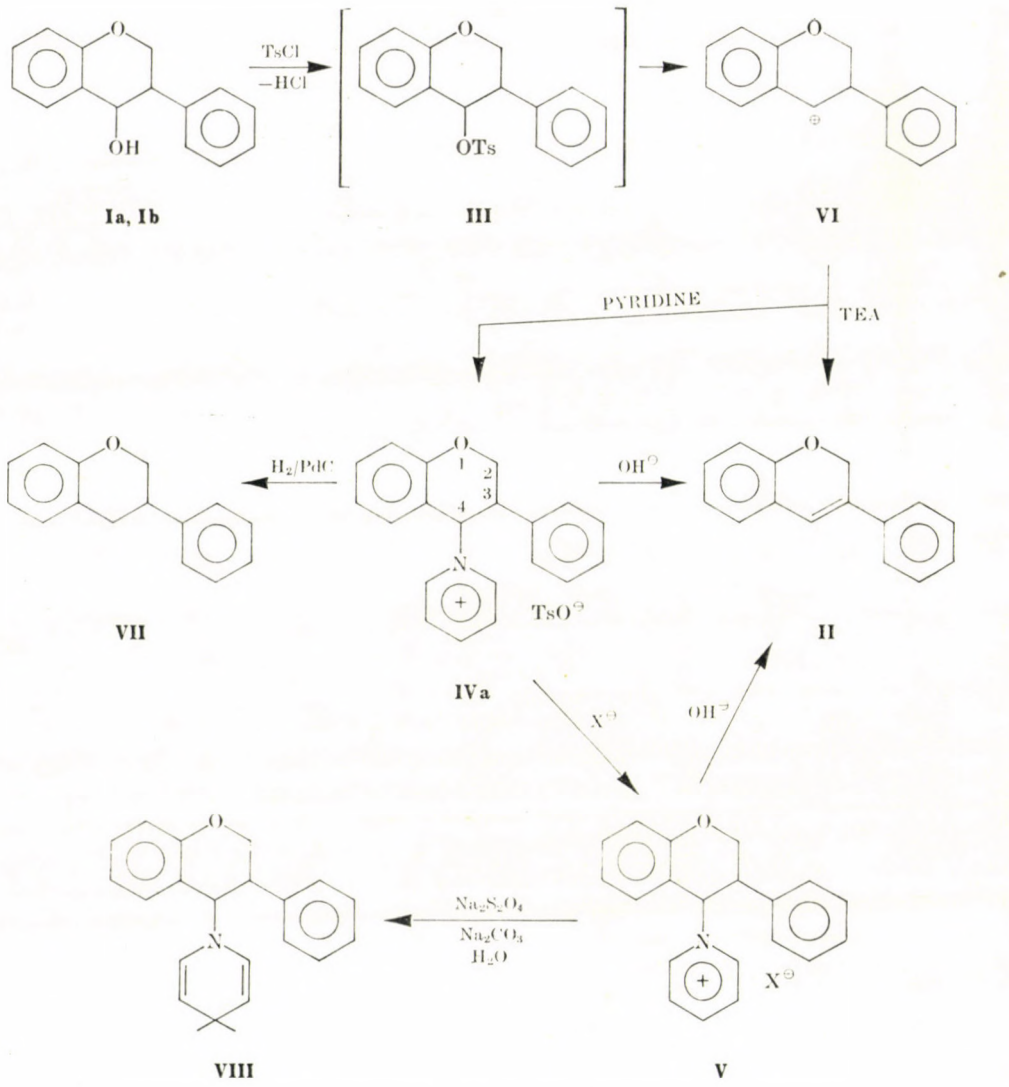

Scheme 1

determinations showed the identity of products from **Ia** and **Ib**. On the basis of these experiments the formation of tosyl esters (**III**) of the alcohols **Ia** and **Ib** is probable. Owing to the mesomeric effect of the tosyloxy group, this compound can decompose to give the carbonium ion **VI** and the tosylate anion. The carbonium cation is then attacked by the non-bonding electron pair of pyridine, so that the pyridine ring occupies the position farther away from the C_3-phenyl group. The process therefore results in the formation of the same **IVa** either from **Ia** or **Ib**.

Table II

PMR data of **Ia, Ib** *and* **VIII***

Compound	Position of protons	Number of protons	Chemical shift (ppm)	Coup. const. (Hz)	Configuration
	C_2	2	4.16–4.52 m		4-OH (a')
Ib	C_3	1	3.32–3.51 m	$J_{3,4} = 3.5$	3-Ph (e)
acetate	C_4	1	5.89 d		
	O-acetyl	3	1.78 s		*cis*
	C_2	2	4.20–4.32 m		4-OH (e')
Ia	C_3	1	3.12–3.28 m	$J_{3,4} = 6.5$	3-Ph (e)
acetate	C_4	1	6.11 d		
	O-acetyl	3	1.90 s		*trans*
	C_2	2	4.32–4.62 m		
	C_3	1	3.80–4.05 m		
Vb	C_4	1	—		
	αH	2	8.68–8.71		
	βH	2	7.81–7.95		
	γH	1	8.31–8.43		
	C_2	2	4.0 –4.4 m		
VIII	C_3	1	3.10–3.36 m	$J_{3,4} = 8.1$	3-Ph (e)
	C_4	1	5.5 d		4-Py (e')
	αH	2	4.0 –4.4 m		*trans*
	βH	2	4.0 –4.4 m		
	γH	2	2.8 m		

* Solvent: DMSO-d_6; reference: sodium 3-trimethylsilylpropionate

Triethylamine, however, is a stronger base than pyridine. In triethylamine solution the proton of **VI** is removed by the solvent yielding **II**.

The structures of **IVa** and **V** have been studied by PMR spectroscopy. The protons of the pyran ring in **IVa** and **V** form an ABMX system, similar to the one found in 3,4-disubstituted chromans [14, 15, 19]. The structures of such compounds can be characterised by the J^{MX} coupling constants, representing the steric relations of C^3—H (M) and C^4—H (X). Unlike the case of 4-hydroxy- and 4-acetoxyisoflavan derivatives, the C_4-proton is strongly influenced by the C^4—N^+ substituent, resulting in a strong paramagnetic shift in compounds such as **IVa** and **V**. Because of this shift, the signal of C^4—H appears in the aromatic region together with aromatic protons, making direct PMR structure determination impossible.

In order to overcome the problem of PMR structure determination, **Vb** was reduced to the corresponding 1.4-dihydropyridil derivative (**VIII**) by the $Na_2S_2O_4$ method [20, 21]. This reduction of known mechanism leaves the stereochemistry at C^3 and C^4 unchanged, therefore this may be regarded as identical in **IVa**, **V** and **VIII**. In the latter compound the C^4—H shows a doublett in the PMR spectrum ($\delta = 5.5$ ppm, $J_{3,4} = 8.1$ Hz). This means that C^3—H and C^4—H are in *trans*-diaxial position, indicating the diequatorial relation of the aromatic C^3- and C^4-substituents in **IVa** and **V** (Fig. 1).

The Pd/C hydrogenation of isoflavan-4-(1-pyridinium) salts takes with a C^4—N bond cleavage, similarly to that observed in *N*-benzylpyridinium salts [16]. **Vb** upon Pd/C hydrogenation gives isoflavan (**VII**) in an almost quantitative yield. In dilute alkaline solution **Vb** decomposes to pyridine and isoflav-3-ene (**II**). Both reaction corroborate the structure assignments of **IVa** and **V**.

Experimental

M.p.'s are uncorrected. PMR spectra were recorded on a JEOL LNM—MH 100 instrument. The TLC adsorbent was of a Merck DC-Alurolle Kieselgel F-254 type; developing solvent systems: benzene: ethanol = 96 : 4, and petroleum ether: ethyl acetate = 91 : 9.

Trans-4-acetoxyisoflavan and *cis*-4-acetoxyisoflavan

Isoflavanone (17.92 g; 0.08 mole) was reduced with sodium borohydride in ethanol at room temperature. The mixture of the resulting 4-hydroxyisoflavans was then acylated by the usual methods [7, 17] (pyridine, Ac_2O) to obtaine a mixture of the *cis*- and *trans*-4-acetoxyisoflavans (19.15 g; 89.5%), m.p. 60—65 °C. The mixture was then fractionated by crystallization from a 10 : 1 mixture of petroleum ether : ethyl acetate to yield 8 g (41.8%) of *cis*-4-acetoxyisoflavan m.p. 94—95 °C (*lit.* [7] m.p. 93 °C), and 1.75 g (9.15%) of *trans*-4-acetoxyisoflavan, m.p. 72—73 °C (*lit.* [18] m.p. 72—73 °C). The PMR data are shown in Table II.

Cis-(β)-4 hydroxyisoflavan (Ib)

Cis-4-acetoxyisoflavan (2.68 g; 0.01 mole) was dissolved in ethanol (20 ml) and 0.011 mole of sodium hydroxide (0.58 ml of a 50% solution) was then added. The solution was refluxed for 5 h* and worked up as given in the literature [7] to obtain 2.0 g (88.5%) of **Ib**, m.p. 75 °C (*lit.* [19] m.p. 75 °C).

PMR: $J_{3,4}$: 3.0 Hz ($CDCl_3$) (*lit.* [19] $J_{3,4}$ 2.9 Hz).

Trans (α)-4-hydroxyisoflavan (Ia)

Trans-4-acetoxyisoflavan (1.34 g; 0.005 mole) was dissolved in ethyl alcohol (10 ml) and 0.0055 mole (0.29 ml of a 50% solution) of sodium hydroxide was added. The solution was refluxed for 5 min.* The usual work-up gave 1.0 g (88.5%) of **Ia**, m.p. 96—97 °C (*lit.* [18] m.p. 97—97.5 °C).

PMR $J_{3,4}$: 8 H_2 ($CDCl_3$) (*lit.* [18] $J_{3,4}$; 8.0 Hz).

* The rates of hydrolysis are very different for *cis*- and *trans*-4-acetoxyisoflavan derivatives. This fact provides a possibility of attaining a high yield in the preparation of **Ia**. This will be reported elsewhere.

Isoflavan-4-(1-pyridinium)*p*-toluenesulfonate (IVa)

4-hydroxyisoflavan (0.92 g; 0.004 mole) (mixture of the *cis*- and *trans* isomers, or either the pure *cis* or *trans* compound) was dissolved in dry pyridine (4 ml) and cooled to 0 °X. *p*-Toluenesulfonyl chloride (1.14 g; 0.006 mole) was then added, the mixture was allowed to react at 0 °C for 1 day, and poured in to water (20 ml). The solution was extracted with 3 × 10 ml of ether, and then with chloroform. The etheral solution contained the unchanged starting material, as well as isoflav-3-ene (TCL). The chloroform solution was dried over $MgSO_4$ and diluted with 30 ml of ethyl acetate. The white crystals wich separated were collected (**IVa**); 1.26 g (68.4%), m.p. 136—137 °C.

$C_{27}H_{25}NO_4S$ (459.5). Calcd. C 70.58 H 5.48; S 6.98; N. 3.05. Found C 69.49; H 5.28 S 6.99; N 2.99%.

Isoflavan-4-(1-pyridinium) chloride (Vb)

IVa (0.46 g; 0.001 mole) was dissolved in 10 ml of $CHCl_3$ saturated with water. This solution was then shaken with 2 g of powdered calcium chloride for 10 min, filtered, and the chloroform solution was diluted with 10 ml of ethyl acetate. The crystals which separated were collected by filtration to obtain 0.28 g (86%) of **Vb**, m.p. 232—235 °C.

$C_{20}H_{18}NOCl$ (328.8). Calcd. N 4.32; Cl 10.94. Found N 4.28; Cl 10.77%.

Isoflavan-4-(1-pyridinium) iodide (Vc)

Compound **IVa** (0.46 g; 0.001 mole) was dissolved in 50 ml of dry acetone. Sodium iodide (1.5 g) was added, and the mixture was shaken for 1 h, filtered, and the filtrate concentrated to 5 ml. Dilution with 10 ml of water resulted in the separation of yellow crystals, 0.25 g (61%), m.p. 171—172 °C.

$C_{20}H_{18}NOI$ (415.3). Calcd. N 3.37; I 30.56. Found N 3.40; I 30.30%.

Isoflavan-4-(1-pyridinium) picrate (Ve)

A solution of **IVa** (0.46 g 0.001 mole) in 10 ml of water was mixed with a 2% aqueos solution of picric acid by adding the latter dropwise until the separation of crystals was complete. The product 0.48 g; (92%) had m.p. 163 °C.

$C_{26}H_{20}N_4O_8$ (516.48). Calcd. C 60.46; H 3.86; N 10.06. Found C 62.74; H 4.60; N 10.10%.

Isoflavan-4-(1-pyridinium) perchlorate (Vd)

Compound **IVa** (0.46 g; 0.001 mole) was dissolved in 10 ml of water, and 60% perchloric acid was added dropwise until the separation of white crystals was complete. The product was 0.38 g (99%) of white crystals, m.p. 182 °C.

$C_{20}H_{18}NO_5Cl$ (373.8). Calcd. C 62.26; H 4.72; N 3.63. Found C 61.27; H 4.70; N 3.55%.

4-[1-(1,4-Dihydropyridyl)]isoflavan (VIII)

To an aqueous solution of (0.324 g 0.001 mole) of **Vb** there was added 0.32 g of anhydrous sodium carbonate, and the solution was cooled to 0 °C. Nitrogen was passed through the solution during the 10-min period of the addition of 0.66 g sodium dithionite dissolved in 20 m of water. The reaction mixture was then allowed to stand for 2 h, and the white mass of crystals was filtered off under nitrogen, washed with water, and dried to obtain 0.21 g (71%) of **VIII**, m.p. 86—88 °C.

$C_{20}H_{19}NO$ (289.6). Calcd. C 83.04; H 6.57; N 4.84. Found C 82.82; H 6.46; H 4.95%.

Catalytic hydrogenation of Vb

Compound **Vb** (0.324 g; 0.001 mole) was dissolved in 30 ml of ethyl alcohol and 0.3 g Pd/C (10% Pd) was added to the solution. Hydrogenation was continued until the absorption of 24.5 ml hydrogen (about 60 min). The catalyst was then removed by filtration and the solution evaporated in vacuum to leave an oil. Crystallization from 80% aqueous ethyl alcohol gave 0.20 g (96.2%) of isoflavan (**VII**), m.p. 55—56 °C (*lit.* [7] m.p. 54—55 °C).

Alcaline decomposition of Vb

Compound **Vb** (0.97 g; 0.003 mole) was dissolved in 10 ml of water, and 0.0033 mole of sodium hydroxide (0.132 g of NaOH in 1 ml of water) was added. After 30 min,the solid, which deposited was removed from the orange solution by filtration. Crystallization from 80% ethyl alcohol gave 0.22 g (28.7%) isoflav-3-ene (**II**), m.p. 89—90 °C (*lit.* [18] m.p. 90—91 °C).

REFERENCES

[1] Carney, R. W., Bencze, V. L., Wojtkunski, J., Renzi, A. A., Dorfman, L., de Stevens, G.: J. Med. Chem., **9,** 516 (1968)
[2] Irmscher, K., Kramer, J., Kraft, H. G., Krieser, H.: Neth. Appl. 6,517,021; C. A. **66,** 28657 (1967)
[3] Irmscher, K., Borck, J.: Ann., **744,** 164 (1971)
[4] Ray, S., Grover, R. K., Anagd, N.: Ind. J. Chem., **9,** 727 (1971)
[5] Ray, S., Grover, R. K., Kamboj, V. P., Setty, B. S., Kar, A. B., Anand, N.: J. Med. Chem., **19,** 276 (1976)
[6] Gopalchari, R., Iyer, R. N.: Ind. J. Chem., **4,** 331 (1966)
[7] Inoue, N.: Bull. Chem. Soc. Japan, **37,** 601 (1964)
[8] Anjaneyulu, A. S., Krishna, C. S., Row, L. R.: Tetrahedron, **21,** 2677 (1965)
[9] Szabó, V., Antal, E.: Tetrahedron letters, **1973,** 1659
[10] Szabó, V., Antal, E.: Acta Chim. (Budapest) **90,** 381 (1976)
[11] Coates, R. M., Chen, J. P.: Tetrahedron, **32,** 2705 (1969)
[12] Kochi, L. K., Hammond, G. S.: J. Am. Chem. Soc., **75,** 3443 (1953)
[13] Tipson, R. S.: J. Org. Chem., **9,** 235 (1944)
[14] Yamaguchi, S., Kabuto, K., Ninomiya, Y., Inoue, N.: Bull. Chem. Soc. Japan, **43,** 3952 (1970)
[15] Kabuto, K., Kikuchi, Y., Yamaguchi, S., Inoue, N.: Bull. Chem. Soc. Japan, **46,** 1839 (1973)
[16] Bergel, F., Cohen, A.: U. S. Pat. 4,932,520 (1950)
[17] Inoune, N.: Bull. Chem. Soc. Japan, **37,** 606 (1964)
[18] Yamaguchi, S., Ito, S., Suzuki, I., Inoue, N.: Bull. Chem. Soc. Japan, **41,** 2073 (1968)
[19] Yamaguchi, S., Ito, S., Namakura, A., Inoue, N.: Bull. Chem. Soc. Japan, **38,** 2187 (1965)
[20] Mauzerall, D., Westheimer, F. H.: J. Am. Chem. Soc., **77,** 2261 (1955)
[21] Acheson, R. M., Paglietti, G.: J. Chem. Soc. Perkin I, **1976,** 45

Vince Szabó
János Borbély
Ërnő Antal
H-4010 Debrecen 10.

Acta Chimica Academiae Scientiarum Hungaricae, Tomus 102 (1), pp. 59—65 (1979)

A NEW ANOMALOUS RACEMATE

L. TŐKE,[1] M. ÁCS,[1] E. FOGASSY,[1] F. FAIGL,[1] S. GÁL[2] and J. SZTATISZ[2]

([1]Department of Organic Chemical Technology, [2]Department of General and Analytical Chemistry, Technical University, Budapest)

Recived July 5, 1978

Accepted for publication October 20, 1978

In the course of the resolution of racemic 6-phenyl-2,3,5,6-tetrahydro-imidazo-[2,1-*b*]thiazole, the physical properties of the racemate, the pure enantiomers and of a composition containing the enantiomers in 3 : 1 ratio were found to be different in both the solid state and in solution. The relatively stable molecular complex containing the antipodes in 3 : 1 ratio is called an 'anomalous racemate'.

In an earlier paper [1] we reported the resolution of racemic 6-phenyl-2,3,5,6-tetrahydro-imidazo[2,1-*b*]thiazole (*R*, *S*-**1**), a compound with antihelmintic effect.

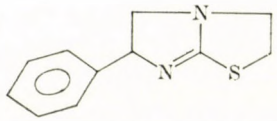

R, *S*–**1**

The optical isomers were separated by means of *O*,*O*-dibenzoyl-*R*,*R*-tartaric acid (DBTA); the method in outline is shown below.

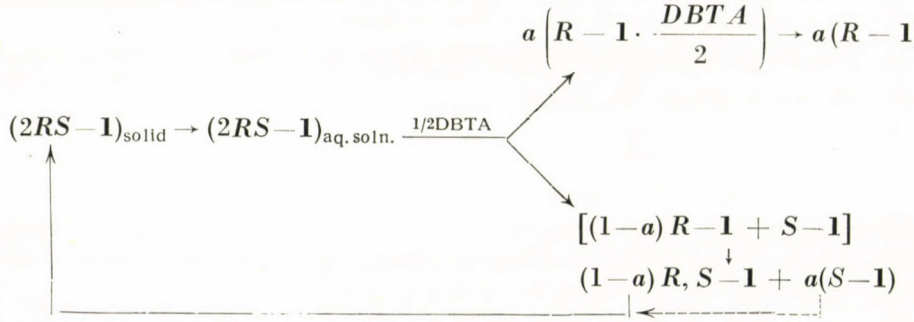

where $a_{max} = 0.7$.

According to our experience, the neutral DBTA salt of *R*-**1** can not be obtained in yield higher than 70%, either by the methods given in the literature [3—6] or by the procedure employed by us.

However, the factor limiting the yield is not the solubility of the salt, as indicated by the following experiments.

(*a*) The neutral salt of *R*-**1** formed with *O,O*-dibenzoyl-*R,R*-tartaric acid is practically insoluble under the experimental conditions of the resolution process.

(*b*) The enantiomer *R*-**1** can be recovered with DBTA from a series of isomeric mixtures prepared from the racemate and pure *R*-**1**, and in each case the yield is determined exclusively by the deviation of the composition of the

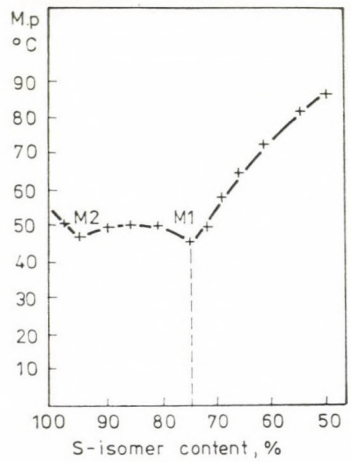

Fig. 1. Dependence of the melting point on the composition

solution from the 3*S* : 1*R* ratio of the enantiomers. (However, in aqueous solution, in the presence of a mineral acid, the excess isomer can be separated from the racemate in high purity and in satisfactory yield [1].)

In order to explain the experimental observations, the dependence of the melting point of the compound on the optical purity was first examined (Fig. 1).

The melting point curve with two minima does not agree with the shape of melting point curves characteristic of true racemates well known from the literature [7]. Strikingly, one of the minima (M1) on the curve numerically agrees with the isomeric composition remaining in solution during the resolution process.

In the IR spectra recorded in KBr pellets, the intensities of the doublets at 1595 cm^{-1} and 1585 cm^{-1} also show extreme values at 75% *S*-**1** enantiomer content (Fig. 2a).

The thermal behaviour of the samples was then examined. The results of the evaluation of the DSC and TG curves are summarized in Table I. The heat consumption observed during the DSC experiments is the sum of the heats of

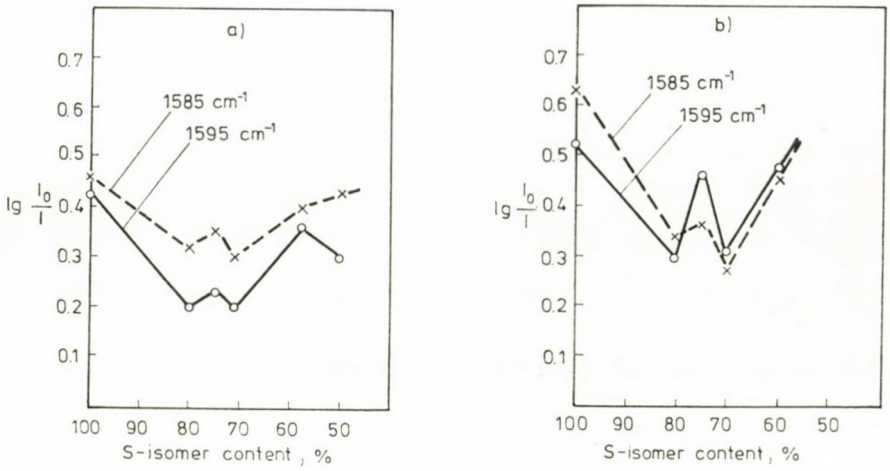

Fig. 2. Intensities of the bands at 1585 cm^{-1} and 1595 cm^{-1} in the IR spectra of compound **1** *vs.* the antipode content (*a*) in KBr; (*b*) in $CHCl_3$

melting of *S*-**1** and *R,S*-**1** and of the heat of dissolution of *R,S*-**1** in the melt. Assuming that these heat quantities are additive in proportion to the ratio of the enantiomers, in the knowledge of the heats of melting of the pure enantio-

Table I

Thermal analysis data and dissolution heat values

No. of sample	S-isomer content %	DSC analysis				Tg analysis		
		Max. I	Max. II	$Q_{measured}$	$Q_{dissoc.}$	Step I till 250 °C	Step II till 400 °C	Step III till 620 °C
		temperature C°		Joule/g				
1	100	59.5	—	91.56	—	67%	16%	—
2	97	56.5	—	104.16	−17.22	25%	56.5%	12%
3	95	56.5	—	82.00	−10.92	28%	47%	10%
4	90	56.5	64.0	88.62	− 9.66	21.5%	55%	13%
5	86	55.0	68.0	84.00	−17.64	18%	57%	14%
6	81	55.5	74.0	88.20	−16.80	19.5%	49%	13.5%
7	78	56.5	78.5	68.88	−38.22	16%	51%	14%
8	75	56.0	82.0	89.46	−19.74	24%	41.5%	11.5%
9	72	55.0	82.0	89.46	−15.54	19%	47.5%	11.5%
10	69	54.5	84.0	81.90	−31.92	15.5%	49%	14.5%
11	66	53.0	85.5	91.56	−41.16	15.5%	49%	12.5%
12	61	53.0	86.5	77.28	−42.00	17%	44.5%	14%
13	55	—	90.0	64.68	−58.80	13%	47%	14.5%
14	50	—	90.5	127.26	—	18.5%	42%	14%

mers and the racemate, the heats of dissolution belonging to the individual compositions can be calculated according to the following correlation:

$$Q_{\text{dissolution}} = Q_{\text{measured}} - xQ_{S-1} - (1 - x)\, Q_{R,S-1}$$

where x is the mole fraction or weight fraction.

When the heats of dissolution calculated ($Q_{\text{dissolution}}$) are plotted as a function of the composition, the curve has a local maximum at 78% *S*-isomer content (Fig. 3).

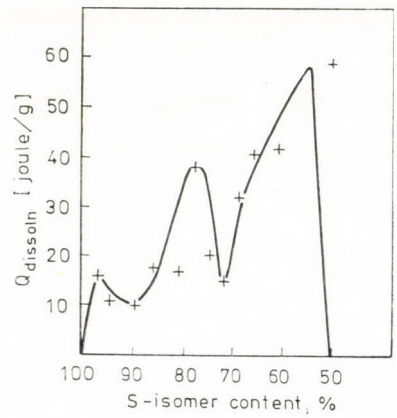

Fig. 3. Calculated heat of solution *vs.* composition

There is an interesting difference in the thermogravimetric behaviour of solid samples of different compositions. As seen from Table I, compound **1** undergoes decomposition, more accurately, loss of weight, in two steps. According to the microanalytical investigations (see Table II) and spectra, no dramatic

Table II

Microanalytical data

	Composition of samples 1 and 14 before heating	Sample 1 after heating to 250 °C	Sample 14 after heating to 250 °C
C	64.7%	62.48%	59.60%
H	5.9%	5.66%	6.00%
N	13.7%	13.72%	11.82%

change in the structures of the substances took place during these processes. The difference in the weight loss of the pure enantiomer and the racemate can be attributed to the different tensions of the two substances. The weight loss of the sample with the critical compositions (3*S* : 1*R*-**1**) (Table I, No. 8) is

rather similar to that of the real racemate, wich indicates a certain extent of similarity between the two substances.

The results of the X-ray diffraction investigations* on the pure *S*-**1** isomer, the racemate and the 3*S* : 1*R*-**1** samples are shown in Table III. The

Table III

X-ray data

R-**1**		*R, S*-**1**		3S:1*R*-**1**	
d (Å)	*I* %	*d* (Å)	*I* ,%	*d* (Å)	*I*, %
10.799	23.4			10.695	16.8
				9.302	10.5
8.838	12.7			8.733	5.8
		8.170	16.5	8.170	6.3
7.237	13.7	7.369	6.5	7.132	9.5
		6.651	2.5	6.421	29.0
5.801	4.4	6.188	34.5	5.771	4.2
5.433	25.4	5.535	4.5	5.407	27.4
		5.394	13.5	5.063	3.7
		5.181	3.5		
4.839	22.4	4.844	44.5	4.818	17.4
4.741	87.8	4.624	13.5	4.716	76.8
		4.572	9.0		
				4.483	100.0
4.436	48.8	4.436	24.5		
4.329	68.3			4.308	46.3
4.243	100.0	4.227	32.0	4.227	76.8
		4.141	100.0	4.151	30.0
4.030	8.8	3.948	5.0	4.008	4.2
3.976	6.3	3.890	7.0	3.928	13.2
3.723	12.2	3.735	36.0	3.717	30.5
3.630	7.8	3.630	7.0	3.630	19.5
3.414	42.9	3.463	7.0	3.411	29.5
3.393	62.9	3.371	16.0	3.376	38.4
		3.324	58.0	3.000	17.4

data indicate that the crystallographic parameters of the three solid samples are different, that is, even the crystal form is altered at the 3*S* : 1*R*-**1** composition.

* The X-ray diffraction spectra were recorded by L. BOGNÁR (Department of Mineralogy, Eötvös Loránd University, Budapest).

During an investigation of the conditions of optical isomerism in malic acid, FREDGA [8] found a molecular complex with a composition deviating from the 1 : 1 isomeric ratio; this he named "anomalous racemate". The existence of this material was confirmed by the melting point *vs.* composition diagram and by X-ray powder diagrams.

On the basis of the preparative facts and instrumental examinations it is now concluded that the substance investigated by us exists not only in the form of the optically pure isomers and the racemate, but also in the form of an associate with deviating physical properties, its composition being 3*S* : 1*R* (or its mirror image 3*R* : 1*S*). On the analogy to FREDGA's work, this molecular complex is also called an "anomalous racemate".

The surprisingly low yield of the resolution process, however, can not be explained by the existence of such a molecular associate if it exists only in the solid state. It was thus assumed that this type of complex must also be present in relatively concentrated solutions, used under the conditions of the resolution.

In Fig. 2b, the doublets at 1595 cm^{-1} and 1585 cm^{-1} in the IR spectra of samples with various ratios of the isomers in chloroform solutions are plotted as a function of the composition. The course of the curve is analogous to that obtained with the solid samples, thus confirming the assumption.

The existence of the molecular complex depends on the pH of the solution and on the nature of the solvent. Weak acids, like DBTA, can not decompose the 3 : 1 complex of the enantiomers in aprotic solvents (*e.g.* $CHCl_3$ or CH_2Cl_2), therefore the yield of resolution can not be increased above the given value under such conditions.

In protic solvents, on the effect of strong acids, the complex undergoes dissociation and the pure enantiomer can be separated in nearly 100% yield (see the method of selective liberation in Ref. [1]).

In his paper dealing with resolution processes, WILEN [9] listed four factors wich determine the yield of resolution. The existence of anomalous racemates should be regarded as a fifth parameter to be considered in planning a resolution processes.

Experimental

6-Phenyl-2,3,5,6-tetrahydro-imidazo[2,1-*b*]thiazole was supplied by Chemical Works Gedeon Richter Budapest; the optical isomers were prepared from it according to the method described in our previous paper [1].

The samples with various isomeric compositions were made by evaporation to dryness in vacuo of methanolic solutions prepared from substances weighed on an analytical balance.

M.p.'s were determined with a Büchi melting point measuring apparatus.

The IR spectra were recorded with a Perkin-Elmer 237 spectrophotometer in KBr pellets or in 0.1 mole/litre chloroform solutions.

Thermal analyses were effected with a DuPont 990 Thermal Analyser DSC and a 951 Thermogravimetric Analyser apparatus (rate of heating: 10 °C/min.)

X-ray diffraction diagrams were obtained with a Siemens Cristalloflex powder diffractometer in a Cu tube.

REFERENCES

[1] FOGASSY, E., ÁCS, M., FELMÉRI, J., ARACS, Zs.: Periodica Polytechnica, **20,** 247 (1976)
[2] ERHART, G., RUSCHIG, H.: Arzneimittel. Vol. V, p. 33 Verlag Chemie, Weinheim (1972)
[3] Brit. Pat. 1, 169, 310 (1967); C. A., **72,** 55453
[4] U. S. Pat. 1,127,852 (1966); C. A., **70,** 11698
[5] Ger. Offen 2,027,030 (1970); C. A., **74,** 53786
[6] Ger. Offen 1,908,802 (1969); C. A., **72,** 21688
[7] NÓGRÁDI, M.: Bevezetés a sztereokémiába. Műszaki Könyvkiadó, Budapest, 1975 (In Hungarian)
[8] ANDERSSON, M., FREDGA, A., JERSLEV, B.: Acta Chem. Scand., **20,** 1060 (1966)
[9] WILEN, S. H., COLLET, A., JACQUES, J.: Tetrahedron, **33,** 2725 (1977)

László TŐKE
Mária ÁCS
Elemér FOGASSY
Ferenc FAIGL
H-1111 Budapest, Műegyetem rkp. 3.

Sándor GÁL
Janisz SZTATISZ
H-1111 Budapest, Gellért tér 4.

Acta Chimica Academiae Scientiarum Hungaricae, Tomus 102 (1), pp. 67—71 (1979)

RING *A* AROMATIZATION OF 3β-ACETOXY-5 α-CHOLESTAN-6-ONE

M. S. AHMAD and NAJM ZAHIR KHAN

(Department of Chemistry, Aligarh Muslim University, Aligarh, India)

Received September 8, 1978

Accepted for publication October 20, 1978

The title compound (**1**) on refluxing with Br_2HBr in ether—acetic acid rearranges to 1-methyl-19-norcholesta-1,3,5(10)-triene-6-one (**2**), together with two other isolable compounds (**3**) and (**4**). These compounds have been identified on the basis of spectral properties and comparison with authentic samples in known cases. A possible mechanism for the conversion **1** → **2** is suggested.

In an attempted preparation of 3β-acetoxy-7-α-bromo-5 α-cholestan-6-one (**5**), following the literature procedure [1], the title compound (**1**) was heated under reflux with bromine and HBr (as catalyst) in ether-acetic acid for 22 hours to furnish compounds with melting points of 140 (**2**), 169 (**3**) and 163 °C (**4**). The structures of these compounds were established by their spectral properties and by comparison with authentic samples where available.

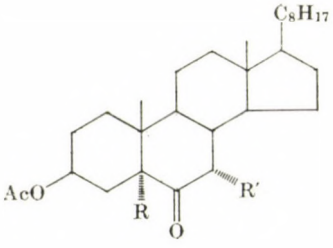

1 R = H; R′ = H

4 R = Br; R′ = H

5 R = H; R′ = Br

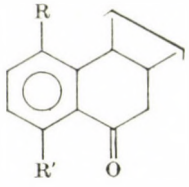

2 R = CH_3; R′ = H

6 R = H; R′ = CH_3

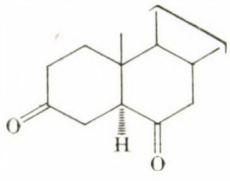

3

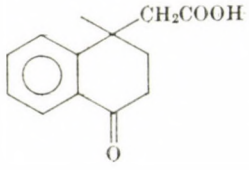

7

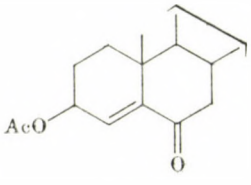

8

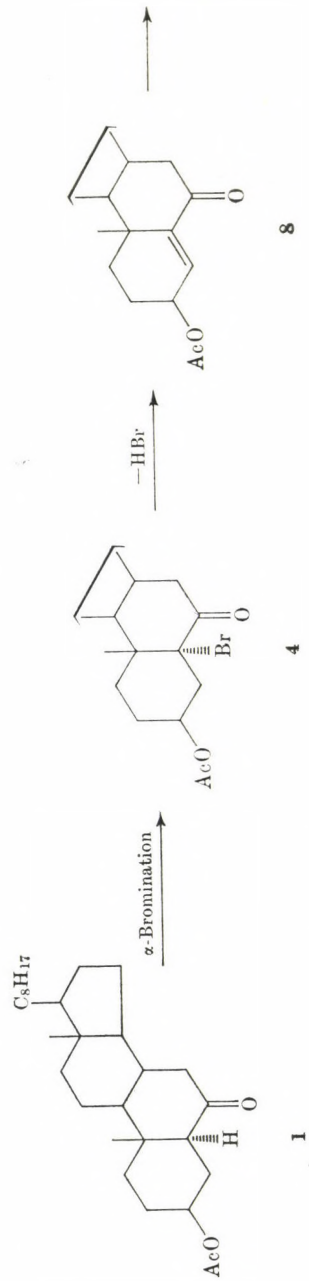

1 4 8 3

Scheme 1

Compound **2** (negative Beilstein test) has the formula $C_{27}H_{40}O$, a composition supported by its mass spectrum (M^+ 380, $C_{27}H_{40}O$). This composition suggests the loss of the acetate function and possible aromatization of ring *A*. The IR spectrum gave bands at 3030w (C=C—H), 1680s (C=C—C=O) and 1585 cm^{-1} (C=C, aromatic); the IR spectrum did not show the presence of acetate or hydroxyl group. The presence of a conjugated carbonyl group was also evident in the UV spectrum of the compound with m.p. 140 °C (λ_{max} 255 nm and a weak band at 335 nm). The presence of an aromatized ring (ring *A*) permits two possibilities, *viz.* (**2**) and (**6**). The NMR spectrum was decisive in determining the structure of this compound. The NMR spectrum (60 MHz; $CDCl_3$) gave signals at delta 7.9d,d (1H, J = 8 Hz, *ortho* coupled and 3 Hz, *meta* coupled, C4—*H*), 7.26m (2H, C2—*H* and C3—*H*), 2.43s (3H, C1—Me), 2.5m (2H, merging with the C1-methyl signal, $COCH_2$), 0.71s (3H, C13—Me), 0.83 and 0.90 ppm (other methyl protons). The downfield signal at δ 7.9 ppm d.d for 1 proton is compatible with a beta proton relative to a carbonyl group as in structure **2**. The NMR spectrum of **2** compared with that of 1-methyl-1-carboxymethyl-4-tetralone (**7**) [2], in the latter case, the beta proton relative to the carbonyl group, as expected, appeared at a relatively lower field. From the NMR values the compound of m.p. 140 °C has been assigned structure **2** rather than that of its isomer **6**.

The compound with m.p. 169 °C was identified as 5 α-cholestane-3,6-dione (**3**) by its spectral properties and by comparison with an authentic sample [3]. The formation of **3** from **1** involves the intermediacy of **4** and **8**, which has been experimentally substantiated [3].

The compound with m.p. 163 °C has been identified as 3 β-acetoxy-5 α-bromocholestan-6-one (**4**) by comparison with an authentic sample [3].

The aromatization of ring *A* requires the presence of three potential sites of unsaturation in rings *A* and *B* [4, 5]. Further, in the presence of a 6-keto function, aromatization of the ring does not involve a C5-cationic and subsequent spiro cationic intermediates [6]. Keeping these observations in view, a possible mechanism for the conversion **1** → **2** is in Scheme 2. This shows involvement of **4** and **8**, which were individually shown to provide the aromatized product **2** under similar reaction conditions.

Experimental

All melting points are uncorrected. IR spectra were determined in KBr with a Perkin—Elmer 237 Spectrophotometer. NMR spectra were run in $CDCl_3$ on a Varian A 60 instrument with $SiMe_4$ as internal standard. UV spectra were taken in 95% ethanol on a Beckman DB Spectrophotometer. Thin-layer chromatographic plates were coated with silica gel. A 20% aqueous solution of perchloric acid was used as the spraying agent. Light petroleum refers to the fraction boiling at 60—80 °C.

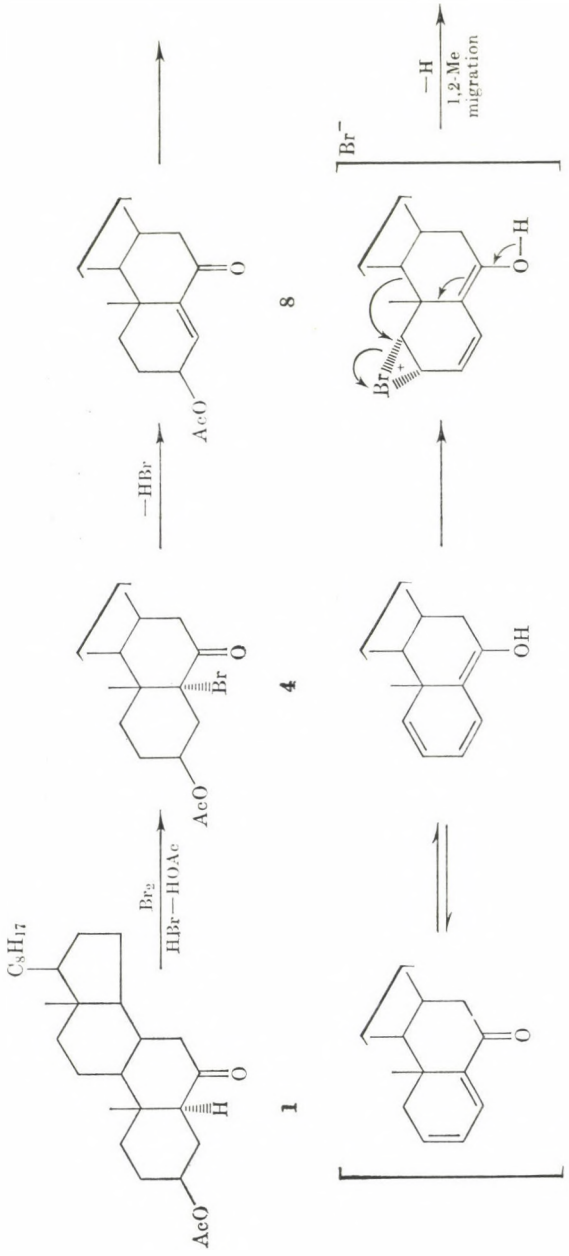
C_8H_{17}
AcO
H
O
1
Br_2
HBr—HOAc
AcO
Br
O
4
—HBr
AcO
O
8
OH
O
Br
Br⁻
—H
1,2-Me
migration
O—H
2

Scheme 2

1-Methyl-19-norcholesta-1,3,5(10)-trien-6-one (2)

To a solution of 3β-acetoxy-5α-cholestan-6-one (**1**) (5.8 g) in either (80 ml) and acetic acid (15 ml) was added dropwise a bromine solution (2.5 g of bromine in 25 ml of acetic acid) over a period of 30 min. The reaction was catalyzed by the addition of HBr (1 ml, 48%) and the mixture heated under reflux for 22 h. The ether was removed under reduced pressure and the acetic acid solution diluted with water to turbidity. It was extracted with ether and the ethereal solution washed with water, sodium bicarbonate solution (5%) and water, and dried over anhydrous sodium sulfate. Removal of the solvent gave an oil (*ca.* 5 g) which was chromatographed on silica gel (100 g, NCL, Poona). Fractions of 20 ml were collected. Eluates from light petroleum-ether (15 : 1) gave **2**, recrystallized frdm light petroleum (0.8 g',m.p. 140 °C.

$C_{27}H_{40}O$. Calcd. C 85.2; H 10.5. Found C 84.9; H. 10.2%.

Further elution with the same solvent system (9 : 1 gave 3 β-acetoxy-5α-bromocholestan-6-one (**4**,, recrystallized from light petroleum (70 mg), m.p. 163 °C; ν_{max} 1740 s ($CH_3CO—O$), 1715 s (C=O) and 1240 s (acetate); δ 5.3 br (1H C3—H, *axial*), 2.4 d ($J = 7$ Hz, 2H, C7—H_2), 2.01 s (3H, CH_3COO), 1.0 s (3H, C10—Me), .070 s (3H, C13—Me), 0.91 and 0.85 ppm (other methyl protons).

Continued elution with the same solvent system (4 : 1 gave the dione (**3**) [3], (120 mg), m.p. and m.m.p. 168 °C; 1710 s (C=O); δ 2.1—2.7 br (7H, C2—H_2, C4—H_2, C5—H, C7—H_2), 0.90 s (3H, C10—Me), 0.70 s (3H, C13—Me), 0.85 and 0.80 pp.m (other methyl protons.

The bromoketone (**4**), when subjected to the same reaction condition afforded **2** and **3**.

*

We are grateful to Professor W. Rahman, Head, Department of Chemistry, for providing the necessary faiclities and to the Department of Atomic Energy, Government of India, for financial assistance to one of us (NZK).

REFERENCES

[1] Corey, E. J., Sneen, R. A.: J. Am. Chem. Soc., **78,** 6269 (1956)
[2] Herz, W., Caple, G.: J. Am. Chem. Soc., **84,** 3517 (1962)
[3] Heilbron, I. M., Jones, E. R. H., Spring, F. S.: J. Chem. Soc., **1937,** 801
[4] Hanson, J. R.: Tetrahedron Lett., **1972,** 4501
[5] Libman, J., Mazur, Y.: Chem. Comm., **1971,** 730
[6] Hanson, J. R.: Chem. Comm., **1971,** 1119

M. S. Ahmad
Najm Zahir Khan
Aligahr Muslim University, Aligarh, India

Acta Chimica Academiae Scientiarum Hungaricae, Tomus 102 (1), pp. 73—83 (1979)

HYDROGEN-BONDED POLY(VINYL-ALCOHOL) GELS,* I

SOLUBILITY STUDIES

J. GYÖRGYI-EDELÉNYI[1], M. NAGY[1] and J. BOGNÁR[2]

([1]Department of Colloid Science, L. Eötvös University, Budapest, [2]BUDALAKK Paint and Synthetic Resin Works Budapest)

Received June 12, 1978
In revised form September 19, 1978

Accepted for publication October 30, 1978

Thermo-instable hydrogels of poly(vinyl aclohol) (PVA) with different structure have been prepared by using dioxane as a precipitant which has been exchanged against water after gelation has taken place The solubility measurements were carried out on temperatures between 298 and 353 K. Calculations based on experimental results allowed to distinguish two types of junction points with different energies. Through changes brought about in the gel structure by the gradual breaking of the junction points exchanging water against *n*-propanol–water mixtures additional information can be obtained. Increasing the *n*-propanol concentration, gel solubility increases and the differences between the two characteristic energies diminish. These statements were supported by the results of thermomechanical measurements.

Introduction

Poly(vinyl alcohol), PVA, is a watersoluble synthetic macromolecule which forms gels easily under favourable conditions, *e.g.* in a concentrated solution. The reversibility of this process suggests that no chemical bonding is involved in the network formation.

Gel formation can occur in pure aqueous solution but also as the result of various additives, *e.g.* dyes, aromatic compounds with several hydroxyl groups, certain precipitating agents (glycerol, ethylene glycol) [1, 2]. Probably, the latter only promote the formation of the physically linked junction zones among the polymer chains without being directly involved in their development. No detailed data concerning the action of such additives are available.

One of the most important papers on this subject is given by SHIBATANI [3] dicussing the formation of PVA gels *via* binary association at suitable sites on the polymer chain and it was stated that the formation of active centers is the rate-determining process. According to his results, a stereo-block composed of five to ten syndiotactic units can be regarded as a site of crosslinking.

* Presented before the Committee on the Physics of Plastics, Hungarian Academy of Sciences, October 1977.

Other studies show that in solvent–precipitant systems first a microphase separation takes place followed by an organization process in the polymer rich regions. This, in turn, produces crystallites with average dimensions of 30 to 70 nm [4].

TAKAHASHI and HIRAMITSU [5] and OGASAWARA *et al.* [6] consider PVA to be a copolymer consisting of atactic sequences and of syndiotactic ones inclined to form crystallites, which are responsible for the formation of thermoreversible gel. The crystallites which consist of syndiotactic sequences are the junction sites in the network; the size of such crystallites can be deduced from the melting point of the gel, using an equation proposed by TAKAHASHI.

The bonding strength of the junction points can be determined from the melting temperatures of the gels (T_m^{gel}), assuming the gel $\rightleftharpoons$ polymer solution transition to be an equilibrium process. Thus, GEMBITSKII *et al.* [7], using FERRY equation [8], found 75.4 kJmol^{-1} for the bonding energy, while TAKAHASHI and HIRAMITSU [5] and SHIBATANI [3] reported 10.9 kJmol^{-1} and 54.5 kJmol^{-1}, respectively.

The relatively great scattering of the above data can be explained partly by the differences in the experimental methods, partly by the diversity of PVA samples studied. The importance of this fact becomes clear if we accept the general opinion that the gelling is caused by the syndiotactic regions of the chains. This is supported by the observation that the PVA rich in syndiotactic sequences is practically insoluble in water due to the strong interaction between the polymer chains of such type of tacticity.

So far, few experimental data have been reported on the structure of physically bonded PVA gels. According to electron microscopic studies by OBOLONKOVA *et al.* [9], globules between 90 and 110 nm in average size form a network in PVA–water systems, while in PVA–glicerol–water systems aggregates with an average cross section of 50 to 60 nm are first arranged in bundles and then gave a cell-like network.

This short survey shows that despite of the diverse studies concerning PVA gels, their behaviour is still far from being well understood.

This paper is concerned with the solubility properties of PVA hydrogels with different supermolecular structures produced by systematically modifying the conditions of gels formation. The investigation of solubility seems to be useful, providing an insight into the nature of gel → polymer solution transition for thermolabile gels and it can give some information on the distribution of bond energies, too.

Experimental

Materials. The gels were prepared from a commercial PVA Rhodoviol 16/20 (Rhone-Poulenc, Paris). The acetate content of the sample was reduced to about 0.3 mol% by hydrolysis in a 2 : 8 mixture of methanol and water, in the presence of NaOH and Na_2SO_3. The homogeneity with respect to molecular weight was increased by removing the fraction of the lowest

molecular weight (about 10%). The average molecular weight of the sample thus prepared was determined by means of ultracentrifuge ($\overline{M}_w = 80 \times 10^3$) and viscosimetry ($\overline{M}_\eta = 83 \times 10^3$).

Analytical grade (REANAL products) dioxane and *n*-propanol were used.

Preparation of PVA hydrogels. The structure of the PVA hydrogels was modified by varying the concentration of the polymer and dioxane, latter used as precipitant. PVA was dissolved in a dioxane–water mixture of known composition in a flask fitted with a reflux condenser at 368 to 373 K. After complete dissolution the heated solution was poured into a horizontal plexiglass cell, covered with a plexiglass plate and placed into a desiccator containing a 1 : 1 mixture of dioxane and water.

In order to follow the process of gel formation, the turbidities of the solutions were measured with a Spectromom 360 type spectrophotometer. Gelation was allowed to proceed until a practically constant turbidity was reached. The time required for gelation varied between 4 and 21 days, depending on the composition of mixture.

Then dioxane was replaced by distilled water. In the solution of the aqueous gels no dioxane could be detected by interferometry, indicating that the solvent exchange proceeded completely. The gels were stored in distilled water at room temperature.

In order to characterize the aqueous gels the approximate dimensions (effective radius, $\bar{r}$) of the supermolecular inhomogeneities were determined by means of the DQ method proposed by SAKURADA *et al.* [10]. This method can also be applied for PVA hydrogel films, as it was shown by NAGY *et al.* [11], since their electron microscopic study proved that the supermolecular inhomogeneities have nearly spherical form. The turbidities of 2 mm thick gel films were measured against water with a Spectromom 360 spectrophotometer, at wavelengths of 430 and 700 mm. The $\bar{r}$ value characteristic of the gel structure and its changes were calculated from the quotient DQ of the two turbidity values according to the DQ *vs.* $\bar{r}$ correlation discussed by SAKURADA.

For determination of the polymer content, the swelling medium adhering to the surface of the gel sample was removed with filter paper and the weights of the sample were measured in this state and after drying to a constant weight in vacuum at 333 K.

The accuracy of this method was $\pm 1\%$. The degree of swelling of the polymer (Q_w) *i.e.* the amount of solvent bound by 1 g dry polymer, together with the volume fraction of the polymer (v_2) in the gel was determine from the polymer content. Calculating v_2 values, the volumes of the polymer and the solvent were considered to be additive [12].

The gels were also characterized by constant C, determined from mechanical measurements [13]. This quantity is proportional to the number of elastically effective network chains and to the modulus of elasticity [14].

The characteristic of the gels studied are listed in Table I, parallel with the composition of the system under gelation (w_{PVA}, $w_{dioxane}$). The producibility of the gel preparation is demonstrated in the case of the gel with $w_{dioxane} = 0.50$ and $w_{PVA} = 0.04$. The gel preparation was reproducible within 5—10%, depending on the methods used for their characterization.

Table I

On gelation		PVA hydrogel					
		1 month			1 year		
$w_{dioxane}$ of medium	w_{PVA} of system	v_2	$\bar{r}$ (nm)	C (kN m^{-2})	v_2	$\bar{r}$ (nm)	C (kN m^{-2})
0.48	0.04	0.0287	200	4.0			
0.48	0.06	0.0477	280	17.3	0.0484	275	18.0
0.48	0.10	0.0715	200	40.3	0.0714	200	41.6
0.50	0.04	0.0299	290	2.8	0.0292	—	3.2
0.50	0.04	0.0292	—	2.7	0.0282	—	3.0
0.54	0.04	0.0301	210	2.8			

Methods

Solubility measurements of PVA hydrogels

A gel sample of known weight and polymer content was placed into the sample holder of a jacketed glass vessel, then a known amount of water or *n*-propanol–water mixture was added. The liquid was stirred magnetically. The temperature was kept within ± 0.1 K by means of an ultrathermostat. Studies were carried out between 298 and 353 K.

The amount of the dissolved PVA in the solution was determined as a function of time for each temperature. After a certain interval (3 to 5 days depending on the temperature) the PVA concentration became constant, subsequently, the temperature was raised in 2.5 or 5.0 K increments.

For the quantitative determination of PVA the colour reaction in aqueous PVA-I_2-KI system in the presence of boric acid was used [15]. Extinction coefficient of the solution was measured at $\lambda = 685$ nm, and the PVA concentration was determined from a calibration curve. The reproducibility of the method was within ± 2 %.

Thermomechanical measurements on PVA hydrogels

In order to compare the results obtained from solubility measurements, the unilateral compression of the gels under constant loading was determined as a function of temperature. The gel sample and the inert medium, (paraffin oil) in a glass cuvette were placed into a thermostated glass vessel and a constant loading (69 Nm^{-2}) was applied by a suitably shaped metal plate placed upon the surface of the gel; at this load the deformation of the sample was homogeneous until the yield point was reached. The changes in the size of the gel sample were determined with a *Brinell*-microscope (magnification $25\times$) within ± 0.02 mm accuracy. This was done every 15 min at first, and later every hour. Deformation equilibrium was usually attained after 24 hrs; subsequently, the temperature was raised in 2.5 or 5.0 K increments. The gel sample was a $10 \times 10 \times 10$ mm cube, test being carried out under the same conditions. Paraffin oil was chosen as the inert medium because it does not dissolve the polymer and does not mix with the swelling medium of the gel.

The shape of the termomechanical curves and the flow point values provide information about the temperature-dependent structural changes. Characteristic temperature values of the curves were reproducible with an accuracy of 1—2 K.

Results and discussion

Solubility of PVA hydrogels

It was expected that the extremely time-consuming solubility studies carried out under equilibrium conditions would furnish information about the energy distribution of the junction sites in the thermolabile gels of various

structures. After a certain period (48—96 hrs) the rate of dissolution falls to zero and a constant concentration is reached (Fig. 1).

In order to verify that the amount of polymer dissolved at various temperatures do not involve fractionation by molecular weight, the molecular weights of these "fractions" have been determined by ultracentrifuge, at temperatures 328, 338 and 350 K, and the $\overline{M}_w$ values were 74×10^3, 75×10^3 and 78×10^3, respectively. The systematic error of the determination of $\overline{M}_w$ and the fact that the samples were derived from comparatively homogeneus sample, excluded the possibility of fractionation by molecular weight.

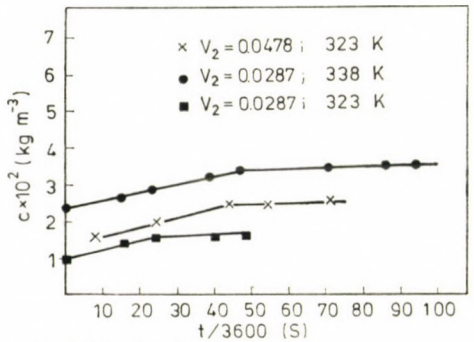

Fig. 1. The amount of PVA dissolved at a given temperature as a function of time

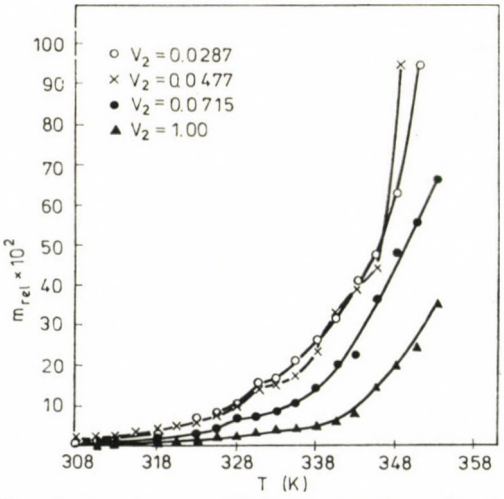

Fig. 2. The relative amount of PVA dissolved as a function of time

To elucidate the correlation between polimer content and gel structure, the temperature dependence of the solubility of the gels prepared at the same dioxane content ($w_{\text{dioxane}} = 0.48$) but various PVA concentration and the solubility of the original PVA film ($v_2 = 1.0$) were compared. Figure 2 shows a set

of curves which represent the relative amount of PVA (m_{rel}) dissolved at different temperatures ($m_{rel} = m/m_0$, where m is the amount of PVA dissolved and m_0 is the initial content of PVA in the system). The structural differences between these gels are shown primarily by their termal stability, *i.e.* by the amount of PVA dissolved at the maximum temperature applied in the experiments. Gels with polymer content $v_2 = 0.0477$ and $v_2 = 0.0287$ are completely dissolved at 348—350 K, while for gel with $v_2 = 0.0715$ $m_{rel} = 0.67$, and for the PVA film $m_{rel} = 0.37$.

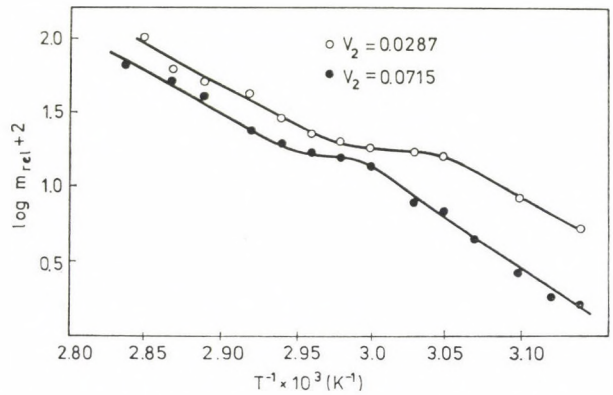

Fig. 3. Logarithm of the relative amount of PVA dissolved as a function of the reciprocal temperature

With increasing temperature the junction zones are gradually rearranged and broken down, and the polymer molecules thus released are dissolved by the solvent present in great excess. The amount of PVA dissolved at a given temperature (c) can be correlated with the bonding strength of the junction points. An attempt is made to calculate, by analogy to the heat of dissolution, the energy characteristic of the forces at the junction sites. The logarithms of the constant PVA concentration (c) or of the corresponding m_{rel} values were plotted against $1/T$. This is illustrated for different gels in Fig. 3. In all experiments, functions composed of two linear sections with different slopes were obtained. This means that within a given temperature range the energy needed for disrupting the junction sites is nearly constant and there is a temperature range where the disruptions do not involve significant dissolving.

On the basis of this findings it seems that the structure of these gels consists of two types of junction sites with different bond energies, which can be characterized by the slopes or apparent energies (E_1 and E_2) calculated by the analogy to the heat of dissolution of solids (Table II). These values, of course, are not absolute measures of the binding forces in the junction sites, still they give valuable information about changes in the structure of these gels.

Table II

v_2	E_1 (kJ mol^{-1})	E_2 (kJ mol^{-1})
0.0287	74.1	90.3
0.0477	97.6	132.3
0.0715	130.2	142.4
1.0	75.4	150.3

The data in Table II also show that increasing the polymer content, the strength and homogeneity of the gel structure also increase.

Two gels prepared with the same polymer content, ($w_{PVA} = 0.04$), but with different dioxane concentrations $w_{dioxane} = 0.50$ (gel 1) and $w_{dioxane} = 0.54$ (gel 2), were selected for further investigation of the structure of PVA hydrogels. These gels differ in their supermolecular organization. The gel 2, prepared with greater dioxane content is most probably built of globular elements with greater bond energy due to the pre-existing order of polymer solution prior to gelling.

Competitive interactions for hydrogen bonds were utilized to detect the differences in the supermolecular structure of these gels. The swelling medium of the gel (the water) was replaced by *n*-propanol–water mixtures ($w_{PrOH} = 0—0.4$). The composition of the *n*-propanol–water mixtures in equilibrium with the gel was determined by refractometry.

Due to the structural changes in the polymer–solvent interactions, the degree of swelling by weight of the gel (Q_w) as a function on *n*-propanol concentration passes through a maximum (Table III).

Table III

w_{PrOH}	gel 1	gel 2
0.0	28.1	23.9
0.06	27.9	23.9
0.12	29.3	25.9
0.25	29.9	25.6
0.35	25.5	22.5
0.40	22.2	20.7

The appearance of the synergetic effect in these mixtures are in good agreement with the results reported by NAGY *et al.* [16, 17].

So solubility experiments were also carried out in *n*-propanol–water mixtures corresponding to the swelling medium of the gel, in order to explore

the structure-breaking effect of *n*-propanol. The results for gel samples 1 and 2 are shown in Figs 4 and 5.

Curves with different slopes are also observed for the aqueous gels, indicating the presence of two types of junction sites with different bond energy. This step-like character disappears for the more homogeneous gel 1 already at $w_{PrOH} = 0.06$, while in the case of gel 2, $w_{PrOH} = 0.12$ is needed for the homogenization of the junction sites.

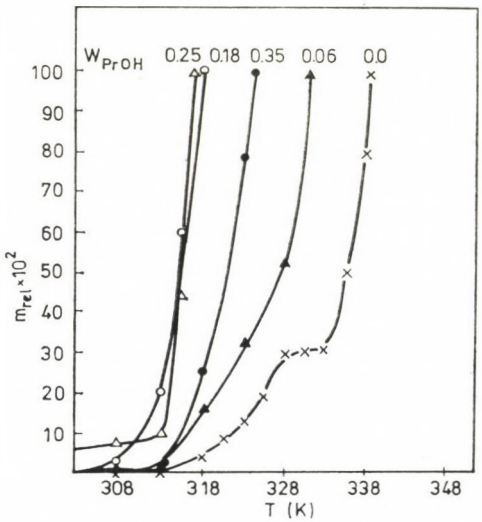

Fig. 4. Relative amount of PVA dissolved from gel 1 as a function of the temperature, at various *n*-propanol contents

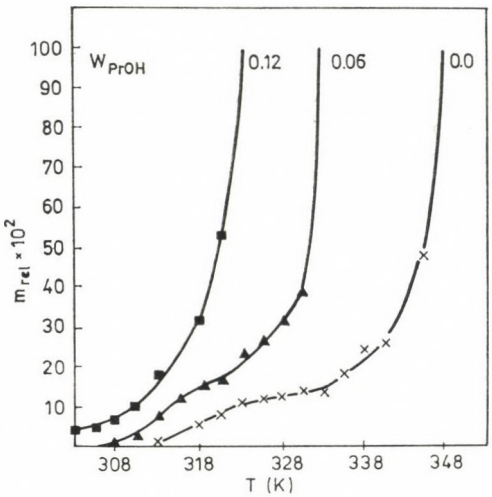

Fig. 5. Relative amount of PVA dissolved from gel 2 as a function of the temperature, at various *n*-propanol contents

The *n*-propanol considerably enhances the solubility of both gels up to $w_{PrOH} = 0.25$, where this effect is reversed. A further increase of the *n*-propanol content diminishes the solubility of the gel. This is in agreement with the results of swelling measurements and with literature data [16, 17].

The temperatures of incipient and complete dissolution and the apparent energies E_1 and E_2 calculated from the log m_{rel} *vs.* $\frac{1}{T}$ plot are collected in Table IV.

Table IV

Gel	w_{PrOH}	Temperature of dissolution (K)		E_1 (kJ mol^{-1})	E_2 (kJ mol^{-1})
		incipient	complete		
1	0.0	313	338	165.8	183.4
	0.06	308	331	92.9	—
	0.0	313	348	191.3	230.3
2	0.06	305	333	170.4	191.3
	0.12	298	323	122.0	—

These data clearly demonstrate the differences in the structures of these gels. *n*-Propanol at a weight fraction of 0.06 suffices to disrupt and homogenize the junction sites in gel 1. Gel 2, produces from a solution containing more precipitant and a preformed structure, it contains more intramolecular bonds and its structure is more heterogenous with respect to the junction sites. In this case the process of homogenization has also appeared at higher *n*-propanol contents, but the formation of a bond type of the same energy occurs only above $w_{PrOH} = 0.12$.

Thermomechanical study of PVA gels

In order to complete and support the results of solubility measurements, thermomechanical studies have been carried out on gel 1 and 2. The relative equilibrium deformation $\left(\frac{\Delta l}{l_0} \cdot 100\right)$ plotted against the temperature resulted in similar curves to those of solubility data (*cf.* Figs 4 and 5). As the *n*-propanol content increases, the deformation of the gel begins at gradually lower temperatures and the step-like behaviour of thermomechanical curves depending on the bond energy distribution inside the gels disappears at different *n*-propanol concentration, *i.e.* in the case of gel 1 at $w_{PrOH} = 0.06$, and gel 2 above $w_{PrOH} = 0.12$, respectively. This tendency is reversed at $w_{PrOH} = 0.25$ because the gel structure becomes more stable in consequence of changes in the polymer—solvent interactions.

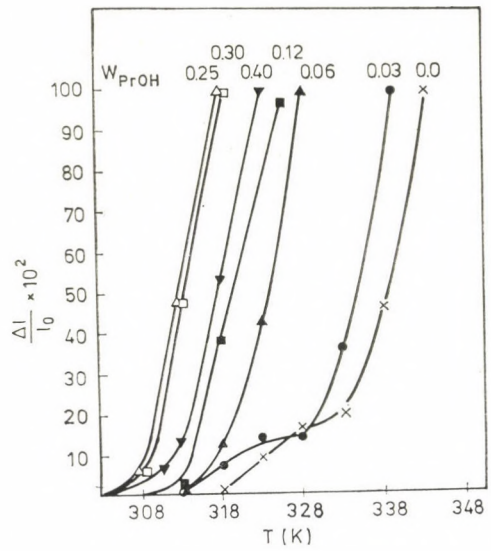

Fig. 6. Thermomechanical curves of gel 1 at various concentrations of *n*-propanol

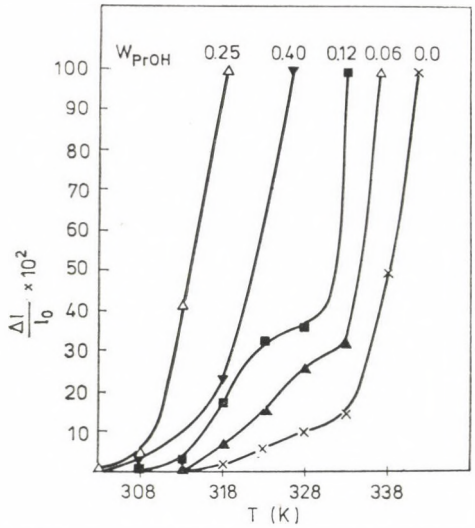

Fig. 7. Thermomechanical curves of gel 2 at various concentrations of *n*-propanol

The results have been in good agreement with the data of solubility measurements supported that the junction sites of these PVA hydrogels could be characterized by two different energies.

*

The author wish to express their thanks to dr. P. Kovács for the UC molecular weight determinations.

REFERENCES

[1] PRITCHARD, J. G.: Poly(vinyl-alcohol). Basic properties and uses. Polymer Monographs, Vol. 4. Gordon and Breach Science Publishers, London 1970
[2] FINCH, C. A.: Poly(vinyl-alcohol). Properties and Application. John Wiley and Sons, London 1973
[3] SHIBATANI, K.: Polymer J., **1,** 348 (1970)
[4] PINES, E., PRINS, W.: Macromolecules, **6,** 888 (1973)
[5] TAKAHASHI, A., HIRAMITSU, S.: Polymer J., **6,** 103 (1974)
[6] OGASAWARA, K., NAKAJIMA, T., YAMAURA, K., MATSUZAWA, S.: Pogr., Colloid & Polymer Sci., **58,** 145 (1975)
[7] GEMBITSKII, L. S., GUBENKOVA, E. N., VERHOTINA, L. N., SPERANSKII, V. V.: Vysokomol. Soed., Ser. A, **12,** 259 (1970)
[8] ELDRIDGE, I. E., FERRY, I. D.: J. Phys. Chem., **58,** 992 (1954)
[9] OBOLONKOVA, E. S., ROGOVINA, L. Z., DIMITRIEVA, N. A., BELAVTSEVA, E. M., SLOMINSKII, G. L.: Koll. Zh., **36,** 284 (1974)
[10] SAKURADA, I., HOSONO, M., TAMAMURA, S.: Bull. Inst. Chem. Res. Kyoto Univ., **42,** 145 (1964)
[11] NAGY, M., WOLFRAM, E., VÁRADI, T.: Progr. Coll. & Polymer Sci., **60,** 138 (1976)
[12] NAGY, M.: Thesis. Budapest 1973
[13] GYÖRGYI-EDELÉNYI, J., NAGY, M. (In press)
[14] DUSEK, K., PRINS, W.: Adv. Polymer Sci., **6,** 1 (1969)
[15] ZWICK, M. M.: J. Polymer Sci. Part A-1, **1966,** 1642
[16] NAGY, M.: Kém. Közl. **29,** 1 (1968)
[17] NAGY, M., WOLFRAM, E., GYŐRFI-SZEMEREI, A.: J. Polymer Sci., Part C, **39,** 169 (1972)

Judit GYÖRGYI-EDELÉNYI
Miklós NAGY
} H-1445 Budapest, P. O. Box 328
János BOGNÁR, H-1044 Budapest, Dunasor 11.

Acta Chimica Academiae Scientiarum Hungaricae, Tomus 102 (1), pp. 85—90 (1979)

PREPARATION OF HOMOGENEOUS TENSIDES*

P. SALLAY,[1] J. MORGÓS,[1] L. FARKAS,[1] I. RUSZNÁK[1] and B. BARTHA[2]

([1]Department of Organic Chemical Technology, Technical University, Budapest and [2]United Chemical Works, Budapest)

Received July 13, 1978

Accepted for publication October 31, 1978

The first six members of the homologous series of polyethylene glycol dodecyl-ethers have been prepared in gas chromatographic purity. It has been found that these compounds can be prepared in better yields and higher purity by means of repeated Williamson syntheses than by an alternate method from dodecyl tosylate. Polyethylene glycol containing at most three glycol units can be used for the synthesis.

Introduction

When reacting dodecyl alcohol with ethylene oxide, no uniform product is obtained; the resulting nonionic tenside is always a mixture of polymer homologues. The first reaction step yields ethylene glycol monododecylether, which, reacting with a further ethylene oxide molecule, is converted into diethylene glycol monoether, *etc.*:

$$R{-}OH + \underset{\diagdown\,O\,\diagup}{CH_2{-}CH_2} \rightarrow R{-}O{-}CH_2{-}CH_2{-}OH$$

$$R{-}O{-}CH_2{-}CH_2{-}OH + \underset{\diagdown\,O\,\diagup}{CH_2{-}CH_2} \rightarrow R{-}O{-}(CH_2{-}CH_2{-}O)_2{-}H$$

$$R{-}(O{-}CH_2{-}CH_2)_n{-}OH + \underset{\diagdown\,O\,\diagup}{CH_2{-}CH_2} \rightarrow R{-}O{-}(CH_2{-}CH_2{-}O)_{n+1}{-}H$$

$(R = -C_{12}H_{25})$

In each step of the reaction ethylene oxide reacts with a primary alcoholic hydroxyl group. Since thehydroxyl groups of the starting alcohol and of the resulting glycol ether have approximately the same reactivity, it can be expect-

* Paper presented at the Conference of the Hungarian Chemical Society, Debrecen 1977

ed that ethylene oxide reacts simultaneously with both types of hydroxyl groups (*i.e.* a consecutive competitive reaction takes place), and the reaction product is therefore a mixture of various oxyethylated derivatives of dodecyl alcohol. The ratio of these oxyethylated homologues in the products may vary with the reaction conditions (temperature, catalyst, *etc.*).

Accurate determination of the concentrations of the components may often be important, since the distribution constants calculated from these concentrations allow conclusions to be drawn on the rates of the partial reactions [1]. The colloid chemical properties, which affect the applicability of tensides, also depend on the distribution of homologues [2].

It is a basic requirement in quantitative analysis that all the homologues should be accessible for analysis, *i.e.* a method should be found for the preparation of the reaction chain (homogeneous tenside). Homogeneous tenside is an oxyethylated product containing only one polymer homologue [3].

Of the methods suitable in principle for the preparation of homogeneous tensides based on dodecyl alcohol, the simples way, oxyethylation of dodecyl alcohol

$$R{-}OH + (CH_2{-}CH_2)_n \rightarrow R{-}O{-}(CH_2{-}CH_2{-}O)_n{-}H,$$

as discussed above, always leads to a mixture of homologues; therefore it is inapplicable for our purposes.

For similar reasons, the synthesis starting from sodium dodecanolate and monochloroethylene glycol derivatives

$$R{-}O{-}Na + Cl{-}(CH_2{-}CH_2{-}O)_n{-}H \rightarrow R{-}O{-}(CH_2{-}CH_2{-}O)_n{-}H + NaCl$$

must also be discarded, since the chlorinated ethylene glycol derivatives are usually prepared by the oxyethylation of ethylene chlorohydrin, which again leads to the formation of homologues [4].

Two reactions appear to be suitable from the practical point of view; one is a Williamson synthesis from dodecyl chloride and the appropriate monosodium ethylene glycolate

$$H{-}(O{-}CH_2{-}CH_2)_n{-}ONa + Cl{-}R \rightarrow R{-}O{-}(CH_2{-}CH_2{-}O)_n{-}H + NaCl,$$

and the other from dodecyl tosylate and the appropriate monosodium ethylene glycolate.

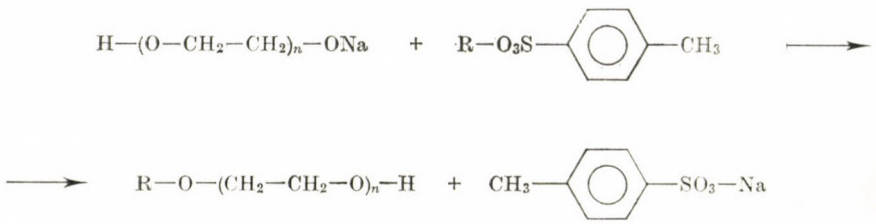

Accordingly, these syntheses have been studied to determine their applicability for the preparation of homogeneous tensides of gas chromatographic purity.

Method

The Williamson synthesis was effected in two different ways.

(1) The polyethylene glycol chain was built up from the monosodium salts of lower ($m = 1$—3) glycols and dodecyl chloride.

$$C_{12}H_{25}Cl + Na—(O—CH_2—CH_2)_m—OH \rightarrow C_{12}H_{25}—(O—CH_2—CH_2)_m—OH + \\ + NaCl$$

I **II** **III**

The hydroxyl group of the resulting ethylene glycol monoether was replaced by halogen *via* treatment with thionyl chloride, and the desired chain length was attained by repeating the Williamson synthesis, using this alkyl chloride.

$$\mathbf{III} + SOCl_2 \rightarrow C_{12}H_{25}—(O—CH_2—CH_2)_{m-1}—O—CH_2—CH_2—Cl$$

IV

(2) According to the second method, the appropriate polyethylene glycol chain was prepared first (again by Williamson synthesis, in which the maximum value of n and m was 3),

$$Cl—(CH_2—CH_2—O)_n—CH_2—CH_2—Cl + 2\ Na—O—(CH_2—CH_2—O)_m—H \rightarrow \\ \rightarrow HO—(CH_2—CH_2—O)_{2m+n+1}—H + 2\ NaCl$$

and then its monosodium glycolate was allowed to react with dodecyl chloride. The characteristics of the homogeneous tensides prepared are shown in Table I. The purity of the products was checked by gas chromatography. The product was accepted as pure only when its gas chromatogram had one peak under the given experimental conditions [5].

Table I

Homogeneous tensides prepared by Williamson synthesis

Formula	m	n	Boiling point		Yield, %
			K/Pa	°C/mmHg	
$C_{12}H_{25}O-CH_2CH_2-OH$	1	0	417/13.3	144/0.1	65
$C_{12}H_{25}(O-CH_2CH_2)_2-OH$	2	0	437/13.3	164/0.1	57
$C_{12}H_{25}(O-CH_2CH_2)_3-OH$	3	0	451/13.3	178/0.1	38
$C_{12}H_{25}(O-CH_2CH_2)_4-OH$	2	2	461/ 6.7	188/0.05	50
$C_{12}H_{25}(O-CH_2CH_2)_5-OH$	2	3	486/ 6.7	212/0.05	23
$C_{12}H_{25}(O-CH_2CH_2)_6-OH$	3	3	506/13.3	233/0.1	26

where

m is the number of glycol units in the first step
n is the number of glycol units in the second step

From dodecyl tosylate, the monoethers of ethylene-, diethylene- and triethylene glycols were prepared only, through the corresponding monosodium glycolates, since the obtained products proved to be inappropriate even after repeated distillations, as gas chromatographic test materials. The yields of the first three tenside homologues prepared by the tosyl ester method are shown in Table II.

Discussion

According to the results of Williamson syntheses in two ways, the first three members of the homologous series of polyethylene glycol monododecyl ethers can be synthesized directly from commercially available ethylene glycol, diethylene glycol and triethylene glycol of appropriate quality. The preparation of higher polyethylene glycol chains, and Williamson synthesis therefrom yields tensides of insufficient quality. Although tetraethylene glycol of gas chromatographical purity was successfully prepared, owing to the more severe reaction conditions necessary for the further synthesis, not only the condensa-

Table II

Homogeneous tensides prepared from dodecyl tosylate

Formula	Boiling point		Yield, %
	K/Pa	°C/mmHg	
$C_{12}H_{25}O-CH_2CH_2O-H$	425/26.6	152/0.2	40
$C_{12}H_{25}O-(CH_2CH_2O)_2-H$	436/13.3	163/0.1	34
$C_{12}H_{25}O-(CH_2CH_2O)_3-H$	452/13.3	179/0.1	13

tion reaction, but also the preparation of monosodium glycolate required higher temperatures. The amounts of by-products increased and, as shown by the gas chromatogram, even after several distillations the product was contaminated. In the case of polyethylene glycols containing more than four units, even the polyethylene glycol could not be prepared in gas chromatographic purity. The procedure is further complicated by the fact that for longer ethylene glycol chains the boiling point of polyethylene glycol is close to that of the monoether, therefore, their separation is imperfect.

With increasing polyethylene glycol chain the yield decreases. In the synthesis starting from tosyl ester, the yield is lower than in the Williamson synthesis, even for the first member of the homologous series. Although the reaction conditions are substantially milder in the former case (80—100 °C instead of 140—160 °C), the product is much more contaminated, and further purification does not yield gas chromatographically uniform product.

It can be stated therefore that for the preparation of homogeneous dodecyl alcohol-based tensides, a multistep Williamson synthesis is more preferable, provided that polyethylene glycols longer than tetraethylene glycol are not applied in the individual reaction steps.

Experimental

Preparation of polyethylene glycol dodecyl ethers by Williamson synthesis

Ethylene glycol (or di- or triethylene glycol) (2.5 moles) was placed into a four-necked flask equipped with reflux condenser, gas inlet tube and dropping funnel. Under nitrogen atmosphere, 0.5 moles (11.5 g) of metallic sodium was added at 80 °C. The temperature of the solution was raised to 140—160 °C, then 0.5 moles of dodecyl chloride was added and the mixture stirred at 140—160 °C for 20—25 h. The precipitated salt was filtered off, the two phases of the reaction mixture were separated, and the upper phase was fractionally distilled in vacuum.

Preparation of tetra- (or hexa-) ethylene glycol

Thionyl chloride (3 moles) was placed into a four-necked flask equipped with a stirrer, and 3 moles of diethylene glycol was added gradually to the boiling reaction mixture. When the temperature of the mixture reached 130 °C, it was stirred for 30 min and then fractionated. The main fraction (82%) had b.p. 176—178 °C. To 0.5 moles of β,β'-dichlorodiethyl ether prepared as described above, 1 mole of monosodium (diethylene)glycolate was added, and the reaction mixture was stirred at 140—160 °C. The precipiatted salt was filtered off and the filtrate fractionally distilled in vacuum. The main fractions were tetraethylene glycol (41%), 386—389 K/20 Pa (113—116 °C/0.15 mmHg), and hexaethylene glycol (17%), 481 K/6.7 Pa (208 °C/0.05 mmHg).

Preparation of polyethylene glycol dodecyl ether from tosyl ester

To a solution of 0.5 moles of monosodium ethylene (di- or tri-) glycolate prepared as described above, 0.5 moles of dodecyl tosylate [6] was added at 80 °C. The mixture was maintained at 80—100 °C for 20 h, then the precipitated solid was filtered off, the filtrate separated, and the upper phase fractionally distilled in vacuum.

REFERENCES

[1] MAGET, H. J. R.: J. Polym. Sci., **57,** 773 (1962)
[2] GROSSMANN, H.: Tenside, **7,** 188 (1970)
[3] SCHICK, M. J.: Nonionic Surfactants, p. 441. Marcel Dekker, New York, 1967
[4] CHAKOVSKY, N., MARTIN, R. H., VAN NECHEL, R.: Bull. Soc. Chim. Belg., A III **65,** 423 (1956)
[5] FARKAS, L., MORGÓS, J., SALLAY, P., RUSZNÁK, I., BARTHA, B.: Kolor. Ért. **20,** 344, 350, (1978)
[6] Org. Synth. **20,** 50 (1940)

Péter SALLAY
Jenő MORGÓS
László FARKAS
István RUSZNÁK
H-1502 Budapest, Műegyetem, P. O. Box 91.
Béla BARTHA, H-1172 Budapest, Cinkotai u. 26.

Acta Chimica Academiae Scientiarum Hungaricae, Tomus 102 (1), pp. 91—100 (1979)

NOTES ON THE MECHANISM OF THE REARRANGEMENT OF 2'-HYDROXYCYCLOPENTENONE DERIVATIVES TO THE 3'-HYDROXY ANALOGUES

STEREO-CONTROLLED SYNTHESES OF PROSTAGLANDIN SYNTHONS

L. NOVÁK,[1] J. ROHÁLY,[1] M. KAJTÁR[3] and CS. SZÁNTAY[1, 2]

([1]Institute for Organic Chemistry, Technical University, Budapest, [2]Central Research Institute for Chemistry, Budapest and [3]Institute for Organic Chemistry, Eötvös Loránd University, Budapest)

Received July 31, 1978

Accepted for publication October 31, 1978

A simple and effective preparation of the 3'(*R*)-hydroxycyclopentenone intermediates for the syntheses of prostaglandins E_1 and E_2 is reported. Also discussed is the mechanism of the rearrangement of the 2'-hydroxycyclopentenone derivatives into the 3'-hydroxy analogues.

During the last years a few elegant methods have been developed for the syntheses of hydroxycyclopentenones of type **1** [1—13]. Among these, special interest is attached to those which lead to optically active compounds (**1a**, **b**) [7—13], because the latter can be conveniently transformed to prostaglandins E_1 and E_2 *via* the conjugate addition of organometallic derivatives.

Recently, FLOYD [3] reported a useful method for the synthesis of the racemic hydroxycyclopentenone **1a** by the kinetically controlled ring opening of the racemic epoxyketone **5a** with a base, followed by rearrangement of the 2'-hydroxycyclopentenone derivative **6a** to the thermodynamically more stable 3'-hydroxy compound (**1a**). Most recently, PIANCATELLI and SCETTRI have described a modified procedure for the conversion of 2'-hydroxy compounds to the racemic 3'-hydroxy cyclopentenones, using column chromatography on neutral or basic alumina [6, 14].

Although the above authors had no direct evidence for the possible mechanism of the rearrangement, they presumed that the reaction proceeded *via* a dehydration—hydration sequence, with the initial formation of a cyclopentadienone derivative (**8**), which immediately underwent hydration to give the 3'-hydroxycyclopentenone.

In the course of our studies on the chemistry of prostaglandins, it was of interest to learn whether this method was adaptable for the synthesis of optically active prostanoid synthons (**1a**, **b**) too. If so, the proposed mechanism of the rearrangement must be erroneous, because the intermediate (**8**) postulated in the crucial step is an achiral compound.

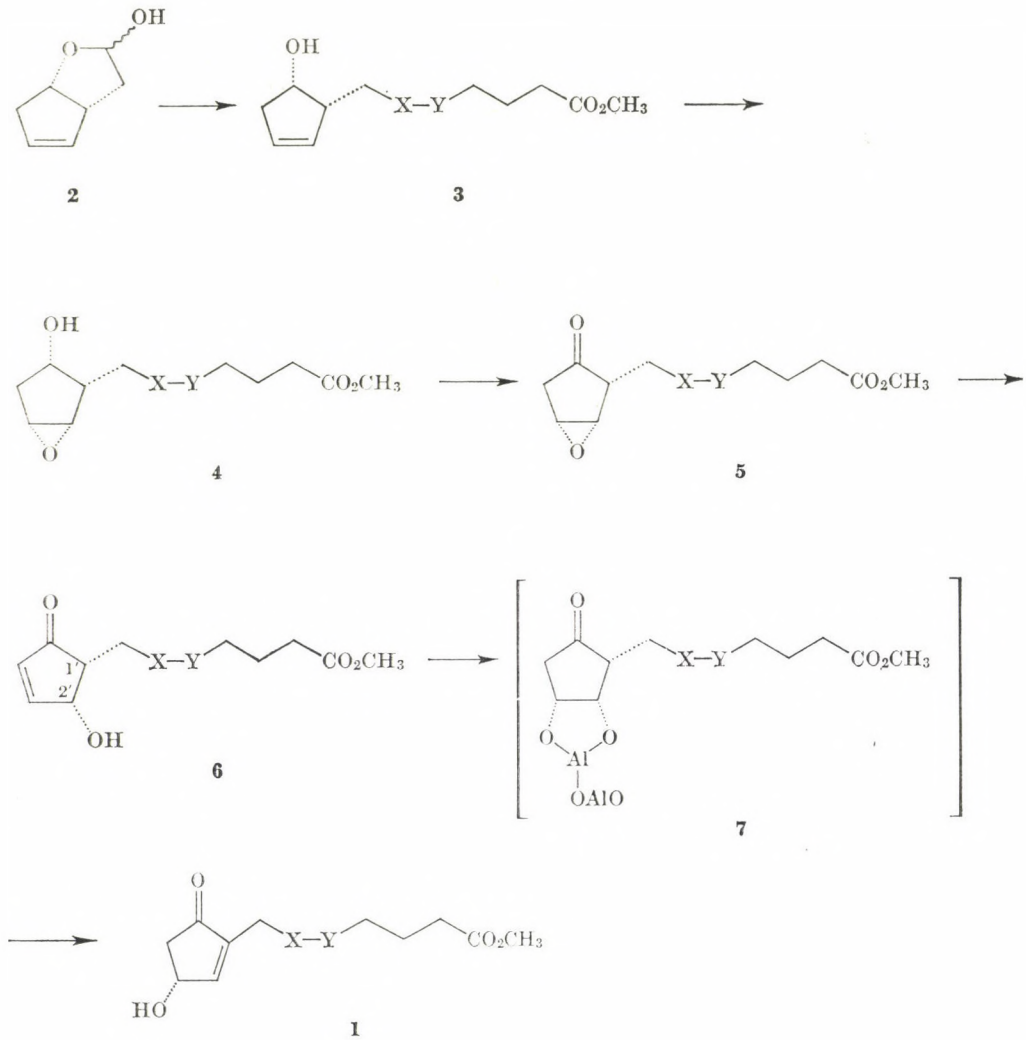

Scheme 1

In order to investigate and answer this question, we prepared the hitherto unknown optically active 2'-hydroxycyclopentenone derivatives **6a**, **b**, using the above methods. The synthetic route is outlined in Scheme I.

First, the optically active unsaturated lactol **2** was converted, by condensation with ylide derived from 4-carboxybutyltriphenylphosphonium bromide and sodio methylsulfinylmethide, to the corresponding cyclopentenol derivative **3** [15]. Epoxydation with *t*-butyl hydroperoxide and vanadyl acetylacetonate [5, 16] gave selectively the α-epoxyalcohol **4a**, which was oxidized with Jones reagent to the corresponding epoxyketone **5**. Exposure of the latter to an ethereal solution of triethylamine furnished, *via* the kinetically formed enolate, the 2'-hydroxycyclopentenone **6a**.

The intermediate of the prostaglandin E_1-type synthon **6b** was prepared in a similar manner, starting with the catalytic reduction of the optically active α-epoxyalcohol **4a**, followed by the oxidation of the resulting saturated compound (**4b**) with Jones reagent. On treatment with triethylamine the epoxycyclopentanone **5b** underwent elimination to yield the 2'-hydroxycyclopentenone **6b**.

The steric course of the reaction steps and the assignment of configurations at the ring carbon atoms of the intermediates were based on NMR and CD studies.

The crucial step in the synthesis of the 2'-hydroxyenones **6** was the transition metal-catalyzed epoxidation of the cyclopentenol **3** by *t*-butyl hydroperoxide. Here, we could isolate only one product, and NMR analysis suggested that its configuration was the required all-*cis* (**4**).

Upon exposure of the epoxyketone **5** to a base, the (1'*R*,2'*R*)-stereoisomer of the 2'-hydroxycyclopentenone **6** was formed*. CD studies confirmed the structural assignments.

For the conversion of the 2'-hydroxycyclopentenones into the 3'-hydroxy analogues, we used essentially the same procedure as PIANCANTELLI and SCETTRI did. The cyclopentenone **6** was adsorbed on alumina (Brockmann grade III, basic) and, after standing overnight, the compound was eluted. The conversion proceeded with a high degree of stereochemical control, because from 2'(*R*)-hydroxy compounds we obtained optically pure 3'(*R*)-hydroxycyclopentenones (**1**) in excellent yields.

The absolute configurations of the chiral centers in compounds **1a**, **1b** and **6b**, deduced from the synthesis, were also supported by a comparsion of their CD spectra with those of natural pyrethrolone (**10**) [17] and another hydroxycyclopentenone derivative of very similar constitution and known absolute configuration (**11**) [18]. All these substances show a weaker (at 320—330 nm) and a stronger (at 220—230 nm) Cotton effect of opposite sign in the investigated spectral range (Table I).

The CD maxima can be assigned to the n-π^* (R-band) and π-π^* (K-band) electronic transitions, respectively, of the non-coplanar α,β-enone chromophore

* The reasonable assumption was made that the configuration at C-1' is retained in the course of this elimination (*cf.* Ref. [4]).

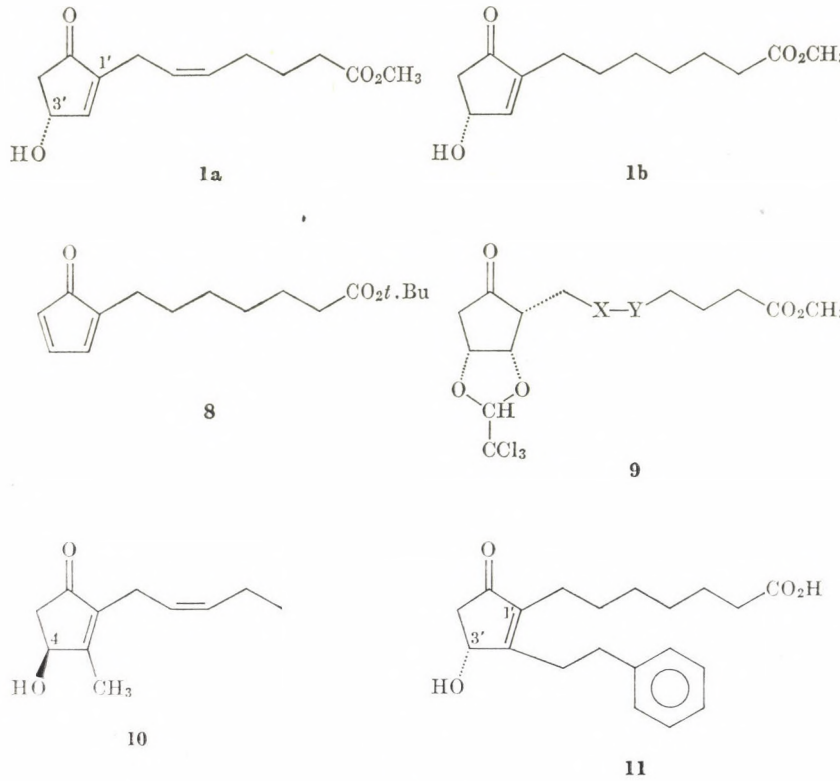

Scheme 2

in the cyclopentenone ring. The signs of the CD maxima in the spectra of compounds **1a**, **1b** and **1a** THP ether are the same as those of 3'(*R*)-**11** and opposite to those of 4(*S*)-**10** [18]. As the chirality of all these molecules is determined only by the configuration of the chiral center, the absolute configuration of **1a**, **1b** and **1a** THP ether must be 3'(*R*).

The 2-cyclopentenone ring can assume two chiral conformations which are mirror images of each other. These conformations are equally populated in the case of 2-cyclopentenone itself and its achiral derivatives. However, the position of the equilibrium between the two possible forms of enantiomeric ring conformation, *i.e.* the preferred absolute conformation of a chirally substituted (at C-4 and/or C-5) 2-cyclopentenone, is determined by the configuration of the chiral center(s). The correlation between the ring conformation (*i.e.* the chirality of the enone chromophore) and the signs of the R- and K-band Cotton effects [19] are shown in Fig. 1. (The ring is viewed from the direction of the axis of the O=C bond.)

Table I

Chiroptical properties of **1, 6b, 10, 11**

Compound	CD Cotton effects							
	λ nm	R-band $\Delta\varepsilon$	$[\Theta]$	λnm	K-band $\Delta\varepsilon$	Solvent $[\Theta]$	$\frac{\Delta\varepsilon\ K}{\Delta\varepsilon\ R}$	$[\alpha]_{D}$ (c = 1, MeOH)
1a	325	−2.68	− 8 840	225	+16.2	+53 500 ethanol	6.05	+11.5
	331.5	−1.55	− 5 120	221	+13.3	+43 900 cyclohexane	8.57	
1a (THP ether)	325	−2.30	− 7 600	225	+13.9	+45 900 cyclohexane--ethanol (1 : 1)	6.04	+20
1b	320	−3.10	−10 230	228	+17.5	+57 800 ethanol	5.65	+17.2
6b	330	+1.45	+ 4 780	224.5	−12.4	−40 800 ethanol	8.54	−48
	335	+2.32	+ 7 660	222.5	−14.7	−48 500 cyclohexane--ethanol (9 : 1)	6.33	
10	312	+3.91	+12 900	227	−19.1	−63 100 methanol	4.89	+12.5[a]
11	314	−4.64	−15 300	238	+14.3	+47 100 methanol	3.08	−30.1

[a] $c = 13.1$, EtOH [17].

R-band
Cotton ($\sim$ 320 nm)
K-band
effects ($\sim$ 230 nm)

10 (4*S*)	R_1=H,	R_2=OH,	R_3=H
11 (3'*R*)	R_1=OH,	R_2=H,	R_3=H
1a (3'*R*)	R_1=OH,	R_2=H,	R_3=H
1b (3'*R*)	R_1=OH,	R_2=H,	R_3=H
6b (1'*R*, 2'*R*)	R_1=H,	R_2=OH,	R_3=$(CH_2)_6COOCH_3$

Fig. 1

According to the above rule [19], the position of the hydroxyl group at C-4 and C-3' in the preferred conformation of the model substances **10** and**11**, as well as in **1a** and **1b**, should be *pseudoaxial*. Based on this assumption, also the configuration of **6b** can be determined. In this compound there is an -methoxycarbonyl-hexyl side chain at C-1' beside the hydroxyl group at C-2'. The two substituents are *cis* to each other. Supposing the alkyl group to be in *pseudoequatorial* position, like in natural prostaglandin E_1 [20] and in its stereoisomers [19], we may conclude that the hydroxyl group at C-2' is *pseudoaxial* in this molecule, too. The signs of the Cotton effects found in the CD spectrum of **6b** can thus be correlated with its 1'(*R*),2'(*R*) configuration. (The position of the hydroxyl group relative to the enone chromophore is opposite to that found in compounds **1a** and **1b**. The identical configurational sign of the chiral center C-2' in all the three compounds is due only to the rules of the CIP conventions. The opposite absolute conformation of the cyclopentenone ring in **1a** and **1b** on the one hand, and in **6b** on the other, is reflected in the opposite signs of the Cotton effects in **6b** and in **1a** and **1b**.)

It is of interest to note that the configurational correlation of substituted 2-cyclopentenone derivatives can only be based on a comparison of their CD (or ORD) spectra. The signs of the $[\alpha]_D$ values are unsuitable for this purpose. As can be seen from the data of Table I, 4(*S*)-**10** is dextrorotatory as well as 3'(*R*)-**1a** or 3'(*R*)-**1b**, although their CD spectra are nearly mirror images. The sign of the optical rotation at 589 nm is very sensitive to the relative intensity of the two ultraviolet Cotton effects of opposite sign. In the case of **10** and **11** the quotients of the values of the K-band and R-band CD maxima are smaller than 5, whereas in the spectra of **1a**, **1b**, **1a** THP ether and **6b** this value is larger than 5. The sign of the optical rotation at the sodium D line of the former sub-

stances is determined by the R-band Cotton effect, which is the weaker one, but relatively stronger than in the other compounds. In the CD spectra of the compounds investigated by us, however, the farther K-band Cotton effect is relatively more intense, and therefore the sign of the rotation at 589 nm is determined by its sign.

From the stereoselectivity of the rearrangement, the possibility of a reaction proceeding *via* dehydration-hydration steps can be ruled out. In the alternative mechanism involving addition-elimination of hydroxide ion, from the 2'(*R*)-compounds we should have got the corresponding 3'(*S*)-hydroxycyclopentenones *via* the (2'*S*,3'*S*)-dihydroxy intermediate. Therefore, we would like to propose a reaction path involving the attack of alumina virtually exclusively from the α-side of the 2'(*R*)-hydroxycyclopentenones (**6**), giving rise to an ester type intermediate (**7**) in the primary step, which then undergoes elimination to produce the thermodinamically more stable 3'(*R*)-hydroxy compound (**1**).*

We could furthermore demonstrate that the rearrangement with a cyclic ester mechanism might proceed stereospecifically. Here, the rearrangement was carried out by Stork's method elaborated also for the racemic 2'-hydroxycyclopentenones. This method consists in the formation of an acetal intermediate, which then undergoes elimination to give the 3'-hydroxy derivative. Treatment of the 2'(*R*)-hydroxycyclopentenone **6** with an ethereal solution of anhydrous chloral led to the corresponding hemiacetal (**9**), which upon addition of triethylamine, afforded the optically pure 3'(*R*)-hydroxycyclopentenone **1**. The yields were comparable with those obtained by the above method.

The successful synthesis of prostaglandin synthons greatly expands the synthetic utility of this simple and convenient method, for the rearrangement results not only in the conversion of a 2'-hydroxycyclopentenone to the corresponding 3'-hydroxy analogue, but also accomplishes this task in a highly stereoselective fashion.

Experimental

IR spectra were obtained with a Spectromom 2000 spectrometer. NMR spectra were recorded at 60 MHz, with TMS internal standard, on a Perkin Elmer R12 spectrometer. MS measurements were taken on a JEOL JGC-20K and JMS-01SG-2 combined GC/MS system. (Ionizing energy 74 eV, acc. voltage 10KV, ionizing current 200 A). Circular dichroism spectra were determined by means of a Jobin-Yvon dichrograph Model-III in quartz cells of 1 mm length at room temperature.

(-)-Methyl [7-(5-hydroxy-2-cyclopentenyl)]-5(*Z*)-heptenoate (3a)

This compound was prepared, according to the method reported for the racemic compound by GRIECO and REAP [15], from (-)-*cis*-2-oxybicyclo[3,3.0]oct-6-en-3-ol (**2**).
$[\alpha]_D^{25} -78°$ ($c = 1.1$, methanol).

* Very recently, a mechanism *via* enolate ion was proposed for this rearrangement: SCETRI, A., PIANCATELLI, G., D'AURIA, M., DAVID, G.: Tetrahedron, **35**, 135 (1979).

(-)-Methyl [7-(5-hydroxy-2,3-α-epoxycyclopentyl)]-5(*Z*)-heptenoate (4a)

To a stirred solution of 31.5 g (0.14 mole) of the cyclopentanol derivative **3a** and 0.4 g of vanadyl acetylacetonate in 285 ml dry benzene, there was added dropwise 30 g (0.33 mole) of freshly prepared *t*-butyl hydroperoxide [20], and the resulting solution was refluxed for 4 h. The solution was cooled to room temperature, filtered, the solvent evaporated and the residue was purified by filtration through a short columm packed with silica gel, using benzene-ethyl acetate 3 : 2 as eluent, to obtain 27.65 g (82%) of the epoxycyclopentanol **4a** [21]; $[\alpha]_D^{25}$ −8° (c = 1.0, methanol). (For the racemic compound, see Ref. [5]).

$C_{13}H_{20}O_4$ (240.3). Cald. C. 64.95; H 8.39. Found C 64.76; H. 8.22%.

IR(film): 3450, 1740, 1370, 1220, 1170, 1100, 1060 cm^{-1}.

NMR(CCl_4): δ 1.7—2.6 (11H, m), 3.5 (2H, d, J = 5 Hz), 3.7 (3H, s), 5.5 (2H, m).

MS: M^+ 240 (5), m/e 222 (6), 209 (7), 192 (8), 149 (16), 148 (14), 141 (20), 140 (90), 136 (12), 135 (40), 125 (41), 119 (25), 117 (20), 100 (19), 99 (14), 98 (28), 95 (25), 93 (28), 91 (36), 83 (40), 81 (100), 80 (100), 79 (90), 67 (70), 55 (50), 43, (48), 41 (90).

(-)-Methyl [7-(2,3-α-epoxy-5-oxo-cyclopentyl)]-5(*Z*)-heptenoate (5a)

A solution of 4.2 g (0.042 mole) of chromium trioxide and 3.6 ml of *conc.* sulfuric acid in 30 ml of water was added to a stirred and cooled solution of 5.35 g (0.023 mole) of the epoxycyclopentanol **4a** in 60 ml of acetone, during 3 h at −10°C. After stirring for further 1 h at −10°C, the reaction mixture was treated successively with 6 ml of isopropanol, 80 ml of saturated sodium carbonate solution (pH ~ 6), and then extracted three times with ether (400 ml). The combined ethereal extracts were washed with brine and dried over anhydrous magnesium sulfate. Removal of the solvent in vacuum afforded 4.25 g (80%) of the crude epoxyketone **5a***; $[\alpha]_D^{25}$ −63° (c = 1.0, methanol). (For the racemic compound, *cf.* Ref.[5].)

IR (film): 1740, 1340, 1220, 1160 cm^{-2}.

NMR (CCl_4): δ 1.7—2.5 (11H, m), 3.6 (5H, s), 5.5 (2H, m).

***R*-(-)-Methyl [7-(2-hydroxy-5-oxo-3-cyclopentenyl)]-5(*Z*)-heptenoate (6a)**

Triethylamine (3 g; 0.029 mole) was added dropwise to a stirred solution of the epoxyketone **5a** (2.75 g; 0.0115 mole) in 1 : 1 ether-methylene chloride (25 ml) and the reaction mixture was allowed to stand overnight. After evaporation of the solvent, ether (30 ml) was added and the resulting solution was succesively washed with 1N HCl, water, brine and then dried over anhydrous magnesium sulfate. Removal of the solvent in vacuum afforded 2.6 g (95%) of the crude 2'-hydroxycyclopentenone **6a**; $[\alpha]_D^{25}$ −40° (c = 1.0; methanol). A sample of this product was purified by filtration through silicic, acid using benzene-ethyl acetate (3 : 2) as eluent to obatin pure **6a**; $[\alpha]_D^{25}$ −43° (c = 1.0; methanol). (For the racemic compound, *cf.* Ref. [5].)

$C_{13}H_{18}O_4$ (238.27). Calcd. C 65.54; H 7.61. Found C 65.44; H 7.49%.

IR(film): 3400, 1740, 1710, 1370, 1220, 1170, 1120 1060 cm^{-1}.

NMR(CCl_4): δ 1.6—2.6 (9H, m), 3.6 (3H, s), 5 (1H, m), 5.5 (2H, m), 6.15 (1H, d, J = 7 Hz), 7.55 (1H, dd, J = 3 Hz).

MS: M^+ 238 (15), m/e 220 (18), 219 (100), 206 (25), 205 (15), 189 (27), 188 (40),160 (42), 146 (57), 140 (45), 133 (60), 123 (44), 119 (25), 107 (42), 97 (90), 81 (60), 80 (45), 67 (60), 55 (65), 41 (65).

***R*-(+)-Methyl [7-(3-hydroxy-5-oxo-cyclopentenyl)]-5(*Z*)-heptenoate (1a)**

Procedure A: To a stirred suspension of alumina (20 g; Brockmann grade I basic) and water (0.9 ml) there was added a solution of 1.2 g (5.05 moles) of the 2'-hydroxycyclopentenone **6a** in ether (20 ml) and the resulting mixture was stirred at room temperature overnight. The reaction mixture was transferred onto a column and eluted with ethyl acetate-methanol (10 : 1); the solution was then concentrated to yield 1.0 g (83%) of the 3'-hydroxycyclopentenone **1a**; $[\alpha]_D^{25}$ +12° (c = 1.0, methanol). *(Lit.* [9] $[\alpha]_D^{25}$ +11.2°; c = 1.92, methanol*)*.

* The epoxyketone decomposed thermally upon attempted distillation. Attempts at purifying the crude epoxyketone by chromatography resulted in an elimination reaction which gave a 1 : 1 mixture of the 2'-hydroxycyclopentenone **6** and 3'-hydroxycyclopentenone **1**.

IR(film): 3400, 1745, 1710, 1640, 1360, 1320, 1240, 1230, 1200, 1140, 1040 cm^{-1}.

NMR(CCl_4): δ 1.4—2.6 (8 H,m), 2.85 (2H, m), 3.7 (3H, s), 4.8 (1H, m), 5.45 (2H, t, $J = 5$ Hz), 7.05 (1H, m).

MS:M^+ 238 (7), *m/e* 220 (100), 208 (6), 207 (21), 192 (8), 189 (30), 188 (40), 161 (16), 160 (56), 147 (23), 146 (63), 133 (46), 131 (12), 121 (23), 119 (52), 118 (20), 117 (20), 107 (22), 105 (20), 95 (24), 94 (54), 91 (38), 85 (23) 79 (36), 67 (38), 55 (28), 43 (64), 41 (48).

Procedure B: Anhydrous chloral (1.2 g; 8.2 mmoles) was added dropvise to a stirred solution of the 2'-hydroxycyclopentenone **6a** (1.7 g; 7.2 mmoles) in dry ether (10 ml), and the reaction mixture was allowed to stand at room temperature for 16 h. Triethylamine (2 g; 19.4 mmoles) was added and the mixture was stirred at room temperature for 1 h. Evaporation of the solvent in vacuum left a yellow oil (3 g), which was chromatographed on silicic acid (benzene-ethyl acetate 3 :2) to give the 3'-hydroxycyclopentenone **1a** (1.2 g; 71%); $[\alpha]_D^{25}$ $+11.5°$ (= 1.0, methanol). The tetrahydropyranyı ether derivative of **1a** was prepared by the standard method; $[\alpha]_D^{25}$ $+20°$ ($c = 2.32$, methanol,.

IR (NaCl,: 1740, 1720, 1640, 1360, 1200, 1150, 1130, 1080, 1030, 990.

NMR(CCl_4,): δ 0.95 (3H, t, $J = 7$ Hz), 1.1—2.5 (14H, m), 2.8 (2H, m), 3.7 (3H, s), 3.9 (2H, t, $J = 6$ Hz), 4.7 (2H m) 5.4 (2H, m), 7.05 (1H, m).

(—)-Methyl [7-(-5-hydroxy-2.3-α-epoxycyclopentyl)]-heptanoate (4b)

The epoxycyclopentanol **4a** (10 g; 0.041 mole) was mixed with 0.5 g of 5% palladium-on-charcoal in 30 ml of methanol, and the mixture was stirred under a hydrogen atmosphere (1 atm) until the theoretical amount of hydrogen (1 l) had been absorbed. The catalyst was removed by filtration and the solvent evaporated in vacuum to give 9.8 g (98%) of the oil epoxycyclopentanol **4b**; $[\alpha]_D^{25}$ $-10°$ ($c = 1.0$, methanol). (For the racemic compound, *cf.* Ref. [5].)

$C_{13}H_{22}O_4$ (242.3). Calcd. C 64.43; H 9.15. Found C 64.27; H 9.22%.

IR (film): 3450, 1740, 1370, 1220, 1200, 1170, 1070 cm^{-1}.

NMR($CDCl_3$): δ 1.2—1.8 (10H, m), 1.9—2.5 (5H, m), 3.5 (2H, d, $J = 5$ Hz), 3.7 (3H, s), 3.8 (1H, m).

MS:M^+ 242 (<1), *m/e* 241 (5), 224 (6), 211 (10), 208 (8), 193 (18), 192 (22), 180 (14), 164 (20), 144 (9), 143 (34), 125 (12), 122 (10), 121 (20), 112 (11), 111 (32), 110 (14), 109 (28), 107 (12), 101 (16), 100 (100), 99 (26), 96 (38), 95 (34), 87 (48), 84 (38), 83 (40), 82 (32), 81 (42), 74 (40), 71 (20), 69 (42), 67 (42), 56 (42), 54 (62), 44 (46), 42 (72).

(—)-Methyl [7-(2,3-α-epoxy-5-oxo-cyclopentyl)]-heptanoate (5b)

The epoxycyclopentanol **4b** (5.3 g; 0.022 mole) was oxidized with standard Jones reagent (45 ml), as described for **4a** to obtain the epoxyketone **5b** in 75% yield;* $[\alpha]_D^{25}$ $-56°$ ($c = 1.0$; metahnol). (For the racemic compound, *cf.* Ref. [5].)

$C_{13}H_{20}O_4$ (240.3). Calcd. C 64.98; H 8.39. Found C 64.56; H 8.15%.

IR(film): 1740, 1370, 1240, 1200, 1170, 1000 cm^{-1}.

NMR($CDCl_3$): δ 1.3—1.8 (10H, m), 2.1—2.5 (3H, m), 2.58 (2H, s), 3.7 (3H, s), 3.8 (2H, s).

R-(—)-Methyl [7-(2-hydroxy-5-oxo-3-cyclopentyl)]-heptanoate (6b)

The epoxyketone **5b** and triethylamine were allowed to react according to the method described for **6a**, to obtain the 2'-hydroxycyclopentenone **6b** in 93% yield; $[\alpha]_D^{25}$ $-48°$ ($c = 1.0$, methanol). (For the racemic compound, *cf.* Ref. [5].)

$C_{13}H_{20}O_4$ (240.3). Calcd. C 64.97; H 8.39. Found C 64.72; H 8.28%.

IR(film): 3400, 1740, 1715, 1370, 1270, 1200, 1170, 1120, 1040 cm^{-1}.

NMR($CDCl_3$): δ 1.2—1.8 (10H, m), 2.1—2.5 (3H, m), 3.7 (3H, s), 3.95 (1H, m), 5.05 (1H, m), 6.15 (1H, d, $J = 6$ Hz), 7.52 (1H, dd, $J = 3$ Hz).

MS:M^+ 240 (10), *m/e* 222 (14), 209 (11), 208 (11), 190 (16), 162 (9), 143 (12), 121 (12), 111 (19), 109 (12), 107 (10), 98 (100), 95 (21), 84 (35), 80 (17), 67 (20), 55 (31), 41 (38).

* Other oxidation methods (*e.g.* with manganese dioxide, barium manganate) were unsuccessful.

R-(+)-Methyl [7-(3-hydroxy-5-oxo-cyclopentyl)]-heptanoate (1b)

The 2'-hydroxycyclopentenone **6b** was converted into the 3'-hydroxycyclopentenone derivative **1b** as described for **1a** (Procedure *A* or *B*) to obtain the product in 75% and 65% yield, respectively; $[\alpha]_D^{25}$ +17.2° (*c* = 1.0; ethanol); m.p. 62 °C (ethyl acetate). (*Lit.* [11] $[\alpha]_D^{24}$ +17.28°; *c* = 0.49, methanol; m.p. 60—61 °C).

IR(KBr): 3350, 1740, 1700, 1370, 1330, 1310, 1210, 1170, 1100, 1080 cm^{-1}.

NMR($CDCl_3$): δ 1.2—1.6 (8H, m), 2—2.8 (6H, m), 3.7 (3H, s), 3.9 (1H, m), 4.9 (1H, m), 7.15 (1H, m).

MS:M^+ 240 (6) *m/e* 224 (4), 223 (21), 222 (58), 209 (7), 208 (15), 191 (42), 190 (100), 172 (15), 163 (32), 162 (46), 149 (24), 137 (15), 136 (26), 135 (24), 122 (25), 111 (30), 110 (22), 97 (30), 96 (48), 95 (72), 94 (26), 93 (20), 87 (16), 79 (32), 67 (42), 55 (54), 43 (74), 41 (82), 39 (38).

The tetrahydropyranyl ether derivative of **1b** was prepared by the standard method; $[\alpha]_D^{25}$ +22° (*c* = 1.0; methanol).

IR(NaCl): 1735, 1715. 1640. 1360, 1200, 1150, 1130, 1080, 1030, 990.

NMR(CCl_4): δ 0.95 (3H, t, *J* = 7 Hz), 1.1—1.9 (14H, m), 2—2.4 (6H, m), 3.7 (3H, m), 3.9 (2H, t, *J* = 6 Hz), 4.7 (2H, m), 7.05 (1H, m).

MS:M^+ 324 (<1), *m/e* 240 (36), 239 (10), 235 (12), 223 (78), 222 (15), 191 (24), 163 (20), 149 (5), 85 (100), 84 (20), 79 (25), 41 (40).

*

The authors' thanks are due to Ilona BATTA, Pál KOLONITS, Tibor MÜLLER and Áron SZÖLLÖSI for the elemental and spectral analyses. Financial assistance from Chinoin Pharmaceutical and Chemical Works Ltd, Budapest, is gratefully acknowledged.

REFERENCES

[1] HESLINGA, L., van GORKOM, M., van DORP, D. A.: Rec. Trav. Chim., **87,** 1421 (1968)
[2] ALVAREZ, F. S., WREN, D., PRICE, A.: J. Am. Chem. Soc., **94,** 7823 (1972)
[3] FLOYD, M. B.: Synth. Commun., **4,** 317 (1974)
[4] STORK, G., KOWALSKI, C., GRACIA, G.: J. Am. Chem. Soc., **97,** 3258 (1975)
[5] KOBAYASHI, M., KUROZUMI, S., TORN, T., ISHIMOTO, S.: Chem. Lett. **1976,** 1341
[6] PIANCATELLI, G., SCETTRI, A.: Tetrahedron Lett., **1977,** 1131
[7] SIH, Ch. J., HEATHER, J. B., PERUZZOTTI, G. P., PRICE, Ph., SOOD, R., LEE, L. F. H.: J. Am. Chem. Soc., **95,** 1676 (1973)
[8] HEATHER, J. B., SOOD, R., PRICE, Ph., PERUZZOTTI, G. P., LEE, S. S., LEE, L. F. H., SIH, Ch. J.: Tetrahedron Lett., **1973,** 2313
[9] GRUBER, L., TÖMÖSKÖZI, I., MAJOR, E., KOVÁCS, G.: Tetrahedron Lett., **1974,** 3729
[10] SIH, Ch. J., SALOMON, R. G., PRICE, Ph., SOOD, R., PERUZZOTTI, G.: J. Am. Chem. Soc., **97,** 857 (1975)
[11] SIH, Ch. J., HEATHER, J. B., SOOD, R., PRICE, Ph., PERUZZOTTI, G., LEE, L. F. H., LEE, S. S.: J. Am. Chem. Soc., **97,** 865 (1975)
[12] BRUHN, M., BROWN, C. M., COLLINS, P. W., PALMER, J. R., DEJANI, E. Z., PAPPO, R.: Tetrahedron Lett., **1976,** 235
[13] YAMADA, S., KITAMOTO, M., TERASHIMA, S.: Tetrahedron Lett., **1976,** 3165
[14] PIANCATELLI, G., SCETTRI, A.: Synthesis, **1977,** 116
[15] GRIECO, P. A., REAP, J. J.: J. Org. Chem., **38,** 3413 (1973)
[16] CHEN, D. M., RADLEY, K., REEVES, L. W.: J. Am. Chem. Soc., **96,** 6136 (1973)
[17] ELLIOT, M.: J. Chem. Soc., **1964,** 5225
[18] MIGANO, M., DORN, C. R.: J. Am. Chem. Soc., **95,** 2664 (1973)
[19] SNATZKE, G., SNATZKE, F.: in "Fundamental Aspects and Recent Developments in Optical Rotatory Dispersion and Circular Dichroism" (Eds) CIARDELLI, F. and SALVADORI, P., p. 109, Heyden and Son, London 1973
[20] DE CLERCQ, P., SAMSON, M., TAVERNIER, D., VAN HARER, D., VANDEWALLE, M.: J. Org. Chem., **42,** 3140 (1977)
[21] BARTLETT, P. D., MCBRIDE, J. M.: J. Am. Chem. Soc., **87,** 1727 (1965)

Lajos NOVÁK
János ROHÁLY
Csaba SZÁNTAY
} H-1521 Budapest, Gellért tér 4
Márton KAJTÁR, H-1443 Budapest, Eötvös Loránd Tudományegyetem

Acta Chimica Academiae Scientiarum Hungaricae, Tomus 102 (1), pp. 101—102 (1979)

THE FORMATION OF ELECTRON TRANSFER PRODUCTS IN THE REACTION OF TRIPHENYLMETHYL CHLORIDE WITH SODIUM METHOXIDE IN 2,2-DIMETHOXYPROPANE

(PRELIMINARY NOTE)

Gy. SIMIG and K. LEMPERT

(Research Group for Alkaloid Chemistry, Hungarian Academy of Sciences, Budapest)

Received February 27, 1979
Accepted for publication March 5, 1979

In continuation of our studies into anomalous reactions of halogen derivatives with nulceophiles [1], triphenylmethyl chloride (**1a**) was allowed to react with sodium methoxide in 2,2-dimethoxypropane to obtain, in addition to the normal methanolysis (**1b**) and hydrolysis products (**1c**), the *cine* product **2** (probably a mixture of the *o*- and *p*-isomers), the reduced product **1d**, and dityrityl peroxide (DTPO) [Experiments 1 and 2, Table I] which, with the exception of compound **2**, were identified by comparison (TLC, IR) with

$Ph_3C—X$ $\quad$ $Ph_2CH—C_6H_4—OMe$ $\quad$ $p\text{-}Ph_3C—C_6H_4—CHPh_2$

1a: X = Cl $\quad$ **2** $\quad$ **3**
1b: X = OMe
1c: X = OH
1d: X = H

authentic samples. Compound **2**, a reluctantly crystallizing oily product, was characterized by its ^1H NMR [$CDCl_3$; δ 3.75s (MeO), 5.50s ($Ar_3C—H$), 6.6—7.45m (14H, ArH's)] and IR spectra [KBr; 840, 810 and 790 cm^{-1}; the spectra of compounds **1b** and **1d** have no bands in this region]. The fully aromatic dimer **3** [2] was not obtained in any of the experiments.

In Experiments 5—8, run in the presence of nitro-or *m*-dinitrobenzene, the yields of compound **1d** and of DTPO were found to decrease significantly, whereas the yield of compound **1b** increased which, together with the structures of these products, appears to indicate that, in contrast to compound **1b**, compound **1d** and DTPO are formed *via* intermediate radical anions and radicals, as shown in Scheme 1. This appears to be the first case of the formation, induced by sodium methoxide (or, in fact, by any similar, hardly oxidizable nucleophile), of radical anions from an arylmethyl halide containing no nitro group in *p*-position (*cf.* Ref. [4]).

$$R-Hlg + CH_3O^{\ominus} \rightarrow (R-Hlg)^{\ominus\bullet} + CH_3O\cdot \rightarrow R\cdot + Hlg^{\ominus} + CH_3O\cdot$$

$$R\cdot + CH_3O^{\ominus} \rightarrow R-H + \cdot CH_2O^{\ominus}$$

$$R\cdot + CH_3O^{\ominus} \rightarrow R:^{\ominus} + CH_3O\cdot \qquad R:^{\ominus} \xrightarrow{\text{work-up}} R-H$$

$$R-Hlg + \cdot CH_2O^{\ominus} \rightarrow (R-Hlg)^{\ominus\bullet} + CH_2O$$

$$R\cdot + CH_3OY \rightarrow R-H + \cdot CH_2OY$$

$$R\cdot + O_2 \rightarrow R-O-O\cdot \xrightarrow{+R\cdot} R-O-O-R$$

$R = (C_6H_5)_3C-$ $\qquad$ $Y = -C(CH_3)_2OCH_3$

Scheme 1. Formation of triphenylmethane (R—H = **1d**) and DTPO (= R—O—O—R) *via* the radical anion–radical mechanism *(cf.* Ref. [3])

Table I

Reaction of triphenylmethyl chloride (**1a**) *with sodium methoxide in 2,2-dimethoxypropane (DMP)*

Run No.[a]	Products and yields (isolated), %					Total yield, %
	1b	**1c**	**2**	**1d**	DTPO	
1[b]	27.8	15.2	[d]	20.5	>2	65.5
2[b]	29.7	15.4	10.2	16.7	5.4	77.4
3[c]	32.9	17.1	7.1	21.0	—[e]	78.1
4[c]	32.6	18.0	5.5	19.4	—[e]	75.5
5[b, f]	37.5	8.6	≤8[g]	11.4	—[e]	57.5[h]
6[b, f]	37.3	20.1	<2.4[g]	11.5	—[e]	71.3
7[b, i]	43.4	24.8	<4[g]	15.0	—[e]	83.2[h]
8[b, j]	44.8	12.2	<1	4.3	—[e]	62.3

[a] Mixtures of **1a** (1.0 g), NaOMe (4 equivalents) and DMP were refluxed for 1 h and worked up by fractional crystallization (DTPO) and preparative TLC (**1b—d, 2**)
[b] In air
[c] Under nitrogen
[d] No attempt was made to isolate compound **2** in Run 1
[e] Not formed in isolable amounts
[f] In the presence of 1 mole of $PhNO_2$ for 1 mole of compound **1a**
[g] Since compound **2** and $PhNO_2$ had almost identical R_f values in the system used, the latter was removed by steam distillation
[h] Yield of compound **2** not included
[i] In the presence of **2** moles of $PhNO_2$ for 1 mole of compound **1a**
[j] In the presence of 1 mole of *m*-dinitrobenzene for 1 mole of compound **1a**; considerable amounts of tarry products were formed

REFERENCES

[1] SIMIG, GY., LEMPERT, K., VÁLI, ZS., TÓTH, G., TAMÁS, J.: Tetrahedron, **34,** 2371 (1978) and references cited therein
[2] ULLMANN, F., BORSUM, W.: Ber. dtsch. chem. Ges., **35,** 2877 (1902)
[3] ZOLTEWICZ, J. A., OESTREICH, T. M., SALE, A. A.: J. Am. Chem. Soc., **97,** 5889 (1975)
[4] KORNBLUM, N.: Angew. Chem., **87,** 797 (1975)

Gyula SIMIG
Károly LEMPERT } H-1111 Budapest, Gellért tér 4.

RECENSIONES

Topics in Current Chemistry, Vol. 73

Organic Chemistry, 271 pp.

Springer Verlag, Berlin, Heidelberg, New York 1978

The series contains comprehensive papers offering a survey of the present state and future trends in modern chemical research. The authors of the individual papers are active workers in the special fields discussed. The present volume contains four independent papers dealing with organic chemistry.

W. S. SHELDRICK: *Stereochemistry of Penta- and Hexacoordinate Phosphorus Derivatives.* The largest development in the stereochemistry of phosphorus compounds has been achieved in the field of penta- and hexacoordinated derivatives. These compounds could hardly be examined earlier owing to their instability and volatility. In the last decade, however, the availability of stable phosphoranes containing one or two rings, as well as the development of electron diffraction and X-ray diffraction techniques have brought about several new results in structure elucidation. In this paper, the stereochemical examination of penta- and hexacoordinated phosphorus derivatives effected by diffraction methods is discussed. After a discussion of the configuration of pentacoordinated phosphorus derivatives and the theory of bonding, the paper deals with acyclic, monocyclic, spirobicyclic, condensed cyclic and tricyclic phosphorus derivatives and some hexacoordinated phosphorus compounds — ionic and non-ionic complexes — and the results obtained up to 1976 in the determination of their structures are described. A critical survey of the ample literature is completed by tabular summary of the data.

P. CAUBÈRE: *Complex Bases and Complex Reducing Agents. New Tools in Organic Synthesis.* In the paper consisting of two chapters the author discusses his own results. The starting point of the examinations has been the observation that certain aromatic nucleophilic substitution reactions cannot be achieved with sodium amide acting as a base in a given solvent and with a given nucleophilc agent, yet the reaction takes place readily on the addition of certain activating agents (alcoholates, enolates). Results of several experiments have confirmed that in these reactions the real active agent is the "complex base" formed from sodium amide and the activating agent. The reactions evoked by means of the complex bases, the role of the nature of the activating agent, the solvent and the optimum ratio of the activating agent and sodium amide are discussed in detail.

In the second chapter, the principle of activation of sodium amide is extended to the case of reductions effected with sodium hydride. Although the detailes of the general rule deduced from these studies await yet elucidation, a large number of the practical examples given provide useful information for the synthetic organic chemists inspiring further application of the method.

J. C. JUTZ: *Aromatic and Heteroaromatic Compounds by Electrocyclic Ring-Closure with Elimination.* In the synthesis of oligo- and polycyclic aromatic and heteroaromatic compounds, increasingly widespread application is found by the method of electrocyclic ring-closure, induced thermally, accompanied by elimination. The prototype of these reactions is the Ziegler-Hafner azulene synthesis, where trialkylamine containing a fulvenoid decapentaene structural part yields azulene on heating by electrocyclic ring-closure and the split-off of dialkylamine. In the development of oligo- and polycyclic aromatic systems, a cyclization of hexatriene—cyclohexadiene type takes place. The most various 1-dialkylamino-1,3,5-hexatrienes can be converted thermally into benzene derivatives with the release of dialkylamine. The field of application of this cyclization reaction has been greatly extended by realizing that 1-dialkylaminohexatrienes, in which the double bond is formally the part of an aromatic or heteroaromatic system, can also be readily subjected to cyclization. *i.e.* ring annelation can be achieved.

Further possibilities are provided by the fact that nitrogen atoms can substitute one or two carbon atoms in the chain of 1-dialkylaminohexatrienes, hence six-membered heteroaromatic systems can be obtained in this way. The paper gives a systematic and detailed survey of the theory of the reaction and its applications.

H. SCHWARZ: *Some Newer Aspects of Mass Spectrometric Ortho Effects.* The *ortho* effect was applied earlier only in diagnostic work in the mass spectrometric structure elucidation of organic compounds, for the identification of 1,2-disubstituted *cis* structural parts. In the present paper the author reports on the most recent examinations aiming at the elucidation of the mechanism of the *ortho* effect and related secondary conversions. The short, concise paper containing a large literature provides valuable help for researchers dealing with mass spectrometry.

J. CSÁSZÁR

Topics in Current Chemistry, Vol. 74

Organic Coumponds, Syntheses, Stereochemistry, Reactivity 133 pp.

Springer Verlag, Berlin, Heidelberg, New York 1978

The present book of the series (*cf.* previous book review) contains four comprehensive papers dealing with organic chemistry.

F. VÖGTE, G. HOHNER: *Stereochemistry of Multibridged, Multilayered and Multistepped Aromatic Compounds. Transannular and Electronic Effects.* In connection with the structure elucidation of cyclophanes (aromatic rings connected by two bridges), analogues with particular structures have been recently prepared: (*a*) aromatic rings linked by three or more bridges (multibridged phanes); (*b*) coupling of several aromatic rings by means of bridges characteristic of phanes so as to make the aromatic rings to form layers above each other (multilayered phanes); (*c*) connection of aromatic rings by means of bridges ensuring stepwise arrangement of the aromatic rings above each other in the systems developed (multistepped phanes). These rigid, sometimes strongly stressed systems are particularly suitable for studies of intramolecular steric and electronic interactions. The present paper provides a short, concise summary of these special phanes, their spectroscopic studies and their geometry, on the basis of the most recent literature data, that is, papers published between 1960 and 1977.

E. S. LEWIS: *Isotope Effects in Hydrogen Atom Transfer Reactions.* The paper deals with hydrogen atom transfer reactions which can be characterized by the general formula $A\cdot + H{:}X \rightarrow A{:}H + X\cdot$, where $A\cdot$ or $X\cdot$ or both are organic free radicals. Hydrogen atom transfer is frequently occurring in organic reactions taking place through free radicals. Since this means the least complicated substitution reaction for the organic chemist, it has been studied in detail, yet several questions have remained unsolved. Studies on the isotope effect in hydrogen atom transfer reactions can be accomplished experimentally and the transition states of the reactions do not give rise to special difficulties in the investigations either; these can also be studied. In a series of systems, which can be characterized by a constant intrinsic barrier, any of the three values, intrinsic barrier, isotope effect and exothermicity, can be calculated in the knowledge of the two other data by the modified Marcus equation, or by means of the hyperbolic correlation not deduced theoretically, but easier to apply. The paper reports on these investigations.

R. J. LEMIRE, P. G. SEARS: *N-Methylacetamide as a Solvent.* Special attention has been paid to the *N*-methylamides of lower carboxylic acids since 1951, when their very high dielectric constants were published. Since then these compounds have gained importance as new, non-aqueous solvents, as they can be purified relatively easily and their properties can well be combined. The member of the group studied in greatest detail is *N*-methylacetamide (NMA). The author collected the experimental results and classified them. The main chapters of the paper give a good picture of the thorough work of the authors: Synthesis and purification; Structure of NMA in the gaseous phase and in solid state; Physical properties and structure of liquid NMA; Electrochemistry (*e.g.*, ion transport, behaviour of electrodes in NMA, *etc.*); Solutions (solubility of electrolytes and non-electrolytes, cryoscopic measurements in NMA); Solvatation; Reactions in NMA. The chapters contain the large majority of literature data in addition to ample references, thus the paper is interesting not only for those already employing NMA and requiring a summary of its properties, but for all who want to find a non-aqueous solvent with excellent and well-known properties.

J. GASTEIGER, C. JOCHUM: *EROS, A Computer Program for Generating Sequences of Reactions*. For long, the application of computers in chemistry was limited to numerical calculations. Recently, the possibilities of this modern technique have also been applied for the solution of chemical problems, such as the design of syntheses, determination of correlation between structure and acitivity and the elucidation of molecular structure from spectroscopic data. These were characteristically such problems, which had been thought to be soluble only by the human mind; the most interesting and most colourful is the design of synthesis paths for organic compounds. In the computer treatment of chemical reactions, mainly the illustration of the molecules and the reactions was assumed to be required. Since illustration of the molecules is more or less a technical task, the central problem was the illustration of chemical reactions. In the systems developed earlier, the synthetic reactions were obtained by combining those known before, thus these systems can be regarded as a library in a computer. The authors with a larger team started the development of a computer program suitable for the design of syntheses in 1972. The molecules are represented by BE matrices (*b*ond and *e*lectron matrices), the reactions are represented by R-matrices. Since the R matrix can also be formed entirely formally, this method is suitable for the production of any possible reaction, irrespective of the fact whether siuch a reaction is really known or is perfectly new. First the CICLOPS (*C*omputers *i*n *C*hemistry, *L*ogic *O*riented *P*lanning of *S*yntheses) program was developed for the design of syntheses and, on the basis of the favourable experience obtained with it, the EROS (*E*laboration of *R*eactions for *O*rganic *S*ynthesis), a new synthesis-planning program has been evolved. The authors shortly review the method and present some illustrative examples of its applicability.

At the end of the book, the Author Index of Vols 26—74 of the series is given.

J. CSÁSZÁR

Recent Results in Chemistry, Vol. 41 (In Hungarian); Editor Béla CSÁKVÁRI, Akadémiai Kiadó, Budapest 1978

P. MÓRITZ: *Calculation-technical Methods for the Examination of Phase and Chemical Equilibria*

220 pages, 376 references

The summary of the content of this book is not a formality in this case because the author has dealt with a much broader field here than what one would expect from the title. This book contains not only useful calculation methods, but also valuable literature surveys, important discussions, good establishments and remarks of the physicochemical characteristics of gases and mono- and multicomponent liquids.

Chapter *1* establishes the fundamentals of the theory of corresponding states and a discussion of efforts making it both more exact and more general. In the next chapter the author reviews the most important approximate methods for the calculation of characteristics which determine the critical states of liquids. These methods make use of the number of carbon atoms in a homologous series of compounds or of certain physical quantities (*e.g.* polarizab'lity, molar refraction, *etc.*). Next, some simple methods suggested by the author are introduced. The topic of Chapter *3* is the calculation of the vapor pressure of liquids. Here is given a very good summary of the equations in the literature for the calculation of this quantity. Also discussed are two simpler methode suggested by the author. One of these methods is based on the use of atomic and bond increments, while the other is based on the atomic group increments. In the next chapter, where the examinations of the gaseous state are reviewed, tabulated summarizations give a very good survey of the gas equations suggested in the literature. Very remarkable are the author's optimalizations of the constants of the van der Waals equation which result in somewhat different but better constants than the well known ones. Also important is that new state parameters are suggested with these new constants, which behave like the critical state parameters of gases, allowing higher accuracy to be obtained. The next chapter deals with the calculation of surface tension and a new calculation method is described, using atomic and bond increments given by the author. The connection of surface tension to viscosity is also examined.

Chapter *6* deals with the calculation of some characteristics of multicomponent liquid mixtures and a computer program is described to determine the equation of the correct boiling point curves. This program finds the optimum values of six constants. The problems discussed here are important in chemical engineering.

The topic of the next chapter is the calculation of the equilibrium conversions from the equilibrium constants. A good calculation method is described, the essence of which is that the equilibrium constants are rewritten with the molar ratios of the reactants and products and the equations obtained are reduced to zero and minimized.

The last chapter deals with the methodology of the determination of phenomenological relations. A computer program is given for the examination of the homogeneityof measured data and for the determination of the largest homogeneous sub-set. Another program is written on the basis of a new method for the examination of the significance and for the detection of systematic trends in the column and rows of tabulated experimental data. Next, there is a very good description on the choice of a function best approaching the measured data. A method is introduced to approach the measured data by multivariable nonlinear functions. Also a computer program is written for this purpose which finds the optimum values of the parameters of a function. Another calculation method is suggested to determine the equation of a family of curves depending on parameters. This method, in essence, deals with the parameters on two levels: as common and group parameters. Finally, methods are given to optimalize physico-chemical models, which is mathematically the determination of the extreme value of scalar vector functions. The author's simple procedure, which is a modified simplex method, has the advantages of the known ones (grid, gradient and search) and can be used to solve numerous problems. The flow chart and the text of the program are given and also the results obtained on some model functions.

This book is a very well written, outstanding work. All the literature surveys are clear and concise, and contain important additional comments in the discussed details. The presentation of the chemical and mathematical problems are very understandable, and their treatment and solution can be easily followed. The author's own results, which are remarkable, both from practical and theoretical points of view, are well incorporated into this book. The calculation-technical methods discussed in the last chapter and the computer programs will be very useful tools to solve various problems. Although the author raises and solves numerous problems from the point of view of chemical engineering practice, I am convinced that the subjects dealt with in this book can also be successfully applied in other fields of chemistry.

J. Tóth and P. Érdi: *The Models, Problems and Applications of Formal Reaction Kinetics*

125 pages, 230 references

Formal reaction kinetics, the topic of this book, is a discipline of reaction kinetics which does not deal with microscopic mechanisms of chemical reactions, even when one of the models is applied in reaction kinetics. On the other hand, formal reaction kinetics — even in the consequences of its abstraction — is not only an applicable mathematical theory, but also an applied one in other areas of sciences in addition to chemistry, *e.g.* in biology. One of the main aims of the authors in writing this book was to introduce and discuss the possible models of formal reaction kinetics and their applicability in various fields of sciences.

In Chapter *1* of the book the authors define the basic concepts with formulations of formal reaction kinetics and they introduce the applicability of these on a "composed chemical reaction" of the Volterra—Lehotka type. After giving the definitions, they make various supplements and restrictions in order to obtain the models of the composed chemical reaction. Eight such models are identified in this book depending on the nature of changes and on the choice of time and space of events as continuous or discrete.

The topic of Chapter *2* is the discussion of the stochastic models of the composed chemical reaction satisfying the generalized law of mass action. The most detailed treatment is given on the model of continuous time and discrete space of events, which is justified by the fact that this model is the most realistic, the best established and also the most frequently used one among the stochastic models. Then the Kolmogorov differential equations referring to the transition probability and absolute distribution functions of the Markov process are introduced and there is also a discussion of the methods used to solve these equations. This survey is more systematic and more complete than in the literature.

In Chapter 3 the authors deal with the deterministic models. The majority of this section is given to the Wilhelmy—Guldberg—Waage model or, as it is defined in the formal reaction kinetics, to the deterministic model of continuous time and continuous space of events. Beside the detailed treatment of this model there are also some mathematically important results here, a brief section is presented on enzyme kinetics and on the methods of concluding the elementary reactions from concentrations *versus* time curves.

The topic of the next chapter is the comparison of the various models. In the last chapter there is a short survey on the application of the formal reaction kinetics. The chemical applications (enzyme kinetics, oscillation reactions, *etc.*) and the physical applications are mentioned only very briefly. The main emphasis of this section is given to the applicabilities for constructing models for population dynamics, for the propagation of epidemics and for microbiological and genetical processes.

In this book the authors discuss the models of the formal reaction kinetics with their treatments on a mathematically well established basis. They introduce not only the past changes in this field, but also point to recent ones and to vivid problems. They make valuable contributions, *e.g.* they managed to demonstrate that the model of continuous time and discrete space of events for the composed chemical reaction fulfilling the generalized law on mass action is a generalized Markov process and that most of the processes applied in the chemistry and biology are its special cases. The book contains 230 citations, but it is a pity that only one third of those belongs to chemistry and biochemistry, which is too little for a book written for this series. I think that a more striking emphasis of the chemical aspects and that examples of the sometimes too abstract discussions would have been advantageous for this book.

F. GAISER

INDEX

ANALYTICAL CHEMISTRY

PHYSICAL AND INORGANIC CHEMISTRY

ORGANIC CHEMISTRY

Printed in Hungary

A kiadásért felel az Akadémiai Kiadó igazgatója. Műszaki szerkesztő: Zacsik Annamária

A kézirat nyomdába érkezett: 1979. III. 28. — Terjedelem: 9,80 (A/5) ív, 57 ábra

79.7007 Akadémiai Nyomda, Budapest — Felelős vezető: Bernát György

ACTA CHIMICA

ТОМ 102—ВЫП. 1

РЕЗЮМЕ

Гидродехлорирование альдрина, диельдрина и токсафена

Р. Б. ЛАПИЕРРЕ, Э. БИРОН, Л. ЛУЦИ, Б. Л. КРАНИХ, А. Х. БЕИС

Реакция гидродехлорирования альдрина, его эпоксида — диельдрина и токсафена была исследована в растворе $C_2H_5OH-NaOH$ при 50 барах H_2, 130°C и, используя никелевый катализатор на Кизельгуре с содержанием никеля 61%. Стехиометрия этих тяжелых мультифункциональных частиц следует правилам, определенным для простых образцов с низким молекулярным весом. Типичными являются синхронные (т. е. многоступенчатые) реакции, в которых промежуточные продукты не десорбируются. Так например, для альдрина:

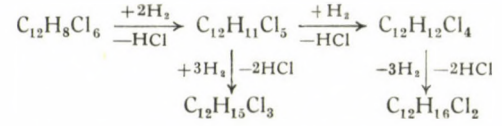

Вначале гидрируется олефиновая группа в молекуле (эпоксид не затрагивается при этих условиях) и одновременно с этим происходит выделение высоко активного геминального дихлорида. Молекула затем реадсорбируется и на одной ступени теряет свои олефиновые атомы хлора и гидрируется по олефиновой связи. Последними, наименее реактивными хлорами, которые выделяются, являются алифатические хлоры. Вследствие их очень низной реактивности, диельдрин, альдрин и токсафен, не легко полностью лишить соответствующего углеводородного скелета.

Источники погрешностей количественного определения твердых кристаллических минералов с помощью ИК спектроскопии

Й. ХЛАВАИ и Я. ИНЦЕДИ

Были изучены возможности количественного определения с помощью ИК спектроскопического и рентгено-диффракционного методов четырех минералов различного происхождения и физических свойств каолиниз (цетлитца), сеги бумажный каолин из Сега, песок из Уркута, шведский земляной ортоклас). Изменение размеров зерен образцов и организованности кристаллического состояния было достигнуто с помощью измода в вибрационной паровой мельнице.

Были определены коррелирующие зависимости количественных параметров, определенных из ИК спектров и рентгенограмм, от размера зерен помола.

Исследование свойств поверхностей раздела в системах петропорфиринов с водой и бензолом

Й. ЛАКАТОШ-САБО

Рассматриваются поверхностные натяжения и способность к образованию пленок в системах углеводородных фракций богатых порфирином, выделенных из характерных отечественных нефтей, с водой и бензолом. Были сделаны попытки определения зависимости этих величин от содержания порфирина, азота, гетероатомов и отношения C/H во фракциях. В качестве сравниваемой модели использовали *мезо*-тетрафенилпорфирин, а

также его ванадиевые и никелевые комплексы. Было установлено, что соединения природных углеводородов с большим содержанием гетероатома уменьшают поверхностное натяжение, а способность и образованию пленок может быть приписана присутствию ненасыщенных углеводородов. Изменение обоих параметров поверхностей раздела совпадает с изменением содержания порфирина в отдельных углеводородных фракциях.

Исследование электронного строения смешанных комплексов железо-диоксим с помощью спектроскопии Мёссбауэра

Л. КОРЕЦ, А. А. САГИЕР, Ч. ВАРХЕИ и К. БУРГЕР

С помощью параметров Мёссбауэра смешанных комплексов железа-диоксима с однокислыми азотными основаниями, а также, исходя из данных, рассчитанных из них с помощью метода МО, было обсуждено влияние отдельных лигандов на электронное строение центрального атома железа (на заселение σ и π орбит и эффективный заряд).

Производные аминофталазинона, V

Синтез 4-гидразино-1(2*H*)-фталазинонов

К. КЁРМЕНДИ, К. А. ЮХАС и Е. ЛЕМБЕРКОВИЧ

3-Оксо-1-иминоизоиндолин (**3**), реагируя с монозамещенными алкилгидразинами дает производные аминофталазинона (**5**), замещенные в положении N(2), структура которых была подтверждена препаративным путем. Замещение при N(2) экранирует обмен аминогруппы на гидразиновую группу, поэтому путь **3** → **5** → **6** является непригодным для продолжения синтеза Кёхлера [1]. Соединение **3** и его алкил-дизамещенные и циклические алкиленгидразины (напр., *N*-аминопиперидин) образуют гидразиноизоиндолиноны (**9**) с удовлетворительным выходом, которые могут быть превращены с помощью гидразингидрата, метилгидразина и 2-гидроксиэтилгидразина в производные гидразинофталазинона со структурой **10** и **11**, соответственно. Аминофталазинон (**4**) и полученные гидразинофталазиноны (**10**) метилируются в положении N(2) с помощью диметилсульфата.

Синтез солей изоглаван-4-(1-пиридиния)

В. САБО, Й. БОРБЕЙ и Е. АНТАЛ

Обработка *транс*(α)-и *цис*(β)-4-гидроксиизофлаванов (**1a**, **1b**) хлористым тозилом в пиридине приводит — вместо ожидаемых тозилатов — к одинаковому изофлаван-4-(1-пиридиний)-тозилату (**IVa**). Анион соединения **IVa** обменивается на другие анионы. Восстановительные методы превращают **IVa** в изофлаван (**VII**) и 4-[1-(1,4-дигидро)-пиридил]-изофлаван (**VIII**); в то время как в щелочных средах он может быть превращен в изофлав-3-ен (**II**).

Новый аномальный рацемат

Л. ТЁКЕ, М. АЧ, Э. ФОГАШИ, Ф. ФЕЙГ, Ш. ГАЛ и Я. СТАТИС

В ходе исследований разделения биологически активного рацемата 6-фенил-2,3,5,6 тетрагидро-имидазо[2,1-*b*]тиазола наблюдались необычные расхождения как в твердом состоянии, так и в растворе между свойствами рацемата (или чистого антипода) и рацемата с составом антиподов 3 : 1.

Было найдено, что при таком соотношении антиподов образуется относительно стабильный молекулярный комплекс, названный аномальным рацематом.

Ароматизация кольца А в 3β-асетокси-5α-холестан-6-оне

М. С. АЗМАД и Н. З. ХАН

Заглавное соединение (1) при кипячении его с Br_2—HBr в смеси эфир-уксусная кислота претерпевает перегруппировку, давая 1-метил-19-норхолеста-1,3,5(10)-триен-6-он (2), вместе с двумя другими изолируемыми соединениями (3) и (4). Идентифицирование этих соединений было произведено на основе их спектральных свойств и сравнением со стандартными образцами известного строения. Приводится возможный механизм превращения (1) → (2).

Исследование гелей поливинилового спирта с водородными связями,

Исследование растворимости

Й. ДЬЁРДИ ЭДЕЛЕНИ, М. НАДЬ и Й. БОГНАР

Термически нестабильные гидрогели поливинилового спирта с различной структурой были приготовлены, используя диоксан в качестве высадителя, который был заменен на воду после того, как произошло гелеобразование. Измерения растворимости производились при температурах между 298—353°К. Расчеты, основанные на экспериментальных результатах позволяют различать два типа точек прилипания в гелях с различными энергиями.

Исходя из изменений в структуре геля за счет постепенного разрыва точек прилипания с помощью замены воды на смеси *н*-пропанола с водой, могут быть получены дополнительные сведения. Увеличивая концентрацию *н*-пропанола, увеличивается растворимость геля и различия между двумя характерными энергиями уменьшаются. Эти заключения подтверждаются результатами термомеханических измерений.

Получение гомогенных тензидов

П. САЛЛАИ, Й. МОРГОШ, Л. ФАРКАШ, И. РУСНАК и Б. БАРТА

Были получены шесть первых членов гомологического ряда эфира додецилового спирта с полигликолем с газовохроматографической чистотой. Было установлено, что с помощью синтеза Виллиамсона желаемые соединения получаются с лучшим выходом и чистотой, чем исходя из тозилового эфира додецилового спирта. Для синтеза использовался полиэтиленгликоль с максимальным числом гликольных единиц, равным трем.

Замечания к механизму перегруппировки производных 2'-гидроксициклопентанонов, приводящей к 3'-гидроксианалогам

Стереоконтролируемый синтез простагаландин синтонов

Л. НОВАК, Й. РОХАИ, М. КАЙТАР и Ч. САНТАИ

Описываются простые и эффективные пути приготовления 3'(*R*)-гидроксициклопентанонов, являющихся промежуточными продуктами в синтезе простагландинов E_1 и E_2. Также обсуждается механизм перегруппировки 2'-гидроксициклопентанонов, приводящей к его 3'-гидроксианалогам.

Les Acta Chimica paraissent en français, allemand, anglais et russe et publient des mémoires du domaine des sciences chimiques.

Les Acta Chimica sont publiés sous forme de fascicules. Quatre fascicules seront réunis en un volume (4 volumes par an).

On est prié d'envoyer les manuscrits destinés à la rédaction à l'adresse suivante:

Acta Chimica
Budapest, P.O. Box 67, H-1450, Hongrie

Toute correspondance doit être envoyée à cette même adresse.

La rédaction ne rend pas de manuscript.

Le prix de l'abonnement: $36,00 par volume.

Abonnement en Hongrie à l'Akadémiai Kiadó (1363 Budapest, P. O. B. 24, C. C. B. 215 11488), à l'étranger à l'Entreprise du Commerce Extérieur « Kultura » (H-1389 Budapest 62, P. O. B. 149 Compte-courant No. 218 10990) ou chez représentants à l'étranger.

Die Acta Chimica veröffentlichen Abhandlungen aus dem Bereich der chemischen Wissenschaften in deutscher, englischer, französischer und russischer Sprache.

Die Acta Chimica erscheinen in Heften wechselnden Umfanges. Vier Hefte bilden einen Band. Jährlich erscheinen 4 Bände.

Die zur Veröffentlichung bestimmten Manuskripte sind an folgende Adresse zu senden:

Acta Chimica
Budapest, Postfach 67, H-1450, Ungarn

An die gleiche Anschrift ist jede für die Redaktion bestimmte Korrespondenz zu richten.

Manuskripte werden nicht zurückerstattet.

Abonnementspreis pro Band: $36,00.

Bestellbar für das Inland bei Akadémiai Kiadó (1363 Budapest, Postfach 24, Bankkonto Nr. 215 11488), für das Ausland bei »Kultura« Außenhandelsunternehmen (H-1389 Budapest 62, P.O.B. 149. Bankkonto Nr. 218 10990) oder seinen Auslandsvertretungen.

«Acta Chimica» издают статьи по химии на русском, английском, французском и немецком языках.

«Acta Chimica» выходит отдельными выпусками разного обектъка, 4 выпус составляют один том и за год выходят 4 тома.

Предназначенные для публикации рукописи следует направлять по адресу:

Acta Chimica
Budapest, P.O. Box 67, H-1450, ВНР

Всякую корреспонденцию в редакцию направляйте по этому же адресу.

Редакция рукописей не возвращает.

Подписная цена — $36,00 за том.

Отечественные подписчики направляйте свои заявки по адресу Издательства Академии Наук (1363 Budapest, P.O.B. 24, Текущий счет 215 11488), а иностранные подписчики через организацию по внешней торговле «Kultura» (H-1389 Budapest 62, P.O.B. 149. Текущий счет 218 10990) или через ее заграничные представительства и уполномеченных.

Reviews of the Hungarian Academy of Sciences are obtainable at the following addresses:

AUSTRALIA
C.B.D. LIBRARY AND SUBSCRIPTION SERVICE. Box 4886, G.P.O., *Sydney N.S.W. 2001*
COSMOS BOOKSHOP, 145 Ackland Street, *St, Kilda (Melbourne), Victoria 3182*

AUSTRIA
GLOBUS, Höchstädtplatz 3, *1200 Wien XX*

BELGIUM
OFFICE INTERNATIONAL DE LIBRAIRIE, 30 Avenue Marnix, *1050 Bruxelles*
LIBRAIRIE DU MONDE ENTIER, 162 Rue du Midi, *1000 Bruxelles*

BULGARIA
HEMUS, Bulvar Ruski 6, *Sofia*

CANADA
PANNONIA BOOKS, P.O. Box 1017, Postal Station "B", *Toronto, Ontario M5T 2T8*

CHINA
CNPICOR, Periodical Department, P.O. Box 50, *Peking*

CZECHOSLOVAKIA
MAD'ARSKÁ KULTURA, Národni třida 22, *115 66 Praha*
PNS DOVOZ TISKU, Vinohradská 46, *Praha 2*
PNS DOVOZ TLAČE, *Bratislava 2*

DENMARK
EJNAR MUNKSGAARD, Norregade 6, *1165 Copenhagen*

FINLAND
AKATEEMINEN KIRJAKAUPPA, P.O. Box 128, *SF-00101 Helsinki 10*

FRANCE
EUROPERIODIQUES S. A., 31 Avenue de Versailles, *78170 La Celle St.-Cloud*
LIBRAIRIE LAVOISIER, 11 rue Lavoisier, *75008 Paris*
OFFICE INTERNATIONAL DE DOCUMENTATION ET LIBRAIRIE, 48 rue Gay-Lussac, *75240 Paris Cedex 05*

GERMAN DEMOCRATIC REPUBLIC
HAUS DER UNGARISCHEN KULTUR, Karl-Liebknecht-Strasse 9, *DDR-102 Berlin*
DEUTSCHE POST ZEITUNGSVERTRIEBSAMT, Strasse der Pariser Kommüne 3—4, *DDR-104 Berlin*

GERMAN FEDERAL REPUBLIC
KUNST UND WISSEN ERICH BIEBER, Postfach 46, *7000 Stuttgart 1*

GREAT BRITAIN
BLACKWELL'S PERIODICALS DIVISION, Hythe Bridge Street, *Oxford OX1 2ET*
BUMPUS, HALDANE AND MAXWELL LTD., Cowper Works, *Olney, Bucks MK46 4BN*
COLLET'S HOLDINGS LTD., Denington Estate. *Wellingborough, Northants NN 2QT*
WM. DAWSON AND SONS LTD., Cannon House, *Folkestone, Kent CT19 5EE*
H. K. LEWIS AND CO., 136 Gower Street, *London WC1E 6BS*

GREECE
KOSTARAKIS BROTHERS, International Booksellers, 2 Hippokratous Street, *Athens-143*

HOLLAND
MEULENHOFF-BRUNA B.V., Beulingstraat 2, *Amsterdam*
MARTINUS NIJHOFF B.V., Lange Voorhout 9—11, *Den Haag*
SWETS SUBSCRIPTION SERVICE, 347b Heereweg, *Lisse*

INDIA
ALLIED PUBLISHING PRIVATE LTD., 13/14 Asaf Ali Road, *New Delhi 110001*
150 B-6 Mount Road, *Madras 600002*
INTERNATIONAL BOOK HOUSE PVT. LTD., Madame Cama Road, *Bombay 400039*
THE STATE TRADING CORPORATION OF INDIA LTD., Books Import Division, Chandralok, 36 Janpath, *New Delhi 110001*

ITALY
EUGENIO CARLUCCI, P.O. Box 252, *70100 Bari*
INTERSCIENTIA, Via Mazzé 28, *10149 Torino*
LIBRERIA COMMISSIONARIA SANSONI, Via Lamarmora 45, *50121 Firenze*
SANTO VANASIA, Via M. Macchi 58, *20124 Milano*
D. E. A., Via Lima 28, *00198 Roma*

JAPAN
KINOKUNIYA BOOK-STORE CO. LTD., 17-7 Shinjuku-ku 3 chome, Shinjuku-ku, *Tokyo 160-91*
MARUZEN COMPANY LTD., Book Department, P.O. Box 5050 Tokyo International, *Tokyo 100-31*
NAUKA LTD. IMPORT DEPARTMENT, 2-30-19 Minami Ikebukuro, Toshima-ku, *Tokyo 171*

KOREA
CHULPANMUL, *Phenjan*

NORWAY
TANUM-CAMMERMEYER, Karl Johansgatan 41—43, *1000 Oslo*

POLAND
WĘGIERSKI INSTYTUT KULTURY, Marszałkowska 80, *Warszawa*
CKP 1 W ul. Towarowa 28 *00-958 Warsawa*

ROUMANIA
D. E. P., *Bucuresti*
ROMLIBRI, Str. Biserica Amzei 7, *Bucureşti*

SOVIET UNION
SOJUZPETCHATJ — IMPORT, *Moscow*
and the post offices in each town
MEZHDUNARODNAYA KNIGA, *Moscow G-200*

SPAIN
DIAZ DE SANTOS, Lagasca 95, *Madrid 6*

SWEDEN
ALMQVIST AND WIKSELL, Gamla Brogatan 26, *S-101-20 Stockholm*
GUMPERTS UNIVERSITETSBOKHANDEL AB, Box 346, *401 25 Göteborg 1*

SWITZERLAND
KARGER LIBRI AG, Petersgraben 31, *4071 Basel*

USA
EBSCO SUBSCRIPTION SERVICES, P.O. Box 1943, *Birmingham, Alabama 35201*
F. W. FAXON COMPANY, INC., 15 Southwest Park, *Westwood, Mass, 02090*
THE MOORE-COTTRELL SUBSCRIPTION AGENCIES, *North Cohocton, N.Y. 14 6*
READ-MORE PUBLICATIONS, INC., 140 Cedar Street, *New York, N. Y. 10006*
STECHERT-MACMILLAN, INC., 7250 Westfield Avenue, *Pennsauken N.J. 0 110*

VIETNAM
XUNHASABA, 32, Hai Ba Trung, *Hanoi*

YUGOSLAVIA
JUGOSLAVENSKA KNJIGA, Terazije 27, *Beograd*
FORUM, Vojvode Mišića 1, *21000 Novi Sad*

30. XI. 1979 HU ISSN 0001—5407 **Index: 26.007**

ACTA CHIMICA

ACADEMIAE SCIENTIARUM HUNGARICAE

TOMUS 102 FASCICULUS 2

AKADÉMIAI KIADÓ, BUDAPEST

1979

ACTA CHIM. ACAD. SCI. HUNG. ACASA2 102 (2) 109–213 (1979)

ACTA CHIMICA

A MAGYAR TUDOMÁNYOS AKADÉMIA KÉMIAI TUDOMÁNYOK OSZTÁLYÁNAK IDEGEN NYELVŰ KÖZLEMÉNYEI

Acta Chimica is a journal for the publication of papers on all aspects of chemistry in English, German, French and Russian.

Acta Chimica is published in 4 volumes per year. Each volume consists of 4 issues of varying size.

Manuscripts should be sent to

Acta Chimica
Budapest, P.O. Box 67, H-1450, Hungary

Correspondence with the editors should be sent to the same address. Manuscripts are not returned to the authors.

Subscription: $36.00 per volume.

Hungarian subscribers should order from Akadémiai Kiadó, 1363 Budapest, P.O. Box 24. Account No. 215 11488.

Orders from other countries are to be sent to "Kultura" Foreign Trading Company (H-1389 Budapest 62, P.O. Box 149. Account No. 218 10990) or its representatives abroad.

Acta Chimica Academiae Scientiarum Hungaricae, Tomus 102 (2), pp. 109—111 (1979)

X-RAY AND ELECTRON MICROSCOPIC STUDIES ON CALCIUM-COPPER HYDROXYLAPATITES

P. N. PATEL and S. V. CHIRANJEEVI RAO

(Post-Graduate Department of Chemistry, G. M. College, Sambalpur, India)

Received January 5, 1978

In revised form March 11, 1978

Accepted for publication September 4, 1978

The lattice constants of calcium-copper hydroxylapatites were found to decrease with increasing copper content of the samples, resulting from the contraction of the unit cell volume. The contraction in crystal dimensions could be observed in the electron microscopic patterns of the samples. The introduction of Cu^{3+} into calcium hydroxylapatite, $Ca_{10}(PO_4)_6(OH)_2$, results in the formation of solid solutions.

Calcium hydroxylapatite, (CaHA), $Ca_{10}(PO_4)_6(OH)_2$, the major inorganic constituent of the human skeletal system [1], belongs to an isomorphous series of compounds known as apatites. It forms solid solutions with isomorphic copper hydroxylapatite, (CuHA), $Cu_{10}(PO_4)_6(OH)_2$, due to the closeness of the ionic radii of Ca^{2+} (0.99 Å) and Cu^{2+} (0.72 Å) [2]. The $Ca^{2+} \rightarrow Cu^{2+}$ replacement in CaHA is of extreme biological significance as it explains the mechanism of incorporation of copper into the human skeletal system according to the following equation:

$$Ca_{10}(PO_4)_6(OH)_2 + nCu^{2+} \rightarrow Ca_{10-n}Cu_n(PO_4)_6(OH)_2 + nCa^{2+}$$

As part of the physico-chemical studies on calcium-copper hydroxylapatites, the present communication deals with X-ray and electron-microscopic studies.

Experimental

The details of preparation and identification of CaHA, CuHA and Ca—CuHA in the form of solid solutions were reported earlier [3]. The X-ray diffraction pattern of powdered samples were obtained with a NORELCO powder diffractometer employing Ni-Filtered Cu—K_a radiation with a graphite monochromator. Sharp peaks separated by less than 0.1 degree (2 Θ) can be resolved with a 0.006 inch entrance slit at a scan rate of 1 degree (2Θ) per minute using a tube voltage of 50 kV and a current of 20 mA. The composition and unit cell dimensions of calcium-copper hydroxylapatites and their solid solutions are given in Table I.

Table I

Composition and unit cell dimensions of calcium-copper hydroxylapatites and their solid solutions

Sample No.	Wt%			Molecular formula	Atom ratio $\left(\frac{Ca + Cu}{P}\right)$	Lattice parameter		Unit cell volume
	Ca	Cu	P			*a*	*c*	
1	39.80	—	18.61	$Ca_{10}(PO_4)_6(OH)_2$	1.68	9.37	6.88	523.1
2	27.39	16.06	17.41	$Ca_{7\cdot3}Cu_{2\cdot7}(PO_4)_6(OH)_2$	1.67	9.26	6.81	505.7
3	21.48	23.66	16.89	$Ca_{5\cdot9}Cu_{4\cdot1}(PO_4)_6(OH)_2$	1.67	9.14	6.74	487.6
4	14.76	32.30	16.30	$Ca_{4\cdot2}Cu_{5\cdot8}(PO_4)_6(OH)_2$	1.67	9.03	6.68	471.7
5	6.02	43.52	15.53	$Ca_{1\cdot8}Cu_{8\cdot2}(PO_4)_6(OH)_2$	1.67	8.92	6.60	454.8
6	—	51.25	15.00	$Cu_{10}(PO_4)_6(OH)_2$	1.67	8.83	6.53	440.9

The inherent error in the lattice parameter is ± 0.01 Å

Results and Discussion

The results of chemical analyses of the sample obtained by applying a method specially worked out for this purpose [4] are given in Table I. Based on the fact that 1 mol of the sample has a total of 10 g atoms of calcium and/or copper, the molecular formulae of the samples were calculated from the results of columns 2—3 and included in column 5 of Table I. The atom ratio, $\frac{Ca + Cu}{P}$ per mol of sample was ~ 1.68 (theoretical 1.67). The molar volume of the end members and those of the intermediate samples, which lie within the range of end members, indicate the formation of homogeneous solid solutions [5]. The homogenity and crystaleinity of the samples were further confirmed by the lattice parameters of the samples. It is a well-established fact that all the members of the apatite family exhibit a hexagonal crystal structure belonging to the hexagonal bipyramidal class 6/m (spaces group $C_{6_3/m}$) [6]. The lattice parameters show unit cell contraction consequent upon the introduction of the smaller Cu^{2+} ion (0.72 Å) in the apatite lattice. The decrease in crystal dimensions could also be observed in the electron-microscopic patterns of a representative set of samples.

*

The authors are grateful to Prof. G. FERRARIS, University of Torino, Italy, for the technical assistance provided with the X-ray diffraction spectra, to Prof. Dr. R. B. CONDRATE, Associate Professor, New York State College of Ceramics, Alfred University, U.S.A., for the Electron-micrographs and to the University Grants Commission for a research grant.

REFERENCES

[1] NEUMAN, W. F., NEUMAN, M. W.: Chem. Rev., **53,** 1 (1953)
[2] COLLIN, R. L.: J. Am. Chem. Soc., **81,** 5275 (1969)
[3] PATEL, P. N., CHIRANJEEVI RAO, S. V.: J. Ind. Chem. Soc. (In press)
[4] PATEL, P. N., CHIRANJEEVI RAO, S. V.: Acta Siencica Indica, **3,** 19 (1977)
[5] PARTINGTON, J. R.: An Advanced Treatise of Physical Chemistry, Vol. **3,** Longmans Green and Co, P. 121—142, London, 1952
[6] VANWAZER, J. R.: Phosphorus and its compounds, Vol. 1, P. 534, Interscience, New York, 1966

Premananda PATEL Post-Graduate Dept. of Chemistry, G. M. College Sambalapur, India
S. V. CHIRANJEEVI RAO Hindustan Zinc Ltd., Visakhapatnam-15 (A. P.) India

Acta Chimica Academiae Scientiarum Hungaricae, Tomus 102 (2), pp. 113–120 (1979)

ANALYTICAL APPLICATION OF SOME OUTER-SPHERE COMPLEXES. SPECTROPHOTOMETRIC DETERMINATION OF TRIFLUOROACETIC ACID AND INORGANIC AZIDES BY SOLVENT EXTRACTION WITH (1,10-PHENANTHROLINE)IRON(II) CHELATE

L. Ilcheva and G. Todorova

(Department of Analytical Chemistry, Chemico-Technological Institute, Sofia, Bulgaria)

Received April 6, 1978
In revised form September 8, 1978
Accepted for publication October 13, 1978

It was found that small amount of CF_3COOH or NaN_3 can be extracted into nitrobenzene when a moderate amount of 1,10 phenanthroline chelate cation was present in the aqueous phase. The absorbance of the extract at λ_{max} was found to be proportional to the CF_3COOH (518 nm) respectively to the NaN_3 (516 nm) concentration in the aqueous phase. To obtain optimum conditions for the determinations, various factors were studied: the pH's of the solution, the effect of the concentration of 1,10-(phenanthrolin)iron(II) chelate and buffer solution, the shaking time, the stability of the color, the presence of the diverse ions. The chemical formulae of the extracted outer-sphere complexes were found to be: $Fe(phen)_3(CF_3COO)_2$ and $Fe(phen)_3(N_3)_2$.

Several methods have been reported for the colorimetric determination of inorganic azides [1—4], but most of them require preliminary treatment and distillation of the sample. There are no data available about the colorimetric determination of small amounts of trifluoroacetic acid.

In the course of our investigations on outer-sphere complexes it has been observed that if a considerable excess of tris(1,10-phenanthroline)iron(II) chelate is added to an aqueous solution containing a small amount of trifluoroacetic acid or inorganic azides, tris(1,10-phenanthroline)iron(II) trifluoroacetate or tris(1,10-phenanthroline)iron(II)azide can be extracted into nitrobenzene. The absorbance of the organic layer is proportional to the amount of trifluoroacetic acid or azide present in the aqueous phase. So, by measuring the absorbance of the organic phase it was possible to determine small amounts of trifluoroacetic acid or inorganic azides.

Experimental

A 0.01 *M* solution of tris(1,10-phenanthroline)iron(II) sulfate was prepared by dissolving analytical grade iron(II) ammonium sulfate and 1,10-phenanthroline in water containing a few drops of sulfuric acid. The trifluoroacetic acid solution was standardized against sodium hydroxide. NaN_3 of analytical grade was used without further purification. Nitrobenzene was purified by distillation before the extraction.

The spectrophotometric measurements were made on a VSU Zeiss Iena model spectrophotometer. The pH measurements were performed using a Seibold pH meter. A horizontal shaker was used for the extraction.

Results and Discussion

Absorption spectra

The absorption spectra of the nitrobenzene phase obtained by the above procedure are shown in Figs 1 and 2. It can be seen that the presence of CF_3COOH and NaN_3 in the aqueous phase leads to a considerable increase in the absorbance of the organic phase. The absorbance maxima of the extracts are at 515—518 nm.

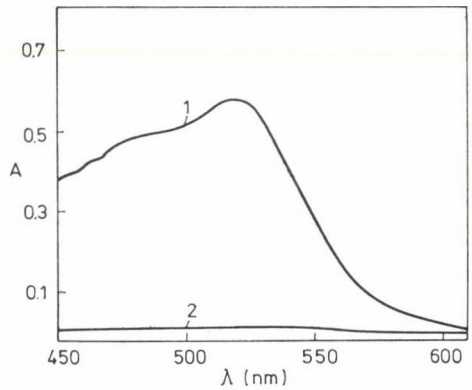

Fig. 1. Absorption spectra of the nitrobenzene phase for the system $Fe(phen)_3^{2+}-CF_3COOH$. Curve 1: $[CF_3COOH] = 4\times10^{-4}$ *M*, $[Fe(phen)_3^{2+}] = 4\times10^{-3}$ *M*, $[KH_2PO_4] = 0.05$ *M*, pH = 4.4, $l = 1.0$ cm; Curve 2: reagent blank, reference: nitrobenzene

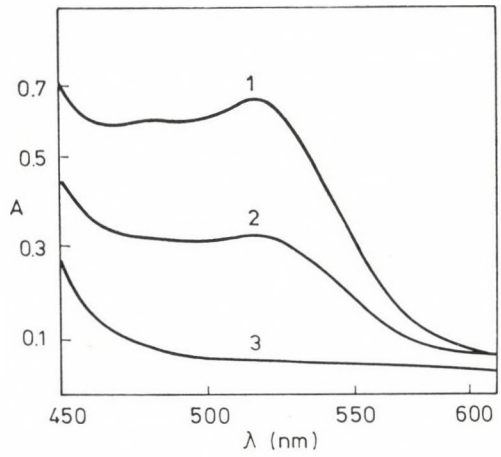

Fig. 2. Absorption spectra of the nitrobenzene phase for the system $Fe(phen)_3^{2+}-NaN_3$. Curve 1: $[NaN_3] = 1\times10^{-3}$ *M*, $[Fe(phen)_3^{2+}] = 8\times10^{-3}$ *M*, $[KH_2PO_4] = 0.06$ *M*, pH = 7.5, $l = 1.0$ cm; Curve 2: reagent blank; Curve 3: nitrobenzene, reference: air

Effect of the pH

The extraction of trifluoroacetic acid was performed at various pH values of the aqueous phase. Fig. 3 shows that the degree of extraction of CF_3COOH is the highest and remains constant in the pH range of 3—5. In more acidic solutions (pH $<$ 2.5) the absorbance trends to decrease presumably because of the decomposition of the phenanthroline iron(II) complex. In more alkaline solutions (pH $>$ 7) the absorbance increases by about 15%. Therefore, we applied a borax buffer (pH = 9.5), but the reproducibiliy of the results was poor. The effect of pH on the system $Fe(phen)_3$—NaN_3 is shown in Fig. 4. The degree of extraction is about the same in the pH range of 7—9.

Effect of tris(1,10-phenanthroline)iron(II) concentration

The absorbance of the nitrobenzene phase in the presence of CF_3COOH is constant at chelate concentrations above $2\times10^{-3}M$. At least a 8 to 10-fold excess of the phenanthroline chelate over trifluoroacetic acid is necessary to

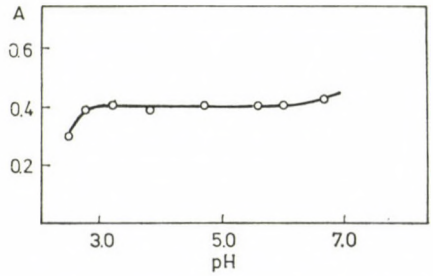

Fig. 3. Effect of pH on the extraction for the system $Fe(phen)_3^{2+}CF_3COOH$. $[CF_3COOH] = 2.5\times10^{-4}$ *M*, $[Fe(phen_3^{2+}] = 3\times10^{-3}$ *M*, $[KH_2PO_4] = 0.05$ *M*, reference: reagent blank

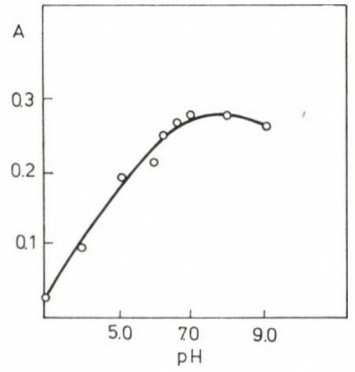

Fig. 4. Effect of pH on the extraction for the system $Fe(phen)_3^{2+}NaN_3$. $[NaN_3] = 1\times10^{-3}$ *M* $[Fe(phen)_3^{2+}] = 8\times10^{-3}$ *M*, $[KH_2PO_4] = 0.05$ *M*, reference: reagent blank

obtain quantitative recoveries. The chelate concentration was kept at $3\times$ $\times 10^{-3}M$ to study the $Fe(phen)_3^{2+}$—CF_3COOH system. Fig. 5 shows the effect of chelate concentration on the extraction of NaN_3. The iron chelate should be maintained at a 6-fold or higher excess over the azide.

Effect of shaking time

Shaking time for the extraction of CF_3COOH varied from 0.5 min to 30 min. It appears that a 1-minute shaking is enough to achieve complete extraction. The absorbance of the nitrobenzene phase in the presence of NaN_3 was measured as a function of shaking time from 1 to 70 min. After 10-min

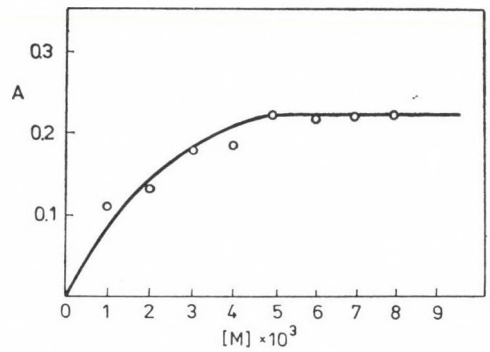

Fig. 5. Effect of the tris(phenanthroline)iron(II) concentration on the extraction of NaN_3 $[NaN_3] = 8\times10^{-4}$ *M*, $[KH_2PO_4] = 0.02$ *M*, pH = 7.0

shaking the results are reproducible but the degree of extraction is a little lower than that after a 1-hr shaking. In this case, however, the separation of the two layers must be performed by centrifugation.

Effect of buffer concentration

Aqueous $Fe(phen)_3^{2+}$—CF_3COOH solutions buffered at pH 4.4 with a phosphate buffer remained unchanged within the concentration range of 0.04—0.2 *M*. In a series containing $8\times10^{-3}M$ $Fe(phen)_3^{2+}$ and $1\times10^{-3}M$ NaN_3 (at pH = 7) the variation of phosphate buffer within the limits 0.02—0.25 *M* did not affect the degree of extraction.

Stability of colour

The absorbance of the extracts was measured as a function of time. The colour of the two extracts was very stable and did not change over 24 hrs for $Fe(phen)_3^{2+}$—CF_3COOH and 48 hrs for $Fe(phen)_3^{2+}$—NaN_3.

Reproducibility and precision

The reproducibility of the methods proposed was estimated considering the results of n sample solutions for the two systems. The mean value of the absorbance of each extract and the standard deviations are given in Table I. It is obvious that the reproducibility of the system $Fe(phen)_3^{2+}$—CF_3COOH is much better than that of the $Fe(phen)_3^{2+}$—NaN_3 system.

Table I

Mean absorbances and standard deviations

$Fe(phen)_3^{2+}-CF_3COOH$			$Fe(phen)_3^{2+}-NaN_3$		
n	A	σ	n	A	σ
10	0.386	0.005	9	0.202	0.007

Anion interferences

A series of anions were checked for possible interference by adding NH_4F, NaCl, CH_3COOH, Na_2SO_4 and $NaNO_3$ to a solution containing $2.5\times$ $\times 10^{-4}M$ CF_3COOH. The solution obtained was normally extracted. The results are given in Table II.

Table II

Determination of CF_3COOH in the presence of different ions
(CF_3COOH concentration 2.5×10^{-4} M)

Added salt	Concentration (mol/dm³)	CF_3COOH (found) (%)
NH_4F	1.4×10^{-3}	100
	1.22×10^{-2}	101
CH_3COOH	2.5×10^{-3}	99
	2.2×10^{-2}	100
Na_2SO_4	2.5×10^{-3}	100
	2.5×10^{-2}	99
NaCl	2.5×10^{-3}	102
$NaNO_3$	1×10^{-4}	103

Sulfide ions interfere in almost every method of azide determination [1—4]. Unfortunately, sulfide also interferes in the present method. The organ-

ic layer turned black and in about 15 min iron sulfide precipitated. The rate of reaction between tris(1,10-phenanthroline)-iron(II) and sulfide ion strongly depends on the pH. At pH = 7 when HS^- ions predominate, the absorbance of the solution practically remaines constant for more than two hours. This fact shows that only S^{2-} enters the inner coordination sphere of tris-(1,10-phenanthroline)iron(II) giving the final black precipitate.

Recommended procedure for the determination of CF_3COOH

Mix 15.00 ml of tris(1,10-phenanthroline)iron(II) sulfate solution ($1\times\times10^{-2}$ *M*), 5.00 ml phosphate buffer solution (0.5 *M*) and 0.4—4.0 ml trifluoroacetic acid solution (5.0×10^{-3} *M*). Dilute the resulting solution to 50.00 ml with doubly distilled water and adjust the pH 4.4. Extract a 25.00 ml aliquot with 10.00 ml nitrobenzene for 5 min. After 30 min, trasfer the organic layer to a flask containing 1 g of anhydrous sodium sulfate and shake it vigorously until the solution becomes transparent. Measure the absorbance at 518 nm using a reagent blank solution as reference. Beer's law is obeyed in the range of 3×10^{-5}—4×10^{-4} *M* trifluoroacetic acid.

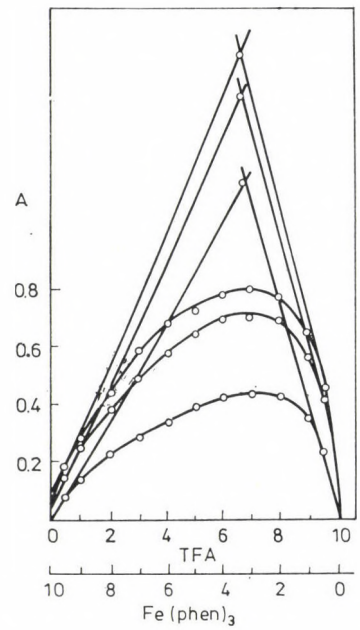

Fig. 6. Composition of the extracted species $Fe(phen)_3(CF_3COO)_2 \cdot [CF_3COOH] + [Fe(phen)_3] = 2\times10^{-3}$ *M*, λ = 490, 518 and 540 nm

Recommended procedure for the determination of sodium azide

Mix 20.00 ml of tris(1,10-phenanthroline)iron(II) sulfate solution ($1.0\times$ $\times 10^{-2}$ *M*), 2.5 ml phosphate buffer (0.5 *M* KH_2PO_4, pH = 7) and 0.25—2.00 ml sodium azide solution (1.0×10^{-2} *M*). Dilute the resulting solution to 25.00 ml. Extract an aliquot of 20.00 ml with 15.00 ml nitrobenzene for 1 hr. After 15—20 min centrifuge the solution and run off the organic layer into a test tube. Add 1 g of anhydrous sodium sulfate and shake it vigorously to remove the traces of water. Measure the absorbance of the solution at 516 nm in a 3 cm cell using a reagent blank as a reference. Beer's law is obeyed in the range of 2×10^{-4}—7×10^{-4} *M* NaN_3 in the aqueous phase.

Composition of the extracted species

The composition of the extracted species for the two systems was found to be 1 : 2 according to the continuous variation method (Figs 6 and 7). This suggests that the chemical formula of the extracted species can be represented as $Fe(phen)_3(CF_3COO)_2$ and $Fe(phen)_3(N_3)_2$. Rao and Sarma [5] proposed another mechanism for the 1,10-phenanthroline azide complex: first ferroin

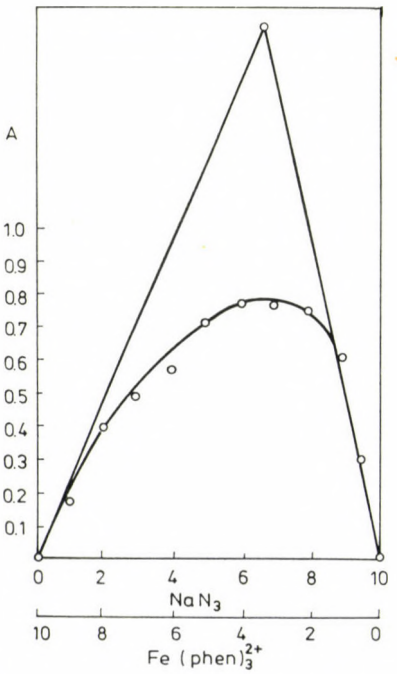

Fig. 7. Composition of the extracted species $Fe(phen)_3(N_3)_2 \cdot [NaN_3] + [Fe(phen)_3^{2+}] =$ $= 0.83\times 10^{-2}$ *M*, pH = 7.0

forms the outer-sphere complex $Fe(phen)_3(N_3)_2$ and extracts into nitrobenzene. Then the two azide ions enter the inner coordination sphere of ferroin, displacing one *o*-phenanthroline molecule and the final extracting species remains $Fe(phen)_2(N_3)_2$. The proposed mechanism, however, is in contrast with all the other similar systems, *viz.* $Fe(phen)_3(SCN)_2$ [6], $Fe(phen)_3(ClO_4)_2$ [7], $Fe(phen)_3(C_6H_5O)_2$ [8] and $Fe(phen)_3(CCl_3COO)_2$ [9].

*

The authors are indebted to Professor M. T. Beck, L. Kossuth University Debrecen for stimulating discussions.

REFERENCES

[1] Roberson, Ch. E., Austin, C. A.: Anal. Chem., **29,** 854 (1957)
[2] Staples, P. J.: Chem. Ind. (London), **39,** 1210 (1960)
[3] Mizushima, Y., Magagama, S.: J. Ind. Explos. Soc. Japan, **17,** 113 (1956)
[4] Clem, R. G., Huffman, E. H.: Anal. Chem., **37,** 366 (1965)
[5] Rao, V. P. R., Bhaskara Sarma, P. V. R.: Michrochim. Acta, **1970,** 783
[6] Rao, V. P. R., Rao, K. V., Bhaskara Sarma, P. V. R.: Talanta, **16,** 277 (1969)
[7] Fritz, S., Abbink, W., Campbell, A.: Anal. Chem., **36,** 11, 2123 (1964)
[8] Yamamoto, Y., Kumamuru, T., Yamate, M.: Japan Analyst, **16,** 1181 (1967)
[9] Yamamoto, Y., Kumamaru, T., Uemura, Y.: Anal. Chim. Acta, **39,** 51 (1967)

Liliana Ilcheva, Gergana Todorova } Chemico-Technological Institute, Sofia-Darvenitsa 1156, Bulgaria

Acta Chimica Academiae Scientiarum Hungaricae, Tomus 102 (2), pp. 121—125 (1979)

STABILITY CONSTANTS OF OUTER-SPHERE COMPLEXES $Fe(phen)_3(CF_3COO)_2$ AND $Fe(phen)_3(CCl_3COO)_2$

L. Ilcheva, G. Todorova and M. Georgieva

(Department of Analytical Chemistry, Chemico-Technological Institute, Sofia, Bulgaria)

Rceeived April 6, 1978

In revised form September 8, 1978

Accepted for publication October 13, 1978

The liquid-liquid partition of $Fe(phen)_3(CF_3COO)_2$ and $Fe(phen)_3(CCl_3COO)_2$ in nitrobenzene, as a function of ligand concentration was studied. Taking into consideration that only the neutral outer-sphere complex was extracted the ratio of the total concentration of the metal ion species, as well as the ratio of the outer-sphere complex concentrations in the two phases was foudn. The estimated outer-sphere stability constants are $k_1 = 1.1 \times 10^2$; $k_2 = 8 \times 10$ for $Fe(phen)_3(CF_3COO)_2$ and $k_1 = 4.2 \times 10^3$; $k_2 = 4.3 \times 10^2$ for $Fe(phen)_3(CCl_3COO)_2$. Having in mind the present study, as well as the other results the following order for the outer-sphere association of $Fe(phen)_3^{2+}$ could be given:

$$CCl_3COO^- > CF_3COO^- \gg CH_3COO^-.$$

The analytical application of $Fe(phen)_3(CF_3COO)_2$ and $Fe(phen)_3 \cdot (CCl_3COO)_2$ based on outer-sphere coordination to tris(1,10-phenanthroline)iron(II) has been described [1, 2]. The determination of outer-sphere stability constants of $Fe(phen)_3^{2+}$ with CCl_3COO^- and CF_3COO^- in water saturated with nitrobenzene is of certain importance for solvent extraction processes.

Experimental

Preparation and standardization of the solutions

A 0.01 *M* solution of tris(1,10-phenanthroline)iron(II) sulfate was prepared by dissolving analytical grade iron(II) ammonium sulfate and 1,10-phenanthroline in water containing a few drops of sulfuric acid. Trifluoroacetic acid and trichloroacetic acid solutions were standardized against sodium hydroxide. Nitrobenzene was purified by distillation and saturated with bidistilled water before use.

Apparatus

The spectrophotometric measurements were performed on a VSU Zeiss Jena model and CF-4A spectrophotometers, using 1 cm glass cells. The pH's were measured with a Seibold pH meter. A horizontal shaker was used for the extraction.

A constant ionic strength in the aqueous phase was maintained with KH_2PO_4. For the system $Fe(phen)_3 - CF_3COO^-$, $I = 0.2$ and for $Fe(phen)_3 - CCl_3COO^-$, $I = 0.15$.

Procedure for Liquid-Liquid Partition of Tris(1,10-Phenanthroline)iron(II) in the Presence of Trifluoroacetic Acid

In a 50.00 ml volumetric flask suitable amounts of 1,10-phenanthroline-iron(II), trifluoroacetic acid and KH_2PO_4 at $I = 0.2$ were mixed [1]. The pH was adjusted 5.0. A 25.00 ml aliquot was extracted with 10.00 ml nitrobenzene for 5 min. After 30 min, the organic layer was transferred to a flask containing 1 g anhydrous sodium sulfate. The solution was vigorously shaken until transparent. The absorbance of the organic layer was measured at 518 nm using a reagent blank solution as reference.

Procedure for Liquid-Liquid Partition of Tris(1,10-phenanthroline)iron(II) in the Presence of Trichloroacetic Acid

In a 50.00 ml volumetric flask suitable amounts of ferroin, trichloroacetic acid and KH_2PO_4 were mixed at $I = 0.15$ and pH = 4.0 [2]. An aliquot of 20.00 ml was extracted with 10.00 ml nitrobenzene for 5 min. After 30 min the organic layer was transferred to a flask containing 1 g anhydrous sodium sulfate and it was shaken vigorously. The absorbance of the organic layer was measured at 515 nm using a reagent blank solution as reference. The extraction procedure was performed in the dark, because the intensity of the colour decreases rapidly in sunlight.

Determination of the Molar Absorptivity of $Fe(phen)_3(CF_3COO)_2$ in Nitrobenzene

25.00 ml of a solution containing 4×10^{-5}—8×10^{-5} M $Fe(phen)_3^{2+}$ and CF_3COOH in excess (4×10^{-3}—38×10^{-3} M) at $I = 0.2$ (KH_2PO_4) and pH = 5.0, was extracted with nitrobenzene and the absorbance of the organic layer was measured. The aqueous phase was treated in a silica bowl with concentrated HNO_3 and H_2SO_4 [3]. The total iron concentration was determined in the aqueous phase left after the extraction [4]. The results of 20 analyses were treated statistically and the 95% confidence interval of the molar absorptivity was found to be $(12.30 \pm 0.06) \times 10^3$.

Determination of the Molar Absorptivity of $Fe(phen)_3(CCl_3COO)_2$ in Nitrobenzene

Exhaustive extractions were performed in the following way. Series of solutions were prepared containing different amounts of ferroin (5×10^{-5}—10×10^{-5} M) and a large excess of CCl_3COOH (2×10^{-3} M) at $I = 0.15$ (KH_2PO_4) and pH = 5.0. An aliquot of 10.00 ml was extracted with 10.00 ml nitrobenzene. The layers were allowed to separate and the organic layer was transferred to a 25.00 ml volumetric flask. The extraction procedure was repeated with the aqueous layer. The organic extracts were combined and diluted in a 25.00 ml volumetric flask with nitrobenzene. The absorbance was measured against a reagent blank solution for every ferroin concentration. Taking into account the dilution factor, the molar absorptivity of outer-sphere complex was calculated. For a set of six observation the 95% confidence interval of the molar absorptivity was found [5] to be $(8.13 \pm 0.08) \times 10^3$.

Results and Discussion

The formation of the outer-sphere complex can be represented by reactions:

$$Fe(phen)_3^{2+} + X^- \rightleftharpoons Fe(phen)_3X^+ \quad (1)$$

$$Fe(phen)_3X^+ + X^- \rightleftharpoons Fe(phen)_3X_2 \quad (2)$$

where X^- is CCl_3COO^- or CF_3COO^-.

With the molar absorptivity of the neutral outer-sphere complex and the absorbance of the organic phase at a given ligand concentration, the ratio

of the total concentrations of the metal species in the two phases can be expressed as (Figs 1 and 2):

$$q = \frac{[MX_2]_{org}}{[MX_2]_{aq} + [MX]_{aq} + [M]_{aq}} = \frac{\lambda_2 \beta_2 [X^-]^2_{aq}}{\sum_0^2 \beta_i [X]^i_{aq}} \tag{3}$$

M is $Fe(phen)_3^{2+}$ and $\beta_2 = K_1 = K_2$, were

$$K_1 = \frac{[Fe(phen)_3 X^+]}{[Fe(phen)_3^{2+}]\,[X^-]}\,; K_2 = \frac{[Fe)phen)_3\, X_2]}{[Fe(phen)_3 X^+][X^-]}$$

$$\lambda_2 = \frac{[MX_2]_{org}}{[MX_2]_{aq}}\,.$$

If K_1 and K_2 are inserted into Eq. (3), after some rearrangement the following expression can be obtained:

$$\left(\frac{\lambda_2}{q} - 1\right)[X^-]^2_i = \frac{1}{K_2} + \frac{1}{\beta_2 X^-}\,. \tag{4}$$

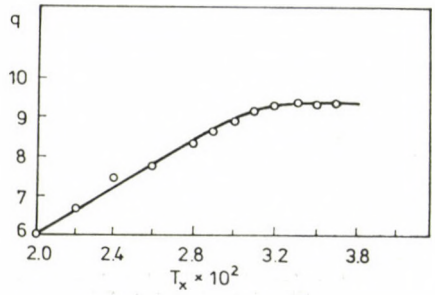

Fig. 1. q as a function of ligand concentration for the system $Fe(phen)_3 - CF_3COO^-$; $[Fe(phen)_3] = 7 \times 10^{-5}\ M$

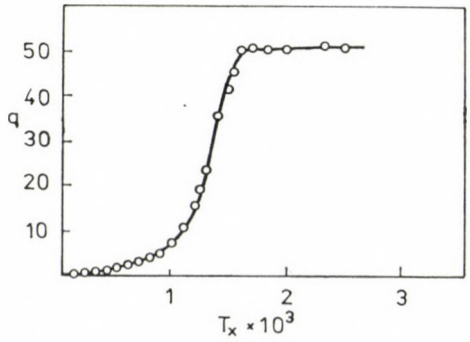

Fig. 2. q as a function of the ligand concentration for the system $Fe(phen)_3 - CCl_3COO^-$; $[Fe(phen)_3] = 8 \times 10^{-5}\ M$

The value of X^- to a good approximation is equal to the total X concentration ($T_X \gg T_M$).

$$\left(\frac{\lambda_2}{q} - 1\right) T_X = \frac{1}{K_2} + \frac{1}{\beta_2 T_X} . \tag{5}$$

λ_2 is obtained from the horizontal part of the curve (Figs 1 and 2). In Figs 3 and 4, the left-hand side of Eq. (5) is shown as a function of the total ligand concentration. Table I summarizes the results obtained for both systems.

It is noteworthy that the extraction measurements did not show evidence for outer-sphere complex formation between tris(1,10-phenanthroline)iron(II) and $H_2PO_4^-$ ions, the reason of which is not clear as yet. This was shown by experiments [1] on the effect of phosphate buffer on the extraction of trifluoroacetic acid. It was found that the variation of phosphate buffer between 0.02 and 0.25 *M* did not affect the degree of extraction.

Developing an extraction procedure for trichloroacetic acid YAMAMOTO, KUMAMURU and UEMURA [2] found that solutions buffered at pH = 4 with phosphate gave constant results over the concentration range of 0.04—0.16 *M*. In the determination of perchlorate ions by solvent extraction with 1,10-phen-

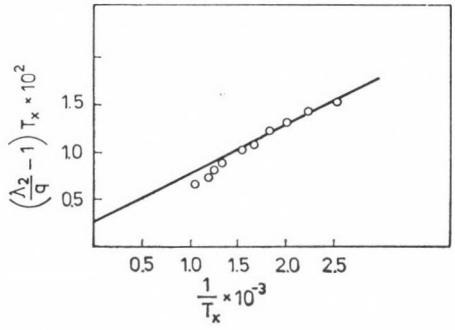

Fig. 3. $(\lambda_2/q - 1)T_X$ as a function of $1/T_X$ for the system $Fe(phen)_3 - CCl_3COO^-$; $[Fe(phen)_3] = 8 \times 10^{-5}$ *M*

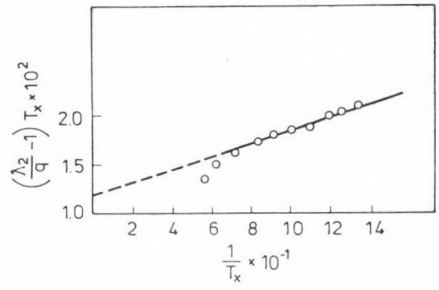

Fig. 4. $(\lambda_2/q - 1)T_X$ as a function of $1/T_X$ for the system $Fe(phen)_3 - CF_3COO^-$; $[Fe(phen)_3] = 7 \times 10^{-5}$ *M*

Table I

Stability constants and other data for the outer-sphere complexes $Fe(phen)_3X_2$

Outer-sphere complex	λ (nm)	Molar absorptivity	K_1	K_2
$Fe(phen)_3(CF_3COO)_2$	518	12.30×10^3	1.1×10^2	8×10
$Fe(phen)_3(CCl_3COO)_2$	516	8.11×10^3	4.2×10^2	4.3×10^2

anthroline-iron(II), it was found [6] that even considerable amounts of phosphate ions did not interfere. Phosphate ions do not interfere in the selective extraction of hexafluoroarsenate [7] or hexafluorophosphate [8] with ferroin.

The results of this work show that outer-sphere complex formation of $Fe(phen)_3^{2+}$ is the strongest with large anions, similary to other outer-sphere complex cations, *e.g.* $Co(NH_3)_6^{3+}$, $CO(en)_3^{3+}$, $Co(dip)_3^{3+}$, $Co(phen)_3^{3+}$ [9, 10, 11, 12]. Considering this and the results in Table I, we can write the following order for the outer-sphere association of $Fe(phen)_3^{2+}$

$$CCl_3COO^- > CF_3COO^- \gg CH_3COO^-$$

These results can hardly be explained by the electrostatic attraction between the inner-sphere complex and the ligand only. It is evident that hydration and solvation of the species may play a very important role too.

*

The authors are indebted to Professor M. T. Beck, L. Kossuth University, Debrecen, for stimulating discussions on the outer-sphere complexes.

REFERENCES

[1] Ilcheva, L., Todorova, G.: Acta Chim. Acad. Sci. Hung. (In press)
[2] Yamamoto, Y., Kumamuru, T., Uemura, Y.: Anal. Chim. Acta, **39,** 51 (1967)
[3] Knizek, M., Musilova, M.: Collect. Czechoslov. Chem. Commun., **33,** 757 (1968)
[4] Welcher, F. L.: Organic Analytical Reagents, Van Nostrand, New York 1947
[5] Dean, R. B., Dixon, W. J.: Anal. Chem., **23,** 636 (1951)
[6] Yamamoto, Y., Kotsuji, K., Kinuwaki, S., Sawamura, H.: Nippon Kagaku Zasshi, **85,** 869 (1964)
[7] Archer, V. S., Doolittle, F. G.: Talanta, **14,** 921 (1967)
[8] Archer, V. S., Doolittle, F. G.: Anal. Chem., **39,** 371 (1967)
[9] Mazzei, M., Lederer, M.: J. Chromatog., **31,** 196 (1967)
[10] Lederer, M., Mazzei, M.: J. Chromatog., **35,** 201 (1968)
[11] Mazzei, M., Lederer, M.: J. Chromatog., **40,** 197 (1969)
[12] Yamamoto, Y., Tarumoto, T., Ywamoto, E.: Anal. Chim. Acta, **64,** 1 (1973)

Liliana Ilcheva
Gergana Todorova
M. Georgieva
Chemico-Technological Institute, Sofia-Darvenitsa 1156, Bulgaria

Acta Chimica Academiae Scientiarum Hungaricae, Tomus 102 (2), pp. 127—133 (1979)

DEBENZO DERIVATIVES OF ALKALOIDS WITH INDOLO[2,3-*c*]QUINAZOLINO[3,2-*a*]-PYRIDINE SKELETON, IX*

DEBENZOEVODIAMINE

Z. PÁL,[1] K. HORVÁTH-DÓRA,[1] G. TÓTH,[2] O. CLAUDER[1] and J. TAMÁS[3]

([1]Institute of Organic Chemistry, Pharmaceutical Faculty, Semmelweis Medical University, Budapest, [2]Institute for General and Analytical Chemistry, Technical University, Budapest, [3]Central Research Institute for Chemistry, Hungarian Academy of Sciences, Budapest)

Received June 12, 1978
Accepted for publication October, 30, 1978

Debenzorutecarpine (**5**) was converted into dehydrodebenzoevodiamine hydroiodide (**6**) with methyl iodide. When treated with ammonia compound **6** yielded the debenzoevodiaminic acid ammonium salt (**7**) through ring cleavage; while reduction produced debenzoevodiamine (**11**). The synthesis of **11** has also been realized by starting from 1,2,3,4-tetrahydro-1-oxo-β-carboline (**9**) and *N*-methyl-β-alanine ethyl ester (**12**). The intermediate in the synthesis, debenzoevodiaminic acid ethyl ester (**13**), was prepared in the form of its hydrochloride. Compound **13** also yielded debenzoevodiamine (**11**) after cyclization and reduction. The structures of the compounds prepared have been confirmed by elemental analysis, UV, IR, ^{1}H—NMR and MS spectroscopic data

In our previous paper [1] the preparation of a new rutecarpine derivative, the so-called debenzorutecarpine (**5**) and reduction investigations on its were described.

As a continuation of this work, the synthesis of debenzoevodiamine (**11**) was to be achieved. The studies were continued in two directions: (i) the conversion of debenzorutecarpine (**5**) into debenzoevodiamine (**11**), and (ii) the direct synthesis of debenzoevodiamine (**11**) were attempted.

Methylation of the N(14) nitrogen of rutecarpine (**1**) was described by NAKASATO *et al.* [2]: dehydroevodiamine (**2**) was formed with dimethyl sulfate in benzene. This compound is one of the intermediates in the evodiamine (**4**) synthesis described by PACHTER *et al.* [3].

Dehydroevodiamine hydrochloride (**2**) transforms into retsinine (**3**) under the effect of bases; the latter can be hydrogenated catalytically to obtain evodiamine (**4**)

Methylation of debenzorutecarpine (**5**) could be effected in satifactory yields with a large excess of methyl iodide in nitromethane. The reaction took place at room temperature and debenzorutecarpine methyl iodide (**6**), also referred to as dehydrodebenzoevodiamine hydroiodide (**6**), separated from the reaction mixture in a crystalline state.

* Part VIII: Acta Chim. Acad. Sci. Hung., **99**, 43 (1979)

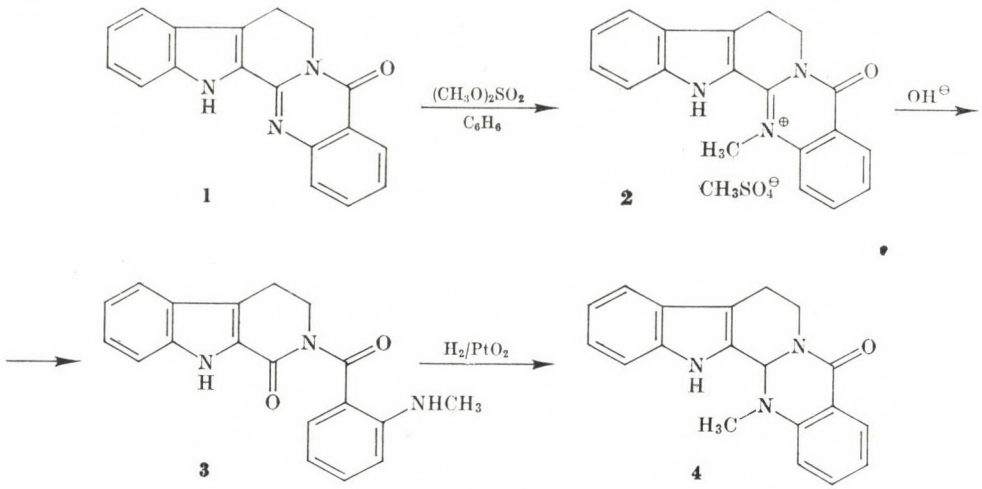

Fig. 1

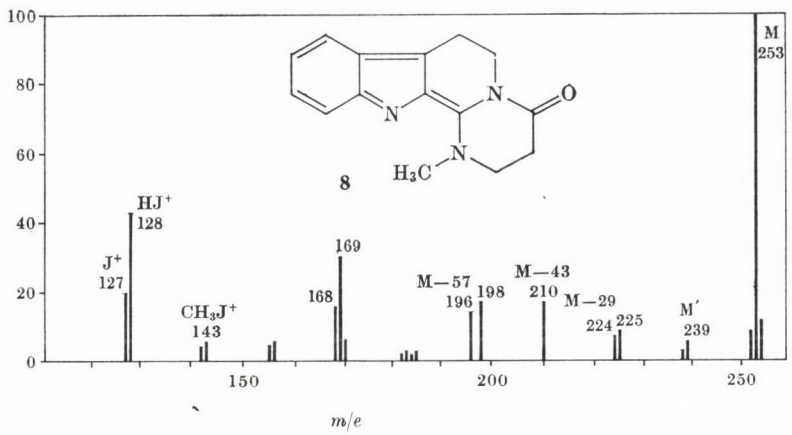

Fig. 2

Mass spectrometric investigation of compound **6** indicated that the corresponding base (**8**) (M^+ 253, base peak) and HI were formed during evaporation. The molecular ion corresponding to the base (**8**) has a significant stability. On the basis of the spectrum, demethylation takes place to a slight extent only (see peak *M*-14 in Fig. 2). The subsequent path of fragmentation is similar to that of debenzorutecarpine (**5**) [1], the formation of the fragment ion of 169 *m/e* with a tetrahydro-β-carboline skeleton is the most significant step here too.

In the IR spectrum of **6**, the carbonyl vibration of the acylamidine group shifts from 1700 cm^{-1} observed in **5** to 1730 cm^{-1}, owing to the presence of a positive charge due to quaternization.

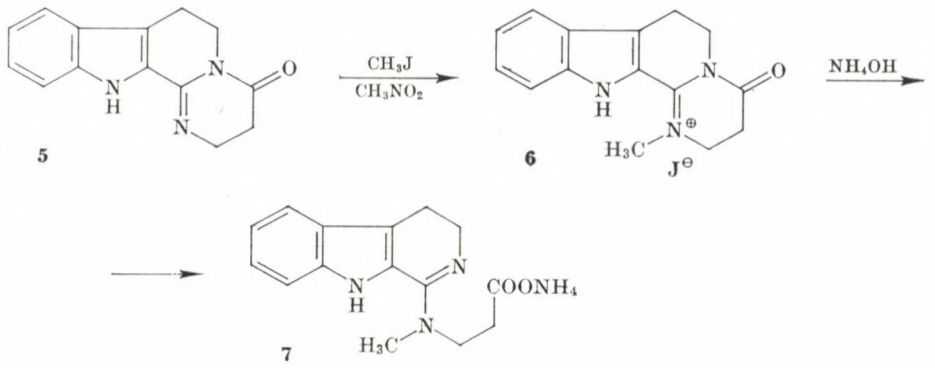

5 6 7

Fig. 3

In the ^1H—NMR spectrum, the $N^+—CH_3$ group appears at δ 4,12 as a singlet. The triplet signal of the methylene protons of rings C and D indicates the high flexibility of these rings and rapid interconversion of the conformers.

Dehydrodebenzoevodiamine hydroiodide (**6**) was then allowed to react with ammonia. Surprisingly the expected ring cleavage did not take place and no debenzorethsinine was formed. The structural investigation of the substance obtained (**7**) has shown that in the case of dehydrodebenzoevodiamine hydroiodide (**6**) the amide bond of the lactam ring was split and, after rearrangement of the double bond, the ammonium salt of debenzoevodiaminic acid (**7**) was formed.

In accordance with this, in the IR spectrum of **7** the characteristic absorption of the carboxylate anion (1560 cm^{-1}) appears and can be evaluated sufficiently well. In the ^1H—NMR spectrum the signal of $N—CH_3$ was shifted to δ 2.93, in accordance with the elimination of the positive charge from the N atom.

This type of ring cleavage has not been described in the literature either for rutecarpine (**1**) or evodiamine (**4**). Upon alkaline treatment of the alkaloids, in addition to norharmane [4—6], *N*-methylanthranilic acid is formed from evodiamine (**4**) while anthranilic acid from rutecarpine (**1**).

In the synthesis of *cis* and *trans*-hexahydrorutecarpine, the two appropriate open-chain aminocarboxylic acids were prepared as intermediates; these yielded the desired compounds on further cyclization [7].

In the preparation of debenzorutecarpine (**5**), the open-chain debenzorutecarpic acid could not be either detected or prepared. Supplementary ring cleavage experiments were carried out under both acidic and alkaline conditions. In both cases the starting compounds of the synthesis, *i.e.* 1,2,3,4-tetrahydro-1-oxo-β-carboline (**9**) and β-alanine (**10**) were recovered.

In continuation of investigations on dehydrodebenzoevodiamine hydroiodide (**6**), the quaternary compound was subjected to reduction. In the reac-

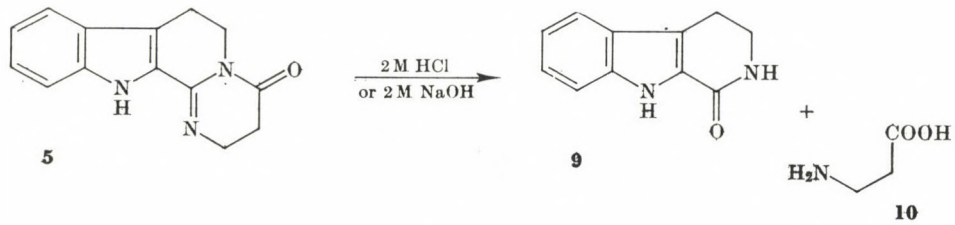

5 9 10

Fig. 4

tion effected in methanol with $NaBH_4$, debenzoevodiamine (**11**) was formed in satisfactory yield.

During spectroscopic investigations of compound **11**, in the mass spectrum the molecular ion was at 255 *m/e* (base peak), in accordance with the formula given. The appearance of the *M*-1 fragment and its nearly 100% intensity indicate the presence of the C(3) proton. This was also confirmed by the ^{1}H—NMR spectrum. The signal of the C(3) proton appears as a singlet at δ 5.60. The chemical shift of the signal of H_e—C(5) is very large in this case, *viz.* 5.08. This indicates that here, similarly to 3,14-dihydrodebenzorutecarpine [1] and *trans*-hexahydrorutecarpine [8] examined earlier, a conformer predominates in the solution in which the H_e—C(5) and C=O groups are coplanar.

The synthesis of debenzoevodiamine (**11**) was also realized by analogy to the synthesis of debenzorutecarpine (**5**) [1]: here the condensation partners were 1,2,3,4-tetrahydro-1-oxo-β-carboline (**9**) and *N*-methyl-β-alanine ester (**12**) [9]. Chromatographic monitoring of the reaction revealed that the condensation took place in two steps. First the open-chain aminocarboxylic acid compound (**13**) was formed and this gradually transformed into the cyclic state. Reduction of the amount of $POCl_3$ employed, and stopping of the reaction at a mixture permitted the isolation of the open-chain intermediate, debenzoevodiaminic acid ethyl ester (**13**) in the form of its hydrochloride.

Spectroscopic examination of compound **13** unambiguously confirmed the structure expected. In the IR spectrum, the stretching vibration of the ester carbonyl appeared at 1720 cm^{-1}. The diffuse absorption between 3300—2700 cm^{-1} refers to the amidinium chloride unit. In the ^{1}H—NMR spectrum the signals of the ethyl ester —O—CH_2—CH_3 group protons were identified at 1.31 (t, 3H) and 4.24 (q, 2H).

Subsequently the isolated debenzoevodiaminic acid ethyl ester hydrochloride (**13**) was refluxed further in the presence of $POCl_3$ in benzene solution. The reaction was monitored chromatographically, then the reaction mixture was processed and dehydrodebenzoevodiamine hydrochloride (**14**) was isolated.

The analytical data of compound **14** agreed perfectly with those of the product of the reactions effected without isolation of the intermediate. Since

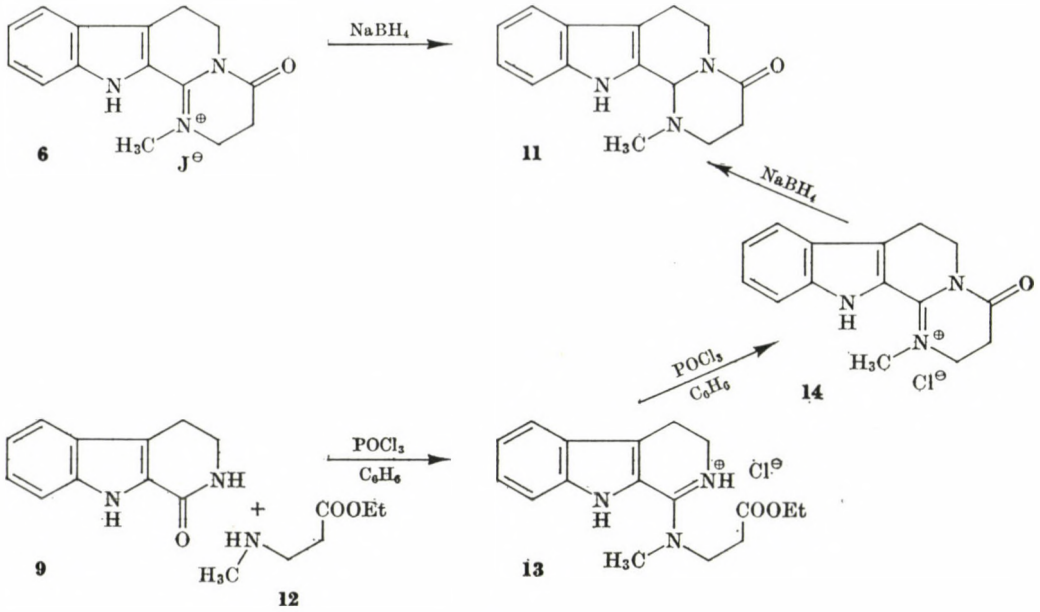

Fig. 5

compound **14** differs from dehydrodebenzoevodiamine hydroiodide (**6**) only in the nature of the halogen, the spectroscopic data were also the same.

Dehydrodebenzoevodiamine hydrochloride (**14**) was then subjected to reduction in the manner discussed earlier, and debenzoevodiamine (**11**) was again obtained.

Experimental

Debenzorutecarpine methyl iodide (6)

Debenzorutecarpine (**5**) (3.00 g, 0.012 mol) was dissolved in nitromethane (200 ml). Freshly distilled methyl iodide (40 ml, 0.6 mol) was added and the mixture was allowed to stand in a dark place at room temperature for 2 days. Yellow needles separated during standing. The mother liquor was concentrated to 2/3 volume and the new crystals formed were filtered off. Recrystallization from ethanol (3.38 g, 70.7%). M.p. 268—270 °C.

$C_{15}H_{16}N_3OI$ (381). Calcd. C 47.24, N 11.02, I 33.35; Found C 47.10, N 11.03, I 33.30%.

UV(EtOH) $\lambda_{max}(\log \varepsilon)$: 242 (4.06); 328 (4.16); 340 (4.00) nm.

IR(KBr): 3520, 3450, 3300 (νNH); 1730 (νC=O); 1615 (νC=N) cm^{-1}.

^1H—NMR (CF_3COOH): H_2—C(6) and H_2—C(16) 3.30 m (4H); H_2—C(5) and H_2—C(15) 4.24 t(2H), 4.48 t, (2H); N^+—CH_3 4.12 s (3H); H—C (9, 10, 11, 12) 7.2—7.8 m (4H); NH 9.76 s (1H).

MS: M^+: 253, 252, 228, 198, 196, 169 *m/e*.

Ammonium salt of debenzoevodiaminic acid (7)

Debenzorutecarpine methyl iodide (**6**) (0.57 g, 0.0015 mol) was dissolved in concentrated ammonium hydroxide (25.0 ml). Compound **6** was dissolved with a yellow colour, then the solution turned into white. It was then extracted with chloroform (2 × 50 and 8 × 25 ml).

The combined chloroform phases were dried over ignited Na_2SO_4, then filtered. After evaporation to dryness, a yellow solid was obtained, which was crystallized from acetone to yield white needles (0.32 g, 74.4%). M. p. 156—158 °C.

$C_{15}H_{20}6N_4O_2$ (288). Calcd. C 62.5, N 19.44; Found C 62.3, N 19.50%.

UV (EtOH): λ_{max}(log ε): 242 (4.43); 320 (4.45) nm.

IR(KBr): 3440, 3200—2700 (νNH and NH_4^+); 1660 (νC=N); 1560, 1400 (νCOO^-) cm^{-1}.

^{1}H—NMR (CD_3OD): H_2—C(16); H_2—C(6) 2.66 t (2H) and 2.7 t (2H); H_2—C(15), H_2—C(5) 3.51 t (2H) and 3.62 t (2H); N—CH_3 2.92 s (3H); H—C (9, 10, 11, 12) 6.95—7.55 m (4H).

MS: M^+ 271 *m/e*.

Debenzoevodiamine (11)

Debenzorutecarpine methyl iodide (**6**) (0.381 g, 0.001 mol) was dissolved in methanol (40 ml), and $NaBH_4$ (0.38 g) was added in small increments. After the evolution of hydrogen had ceased, the deep yellow solution turned into almost colourless, and it was then refluxed on a water bath for 1 hr, and evaporated to dryness in vacuum. The solid residue was dissolved in 2*M* HCl (3 ml) then made alkaline with 2*M* NaOH (4 ml). The alkaline solution was extracted with chloroform (1 × 30 and 4 × 25 ml), the combined chloroform fractions were dried over ignited Na_2SO_4, filtered and evaporated to dryness in vacuum. The residual yellowish-brown oil crystallized under the effect of ethanol; the white crystals were recrystallized from ethanol (0.22 g, 86.2%). M. p. 240—242 °C.

$C_{15}H_{17}N_3O$ (225). Calcd. C 70.75, N 16.47; Found C 70.8, N 16.45%.

UV (EtOH): λ_{max}(log ε): 226 (4.40); 274 (3.95); 282 (3.96) nm.

IR(KBr): 3280 (νNH); 1630 (νC=O) cm^{-1}.

^{1}H—NMR ($CDCl_3$): H_2—C(16) 2.56 t (2H); H_2—C (15) and H_a—C(5) 2.8—3.4 m (5H); H_e—C(5) 5.08 m (1H); H—C(3) 5.60 s (1H); H—C(9, 10, 11, 12) 7.00—7.55 m (4H); NH 8.30 s (1H); N—CH_3 2.41 s (3H).

MS: M^+ 255, 254, 212, 211, 170, 169 *m/e*.

Debenzoevodiaminic acid ethyl ester. HCl (13)

1,2,3,4-Tetrahydro-1-oxo-β-carboline (**9**) (0.93 g, 0.005 mol) was dissolved in a mixture of anhydrous benzene (12.5 ml) and $POCl_3$(4 ml). After dissolution of the substances, *N*-methyl-β-alanine ethyl ester (**12**) was added dropwise. The mixture was then refluxed on a water bath for 3 hrs. The solvent was distilled in vacuum and 15 ml of water was added. The mixture was made alkaline with concentrated NH_4OH and the alkaline solution was extracted with chloroform (2 × 40 and 3 × 20 ml). The combined chloroform fractions were dried over ignited Na_2SO_4 and filtered. A thick oil was obtained after distillation of the chloroform, this was crystallized from acetone. The white crystals were recrystallized from some hot ethanol (1.5 g, 68.8)%. M.p. 187—189 °C.

$C_{17}H_{22}N_3O_2Cl$ (335.5). Calcd. C 60.80, N 12.51, Cl 10.58; Found C 60.95, N 12.70, Cl 10.30%.

UV (EtOH): λ_{max}(log ε): 242 (4.12); 324 (4.30) nm.

IR (KBr): 3300—2700 (νNH indol and amidinium); 1720 ($\nu C{=}O_{ester}$); 1680 ($\nu C{=}N^+_{amidinium}$) cm^{-1}.

^{1}H—NMR ($CDCl_3$ + CD_3OD(9 : 1)): EtO—1.31 t (3H); 4.24 q (2H); H_2—C(16) 2.96 t (2H); H_2—C(6) 3.14 t (2H); H_2—C(5) and H_2—C(15) 3.64 m (2H) and 3.76 t (2H); N—CH_3 3.97 s (3H); H—C(9, 10, 11, 12) 7.05—7.65 m (4H).

MS: M^+ 299 *m/e*.

Dehydrodebenzoevodiamine hydrochloride (14)

a) 1,2,3,4-Tetrahydro-1-oxo-β-carboline (**9**) (3.72 g, 0.02 mol) was dissolved in a mixture of anhydrous benzene (50 ml) and $POCl_3$ (20 ml). *N*-methyl-β-alanine ethyl ester (**12**) (3.1 ml, 0.04) mol was added under cooling. The mixture was refluxed on a water bath for 5 hrs. After the reaction period the solution was cooled and a yellow crystalline substance separated, this was filtered off, washed with benzene and recrystallized from methanol (4.1 g, 71%). M.p. 181—184 °C.

b) Debenzoevodiaminic acid ethyl ester hydrochloride (**13**) (0.35 g, 0.001 mol) was dissolved in a mixture of anhydrous benzene (15 ml) and $POCl_3$ (4 ml). The clear solution was refluxed on a water bath for 2 hrs. After cooling, yellow crystals separated, these were filtered off and recrystallized from ethanol (0.25 g, 82.7%). M.p. 182—184 °C.

$C_{15}H_{16}N_3OCl$ (289.5). Calcd. C 62.10, N 14.50, Cl 12.20; Found C 62.3, N 14.31, Cl 12.00%.

UV(EtOH): ν_{max}(log ε): 242 (4.06); 326 (4.16) nm.

IR (KBr): 3520, 3450 (νNH); 1730 (νC=O); 1615 (νC=N) cm^{-1}.

REFERENCES

[1] PÁL, Z., HORVÁTH-DÓRA, K., TÓTH, G., TAMÁS, J., CLAUDER, O.: Acta Chim. Acad. Sci. Hung., **99**, 43 (1979)
[2] NAKASATO, T., ASADA, S., MARNI, K.: Jakugaka Zasshi, **82**, 619 (1962)
[3] PACHTER, I. J., SULD, G.: J. Org. Chem., **25**, 1680 (1960)
[4] ASAHINA, Y., MAYEDA, S.: J. Pharm. Soc. Japan, **416**, 871 (1916)
[5] ASAHINA, Y., FUJITA, A.: J. Pharm. Soc. Japan, **476**, 863 (1921)
[6] ASAHINA, Y.: J. Pharm Soc. Japan, **503**, 1 (1924)
[7] HORVÁTH-DÓRA, K., TÓTH, G., TAMÁS, J., CLAUDER, O.: Acta Chim. Acad. Sci. Hung., **94**, 345 (1977)
[8] TÓTH, G., HORVÁTH-DÓRA, K., CLAUDER, O., DUDDECK, M.: Ann. Chem., **1977**, 529
[9] LINDSAY, R. D., CHELEDIN, V. H.: J. Am. Chem. Soc., **72**, 828 (1950)

Zoltán PÁL
Klára HORVÁTH-DÓRA
Ottó CLAUDER
H-1092 Budapest, Hőgyes E. u. 7.

Gábor TÓTH
H-1521 Budapest, Gellért tér 4.

József TAMÁS
H-1088 Budapest, Puskin u. 11—13.

Acta Chimica Academiae Scientiarum Hungaricae, Tomus 102 (2), pp. 135—140 (1979)

SEX PHEROMONE OF THE CABBAGE ARMYWORM, *MAMESTRA BRASSICAE*: ISOLATION, IDENTIFICATION AND STEREOCONTROLLED SYNTHESIS

L. NOVÁK,[1] M. TÓTH,[2] J. BALLA[3] and Cs. SZÁNTAY[1]

([1]Institute for Organic Chemistry, Technical University, Budapest and Central Research Institute for Chemistry; [2]Research Institute for Plant Protection, Budapest, and [3]Institute for General and Analytical Chemistry, Technical University, Budapest)

Received October 3, 1978
Accepted for publication October 31, 1978

Two major components of the cabbage armyworm's sex pheromone, (*Z*)-11-hexadecenyl acetate and (*Z*)-11-heptadecenyl acetate, were isolated, identified and then synthesized employing the stereoselective Wittig-olefination as the key step.

The existence of a female sex pheromone in the cabbage armyworm (*Mamestra brassicae* L., Lepidoptera, Noctuidae) was evidenced by two research groups [1, 2]. Recently, BESTMANN *et al.* [3, 4], and MARTIN *et al.* [5] have identified and synthesized the major component of the pheromone as (*Z*)-11-hexadecen-1-yl acetate (**1a**), but the minor component(s) remained still unknown. The present work was completed in order to achieve a more detailed knowledge of the chemical nature of all components in the pheromonal secretion of female *Mamestra brassicae*.

The moths used originated from a laboratory culture maintained on a semisynthetic diet [6] at 28 °C and 60—80% rel. hum. The pupae were sexed and the emerging adults were held at a reversed 18/6 light/dark photoregime.

The isolation of the pheromone was made by excising the abdomen tips of approximately 300 calling virgin females and extracting them in hexane. Beside this method, Porapak Q collection of volatiles originating from about 160 3 to 5 days old females was also conducted [7].

In our laboratory bioassay the precopulatory behaviour response of males was monitored. Walking with wing fanning and flying were chosen as the key responses. In every repetition four 3 to 5 days old unmated males were used and at every test this treatment was replicated at least 15 times. Data were also corrected for basic activity.

Gas chromatographic analysis of the concentrated hexane extract showed a multicomponent mixture, which consisted of two major components in a 95 : 5 ratio.

The principal component proved to be (*Z*)-11-hexadecenyl acetate (**1a**), as recently reported by BESTMANN *et al.* [3, 4]. The minor component had a

longer retention time on the non-polar silicone column, and it was assumed that it might have a structure similar to **1a**, but a higher molecular weight.

The GC—MS analysis of the extract exhibited a characteristic mass spectrum of the minor component and indicated that the molecular weight was 296. Furthermore, there was a dominating fragment at *m/e* 236 resulting from the loss of CH_3COOH from the molecular ion. A weak but typical ion for acetates was also present at *m/e* 61 ($CH_3COOH_2^+$). Signals at *m/e* 192 and 96 indicated that the unsaturation in the long-chain acetate was in position 11. (For details, see Experimental.)

Because the molecular weight of the compound indicated a chemical composition of $C_{19}H_{36}O_2$, and the mass spectrum was very similar to the spectrum of **1a**, we synthetized the (*Z*)-11-heptadecenyl acetate (**1b**), and run its spectrum. The two spectra showed excellent agreement, which proved that the minor component of the pheromone system was (*Z*)-11-heptadecenyl acetate (**1b**).

The method used for the preparation of the pheromone components (**1a** and **1b**) is shown in Chart I. The hydroxyl group of 11-bromo-undecen-1-ol (**2**; X=H) was protected by conversion to the tetra-

Chart I

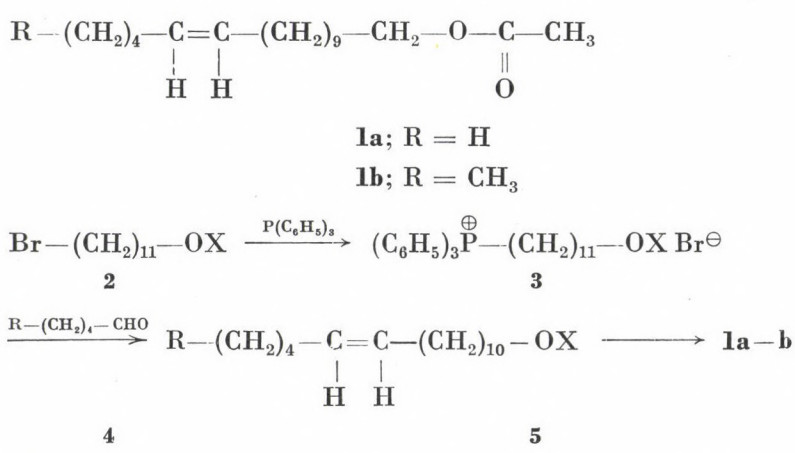

hydropyranyl ether (**2**; X=THP) [8], which was then treated with triphenylphosphine.

The resulting triphenylphosphonium salt (**3**; X=THP) was converted to an ylide with sodium methylsulfinylmethide in dimethyl sulfoxide and allowed to react with hexanal (**4**; R=CH_3) to form the tetrahydropyranyl ether of (*Z*)-11-heptadecen-1-yl acetate (**5**; R=CH_3; X=THP). Subsequent refluxing with acetyl chloride in acetic acid cleaved the protecting group to form the desired (*Z*)-11-heptadecen-1-yl acetate (**1b**).

In an alternative synthetic route, the bromohydrin (**2**; R=H) was transformed by treatment with ethyl vinyl ether into the ethoxy ether derivative [**2**; X=CH(CH_3)OEt], which was treated with triphenylphosphine. The resulting phosphonium salt [**3**; X=CH(CH_3)OEt] was made to react with potassium metal predissolved in hexamethylphosphoric triamide to form the ylide, and this was condensed with hexanal to give the ethoxy ether derivative of (*Z*)-11-heptadecenyl acetate [**5**; R=CH_3; X=Ch(CH_3)OEt]. Removal of the protecting group by reaction with an acid in methanol, followed by acetylation afforded the pheromone component **1b**.

The method of preparing the main component of the sex attractant (**1a**) was somewhat more direct. Acetylation of the bromohydrin (**2**; R=H), followed by treatment with triphenylphosphine afforded the triphenylphosphonium salt (**3**; X=Ac). This was converted to the corresponding ylide using sodium methylsulfinylmethide, which was allowed to react with pentanal (**4**; R=H) to give (*Z*)-11-hexadecen-1-yl acetate (**1a**).

The above synthesis was simpler than the previous one [4], but the yield was rather moderate (25%, based on the phosphonium salt used).

The stereochemical homogeneity of the samples was proved by gas chromatography and TLC analysis ($AgNO_3$-impregnated silica gel). The substances (**1a** and **1b**) were homogeneous as judged by VPC with $< 2\%$ impurities present.

In laboratory bioassays, a mixture of **1a** and **1b** in the natural ratio (9.5 : 0.5) induced a 50% response at a 4.2 ng dose, whereas by **1a** alone the same response could be elicited only with 47 ng. Compound **1b** tested alone though exhibited some activity, a 50% response could be achieved only by a dose of about 350 ng.

Beside proving the synergistic effect of **1b**, our laboratory bioassay was not suitable for clarifying other aspects of biological function(s) of the components; for completing this more extensive field testing is needed.

Although there are a number of other Noctuidae in which multicomponent pheromone systems have been identified [9, 10], this is the first report of a pheromone mixture containing two acetates of which the first has an even numbered and the second on odd numbered carbon chain.

Experimental

Boiling points are uncorrected. IR spectra refer to films and were determined on a Spektromom 2000 spectrometer. NMR spectra were recorded in CCl_4 solutions at 60 MHz, with TMS internal standard, on a Perkin Elmer R12 spectrometer. GLC analyses were performed on a Pye 105 gas chromatograph (4% SE-30 and 6% OV-210 on chromosorb W 60—80 mesh, 2 mm × 2 m glass column; carrier gas He; 195 °C), GC/MS measurements were taken on a JEOL JGC-20K and JMS-O1SG-2 combined system (ionizing energy 75 eV, acc. voltage 10 kV, ionizing current 200 A). Compounds **2** (R=H) and **4** were obtained commercially and purified by standard procedures.

11-Bromo-1-undecyl acetate (2; X = Ac)

Ac_2O (15 ml; 0.15 mole) was added to a solution of 11-bromo-1-undecanol (30 g; 0.12 mole) in dry benzene (100 ml) and the mixture was allowed to stand overnight at room temperature. Removal of the solvent and distillation of the residue gave 31.4 g (90%) of **2** (X = Ac), b.p. 120 °C/0.1 mm; ν_{max} 1735, 1360, 1230, 1040 cm^{-1}; δ 1.3 (18H, m), 1.96 (3H, s), 3.35 (2H, t, J = 7 Hz), 3,95 (3H, t, J = 7 Hz).

11-Acetoxy-1-undecyl-triphenylphosphonium bromide (3; X = Ac)

A mixture of the bromide **2** (X=Ac; 30 g; 0.1 mole) and tripenylphosphine (26 g; 0.1 mole) in dry acetonitrile (100 ml) containing anhydrous potassium carbonate (1 g) was refluxed on a water bath for 15 h. The reaction mixture was cooled, filtered and the acetonitrile evaporated. The residue was extracted three times with dry ether (300 ml) and dried in vacuum at room temperature overnight to obtain 45.3 g (80%) of **3** (X=Ac) as a pale yellow material; ν_{max} 1740, 1360, 1240, 1150, 1040 cm^{-1}; δ 1.2 (14H, m), 1.5 (4H, m), 2 (3H, s), 3.5 (2H, m), 4 (3H, t, J = 7 Hz), 7.7 (15H, m).

(Z)-11-Hexadecen-1-yl acetate (1a)

To a solution of sodium methylsulfinylcarbanion (prepared from 2.5 g; 0.13 mole of sodium hydride) in dimethyl sulfoxide (30 ml) was added a solution of 11-acetoxy-1-undecyl-triphenylphosphonium bromide (**3**; X=Ac; 20 g; 0.036 mole) in dimethyl sulfoxide (40 ml) with stirring at room temperature. After the mixture had been stirred for 30 min, the dark orange solution of the resulting ylide was cooled to +5 °C and pentanal (4.0 g; 0.04 mole), in dimethyl sulfoxide (10 ml) was added. The suspension was stirred for 10 h at room temperature, then poured into water, and the resulting mixture was extracted with hexane (200 ml). The organic phase was washed succesively with water, 5% sulfuric acid, water, aqueous sodium hydrogen sulfate, water and then dried over magnesium sulfate. The hexane was evaporated and the residue fractionally distilled to afford **1a** (2.5 g; 25%), b.p. 120—122 °C/0.25 mm (*lit.* [4] 108 °C/0.1 mm); ν_{max} 1740, 1380, 1365, 1235 cm^{-1}; δ 0.9 (3H, t, J = 7 Hz), 1.3 (20H, m), 2 (7H, s + m), 4.05 (2H, t, J = 7 Hz), 5.35 (2H, m).

GC: *Rt* 11.9 min.

MS: M^+ 282 (<1), *m/e* 223 (31), 138 (15), 124 (21), 110 (43), 97 (96), 83 (100), 82 (75), 70 (57), 69 (69), 57 (13), 55 (99), 44 (69), 42 (57), 28 (53).

11-Bromoundecan-1-ol tetrahydropyranyl ether (2; X = THP)

A mixture f 5 g (0.059 mole) of dihydropyran, 10 g (0.04 mole) of 11-bromo-1-undecanol, and 3 drops of *conc.* HCl was stirred at room temperature overnight. The mixture was then stirred a few minutes with solid potassium carbonate, dried ($MgSO_4$) and concentrated in vacuum to give 10.5 g of **2** (X=THP); δ 1.25—2.2 (24H, m), 3.5 (6H, m), 4.5 (1H, m). This was employed for the next step without further purification.

11-(2-Tetrahydropyranyloxy)-1-undecyl-triphenyl-phosphonium bromide (3; X = THP)

The bromide **2** (X=THP) (13 g; 0.039 mole) was added to a solution of triphenylphosphine (11 g; 0.04 mole) in dry acetonitrile (30 ml) and heated under reflux for 10 h, in the presence of potassium carbonate (0.5 g). The mixture was filtered, concentrated in vacuum and then vigorously shaken with ether followed by decantation (three portions of 100 ml each). The remaining residue was dried in vacuum at room temperature overnight to obtain 19 g (82%) of **3** (X=THP); δ 1.2—2 (24H, m), 3—4 (6H, m), 4.5 (1H, m), 7.5—8.3 (15H, m).

(Z)-11-Heptadecen-1-ol terahydropyranyl ether (5; R = CH_3; X = THP)

Sodium methylsulfinylcarbanion (dimsylsodium) was prepared in the usual manner from sodium hydride (1.1 g; 0.037 mole) and dimethyl sulfoxide (15 ml). A solution of 11-(2-tetrahydropyranyloxy)-1-undecyl-triphenylphosphonium bromide (**3**; X=THP) (10.5 g; 0.017 mole) in dry dimethyl sulfoxide (20 ml) was added with stirring at room temperature. The mixture turned dark orange; it was stirred for 0.5 h at 50 °C and then a solution of freshly

distilled hexanal (1.7 g; 0.017 mole) in dimethyl sulfoxide (5 ml) was added. All these operations were carried out under an argon atmosphere and the solutions were introduced through a rubber septum. The mixture was strirred at room temperature for 5 h, the reaction was then quenched by adding water (30 ml) with cooling, and the resulting solution was extracted with hexane (150 ml). The hexane solution was washed successively with water, 5% sulfuric acid, saturated sodium chloride solution and dried. Removal of the solvent gave **5** (R=CH_3; X=THP), (4.65 g; 82%); δ 0.9 (3H, t, J = 7 Hz), 1.1—1.7 (28H, m), 1.9 (4H, m), 3.5 (4H, m), 4.5 (1H, m), 5.25 (2H, t, J = 6 Hz).

$C_{22}H_{42}O_2$. Calcd. C 78.04; H 12.51. Found C 77.86; H 12.37%.

(*Z*)-11-Heptadecen-1-yl acetate (1b)

A solution of the tetrahydropyranyl ether (**5**; R=CH_3; X=THP; 5.7 g; 0.016 mole), acetic acid (10 ml) and acetyl chloride (3 ml) was refluxed for 4 h and then allowed to stand overnight. The solution was poured into ice and extracted with hexane (100 ml). The ethereal extract was washed with water and dried over $MgSO_4$. After removal of the solvent, the residue was distilled to give oily **1b** (2.6 g; 52%); b.p. 122—126 °C/0.25 mm; ν_{max} 1740, 1380, 1360, 1230, 1040 cm^{-1}; δ 0.9 (3H, t, J = 7 Hz), 1.3 (22H, m); 2 (7H, s + m), 4.05 (2H, t, J = 7 Hz), 5.35 (2H, m).

$C_{19}H_{36}O_2$. Calcd. C 76.97; H 12.24; Found C 76.72; H 11.98%.

GC: *Rt* 15.4 min.

MS: M^+ 296 (<1), *m/e* 236 (27), 192 (5.2), 152 (10), 138 (14), 124 (17), 110 (39), 96 (76), 83 (37), 82 (81), 69 (42), 61 (12), 55 (69), 43 (46), 28 (100).

1-Bromo-11-(1-ethoxy-ethoxy)undecane [2; X = $CH(CH_3)OEt$]

To a cooled mixture of 11-bromo-1-undecanol (10 g; 0.04 mole), and freshly distilled ethyl vinyl ether (3.6 g; 0.05 mole) was added 2 drops of *conc.* HCl, and the resulting solution was stirred at room temperature for 1 h. The mixture was then stirred a few minutes with solid potassium carbonate, filtered and the excess of ethyl vinyl ether was evaporated in vacuum to leave 11 g of **2** [X=$CH(CH_3)OEt$], a viscous, yellowish oil; δ 1.3 (24H, m), 3.45 (6H, m), 4.65 (1H, q, J = 6 Hz). The compound suffered thermal decomposition upon attempted distillation.

11-(1-Ethoxy-ethoxy)-1-undecyl-triphenylphosphonium bromide [3; X=$CH(CH_3)OEt$]

The bromide **2** [X=$CH(CH_3)OEt$; 9.69 g; 0.03 mole] was added to a solution of triphenylphosphine (7.86 g; 0.03 mole) and potassium carbonate (0.5 g) in dry acetonitrile (40 ml), and the mixture was heated under reflux for 16 h. After filtration, the solvent was evaporated in vacuum and the residue shaken with ether followed by decantation (two 150-ml portions). The viscous residue was dried in vacuum overnight to obtain 13 g (74%) of **3** [X=$CH(CH_3)OEt$]; δ 1.3 (24H, m), 3.45 (6H, m), 4.65 (1H, q, J = 6 Hz), 7.5—8.3 (15H, m).

(*Z*)-1-(1-Ethoxy-ethoxy)-11-heptadecenol [5; R = CH_3; X = $CH(CH_3)OEt$]

Potassium metal (1.4 g; 0.036 g-atom) was added with stirring to dry hexamethylphosphoric triamide (40 ml) and the mixture was stirred at room temperature for 1 h under an argon atmosphere. A solution of the phosphonium bromide **3** [X=$CH(CH_3)OEt$; 11.7 g; 0.02 mole] in dry hexamethylphosphoric triamide (15 ml) was added and the mixture was stirred at room temperature for 1 h in vacuum in order to remove the dimethylamine generated in the reaction. Then freshly distilled hexane (2 g; 0.02 mole) was added dropwise at 0 °C and the resulting mixture was stirred at room temperature for 8 h. The reaction was quenched by adding water with cooling and the solution was extracted with hexane (150 ml). The organic phase was washed successively with water, cold 5% sulfuric acid, water, aqueous sodium hydrogen sulfite, saturated brine, and dried over magnesium sulfate, finally concentrated in vacuum to give **5** [R=CH_3; X=$CH(CH_3)OEt$; 4.4 g; 67%]; δ 0.9 (3H, t, J = 7 Hz), 1.3 (28H, m), 3.5 (4H, m), 4.65 (1H, q, J = 6 Hz), 5.45 (2H, m). This product was used in the next step without further purification.

(*Z*)-11-Heptadecen-1-yl acetate (1b)

To a solution of the ethoxy ether **5** [R=CH_3; X=$CH(CH_3)OEt$; 5 g) in methanol (20 ml) was added 4 drops of *conc.* HCl, and the resulting solution was stirred at room temperature for 4 h. The mixture was then poured into water and extracted with ether. The ethereal extract was washed with water, dried ($MgSO_4$), concentrated and the residue distilled in vacuum to give (*Z*)-11-heptadecen-1-ol (**5**; R=CH_3; X=H; 2.5 g, 58%), b.p. 165 °C/0.25 mm; ν_{max} 3400, 1380, 1050 cm^{-1}; δ 0.9 (3H, t, J = 7 Hz), 1.3 (22H, m), 2 (4H, m), 3.5 (2H, m), 4.5 (1H, m), 5.3 (2H, m).

$C_{17}H_{34}O$. Calcd. C 80.24; H 13.47. Found C 80.04; H 13.35%.

Acetic anhydride (3 ml) was added to a stirred, ice-cooled mixture of the alcohol **5** (R=CH_3; X=H; 2.5 g) in dry pyridine (5 ml). After 3 h at room temperature, the solution was poured onto ice and the resulting mixture was extracted with ether. The organic phase was washed successively with water, 5% sulfuric acid, water and dried. The residue obtained after removal of the solvent in vacuum was distilled to give **1b** (2.25 g; 42% based on the ethoxy ether used), b.p. 122—125 °C/0.25 mm. The compound proved to be identical with the one prepared above.

REFERENCES

[1] SZENTESI, A., TÓTH, M., DOBROVOLSZKY, A.: Acta Phytopathol. Acad. Sci. Hung., **10,** 425 (1975)
[2] OTTO, D., PILZ, R., BEHNISCH, I.: Arch. Phytopathol. und Pflanzenschutz, Berlin, **12,** 197 (1976)
[3] BESTMANN, H. J., VOSTROWSKY, O., KOSCHATZKY, K. H., PLATZ, H., SZYMANSKA, A., KNAUF, W.: Tetrahedron Letters, **1978,** 605
[4] BESTMANN, H. J., KANTARDJIEW, I., RÖSEL, P., STRANSKY, W., VOSTROWSKY, O.: Chem. Ber., **111,** 248 (1978)
[5] DESCOINS, C., PRIESNER, E., GALLOIS, M., ARN, H., MARTIN, G.: Compt. Rend. Acad. Sci. Ser. D, **286,** 77 (1978)
[6] NAGY, B.: Acta Phytopathol. Acad. Sci. Hung., **5,** 73 (1970)
[7] BYRNE, K. J., GORE, W. E., PEARCE, G. T., SILVERSTEIN, R. M.: J. Chem. Ecol., **1,** 1 (1975)
[8] SCHILL, G., MURJAHN, K.: Chem. Ber., **104,** 3587 (1971)
[9] NESBITT, B. F., BEEVOR, P. S., COLE, R. A., POPPI, R. G.: Nature (New Biol.), **244,** 208 (1973)
[10] TAMAKI, Y., NOGUCHI, H., YUSHIMA, T.: Appl. Entomol. Zool., **8,** 200 (1973)

Lajos NOVÁK, Csaba SZÁNTAY } H-1521 Budapest, Gellért tér 4.

Miklós TÓTH H-1022 Budapest, Hermann Ottó u. 15.
József BALLA H-1521 Budapest, Gellért tér 4.

Acta Chimica Academiae Scientiarum Hungaricae, Tomus 102 (2), pp. 141—142 (1979)

OXAZEPINES AND THIAZEPINES, VI*

A CONVENIENT SYNTHESIS OF BENZOTHIAZEPINE SULFOXIDES *(SHORT COMMUNICATION)*

A. LÉVAI

(Institute of Organic Chemistry, Kossuth Lajos University, Debrecen)

Received September 22, 1978
Accepted for publication November 3, 1978

In spite of the fact that various methods are known for the synthesis of the sulfoxides of sulfur-containing heterocyclic compounds [2—5], the preparation of benzothiazepine sulfoxides are hardly mentioned in the literature. Very few representatives of such derivatives have yet been described; these were synthesized by the sodium periodate oxidation of the corresponding

Table I

Physical constants and analysis data of the compounds prepared

	Compound	M.p., °C	Yield, %	Overall formula	Analysis, %			
					Calculated		Found	
					N	S	N	S
I	2,3-Dihydro-2-phenyl-1,4-benzothiazepin-5(4*H*)-one-1-oxide	290 decomp.	63.4	$C_{15}H_{13}O_2NS$	5.16	11.80	5.02	11.74
II	2,3-Dihydro-2-phenyl-1,5-benzothiazepin-4(5*H*)-one-1-oxide	201—202 (d.)	77.8	$C_{15}H_{13}O_2NS$	5.16	11.80	5.09	11.57
III	2,3-Dihydro-2-phenyl-3-methyl-1,5-benzothiazepin-4(5*H*)-one-1-oxide	276—277	56.6	$C_{16}H_{15}O_2NS$	4.91	11.22	4.86	10.86
IV	2,3-Dihydro-2-phenyl-3-acetamino-1,5-benzothiazepin-4(5*H*)-one-1-oxide	267—268	76.9	$C_{17}H_{16}O_3N_2S$	8.56	9.75	8.61	9.71
V	2-Phenyl-3-bromo-1,5-benzothiazepin-4(5*H*)-one-1-oxide	171—172	76.3	$C_{15}H_{10}O_2NSBr$	4.01	9.19	4.03	9.11

* For Part V, see Ref. [1]

benzothiazepines [6—8]. By means of the oxidation of benzothiazepines with hydrogen peroxide only sulfones have hitherto been obtained [9—11].

Recently MAGNIA [12] worked out a simple and convenient method for the synthesis of penicillin and cephalosporin sulfoxides with the help of oxidation with hydrogen peroxide in the presence of formic acid or acetic acid. This procedure has now been applied for the preparation of benzothiazepine sulfoxides. 2,3-Dihydro-2-phenyl-1,4-benzothiazepin-5(4*H*)-one, 2,3-dihydro-2-phenyl-1,5-benzothiazepin-4(5*H*)-one, its 3-methyl and 3-acetamino derivatives and 2-phenyl-3-bromo-1,5-benzothiazepin-4(5*H*)-one, respectively, were allowed to react with hydrogen peroxide in the presence of formic acid; the products were the corresponding sulfoxides (**I**—**V**) (Table I). The sulfoxide character of the compounds prepared is unequivocally proved, besides the analyses, by the $\nu S{=}O$ bands appearing in their IR spectra at about 1040 and 1070 cm^{-1}. Sulfone formation was not observed; this is in accordance with the results of MAGNIA obtained for penicillin and cephalosporin derivatives [12].

Experimental

M.p.'s are uncorrected.
IR spectra were recorded with a Perkin-Elmer 283 instrument in KBr discs.

Oxidation of Benzothiazepines — General Procedure

Benzothiazepine (10 mmoles) was dissolved in dichloromethane (150 ml) and 30% hydrogen peroxide (12 mmoles) and formic acid (40 mmoles) were added to the solution. The reaction mixture was stirred for 7 h at room temperature. The solvent was then evaporated in vacuum and the residue crystallized from ethanol to obtain the product as white crystals (Table I).

*

The author's thanks are due to Dr. Z. DINYA for the IR spectra and to the Hungarian Academy of Sciences for financial support of this research.

REFERENCES

[1] LÉVAI, A., BATA, GY.: Acta Chim. Acad. Sci. Hung. **99,** 331 (1979)
[2] CHOW, A. W., HALL, N. M., HOOVER, J. R. E.: J. Org. Chem., **27,** 1381 (1962)
[3] KAISER, G. V., COOPER, R. D. G., KOEHLER, R. E., MURPHY, C. F., WEBBER, J. A., WRIGHT, I. G., VAN HEYNINGEN, E. M.: J. Org. Chem., **35,** 2430 (1970)
[4] SPRY, D. O.: J. Org. Chem., **37,** 793 (1972)
[5] MICETICH, R. G.: Synthesis, **1976,** 264
[6] STERNBACH, L. H., LEHR, H., REEDER, E., HAYES, T., STEIGER, N.: J. Org. Chem., **30,** 2818 (1965)
[7] THOMAS, P. C., PAUL, I. C., WILLIAMS, T., GRETHE, G., USKOKOVIC, M.: J. Org. Chem., **34,** 365 (1969)
[8] BOSE, A. K., HOFFMAN III, W. A., MANHAS, M. S.: J. Chem. Soc. Perkin I, **1976,** 2343
[9] HIDEG, K., HANKOVSZKY, O. H.: Acta Chim. Acad. Sci. Hung., **56,** 405 (1968)
[10] WÜNSCH, K. H., EHLERS, A.: Chem. Ber., **102,** 1869 (1969)
[11] WÜNSCH, K. H., STAHNKE, K. H., EHLERS, A.: Chem. Ber., **103,** 2302 (1970)
[12] MAGNIA, A.: Synthesis, **1978,** 361

Albert LÉVAI H-4010 Debrecen P. O. Box 20.

Acta Chimica Academiae Scientiarum Hungaricae, Tomus 102 (2), pp. 143—150 (1979)

INDIRECT POLAROGRAPHIC STUDY OF ACID — BASE EQUILIBRIA OF SOME BENZOIC ACID DERIVATIVES

É. GYÁRFÁS, B. TŐKÉS and L. KÉKEDY[1]

(Laboratory of Physical Chemistry, Medical and Pharmaceutical Institute, Tîrgu Mureş, Romania, [1]Department of Inorganic and Analytical Chemistry, "Babeş-Bolyai" University, Cluj-Napoca, Romania)

Received April 12, 1978
In revised form October 22, 1978
Accepted for publication November 14, 1978

Dissociation and recombination rate constants of benzoic acid and ten derivatives have been determined using RÜETSCHI's indirect polarographic method in the presence of azobenzene and/or *p*-nitraniline, respectively. The quantitative data obtained are correlated with structural considerations.

Introduction

In a previous paper [1] we have reported on the acid-base behaviour of benzoic acid and some derivatives based on the direct polarographic investigation of the kinetic current of H^+-ions formed in the equilibrium reaction:

$$HA \underset{k_r}{\overset{k_a}{\rightleftharpoons}} H^+ + A^- \tag{1}$$

characterized by the acidity constant

$$K_a = \frac{k_d}{k_r}, \tag{2}$$

k_d and k_r being the dissociation and the recombination rate constants, respectively. However, with very weak acids the kinetic hydrogen wave appears at too negative potentials, being masked by the supporting electrolyte. In this case RÜETSCHI's indirect method [2, 3], in accordance with the WEBER—KOUTECKÝ theory [4] can be applied. It is based on the property of some organic compounds, like azobenzene [2, 3], or *p*-nitraniline [5] (mediators), which in the presence of H^+-ions yield double reduction waves (Fig. 1). The first wave is determined both by the rate of the dissociation of the weak acid present and diffusion, allowing the evaluation of the respective rate constants, k_d and k_r, respectively. The second wave is diffusion-controlled and corresponds to the

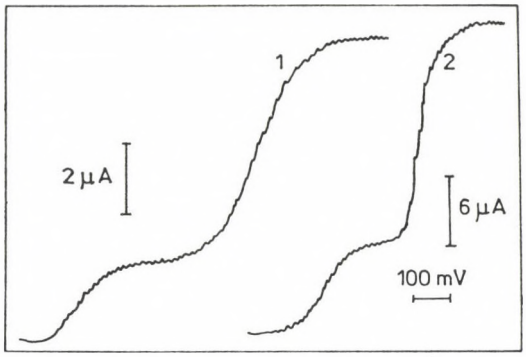

Fig. 1. The double reduction wave of azobenzene (1) and of *p*-nitraniline (2) in the presence of benzoic acid. Experimental conditions: see in the text

reduction of the organic mediator compound unaffected by protons. The limiting current of the first wave is given by the equation [2]:

$$\frac{i}{kt_1^{1/2}} = 0.87MD^{1/2}\,\alpha\sqrt{\frac{K_a k_d}{[A^-]}} - 0.87M\sqrt{\frac{K_a k_d}{[A^-]}}\cdot\frac{i}{k} \tag{3}$$

where

$$k = 0.627\cdot 10^{-3}\, nFm^{2/3} t_1^{1/6} \tag{4}$$

$$\alpha = \frac{D_{H^+}[H^+] + D_{HA}[HA]}{D} \tag{5}$$

$$D = \frac{D_{H^+} + \dfrac{[A^-]}{K_a} D_{HA}}{1 + \dfrac{[A^-]}{K_a}} \tag{6}$$

$$M = \frac{D}{D_{HA}}\sqrt{\frac{D_{H^+}}{D_{HA}}} \approx \sqrt{\frac{D_{H^+}}{D_{HA}}}\,. \tag{7}$$

This indirect method can be applied to electrochemically inactive weak acids. The kinetic current can be observed if it differs from the diffusion current at least by 10%, *i.e.*:

$$i/i_d \leqslant 0.9 \tag{8}$$

Considering equation (3), the above inequality can be written in the form:

$$\lambda = 0.87\sqrt{\frac{k_d K_a t_1}{[A^-]}\cdot\frac{D_{H^+}}{D_{HA}}} \leqslant 9\,. \tag{9}$$

Since in general $t_1 \sim 3$ s and $D_{H+}/D_{HA} \sim 3$, condition (9) is equal to:

$$\frac{k_d K_a}{[A^-]} \leqslant 4 . \tag{10}$$

The minimal value of λ in equation (9) being $\lambda \geqslant 1/100$, it follows that with the indirect polarographic method electrochemically inactive acids with $5 > > pK_a > 10$ can be investigated. Equation (3) is valid if the dissociation reaction (1) is pseudo-monomolecular, and the recombination one is monomolecular. This condition is fulfilled if the investigations are performed in well buffered solutions containing a large excess of anion (at least ten times the concentration of the acid). In order to avoid the influence of the electric field of the electrode on the rate of dissociation, the thickness of the reaction layer (μ), *i.e.* the distance traversed by the H^+-ions during their mean lifetime should be considerably greater than the diffuse part of the electric double layer (δ):

$$\mu \gg \delta \tag{11}$$

The minimal value of the bulk anion concentration is 10^{-2} *M*, otherwise the concentration of the anions in the reaction layer $[A^-]_\mu$ would differ considerably from that in the solution. At these relatively small concentrations the effective thickness of the reaction layer is small, relationship (11) obeys only in more concentrated supporting electrolyte. The best results have been obtained in 1.9 *M* LiCl. In this case

$$\mu = \left(\frac{D_{H^+}}{k_r[A^-]}\right)^{1/2} = \left(\frac{4.94 \times 10^{-6}}{1.6 \times 10^9 \times 2.3 \times 10^{-2}}\right)^{1/2} = 3.7 \times 10^{-7}\ \text{cm}$$

and

$$\delta = \left(\frac{1000\, \varepsilon\, kT}{8e_0^2 N_A I}\right)^{1/2} = \left(\frac{1000 \times 3i \times 5 \times 1.38 \times 10^{-16}\, 298}{8 \times 3.14(4.8 \times 10^{-10})^2\, 6.023 \times 10^{23} \times 1.93}\right)^{1/2} =$$

$= 1.4 \times 10^{-8}$ cm, respectively. The symbols have their usual meaning [6].

Experimental

Benzoic acid and ten derivatives were investigated in 2×10^{-3} *M* concentration in 1.9 *M* LiCl in 85% aqueous ethanol (to decrease the strength of the acids) at 25° in the presence of either azobenzene (2.5×10^{-3}), or *p*-nitraniline (2.0×10^{-3} *M*), (mediators). The supporting electrolyte contained the respective Na-salts of the acids in 2.3×10^{-3} *M* concentration. The reduction waves of the organic mediators have been recorded with an LP-55 Type Polarograph using an EZ-2 Type recorder. A water-jacketed H-cell was used with a S.C.E. reference electrode and an agar bridge containing sat. KCl. In the course of the corresponding experiments the drop time varied between 2.30 and 4.70 s. Constant working temperature of 25± 0.05 °C was assured using an U-10 Type thermostat. The acidity constants in the conditions of our experiments were determined potentiometrically using a Präcitronic MV 85 electronic potentiometer (Dresden).

Results and Discussion

The dissociation rate constant k_d has been computed from equation (3) using the drop time method [2]: the variation of the kinetic current (first wave) being followed as a function of drop time (the same capillary), (Fig. 2). In this

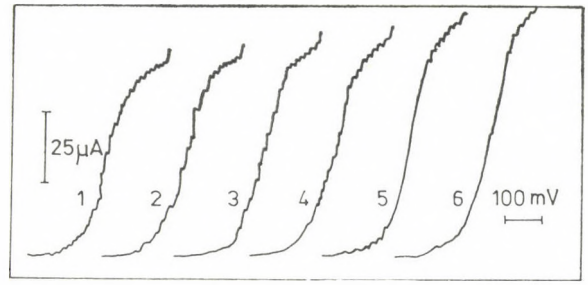

Fig. 2. The variation of the kinetic current of *p*-nitraniline (first wave) in the presence of benzoic acid as a function of drop time. Drop times in s: 1 — 4.71; 2 — 4.21; 3 — 3.75; 4 — 3.10; 5 — 2.60; 6 — 2.30

case

$$k = \text{const.}\ m^{2/3} t_1^{1/6} \tag{12}$$

and since

$$mt_1 = \text{const.} \tag{13}$$

equation (3) becomes:

$$it_1^{1/2} = \text{cont.} - \frac{[A^-]}{0.87\, M(K_a\, k_d)^{1/2}}\, i\,. \tag{14}$$

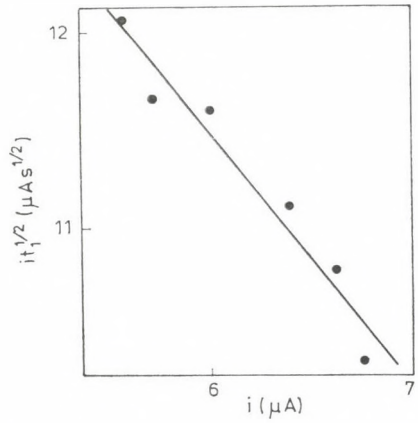

Fig. 3. Variation of $it_1^{1/2}$ a a function of i (equation 14) for the *p*-nitraniline — benzoic acid system

Thus k_d can be calculated from the slope of the line $it^{1/2}$ *vs.* i. (Fig. 3). The experimental data obtained are given in Tables I and II, respectively.

Table I

Experimental data obtained in the presence of azobenzene

R–C_6H_4–COOH (R)	$it_1^{1/2}$ (Equation 14)	Statistical data	
		r	S_0
H	$-(1.23 \pm 0.22)i + (8.73 \pm 0.62)$	−0.956	±0.113
2-Cl	$-(0.596 \pm 0.069)i + (7.47 \pm 0.21)$	−0.980	±0.033
4-Cl	$-(0.665 \pm 0.018)i + (9.57 \pm 0.071)$	−0.9993	±0.011
4-Br	$-(0.585 \pm 0.095)i + (6.84 \pm 0.28)$	−0.962	±0.057
2-CH_3	$-(0.851 \pm 0.083)i + (11.64 \pm 0.35)$	−0.986	±0.058
3-CH_3	$-(1.490 \pm 0.063)i + (9.54 \pm 0.19)$	−0.9965	±0.034
4-CH_3	$-(2.402 \pm 0.092)i + (15.05 \pm 0.32)$	−0.9978	±0.033
3-OH	$-(0.885 \pm 0.025)i + (9.93 \pm 0.091)$	−0.9984	±0.015
4-OH	$-(3.84 \pm 0.12)i + (15.29 \pm 0.31)$	−0.9982	±0.031
4-OCH_3	$-(3.07 \pm 0.24)i + (12.83 \pm 0.64)$	−0.991	±0.072
2-NH_2	$-(1.22 \pm 0.31)i + (8.56 \pm 0.86)$	−0.940	±0.101
3-NH_2	$-(2.10 \pm 0.18)i + (21.30 \pm 0.96)$	−0.986	±0.128
4-NH_2	$-(3.55 \pm 0.24)i + (14.23 \pm 0.62)$	−0.9955	±0.033

Table II

Experimental data obtained in the presence of p-nitraniline

R–C_6H_4–COOH (R)	$it_1^{1/2}$ (Equation 14)	Statistical data	
		r	S_0
H	$-(1.304 \pm 0.096)i + (19.26 \pm 0.59)$	−0.981	±0.107
2-Cl	$-(0.41 \pm 0.11)i + (18.63 \pm 0.91)$	−0.910	±0.410
4-Cl	$-(0.622 \pm 0.080)i + (24.59 \pm 0.79)$	−0.968	±0.139
4-Br	$-(0.562 \pm 0.018)i + (12.766 \pm 0.097)$	−0.998	±0.020
2-CH_3	$-(0.87 \pm 0.11)i + (17.81 \pm 0.74)$	−0.968	±0.146
3-CH_3	$-(1.414 \pm 0.052)i + (17.91 \pm 0.31)$	−0.998	±0.044
4-CH_3	$-(2.19 \pm 0.25)i + (18.03 \pm 0.15)$	−0.9803	±0.100
3-OH	$-(0.875 \pm 0.066)i + (13.76 \pm 0.34)$	−0.9889	±0.066
4-OH	$-(4.25 \pm 0.48)i + (29.03 \pm 2.30)$	−0.9815	±0.147
4-OCH_3	$-(3.04 \pm 0.16)i + (39.12 \pm 1.31)$	−0.994	±0.14
2-NH_2	$-(2.07 \pm 0.23)i + (22.77 \pm 1.34)$	−0.971	±0.193
3-NH_2	$-(2.06 \pm 0.12)i + (30.04 \pm 0.91)$	−0.971	±0.129
4-NH_2	$-(2.91 \pm 0.27)i + (14.68 \pm 1.47)$	−0.9871	±0.080

In order to calculate k_d from equations (14) and (7) the values of the diffusion coefficients D_{HA} and D_{H^+} must be known. The former has been calculated from the Einstein—Smoluchowski equation:

$$D_{HA} = \frac{2.96 \times 10^{-7}}{\eta V_M^{1/3}} \tag{15}$$

η being determined with a Höppler viscosimeter. D_{H^+} was also determined experimentally from the reduction waves of the H^+-ions of HCl solutions in the same medium, using the Ilkovič equation:

$$i = (2.864 \pm 0.070) \times 10^{-3} c - (0.53 \pm 0.21) \times 10^{-6}$$
$$r = 0.9980 \qquad S_0 = \pm 0.27 \times 10^{-6}$$

(i and S_0 in μA; c in mol/l). From the slope of the regression line the value of $D_{H^+} = 4.94 \times 10^{-6}\ cm^2 s^{-1}$ has been calculated. The rate constant values obtained, together with the diffusion coefficient and the acidity constant values (determined potentiometrically), respectively, are given in Table III. The correlation between the rate constants and constitution is reflected by the linear relationship between K_a, k_d or k_r and the substitution coefficient [7], respectively (Fig. 4):

Table III

Experimental diffusion coefficient, acidity constant and rate constant values

Indexes A and N refer to azobenzene and/or *p*-nitraniline, respectively

R—C_6H_4—COOH R	$D_{HA} \cdot 10^6$ $cm^2 s^{-1}$	$K_a \cdot 10^6$ $M l^{-1}$	$k_{d(A)} \cdot 10^{-3}$ s^{-1}	$k_{r(A)} \cdot 10^{-9}$ $M^{-1} l s^{-1}$	$k_{d(N)} \cdot 10^{-3}$ s^{-1}	$k_{r(N)} \cdot 10^{-9}$ $M^{-1} l s^{-1}$
H	1.888	2.12	3.54	1.67	3.22	1.52
2-Cl	1.854	19.16	0.63	0.034	3.49	0.18
4-Cl	1.853	4.45	5.79	1.30	6.62	1.49
4-Br	1.830	4.28	7.69	1.80	6.19	1.45
2-CH_3	1.696	1.92	7.34	3.82	7.20	3.75
3-CH_3	1.714	1.76	2.70	1.53	3.00	1.70
4-CH_3	1.714	1.27	1.44	1.13	1.73	1.36
2-OH	1.890	81.64	—	—	—	—
3-OH	1.903	2.79	5.36	1.92	5.48	1.96
4-OH	1.980	0.61	1.26	2.07	1.03	1.69
4-OCH_3	1.805	0.93	1.27	1.37	1.30	1.40
2-NH_2	1.919	0.62	1.30	2.13	0.45	0.74
3-NH_2	1.924	1.37	1.97	1.44	2.03	1.48
4-NH_2	1.924	0.32	1.14	3.57	1.71	5.33

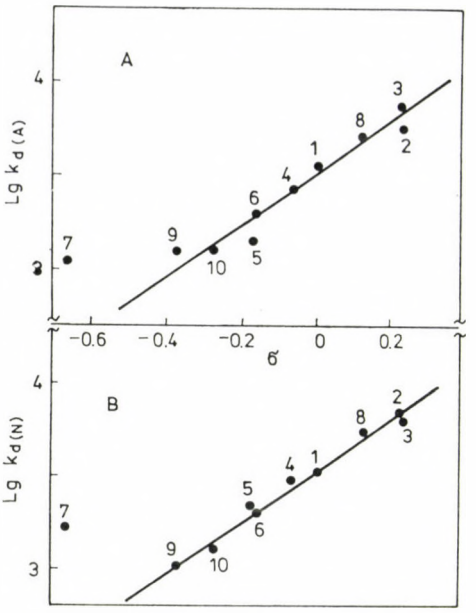

Fig. 4. $\log k_d - \sigma$ (substituent constant) dependence. Mediators used: A — azobenzene; B — *p*-nitraniline. The compound investigated (R in $R-C_6H_4-COOH$); 1 — H; 2 — 4 Cl; 3 — 4 Br; 4 — 3 CH_3; 5 — 4 CH_3; 6 — 3 NH_2; 7 — 4 NH_2; 8 — 3 OH; 9 — 4 OH; 10 — 4 OCH_3

$$\lg K_a = (0.987 \pm 0.058) \lg K_{d(N)} - (9.06 \pm 0.20)$$
$$r = 0.987 \qquad S_0 = \pm 0.049$$

$$\lg K_a = (0.947 \pm 0.098) \lg K_{d(A)} - (9.01 \pm 0.34)$$
$$r = 0.963 \qquad S_0 = \pm 0.083$$

$$\lg K_a = (1.329 \pm 0.035)\sigma - (6.03 \pm 0.10)$$
$$r = 0.9979 \qquad S_0 = \pm 0.026$$

$$\lg k_{d(N)} = (1.386 \pm 0.065)\sigma + (3.516 \pm 0.013)$$
$$r = 0.9924 \qquad S_0 = \pm 0.039$$

$$\lg k_{d(A)} = (1.37 \pm 0.12)\sigma + (3.517 \pm 0.025)$$
$$r = 0.975 \qquad S_0 = \pm 0.072$$

The reaction constants calculated from the slope of the regression lines have appropiate values: $\varrho_{K_a} = 1.33$; $\varrho k_{d(N)} = 1.37$. This is consistent with the fact that the *meta* and *para* substituted benzoic acid derivatives manifest a normal behaviour [8], *i.e.* the rate determining step of the recombination is the diffusion-controlled mutual approach of the H^+ and A^- ions, respectively, until a critical distance with the formation of a so-called latent ion-pair (H^+aqA^-). The corresponding rate constant is practically identical for all the derivatives

investigated ($\bar{k}_r = 1.60 \times 10^9 M^{-1}ls^{-1}$), regardless of the substituent and the nature of the mediator organic compound used. Deviations from the $K_a - k_d$ parallelism appear owing to the *orto*-effect of some substituents (*o*-Cl, *o*-NH_2), as well as in the case of *p*-NH_2 benzoic acid. Salicylic acid cannot be investigated by this method, since its pK_a is lower than 5.

The smaller value for $\bar{k}_r$ obtained in 1.9 *M* LiCl, compared with that determined in 0.05 *M* LiCl ($\bar{k}_r = 2.35 \times 10^{10}\ M^{-1}ls^{-1}$) is due to the increased viscosity of the former solution, as well as to the destruction of the normal structure of water, which in more concentrated LiCl solutions (>1 *M*) is appreciable [9]. Beside this, Li^+-ions owing to their high charge density, exert a strong polarization effect on the carboxyl group. Contrary to the expectations the k_d values are approximately three times smaller than those obtained in 0.05 *M* LiCl. The observed linear correlation between the dissociation rate constants and the substituent constants σ of the weak acids, as well as the fact that the reaction rate constants (ϱ) obtained are nearly independent on the mediator used indicate, that in this case, from the chemical steps preceeding the electrode reaction, the dissociation of the weak acid is rate determining. If the protonation of the mediator would be the rate determining step (MAIRANOVSKII [10]), the parameters of the kinetic current would depend on the nature of the mediator used, and not on that of the weak acid.

REFERENCES

[1] TŐKÉS, B., GYÁRFÁS, É., KÉKEDY, L.: Z. phys. Chem. **260,** 1 (1979)
[2] RÜETSCHI, P., VIELSTICH, W.: Z. phys. Chem. (Neue Folge), **4,** 124 (1955)
[3] RÜETSCHI, P.: Z. phys. Chem. (Neue Folge), **5,** 323 (1955)
[4] WEBER, J., KOUTECKÝ, J.: Coll. Czech. Chem. Comm., **20,** 980 (1955)
[5] NÜRNBERG, H. W., VAN RIESENBECK, G., VON STACKELBERG, M.: Coll. Czech. Chem. Comm., **26,** 126 (1961)
[6] MOELWYN-HUGHES, E. A.: The Chemical Statics and Kinetics of Solutions. Academic Press, London, New York, 1971
[7] HAMMETT, L. P.: Physical Organic Chemistry. 2nd Ed. McGraw-Hill, New York, 1970
[8] NÜRNBERG, H. W., DÜRBECK, H. W.: Z. Anal. Chem., **205,** 217 (1964)
[9] GOOD, W.: Electrochim. Acta, **9,** 203 (1964)
[10] MAIRANOVSKII, S. G.: Kataliticheskie i kineticheskie volny v polyarografii. Nauka, Moskva, 1966

Éva GYÁRFÁS
Béla TŐKÉS } R-4300 Tîrgu Mureş, Str. Gh. Marinescu nr. 38. Romania

László KÉKEDY R-3400 Cluj-Napoca, Str. Arany J., nr. 11, Romania

Acta Chimica Academiae Scientiarum Hungaricae, Tomus 102 (2), pp. 151—156 (1979)

THE ANODIC DISSOLUTION OF COPPER IN THE PRESENCE OF DIPHOSPHATE

R. K. ASTAKHOVA,[1] J. SZALMA,[2] J. FARKAS[2] and L. KISS[2]

([1]Department of Electrochemistry, University of Leningrad, [2]Department of Physical Chemistry and Radiology, Eötvös Loránd University, Budapest)

Received September 27, 1978

Accepted for publication November 14, 1978

The anodic dissolution of copper has been studied by means of a rotating ring disc electrode in diphosphate media at pH 8.6 and 4.8. The ionization of copper occurs in a stepwise mechanism, under the conditions studied, *i.e.* in two one-electron steps. The changes hereby ensuing in pH and in the composition of the complex which participates in the reaction significantly affect the kinetics of the process.

Copper baths which contain diphosphate (pyrophosphate) are used extensively in recent years. Accordingly, quite a number of communications [1, 2] deals with the details of the cathodic process that occurs in diphosphate baths; with its mechanism and also with the various parameters which affect this process. Comparatively few in number are the papers which discuss the anodic process in this bath [1, 3, 4]. These papers deal chiefly with the passivation of copper anodes, respectively, with the prevention of this, in a diphosphate medium.

No data in the literature reveal whether the anodic dissolution of copper in diphosphate media occurs, like in sulphuric acid [5] or in perchlorate [6], as two one-electron steps in series, therefore the study of this point has been the aim of the present investigations.

A rotating ring disc electrode was used in these experiments. The disc electrode was made of electro-deposited copper, the ring electrode was platinum. The radius of the disc electrode was 0.25 cm. The chemicals used were analytically pure.

The glass apparatus was one described in an earlier paper [7]. Measurements were carried out potentiostatically by means of a double potentiostat. The electrode potentials given below refer to normal calomel electrode potential.

The tests were carried out in mixtures of a 0.5 mol $\cdot$ dm^{-3} solution of $K_4P_2O_7$ and a 0.25 mol $\cdot$ dm^{-3} solution of K_2SO_4, at pH 8.6 and 4.8. Sulphuric acid was used to adjust the pH of the medium to 4.8. Most of the experiment, were carried out at pH 8.6 since this is the pH of the diphosphate solutions used in industrial practice [1].

Results

Polarization curves recorded in the pH 8.6 solution, at 20, 40, and 60 °C, at 520 r.p.m. are shown in Fig. 1. As expected, the rate of anodic dissolution at the same ε potential of the electrode increases with temperature. The initial sections of the curves are linear; the Tafel constants b vary between 45 mV (20 °C) and 50 mV (60 °C). With higher current intensities the curves will deviate towards the ordinate; at higher electrode potentials ε passivation occurs. A variation of the number of revolutions of the disc electrode does not affect the shape of the curves.

Figure 2 shows the changes of the oxidation limiting current I_R at the ring in a function of anodic disc current, at 60 °C and at various r.p.m. of the elec-

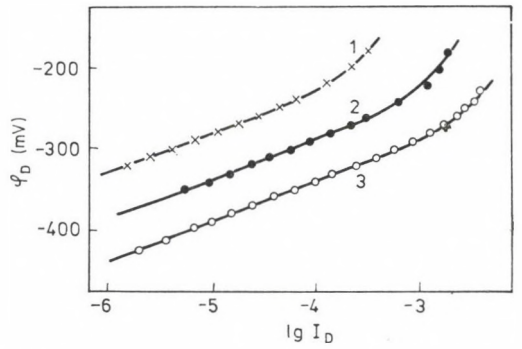

Fig. 1. Polarization curves on copper disc electrode at 520 r.p.m. at different temperatures 20 °C(1) 40 °C(2) 60 °C(3) the composition of solution 0.5 mol · dm^{-3} $K_4P_2O_7$ + 0.25 mol · dm^{-3}. pH = 8.6

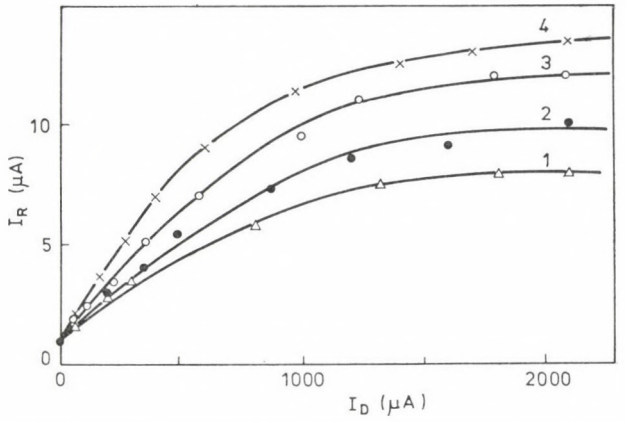

Fig. 2. Oxidation limiting current on the ring electrode *vs.* anodic disc current at pH = 8.6 and 60 °C. R.p.m. were 140 min^{-1} (1), 290 min^{-1} (2), 520 min^{-1} (3), and 1080 min^{-1} (4) the composition of solution: 0.5 mol · dm^{-3} $K_4P_2O_7$ + 0.25 mol · dm^{-3} K_2SO_4

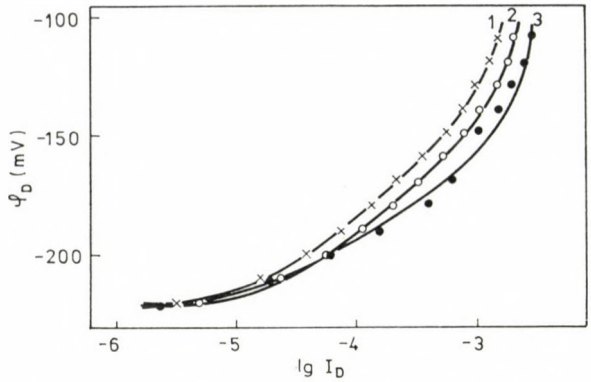

Fig. 3. Polarization curves on a copper disc electrode at pH = 4.8 and 40 °C. R.p.m. were 140 min^{-1} (1), 520 min^{-1} (2), and 1080 min^{-1} (3) the composition of solution 0.5 mol · dm^{-3} $K_4P_2O_7$ + 0.25 mol · dm^{-3} K_2SO_4

trode. The curves belonging to the various r.p.m. do not coincide: the limiting currents increases at higher r.p.m. The I_R *vs* I curves approximate a course parallel to the abscissa at an intensity value where the ε *vs* lg I curve deviates from the linear; *cf.* curve 3 in Fig. 1. There is a correlation between I_R and I, similar to that shown in Fig. 2, also at lower temperatures, but the limiting currents I_R are smaller and cannot be measured accurately.

Polarization curves for pH 4.8 at 40 °C and at various r.p.m. are shown in Fig. 3. These are shifted towards more negative potentials when r.p.m. increases. This suggests that the kinetics of anodic dissolution is affected also by diffusion process.

Also I_R values have been determined and found to be lower by a factor of 5 at pH 4.8 than at pH 8.6, other conditions being equal. When $I = 3 \ldots 4$ mA, $I_R = 1 \ldots 3$ μA, therefore I_R figures are not well reproducible: yet it is certain that with higher disc current also I_R increases.

Discussion

That copper is dissolved by a stepwise mechanism also in diphosphate media [8] is suggested by the experimental results given on Figures 1 and 2; notably by the slopes of the polarization curves and by the dependence of the limiting current at the ring as a function of the disc current, on the r.p.m. of the electrode. The very low limiting current measured on the ring electrode suggests that the rate of diffusion of Cu^+ ions, or that of the Cu^+-complex, into the bulk of the solution is much lower than the rate of oxidation of Cu^+ to Cu^{++}.

The polarization curve of a metal ionization process which proceeds in two one electron steps, if the solution does not contain the ions of the given

metal, is described, for the conditions just explained, by the following correlation [8]:

$$j = \frac{2\, k_{a_1} k_{a_2}}{k_{k_1}\left(1 + \dfrac{k_{k_2}}{X_2}\right) + k_{a_2}} \tag{1}$$

where j stands for current density; k_{a_i}, k_{k_i} stand for the rate constants of the i^{th} anodic and catodic charge transfer processes ($i = 1, 2$), X_2 stands for the rate constant of diffusion of the Cu^{2+}-complex. In the case of a rotating disc electrode this is

$$X_2 = 0.62\, D_2^{2/3}\, \nu^{-1/6} \left(\frac{2\pi}{60}\right)^{1/2} f^{1/2} = X_2' f^{1/2} \tag{2}$$

where D_2 is the diffusion coefficient of the given metal ion; ν is the kinematic viscosity of the solution; and f is the r.p.m. of the electrode. The rate constants of the elementary reaction steps depend on the electrode potentials as follows.

$$\begin{aligned} k_{a_i} &= k'_{a_i} \exp \frac{\alpha_i F\varepsilon}{RT} \\ k_{k_i} &= k'_{k_i} \exp - \frac{(1-\alpha_i) F\varepsilon}{RT}, \quad i = 1, 2 \end{aligned} \tag{3}$$

where k'_{a_i} and k'_{k_i} are the respective rate constants when $\varepsilon = 0$, thus their value depends also on the reference electrode used; α_i is the transfer coefficient, the other symbols are usual.

The shape of the polarization curves recorded at pH 8.6 is invariant to changes of r.p.m. of the electrode, this prompts the conclusion that

$$k_{k_2} \ll X_2 . \tag{4}$$

At not too high anodic current densities the Tafel constant b of the polarization curves varies between 45 mV and 50 mV in the function of temperature. This indicates that

$$k_{k_1} \gg k_{a_2} . \tag{5}$$

Thus, under given conditions, the equation of the polarization curve can be written, on the basis of correlations (1) and (3), as

$$\varepsilon = \frac{RT}{(1+\alpha_2) F} \lg \frac{k'_{k_1}}{k'_{a_1} k'_{a_2}} + \frac{RT}{(1+\alpha_2) F} \ln j . \tag{6}$$

Experimental results give $\alpha_2 = 0.29 - 0.32$.

Instead of the inequality (5),

$$k_{K_1} \ll k_{a_2} \tag{7}$$

is realized when anodic polarization is increased, because the potential is shifted towards the positive direction. Thus, in conformity with correlations (1) and (3), the polarization curves becomes steeper. It must be noted, however, that this is not the only cause why the polarization curve becomes steeper in the case here studied but also because the passivation of the metal surface begins, as already mentioned.

Also the polarization curve recorded at pH 4.6 can be interpreted in terms of a stepwise mechanism, on the basis of the Eq. (1). That the polarization curve is effected by the r.p.m. of the electrode suggests that inequality (4) are not fulfilled and that

$$k_{K_2} \geqslant X_2 \tag{8}$$

It is supposed that inequality (5) subsist also in this instant if anodic polarization is not too great. At any further increase of anodic polarization correlation (1) does not suffice any more. Then kinetics is affected most probably by the solubility of the complex formed at the anode surface and by the partial blocking of the electrode surface with the precipitated salt layer.

The comparison of the polarization curves belonging to 40 °C, shown in Figs 1 and 3, allow also the statement that, potentials being the same, the ionization of copper proceeds at a higher rate at pH 8.6 than at pH 4.8. According to experimental data (*cf.* Fig. 3), the ionization of copper occurs at more positive potentials when pH is 4.8, and the exchange current of this process is higher than in a solution of pH 8.6. Also inequality (8) refers to this, and is in accordance with the statement [10] that protonated complexes are more easily reducible than the unprotonated ones. According to data in the literature [11] the copper complex formed in diphosphate solutions at pH 4.8 consist chiefly of

$$CuH_2(P_2O_7)_2^{4-}$$

and at pH 8.6, of

$$Cu(P_2O_7)_2^{6-}$$

ions only.

Thus experimental results show that the rate of the cathode process increases and that of the anode process decreases in consequence of the protonation of the diphosphate (with the decrease of pH).

Experimental data suggest that the ionization of copper also in diphosphate media takes place in two one-electron steps. The details of this mecha-

nism cannot be clarified on the basis of available data. Thus, for instance, it can be surmised that the adsorption of the ligand precedes the charge transfer and that the stable copper complex in the solution is formed in a chemical reaction coupled with the charge transfer [9] process.

REFERENCES

[1] PURIN, B. A.: Elektroosazhdenie metallov iz pirofosfatnikh elektrolitov. Izd. "Zinatne" Riga, 1975
[2] BEK, R. Yu., SORKIN, G. N.: Izv. Sib. Otd. AN SSSR ns 12, 142 (1970); RADOVICI, O., VASS, C.: Rev. Roum. Chim., **18,** 1105 (1973); RADOVICI, O., VASS, C., SOLACOLU, I.: Rev. Roum. Chim., **18,** 1325 (1973); **18,** 2021 (1973)
[3] GURILEV, V. V., LEVIN, A. J.: Zhurn. Prikl. Khim., **37,** 2625 (1977)
[4] PILAVOV, Sh. G., EGOROVA, A. I.: Zashchita Met., **13,** 734 (1977)
[5] KISS, L., FARKAS, J.: Acta Chim. Acad. Sci. Hung., **66,** 395 (1970)
[6] MOLODOV, A. I., MARKOSYAN, G. N., LOSEV, V. V.: Elektrokhimiya, **7,** 263 (1971)
[7] KISS, L., FARKAS, J., KŐRÖSI, A., MANDL, J.: Acta Chim. Acad. Sci. Hung., **79,** 43 (1973)
[8] KISS, L., FARKAS, J.: Kémiai Közlemények, **34,** 261 (1970)
[9] KISS, L., VARSÁNYI, M.: Acta Chim. Acad. Sci. Hung., **88,** 259 (1976)
[10] KORYTA, J.: Adv. in Electrochem. and Electrochem. Eng., **6,** 289 (1967; ed.: P. DELAHAY); BEREZINA, S. I., VOITSEKHOVSKAYA, R. N., VOITSEKHOVSKII, Yu. G., GUDIN, N. V.; Prikladnaya Elektrokhimiya, Vyp. 6. Kazan' 1977 Str. 6. — Ref. Zh. Khim. 191229 (1977)
[11] BEK, R. Yu.: Izv. Sib. Otd. AN SSSR Ser. Khim. n° 4, vyp 2, 118 (1976)

Ravsat Kamilovna ASTAKHOVA SU-199004 Leningrad, Srednii pr. 41/43.

József SZALMA
József FARKAS
László KISS
H-1088 Budapest, Puskin u. 11—13.

Acta Chimica Academiae Scientiarum Hungaricae, Tomus 102 (2), pp. 157—164 (1979)

DETERMINATION OF KUHN-MARK-HOUWINK CONSTANTS FOR SEVERAL POLYMERS AND THEIR APPLICATION IN GEL PERMEATION CHROMATOGRAPHY

G. SAMAY

(Research Institute for Plastics Industry, Budapest)

Received September 8, 1978
Accepted for publication November 21, 1978

Intrinsic viscosity *vs.* molecular weight relations are reported for several polymer types, measured under conditions pertinent to routine gel permation chromatography. In possession of the data, the universality of two calibrating methods in gel permeation chromatography could be confirmed.

The easiest way to determine the molecular weight of a macromolecular material is to measure the intrinsic viscosity of the sample and calculate the molecular weight via the KUHN-MARK-HOUWINK relation:

$$[\eta] = KM^a \tag{1}$$

where K and a are constants at a given temperature in the solvent used. These constants (often called the KMH-constants) are enumerated in international tables [1] or monographs [2] for many polymer types under different conditions, therefore, the routine estimation of the molecular weight average of the most frequently used polymers is easy for the industrial laboratories. The molecular weight average obtained is the so called viscosity-average molecular weight and is defined as:

$$M_v = \left(\sum_i M_i^a w_i / \sum_i w_i \right)^{1/a} \tag{2}$$

This average falls between the weight- and the number-average molecular weights of the polydisperse sample, and if the polydispersity is not high, it is roughly equal to the weight average. Having no KMH-constants at disposal for the material tested, they can be determined by absolute measurements of the molecular weight and the intrinsic viscosity of several fractions of the polymer and, according to Eq. (1), the log $[\eta]$ *vs.* log M plot yields the desired factors (the slope of the straight line is a, while the intercept gives log K).

The KMH-constants are often used in the practice of gel permeation chromatography. The universal calibration according to BENOIT [3] applies the product of the molecular weight and the intrinsic viscosity of the samples.

Hence the molecular weight can be directly obtained if the KMH-constants are known for the material examined by GPC. For this reason, many measurements were carried out in the last years to obtain KMH-constants for the conditions which are most frequently used in gel permeation chromatography [tetrahydrofuran (THF), 298 K and 1.2,4-trichlorbenzene (TCB), 403 K].

The aim of this work is to report on several series of measurements in GPC-solvents and give experimental KMH-constants for further use. On the basis of viscometric data also the universality of the "universal" calibrations used in GPC could be confirmed.

Experimental

Viscometry

The viscosities were measured by a modified Ubbelohde-type capillary viscometer; the geometry of this device was chosen so that the dynamic factors could be neglected. (The length of the capillary was 20 cm and the inner diameter 0.3 mm.) The volume of the measuring bulb was 1 cm^3. Thus quantities of solutions as small as 3 cm^3 could be tested in this apparatus. Dilutions were carried out in the solution reservoir of the device. The times of effusion were measured at four concentrations: 0.5—0.4—0.3—0.2 g/100 cm^3, and the viscosity numbers (specific viscosity *per* concentration) were plotted against the concentration and extrapolated to zero concentration by a least-squares method.

The measurements were performed in thermostated vessels in THF solution at 298 K and in TCB solution at 403 K. The KMH-constants were obtained by linear regression of the log $[\eta]$ *vs.* log M values of the fractions. The calculations were performed on a HP 9830 programmable calculator.

Gel Permeation Chromatography

The GPC measurements were performed in two GPC instuments. A WATERS GPC 200 apparatus worked at 403 K with TCB solvent equipped with 5 Styragel columns (6.5×10^3, 2.5×10^3, 9×10^2, 100, 25 nm). The GPC runs at ambient temperature were performed in an apparatus constructed in this Institute using THF as a solvent and three Styragel columns (10^4, 10^3 and 3×10^2 nm respectively). The volume of the syphon counter was 5 cm^3 in the former apparatus and 1.67 cm^3 in the latter; the flow rate was 1 cm^3/min in each case.

Materials

The THF solvent was of REANAL analytical grade and was distilled from CuCl crystals to destroy its possible peroxide content. TCB was purchased from MONTEDISON in "puro erba reagente" quality. It was used without further purification, using "Santonox R" as a stabilizer.

The polymer materials were as follows.

Polystyrene fractions of known molecular weights were purhased from WATERS. The polyethylene fractions were produced and characterized by S.N.P.A. (France). The polypropylene fractions were made by Baker-Williams fractionation of an industrial polymer and characterized by viscometry in tetrahydronaphthalene to estimate the molecular weights of the fractions. (For the KMH-constants for these measurements see Ref. [4].) Poly(*n*-alkyl methacrylate) fractions (where alkyl is ethyl, buthyl and octyl) together with equimolar random and alternating copolymer fractions of styrene with these alkyl methacrylates were made and characterized in the Institute of Macromolecular Chemistry, Czechoslovak Academy of Sciences; the detailed characterization of these fractions was given elsewhere [5]. Also the poly(vinyl chloride) fractions were delivered by this institute.

For constructing the GPC universal calibration curves, WATERS polypropylene oxide fractions and REANAL *n*-paraffins were used, too.

Results

KMH plots

In Figs 1, 2 and 3 the log $[\eta]$ *vs.* log M plots are shown for the different methacrylate homo- and copolymers, measured in THF at 298 K. In the upper parts of the Figures the regression lines and the confidence limits are shown for the alternating and random type copolymers of the same chemical composition. These lines show that on the basis of our mesurements no difference can be observed between the KMH plots for the two types of copolymers, therefore, a common regression line was drawn for all copolymer fractions of the same composition, irrespective of the sequential structure of the molecules. These lines are shown together with the measured points in the lower part of the Figures together with the homopolymer points.

In Fig. 4 the data of further measurements are shown for THF at 298 K, *viz.* the KMH plots for PVC and polystyrene. For comparison, the data for polystyrene measured at 403 K in TCB are also indicated together with the confidence limits (on a 95% level of significance) of the least-squares fit to these four points (dotted line). The points obtained at 403 K fall close to the other points, therefore, it can be supposed that the same relation is valid for both the high-temperature and low-temperature measurements in this case.

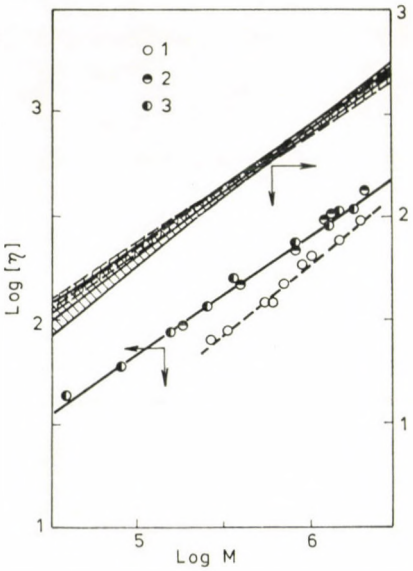

Fig. 1. Kuhn-Mark-Houwink plot for poly(ethyl methacrylate) (1) and poly(styrene-co-ethyl methacrylate) alternating (2) and random (3) copolymers in THF at 298 K. The upper part shows the regression lines and the confidence intervals of the alternating (——) and random (---) copolymers

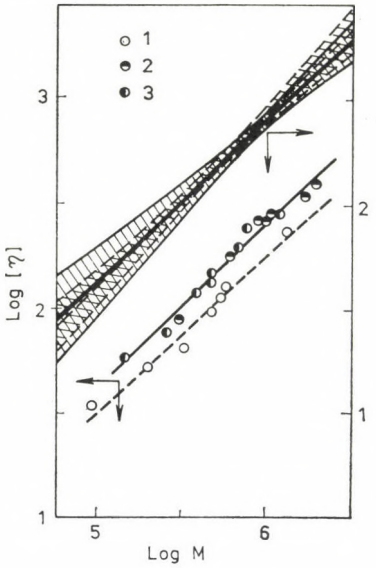

Fig. 2. Kuhn-Mark-Houwink plot for poly(butyl methacrylate) (1) and poly(styrene-co-butyl methacrylate) alternating (2) and random (3) copolymers in THF at 298 K. The upper part shows the regression lines and the confidence intervals of the alternating (——) and random (---) copolymers

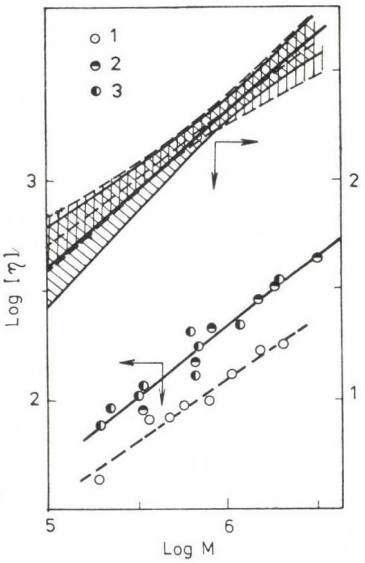

Fig. 3. Kuhn-Mark-Houwink plot for poly(*n*-octyl methacrylate) (1) and poly(styrene-co-*n*-octyl methacrylate) alternating (2) and random (3) copolymers in THF at 298 K. The upper part shows the regression lines and the confidence intervals of the two copolymer types: —— alternating, ------ random

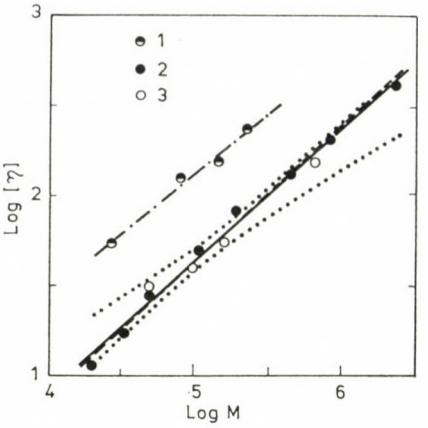

Fig. 4. Kuhn-Mark-Houwink plot for poly(vinyl chloride) (1) and polystyrene (2) in THF at 298 K. 3 — the points for polystyrene measured in TCB at 403 K, —— regression line for points measured at 298 K, ------ regression line for all polystyrene points, ... confidence interval of the regression line for the four high-temperature polystyrene points

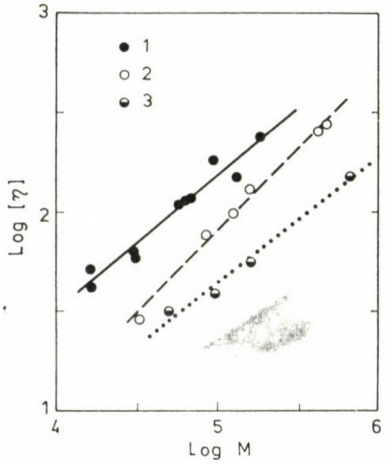

Fig. 5. Kuhn-Mark-Houwink plot measured at 403 K in TCB for polyethylene (1), polypropylene (2) and polystyrene (3)

Hence a common relation for all the points for polystyrene was also calculated and drawn in the Figure by a dashed line.

In Fig. 5 the high-temperature measurements in TCB are illustrated for polyethylene, polypropylene and polystyrene samples.

The KMH-constants together with the $f(a)$ values in Eq. (3) (see later) are summarized in Table I. For polystyrene also the data calculated for low- and high-temperature measurements, are indicated in parentheses.

Table I

Kuhn-Mark-Houwink constants and related f(a) values

Material	a	K 10^2 cm³/g	f(a)	Conditions
Polystyrene	0.76 (0.74)	0.609 (0.832)	0.6215	
Poly(ethyl-methacrylate)	0.67	1.549	0.7004	
Poly(butyl-methacrylate)	0.75	0.503	0.6323	THF
Poly(octyl-methacrylate)	0.56	5.556	0.9000	298 K
Styrene/ethyl methacrylate copolymer	0.56	10.500	0.8931	
Styrene/butyl methacrylate copolymer	0.80	0.370	0.5859	
Styrene/octyl methacrylate copolymer	0.64	2.394	0.7759	
Poly(vinyl chloride)	0.70	4.480	0.7047	
Polystyrene	0.64 (0.74)	2.80 (0.832)	—	TCB
Polypropylene	0.83	0.74	—	403 K
Polyethylene	0.67	6.14	—	

For the common polymer types (polystyrene, polyethylene, polyvinil chloride and polypropylene) some data can be found in handbooks [1, 2]. The scatter of the data reported for the same material under the same conditions is large; thus our data can be considered as reliable in comparison with the literature values.

Application of the data for GPC purposes

Many attempts have been made in gel permeation chromatography to find a universal calibration curve, which would be independent of the test material. Two of the methods are accepted and widely used, namely calibration according to BENOIT, where the product of the molecular weight and the intrinsic viscosity is treated as a universal size parameter, and the COLL—PRUSINOWSKY [6] calibration, which expresses the universal size parameter, Q, with the help of the Ptytsin-Eisner equation:

$$Q = M[\eta]/\mathrm{f}(a) \tag{3}$$

where

$$\mathrm{f}(a) = 1 - 2{,}63\frac{2a-1}{3} + 2{,}86\left(\frac{2a-1}{3}\right)^2$$

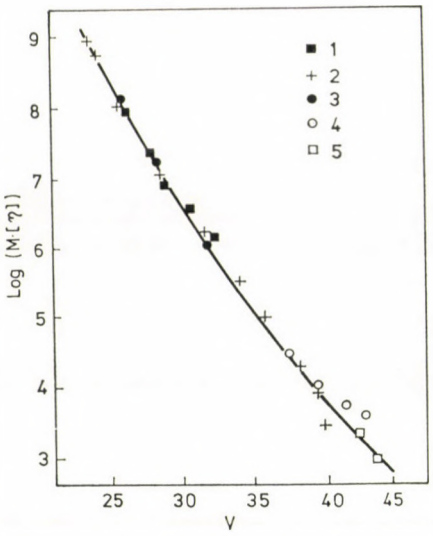

Fig. 6. Universal calibration according to BENOIT for the high-temperature GPC apparatus; 1 — polyethylene, 2 — polystyrene, 3 — polypropylene, 4 — poly(propylene oxide), 5 — *n*-paraffin

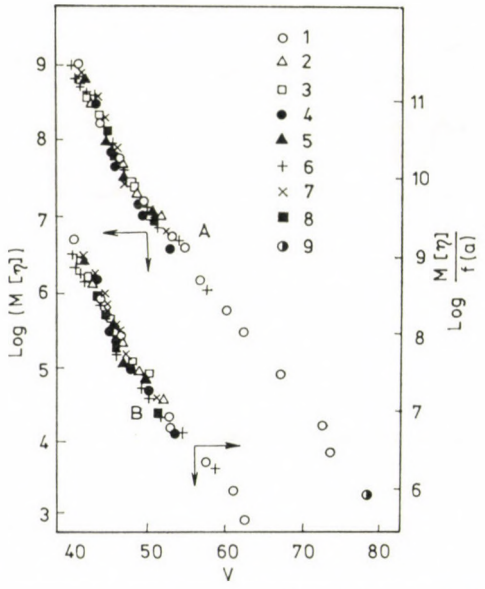

Fig. 7. Universal calibration according to BENOIT — A, and COLL and PRUSINOWSKY — B for the room-temperature GPC apparatus; 1 — polystyrene, 2 — poly(vinyl chloride), 3 — poly(ethyl methacrylate), 4 — poly(butyl methacrylate), 5 — poly(*n*-octyl methacrylate), 6 — poly(styrene-co-ethyl methacrylate), 7 — poly(styrene-co-butyl methacrylate), 8 — poly(styrene-co-*n*-octyl methacrylate), 9 — squalane

With many data at disposal, the universality of these calibrating methods can be confirmed. In Fig. 6 BENOIT's universal calibration is shown for the high-temperature apparatus, while both types of calibration curves are given for the low-temperature apparatus in Fig. 7.

The universality of BENOIT's calibration both at elevated and ambient temperatures is clearly seen from the Figures, and the COLL—PRUSINOWSKY method is also confirmed for low-temperatures.

On the basis of these measurements, it can be supposed that both calibrations are equivalent from the point of view of universality, nervertheless, they are not equivalent from the point of view of their applicability. If the latter method is used, also the KMH-constants must be known in addition to the directly measured intrinsic viscosity of the sample of species, and these constants must be taken either from the literature or determined by tedious and time-consuming measurements. Conversely, the use of the COLL-PRUSINOWSKY calibration requires knowledge of the KMH exponent for the test material, therefore, for example with automatic viscosity detection of the eluate, this latter calibration does not directly give molecular weights. Thus, for routine purposes BENOIT's calibration is recommended.

*

The author is indebted to Dr. J. PODEŠVA and Dr. J. JANČA, Institute of Macromolecular Chemistry, Czechoslovak Academy of Sciences, for the well characterized polymer fractions.

REFERENCES

[1] BRANDRUP, J., IMMERGUT, E. H.: Polymer Handbook. John Wiley and Sons, New York 1975
[2] KURATA, M., STOCKMAYER, W. H.: Fortschr. Hochpolym. Forsch. **3,** 196 (1963)
[3] BENOIT, H., GRUBISIC-GALLOT, Z., REMPP, P., DECKER, D., ZILLOIX, Z. G.: J. Chim. Phys., **63,** 1507 (1966)
[4] RAFF, R. A. V., DOAK, K. W.: Crystalline Olefin Polymers. Intersience, New York 1964
[5] PODEŠVA, J., KRATOCHVIL, P., BOHDANECKY, M., SAMAY, G.: J. Polym. Sci., Phys., **15,** 1521 (1977)
[6] COLL, H., PRUSINOWSKY, L. R.: J. Polym. Sci., A-1, **5,** 987 (1967)

Géza SAMAY H-1950 Budapest, Hungária krt. 114.

Acta Chimica Academiae Scientiarum Hungaricae, Tomus 102 (2), pp. 165—170 (1979)

STUDY OF THE LINEAR CORRELATION FACTOR OF DIELECTRIC POLARIZATION AND FLUID STRUCTURE

R. SABESAN,[1] R. VARADARAJAN[1] and M. SARGURUMOORTHY[2]

([1]Department of Physics, National College, Tiruchirapalli, [2]Department of Physics, Periyar E.V.R. College, Tiruchirapalli, India)

Received September 22, 1978
Accepted for publication November 21, 1978

The variation of the linear correlation factor of dielectric polarization (g) was determined experimentally for several associated liquids in carbon tetrachloride using the Kirkwood-Fröhlich equation for solutions. The fluid structures of these systems were analyzed in the light of the results obtained. The non-ideal behaviour of the so-called nonpolar solvents in dielectric measurements is pointed out.

Introduction

One of the important problems in liquid state physics is that concerning the structure of multimers in associated liquids in the pure state and in different solvents. The tools available are generally the concentration dependence of the dielectric constant, the infrared absorption bands or the position of the hydroxy peak in the N.M.R. spectra. The I.R. and N.M.R. studies do not give any information concerning the alignment of neighbouring solute molecules, which is essential for the full knowledge of the configuration of the multimer species. It was pointed out by COLE [1] that the Kirkwood-Fröhlich [2] linear correlation factor of dielectric polarization g is a measure of the short range intermolecular forces that lead to dipole-dipole interactions.

The factor g cannot be explicitly calculated from its statistical-mechanical expression [2] due to unknown parameters like the mutual dipole orientations and the number of nearest neighbours. However, an experimental determination of g could give quantitative information regarding intermolecular association in polar liquids [3—5]. The basis of the experimental determination of the linear correlation factor g for various concentrations of polar solutes such as alcohols, acids and amines is the Kirkwood-Fröhlich relation extended to solutions:

$$g = \frac{9kT}{4\pi N\mu^2 x_2} \frac{(2\varepsilon + \varepsilon_\alpha)^2}{(\varepsilon_\alpha + 2)^2 (2\varepsilon + 1)} \left[\Phi \frac{\varepsilon - 1}{\varepsilon} - \frac{3x_1 \Phi_1 (\varepsilon_1 - 1)}{2\varepsilon + \varepsilon_1} - \frac{3 x_2 \Phi_2 (\varepsilon_\alpha - 1)}{2\varepsilon + \varepsilon_\alpha} \right] \ldots \quad (1)$$

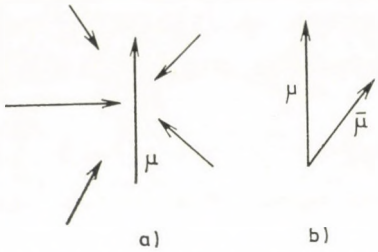

Fig. 1. Correlation between the molecular dipole vector and the neighbouring dipoles

where Φ is the molar volume of the solution; ε is the dielectric constant of the solution; x_1 is the mole fraction of the pure solvent, x_2 that of the solute and ε_α the dielectric constant of induced polarization of the polar component in the pure state, μ is the dipole moment of the solute in the gaseous state.

The static dielectric behaviour of monohydric alcohols and their solutions in nonpolar solvents have been studied with special reference to the variation of g [6—11] but no such extensive studies were made on carboxylic acids, phenols and amines. Prior to studying the polarization of specific complexes of tertiary systems of these acids and amines, we have investigated the variation of g with the concentration in a low dielectric solvent such as carbon tetrachloride.

Materials and Methods

The dielectric measurements were carried out using a Toshniwal RL09 dipole meter at a frequency of 300 kHz with the cell temperature controlled at 35 $\pm$ 0.1 °C. The refractive indices were measured using an Abbe refractometer. The phenols were first treated with anhydrous sodium sulfate and distilled at reduced pressure. The amines were shaken with KOH pellets and distilled before use. AnalaR acetic acid was recrystallized and distilled to eliminate absorbed moisture. BDH AnalaR carbon tetrachloride was used as the solvent.

Results and Discussion

The results are shown in Table I.

The value of g is directly related to the correlation between the direction of a molecule and the molecules in the immediate neighbourhood. The multimers which give $g > 1$ have a positive correlation and the aggregates have a parallel orientation due to dipole-dipole interactions and they are named α-multimers.

The multimers whose dipole-dipole interactions lead to a negative correlation (an anti-parallel orientation) resulting in $g < 1$ are referred to as β-multimers. Several early investigators [12, 13] have found that the concentration dependence of g for monohydric alcohols can be represented by a graph showing a minimum and OSTER's theoretical curve [14] for associated liquids is generally obeyed. However, in the interpretation of the curves there is no unanimity. DANNHAUSER and COLE [15] proposed a model in which the α-mul-

Table I

Variation of ε, n, ϱ, Φ and g with the concentration of solutes in carbon tetrachloride

Solute	Concentration (mol/l)	ε	n	ϱ	Φ	g
	1.0	2.2630	1.4469	1.519	95.49	0.26
	1.4	2.2755	1.4448	1.499	94.56	0.23
Acetic Acid	1.6	2.2955	1.4435	1.496	93.82	0.27
	1.8	2.3105	1.4421	1.491	93.11	0.28
	2.0	2.3180	1.4410	1.485	92.27	0.27
	2.5	2.3655	1.4378	1.469	90.49	0.30
	0.2	2.2955	1.4556	1.550	98.48	1.69
	0.4	2.3305	1.4582	1.535	98.70	1.21
	0.6	2.3580	1.4608	1.527	98.43	0.94
	0.8	2.4020	1.4636	1.520	98.18	0.91
Aniline	1.0	2.4455	1.4659	1.512	97.94	0.89
	1.4	2.5780	1.4721	1.488	97.92	0.96
	1.6	2.6508	1.4751	1.475	98.08	1.02
	1.8	2.6880	1.4782	1.459	97.84	0.89
	2.0	2.7230	1.4798	1.448	98.21	0.91
	0.1	2.2680	1.4461	1.562	98.01	1.01
	0.2	2.3280	1.4469	1.552	98.22	0.99
	0.4	2.4580	1.4480	1.549	97.40	0.97
	0.6	2.5430	1.4491	1.531	97.64	0.87
Pyridine	0.8	2.6530	1.4501	1.526	97.19	0.80
	1.0	2.7830	1.4512	1.516	96.82	0.88
	1.2	2.8880	1.4524	1.512	96.21	0.86
	1.4	3.0180	1.4534	1.505	95.76	0.87
	1.6	3.1280	1.4544	1.492	95.69	0.86
	1.8	3.2680	1.4556	1.477	95.63	0.86
	2.0	3.3780	1.4568	1.474	94.95	0.85
	0.1	2.2392	1.4490	1.552	98.69	0.87
	0.2	2.2548	1.4482	1.538	99.26	0.69
	0.4	2.2912	1.4475	1.524	99.34	0.60
	0.8	2.3874	1.4457	1.494	101.37	0.62
	1.0	2.4212	1.4445	1.477	99.85	0.58
	1.5	2.5460	1.4418	1.437	100.53	0.61
3-Methylbutan-1-01	2.0	2.7072	1.4391	1.394	101.18	0.65
	2.5	2.8736	1.4368	1.355	101.88	0.70

Table I (contd.)

Solute	Concentration (mol/l)	ε	n	ϱ	Φ	g
	3.0	3.0868	1.4346	1.319	102.33	0.76
	3.5	3.4092	1.4318	1.276	102.87	0.85
	4.0	3.7862	1.4295	1.236	103.62	0.95
	0.1	2.2236	1.4492	1.560	97.90	0.56
	0.2	2.2392	1.4489	1.553	97.66	0.62
	0.4	2.2938	1.4478	1.547	96.40	0.73
	0.8	2.3848	1.4462	1.536	94.82	0.83
	1.0	2.4654	1.4450	1.528	93.49	0.88
Methanol	1.5	2.6552	1.4425	1.516	91.30	1.03
	2.0	2.8840	1.4401	1.498	89.27	1.14
	2.5	3.2038	1.4373	1.475	87.27	1.29
	3.0	3.4638	1.4356	1.470	85.37	1.38
	3.5	3.8070	1.4337	1.455	83.41	1.47
	4.0	4.2750	1.4305	1.438	81.22	1.59
	0.1	2.2340	1.4510	1.542	99.30	0.86
	0.2	2.2548	1.4517	1.535	99.47	0.89
	0.4	2.3172	1.4535	1.522	99.44	0.95
	0.8	2.4212	1.4570	1.514	98.42	0.99
Phenol	1.0	2.4836	1.4595	1.504	98.44	1.01
	1.5	2.6708	1.4628	1.485	99.69	1.05
	2.0	2.8632	1.4670	1.458	97.83	1.23
	2.5	3.0920	1.4718	1.438	97.28	1.26
	3.0	3.3728	1.4764	1.417	96.67	1.33
	3.5	3.5860	1.4803	1.400	96.00	1.36
	4.0	3.9656	1.4850	1.367	96.34	1.47
	0.1	2.2756	1.4512	1.545	99.39	0.85
	0.2	2.3172	1.4525	1.543	99.37	0.77
	0.4	2.4160	1.4555	1.533	99.69	0.70
	0.8	2.5980	1.4605	1.520	99.84	0.65
	1.0	2.7072	1.4635	1.514	99.85	0.64
4-Chlorophenol	1.5	2.9828	1.4698	1.499	99.91	0.64
	2.0	3.2012	1.4759	1.486	99.98	0.61
	2.5	3.4872	1.4820	1.467	100.38	0.62
	3.0	3.8044	1.4885	1.439	101.48	0.64
	3.5	4.1476	1.4949	1.427	101.36	0.65
	4.0	4.5012	1.5014	1.411	101.53	0.66

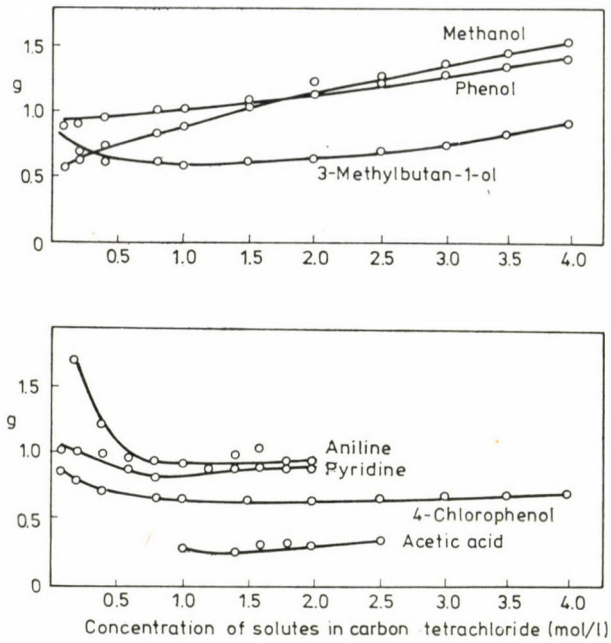

Fig. 2. Variation of g with the concentration of solutes in carbon tetrachloride

timers were open chains of all sizes. At low concentrations, it has been presumed that β-multimers do exist resulting in a dip in the g values. However, BORDEWIJK [6, 16] proposed a 1, 2—4 model for alcohols, in which the α-multimers are cyclic tetramers with out-of-plane O—H. . .O bond and the β-multimers are present as closed dimers at low concentrations. This is in contrast with the conclusion of IBBITSON and MOORE [17] and BELLAMY and PACE [18] from I.R. studies that the smallest multimers are generally linear. The rapid fall of g in methanol and 3-methylbutan-1-ol as the concentration is decreased can be explained assuming the conversion of α-multimers to β-multimers. As a closed dimer will have a negligible g value, in contrast to what is observed here, it may be concluded that an open dimer with restricted rotation around the H-bond can adequately represent the β-multimer.

In carboxylic acids the predominance of *cis*-configuration and the coplanarity of the C—CH_3 bond with the carbonyl bond will minimize the deviation of the bond angle from the ideal value, if cyclic dimers are formed. However, in phenols, the H-bond is stronger in cyclic multimers than in cyclic dimers since the deviation from the ideal bond angles is smaller in the former. The low g values in 4-chlorophenol indicate that these cyclic β-multimers are stabilized in the O—H. . .O plane. The concentration dependence of g for phenol also indicates that the equilibrium between α-multimers and β-multimers is stabilized compared to alcohols, due to the stronger acidity of the former.

One major obstacle in the interpretation of fluid structure is the non-ideal behaviour of the so-called nonpolar solvents. For example, we have shown [4] that the dependence of g on the concentration of acetic acid is different in different solvents which are considered inert. It has been found that g increases in the order hexane $>$ cyclohexane $>$ carbon tetrachloride $>$ benzene (Fig. 1 of Ref. 4). The self-associated monomer-dimer equilibrium of the solute acetic acid is highly concentration dependent in cyclohexane since the monomers are not stabilized and hence leave more terminal groups. However, the low and almost constant g values in carbon tetrachloride and benzene suggest that the monomer is stabilized by association with solvent species. Similar results were obtained by CAMPBELL *et al.* [19], FLETCHER [20], MULLENS *et al.* [21] and BORDEWIJK *et al.* [22] for alcohols.

The behaviour of aniline and pyridine is characteristic of an ideal, weakly associated system. The higher values of g at low concentrations of pyridine and aniline may perhaps be due to the interaction of the lone pair of electrons of the nitrogen atom with the positive charge of the carbon in carbon tetrachloride.

REFERENCES

[1] COLE, R. H.: Ann. Rev. Phys. Chem., **11,** 149 (1961)
[2] BÖTTCHER, C. J. F.: Theory of Electrical Polarization, revised by van BELLE, O. C., BORDEWIJK, P., RIP, A., Vol. I, Elsevier, Amsterdam 1973
[3] MAHROTRA, S. C., SRIVASTAVA, S. L.: Ind. J. Pure Appl. Phys., **10,** 456 (1972)
[4] SABESAN, R., VARADARAJAN, R., SARGURUMOORTHY, M.: Ind. J. Pure Appl. Phys., **15,** 538 (1977)
[5] TJIA, T. H.: Thesis, University of Leiden, 1974
[6] BORDEWIJK, P., Ph. D. Thesis, University of Leiden, 1968
[7] DANNHAUSER, W., GUERING, R., FLUECKINGER, A. F.: J. Chem. Phys., **52,** 6447 (1970)
[8] GRUNWALD, E., CHUAN PAN, K.: J. Phys. Chem., **80,** 2929 (1976)
[9] SINGH, B., VIJ, J. K.: Bull. Chem. Soc., Japan, **49,** 1824 (1976)
[10] SALAMON, T., LISZI, J., RATKOVICS, F.: Acta Chim. Acad. Sci. Hung., **87,** 136 (1975)
[11] STOKES, R. H., MARSH, K. N., TOMLINS, R. D.: Conf. Int. Thermodyn. Chim., **9,** 120 (1975)
[12] MECKE, R., REUTER, A., SCHUPP, R. L.: Z. Naturforsch., **4a,** 182 (1949)
[13] HUYSKENS, P., CRACCO, F.: Bull. Soc. Chim. Belg., **69,** 422 (1960)
[14] OSTER, G.: J. Am. Chem. Soc., **68,** 2036 (1946)
[15] DANNHAUSER, W., COLE, R. H.: J. Chem. Phys., **23,** 1762 (1955)
[16] BORDEWIJK, P., KUNST, M., RIP, A.: J. Phys. Chem., **77,** 548 (1973)
[17] IBBITSON, B. A., MOORE, L. E.: J. Chem. Soc., (B), **1967,** 76
[18] BELLAMY, L. J., PACE, W.: Spectrochim. Acta, **22,** 535 (1966)
[19] CAMPBELL, C., BRINK, G., GLASSER, L.: J. Phys. Chem., **79,** 660 (1975)
[20] FLETCHER, A. N.: J. Phys. Chem., **73,** 2217 (1969)
[21] MULLENS, J., HANSSENS, L., HUYSKENS, P.: Bull. Soc. Chim. Belg., **79,** 539 (1971)
[22] BORDEWIJK, P., KUNST, M., RIP, A.: Ber. Bunsenges. Phys. Chem., **80,** 839 (1976)

Ramamoorthy SABESAN, Ramanatha VARADARAJAN } Department of Physics, National College, Tiruchirapalli-620 001. Tamil Nadu. S. India

Marudanayagam SARGURUMOORTHY Department of Physics, Periyar E.V.R. College, Tiruchirapalli-620 020. Tamil Nadu. S. India

Acta Chimica Academiae Scientiarum Hungaricae, Tomus 102 (2), pp. 171—177 (1979)

INVESTIGATION OF PRODUCT DISTRIBUTION IN THE OXYETHYLATION OF DODECYL ALCOHOL CATALYZED BY MAGNESIUM PERCHLORATE

P. SALLAY, J. MORGÓS, L. FARKAS and I. RUSZNÁK

(Department of Organic Chemical Technology, Technical University, Budapest)

Received September 22, 1978
Accepted for publication November 21, 1978

The oxyethylation of dodecyl alcohol catalyzed by magnesium perchlorate has been investigated in an oxyethylating apparatus based on the measurement of volume flow. It has been established on the basis of the gas-chromatographic analysis of product composition that the distribution is of the FLORY type and is virtually independent of catalyst concentration and reaction temperature. Compared with a reaction mixture catalyzed with potassium hydroxide, the distribution is more favourable. The catalytic effect of magnesium perchlorate can be explained by complex formation between magnesium ions and ethylene oxide.

Oxyethylation reactions never lead to a uniform product, because the reactivity of the glycol hydroxy group formed in the reaction is almost the same as that of the initial compound. As the product of a consecutive, competitive reaction series, a mixture of homologues with different extents of oxyethylation is formed. Thus, the properties of an oxyethylated non-ionic tenside will depend not only on the quantity of ethylene oxide taken up by 1 mol of the initial compound (on the average degree of oxyethylation), but also on the concentration of the individual homologues, *i.e.* on the product distribution.

The individual distributions measured can by characterized the closeness of their approach to the theoretical distributions deduced from kinetic considerations. Thus, two fundamental types can be ditinguished, *viz.* the FLORY [1] and the WEIBULL—NYCANDER—GOLD [2, 3] distribution. In the general case, it is expedient to calculate the distribution coefficients according to NATTA and MANTICA [4].

In a GFR patent [5] published in 1977, WEIBULL and THORSELL describe a new type of catalyst for the oxyethylation of compounds containing active hydrogens of various types. Instead of the usual basic or acidic catalysts, they used neutral inorganic salts (magnesium perchlorate, calcium perchlorate, *etc.*) as catalyst. They found that the distribution of the molecular weight of the products obtained is more favourable than in the case of basic catalysts, and the reaction mixture does not contain by-products characteristic of mixtures obtained with acidic catalysts. They did not investigate the type of distribution and the effect of the reaction conditions on oxyethylation and on the products.

In this work concerned with the oxyethylation of dodecyl alcohol in the presence of magnesium perchlorate, we investigated the type of molecular weight distribution in the product mixture and the effect of reaction conditions on oxyethylation and on the product.

Experimental

The experiments were carried out in the oxyethylation apparatus used earlier [6], based on the measurement of volume flow. For one oxyethylation 0.02 mol of dodecyl alcohol was used. The product composition was determined by the direct gas chromatography of the reaction mixture [7]. The main gas chromatographic characteristics are listed in Table I.

Table I

Parameters of gas-chromatographic analysis

Chromatograph	Model Chrom-31
Column	Stainless steel, ∅6 mm, length 1.4 m 10% SE 301 on Chromosorb W AW DMCS (60—80 mesh)
Temperature	190—290 °C, 10 °C/min
Detection	Flame ionization
N_2 flow rate	45 cm³/min

The compositions measured were compared with the theoretically calculated distributions

FLORY distribution [1]:

$$x_i = e^{-v} \frac{v^i}{i!}$$

where x_i is the mole fraction of the i-th homologue, v is the average degree of oxyethylation

WEIBULL—NYCANDER—GOLD distribution [2, 3]:

$$v = -c \ln x_0 - (c - 1)(1 - x_0)$$

$$x_i = \frac{c^{i-1}}{(c-1)^i} \left\{ x_0 - x_0^c \sum_{j=0}^{i-1} \frac{1}{j!} [(1-c) \ln x_0]^j \right\}$$

where x_0 is the mole fraction of the initial substance in the reaction mixture, c is the distribution coefficient calculated according to WEIBULL, NYCANDER and GOLD. The distribution coefficients determined separately for each component (c_i) have been calculated according to NATTA and MANTICA [4]:

$$x_i = (-1)^i \prod_{j=0}^{i-1} c_j \sum_{j=0}^{i} \frac{1}{\prod_{\substack{k=0 \\ k \neq j}}^{i} (c_k - c_j)} x_0^{c_j}.$$

Results and Discussion

The variation of ethylene oxide uptake with reaction time is shown in Fig. 1. The ethylene oxide uptake under different reaction conditions (temperature, catalyst concentration) is proportional to the reaction time.

In all the cases the distribution of the oxyethylated products is of the FLORY type [1] (Fig. 2), which is clearly shown also by the fact that the distri-

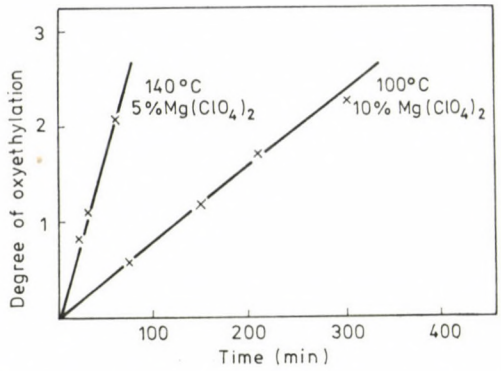

Fig. 1. Variation of ethylene oxide uptake with time

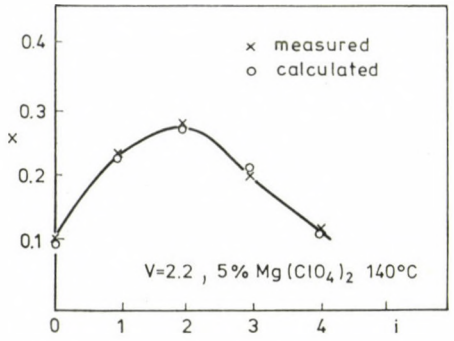

Fig. 2. Distribution of oxyethylated reaction products

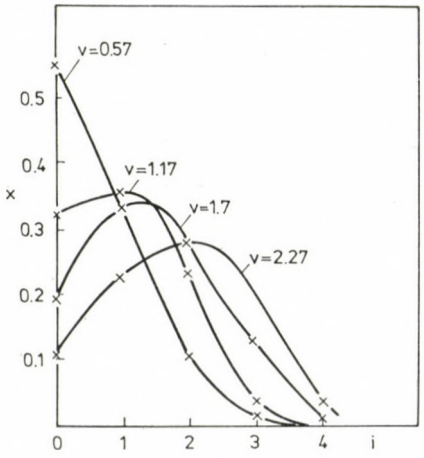

Fig. 3. Variation of the distribution with the average degree of oxyethylation (10% catalyst, 100 °C)

Table II

Effect of the degree of oxyethylation on the distribution (100 °C, 10% catalyst)

v	c	x_0			x_1			c_1	x_2			c_2
		m	calcd. (F)	calcd. (W)	m	calcd. (F)	calcd. (W)		m	calcd. (F)	calcd. (W)	
0.57	0.74	0.544	0.565	0.544	0.334	0.322	0.358	0.970	0.103	0.092	0.083	0.97
1.17	1.08	0.322	0.310	0.322	0.359	0.363	0.348	1.030	0.230	0.212	0.210	0.77
1.70	1.03	0.188	0.182	0.188	0.332	0.310	0.305	0.930	0.288	0.263	0.261	0.78
2.27	1.02	0.106	0.103	0.106	0.230	0.235	0.233	1.030	0.279	0.266	0.264	0.95

x_3			c_3	x_4			c_4
m	calcd. (F)	calcd. (W)		m	calcd. (F)	calcd. (W)	
0.015	0.017	0.013	1.66	0.000	0.002	0.001	—
0.036	0.083	0.086	3.64	0.000	0.024	0.035	—
0.129	0.149	0.151	0.84	0.005	0.063	0.108	2.8
0.190	0.201	0.207	1.07	0.034	0.114	0.124	5.5

v = average degree of oxyethylation (mol ethylene oxide/mol initial alcohol)
m = measured
x_i = mole fraction of the i-th component
calcd.(F) = calculated (according to FLORY [1])
calcd.(W) = calculated (according to WEIBULL, NYCANDER and GOLD [2, 3])
c = distribution coefficient (according to WEIBULL, NYCANDER and GOLD [2, 3])
c_i = distribution coefficient (according to NATTA and MANTICA [4])

Table III

Effect of catalyst concentration (c_k) on oxyethylation

c_k (%)	v	c	x_0			x_1			c_1	x_2			c_2
			m	calcd. (F)	calcd. (W)	m	calcd. (F)	calcd. (W)		m	calcd. (F)	calcd. (W)	
5*	2.26	0.93	0.094	0.104	0.094	0.245	0.236	0.242	0.92	0.270	0.266	0.273	0.94
10*	2.27	1.02	0.106	0.103	0.106	0.230	0.235	0.233	1.03	0.279	0.266	0.264	0.95
15*	2.50	1.03	0.087	0.082	0.087	0.227	0.205	0.203	0.95	0.259	0.256	0.253	0.98
5**	2.27	0.93	0.106	0.103	0.106	0.237	0.235	0.233	1.00	0.275	0.266	0.264	0.96
10**	1.93	1.03	0.150	0.145	0.150	0.234	0.280	0.276	1.21	0.277	0.270	0.267	1.06

x_3			c_3	x_4			c_4
m	calcd. (F)	calcd. (W)		m	calcd. (F)	calcd. (W)	
0.188	0.201	0.203	1.10	0.048	0.113	0.110	3.94
0.190	0.201	0.207	1.07	0.034	0.114	0.118	5.50
0.201	0.213	0.216	1.00	0.051	0.134	0.123	0.98
0.194	0.201	0.207	1.06	0.119	0.114	0.118	0.69
0.180	0.174	0.176	1.15	0.078	0.084	0.091	1.74

* 100 °C
** 140 °C

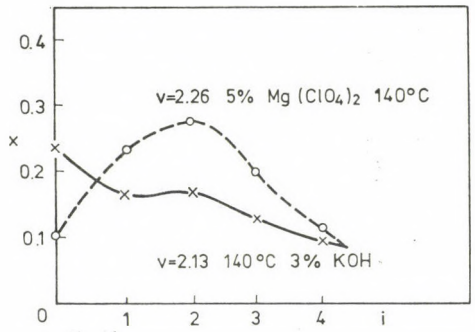

Fig. 4. Comparison of the distribution of reaction mixtures catalyzed by KOH and $Mg(ClO_4)$

bution coefficients calculated according to WEIBULL, NYCANDER and GOLD [2, 3], and NATTA and MANTICA [4], are close to unity (0.9—1.1) (only the value of c_4 differing in some of the cases).

(The figure shows only the distribution calculated according to FLORY, because at a value of $c \sim 1$ the WEIBULL—NYCANDER—GOLD distribution is practically the same.)

With increasing degree of oxyethylation, the character of the distribution (FLORY) does not change, but the maximum shifts to the right and the distribution becomes broader (Table II, Fig. 3).

The distribution is not affected by the concentration of the catalyst (Table III).

Moreover, the distribution is virtually independent of the temperature (Table III).

The product distributions obtained with magnesium perchlorate and KOH were compared (Fig. 4). It has been established that the product distribution with $Mg(ClO_4)_2$ catalyst is more favourable than in the case of KOH, because the quantity of initial substance is considerably lower and the distribution is narrower. In both cases there is no important by-product formation. In the case of magnesium perchlorate no subsequent neutralization is needed. Under identical conditions (140 °C, 5% catalyst) the rate of oxyethylation with $Mg(ClO_4)_2$ is half of that of the reaction with KOH [in the case of 0.088 mol EO/min mol KOH and 0.036 mol EO/min mol $Mg(ClO_4)_2$].

The catalytic effect of magnesium perchlorate can be attributed to complex formation between magnesium ions and ethylene oxide. Perchlorate ions have no effect on the reaction. This is proved by the fact that when alkali perchlorates insoluble in dodecyl alcohol (Na, K) are solubilized with crown ethers, the salt introduced in this way has no catalytic action, because the alkali ion included in the crown compound cannot form a bond with ethylene oxide, while the perchlorate ion has no catalytic effect.

REFERENCES

[1] FLORY, P. J.: J. Am. Chem. Soc., **62,** 1561 (1940)
[2] WEIBULL, B., NYCANDER, B.: Acta Chem. Scand., **8,** 847 (1954)
[3] GOLD, L.: J. Chem. Phys., **20,** 1651 (1952); **28,** 91 (1958)
[4] NATTA, G., MANTICA, E.: J. Am. Chem. Soc., **74,** 3152 (1952)
[5] Ger. 2 639 564 (1977)
[6] RUSZNÁK, I., MORGÓS, J., SALLAY, P.: Wissensch. Zeitschrift T. U. Dresden, **20,** 743 (1971)
[7] FARKAS, L., RUSZNÁK, I., MORGÓS, J., SALLAY, P.: Kolorisztikai Értesítő, **16,** 198 (1974)

Péter SALLAY
Jenő MORGÓS
László FARKAS
István RUSZNÁK

H-1502 Budapest, Műegyetem rkp. 3.

Acta Chimica Academiae Scientiarum Hungaricae, Tomus 102 (2), pp. 179—185 (1979)

STRUCTURE INVESTIGATION OF SUBSTITUTED SCHIFF-BASE DERIVATIVES

Á. I. KISS,[1] M. RÉVÉSZ,[2] J. CSÁSZÁR[2] and M. I. BÁN[2]

([1]Institute of Physical Chemistry, Technical University, Budapest, [2]Institute of General and Physical Chemistry, JATE, Szeged)

Received July 5, 1978

In revised form October 16, 1978

Accepted for publication November 22, 1978

The electronic absorption band appearing between 400 and 450 nm in the spectra of substituted benzylidene-anilines is interpreted in terms of approximate quantum chemical calculations and attributed to the quinonoid structure formed by hydrogen bridge in Schiff-base derivatives where the aldehyde ring has a hidroxy group in *o*- or *p*-position.

Introduction

Spectroscopic studies on Schiff-bases deal primarily with the interpretation of the electronic transitions between 200 and 400 nm [1, 2]. From the behaviour of these bands conclusions are drawn to the electronic structure and the geometry of the molecules. Much less information is available on the electronic transitions above 400 nm. The electronic spectra of substituted benzylidene-anilines show in nonpolar solvents three band systems, in the spectral ranges between 220—240 nm, 260—290 nm and 310—360 nm, belonging to $\pi \rightarrow \pi^*$ transitions. Substituents and solvents have considerable influence only on the longest wavelength transition.

In highly polar hydrogen-bridging solvents an additional band between 400 and 450 nm of medium intensity appears [3]. This band can be attributed to the quinonoid structure formed by hydrogen bonding [4]. The band appears only in spectra of derivatives where the aldehyde group has a hydroxy substituent in 2- (or 4-) position (Fig. 1). In the former case intramolecular and in the latter intermolecular hydrogen bond is assumed. The hydrogen bond formation is very likely reducing the charge density on the oxygen atom of the hydroxy group in the aldehyde ring, and if the aniline ring bears no strong electron acceptor substituents, the azomethine nitrogen atom will bind the phenolic hydrogen thereby accomplishing the quinonoid structure. In the mixture of polar and non-polar solvents an equilibrium between the benzenoid and quinonoid forms is set (Fig. 2).

It seems that all the effects which favour the formation of the quinonoid structure will increase the intensity of the new band. This band is dependent on the nature of the substituent in the aniline ring and quite independently

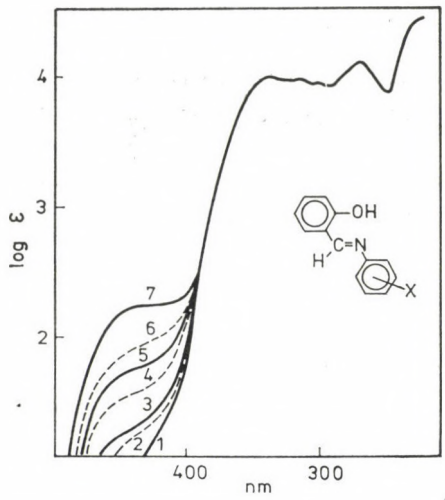

Fig. 1. Electronic absorption spectrum of unsubstituted (X=H) salicylidene-aniline in various solvents (1: in benzene, 7: in methanol, 2—6: in methanol-benzene mixtures)

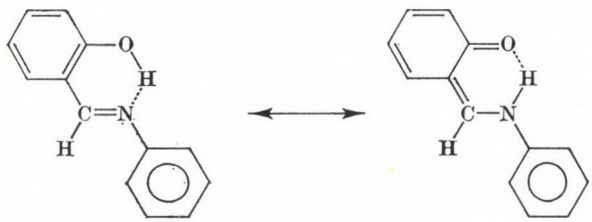

A *B*

Fig. 2. Two forms of salicylidene-aniline (A: benzenoid structure, B: quinonoid structure)

of the substituents — others than hydroxy group — on the aldehyde ring it does not appear when the aniline ring has a strong electron acceptor group on it.

From the spectra the conclusion can be drawn that the necessary conditions for the appearance of the band between 400 and 450 nm are as follows: i) the presence of —OH group in *o*- or *p*-position on the aldehyde ring, and ii) sufficiently large charge density on the azomethine nitrogen this being dependent mainly on the substituent of the aniline ring.

In order to obtain further informations on the problem raised, quantum chemical calculations* by the PPP and CNDO/2 approximations have been performed.

* The observation mentioned has not been interpreted by former calculations [5].

Experimental

The Schiff-base derivatives were prepared by reacting stoichometric quantities of 2- and 4-hydroxy benzaldehyde and substituted anilines in methanolic solutions. The crude products were purified by recrystallizations from methanol and their purities checked by m.p. and C, H-assays. The absorption spectra were taken by using BECKMAN DU and SPECORD UV-VIS spectrophotometers.

Calculations

First PPP calculations on the electronic spectra of benzylidene-anilines having different substituents on the aniline ring have been carried out. As examples the calculated and experimental spectral data for the unsubstituted salicylidene-aniline and the *p*-chloro derivative are given in Table I. It can be

Table I

Molecule	Electronic transitions (energies in eV, oscillator strengths in parentheses)			
	1.		2.	
	Exp.	Calcd.	Exp.	Calcd.
Salicylidene-aniline	3.625	4.015	4.492	4.881
	(0.138)	(0.509)	(0.174)	(0.458)
Salicylidene-4-chloroaniline	3.594	3.997	4.575	4.729
	(0.282)	(0.631)	(0.275)	(0.406)

seen that the substituent effect by the *p*-chloro group is well represented in the calculations: the 340 nm band shows slight red shift and intensity increase on the substitution. Similar substituent effect could be observed and calculated in case of methyl and hydroxy groups and also in *o*- and *m*-substituted derivatives. However, the PPP calculations reproduces only the spectra in nonpolar media and are not able to give any information on the band over 400 nm.

By substitution only very slight changes in the π-charges occur either on the azomethine nitrogen or on the oxygen atom of the hydroxy group on the aldehyde ring (Table II). It seems that the charges on the aldehyde ring and on the azomethine group are not very sensitive to the changes in the aniline ring.

The charge distributions of the enol- and keto-forms of 2-hydroxy-benzylidene-aniline have been calculated by the CNDO/2 method [6]. The geometry of the enol- (benzenoid) form is known from the literature [7] but that of the keto-(quinonoid) form had to be approximated by analogues. The bond distances and angles in the aniline ring of the quinonoid form were supposed to be equal to those in the benzenoid form, however, these structural data for the aldehyde ring were taken from those of butadiene and acrolein [8]. By presuming a symmetry plane bisecting the bonds C_1—C_2 and C_4—C_5,

Table II

Molecule	π-charges (numbering of atoms as in Fig. 4)	
	N_8	O_{15}
Salicylidene-aniline	−0.253	0.189
Salicylidene-2-hydroxy-aniline	−0.254	0.184
Salicylidene-3-hydroxy-aniline	−0.249	0.188
Salicylidene-4-hydroxy-aniline	−0.245	0.188
Salicylidene-2-chloro-aniline	−0.252	0.186
Salicylidene-3-chloro-aniline	−0.250	0.188
Salicylidene-4-chloro-aniline	−0.248	0.188
Salicylidene-4-methyl-aniline	−0.248	0.188

closing of the aldehyde ring was achieved by the simultaneous variation of the bond distances and bond angles (Fig. 3). The C—C bond distances in the benzene rings of 2-hydroxy-benzylidene-aniline were taken to be 1.397 Å. For the two forms of 2-hydroxy-benzylidene-aniline the calculated net charges on the atoms numbered as in Fig. 4 can be found in Table III.

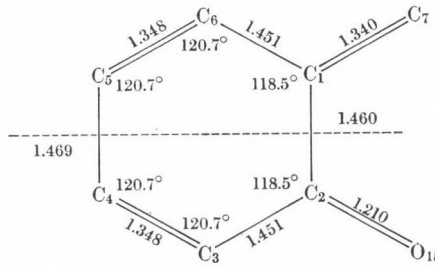

Fig. 3. Bond lengths and bond angles in the aldehyde ring of the quinonoid form of salicylidene-aniline (presumed symmetry plane is indicated by broken line)

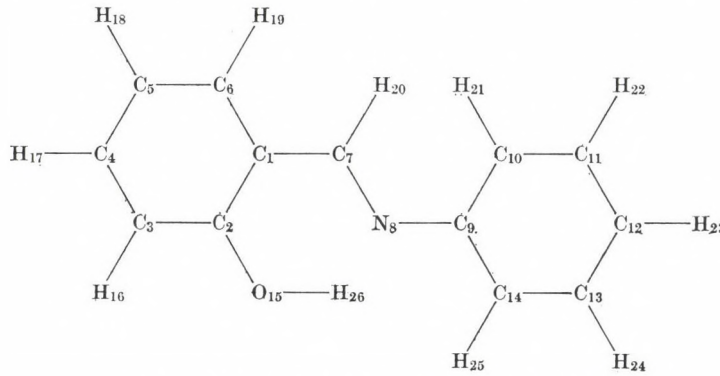

Fig. 4. Numbering of the atoms in salicylidene-aniline

Table III

No.	Atom	Net charges by CNDO/2	
		Benzenoid form	Quinonoid form
1.	C	−0.069	−0.100
2.	C	0.224	0.270
3.	C	−0.071	−0.081
4.	C	0.040	0.050
5.	C	−0.035	−0.037
6.	C	0.034	0.036
7.	C	0.136	0.169
8.	N	−0.186	−0.221
9.	C	0.121	0.134
10.	C	−0.037	−0.038
11.	C	0.021	0.020
12.	C	−0.016	−0.011
13.	C	0.021	0.020
14.	C	−0.038	−0.038
15.	O	−0.277	−0.328
16.	H	0.009	0.011
17.	H	−0.005	−0.007
18.	H	−0.005	−0.004
19.	H	−0.007	−0.011
20.	H	−0.033	−0.002
21.	H	−0.001	0.004
22.	H	−0.007	−0.004
23.	H	−0.007	−0.004
24.	H	−0.007	−0.005
25.	H	−0.001	0.002
26.	H	0.192	0.172
Total electronic energy		−130.687555 a. u.	−130.581973 a. u.
Dipole moment		2.911 Debye	2.549 Debye

The charge density values of the benzenoid form come up to expectations: on the C-atoms of the benzene rings there are small charges which are negative on the 3, 5, 10, 12 and 14 atoms (in *o*- and *p*-positions to the —OH and =N— groups) and positive on the 4, 6, 11 and 13 atoms (in *m*-position to the —OH and =N— groups). The largest polarization effect occurs on the —OH group,

the negative charge on the O-atom being significantly greater than the positive charge on the H-atom. This is in accordance with the loosened character of the proton of the hydroxy group observed experimentally. There is also considerable charge on the N-atom and somewhat smaller positive charge on the C-atom of the azomethine group.

The experimental dipole moment of the unsubstituted salicylidene aniline is 2.39 D [9]. This value is in good agreement with that (2.30 D) calculated by vectorial addition from experimental values for benzalaniline and *o*-hydroxybenzaldehyde [10]. The dipole moments of the two forms calculated by CNDO/2 (4. column in Table IV) show close resemblance to those calculated from ex-

Table IV

Substance	Dipole moment (in Debyes)		
	Exp.	Calcd.	This work
Salicylidene aniline	2.39[a]	2.30[b]	
quinonoid form		2.8[a]	2.55
benzenoid form		2.7[a]	2.91

[a] MINKIN, V. I. *et al.*: Dokl. Akad. Nauk. USSR, *145*, 336 (1962)
[b] MAKÁRY, A.: Unpublished result

perimental data (3. column in Table IV) though they are in reversed order. Unfortunately the small difference in the experimental values of the two forms does not allow establishing the real trend in the change of dipole moments.

The quinonoid form is found by the CNDO/2 calculations to be less stable than the benzenoid one the difference in total electronic energies being $\sim$0.1 a.u. (Table III). Though there are larger charges on the atoms of the quinonoid form, still the resulting dipole moment of it is smaller than that of the benzenoid form. By comparing the charge distributions, it can be seen that the charges on the C_2 and O_{15} atoms as well as on the azomethine nitrogen of the quinonoid form are larger than those on the corresponding atoms in the benzenoid form. On the other hand, the positive charge on the H_{26} atom of the keto-form is smaller than that of the enol-form. The absolute value of the difference in the charges is smaller for the covalently bonded N—H atoms in the quinonoid form (0.049) than for the covalently bonded O—H atoms in the benzenoid form (0.085). From this fact, one can come to the conclusion that the H_{26} atom is bound by the N-atom of the quinonoid form more strongly than by the O-atom of the benzenoid form. The appearance and the intensity of the new band over 400 nm is very likely in close relation with the shift of the equilibrium between the two forms, in favour of the quinonoid form, by the effects mentioned earlier.

*

The authors are greatly indebted to Dr. F. CSER of the Research Institute for Plastic Technology, Budapest for lending them his CNDO/2 program.

REFERENCES

[1] SMITH, H. E., COOK, S. L., WARREN, M. E.: J. Org. Chem., **29,** 2265 (1964)
[2] MURRELL, J.: Tetrahedron Suppl., **2,** 277 (1963)
[3] MINKIN, V. I. *et al.:* Zh. Fiz. Khim., **38,** 1718 (1964); Zh. Org., Khim., **7,** 2364 (1971)
[4] CSÁSZÁR, J., NOVÁK-BIZONY, M.: Acta Chim. Acad. Sci. Hung., **86,** 9 (1975)
[5] TINLAND, B.: Tetrahedron, **26,** 4795 (1970); MINKIN, V. I.: Zh. Fiz. Khim., **41,** 556 (1967); BEZUGLIJ, V. D. *et al.:* Zh. Obs. Khim., **42,** 1102 (1972); MINKIN, V. I. *et al.:* Theor. i Exp. Khim., **11,** 477 (1975); see also [3]
[6] POPLE, J. A., BEVERIDGE, D. L.: Approximate Molecular Orbital Theory, McGraw-Hill Book Co., New York, 1970
[7] WARREN, C. H., WETTERMARK, G., WEISS, K.: J. Amer. Chem. Soc., **93,** 4658 (1971)
[8] KUCHITSU, K., FUKUYAMA, T., MORINO, Y.: J. Mol. Struct., **1,** 483 (1968)
[9] MINKIN, V. I. *et al.:* Dokl. Akad. Nauk USSR, **145,** 336 (1962); OSIPOV, O. A., MINKIN V. I., KOGAN, V. A.: Zh. Fiz. Khim., **37,** 1492 (1963); MINKIN, V. I., OSIPOV, O. A., ZHDANOV, Yu. A.: Dipole Moments in Organic Chemistry., Plenum Press, New York—London, 1970
[10] MAKÁRY, A.: Unpublished result

Árpád István KISS H-1111 Budapest, Budafoki út 8.

Márta RÉVÉSZ
József CSÁSZÁR } H-6701 Szeged, P. O. B. 105
Miklós I. BÁN

Acta Chimica Academiae Scientiarum Hungaricae, Tomus 102 (2), pp. 187—194 (1979)

SPEKTROPHOTOMETRISCHE UNTERSUCHUNG DER BASE-KATALYSIERTEN OXIDATION DES 3-HYDROXY- UND 3-AMINO-FLAVANONS

É. R. DÁVID, M. RÁKOSI, G. B. SZABÓ und R. BOGNÁR

(Lehrstuhl für Organische Chemie der Lajos Kossuth Universität, Debrecen)

Eingegangen am 12. April 1978

Zur Veröffentlichung angenommen am 23. November 1978

Die Untersuchung der Veränderung der Spektren von 3-Hydroxy-flavanon und 3-Amino-flavanon in Abhängigkeit vom pH zeigte, daß beide Verbindungen sich in alkalischen Pufferlösungen in Derivate höherer Oxidationsstufen, namentlich in 3-Hydroxy-flavon bzw. 3-Amino-flavon umsetzen. Es wurde festgestellt, daß der Prozeß eine irreversible, basenkatalysierte, durch Luftsauerstoff hervorgerufene Oxidation ist.

Die natürlichen und synthetischen Flavonoidverbindungen können auf Grund der Oxidationsstufe der die zwei aromatischen Ringe verbindenden Propankette in verschiedene Gruppen eingeordnet werden [1, 2, 3]. Alle Flavonoide verfügen über ein charakteristisches UV-Spektrum mit gut definierten Banden [3, 4], wodurch sie voneinander gut unterschieden werden können. Diese spektralen Eigenschaften sind gleichzeitig auch dazu geeignet, Flavonoidverbindungen mit verschiedenen Oxidationsstufen in Oxidations- oder Reduktionsvorgängen zu verfolgen.

Bei den Untersuchungen der Veränderung der Spektren von den in Stellung 3 mit einer Hydroxyl- bzw. Aminogruppe substituierten Flavon- und Flavanonderivaten mit dem pH-Wert und der Stabilität haben wir gezeigt, daß — unter bestimmten und verhältnismäßig einfachen Bedingungen — das 3-Hydroxy-flavanon und das 3-Amino-flavanon sich in einer Pufferlösung mit alkalischem pH irreversibel zu einer einheitlichen Verbindung mit einer höheren Oxidationsstufe, zu 3-Hydroxy-flavon bzw. 3-Amino-flavon oxidiert. Wir haben die Oxidation nicht nur spektrophotometrisch sondern auch auf präparativem Wege nachgewiesen.

Experimenteller Teil

Die zu den Spektrenaufnahmen verwandten Substanzen wurden auf die von uns früher beschriebene Weise hergestellt [5]. Die Spektren wurden mit einem UNICAM SP 800 Spektrophotometer gemessen, die äthanolischen Stammlösungen mit einer Konzentration von 1.10^{-3} *M* wurden entsprechend verdünnt. Zur pH-Messung wurde ein METHROM-Apparat und eine kombinierte Glaselektrode mit "U" Bezeichnung angewandt. Die Pufferlösungen wurden nach BRITTON—ROBINSON bereitet [6]. Die kinetischen Messungen wurden in Pufferlösungen mit einer Konzentration von 1.10^{-4} bzw. 5.10^{-5} *M* durchgeführt [7].

Zur präparativen Kontrolle des Oxidationsvorganges wurden etwa 500 mg 3-Hydroxy-flavanon bzw. 3-Amino-flavanon. HCl in 25 ml Äthanol bzw. in 25 ml 2*N* äthanolischer Natronlauge unter gelinder Erwärmung gelöst. Die äthanolische Lösung des 3-Hydroxy-flavanons wurde auf pH 11 eingestellt und nach etwa einstündigem Stehen wurde die Lösung mit einigen Tropfen konzentrierter Salzsäure angesäuert. Analog wurde auch die alkalische Lösung des 3-Amino-flavanons behandelt. Die leicht sauren Lösungen wurden in Vakuum kalt konzentriert und die ausgeschiedenen Substanzen aus Äthanol kristallisiert. Die erhaltenen Produkte, 3-Hydroxy-flavon bzw. 3-Aminoflavon. HCl wurden spektrophotometrisch und durch Schmelzpunktsbestimmung identifiziert.

Ergebnisse und Diskussion

Die Veränderung der UV-Spektren in Abhängigkeit des pH-Wertes

Die Spektrendaten des 3-Hydroxy-flavons sind in Tabelle I angegeben.

Das Spektrum zeigt in einer Pufferlösung mit saurem pH keine wesentliche Veränderung im Vergleich mit der in äthanolischer Lösung gemessenen Kurve, eine Verschiebung des pH in den alkalischen Bereich bringt jedoch eine bedeutende Veränderung des Charakter des Spektrums mit sich (Abb. 1). Wenn die alkalische Pufferlösung angesäuert wird, kann das unveränderte Spektrum des 3-Hydroxy-flavons gemessen werden.

Die Veränderung des UV-Spektrums mit dem pH-Wert ist auf die Dissoziation der C_3-Hydroxylgruppe zurückzuführen. Während die Absorption der molekularen Form in das Gebiet der kürzeren Wellenlängen fällt (344 nm), absorbiert die ionische Form bei längeren Wellenlängen (405 nm).

Die Spektren des 3-Hydroxy- und des 3-Amino-flavanons sind in äthanolischer Lösung sehr ähnlich, unterscheiden sich aber wesentlich von dem Spektrum des 3-Hydroxy-flavons (Tabelle I).

Das Spektrum des 3-Hydroxy-flavanons zeigt im pH-Bereich von 1 bis 8 praktisch keine Veränderungen, in einer Pufferlösung über pH 9 jedoch er-

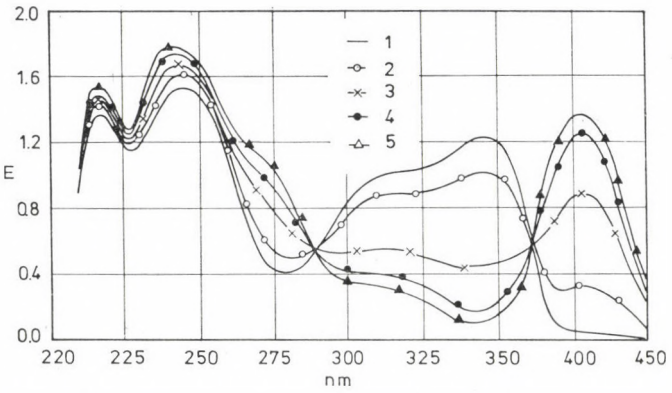

Abb. 1. Spektrumveränderung des 3-Hydroxy-flavons in einer Pufferlösung mit alkalischem pH. *M:* $1 \cdot 10^{-4}$; (1) pH 7; (2) pH 8; (3) pH 9; (4) pH 10; (5) pH 11

Tabelle I

Spektrendaten von 3-Hydroxy-flavon sowie 3-Hydroxy- und 3-Amino-flavanon (M: $1 \cdot 10^{-4}$)

3-Hydroxy-flavon		3-Hydroxy-flavanon		3-Amino-flavanon · HCl	
Äthanol	0,01*N* NaOH	Äthanol	0,01*N* NaOH	Äthanol	0,01*N* NaOH
344 (4,10)	405 (4,13)	322 (3,53)	405 (4,13)	320 (3,62)	360 (3,95)
306 (4,00)	320 (3,60)*	252 (3,94)	320 (3,60)*	253 (4,06)	305 (3,78)*
243 (4,18)	275 (4,00)*	216 (4,46)	275 (4,00)*	216 (4,48)	245 (4,30)
216 (4,28)	235 (4,26)		235 (4,26)		

* Inflexion

scheint die auch bei 3-Hydroxy-flavon auftretende neue Band bei 405 nm (Abb. 2). Die Zunahme der Extinktion dieser Bande mit der Zeit ist gut zu verfolgen. Somit können die zu den einzelnen pH-Werten gehörenden kinetischen Kurven erhalten werden (Abb. 3 und 4).

Wenn man die Pufferlösungen des 3-Hydroxy-flavanons mit einem pH von 10—12 nach der Stabilisierung der Extinktion mit Salzsäure ansäuert (Abb. 3), wird das Spektrum des 3-Hydroxy-flavons erhalten. Dies weist darauf hin, daß in der alkalischen Pufferlösung ein Oxidationsvorgang vor sich geht und die Veränderung des Spektrums eine Folge der durch Oxidation eingetretenen Strukturveränderung ist.

Aus den auf Grund der Zunahme der Extinktion der Bande bei 405 nm konstruierten Kurven (Abb. 4) kann die vom pH abhängende Stabilitätskonstante des 3-Hydroxy-flavanons bzw. die vom pH abhängende Oxidationsgeschwindigkeit berechnet werden (Tabelle II). Außerhalb des alkalischen pH-Bereichs geht die Oxidation weder in polaren, noch in apolaren Lösungsmitteln vor sich.

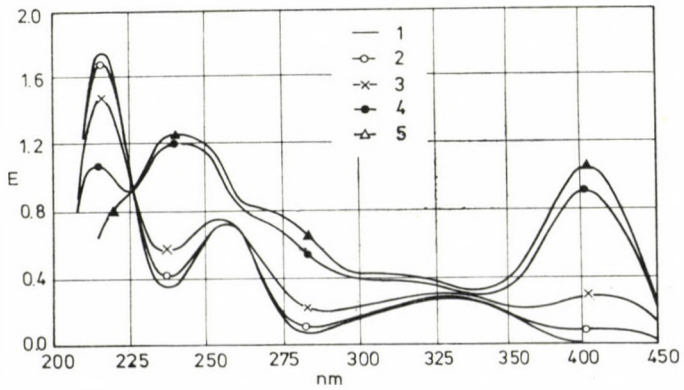

Abb. 2. Spektrumveränderung des 3-Hydroxy-flavanons in einer Pufferlösung mit alkalischem pH. M: $1 \cdot 10^{-4}$; (1) pH 7; (2) pH 8; (3) pH 9; (4) pH 10; (5) pH 11

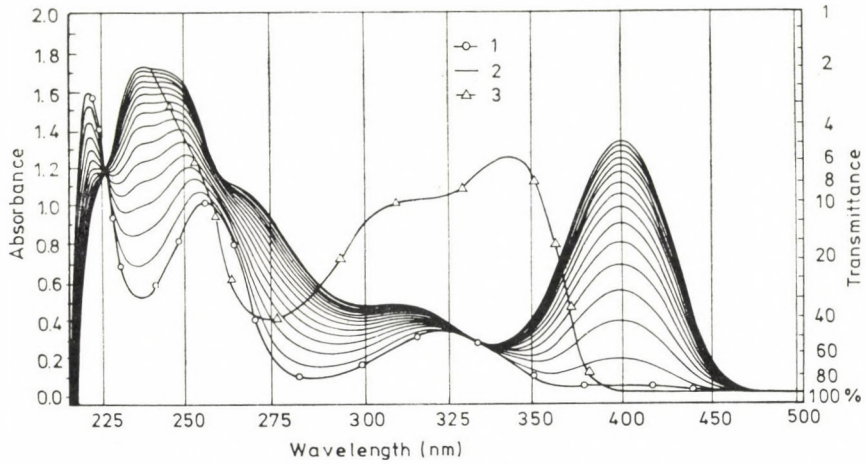

Abb. 3. Zeitliche Veränderung des Spektrums von 3-Hydroxy-flavanon in einer Pufferlösung nach Britton-Robinson mit einem pH von 10. *M:* $1.33 \cdot 10^{-4}$; $t = 0$ (1); $\Delta t = 15$ Min. (2); Spektrum der nach 160 Min. angesäuerten Lösung (3)

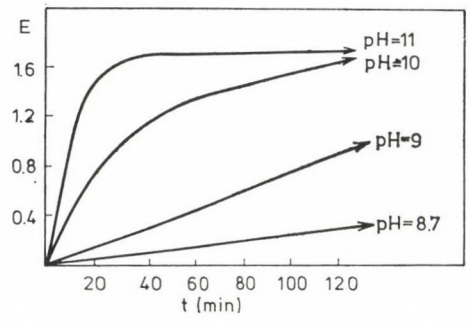

Abb. 4. Zunahme der Extinktion der Bande bei 405 nm des 3-Hydroxy-flavanons in Abhängigkeit von der Zeit in Pufferlösungen mit pH-Werten von 8, 7, 9, 10 und 11

Tabelle II

Geschwindigkeit der vom pH abhängenden Oxidation des 3-Hydroxy- und 3-Amino-flavanons (t =25 C°)

pH	$k \cdot \text{sec}^{-1} \cdot 10^{-2}$	3-Hydroxy-flavanon %	pH	$k \cdot \text{sec}^{-1} \cdot 10^{-2}$	3-Amino-flavanon %
9	0,145	26			
10	2,655	86	10	1,590	36,4
11	7,179	100	11	6,020	69,8
1*N* NaOH	10,425	100	11,8	25,300	100
2*N* NaOH	sehr schnell	100	1*N* NaOH	sehr schnell	100

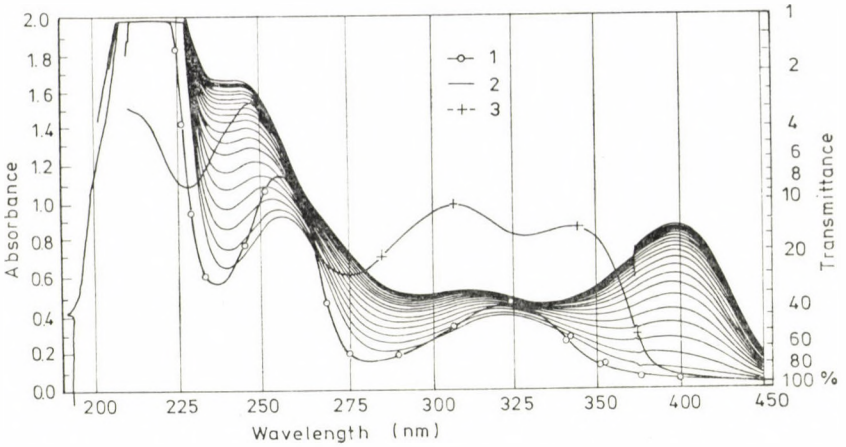

Abb. 5. Zeitliche Veränderung des Spektrums von 3-Amino-flavanon · HCl in einer Pufferlösung nach Britton-Robinson mit einem pH von 10. M: $1.05 \cdot 10^{-4}$; $t = 0$ (1); $\Delta t = 5$ Min. (2); Spektrum der nach 100 Min. angesäuerten Lösung (3)

Ein ähnlicher Oxidationsvorgang wurde auch bei der Untersuchung der vom pH abhängenden Spektrumveränderung des 3-Amino-flavanons beobachtet.

Das 3-Amino-flavanon ist als Base eine sehr labile Verbindung und kann nur in Form des Chlorhydrats aufbewahrt werden. Die Base wird in Gegenwart von Luftsauerstoff oxidiert und je nach den Bedingungen können als Reaktionsprodukte 3-Hydroxy- bzw. 3-Amino-flavon nachgewiesen werden. Außer der Oxidation kann also auch von der Hydrolyse der Aminogruppe gesprochen werden. In Lösung kann die Anwesenheit von Ammonium mit Hilfe des Nessler-Reagens nachgewiesen werden.

Die Hydrolyse muß hier der Oxidation vorausgehen, weil unseren spektroskopischen Messungen nach 3-Amino-flavon — in oxidierter Form — unter den von uns angegebenen Bedingungen nicht hydrolysiert wird.

Dementsprechend entsteht im pH-Bereich von 9—11 neben 3-Hydroxyflavon nur eine kleine Menge 3-Amino-flavon, während nach den spektrophotometrischen Messungen bei pH-Werten über 11 nur 3-Amino-flavon in einer sehr schnellen Reaktion gebildet wird (Abb. 5 und 6, bzw. Tabelle II).

Beschreibung des Mechanismus des Oxidationsvorganges

Die Oxidation des 3-Hydroxy- und 3-Amino-flavanons kann man sich ähnlich wie die Oxidation der α-Hydroxycarbonylverbindungen, der sogenannten Acylcarbinole, vorgestellen. Diese Verbindungen bilden im alkalischen Medium ein tautomeres "Endiol" bzw. "Endiolat-dianion", die befähigt sind, außerst schnell zu den entsprechenden Dicarbonylverbindungen zu oxidieren

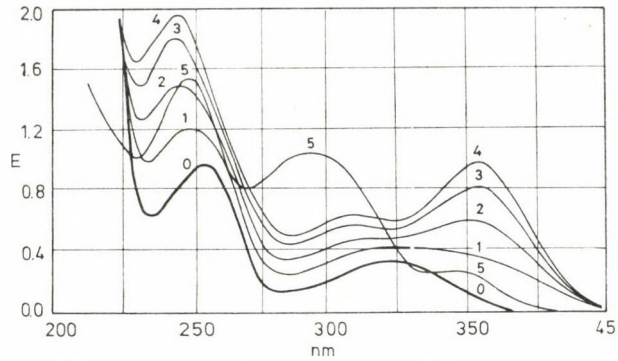

Abb. 6. Zeitliche Veränderung des Spektrums von 3-Amino-flavanon · HCl in einer Pufferlösung nach Britton-Robinson mit einem pH von 11,8. M: $1 \cdot 10^{-4}$; $t = 0$ (0); $\Delta t = 2$ Min. (1, 2, 3, 4); Spektrum der nach 30 Min. angesäuerten Lösung (5)

bzw. sich unter den gegebenen Umständen weiter umzuwandeln [8]. Eben deshalb ist die wichtigste Eigenschaft der Endiole das Reduktionsvermögen, sie werden auch "Reduktone" genannt. Die Oxidation der Endiole kann auch in neutralem oder leicht saurem Milieu unter verhältnismäßig milden Bedingungen (z. B. Luftsauerstoff) vor sich gehen, während das im alkalischem Medium entstehende Endiolat-dianion noch leichter oxidiert wird [9].

Die Oxidation des 3-Hydroxy-flavanons im alkalischen Medium kann nach unserer Annahme wie oben beschrieben werden, aber die Oxidation geht nach den Spektrenmessungen nur in Pufferlösung mit verhältnismäßig hohem pH vor sich, was nahe legt, daß die Bildung der tautomeren Endiol-Form eine Voraussetzung ist:

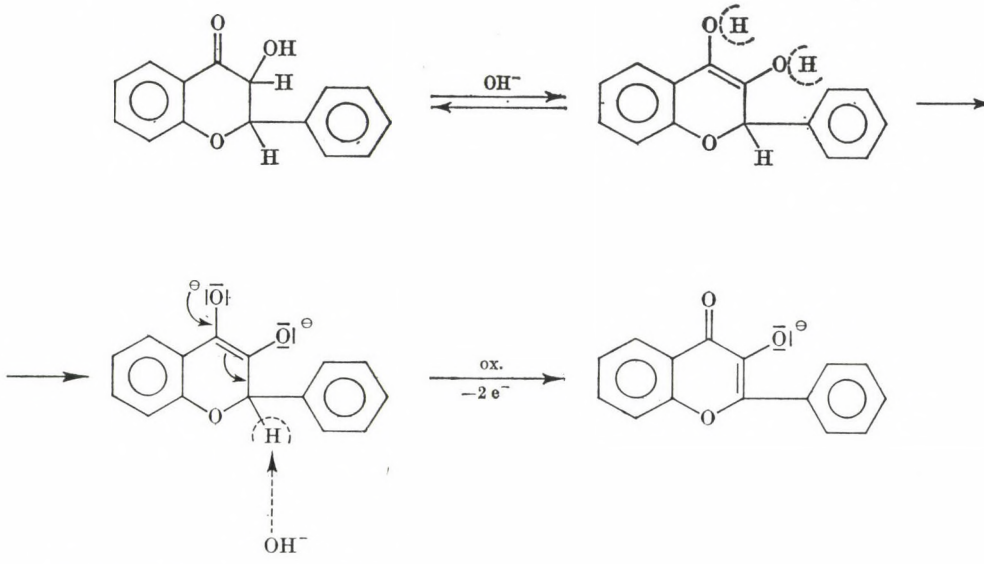

Im alkalischen Medium wird dann das entstandene Endiolat-dianion zu dem entsprechenden Diketon bzw. zu seiner stabileren Form, zu 3-Hydroxy-flavon oxidiert, das in alkalischer Pufferlösung das Spektrum der ionischen Form gibt.

3-Amino-flavanon liefert — je nach dem pH — zwei Oxidationsprodukte: das 3-Hydroxy-flavon bei niedrigem pH (pH 9—10) und das 3-Amino-flavon bei höherem pH (über pH 11). Zwischen pH 10 und 11 kann man beide Produkte finden. Weil die Bildung des 3-Amino-flavons mit größerer Geschwindigkeit als die des 3-Hydroxy-flavons vor sich geht, kann angenommen werden, daß die α-ständige Aminogruppe die Bildung der tautomeren enolischen Form begünstigt und dadurch die Geschwindigkeit des Oxidationsvorganges erhöht wird:

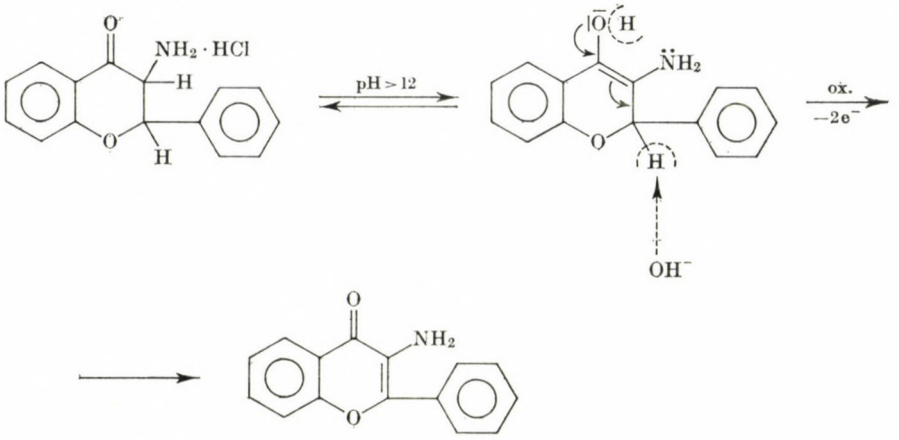

Die Bildung des 3-Hydroxy-flavons zwischen pH 10 und 11 kann folgendermaßen angegeben werden:

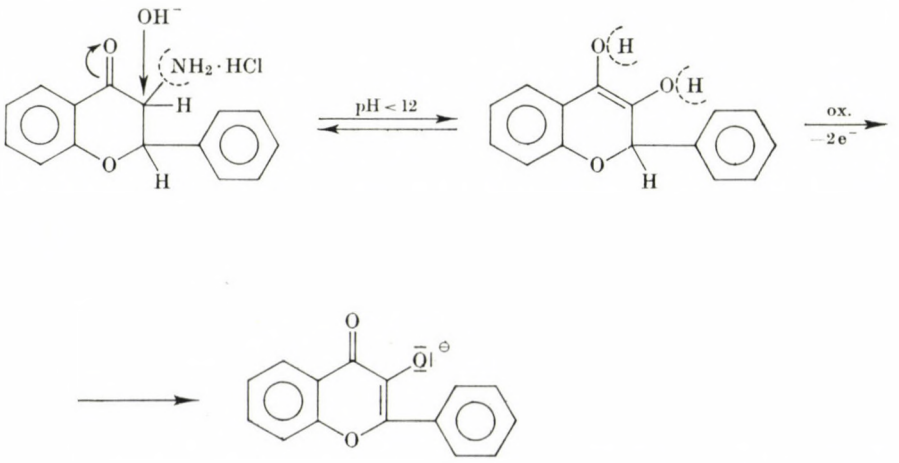

Einen ähnlichen Oxidationsvorgang haben wir auf Grund der Spektrenmessungen auch bei den im Ring "B" in Position C_4, mit einer Hydroxy- bzw. Methoxygruppe substituierten 3-Hydroxy-flavanonderivaten bzw. beim 3-Cyclohexylamino-flavanon beobachtet. Bei diesen Verbindungen entstand — bei gegebenem pH-Wert — einheitlich und irreversibel das entsprechend substituierte Derivat des Produktes mit höherer Oxidationsstufe.

LITERATUR

[1] BOGNÁR, R.: M. T. A. Kém. Tud. Oszt. Közl., **6**, 227 (1955)
[2] BÖHM, K.: »Die Flavonoide« (ed. CANTOR), Aulendorf, 1967
[3] BOGNÁR, R. and his collaborators: »Recent Flavonoid Research« in »Recent Developments in the Chemistry of Natural Carbon Compounds« Vol. **5** (eds. BOGNÁR, R., BRUCKNER, V., SZÁNTAY, Cs.), Akadémiai Kiadó, Publishing House of Hungarian Academy of Sciences, Budapest, 1973
[4] JURD, L.: »Spectral Properties of Flavonoid Compounds« in »The Chemistry of Flavonoid Compounds« (ed. GEISSMAN, T. A.), Pergamon Press, Oxford, London, New York, Paris, 1962
[5] BOGNÁR, R., RÁKOSI, M.: Liebigs Ann. Chem., **693**, 225 (1966); LITKEI, Gy., BOGNÁR, R., DINYA, Z., DÁVID, É. R.: »Oxidation Experiments in the Group of Flavonoids (Algar-Flynn-Oyamada Oxidations)« in »Topics in Flavonoid Chemistry and Biochemistry« (eds. FARKAS, L., GÁBOR, M., KÁLLAY, F.), Akadémiai Kiadó, Publishing House of Hungarian Academy of Sciences, Budapest, 1975
[6] »Puffertabellen« in »Analitikai Zsebkönyv«, Műszaki Kiadó, Budapest, 1971, S.: 394
[7] SCHWETLICK, K.: in »Kinetische Methoden zur Untersuchung von Reaktionsmechanismen«, VEB. Deutscher Verlag der Wissenschaften, Berlin, 1971
[8] HOUBEN-WEYL: »Methoden der organischen Chemie, II. Band, Thieme, G. Verlag, Stuttgart, 1953, S.: 392
[9] JAMES, T. H., WEISSBERGER, A.: J. Am. Chem. Soc., **59**, 2040 (1937)

Éva R. DÁVID
Miklós RÁKOSI
Gizella B. SZABÓ
Rezső BOGNÁR

H-4010 Debrecen, P. O. Box 20.

Acta Chimica Academiae Scientiarum Hungaricae, Tomus 102 (2), pp. 195—200 (1979)

INVESTIGATION OF COMPOUNDS CONTAINING Si—S AND S—Si—S BONDS BY ULTRAVIOLET SPECTROSCOPY, II

AROMATIC COMPOUNDS

T. VESZPRÉMI, M. EL-KERSH and J. NAGY

(Department of Inorganic Chemistry Technical University, Budapest)

Received July 10, 1978
Accepted for publication November 23, 1978

Studies on the through conjugation of sulfur atom over silicon and on the existence of "through-bond" interaction between sulfur atoms in compounds containing S—Si and S—Si—S bonds do not give unambigous results if only aliphatic or alicyclic compounds are investigated by UV spectroscopy. Therefore the investigations were extended to the UV spectra of compounds containing Ar—Si—S grouping in order to draw conclusions on the basis of the changes observed in the spectra of the aromatic systems. An interaction of the sulfur atoms with the aromatic system may be deduced from the spectra. The extent of this effect is similar in the analogous silicon and carbon derivatives. On the other hand, the bathochromic shift of the α and p bands for the silicon compounds indicates that the lone pairs of sulfur atom can form a conjugative connection with the aromatic ring, making use of the vacant silicon d orbitals. The degree of the effect of the lone pairs is rather similar to that of chlorine in the analogous derivatives.

Introduction

In our previous paper[1] a study of the ultraviolet spectra of some aliphatic and saturated cyclic compounds containing S—Si or S—Si—S bond was reported. The interpretation of the ultraviolet spectra and our conclusions were supported by PES results. The absorption band found between 220 and 240 nm in the spectra was shown to have $n \rightarrow \sigma^*$ character. The $n \rightarrow \sigma^*$ transition has a hypsochromic shift in the spectra of silicon compounds as compared with the spectra of the corresponding carbon derivatives; this can be explained by $(d - p)\pi$ interaction between the lone pair of the sulfur atom and the vacant silicon d orbital.

Consideration of a through conjugation of the sulfur atoms over silicon or of a through-bond interaction between sulfur atoms did not lead to any unambiguous result. The spectra of the compounds belonging to the series $(CH_3CH_2S)_nSi(CH_3)_{4-n}$ differ from one another only in the intensity of the bands, indicating the isolation of the sulfur atoms. On the other hand, in compounds where the two sulfur atoms are far from each other (in 1 and 4 positions), only a weak shoulder can be observed in the region 220 to 240 nm. This experimental fact points to the mutual effect of the near sulfur atoms. No unambiguous conclusions can be drawn on the basis of photoelectron

spectral data, either. According to these spectra, the degeneration of the *n* levels of sulfur atoms in S—C—S bond is raised; the levels are split in a small degree. This slight splitting, however is within the experimental error.

In this paper we return to this problem and try to give a correct answer. Our hypothesis is the following. The investigation of the far interactions in aliphatic systems is troublesome because of the relative simplicity and insensibility of the ultraviolet spectra. Aromatic systems are, however, very sensitive to the effect of mobile lone pairs. Thus, *e.g.* the spectrum of benzene is entirely "distorted" in the case of C_6H_5SH owing to a very strong charge transfer interaction. Therefore our recent conclusions are based on the ultraviolet spectra of aromatic systems with Si—S or S—Si—S fragment in the molecule.

Experimental

Compounds **1**—**9** in Table I were prepared by the reaction of the appropriate alkylmercaptan and chlorosilane derivatives in the presence of triethylamine in benzene solution [2, 3]. The purity of the compounds was checked by gas chromatography and by determination of the silicon content.

The UV spectra were recorded with a Spektromom 201 instrument in *n*-hexane using quartz cells of 1 and 0.2 cm thickness. The ultraviolet maxima of the compounds and the intensities of the absorption bands are summarized in Table I.

Results and Discussion

The UV spectra reflect the aromatic structure. The α band with vibrational fine structure (between 260 and 270 nm) and the *p* band (between 216 and 223nm) can readily be distinguished. For some compounds, the position of the β band can also be observed; in other cases the position of the maximum can be concluded from the shape of the spectrum.

The spectra of the linear, the five-membered and six-membered cyclic compounds do not show characteristic differences. The spectra of mono- and diphenyl compounds differ from each other — as expected — first of all in intensity, which increases for the diphenyl derivatives. In addition, a slight bathochromic shift is observed for the diphenyl derivatives in comparison with the monosubstituted compounds; the shift is 1 to 7 nm in the *p* band and somewhat smaller in the α band. This fact indicates conjugation of the phenyl groups in a small degree, through the silicon atom.

The spectra of compounds **8** and **9** indicate that an increase of the number of sulfur atoms results in the increased intensity of the bands.

Table II gives a comparison of the ultraviolet maxima of some compounds with the general formula $C_6H_5Si(CH_3)X_2$ ($X = CH_3$, F, Cl, SC_2H_5) [4, 5]. A bathochromic displacement can be seen from the data for silicon compounds as compared with the analogous carbon derivatives. This is caused by the in-

Table I

UV maxima and intensities of the compounds investigated

(The asterisk indicates a shoulder at the given position)

No.	Compound	α band		CT band		*p* band		β band	
		λ_{max} [nm]	lg ε	λ_{max} [nm]	lg ε	λ_{max} [nm]	lg ε	λ_{max} [nm]	lg ε
1	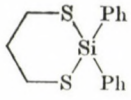	273 266 260*	2.79 2.91 2.94			220	4.15	194	4.73
2	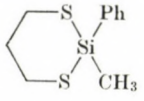	272	2.55	236*	3.43	218	4.14	198	4.51
3	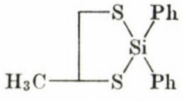	273	2.86	245*	3.63	223	4.27		
4	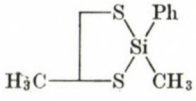	272 266	2.44 2.58	245*	3.05	217	3.88	192	4.44
5	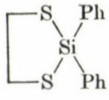	274 267	2.88 3.05	245*	3.55	221	4.20	197	4.83
6	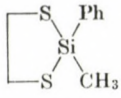	274 266	2.45 2.61	245*	3.13	220*	3.86	194	4.52
7	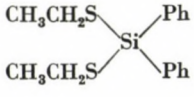	273 266 261	2.85 2.99 3.01	245*	3.50	222*	4.28	195	4.85
8	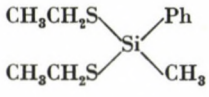	272 265	2.44 2.59	238*	3.24	216*	3.91		
9	$(CH_3CH_2S)_3SiPh$	273 266	2.70 2.84	240*	3.43	218*			

Table II

UV data for some methylphenylsilanes
(λ_{max} in nm)

Band	$PhC(CH_3)_3$		$PhSi(CH_3)_3$		$PhSi(CH_3)F_2$		$PhSi(CH_3)Cl_2$		$PhSi(CH_3)Br_2$		$PhSi(CH_3)(SCH_2CH_3)_2$	
	λ_{max}	lg ε	λ_{max}	lg ε	λ_{max}	lg ε	λ_{max}	lg ε	λ_{max}	lg ε	λ_{max}	lg ε
	266	2.07	270	2.10	270	2.66	272	2.58	273	2.52	272	2.44
α	263	2.13	265	2.24	264	2.74	265	2.68	266	2.64	265	2.59
	257	2.20	258	2.26	258	2.60	259	2.56	260	2.55		
	251	2.14	252	2.23	253*	2.39	254*	2.37	255*	2.39		
CT	—		—		—		—		—		238*	3.24
p	208	3.98	211	4.00	211	3.83	216	3.88	218	3.73	216	3.91
β					~185		~191		~192			

ductive effect of the silicon and $(d - p)\pi$ bond between the silicon atom and the phenyl group. The difference of the spectra with the variation of substituent X can be explained by the change in the inductive effect of X; in addition, the lone pair of X can form a conjugative connection of varying extent with the silicon [5]. On the basis of the data in Table II it is evident that the effect of $-SC_2H_5$ groups is about the same as that of chlorine.

The spectra differ from those of benzene derivatives with weak substituents in the disappearance of the minimum between the α and *p* bands, thus a monotonic increase of the extinction coefficient is observed towards the shorter wavelengths. Since the intensity of $n - \sigma^*$ transitions expected in this regions is much smaller [1], these cannot be responsible for the disappearance of the minimum. Thus the formation of a new band in the range of 230 to 250 nm seems to be a reasonable assumption, which is supported by the appearance of a shoulder in the spectra. Figure 1 and Table III give an explanation for the formation of this band. The data for the carbon derivatives in the Table were taken from the paper of FEHNEL and CARMACK [6].

For $C_6H_5SC_2H_5$ a very intense band is observed at 256 nm, which can be attributed to charge transfer interaction of the lone pair of sulfur with the phenyl group. The α band appears in the spectrum only as an inflexion at 270 nm. If the aromatic ring is isolated from the sulfur atom, the intensity of the CT bands will gradually decrease and a usual spectrum of aromatic character will develop. It can be seen that one carbon atom is not enough to isolate the aromatic ring, but the intensity of the CT band will diminish and the α band begins to appear. In the case of two carbon atoms, the CT band is no longer observed and at the same time the fine structure of the α band can be

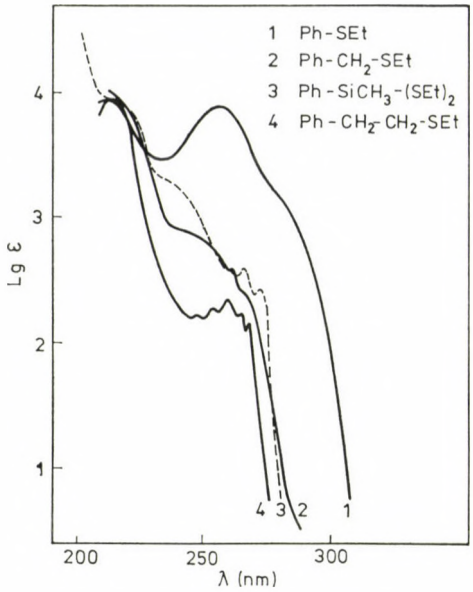

Fig. 1. The appearance of the CT band in the presence of various isolating groups

Table III

UV maxima (in nm) and intensities of aromatic systems containing sulfur

Band	$PhSCH_2CH_3$		$PhCH_2SCH_2CH_3$		$Ph(CH_2)_2SCH_2CH_3$		$PhSi(CH_3)(SCH_2CH_3)_2$	
	λ_{max}	lg ε	λ_{max}	lg ε	λ_{max}	lg ε	λ_{max}	lg ε
	270*	3.40	265	2.40	268	2.15	272	2.44
			260*	2.58	265	2.25	265	2.59
α					259	2.35		
					253	2.28		
					248	2.22		
CT	256	3.90	240	3.90	—		238	
p	210				212	3.95	216*	3.91

distinguished. The isolating effect of a silicon atom is roughly equivalent to that of carbon. Although the distance between the aromatic ring and the sulfur atom is larger in the presence of a silicon atom, at the same time the size of the lone pair of the sulfur is increased [7] because of the smaller electronegativity of silicon; therefore the extent of CT interaction remains unchanged.

REFERENCES

[1] VESZPRÉMI, T., EL-KERSH, M., NAGY, J.: Acta Chim. Acad. Sci. Hung. (In the press)
[2] WIEBER, M., SCHMIDT, M.: Z. Naturforsch., **18b,** 846 (1963)
[3] WIEBER, M., SCHMIDT, M.: J. Organometal. Chem., **1,** 336 (1964)
[4] HENCSEI, P., MESTYANEK, Ö., RÉFFY, J., VESZPRÉMI, T., NAGY, J.: Kémiai Közl., **46,** 414 (1976)
[5] VESZPRÉMI, T., RÉFFY, J., NAGY, J.: Kémiai Közl., **46,** 418 (1976)
[6] FEHNEL, E. A., CARMACK, M.: J. Am. Chem. Soc., **71,** 84 (1949)
[7] COULSON, C. A.: Nature, **221,** 1106 (1969)

Tamás VESZPRÉMI
Mokhtar EL-KERS
József NAGY
H-1521 Budapest, Műegyetem.

Acta Chimica Academiae Scientiarum Hungaricae, Tomus 102 (2), pp. 201—204 (1979)

SOME ASPECTS OF THE SYNERGIC EXTRACTION WITH PARTICIPATION OF MIXTURES OF A CHELATE- AND A DONOR EXTRACTING AGENT

I. L. DUKOV and L. Ch. GENOV

(Department of Inorganic Chemistry, Higher Institute of Chemical Technology, Sofia)

Received May 8, 1978
In revised form October 10, 1978
Accepted for publication November 24, 1978

The influence of the donor extracting agent and the solvent with respect to adduct formation, containing one or two molecules of the synergist, has been followed. Some considerations are expressed about the mechanism of the synergic extraction with mixtures of a chelate- and a donor extracting agent.

The extraction with mixtures containing a chelate extracting agent of β-diketone type and neutral organo-phosphorus extracting agents or heterocyclic nitrogen-containing bases has been the subject of numerous studies. It has been established that in a number of cases the simultaneous formation of adducts is possible, which contain one or two molecules of the donor extracting agent [1—10].

The questions about the adduct formation in the organic phase are not quite clear yet, despite the analysis in some of the investigations [1—6] of a number of factors affecting this process. Consequently, the present paper is an attempt, on the basis of known experimental data analysis, to give a more complete picture about the influence of some of these factors on the composition and stability of the adducts formed in the organic phase.

The adduct formation in the organic phase may be expressed by the following equations:

$$MX_n + S \rightleftharpoons MX_nS \quad (1)$$

$$MX_n + 2\,S \rightleftharpoons MX_nS_2 \quad (2)$$

$$MX_nS + S \rightleftharpoons MX_nS_2 \quad (3)$$

with equilibrium constants, β_1 for equation (1), β_2 for equation (2) and β for equation (3), respectively. In the above equations MX_n is a metal chelate and S is a donor extracting agent (synergist).

When a certain chelate extracting agent is employed (thenoyltrifluoroacetone is used in most studies), the composition and stability of the adducts formed depend not only on the synergist but also on the organic solvent employed. If more inert solvents are applied, which hardly react with the donor extracting agent, one could expect that the predominating adducts would contain two molecules of each synergist, as these solvents almost do not hinder

coordination of the donor molecules to the metal chelate. And vice versa, the concentration of adducts containing two molecules of synergist will decrease with the increase of solvation ability of the solvent employed. In this case, the formation of both adduct kinds will be hindered, but but the second donor molecule would be hampered much more. Therefore, the constant β_2 would be higher, the more basic the synergist used and the more inert the organic solvent. The constant β_1 will be altered in the same manner, however, it would decrease more slowly than β_2 in the transition from a more inert to a more active solvent. Consequently, the ratio between the equilibrium constants β_2/β_1 which actually represents the equilibrium constant β will be greatest in the application of the most inert solvent and the most basic synergist and will decrease with the increase of solvation ability of the solvent.

The above considerations may be illustrated by the experimental results of various authors, included in Table I. The Table gives data on the extraction of different metals with mixtures of thenoyltrifluoroacetone(HTTA) and donor extracting agents. Unfortunately, the Table includes only a small part of the experimental data known to us, mainly concerning the synergic extraction of rare earths, as in most publications the synergists and solvents used were few in number which offers no possibility of following their influence on the formation of the adducts. Furthermore, in some cases, the equilibrium constant of only one of the adducts (β_1 or β_2) was determined although at least for the lanthanides the formation of both kinds of adduct has been established [6—8]. Despite these restrictions, the analysis of the data compiled in Table I confirmed the considerations expressed. The latters are confirmed also by the data on the synergic extraction with participation of the chelate extracting agents 1-phenyl-3-methyl-4-acyl-5-pyrazolones which likewise are β-diketones [10]. This offers a possibility to draw a conclusion that the adduct formation in the organic phase is a stepwise process. Presumably, a complex is primarily formed which contains one molecule of synergist by replacing (partly or completely) of the water coordinated to the metal chelate [6, 8]. Then, depending on the conditions under which the extraction takes place, the addition of a second donor molecule will be possible.

As far as the rare earth elements are capable of forming both kinds of adducts (Table I contains a relatively large number of experimental data on the extraction of europium with mixtures of HTTA and different synergists in various solvents), it is of interest to follow the relationship between the constants β_1 and β_2, obtained in the extraction of europium. Figure 1 illustrates the relationship $\log \beta_2 = f(\log \beta_1)$. It is evident that the relationship under consideration represents a straight line, while the constants β_1 and β_2 are related by the equation $\log \beta_2 = 1.8 \log \beta_1 - 0.60$.

An almost identical relationship is obtained by the statistical interpretation of the stability constants. Since statistically $\beta_1/\beta = 4$, $\beta_1\beta = 1/4\ \beta_1^2$ and

Table I

Equilibrium constants β_1, β_2 and β of thenoyltrifluoroacetonate adducts of some metals

Adduct	Ligand	Cyclohexane			Carbon tetrachloride			Benzene			Chloroform			Reference
		$\log\beta_1$	$\log\beta_2$	$\log\beta$	$\log\beta_1$	$\log\beta_2$	$\log\beta$	$\log\beta_1$	$\log\beta_2$	$\log\beta$	$\log\beta_1$	$\log\beta_2$	$\log\beta$	
$La(TTA)_3S_m$	TBP	—	—	—	4.83	9.33	4.50	—	—	—	—	—	—	5
	MIBK	—	—	—	2.0	2.9	0.9	—	—	—	—	—	—	
$Eu(TTA)_3S_m$	TOPO	—	—	—	7.49	12.26	4.77	5.56	8.60	3.04	5.40	7.60	2.20	5, 8
	TBP	—	—	—	5.36	8.96	3.60	4.27	7.13	2.86	3.63	5.40	1.77	
	DBSO	—	—	—	5.09	8.58	3.49	—	—	—	—	—	—	
	MIBK	—	—	—	1.71	2.34	0.63	—	—	—	1.16	1.52	0.36	
	QUIN	—	—	—	3.48	5.16	1.68	—	—	—	—	—	—	
	DPSO	—	—	—	—	—	—	3.17	5.35	2.18	—	—	—	
$Tm(TTA)_3S_m$	TBP	5.2	8.2	3.0	5.39	7.23	1.84	—	—	—	—	—	—	1, 7
	TOPO	6.84	11.32	4.48	—	—	—	—	—	—	—	—	—	
$La(TTA)_3S_m$	2,2DIP	—	—	—	—	—	—	4.77	6.70	1.93	—	—	—	6
$Nd(TTA)_3S_m$	2,2DIP	5.22	7.76	2.54	5.64	7.63	1.99	5.21	6.71	1.50	4.86	5.62	0.76	
$Gd(TTA)_3S_m$	2,2DIP	—	—	—	—	—	—	6.38	8.59	2.21	—	—	—	
$Lu(TTA)_3S_m$	2,2DIP	5.99	9.06	3.07	5.52	8.86	3.34	6.49	8.63	2.14	3.62	5.70	2.08	
$Am(TTA)_3S_m$	TBP	—	—	—	5.06	8.89	3.83	—	—	—	—	—	—	5
	DBSO	—	—	—	4.97	8.48	3.51	—	—	—	—	—	—	
	MIBK	—	—	—	1.8	2.4	0.6	—	—	—	—	—	—	
$Ca(TTA)_2S_m$	TOPO	—	—	—	5.64	10.68	5.04	—	—	—	—	—	—	1
	TBP	—	—	—	4.11	8.22	4.11	—	—	—	—	—	—	
	MIBK	—	—	—	1.83	2.66	0.83	—	—	—	—	—	—	
$Sr(TTA)_2S_m$	TOPO	—	—	—	5.39	9.78	4.39	—	—	—	—	—	—	1
	TBP	—	—	—	3.76	7.23	3.76	—	—	—	—	—	—	
	MIBK	—	—	—	1.80	2.60	0.80	—	—	—	—	—	—	

TBP — Tributylphosphate
TOPO — Trioctylphosphine oxide
DBSO — Dibutyl sulphoxide
DPSO — Diphenyl sulphoxide
MIBK — Methyl isobutyl ketone
QUIN — Quinoline
2,2DIP — 2,2-Dipyridil

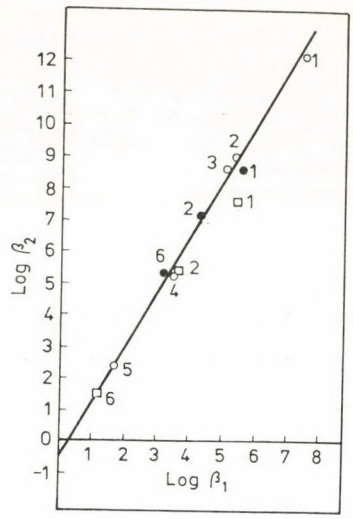

Fig. 1. Dependence of log β_2 on log β_1 in the extraction of Eu with mixtures of HTTA and various synergists. (1) TOPO; (2) TBP; (3) DBSO; (4) QUIN; (5) MIBK; (6) DPSO. Solvent: CCl_4 (open circles); C_6H_6 (closed circles); $CHCl_3$ (squares)

$\beta_1\beta = \beta_2$, therefore $\beta_2 = 1/4\,\beta_1$ of log $\beta_2 = 2$ log $\beta_1 - 0.60$. However, the similarity of the linear relationships is not a sufficient proof that the statistical operations are valid for the systems discussed since the small deviation of the slope of the experimentally obtained relationship from the slope of the theoretical relation ship is due to the significant deviation of the ratio β_1/β from the theoretical value. Indeed, the data contained in Table I show that in most cases the ratio β_1/β differs significantly from the value four, which confirms the statement that the systems under consideration are not ideal.

REFERENCES

[1] MARCUS, Y., KERTES, A. S.: Ion Exchange and Solvent Extraction of Metal Complexes, chapter **11**, Willey-Interscience, New York, 1969
[2] HEALY, T. V.: In Solvent Extraction Research (Edited by A. S. KERTES and Y. MARCUS), p. 257, Wiley-Interscience, New York, 1969
[3] IRVING, H.: In Solvent Extraction Chemistry (Edited by D. DYRSSEN, J. O. LILJENZIN and J. RYDBERG), p. 91, North Holland, Amsterdam, 1967
[4] KERTES, A. S.: Recent Advances in Liquid-liquid Extraction (Edited by C. HANSON), p. 16, Pergamon Press, Oxford, 1971
[5] SEKINE, T., DYRSSEN, D.: J. Inorg. Nucl. Chem., **29**, 1457, 1475, 1481 (1967)
[6] KASSIERER, E. F., KERTES, A. S.: J. Inorg. Nucl. Chem., **34**, 778, 3221 (1972)
[7] FARBU, L., ALSTAD, J., AUGUSTONSON, J. H.: J. Inorg. Nucl. Chem., **36**, 2091 (1974)
[8] MATHUR, J. N., PAI, S. A., KHOPKAR, P. K., SUBRAMANIAN, M. S.: J. Inorg. Nucl. Chem., **39**, 653 (1977)
[9] SEKINE, T., ONO, M.: Bull. Chem. Soc. Japan, **38**, 2087 (1965)
[10] NAVRATIL, O.: Radiohimia, **19**, 626 (1977)

I. L. DUKOV, L. Ch. GENOV } Department of Inorganic Chemistry, Higher Institute of Chem. Techn., 1156 Sofia, Bulgaria

Acta Chimica Academiae Scientiarum Hungaricae, Tomus 102 (2), pp. 205—209 (1979)

OXIDATIVE REARRANGEMENT OF CHALCONES WITH THALLIUM(III) NITRATE, X*

IS NITRATION A SIGNIFICANT SIDE REACTION IN THE OXIDATION OF 2'-HYDROXYCHALCONES WITH THALLIUM(III) NITRATE? (A POLEMIC)

S. ANTUS, L. FARKAS and Á. GOTTSEGEN

(Research Group of Alkaloid Chemistry of the Hungarian Academy of Sciences, Budapest)

Received October 12, 1978
Accepted for publication November 25, 1978

GOTTLIEB and co-workers claimed that the rearrangement of 2'-hydroxychalcones with methanolic $Tl(NO_3)_3$ followed by treatment with acid or alkali provided, instead of the expected isoflavones **2a—c**, their 2'-nitro congeners **3a—c**. We found that under standard conditions nitrated products did not form at all.

We have found and applied in the synthesis of a large number of naturally occurring isoflavonoids the method according to which simple 2'-hydroxychalcones are smoothly converted by thallium trinitrate (TTN) in methanol into 1,2-diaryl-3,3-dimethoxypropan-1-ones which, on acid- or base-catalyzed ring closure, give the corresponding isoflavones [1—6].

For supporting the structures of the natural isoflavones **2h** and **2i** GOTTLIEB *et al.* [7] attempted the synthesis of their methyl- and ethyl ethers by our method. Under non-specified conditions but with reference to our publications [2], they claimed to have obtained from the chalcones **1a—c** the corresponding 2'-nitroisoflavones **3a—c**, instead of the desired products **2a—c**.

Since no such reaction has been observed in our laboratory, we subjected the same chalcones, and several more (**2d—g**) of the same substitution pattern, to our standard oxidation procedure (TTN in methanol). Because of their poor solubility, **1e—g** were oxidized in a mixture of trimethyl orthoformate-methanol [3]. The non-isolated acetals (1,2-diaryl-3,3-dimethoxypropan-1-ones) gave on treatment with sodium methoxide [14] the expected isoflavones **2a—g**. The analytical and spectroscopic data (especially PMR) supported the expected structures and excluded the presence of a nitro group at position 2'. Dealkylation of **2a—d** resulted in 3',4',7-trihydroxyisoflavone (**2j**) [15] which we also obtained by catalytic debenzylation of **2g**. Debenzylation of **2e** in turn gave calycosin (**2h**) [16], whereas by the same procedure **2f** gave 3'-methoxy-4',7-dihydroxyisoflavone (**2i**) [17]. TLC of the crude products obtained from the oxidative rearrangement did not show any traces of a by-product.

* For Part IX, see Ref. [1]

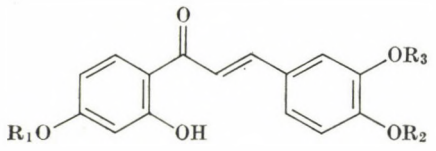

1

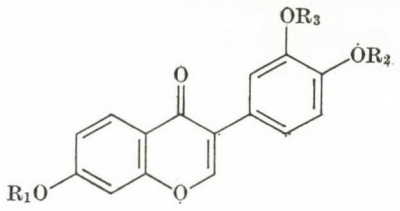

2

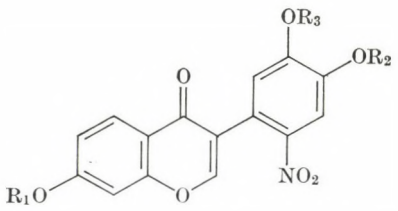

3

	R_1	R_2	R_3
a	Et	Me	Et
b	Et	Et	Me
c	Me	Me	Me
d	Et	Et	Et
e	$PhCH_2$	Me	$PhCH_2$
f	$PhCH_2$	$PhCH_2$	Me
g	$PhCH_2$	$PhCH_2$	$PhCH_2$
h	H	Me	H
i	H	H	Me
j	H	H	H

We conclude therefore that if the experiments are carried out under the conditions specified by us [2], the oxidative rearrangement of 2'-hydroxychalcones with TTN does not result in the formation of nitroisoflavones.

In the syntheses of the required chalcones, the appropriate acetophenone derivative (*i.e.* for **1a**, **1b** and **1d** 2-hydroxy-4-ethoxy- [8], for **1c** 2-hydroxy-4-methoxy- [9], for **1e**, **1f** and **1g** 2-hydroxy-4-benzyloxyacetophenone [10]) was condensed in alkali with the corresponding aldehyde (for **1b** and **1a** vanillin and isovanillin ethyl ethers [11, 12], for **1c** veratraldehyde, for **1d** protocatechualdehyde diethyl ether [13]).

Experimental

The purity of all compounds was checked by TLC and their structures were confirmed by IR and PMR spectra. PMR spectra were recorded on a Perkin-Elmer R-12 (60 MHz) spectrometer in $CDCl_3$; IR spectra were obtained in KBr discs with a Spectromom 2000. M.p.'s were determined on a Kofler micro-hot-stage.

Table I

Physical and analytical data of chalcones **1a—g**

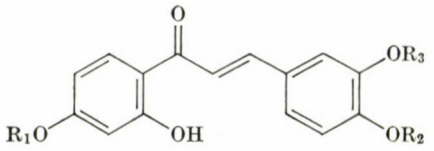

No.	M.p., °C	Solvent	Calcd.		Mol. formula	Found		Yield, %	Method
			C	H		C	H		
1a	129—130	EtOH	70.16	6.48	$C_{20}H_{22}O_5$	70.09	6.40	46	*B*
1b	120—121	EtOH	70.16	6.48	$C_{20}H_{22}O_5$	69.68	6.60	27	*B*
1c	154—156	EtOH	68.78	5.77	$C_{18}H_{18}O_5$	68.65	5.46	69	*A*
1d	121—123	EtOH	70.76	6.79	$C_{21}H_{24}O_5$	71.43	6.99	29	*B*
1e	157—160	C_6H_6	77.23	5.62	$C_{30}H_{26}O_5$	77.23	5.62	50	*B*
1f	172—174	AcOH	77.23	5.62	$C_{30}H_{26}O_5$	76.76	6.01	26	*B*
1g	137—138	C_6H_6	79.68	5.57	$C_{36}H_{30}O_5$	79.74	5.67	50	*A*

Table II

Physical and analytical data of isoflavones **2a—g**

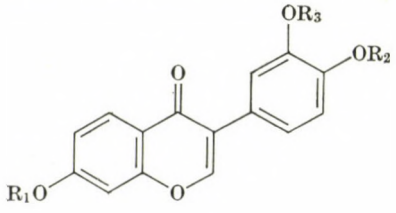

No.	M.p., °C	Solvent	Calcd.		Mol. formula	Found		Yield, %	Method
			C	H		C	H		
2a	135—136	MeOH	70.57	5.92	$C_{20}H_{20}O_5$	70.39	6.09	38	*A*
2b	150—152	MeOH	70.57	5.92	$C_{20}H_{20}O_5$	71.08	6.28	44	*A*
2c	164—165*	MeOH	69.22	5.15	$C_{18}H_{16}O_5$	68.70	4.85	46	*A*
2d	125—126	MeOH	71.17	6.26	$C_{21}H_{22}O_5$	71.04	6.26	22	*A*
2e	126—128	EtOH	77.57	5.21	$C_{30}H_{24}O_5$	77.26	5.13	15	*B*
2f	119—120	MeOH	77.57	5.21	$C_{30}H_{24}O_5$	77.07	5.12	25	*B*
2g	123—125	MeOH	79.98	5.22	$C_{36}H_{28}O_5$	79.21	5.21	23	*B*

* *Lit.* [15] m. p. 163—165 °C

General method of preparating the chalcones
(*cf.* Table I)

Equimolar amounts (0.01 mole) of the appropriate aldehyde and acetophenone were stirred in 15 ml ethanol with 7.5 ml of 25% aqueous NaOH for 24 h at room temperature (Method *A*), or at 70 °C for 3 h (Method *B*); the mixture was acidified with 10% HCl, the solid separated, dried and recrystallized from the solvent given in Table I.

General method for the synthesis of isoflavones by oxidative rearrangement of the starting chalcones and subsequent ring closure

(*cf.* Table II)

A stirred solution of the chalcone (1 mmole) and TTN · 3 H_2O (1.1 mmole) in methanol at room temperature (Method *A*), or in a mixture of trimethyl orthoformate-methanol (2 : 1) at 39 °C (Method *B*) was allowed to react; the reaction was followed by TLC. After the disappearance of the chalcone, the reaction mixture evaporated at 30 °C. The oily crude product was dissolved in chloroform, extracted with water, the organic layer was dried and the solvent evaporated. The residue was boiled in 10 ml 0.1 *N* sodium methoxide for 15 min. The isoflavone precipitated on cooling; it was recrystallized from the solvent given in Table II.

3',4',7-Trihydroxyisoflavone (2j)

(*a*) **2a—d** (1 mmole) was refluxed in a mixture of 3 ml hydriodic acid and 1.5 ml acetic anhydride for 10 h, poured into a saturated solution of $NaHSO_3$, the precipitated substance was separated, washed with water and dried. Recrystallization of the crude product from methanol gave **2j**, m.p. 275—278 °C (*lit.* [15] m.p. 245—248 °C).

(*b*) Hydrogenation of 240 mg of **2g** in 20 ml ethanol was carried out in the presence of Pd/*C* catalyst until the calculated amount of hydrogen had been absorbed. After filtration and partial evaporation an isoflavone precipitated, which gave no m.p. depression with **2j** obtained by procedure (*a*). The m.p. (176—177°) of the triacetate prepared from the isoflavone synthesized above agreed with the literature value (m.p. 175—177 °C [15]).

3',7-Dihydroxy-4'-methoxyisoflavone, calycosin (2h)

Catalytic debenzylation of **2e** resulted in **2h**, m.p. 247—249 °C (*lit.* [16] m.p. 248—249 °C, from methanol). No depression was observed with an authentic sample of calycosin.

4',7-Dihydroxy-3'-methoxyisoflavone (2i)

Catalytic debenzylation of **2f** gave **2i**, m.p. 190—192 °C (*lit.* [17] m.p. 191—192 °C.

*

Spectra were kindly recorded by Drs. P. Kolonits and E. Baitz-Gács and microanalyses were made by Miss K. Ófalvi and Mrs. S. Viszt. We thank Dr. M. Nógrádi for his interest and heplful discussions, and Dr. A. Wolfner for a sample of calycosin.

REFERENCES

[1] Antus, S., Nógrádi, M.: Acta Chim. Acad. Sci. Hung. (In the press)
[2] Farkas, L., Gottsegen, Á., Nógrádi, M., Antus, S.: J. C. S. Chem. Commun., **1972**, 825; J. Chem. Soc. Perkin I, **1974**, 305
[3] Antus, S., Farkas, L., Kardos-Balogh, Zs., Nógrádi, M.: Chem. Ber., **108**, 3883 (1976)
[4] Kardos-Balogh, Zs., Farkas, L., Wolfner, A.: Acta Chim. Acad. Sci. Hung., **94**(1), 75 (1977)
[5] Farkas, L., Wolfner, A.: Chem. Ber., **107**, 3966 (1974)
[6] Antus, S., Nógrádi, M.: Chem. Ber. (In the press)
[7] de Oliveira, A. B., de Oliveira, G. G., Pimenta, L. O., de P. Reis, J. E., Gottlieb, O. R.: Poster Session of the First Joint symposium of the Phytochemical Society of Europe and the Phytochemical Society of North America, Gent (Belgium) 1977

[8] KOSTANECKI, S. V., TAMBOR, J.: Ber., **28,** 2306 (1895)
[9] TAHARA, Y.: Ber., **24,** 2460 (1891)
[10] GULATI, K. C., SETH, S. R., VENKATARAMAN, K.: J. Chem. Soc., **1934,** 1765
[11] TIEMANN, F.: Ber., **8,** 1129 (1875)
[12] SPÄTH, E., BERNAUER, E.: Ber., **58,** 203 (1925)
[13] GATTERMAN, L.: Ann., **357,** 368 (1907)
[14] ANTUS, S., BOROSS, F., NÓGRÁDI, M.: J. C. S. Chem. Commun., **1977,** 333; Ann., **978** (107) (1978)
[15] DHAR, M. L., NARASIMHACHARI, N., SESHADRI, T. R.: J. Sci. Ind. Res., **14B,** 73 (1955)
[16] FARKAS, L., OLECHNOWITZ-STEPIEN, V., WOLFNER, A.: Acta Chim. Acad. Sci. Hung., **74**(3), 367 (1972)
[17] TAKAI, M., YAMAGUCHI, H., SAITOH, T., SHIBATA, S.: Chem. Pharm. Bull., **20** (11), 2488 (1972)

Sándor ANTUS
Loránd FARKAS
Ágnes GOTTSEGEN
H-1111 Budapest, Gellért tér 4.

RECENSIONES

J. C. JOHNSON: *Amino Acids Technology — Recent Development — Chemical Technology Reviews No. 108*

Noyes Data Corporation, Park Ridge, New Jersey, USA, 1978

XII + 369 pages

In the 108th volume of the well-known series, Chemical Technology Reviews, the author discusses 253 US patents published since 1974, dealing with the synthetic and microbiological preparation of amino acids, as well as with their application. The patents between numbers 3,787,287 and 4,060,603 are dealt with here.

The book contains 11 larger chapters (unnumbered) and three indices.

— Amino Acids — Preparative Methods
— Amino Acids and Peptides — Uses
— Aliphatic Amino Acids
— Hydroxyaliphatic Amino Acids
— Sulfur-containing Amino Acids
— Diamino Acids
— Monoamino Dibasic Acids
— Heterocyclic Amino Acids
— Aromatic Amino Acids (of Proteins)
— L-Dopa
— Other Aromatic Amino Acids
— Company Index
— Inventor Index
— US Patent Number Index

The book seems to be very useful primarily for chemists working in this field of industry. Its applicability is two-fold. One hand, it discusses the individual procedures in such a great detail — also giving actual prescriptions — that the original text is no longer required; on the other hand, it presents literature data which are not entirely obtainable from periodicals. The most comprehensive and most extensive information on the technical knowledge of world is offered by the US patents.

This book greatly helps orientation in the large subject and will serve as an excellent guide. The author himself very clearly lists in 15 paragraphs the importance of the US patent literature; the following items can be cited:

5. Patents, unlike periodical literature, are bound by definition to contain new information, data and ideas.

6. It can serve as a source of new ideas in a different but related field, and may be outside the patents protection offered the original invention.

11. Patents provide an excellent starting point for the next investigator.

The author emphasizes aspects of application in a comprehensive and detailed discussion, with special reference to actual new methods. It is noteworthy that most of these patents are used in industry.

Direct application of amino acids and peptides in pharmacy and nutrition has gained increasing importance all over the world, for both man and animal. The use of some amino acids (*e.g.*, tryptophan, threonine, *etc.*) has achieved extraordinary significance in certain countries in the feeding of animals. In human therapy, special amino acids and combinations of amino acids are known.

For these reasons, all books, reviews, *etc.*, which treat the pertaining literature in a comprehensive manner are very important for chemists concerned with amino acids is practice; the present book will be read by them — in the reviewer's opinion — with particular benefit.

G. GÁLL

Structure and Bonding, Vol. 35

Editors: J. D. DUNITZ, J. B. GOODENOUGH, P. HEMMERICH, J. A. IBERS C. K. JØRGENSEN, J. B. NEILANDS, D. REINEN, R. J. P. WILLIAMS

Springer-Verlag, Berlin—Heidelberg—New York, 1978, pp. 176

This new volume of Structure and Bonding contains the following four review articles

J. F. LABARRE: *Conformational Analysis in Inorganic Chemistry: Semi-Empirical Quantum Calculation vs. Experiment.*

The stated purpose of this paper is "to demonstrate that . . . the CNDO/2 and extended CNDO/2 formalisms are definitely reliable tools for theoretical conformational analyses in inorganic and coordination chemistry." This is indeed amply demonstrated on several examples $F_3P{\cdot}BH_3$ and its methyl derivatives as well as similar other Lewis adducts, inorganic ring systems, transition metal complexes, *etc.* As a remarkable theoretical result, the importance of through-space interactions is emphasized. In spite of these nice results, however, the reader has the feeling that a more critical discussion, including examples where the CNDO method is less satisfactory, would be more convincing. Also, inclusion of other semiempirical calculations would have covered the title better than did the presentation of only CNDO results.

D. B. COOK: *The Approximate Calculation of Molecular Electronic Structure as a Theory of Valence*

The aim of this paper is to develop a method which, beyond the capability of calculating molecular properties, is *interpretable* and can be used as a theory of valence. The author's main concept is that "it is, for example, more important to understand the physical processes occurring on bood formation than it is to be able to compute the corresponding bond energies accurately."

The general discussion starts with the variational principle. Following this, constraints arising from a given model and from numerical approximations are discussed. In the end, the author arrives at a fairly plausible model: Generalized Hybrid Orbitals (GHO) The basic difference between these GHO's and the familiar hybrid orbitals is that no a priori symmetry is built in: *e.g.* the generalized sp^3 hybrid orbitals in ammonia are different for the NH bonds and for the lone pair, respectively. Direction and optimal exponents of the GHO's are determined by energy minimization.

It seems doubtful, whether the GHO's can be of any practical use in ab initio calculations: even from the point of view of interpretability, the familiar LCAO method, if the transformation to localized orbitals is carried out, is readily interpretable. On the other hand, the suggested method, as stressed also by the author, may have advantages in NDO (Neglect of Differential Overlap) type approximate calculations.

The paper is written in an exceptionally elegant style and is certainly an enjoyable piece of reading for chemists interested in theoretical chemistry.

D. W. SMITH: *Applications of the Angular Overlap Model*

The angular overlap model (AOM) is a simple, approximate method for the calculation of orbital splittings in transition metal complexes. The splittings are expressed by parameters directly related to σ-, π- and δ-bonding.

The scope of the paper can be best seen from the following section headings: 1. Introduction; 2. d-d Spectra; 3. f-f Spectra; 4. Other Spectra and Optical Properties; 5. Magnetic and E.S.R. Properties; 6. Miscellaneous Applications; 7. Concluding Remarks.

Because the underlying theory is not even outlined and the applications are listed in a very concise form, the paper is hardly understandable for the average reader. However, with its 164 references, the review is certainly useful for specialists who want to have a good literature survey of the subject.

C. FURLANI and C. CAULETTI: *He(I) Photoelectron Spectra of d-Metal Compounds*

This is an excellent review on photoelectron (P. E.) spectroscopy of transition metal complexes, listing results up to 1977. In the introduction, the fundamentals of P. E. spectroscopy are summarized in a clear, easily readable form, and its relative merits and limitations, as compared to electron absorption spectroscopy, are discussed.

Recent results are then discussed in two sections. The first one deals with carbonyl, trifluorophosphine complexes, sandwich complexes, mixed carbonyl-cyclopentadienyl and carbonyl-arene complexes of d-metals in low oxidation states. The second section discusses results on complexes of metals in higher oxidation states with more electronegative ligands, like oxo and halide complexes, nitrogen, oxygen and sulfur containing complexes, amide complexes, *etc.*

Detailed P.E. data on a huge number of complexes are compiled in six tables, and 120 references are listed.

G. FOGARASI

Philip S. BAILEY: *Ozonation in Organic Chemistry, Volume I Olefinic Compounds*

Plenum Press, New York and London

The 39th volume written by Philip S. BAILEY, of this Monograph Series edited by Harry H. WASSERMANN, is an excellent comprehensive treatise making available in one convenient source our complete knowledge of today concerning the reactions of ozone with organic substances. An effort is made to show the development of the present-day thought about the still existing problems of the mechanism of these reactions.

Volume *I* starts with a description of ozone itself, giving a historical background of its action on organic compounds, followed by a study of the mechanism of these reactions. The book clearly shows the development of the step-by-step mechanism of classical ozonolysis, pointing out the remaining, yet unsolved questions of the detailed mechanism.

The ozonolysis of olefins is treated in chronological order, starting from the ozone attack to the final products, in both liquid- and gas-phase reactions.

No doubt, this book covering more than 700 references will serve as an indispensable source of information to all chemists dealing with ozone chemistry.

Chapters: Introduction; The Ozone Molecule; Ozonolysis of Olefins: Introduction, Initial Ozone Attack and Adduct, The Peroxidic Products, Routes to Peroxidic Products, Competitions in Peroxidic Product Formation, Routes from Peroxidic to Non-peroxidic Products; "Anomalous" Ozonolysis of Olefins; "Special" Liquid-Phase Ozonolysis; Electrophilic Ozone Attack on Olefins. Epoxides and Other "Partial Cleavage" Products; Gas-Phase Ozonation of Olefins; Overview and New Developments.

J. REITER

INDEX

ANALYTICAL CHEMISTRY

PHYSICAL AND INORGANIC CHEMISTRY

ORGANIC CHEMISTRY

Printed in Hungary

A kiadásért felel az Akadémiai Kiadó igazgatója — Műszaki szerkesztő: Zacsik Annamária

A kézirat nyomdába érkezett: 1979. IV. 9. — Terjedelem: 9,45 (A/5) ív, 60 ábra

79.7032 Akadémiai Nyomda, Budapest — Felelős vezető: Bernát György

ACTA CHIMICA

ТОМ 102—ВЫП. 2

РЕЗЮМЕ

Рентгеновские и электроно-микроскопные исследования гидроксилацетатов кальция-меди

П. Н. ПАТЕЛЬ и С. В. Х. РАО

Постоянные решетки гидроксилапатитов кальция-меди уменьшаются с увеличением содержания меди в образце, приводя к сокращению объема единичной ячейки. Сокращение размеров кристалла наблюдалось на съемках образцов с помощью электронного микроскопа. Введение Cu^{+2} в гидроксилапатит кальция $Ca_{10}(PO_4)_6(OH)_2$ приводит к образованию его твердых растворов.

Аналитическое применение некоторых внешнесферных комплексов

Спектрофотометрическое определение трифторуксусной кислоты и неорганических азидов экстракцией 1,10-фенантролин-железом

Л. ИЛЧЕВА и Г. ТОДОРОВА

Установлено, что малые количества CF_3COOH и NaN_3 экстрагируются нитробензолом если водная фаза содержит значительный избыток $Fe(phen)_3^{2+}$. Абсорбция органического экстракта (при $\lambda = 518$ nm) пропорциональна концентрации CF_3COOH в водной фазе или концентрации NaN_3 (при $\lambda = 516$ nm). Для установления оптимальных условий определения, было исследовано влияние различных факторов: pH, концентрации $Fe(phen)_3^{2+}$, концентрации буферного раствора, времени встряживания, устойчивости окрашивания, мешающего влияния ионов. Установлен состав экстрагирующихся внешнесферных комплексов: $Fe(phen)_3\,(CF_3COO)_2$ и $Fe(phen)_3\,(N_3)_2$.

Константы стойкости внешнесферных комплексов $Fe(phen)_3(CF_3COO)_2$ и $Fe(phen)_3(CCl_3COO)_2$

Л. ИЛЧЕВА, Г. ТОДОРОВА и М. ГЕОРГИЕВА

Изучена экстрагируемость внешнесферных комплексов $Fe(phen)_3(CF_3COO)_2$ и $Fe(phen)_3(CCl_3COO)_2$ в нитробензол в зависимости от концентрации лиганда. Так как в органическую фазу экстрагируется нейтральный внешнесферный комплекс, были определены коэффициент распределения комплексного металлического катиона и константа распределения нейтрального комплекса между двумя фазами.

Рассчитаны внешнесферные константы стойкости: для $Fe(phen)_3(CF_3COO)_2$ $K_1 = 1{,}1\times 10^2$ и $K_2 = 8\times 10$; для $Fe(phen)_3$—$(CCl_3COO)_2$ $K_1 = 4{,}2\times 10^2$ и $K_2 = 4{,}3\times 10^2$. Результаты настоящих исследований, а также некоторые другие данные показывают, что степень внешнесферной ассоциации комплексного катиона $Fe(phen)_3^{2+}$ уменьшается в ряду

$$CCl_3COO^- > CF_3COO^- \gg CH_3COO^-$$

Дезбензо-производные алкалоидов со скелетом индоло [2,3-*c*] хиназолино [3,2-*a*] пиридина, IX

Дезбензоэводиамин

З. ПАЛ, К. ДОРАНЕ-ХОРВАТ, Г. ТОТ, О. КЛАУДЕР и Й. ТАМАШ

Из дезбензорутекарпина с помощью метилиодида был получен дегидро-дезбензоэводинамин-гидроидид (**6**). При аммонийной обработке соединение **6** с раскрытием кольца превращается в аммонийную соль дезбензоэводиаминовой кислоты; а при восстановлении дает дезбензоэводиамин (**11**). Синтез **11** был осуществлен, исходя из 1,2,3,4-тетрагидро-1-оксо-β-карболина (**9**) и *N*-метил-β-аланин-этилового эфира (**12**). Промежуточный продукт синтеза — этиловый эфир дезбензоэводиаминовой кислоты (**13**) был приготовлен в виде солянокислой соли. Соединение **13** после закрытия кольца и восстановления также дает соединение **11**. Строение полученных соединений было подтверждено с помощью элементарного анализа, УФ, ИК, ЯМР—H^1 и МС-спектроскопических исследований.

Половой феромон капустной американской полковой гусеницы. Mamestra brassicae: Изолирование, идентифицирование и стереоконтролируемый синтез

Л. НОВАК, М. ТОТ, Й. БАЛЛА и Ч. САНТАИ

Два основных компонента полового феромона капустной американской полковой гусеницы, (*Z*)-11-гексадеценил ацетат и (*Z*)-11-гептадеценил ацетат были изолированы, идентифицированы, а затем синтезированы, применяя стереоселективное олефинирование Виттига, как ключевую ступень.

Полярографическое исследование равновесия кислота-основание некоторых производных бензойной кислоты

Е. ДЬЯРФАШ, Б. ТЁКЕШ и Л. КЕКЕДИ

Константы скорости диссоциации и рекомбинации бензойной кислоты и ее десяти производных были определены, используя косвенный полярографический метод Рютши в присутствии азобензола и/или *n*-нитроанилина. Количественные данные коррелируются со структурой.

Изучение анодного растворения меди в пирофосфатных растворах

Р. К. АСТАХОВА, Й. САЛМА, Й. ФАРКАШ и Л. КИШ

С помощью вращающегося дискового электрода с кольцом изучалось анодное растворение меди в водных растворах пирофосфата при pH = 8,6 и 4,8. Полученные данные указывают на то, что в изученных экспериментальных условиях ионизация меди представляет собой процесс, заключающийся в двух последовательных одноэлектронных реакциях (ступенчатый механизм). При изменении pH раствора, вследствие изменения состава комплексов, участвующих в электродных реакциях, существенно изменяются кинетические параметры реакции.

Измерение константы Куна—Марка—Хоувинка для некоторых полимеров и их использование в гель-проникающей хроматографии

Г. ШАМАИ

Представлена зависимость характеристической вязкости от молекулярного веса некоторых полимеров, измеренная при условиях рутинной гель-проникающей хроматографии. С помощью приведенных данных доказана универсальность двух методов калибровки.

Исследование фактора линейной корреляции диэлектрической поляризации и структуры жидкостей

Р. САБЕСАН, Р. ВАРАДХАРАЯН и М. САГУРУМУРФИ

Изменение фактора линейной корреляции диалектрической поляризации (g) было определено экспериментально для некоторых ассоциированных жидкостей в четыреххлористом углероде, используя выражение Кёрквуда—Фрёлиха для растворов. На основе полученных результатов была анализирована жидкая структура этих систем. Было сделано заключение о неидеальном поведении т. наз. аполярных растворителей в диэлектрических измерениях.

Исследование распределения продуктов в ходе оксиэтилирования додецилового спирта, катализированного перхлоратом магния

П. ШАЛЛАИ, Й. МОРГОШ, Л. ФАРКАШ и И. РУСНАК

Оксиэтилирование додецилового спирта, катализированное перхлоратом магния, было исследовано в установке оксиэтилирования измерением объемного потока. На основе газовохроматографического определения состава продуктов было установлено, что это распределение типа Флоти и практически не зависит от концентрации катализатора и температуры реакции. Сравнивая с реакционной системой, катализированной щелочью калия, данное распределение более благоприятно. Каталитическое влияние перхлората магния объясняется образованием комплеска между ионами магния и окислом этилена.

Исследование структуры производных замещенных оснований Шиффа

А. И. КИШ, М. РЕВЕС, Й. ЧАСАР и М. И. БАН

Полосы электронной абсорбции, появляющиеся в области 400—450 нм в спектрах замещенных бензилиденанилинов, интерпретируются на основе приближенных квантовохимических расчетов и приписываются хиноидной структуре, образующейся за счет водородного мостика в основаниях Шиффа, содержащих гидроксильную группу в *орто-* или *пара*-положениях в альдегидном кольце.

Спектрофотометрическое исследование окисления 3-гидрокси- и 3-аминофлаванонов, катализированного основаниями

Е. Р. ДАВИД, Р. БОГНАР, М. РАКОШИ и Б. Г. САБО

При исследовании изменений спектров 3-гидроксифлаванона и 3-аминофлаванона в зависимости от pH было найдено, что в буферном растворе и щелочным pH оба соединения превращаются в производные с более высокой степенью окисления, а именно в 3-гидроксифлавон и 3-аминофлавон, соответственно. Было найдено, что в присутствии кислорода воздуха процесс является необратимой реакцией окисления, катализируемой основаниями.

Исследование соединений, содержащих связи Si—S и S—Si—S, с помощью УФ спектроскопии, II

Ароматические соединения

Т. ВЕСПРЕМИ, М. ЭЛЬ-КЕРШ и Й. НАДЬ

Изучение пропускного сопряжения атомов серы через кремний и существование взаимодействий «пропускной связи» между атомами серы в соединениях, содержащих связи S—Si и S—Si—S не дает однозначных результатов при исследовании с помощью УФ спек-

троскопии лишь алифатических и алициклических соединений. Поэтому исследования были распространены на УФ спектры соединений с группой Ar—Si—S с целью выяснения проблемы, исходя из изменений, наблюдаемых в спектрах ароматических систем. О взаимодействии атомов серы с ароматической системой можно судить по данным спектров. Проявление этого эффекта является подобным в аналогичных производных кремния и углерода. С другой стороны, батохромный сдвиг α и p полос для кремниевых соединений указывает на то, что одиночные пары электронов атома серы участвуют в сопряжении с ароматическим кольцом, используя свободные d-орбитали кремния. Степень влияния одиночных пар довольно-таки подобна наблюдаемой в аналогичных хлористых производных.

Некоторые вопросы синергической экстракции смесями хелатных и донорных экстрагирующих реагентов

И. ДУКОВ и Л. ГЕНОВ

Было исследовано влияние донорного экстрагирующего реагента и растворителя на образование аддукта, содержащего одну или две молекулы синергиста. Приводятся некоторые соображения относительно механизма синергической экстракции смесями хелатных и донорных экстрагирующих реагентов.

Окислительная перегруппировка халконов с нитратом таллия(III), X

Является-ли нитрование значительной побочной реакцией в окислении 2'-гидроксихалконов нитратом таллия(III)? (Полемика)

Ш. АНТУШ, Л. ФАРҚАШ и А. ГОТСЕГЕН

Готлиб и сотрудники нашли, что при перегруппировке 2'-гидроксихалконов в метанольном растворе $Tl(NO_3)_3$ с последующей кислой или щелочной обработкой, вместо ожидаемых изофлавонов **2a—c**, образуются из 2'-нитропроизводные **3a—c**. Нами было найдено, что при стандартных условиях продукты нитрования совсем не образуются.

Les Acta Chimica paraissent en français, allemand, anglais et russe et publient des mémoires du domaine des sciences chimiques.

Les Acta Chimica sont publiés sous forme de fascicules. Quatre fascicules seront réunis en un volume (4 volumes par an).

On est prié d'envoyer les manuscrits destinés à la rédaction à l'adresse suivante:

Acta Chimica
Budapest, P.O. Box 67, H-1450, Hongrie

Toute correspondance doit être envoyée à cette même adresse.

La rédaction ne rend pas de manuscript.

Le prix de l'abonnement: $ 36,00 par volume.

Abonnement en Hongrie à l'Akadémiai Kiadó (1363 Budapest, P.O.B. 24, C. C. B. 215 11488), à l'étranger à l'Entreprise du Commerce Extérieur « Kultura » (H-1389 Budapest 62, P. O. B. 149 Compte-courant No. 218 10990) ou chez représentants à l'étranger.

Die Acta Chimica veröffentlichen Abhandlungen aus dem Bereich der chemischen Wissenschaften in deutscher, englischer, französischer und russischer Sprache.

Die Acta Chimica erscheinen in Heften wechselnden Umfanges. Vier Hefte bilden einen Band. Jährlich erscheinen 4 Bände.

Die zur Veröffentlichung bestimmten Manuskripte sind an folgende Adresse zu senden

Acta Chimica
Budapest, Postfach 67, H-1450, Ungarn

An die gleiche Anschrift ist jede für die Redaktion bestimmte Korrespondenz zu richten.

Manuskripte werden nicht zurückerstattet.

Abonnementspreis pro Band: $ 36,00.

Bestellbar für das Inland bei Akadémiai Kiadó (1363 Budapest, Postfach 24, Bankkonto Nr. 215 11488), für das Ausland bei »Kultura« Außenhandelsunternehmen (H-1389 Budapest 62, P.O.B. 149. Bankkonto Nr. 218 10990) oder seinen Auslandsvertretungen.

«Acta Chimeca» издают стильи по химии на русском, английском, французском и немецком языках.

«Acta Chimica» выходит отдельными выпусками разного объекта, 4 выпуска составхяют одинтом и за год выходят 4 тока.

Предназначенные для публикации рукописи следует направлять по адресу:

Acta Chimica
Budapest, P.O. Box 67, H-1450, BHP

Всякую корреспонданцию в редакцию направляйте по этому же адресу.

Редакция рукописе не;возвращает.

Подписная цена — $36,00 за том.

Отечественные подписчики направляйте свои заявки по адресу Издательства Академии Наук (1363 Budapest, P.O.B. 24. Текущий счет 215 11 488), а иностранные подписчики через организацию по внешней торговле «Kultura» (H-1389 Budapest 62, P.O.B. 149. Текущий счет 218 10990) или через ее заграничные представительства и уполномеченных.

Reviews of the Hungarian Academy of Sciences are obtainable at the following addresses:

AUSTRALIA
C.B.D. LIBRARY AND SUBSCRIPTION SERVICE, Box 4886, G.P.O., *Sydney N.S.W. 2001*
COSMOS BOOKSHOP, 145 Ackland Street, *St. Kilda (Melbourne), Victoria 3182*

AUSTRIA
GLOBUS, Höchstädtplatz 3. *1200 Wien XX*

BELGIUM
OFFICE INTERNATIONAL DE LIBRAIRIE, 30 Avenue Marnix, *1050 Bruxelles*
LIBRARIE DU MONDE ENTIER, 162 Rue du Midi, *1000 Bruxelles*

BULGARIA
HEMUS, Bulvar Ruszki 6, *Sofia*

CANADA
PANNONIA BOOKS, P.O. Box 1017, Postal Station "B", *Toronto, Ontario M5T 2T8*

CHINA
CNPICOR, Periodical Department, P.O. Box 50, *Peking*

CZECHOSLOVAKIA
MAĎARSKÁ KULTURA, Národní třda 22, *115 33 Praha*
PNS DOVOZ TISKU, Vinohradská 46, *Praha 2*
PNS DOVOZ TLAČE, *Bratislava 2*

DENMARK
EJNAR MUNKSGAARD, Norregade 6, *1165 Copenhagen*

FINLAND
AKATEEMINEN KIRJAKAUPPA, P.O. Box 128, *SF-00101 Helsinki 10*

FRANCE
EUROPERIODIQUES S.A., 31 Avenue de Versailles, *78170 La Celle St.-Cloud*
LIBRAIRIE LAVOISIER, 11 rue Lavoisier, *75008 Paris*
OFFICE INTERNATIONAL DE DOCUMENTATION ET LIBRAIRIE, 48 rue Gay-Lussac, *75240 Paris Cedex 05*

GERMAN DEMOCRATIC REPUBLIC
HAUS DER UNGARISCHEN KULTUR, Karl-Liebknecht-Strasse 9, *DDR-102 Berlin*
DEUTSCHE POST ZEITUNGSVERTRIEBSAMT, Strasse der Pariser Kommüne 3—4, *DDR-104 Berlin*

GERMAN FEDERAL REPUBLIC
KUNST UND WISSEN ERICH BIEBER, Postfach 46, *7000 Stuttgart 1*

GREAT BRITAIN
BLACKWELL'S PERIODICALS DIVISION, Hythe Bridge Street, *Oxford OX1 2ET*
BUMPUS, HALDANE AND MAXWELL LTD., Cower Works, *Olney, Bucks MK46 4BN*
COLLET'S HOLDINGS LTD., Denington Estate, *Wellingborough, Northants NN8 2QT*
WM. DAWSON AND SONS LTD., Cannon House, *Folkestone, Kent CT19 5EE*
H. K. LEWIS AND CO., 136 Gower Street, *London WC1E 6BS*

GREECE
KOSTARAKIS BROTHERS, International Booksellers, 2 Hippokratous Street, *Athens-143*

HOLLAND
MEULENHOFF-BRUNA B.V., Beulingstraat 2, *Amsterdam*
MARTINUS NIJHOFF B.V., Lange Voorhout 9—11, *Den Haag*
SWETS SUBSCRIPTION SERVICE, 347b Heereweg, *Lisse*

INDIA
ALLIED PUBLISHING PRIVATE LTD., 13/14 Asaf Ali Road, *New Delhi 110001*
150 B-6 Mount Road, *Madras 600002*
INTERNATIONAL BOOK HOUSE PVT. LTD., Madame Cama Road, *Bombay 400039*
THE STATE TRADING CORPORATION OF INDIA LTD., Books Import Division, Chandralok, 36 Janpath, *New Delhi 110001*

ITALY
EUGENIO CARLUCCI, P.O. Box 252, *70100 Bari*
INTERSCIENTIA, Via Mazzé 28, *10149 Torino*
LIBRERIA COMMISSIONARIA SANSONI, Via Lamarmora 45, *50121 Firenze*
SANTO VANASIA, Via M. Macchi 58, *20124 Milano*
D. E. A., Via Lima 28, *00198 Roma*

JAPAN
KINOKUNIYA BOOK-STORE CO. LTD., 17-7 Shinjuku-ku 3 chome, Shinjuku-ku, *Tokyo 160-91*
MARUZEN COMPANY LTD., Book Department, P.O. Box 5050 Tokyo International, *Tokyo 100-31*
NAUKA LTD., IMPORT DEPARTMENT, 2-30-19 Minami Ikebukuro, Toshima-ku, *Tokyo 171*

KOREA
CHULPANMUL, *Phenjan*

NORWAY
TANUM-CAMMERMEYER, Karl Johansgatan 41—43, *1000 Oslo*

POLAND
WĘGIERSKI INSTYTUT KULTURY, Marszałkowska 80, *Warszawa*
CKP I W ul. Towarowa 28 *00-958 Warsaw*

ROMANIA
D. E. P., *Bucureşti*
ROMLIBRI, Str. Biserica Amzei 7, *Bucureşti*

SOVIET UNION
SOJUZPETCHATJ — IMPORT, *Moscow*
and the post offices in each town
MEZHDUNARODNAYA KNIGA, *Moscow G-200*

SPAIN
DIAZ DE SANTOS, Lagasca 95, *Madrid 6*

SWEDEN
ALMQVIST AND WIKSELL, Gamla Brogatan 26, *101 20 Stockholm*
GUMPERTS UNIVERSITETSBOKHANDEL AB, Box 346, *401 25 Göteborg 1*

SWITZERLAND
KARGER LIBRI AG, Petersgraben 31, *4011 Basel*

USA
EBSCO SUBSCRIPTION SERVICES, P.O. Box 1943, *Birmingham, Alabama 35201*
F. W. FAXON COMPANY, INC., 15 Southwest Park, *Westwood, Mass, 02090*
THE MOORE-COTTRELL SUBSCRIPTION AGENCIES, *North Cohocton, N. Y. 14868*
READ-MORE PUBLICATIONS, INC., 140 Cedar Street, *New York, N. Y. 10006*
STECHERT-MACMILLAN, INC., 7250 Westfield Avenue, *Pennsauken N.J. 08110*

VIETNAM
XUNHASABA, 32, Hai Ba Trung, *Hanoi*

YUGOSLAVIA
JUGOSLAVENSKA KNJIGA, Terazije 27, *Beograd*
FORUM, Vojvode Mišića 1, *21000 Novi Sad*

11. XII. 1979 HU ISSN 0001—5407 Index: 26.007

ACTA CHIMICA

ACADEMIAE SCIENTIARUM HUNGARICAE

TOMUS 102 FASCICULUS 3

AKADÉMIAI KIADÓ, BUDAPEST

1979

ACTA CHIM. ACAD. SCI. HUNG. ACASA2 102 (3) 215–320 (1979)

ACTA CHIMICA

A MAGYAR TUDOMÁNYOS AKADÉMIA KÉMIAI TUDOMÁNYOK OSZTÁLYÁNAK IDEGEN NYELVŰ KÖZLEMÉNYEI

Acta Chimica is a journal for the publication of papers on all aspects of chemistry in English, German, French and Russian.

Acta Chimica is published in 4 volumes per year. Each volume consists of 4 issues of varying size.

Manuscripts should be sent to

Acta Chimica
Budapest, P.O. Box 67, H-1450, Hungary

Correspondence with the editors should be sent to the same address. Manuscripts are not returned to the authors.

Subscription: $ 36.00 per volume.

Hungarian subscribers should order from Akadémiai Kiadó, 1363 Budapest, P.O. Box 24. Account No. 215 11488.

Orders from other countries are to be sent to "Kultura" Foreign Trading Company (H-1389 Budapest 62, P.O. Box 149. Account No. 218 10990) or its representatives abroad.

Acta Chimica Academiae Scientiarum Hungaricae, Tomus 102 (3), pp. 215—222 (1979)

STABILITY OF OUTER-SPHERE HEXAKIS (DIMETHYL SULFOXIDE) CHROMIUM(III) COMPLEXES

Zs. Ákos-Szabó[1], I. Országh[2] and Gy. Bazsa[2]

([1]*Institute of General and Analytical Chemistry, Technical University, Budapest,* [2]*Institute of Physical Chemistry, L. Kossuth University, Debrecen)*

Received June 30, 1978
Accepted for publication December 7, 1978

Outer-sphere hexakis(DMSO)chromium(III) complexes have been studied in water and DMSO.

On the basis of solubility measurements in aqueous medium at 25 °C the stability constants were determined at the value of $I = 1$. The following results have been obtained:

F^-: $\beta_1 < 0.2$;

NO_3^-: $\beta_1 = 5$, $\beta_2 = 19$;

SCN^-: $\beta_1 = 3$, $\beta_2 = 60$.

The order of stability in DMSO is

$$NO_3^- \ll ClO_4^- < SCN^-.$$

During recent years, several papers have been published on outer-sphere complexes of $Cr(DMSO)_6^{3+}$ (henceforth M^{3+}) with various ligands. Some papers deal with methods of preparation, determination of the composition of individual compounds [1—3]; others draw conclusions on the structure of the compounds by using different methods. Spectrochemical studies deal with the symmetry of M^{3+} and have unambiguously demonstrated an octahedral symmetry [4—6]. Glavas *et al.* [7] determined thermochemical properties of the nitrate, perchlorate and halides of M^{3+} by derivatography. Only qualitative data are available as far as the solubility of these compounds is concerned [2]; no data have been found on their stability. The compounds described in the above papers (nitrate, perchlorate, halides) can be prepared in the solid state with relative ease.

In the present work, we have studied the effect of thiocyanate, nitrate and perchlorate ligands on the solubility and determined the stability constants of the outer-sphere complexes formed with the participation of these ligands by means of solubility measurements. At the same time, quantitative data have been obtained with respect to the solubility of the slightly soluble complex salts used in our experiments.

Experimental

1. Materials

Preparation of $M(NO_3)_3$ solutions. $M(NO_3)_3$ served as the starting material prepared by a well-known method from $Cr(NO_3)_3 \cdot 9H_2O$ [1]. ASHLEY *et al.* [9] reported a very slow water-DMSO exchange in the inner coordination sphere. The chromium to DMSO ratio in the compounds synthesized by them was only 1 : 5.1—1 : 5.9. The statements of ASHLEY *et al.* have been supported by our own experiments, too; $M(NO_3)_3$ prepared according to Ref. [1] contained water impurity in each case.

Since our experiments were disturbed by the presence of water as well as the eventual iron impurity of the starting substances, we have developed a procedure for purification. As a result of this, we succeeded in the preparation of an iron-free solution with a chromium to DMSO ratio equal to 1 : 6. The principle of this purification process is that inert M^{3+} does not interact with sodium hydroxide, but a mixed chromium(III)-DMSO-aqua complex containing water in its inner coordination sphere gives a precipitate under the effect of NaOH, consisting of chromium(III)-hydroxide. Sodium hydroxide brings about also the precipitation of iron(III) ion impurities. After filtration the solution is iron-free and the total amount of chromium is bound to six molecules of DMSO. The solution was then re-acidified to pH < 3 and used in further experiments.

Preparation of $Cr(DMSO)_6(ClO_4)_3$

The solution of M nitrate purified as above was mixed with a solution of sodium perchlorate; $M(ClO_4)_3$ precipitated because its solubility in water is low. The precipitate was filtrated, washed nitrate-free with distilled water and dried at 105 °C.

Preparation of $Cr(DMSO)_6Br_3$

$M(ClO_4)$ was dissolved in DMSO and a solution of potassium bromide in DMSO was added in a 1 : 3 mole ratio. (The solubility of KBr in DMSO is 65 g dm^{-3} [10].) The resulting MBr_3 is very slightly soluble in DMSO. The precipitate was filtrated, washed with DMSO and dried.

Further chemicals used:

NaF *p.a.* product of First Chemical Industria
NaSCN *purum* product of REANAL.
$NaNO_3$ *p.a.* product of REANAL.
$NaClO_4 \cdot H_2O$ *puriss.* product of REANAL.
KNO_3 *p.a.* product of REANAL.
KSCN *p.a.* product of REANAL.
$KClO_4$ *p.a.* product of MERCK.
KBr *p.a.* product of REANAL.
DMSO *puriss.* product of REANAL.

2. Instruments

Dual beam Perkin—Elmer 402 recording spectrophotometer.
Warburg apparatus.

3. Solubility measurements

a) *Measurements in aqueous medium*

Solubility measurement is a well known method to establish the extent of complex formation [11]. We investigated the solubility of $M(ClO_4)_3$ in the presence of various ligands. A constant ionic strength had to be ensured for the measurements, therefore, preliminary experiments were carried out to select an appropriate compound. 200 mg $M(ClO_4)_3$ was shaken in each run, first in 25.0 cm^3 water, then in 25.0 cm^3 total volume, with increasing amounts of 1 mol dm^{-3} sodium thiocyanate, sodium nitrate and sodium fluoride added. The shaking

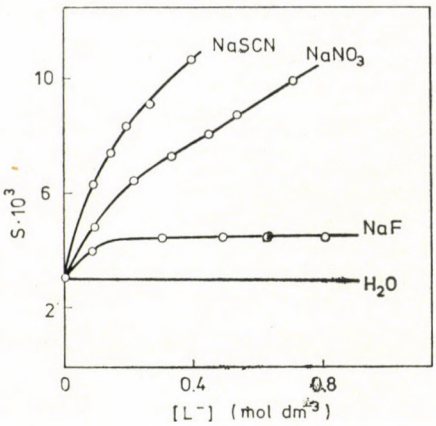

Fig. 1. Solubility of $M(ClO_4)_3$ in water, in the presence of various ligands. (t = 23 °C, ionic strength is not constant)

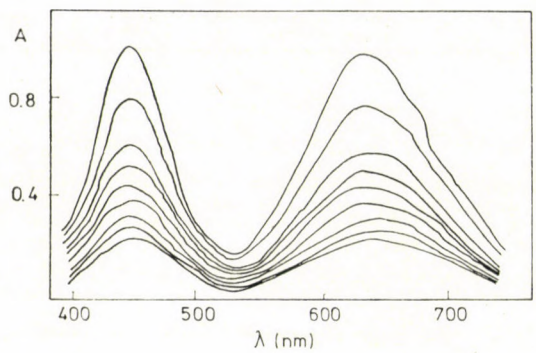

Fig. 2. Spectra of saturated M^{3+} solutions in aqueous NaSCN solutions of various concentrations. (t = 25 °C, I = 1 mol dm^{-3}, adjusted with NaF). NaSCN concentrations (from bottom to top in the Figure): 0, 0.1, 0.2, 0.3, 0.4, 0.5, 0.6, 0.8, 1.0 mol dm^{-3}; d = 1 cm

was performed in a Warburg apparatus at 25 °C. After the dissolution equilibrium had been established, a rapid filtration followed, then the concentration of dissolved chromium complexes was measured spectrophotometrically. Figure 1 shows the effect of various ligands.

It has been shown that the complexing effect of fluoride ion is much less than that of nitrate and thiocyanate ligands.

Preliminary experiments were carried out also to determine the time necessary for equilibration. 200 mg $M(ClO_4)_3$ was shaken in each run with a 0.5 mol dm^{-3} sodium thiocyanate solution for 20, 40, . . . 120 min. These runs indicated an optimum period of 60 min. This time is sufficient for reaching dissolution equilibrium without observable substitution of DMSO in the inner coordination sphere.

On the basis of these preliminary experiments, the measurement of solubility was carried out as follows.

200 mg of $M(ClO_4)_3$ was place into a stoppered flask, then a total amount of 25.0 cm^3 was added of solutions of sodium thiocyanate and sodium fluoride as well as of sodium nitrate and sodium fluoride in various mole ratios. The suspensions were shaken for 1 hr at 25 °C in a Warburg apparatus. After filtration, the absorption spectra were determined. The solubility of $M(ClO_4)_3$ in bidistilled water was measured under analogous conditions.

Figure 2 shows the spectra of solutions containing thiocyanate and fluoride in various ratios as examples.

The absorption maxima at 444 nm were used for evaluation ($\varepsilon = 31.6$ mol^{-1} dm^3 cm^{-1}) [12].

b) *Measurements in DMSO*

Preliminary experiments were carried out in DMSO, too, to determine the optimum experimental conditions, like in case *a*. It was shown that the order of solubility in DMSO is

$$MBr_3 < M(NO_3)_3 < M(ClO_4)_3 < M(SCN)_3$$

On this basis, we studied the solubility with MBr_3. The concentration of dissolved M-compounds was determined by means of the absorption maximum at 443.5 nm ($\varepsilon = 33.5$ mol^{-1} dm^3 cm^{-1} [12]).

Calculation of Stability Constants of Complexes from Solubility Data

Earlier studies [12] indicate that outer-sphere complexes of M^{3+} with the given anions possess an identical visible spectrum independent of the ligand. Thus, the following equations can be written for solute concentrations calculated from the spectra considering the complex product and the solubility product of the perchlorate salt (assuming the formation of ML^{2+} and ML_2^+ outer-sphere complexes):

$$S = [M^{3+}] + [ML^{2+}] + [ML_2^+] \ (S \text{ denotes the solubility});$$

$$\beta_1 = \frac{[ML^{2+}]}{[M^{3+}]\,[L^-]}$$

$$\beta_2 = \frac{[ML_2^+]}{[M^{3+}]\,[L^-]^2}$$

$$K_{0,ClO_4} = [M^{3+}][ClO_4^-]^3 = 5.43 \times 10^{-9}$$

After rearrangement and substitution we obtain the following expression:

$$Y = \left(\frac{27\,S^4}{K_{0,ClO_4}} - 1\right)\frac{1}{[L^-]} = \beta_1 + \beta_2[L^-]$$

If the plot of the left-hand side (Y) against $[L^-]$ gives good straight line, the system can be described adequately by assuming M, ML and ML_2 and the intercept gives directly β_1 and the slope gives β_2. (This was found in water if $[SCN^-] \leqq 0.3$ mol dm^{-3}, $[NO_3^-] \leqq 0.5$ mol dm^{-3}). At higher $[L^-]$ values, even the introduction of another stability constant β_3 does not help to approximate the experimental values better. This does not mean that it is necessary to assume the formation of further (1 : 4, 1 : 5 *etc.)* complexes but there is rather a significant change in the medium which cannot be described quantitatively.

Results and Discussion

1. *Solubility determination in pure solvents*

The solubility of slightly soluble salts has been determined in water and DMSO at 25 °C, by the method described in the Experimental. Results are summarized in Table I.

Table I

Solubilities of some salts of $Cr(DMSO)_6^{3+}$ in water and pure DMSO

$t = 25$ °C, no other salt added

Solvent	Solubility (mol dm^{-3})		
	$M(ClO_4)_3$	$M(NO_3)_3$	MBr_3
H_2O	2.85×10^{-3}	>1	>1
DMSO	1.40×10^{-1}	1.91×10^{-2}	7.46×10^{-4}

2. *Effect of anions on the solubility of $M(ClO_4)_3$ in aqueous medium*

a) Effect of fluoride ions. It has been found that fluoride ions too increase the solubility of $M(ClO_4)_3$. Figure 1 shows that there is a slight but unmistakable increase in the solubility when even large amounts of fluoride ion are added. Our measurements indicate that $\beta_1 < 0.2$ mol^{-1} dm^3. The assumption of the MF^{2+} complex is supported also by kinetic measurements [12]. Further experiments involved sodium fluoride to ensure a constant ionic strength because the complexing ability of fluoride is lower by an order of magnitude than that of the other ligands studied. The formation of an MF^{2+} complex was always taken into consideration.

b) Effect of nitrate ions. According to the solubility studies described in the "Experimental" section, the solubility was measured spectrophotometrically in 0, 0.1, 0.2, . . . 1.0 mol dm^{-3} sodium nitrate solutions with a constant ionic strength of $I = 1$ mol dm^{-3} (adjusted with sodium fluoride). The following values have been obtained for the complex products (Fig. 2):

$$\beta_1 = 5\,; \quad \beta_2 = 19\,.$$

Using these values, the solubility as a function of ligand concentration has been re-calculated. The experimental data fit well to the calculated curve up to a ligand concentration of 0.5 mol dm^{-3} (Fig. 4).

c) Effect of thiocyanate ions. Similarly to nitrate ions, the solubility was determined also in sodium thiocyanate solutions of 0, 0.1, 0.2, . . . 1.0 mol dm^{-3}

concentration, at a constant ionic strength of $I = 1$. The following values were obtained for the stability constants (Fig. 3):

$$\beta_1 = 3\,; \quad \beta_2 = 60\,.$$

The reliability of results has been checked here, too, by fitting the calculated curve to the experimental points (Fig. 4). The fit is very good up to a concen-

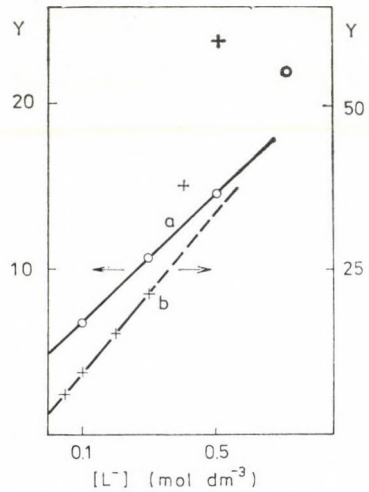

Fig. 3. Determination of the complex products in aqueous (a) $M^{3+} + NO_3^-$ and (b) $M^{3+} + + SCN^-$ systems ($t = 25$ °C, $I = 1$ mol dm^{-3}, adjusted with NaF)

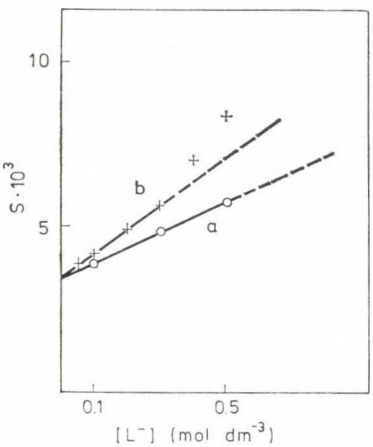

Fi:. 4. Comparison of experimental and calculated solubility values for checking the complex products in (a) $M^{3+} + NO_3^-$ and (b) $M^{3+} + SCN^-$ systems. Symbols denote experimental points, solid line: solubility plot calculated with the constants determined in this work

tration of $[SCN^-] \leqq 0.3$ mol dm^{-3}; on this basis the error in calculating the complex products can be estimated to be less than 10%.

d) Effect of perchlorate ions. The eventual complexing effect of perchlorate has been checked by solubility studies in sodium perchlorate solutions of various

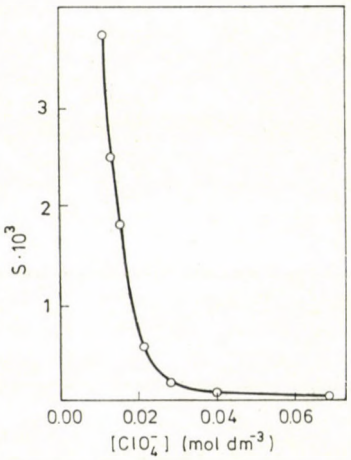

Fig. 5. Solubility of $M(ClO_4)_3$ under the effect of $NaClO_4$ in aqueous medium ($t = 25$ °C, $I =$ $= 1$ mol dm^{-3}, adjusted with NaF). Symbols denote experimental results, solid line: solubility curve calculated from the solubility product $K_{0,ClO_4} = 5.43 \times 10^{-9}$

concentrations. To do so, the solubility values at various perchlorate concentrations have been calculated on the basis of the solubility products measured in a 1 mol dm^{-3} NaF solution. These values were plotted as a function of the perchlorate concentration. Calculated and measured values fit each other well indicating that no outer-sphere complex is formed with perchlorate ions. The results are shown in Fig. 5.

e) Comparison. The data obtained for the four systems studied indicate the following order as far as the stability of outer sphere-complexes is concerned:

$$ClO_4^- \ll F^- \ll NO_3^- < SCN^-$$

3. *Effect of anions on the solubility of MBr_3 in DMSO*

Both perchlorate and thiocyanate ions increase the solubility of MBr_3 in DMSO. ClO_4^- and SCN^- increase the solubility by factors of 9 and 15, respectively, at a 1 mol dm^{-3} concentration. This can also be interpreted in terms of the formation of outer-sphere complexes. The calculation of stability constants

from the concentration dependence of solubility was, however, not possible, because of the large scatter of experimental data.

The solubilities of $M(NO_3)_3$ and $M(ClO_4)_3$ are too high to permit to determine stability constants by this method. Thus, only the following relative stability order can be given

$$NO_3^- \ll ClO_4^- < SCN^-.$$

REFERENCES

[1] COTTON, F. A., FRANCIS, R.: J. Amer. Chem. Soc., **82,** 2986 (1960)
[2] SCHLAFER, L., OPITZ, H. P.: Z. anorg. allg. Chem., **313,** 178 (1961)
[3] SELBIN, J., BULL, W. E., HOLMES, L. H.: J. Inorg. Nucl. Chem., **16,** 219 (1960)
[4] MEEK, D. W., DRAGO, R. R., PIPER, T. S.: Inorg. Chem., **1,** 285 (1962)
[5] VERNEY, Ch. V., WEBER, J. H.: Inorg. Chem., **7,** 283 (1968)
[6] SCHLAFER, L., OPITZ, H. P.: Elektrochem., **65,** 372 (1961)
[7] GLAVAS, M., SKERLAK, T.: Glas Hem. Tehnol. Bosne Hercegovine, **15,** 41 (1967); C. A. **69,** 64250 p (1968)
[8] GLAVAS, M., SKERLAK, T.: Glas. Hem. Tehnol. Bosne Hercegovine, **15,** 31 (1967); C. A. **69,** 48796 r (1969)
[9] ASHLEY, K. R., HAMM, R. E., MAGNUSON, R. H.: Inorg. Chem., **6,** 412 (1967)
[10] MARTIN, D., HAUTHAL, H. G.: Dimethylsulfoxid. Akad. Verlag, Berlin 1971
[11] BECK, M. T.: Chemistry of Complex Equilibria. Akadémiai Kiadó, Budapest 1970
[12] RÁBAI, Gy.: Thesis, Debrecen 1973

Zsuzsa ÁKOS-SZABÓ H-1521 Budapest, Műegyetem

István ORSZÁGH
György BAZSA } H-4010 Debrecen, P. O. Box 7.

Acta Chimica Academiae Scientiarum Hungaricae, Tomus 102 (3), pp. 223—234 (1979)

KINETICS OF FORMATION AND EQUATION OF HEXAKIS-(DIMETHYL SULFOXIDE)-CHROMIUM(III) IN CATALYTIC AND NON CATALYTIC REACTIONS

Gy. RÁBAI, Gy. BAZSA and M. T. BECK

(Institute of Physical Chemistry, L. Kossuth University, Debrecen)

Received June 30, 1978
Accepted for publication December 7, 1978

The kinetics of the reaction of $Cr(H_2O)_n(DMSO)_{6-n}^{3+}$ complexes with water and dimethyl sulfoxide, as well as the effect of nitrite ions and carbon dioxide on the rate of these processes were studied. The kinetic equation of solvolysis in the case of $n = 6$ and the reaction mechanism were determined. The penetration of both water and DMSO into the coordination sphere is accelerated by both nitrite and carbon dioxide in the case of $n = 2-6$, whereas if $n = 0$, aquation is not catalyzed by either nitrite or CO_2. The accelerating effect is interpreted in terms of the enhanced reactivity of carbonato- and nitrito chromium(III) complexes, presumably formed in a rapid pre-equilibrium. The appearance of new ligands in the coordination sphere obviously loosens the chromium-oxygen bonds. The stability constant of the $Cr(H_2O)_5(OCO_2H)^{2+}$ complex has been determined on the basis of kinetic data.

The inert hexaaquachromium(III) ion reacts surprisingly readily with some oxyanions. Rapid complex formation with sulfite [1], iodate [2], nitrite [3], and chromate [4] has been demonstrated spectrophotometrically, that with molybdate [5] both spectrophotometrically and conductometrically. The assumption of an interaction with hydrogen carbonate ions is justified by its catalytic effect observed in the reaction between thiocyanate and chromium(III) [6]. Since the anions mentioned rapidly exchange their oxygen atoms with those of water molecules, it is obvious to assume that rapid complexing occurs without cleavage of the original chromium-oxygen bond, via the exchange of oxygen atoms between coordinated water molecules and oxyanions:

$$(H_2O)_5—Cr—\overset{*}{O}H_2^{3+} + OXO_z^{n-} \rightleftharpoons (H_2O)_5—Cr\overset{*}{O}XO_z^{(3-n)+} + H_2O \qquad (1)$$

This mechanism is identical with that between pentaamminemonoaquacobalt(III) and nitrite, proven by means of ^{18}O isotope [7]. Such evidence, however, has not yet been reported for chromium, and this is the reason why we decided to study this system. A chromium complex was selected in which there is an inert chromium-oxygen bond like in the aqua complex but the ligand — unlike water — is unable to exchange its oxygen atoms rapidly with the oxyanions mentioned. If our hypothesis is correct, no rapid complexing should be observed. The chromium complex of dimethyl sulfoxide (DMSO) is suitable

for this purpose. Infrared spectroscopy points to the coordination of dimethyl sulfoxide to chromium through its oxygen atom [8]. It is also well known that the rate of oxygen exchange in DMSO is very small [9].

Equilibrium data with respect to the solvation of chromium(III) in water, DMSO and the mixture of these two solvents are well known [10]. No quantitative data have so far been reported, however, on the kinetics of the processes involved. The present paper deals with the kinetic study of these processes as well as with the detailed study of the effect of nitrite ions and carbon dioxide on these reactions.

Experimental

Materials

Commercial DMSO (Reanal, technical grade) was purified by vacuum distillation just before the experiments. Hexaaquachromium(III) perchlorate was prepared from chromium(VI) oxide in a perchloric acid medium by its reduction with hydrogen peroxide. It was stored a 1 mol dm^{-3} aqueous solution containing also perchloric acid.

Hexakis(DMSO)chromium(III) was prepared as its nitrate salt by the following procedure. Crystalline chromium(III) nitrate was dissolved in a tenfold molar amount of dimethyl sulfoxide. Carbon dioxide was bubbled through the solution for 2—3 hrs. Then it was heated up to 100—105 °C and mixed at this temperature for 6—8 hrs. A green oily material was obtained after cooling; upon adding absolute ethanol, well filtrable light green crystals precipitated. This substance was purified further as described in Ref. [11]. Further materials: $HClO_4$, HNO_3, $NaNO_3$, $NaNO_2$, CO_2 gas and N_2 gas were of analytically pure grades. These substances were used without further purification.

Methods of Kinetic Studies

Reactions were followed spectrophotometrically at 25 °C, except for the measurement of the activation energy, where the temperature was varied. Water was used as the solvent in aquation reactions and DMSO in the anation processes; in some cases mixtures of DMSO with water were applied. The hydrogen ion concentration in DMSO solutions was adjusted by means of perchloric acid whereas the ionic strength by sodium perchlorate. Nitric acid and sodium nitrate were used for this purpose in aqueous solutions because the DMSO-chromium(III) complex gives a very slightly water-soluble salt with perchlorate ion [11]. The hydrogen ion concentration in DMSO solutions was regarded as equal to the analytical concentration of acid added. The concentration of CO_2 was varied by saturating the reaction mixture containing all components except for the chromium complex by a gas mixture consisting of known amounts of carbon dioxide and nitrogen. The concentration of CO_2 dissolved in DMSO was determined by bubbling nitrogen through the solution. The CO_2 leaving was absorbed in a KOH solution and measured gravimetrically as barium carbonate. It was shown that the solubility of CO_2 in DMSO is independent of the hydrogen ion concentration in the concentration range applied for kinetic measurements.

The reaction was started by adding chromium complex to the mixture. It was carried out in a thermostated, air-tight, stoppered cuvette. The spectrum of the mixture was recorded periodically on a Perkin—Elmer 402 spectrophotometer. A typical group of spectra is shown in Fig. 1.

The log $(A_\infty - A_t)$ values at 460 nm (A_∞ is the absorbance in equilibrium, A_t that at t time) gave a straight line as a function of the time, at least in the initial section of the time scale. The slopes of these line gave the apparent first-order rate constants. If this condition was not fulfilled, the initial slope of the absorbance *vs.* time curve (640 nm) was taken as the measure of the initial rate. These two quantities are related to each other by the following definition:

$$v_0 = \frac{1}{\Delta\varepsilon}\left(\frac{dA}{dt}\right)_0 \tag{2}$$

The value of $\Delta\varepsilon$ in Eq. (2) is not equal to the difference of molar absorbances referred to the total chromium(III) in the equilibrium and the starting mixture, respectively, but is rather

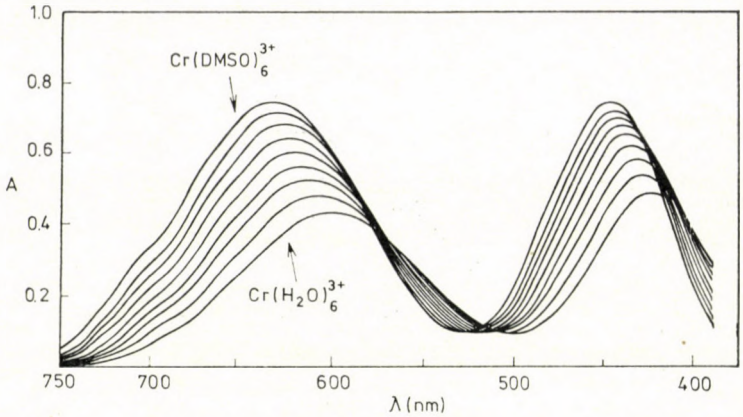

Fig. 1. Spectrum of a $Cr(H_2O)_6^{3+}$ + DMSO reaction mixture as a function of time. $[Cr(H_2O)_6^{3+}] = 0.025$ mol dm^{-3}, $[H^+] = 0.02$ mol dm^{-3}, $I = 1.0$ mol dm^{-3}, $d = 1$ cm

the difference between the molar absorbances of hexaaqua- and mono(DMSO)pentaaquachromium(III). Since this latter complex has not been isolated in the pure state, the valuc of $\Delta\varepsilon$ was estimated on the basis of available literature data [10] and our own measurements as $\Delta\varepsilon = 7 \pm 1$. If this value of 7 ± 1 is substituted into Eq. (2) for $\Delta\varepsilon$, the rate of penetration of the first DMSO molecule can be calculated. This is possible because two conditions are fulfilled with respect to the system studied. If ε_n is the molar absorbance of a mixed-ligand complex containing n DMSO molecules, k_n is the rate constant of the reaction between the same complex and DMSO ($0 \leq n \leq 6$), then

$$\varepsilon_1 - \varepsilon_0 > \varepsilon_2 - \varepsilon_1$$

$$k_1 \gtrsim k_2, k_3$$

As was verified by model calculations, the values of k_4, k_5, k_6 (however large or small they are) do not influence the determination of k_1. The variation of ε_n ($n > 2$) does not influence the accuracy of determination of k_1, either, if the model does not contain an unrealistically large ε_2 value (such as $\varepsilon_2 > 10\varepsilon_1$).

The value of k_1 cannot be determined in such systems if $\varepsilon_1 - \varepsilon_0 < \varepsilon_2 - \varepsilon_1$ and also if $k_1 < k_2, k_3$. If, however, $k_1 \ll k_2, k_3, \ldots k_6$, then, provided that $\Delta\varepsilon = \varepsilon_6 - \varepsilon_0$, the values of k_1 can be calculated correctly. In this case the symbol $\ll$ should represent at least a twenty-fold difference.

Results and Discussion

Solvolysis of $Cr(H_2O)_6^{3+}$ in DMSO

The kinetic parameters of the noncatalytic reactions have been determined first. To ensure a carbon dioxide-free medium, nitrogen gas was bubbled through the solution. The initial rate does not change observably if the ionic strength increases 0.1 to 1.0 mol dm^{-3}. In spite of this fact, the ionic strength was kept constant in further experiments. Figure 2 shows that the initial rate is directly proportional to the concentration of chromium(III) ions. An inverse proportionality is valid for hydrogen ions (Fig. 3). The intercept of the plot in Fig. 3 has a positive value, indicating that the kinetic equation should

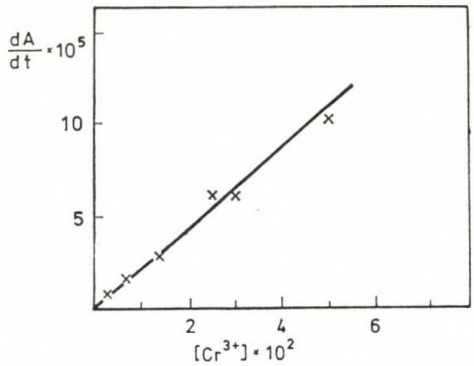

Fig. 2. Rate of the noncatalytic reaction $Cr(H_2O)_6^{3+}$ + DMSO as a function of chromium concentration. $[H^+] = 0.02$ mol dm^{-3}, $I = 1.0$ mol dm^{-3} $NaClO_4$, $\lambda = 640$ nm

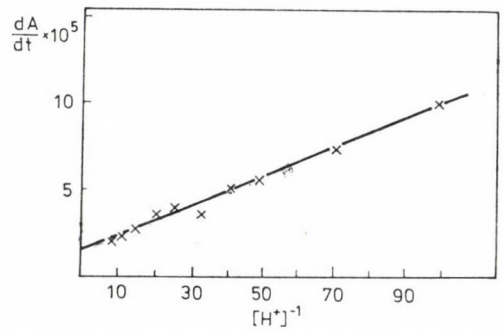

Fig. 3. Rate of the noncatalytic reaction as a function of the reciprocal hydrogen ion concentration. $[Cr(H_2O)_6^{3+}] = 0.025$ mol dm^{-3}, $I = 1.0$ mol dm^{-3} $NaClO_4$, $\lambda = 640$ nm

contain a term independent of the proton concentration. The following kinetic equation describes the experimental results:

$$-\frac{d[Cr(H_2O)_6^{3+}]}{dt} = [Cr(H_2O)_6^{3+}](k + k'[H^+]^{-1}) \qquad (3)$$

If $t = 25$ °C, and $I = 1$ mol dm^{-3}, the values of the constants in Eq. (3) are as follows:

$$k = 8.4 \times 10^{-5} \text{ min}^{-1}, \quad k' = 5.2 \times 10^{-6} \text{ min}^{-1} \text{ mol dm}^{-3}.$$

The difference between the initial rates calculated by means of this equation and found experimentally is not larger than 10%. If the hydrogen ion concentration is 0.01 mol dm^{-3}, the activation energy of the reaction is 129 kJ mol^{-1}.

The results can be interpreted in terms of two simultaneous pathways:

$$Cr(H_2O)_6^{3+} + DMSO \xrightarrow{slow} \text{products} \quad (4)$$

$$Cr(H_2O)_6^{3+} \underset{\leftarrow}{\overset{fast}{\rightleftharpoons}} Cr(H_2O)_5OH^{2+} + H^+ \quad (5)$$

$$Cr(H_2O)_5OH^{2+} + DMSO \xrightarrow{slow} \text{products} \quad (6)$$

Rapid pre-equilibrium (5) is so much shifted to the left in the $[H^+]$ range studied ($K = 3.5 \times 10^{-4}$ mol dm^{-3}) that only 0.1—1% of the total amount of chromium is present as the monohydroxo complex. In spite of this fact, the rates of steps (4) and (6) are comparable. This is in agreement with the fact known from the literature that the substitution reactions of monohydroxochromium(III) are faster by 2—3 orders of magnitude than those of the hexaaqua complex [12].

Effect of Carbon Dioxide on the Rate

It was observed that the rate of formation of DMSO-chromium(III) complexes increases in the presence of carbon dioxide. Figure 4 shows the initial rates together with the ratio of the initial rates of the catalytic and noncatalytic reactions as a function of the CO_2 concentration. This figure demonstrates that solvolysis in a DMSO-solution saturated with CO_2 is nearly four hundred times faster than without CO_2, under otherwise identical conditions. If the concentration of hydrogen ions increases, the rate of the catalytic reaction decreases. The quantitative correlation is depicted in Fig. 5 where the initial rates are plotted as a function of the reciprocal hydrogen ion concentration. The partial reaction order with respect to chromium is 1. The ionic strength has no observable effect in this case, either.

We have determined the energy of activation for the overall process accelerated by CO_2. Since the solubility of CO_2 changes considerably as a function of the temperature, the following procedure was applied. We saturated the liquid mixture containing no chromium complex with CO_2 at 25 °C, then cooled the almost full cuvette to the required lower temperature. Reaching this value, we added a small volume of concentrated chromium(III) solution to the mixture. Thus, the temperature effect was studied at constant CO_2 concentration in the 10—25 °C temperature range. Since the catalytic process is about four hundred times faster than the noncatalytic one, the value obtained ($E_a = 62$ kJ mol^{-1}) corresponds to the energy of activation of the catalytic process. This is less than one half of the activation energy of the noncatalytic process.

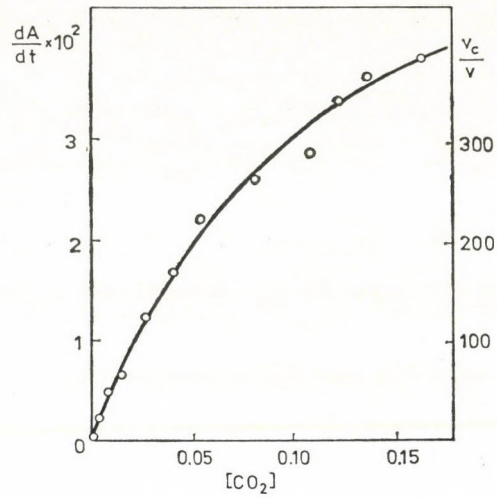

Fig. 4. Reaction rate as a function of the $[CO_2]$ concentration. Right hand axis shows the ratio of the catalytic and noncatalytic reaction. $[Cr(H_2O)_6^{3+}] = 0.025$ mol dm^{-3}, $I = 1.0$ mol dm^{-3} $NaClO_4$, $[H^+] = 0.005$ mol dm^{-3}, $\lambda = 640$ nm

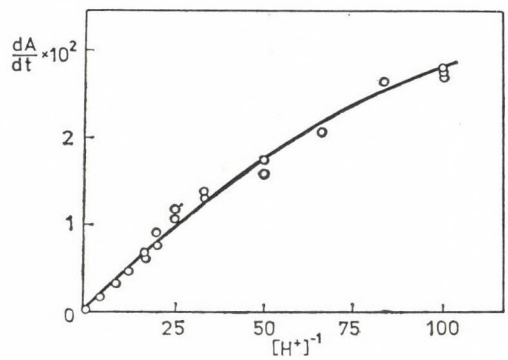

Fig. 5. Rate of reaction catalyzed by carbon dioxide as a function of $[H^+]^{-1}$, $[Cr(H_2O)_6^{3+}] =$ $= 0.025$ mol dm^{-3}, $[CO_2] = 0.165$ mol dm^{-3}, $I = 1.0$ mol dm^{-3}, $\lambda = 640$ nm

The experimental results allow to write the following equation for the catalytic process:

$$-\frac{d[Cr(H_2O)_6^{3+}]}{dt} = v = \frac{k_1 K[CO_2]}{[H^+] + K[CO_2]}\,[Cr(H_2O)_6^{3+}] \qquad (7)$$

Equation (7) can be transformed as follows:

$$[H^+]\frac{v}{[CO_2]} = Kk_1[Cr(H_2O)_6^{3+}] - Kv \qquad (8)$$

Considering also Eq. (2), the values of the constants in Eq. (8) can be determined using the method of least squares: $k_1 = 0.393$ min^{-1} and $K = 0.0425$. Re-calculating the initial rates with these constants, a good agreement was found with the experimental data. The full lines in Figs. 4 and 5 correspond to calculated and the symbols to experimental values. Kinetic evidence is in agreement with the following simple mechanism, in the first step of which a carbonato chromium complex is produced in a rapid reaction:

$$Cr(H_2O)_6^{3+} + CO_2 \overset{K}{\rightleftharpoons} (H_2O)_5Cr(OCO_2H)^{2+} + H^+ \qquad (9)$$

This carbonato complex reacts with DMSO much more rapidly than the hexaaqua complex:

$$(H_2O)_5Cr(OCO_2H)^{2+} + DMSO \xrightarrow{k_1} \text{products} \qquad (10)$$

Considering that an amount of H^+ equivalent to that of ML is formed and the concentration of [ML] can be neglected as compared with $[L]_T$ of carbon dioxide, the following expression is obtained for the equilibrium constant of (9):

$$K = \frac{ML(H_T + ML)}{(M_T - ML)\,L_T} \qquad (11)$$

Here H_T denotes the hydrogen ion concentration added, M_T the total concentration of chromium and ML that of the carbonato complex formed. Rearranging Eq. (11), we obtain

$$ML^2 + ML\,H_T + ML\,L_T K - M_T L_T K = 0 \qquad (12)$$

The quadratic term ML^2 can be neglected. Then the concentration of the carbonato complex will be:

$$ML = \frac{K M_T L_T}{H_T + K L_T} \qquad (13)$$

The rate of reaction will be the product of the carbonato complex concentration and rate constant k_1. If Eq. (13) is multipled by the rate constant of process (10), we obtain an equation identical to that found experimentally (*i.e.* Eq. 7). The contribution of the noncatalytic reaction to the overall rate is not significant. If H_T is large, the importance of $K\,L_T$ in the denominator decreases and the initial rate as a function of the carbon dioxide concentration can be approximated by a straight line. This is shown in Fig. 6, where initial rates observed for a H^+ concentration of 0.10 mol dm^{-3} are plotted as a function of the CO_2 concentration.

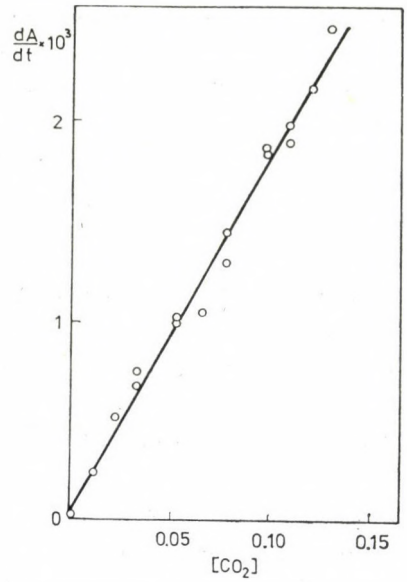

Fig. 6. Reaction rate as a function of the CO_2 concentration. $[Cr(H_2O)_6^{3+}] = 0.025$ mol dm^{-3} $I = 1.0$ mol dm^{-3} $NaClO_4$ $[H^+] = 0.10$ mol dm^{-3}, $\lambda = 640$ nm

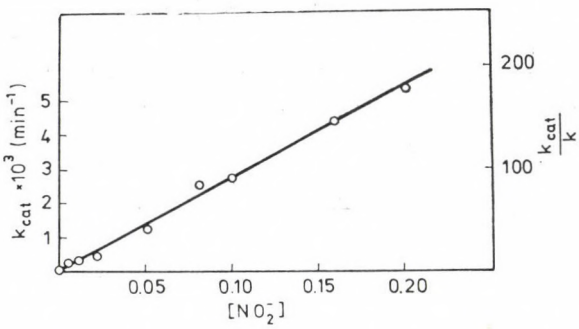

Fig. 7. Reaction rate as a function of the nitrite ions concentration. The right hand axis shows the ratio of the rate constants of the catalytic and the noncatalytic reaction. $[Cr(H_2O)_6^{3+}] =$ $= 0.025$ mol dm^{-3}, $[H^+] = 0.50$ mol dm^{-3}, $I = 1.0$ mol dm^{-3} $NaClO_4$, $\lambda = 640$ nm

Effect of Nitrite ion on the Rate

If the values of $\lg (A_\infty - A_t)$ are plotted as a function of time in the case of the reaction catalyzed by nitrite ions, the points determine a straight line up to a conversion of 60%. This permits to calculate apparent first order rate constants. Since sodium nitrite suffers alkaline hydrolysis, a higher acid concentration had to be applied to avoid the formation of chromium hydroxo complexes. Because of the decomposition of nitrite to gaseous products, the acid concentration could be increased up to a certain limit. Figure 7 shows the

rate as a function of the nitrite ion concentration. The figure contains also the ratio of the rate constants of catalytic and noncatalytic reactions. It can be seen that nitrite in a concentration of 0.2 mol dm^{-3} increases the reaction rate by a factor of almost 200. As opposed to the plot observed with CO_2, no sat-

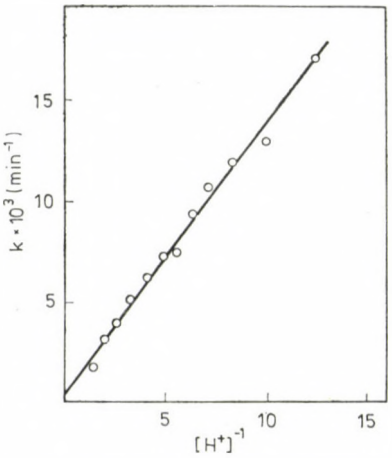

Fig. 8. Rate of the reaction catalyzed by nitrite ions, as a function of $[H^+]^{-1}$. $[Cr(H_2O)_6^{3+}] = 0.025$ mol dm^{-3} $[NO_2^-] = 0.10$ mol dm^{-3}, $I = 1.0$ mol dm^{-3} $NaClO_4$, $\lambda = 640$ nm

uration appears here. If the enhancement of the reaction rate is interpreted in terms of the rapid formation of a nitrito complex (like in the case of carbon dioxide) then the straight line suggests a smaller stability for the nitrito complex, the constant of which cannot be determined even from the kinetic data. According to Fig. 8, at constant nitrite ion concentration, the rate is directly proportional to the reciprocal hydrogen ion concentration. The following equation describes the rate of solvolysis in the presence of nitrite:

$$-\frac{d[Cr(H_2O)_6^{3+}]}{dt} = [Cr(H_2O)_6^{3+}]\,(k + k'[H^+]^{-1} + k_2[NO_2^-]\,[H^+]^{-1}) \quad (14)$$

where $k_2 = 5.4 \times 10^{-2}$ min^{-1}; t = 25 °C; $I = 1.0$ mol dm^{-3} ($NaClO_4$).

The effect of nitrite can be attributed to the formation of a nitritochromium(III) complex without cleavage of the original chromium-oxygen bond, which has an enhanced reactivity. The dependence of the rate on the hydrogen ion concentration indicates that the concentration of the nitrito complex decreases with increasing acidity. It can be concluded that free nitrite ions and not their protonated forms are in equilibrium with the hexaaquachromium(III) ion:

$$H^+ + NO_2^- \rightleftharpoons HNO_2 \quad (15)$$

$$Cr(H_2O)_6^{3+} + NO_2^- \rightleftharpoons Cr(H_2O)_5ONO^{2+} + H_2O \quad (16)$$

The oxygen of the water molecule leaving the complex comes from the nitrite ion.

No nitrito complex formation can be observed spectrophotometrically in a dimethyl sulfoxide medium. The equilibrium [13] and kinetic [14] behaviour of the process has been studied in aqueous medium. It was shown that the reaction assumed above, although not instantaneous is unusually rapid as compared with other substitution reactions of chromium(III). The cleavage of the chromium-oxygen bond in the nitritochromium(III) complex requires less energy than in the hexaaquachromium(III) complex. This is supported by the value of activation energy determined in the presence of 0.1 mol dm^{-3} nitrite ion, which is equal to $E_a = 90$ kJ mol^{-1}.

Effect of NO_2^- and CO_2 on the Coordination and Elimination of the Second, Third, . . . n-th (up to n = 5) DMSO Molecule

It has been shown experimentally that CO_2 and NO_2^- accelerate not only the reaction between hexaaquachromium(III) and DMSO — *i.e.* the incorporation of the first DMSO molecule into the coordination sphere of chromium — but also that of further DMSO molecules. In order to study this problem, a water—DMSO—chromium(III) system has been chosen as the starting material, in which — according to ASHLEY [15] — the average number of both water and DMSO molecules in the coordination sphere is equal to three. The corresponding concentration is 6.4 mol dm^{-3} DMSO in water. If further DMSO is added to the equilibrium mixture corresponding to $\bar{n} = 3$, the new equilibration is much more rapid in the presence of carbon dioxide and nitrite ion than without them. The equilibrium system $\bar{n} = 3$ contains mainly mixed-ligand complexes (water and DMSO). The concentration of hexaaquachromium(III) is negligible, thus its reactions should not be considered. If we add water to the $\bar{n} = 3$ equilibrium system, the equilibrium is shifted in the reverse direction. This occurs at a higher rate if the solution contains carbon dioxide or nitrite ions. Figure 9 shows the reaction of the $\bar{n} = 3$ equilibrium system with water and DMSO. The spectrum of a solution without any nitrite remains unchanged for 400 min. In the presence of nitrite, the same period is sufficient for a considerable change to occur. The experiment proves that both CO_2 and NO_2^- accelerates the coordination and elimination of the 2nd, 3rd, . . . n-th DMSO molecule, respectively. Elimination prevails with $n < 5$.

Aquation of $Cr(DMSO)_6^{3+}$

Aquation is a very slow process at room temperature. The spectrum of the reaction mixture at various reaction times is shown in Fig. 10. Three isosbestic points can be found on the groups of spectra indicating that only the starting $Cr(DMSO)_6^{3+}$ and the final product are present in significant concentrations at

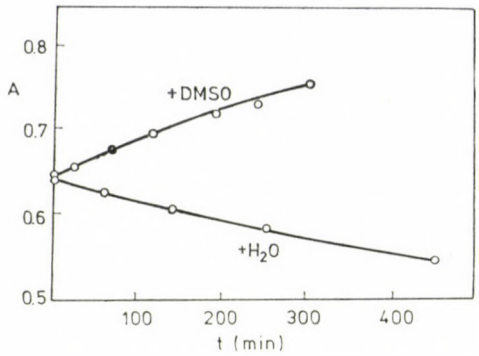

Fig. 9. Reaction of an equilibrium mixture with water and DMSO for $\bar{n} = 3$. [DMSO] = 6.4 mol dm^{-3}, $[Cr^{3+}_{\bar{n}=3}] = 0.025$ mol dm^{-3}, $[H^+] = 0.50$ mol dm^{-3}, $[NO_2^-] = 0.10$ mol dm^{-3}, $\lambda = 640$ nm.
+ DMSO: 1 volume of reaction mixture + + 3 volume of DMSO;
+ H_2O: 1 volume of reaction mixture + + 3 volume of H_2O

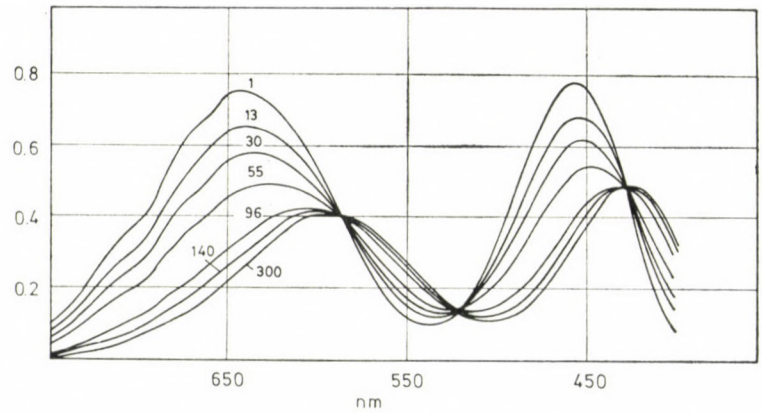

Fig. 10. Change of the spectrum of $Cr(DMSO)_6^{3+}$ during aquation. Numbers written at the curves show the duration of the reaction (min). [Cr(III)] = 0.025 mol dm^{-3}, $t = 80$ °C, pH = = 3.5

all times, and intermediate mixed complexes do not accumulate in observable ammounts. A straight line is obtained if $\lg (A_t - A_\infty)$ at any appropriate wavelength is plotted as a function of time. No isosbestic points are found at higher hydrogen ion concentrations ($[H^+] > 0.01$), neither is the plot of $\lg (A_t - A_\infty)$ against time a straight line. This can be explained by the slow incorporation of the first water molecule at low hydrogen ion concentrations as compared with that of subsequent water molecules. This is not surprising since the hydroxo complex produced by deprotonation of the mixed water-DMSO complex formed in the first step reacts much more rapidly than the

aqua complex. This is in agreement with the general behaviour of chromium complexes. The increase of hydrogen ion concentration suppresses the formation of hydroxo complexes, thus the rate of subsequent steps decreases. The intermediates have an appreciable absorption, thus no isosbestic points appear in the spectrum.

The first order rate constant of aquation of $Cr(DMSO)_6^{3+}$ in water is $k_{aq} = 6.6 \times 10^{-5}$ min^{-1} (at $t = 25$ °C, $I = 2.0$ mol dm^{-3} $NaNO_3$, pH $= 3.5$). This rate does not increase if sodium hydrogen carbonate, carbon dioxide or sodium nitrite is added. This means that the aquation of $Cr(DMSO)_6^{3+}$ ions is not catalyzed by carbon dioxide or nitrite ions.

The results indicate that CO_2 and NO_2^- show a catalytic effect on the processes occurring in the DMSO—chromium(III)—water system if the coordination sphere of chromium contains water molecule(s) too. This is indirect evidence supporting the mechanism of oxygen exchange mentioned in the Introduction since this is the only possibility of rapid complexing *via* oxygen exchange. In this case a carbonato and nitrato complex is produced in a rapid pre-equilibrium and the appearance of a new ligand in the coordination sphere loosens the chromium—oxygen bonds. This is evidenced by the significant decrease of the activation energy of the $Cr(H_2O)_6^{3-}$ + DMSO reaction in the presence of nitrite ions and especially carbon dioxide.

REFERENCES

[1] King, E. L., Carlyle, D. W.: Inorg. Chem., **9,** 2333 (1970)
[2] Mercer, E. E., Hormuth, J. A.: J. Inorg. Nucl. Chem., **31,** 2145 (1969)
[3] Matts, T. C., Moore, P.: J. Chem. Soc. (A), **1969,** 1997
[4] King, E. L., Neptune, J. A.: J. Am. Chem. Soc., **77,** 3186 (1955)
[5] Hall, H. T., Eyring, H.: J. Am. Chem. Soc., **72,** 782 (1950)
[6] Beck, M. T.: J. Inorg. Nucl. Chem., **31,** 2145 (1960)
[7] Murmann, R. K., Taube, H.: J. Am. Chem. Soc., **78,** 4886 (1956)
[8] Cotton, F. A., Francis, R.: J. Inorg. Nucl. Chem., **17,** 62 (1961)
[9] Margin, D., Hauthal, H. G.: Dimethylsulfoxid. Akademie-Verlag, Berlin 1971
[10] Scott, L. P., Weeks, T. J., Bracken, D. E., King, E. L.: J. Am. Chem. Soc., **91,** 5219 (1969)
[11] Szabóné Ákos Zs., Országh, I., Bazsa Gy.: Magy. Kém. Folyóirat, **81,** 53 (1975); Acta Chim. Acad. Sci. Hung. (In press)
[12] Espenson, I.: Inorg. Chem., **8,** 1554 (1969)
[13] Garnier, A.: C. R. Ser. B, **265,** 198 (1967)
[14] Kormos, K.: Thesis, Debrecen, KLTE 1974
[15] Ashley, K. R., Hamm, R. A., Magnusson, R. H.: Inorg. Chem., **6,** 413 (1967)

Rábai Gyula
Bazsa György
Beck Mihály
H-4010 Debrecen, P. O. Box 7.

Acta Chimica Academiae Scientiarum Hungaricae, Tomus 102 (3), pp. 235—246 (1979)

REACTIONS OF AMIDE CHLORIDES WITH UREAS, II

REACTIONS WITH ASYMMETRICALLY DISUBSTITUTED UREAS

I. BITTER, É. KÁRPÁTI-ÁDÁM and L. TŐKE

(Department of Organic Chemical Technology, Technical University, Budapest)

Received July 5, 1978
Accepted for publication December 11, 1978

The reactions of asymmetrically disubstituted ureas with chloromethylenedimethylammonium chloride were investigated. The resulting carbamoylamidinium chloride could not be isolated in the crystalline state but the products of their decomposition formed on thermal treatment, on treatment with a tertiary base and on hydrolysis, have been identified, their structures elucidated and their formation explained. According to the experimental results, direct *N*-acylation seems to be probable.

In a previous paper [1], the reactions of symmetrically disubstituted ureas with chloromethylenedimethyl-ammonium chloride and chlorodimethylaminomethylenedimethyl-ammonium chloride were described. It was found that in the first case *N*-carbamoylformamidinium chlorides, in the second case *N,N'*-diarylchloroformamidinium chlorides were formed

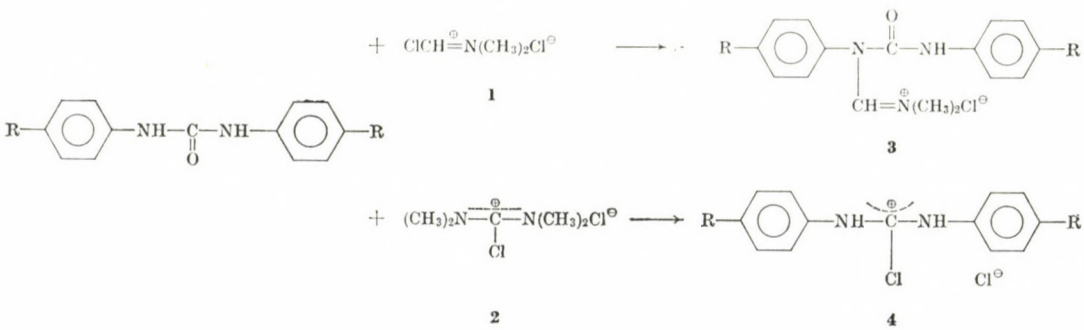

When considering the similar reactivities and structures of reagents **1** and **2** and their different space requirements, the formation of compounds **3** and **4** can be explained as follows. On the analogy of the acylation of ureas, the first step of the reaction is assumed to be the acylation of the carbonyl oxygen with either of the reagents; however, stabilization of the *O*-acyl intermediate takes place in different ways: in the case of **1** an $O \rightarrow N$ acyl migration occurs, whereas with **2**, having a larger space requirement, the process is oxygen chlorine exchange by disproportionation. It must be noted that in the case of **1** there is no reason why to exclude the possibility of direct acylation at the urea nitro-

gen. Unfortunately, the same product (**3**) is formed in either reaction path, owing to the equivalence of the nitrogen atoms.

It was expected that a study of the reactions of a series of asymmetrically disubstituted ureas with amide chlorides would yield further data to substantiate one or the other of the reaction paths outlined above.

According to the working hypothesis, if there is a sufficiently large difference between the basicities of the urea nitrogens, the formation of a homogeneous product can be expected, whose structure is unambiguously dependent on whether *O*- or *N*-acylation has first occurred. (The basicity of the nitrogens in ureas can be compared by the pK_a values of the corresponding amines, as shown by MUKAIYAMA in a kinetic examination of the thermal dissociation of ureas in solution [2]). Our concept is illustrated by the reaction equations below. (In the formulas, an arrow pointing to the nitrogen atom represents the electron donating character of R_1, while an arrow of opposite direction denotes the electron-withdrawing nature of R_2.)

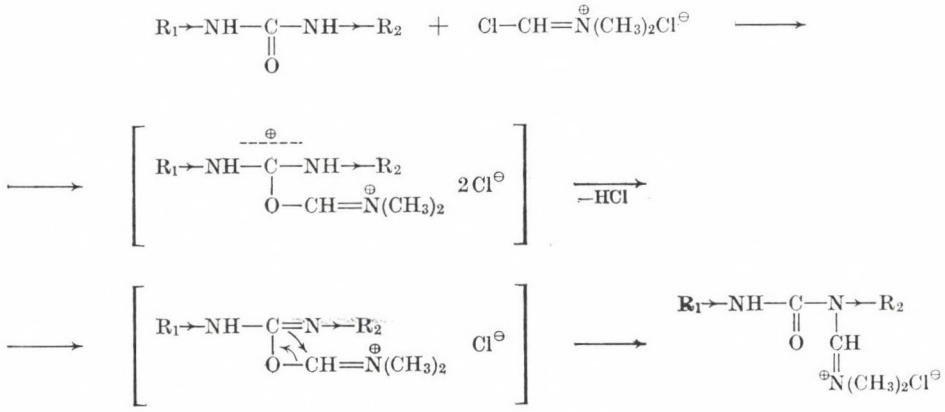

3

Reaction path with *O*-acylation (I)

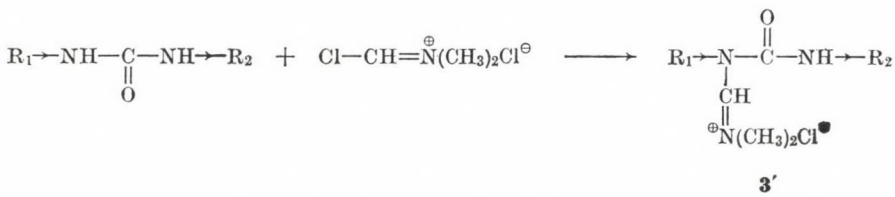

3′

Reaction path with *N*-acylation (II)

On the basis of the two reaction paths it can be concluded that the relative basicity of the nitrogen atoms is of importance, since this will determine the direction of the stabilization of the immonium salt intermediate,

i.e. the direction of the $O \rightarrow N$ acyl migration in the case of *O*-acylation, or the site and result of direct nucleophilic attack in the *N*-acylation reaction path.

The above two reaction paths yielding the different isomers **3** and **3'**, should, of course, be regarded as limiting cases, which have reality only if there is a significant difference between the pK_a values. When these are in the same order of magnitude, certainly an isomeric mixture is obtained, irrespective of the mechanism of formation.

The urea-amide chloride reactions were effected with three groups of asymmetric derivatives:

(a) *N*-phenyl-*N'*-methylurea, *N*-phenyl-*N'*-butylurea, *N*-phenyl-*N'*-cyclohexylurea, *N*-4-nitrophenyl-*N'*-cyclohexylurea;

(b) *N*-phenyl-*N'*-4-chlorophenylurea, *N*-phenyl-*N'*-3,4-dichlorophenylurea, *N*-phenyl-4-tolylurea, *N*-phenyl-4-anisylurea, *N*-4-tolyl-*N'*-3,4-dichlorophenylurea, *N*-phenyl-*N'*-4-nitrophenylurea;

(c) *N*-2-pyridyl-*N'*-phenylurea, *N*-2-pyridyl-*N'*-4'-chlorophenylurea, *N*-2-pyridyl-*N'*-butylurea.

The reagents were allowed to react in equimolar ratio in anhydrous chloroform at 25 °C. After cautious evaporation of the solvent viscous substances were obtained in the case of ureas in groups *(a)* and *(b)* these were purified by washing with ether, but none of them could be crystallized. The accomplishment of the reaction was checked by the determination of the chloride ion content of the product, and by its IR spectrum recorded in chloroform. Two intense bands, characteristic of the carbamoylamidinium structure, could always be found at 1710—1740 cm^{-1} and 1670—1690 cm^{-1} in the spectra. These data and PMR spectroscopy did not yet reveal whether the products had structure **3** or **3'**, and whether they were uniform or a mixture of isomers. Therefore a chemical method of identification was needed. Earlier it was found that compounds of type **3** gave unambiguously isocyanate and *N*-aryl-*N'N'*-dimethylformamidinium chloride on thermal decomposition. This reaction seemed to be suitable for the solution of the problem, since formamidinium chlorides are very stable and their identification makes possible drawing conclusions regarding structure **3** or **3'**.

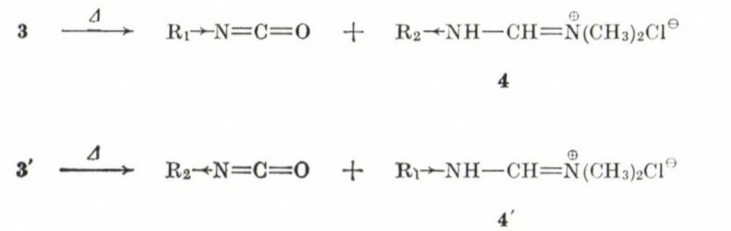

Table I

Thermal decomposition of carbamoylamidinum chlorides

3	$R_1NHCONHR$		pK_a		$R—NH—CH=^+N(CH_3)_2Cl^-$			M.p., °C	Cl⁻, %	
	R_1	R_2	R_1NH_2	R_2NH_2	I*	II*	Formed		calcd.	Found
a	CH_3	C_6H_5	10.64	4.58	C_6H_5	CH_3	C_6H_5	228—230	19.20	19.15
b	C_4H_9	C_6H_5	10.61	4.58	C_6H_5	C_4H_9	C_6H_5	227—230	19.20	19.22
c	4-CH_3—C_6H_4	3,4-Cl_2—C_6H_3	5.10	3.25	3,4-Cl—C_6H_3	4-CH_3—C_6H_4	3,4-Cl_2—C_6H_3	242—246	14.00	14.10
d	C_6H_5	4-NO_2—C_6H_4	4.58	2.04	4-NO_2—C_6H_4	C_6H_5	4-NO_2—C_6H_4	265—268	15.50	15.50
e	C_6H_{11}	C_6H_5	10.68	4.58	C_6H_5	C_6H_{11}	C_6H_5	230—231	19.20	19.10
f	C_6H_5	4-Cl—C_6H_4	4.58	3.9	4-Cl—C_6H_4	C_6H_5	C_6H_5 + 4-Cl—C_6H_4	196—204	19.20 16.20	18.90
g	C_6H_5	3,4-Cl_2—C_6H_3	4.58	3.25	3,4-Cl_2—C_6H_3	C_6H_5	3,4-Cl_2—C_6H_3 + C_6H_5	214—219	19.20 14.0	16.2
h	C_6H_{11}	4-NO_2—C_6H_4	10.68	2.04	4-NO_2—C_6H_4	C_6H_{11}	4-NO_2—C_6H_4	262—265	15.60	15.50
i	4-CH_3—C_6H_4	C_6H_5	5.10	4.58	C_6H_5	4-CH_3—C_6H_4	4-CH_3—C_6H_4 + C_6H_5	210—220	17.90 19.20	18.1
j	4-CH_3O—C_6H_4	C_6H_5	5.31	4.58	C_6H_5	4-CH_3O—C_6H_4	4 · CH_3O—C_6H_4 + C_6H_5	200—202	16.50 19.20	17.0
k	2-CH_3—C_6H_4	C_6H_5	4.39	4.58	mixture	C_6H_5		204—208	19.2	19.2

* I and II represent the products expected on the basis of the two different mechanisms

Thermal decomposition of the carbamoylamidinium chlorides was effected in tetrachloroethane at reflux temperature (140 °C). The course of the reaction was followed by the IR spectrum of the solution observing the intense absorption of the isocyanate formed at 2260—2270 cm^{-1}. It was found that the *N,N'*-diaryl derivatives completely decomposed on refluxing for 20—30 min, while the *N*-aryl-*N'*-alkyl compounds required a reflux time of several hours to achieve complete decomposition. After the accomplishment of the reaction, the solvent was evaporated in vacuum and the trisubstituted formamidinium chlorides were crystallized from the residue with acetone. They were identified by determination of their Cl^- content and by comparison (m.p., IR) with authentic samples prepared from the corresponding amine and chloromethylenedimethylammonium chloride.

The results are summarized in Table I.

As readily seen from the Table, in the cases where the difference in the *K*- values of the N_1 and N_2 atoms exceeded two orders of magnitude, the products expected on the basis of the *O*-acylation mechanism were formed. In the case of compounds **3f, 3g, 3i,** and **3j,** this difference was between 0.5 and 1.3; here a mixture of amidinium chlorides was obtained, which is not in contradiction with either of the mechanisms assumed, although the mixture ratios calculated on the basis of the Cl^- content rather support *N*-acylation (Table II). The behaviour of the *o*-tolyl derivative is remarkable: here the pK_a values are practically the same, yet the product is not a mixture but a homogeneous compound acylated at the nitrogen atom adjacent to the phenyl group. This can be explained by the strong steric hindrance of the *ortho* methyl group.

Table II

Composition of mixtures of N-aryl-N,N'-dimethylformamidinium chlorides

No.	Cl^-, %	Calculated ratio in the mixture, %	
		I	II
3f	18.9	4-Cl—C_6H_4NH—CH=$\overset{+}{N}(CH_3)_2Cl^-$ 10%	C_6H_5NH—CH=$\overset{+}{N}(CH_3)_2Cl^-$ 90%
3g	16.2	3,4-$Cl_2C_6H_3NH$—CH=$\overset{+}{N}(CH_3)_2Cl^-$ 58%	C_6H_5NH—CH=$\overset{+}{N}(CH_3)_2Cl^-$ 42%
3i	18.1	$C_6H_5NHCH=\overset{+}{N}(CH_3)Cl_2^-$ 15%	4-CH_3—$C_6H_4CH=\overset{+}{N}(CH_3)_2Cl^-$ 85%
3j	17.0	C_6H_5NH—CH=$\overset{+}{N}(CH_3)_2Cl^-$ 18%	4-CH_3O—$C_6H_4CH=\overset{+}{N}(CH_3)_2Cl^-$ 82%

On the basis of the results of thermal decomposition, the predominating character of the *O*-acylation mechanism could be advocated — without excluding direct *N*-acylation — if it were sure that no rearrangement can occur under the vigorous conditions (140 °C) used. In order to decide this problem, the identification of the primary product of the urea amide chloride reaction had to be attempted. Earlier it was reported that the solvolysis of the crystalline carbamoylamidinium chlorides prepared by the amide chloride reaction of symmetric diarylureas yielded the starting diarylureas [1]. It was assumed that there may be a possibility for the splitting of the C=N$^+$ bond without the cleavage of the C—N bond, depending on the strength of the bonds which can be attacked hydrolytically, and on the conditions of the hydrolysis.

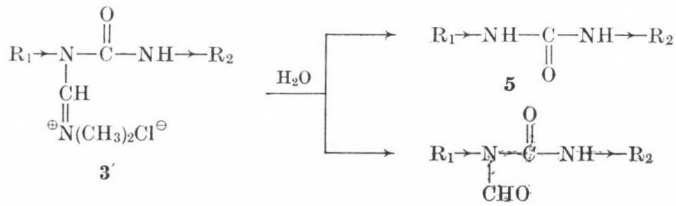

3′ **5** **6**

When the products were treated with alcohol at ambient or reflux temperatures the starting ureas (**5**) were recovered in each case, but when the hydrolysis was effected with water under mild conditions, in some cases the *N*-formylurea of type **6** could be prepared. The two sharp CO bands in the IR spectra (between 1730 and 1680 cm^{-1}) and the CHN analysis data did not yet allow decision which of the N-atoms was carrying the formyl group; therefore, identification was achieved by comparison with authentic samples prepared in an independent way. These were made from the appropriate isocyanates and formanilides by refluxing them in anhydrous toluene.

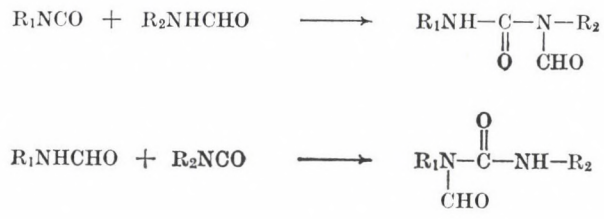

Thus in the case of compounds **3f, 3i** and **3j** it could be established that the formyl group, and consequently the primary dimethylaminomethlyene group, were attached to the more basic nitrogen atom.

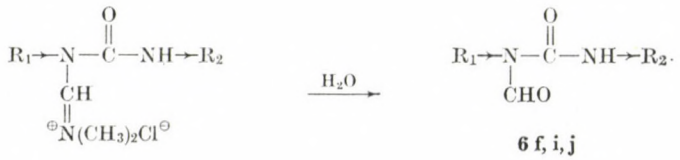

3′ 6 f, i, j

f $R_1 = C_6H_5$, $R_2 = 4\text{-Cl—}C_6H_4$

i $R_1 = 4\text{-}CH_3\text{—}C_6H_4$, $R_2 = C_6H_5$

j $R_1 = 4\text{-}CH_3O\text{—}C_6H_4$, $R_2 = C_6H_5$

k $R_1 = 2\text{-}CH_3\text{—}C_6H_4$, $R_2 = C_6H_5$

Compounds **6** prepared were not entirely homogeneous; they contained 10—20% of the other isomer, as shown by the data in Table II. In the methyl- and methoxy-containing ureas if compounds **3** and the hydrolysis products **6** were mixtures of isomers, this was indicated by the PMR spectra. On the basis of the integrated signal, the approximate ratio of the isomers could also be calculated (Table III).

Table III

PMR data of carbamoylamidinium chlorides and their hydrolysis products in $CDCl_3$ solution ($\delta_{TMS} = 0$)

	3		6	
δ	$N(CH_3)_2$	CH_3 or CH_3O	CH_3	CH_3O
f	2.60; 3.50			
i	2.65; 3.53	2.27; 2.38 25%/75%	2.30; 2.40 20%/80%	
j	2.67; 3.56	3.75; 3.80 15%/85%		3.78; 3.83 19%/81%
k	2.55; 3.45	2.12	2.25	

The spectra were recorded in $CDCl_3$ using TMS as internal standard; the values are given in δ units.

The distant doublet of the $N(CH_3)_2$ group is insensitive to the presence isomers, but the methyl and methoxy groups produce two singlets, and the isomeric ratio calculated on this basis is in accordance with the composition of the mixture calculated from the Cl^- content of the formamidinium chlorides.

Unfortunately, in the case of **3a**, **3b** and **3c**, gentle hydrolysis remained unsuccessful, and ureas **5** could be isolated on heating. Compounds **3d** and **3h** suffered hydrolysis immediately after dissolution in water, however, here again only ureas **5** were formed.

This evidence points to the *N*-acylation mechanism, but it is not sufficient alone; therefore, further possibilities were tried to support this concept: the decomposition of compounds of type **3** was examined on the effect of triethylamine.

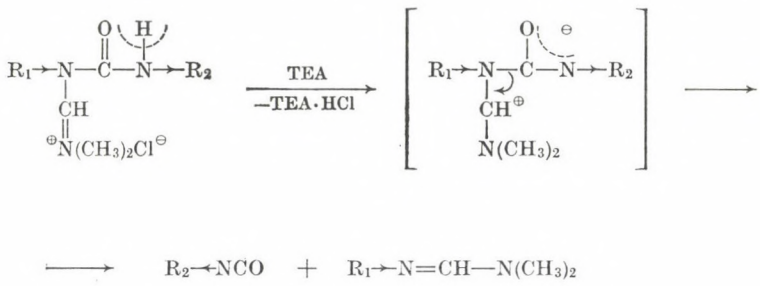

$$\longrightarrow \quad R_2{-}NCO \; + \; R_1{-}N{=}CH{-}N(CH_3)_2$$

In the case of compounds **3c**, **3d**, **3f**, **3g**, **3h**, **3i** and **3j**, the decomposition took place already at room temperature. The resulting isocyanate in the reaction mixture was allowed to react with aniline and thus identified in the form of urea. In this way, it could be established that in all cases the isocyanate containing the less nucleophilic nitrogen atom had been formed on disproportionation with triethylamine, which yielded further evidence for the direct *N*-acylation (Table IV).

Table IV

Decomposition of carbamoylamidinium chlorides with triethylamine

No.	R_1	R_2	$R{-}NH{-}\underset{\underset{O}{\|}}{C}{-}NHC_6H_5$	M.p., °C	Notes
3'c	$4\text{-}CH_3{-}C_6H_4$	$3,4\text{-}Cl_2{-}C_6H_3$	$3,4\text{-}Cl_2{-}C_6H_3$	214—217	
3'd	C_6H_5	$4\text{-}NO_2{-}C_6H_4$	$4\text{-}NO_2{-}C_6H_4$	204—207	
3'f	C_6H_5	$4\text{-}Cl{-}C_6H_4$	$4\text{-}Cl{-}C_6H_4$	237—240	Little $C_6H_5NHCONHC_6H_5$
3'g	C_6H_5	$3,4\text{-}Cl_2{-}C_6H_3$	$3,4\text{-}Cl_2C_6H_3$	215—218	
3'h	C_6H_{11}	$4\text{-}NO_2{-}C_6H_4$	$4\text{-}NO_2{-}C_6H_4$	203—205	
3'i	$4\text{-}CH_3{-}C_6H_4$	C_6H_5	C_6H_5	236—238	Little $C_6H_5NHCONH$ $4\text{-}CH_3C_6H_4$
3'j	$4\text{-}CH_3O{-}C_6H_4$	C_6H_5	C_6H_5	236—239	Little $C_6H_5NHCONH$ $4CH_3OC_6H_4$

Now an explanation was sought for the appearance of such decomposition products on thermal decomposition of compounds of type **3'** which were contradictory to the *N*-acylation mechanism (II). The following working hypothesis was constructed: in the primary reaction, the amide chloride attacks at the more basic N-atom, and the resulting carbamoylamidinium chloride can undergo dissociation on the effect of heat in two ways. According to the first, the expected splitting of the tertiary $-\overset{|}{\underset{|}{N}}-C=O$ bond takes place with the formation of the trisubstituted amidinium chloride containing the electron donating group and the isocyanate carrying an electron-withdrawing substituent; these two compounds react then with each other at the temperature of the decomposition (140 °C), whereupon the two groups mentioned are interchanged (Pathway A).

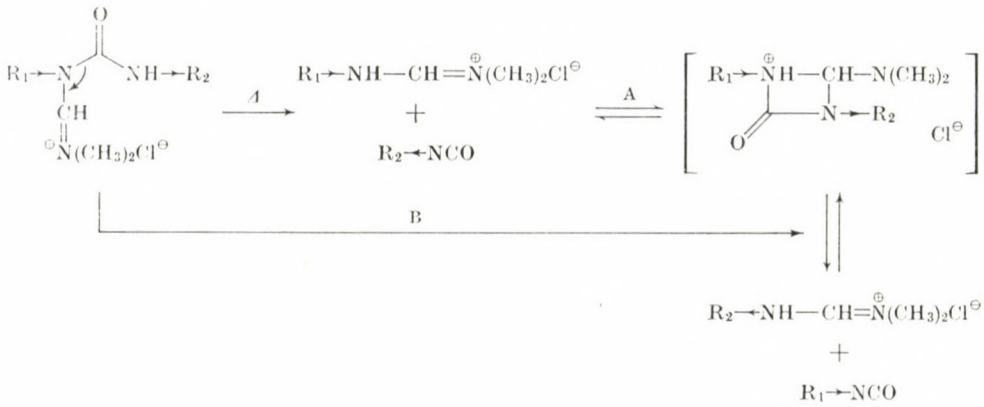

According to Pathway B assumed, the exchange of groups is preceded by an intramolecular rearrangement through an urethidinone ring. As a piece of evidence for this, one experiment is mentioned here, which was effected with 3,4-dichlorophenyl isocyanate and *N*-4-tolyl-*N'*-dimethylformamidinium chloride at reflux temperature in tetrachloroethane. The exchange of the groups in question certainly took place. This reaction will be discussed in detail in a following paper; here any suggestion about even the mechanism is omitted. However, the result of the experiment supports the concept that the reactions of ureas with amide chlorides take place not by *O*-, but by *N*-acylation mechanism.

Finally, a strange but unambiguous reaction is to be reported, which takes place between ureas belonging to group *(c)* and chloromethylenedimethyl-ammonium chloride. The reaction was carried out as described above, and in each case a white crystalline substance separated in a short time which, on the basis of the Cl^- content and comparison with samples prepared in another way, proved to be *N*-2-pyridylium-*N'*, *N'*-dimethylformamidinium di-

chloride (**8**). Thus the reaction yielded a product independent of the nature of R_2, being a good example for the case how the N-2 atom in the pyridine ring can direct the attack of the electrophilic reagent.

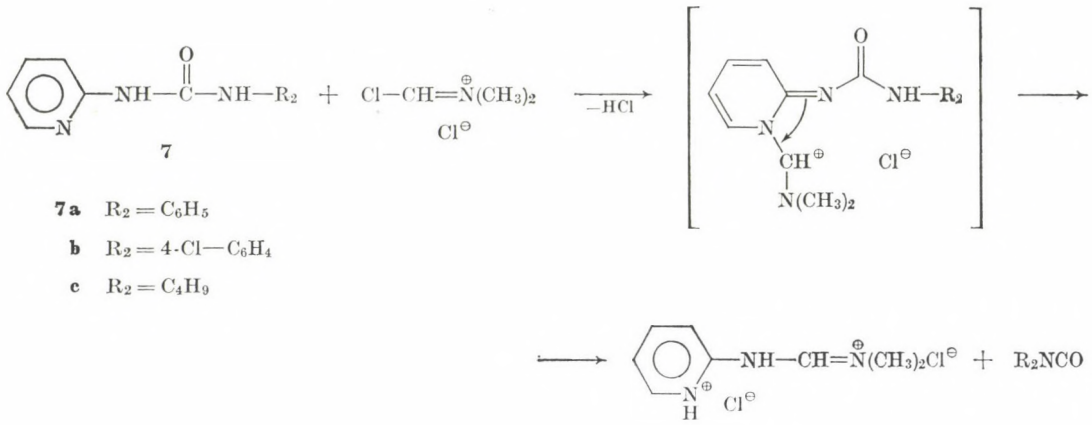

7a $R_2 = C_6H_5$

b $R_2 = 4\text{-Cl}—C_6H_4$

c $R_2 = C_4H_9$

8

The site of the primary reaction is the most basic N atom, the nitrogen in the pyridine ring; the resulting very reactive immonium salt effects then the intramolecular acylation of the neighbouring acyl nitrogen. The presence of the protonated pyridine ring gives rise to spontaneous splitting of the adjacent N—CO bond even at room temperature, thus **8** is formed. Such a directing action of the pyridine ring has been described in the chlorosulfonation of *N*-phenyl-*N*'-2-pyridylureas [3].

Experimental

1. Ureas were prepared according to the following general procedure;

The amine (0.1 mole) in anhydrous benzene (50 ml) was mixed with the isocyanate (0.1 mole) in benzene (50 ml) added dropwise. The reaction mixture was allowed to stand for 1 day, the crystalline substance which separated was filtered off, washed with benzene and dried

1.1	*N*-phenyl-*N*'-methylurea	m.p.	150—151 °C;	*lit.* m.p.	150 °C
1.2	*N*-phenyl-*N*'-butylurea		129—130 °C	,,	130 °C
1.3	*N*-3,4-dichlorophenyl-*N*'-4'-tolylurea		258—260 °C		
1.4	*N*-phenyl-*N*'-nitrophenylurea		205—208 °C	,,	209 °C
1.5	*N*-phenyl-*N*'-cyclohexylurea		162—165 °C		
1.6	*N*-phenyl-*N*'-4-chlorophenylurea		240—243 °C		
1.7	*N*-phenyl-*N*'-3,4-dichlorophenylurea		215—217 °C		
1.8	*N*-cyclohexyl-*N*'-4-nitrophenylurea		163—168 °C		
1.9	*N*-phenyl-*N*'-4-tolylurea		216 °C		
1.10	*N*-phenyl-*N*'-4-anisylurea		193—194 °C		
1.11	*N*-phenyl-*N*'-*o*-tolylurea		199—200 °C		
1.12	*N*-phenyl-*N*'-2'-pyridylurea		180—181 °C		
1.13	*N*-4-chlorophenyl-*N*'-2'-pyridylurea		203—204 °C		
1.14	*N*-butyl-*N*'-2'-pyridylurea		82—84 °C		

2. The reaction of ureas and chloromethylenedimethylammonium chloride was effected in all cases with the same quantities under identical conditions: the latter reagent was prepared from DMF and phosgene "*in situ*", as follows.

A solution of dimethylformamide (1.53 g; 0.021 mole) in chloroform was added dropwise to a 0.5 mole/litre solution of phosgene in chloroform (40 ml), under cooling in ice; the urea (0.02 mole) was then added and the mixture was stirred at 25 °C for 1 h. The solvent was evaporated in vacuum, the residue washed with anhydrous ether and dried over NaOH in a vacuum desiccator.

Characteristic data of the carbamoylamidinium chlorides (**3**) are the following:

3a Calcd. Cl^- 14.69. Found Cl^- 14.85%.
IR ($CHCl_3$): νCO 1725 cm^{-1}; $\nu C{=}\overset{+}{N}$ 1680 cm^{-1}.
3b Calcd. Cl^- 12.52. Found Cl^- 12.90%.
IR ($CHCl_3$) 1725 (νCO); 1680 cm^{-1} ($\nu C{=}\overset{+}{N}$).
3c Calcd. Cl^- 9.18. Found Cl^- 9.72%.
IR ($CHCl_3$): 1725 (νCO); 1680 cm^{-1} ($\nu C{=}\overset{+}{N}$).
3d Calcd. Cl^- 10.18. Found Cl^- 10.60%
IR ($CHCl_3$): 1725 (νCO); 1675 cm^{-1} ($\nu CO{=}\overset{+}{N}$).
3e Calcd. Cl^- 11.47. Found Cl^- 12.10%.
IR ($CHCl_3$): 1720 (νCO); 1675 cm^{-1} ($\nu C{=}\overset{+}{N}$).
3f Calcd. Cl^- 10.50. Found Cl^- 10.85%.
IR ($CHCl_3$): 1730 (νCO); 1680 cm^{-1} ($\nu C{=}\overset{+}{N}$).

3. Thermal decomposition of carbamoylamidinium chlorides

Compound **3** (0.01 mole) was refluxed in anhydrous tetrachloroethane (20 ml) until the ν-N=C=O band of isocyanat appearing at 2260 cm^{-1} in the IR spectrum remained unchanged in the samples taken. The reaction mixture was then cooled, the solvent evaporated in vacuum and the residue crystallized from acetone. The yields calculated for the mixtures and obtained for the homogeneous substances exceeded 90%. TLC of the acetone mother liquor indicated the presence of some diarylurea contaminants and the spot of the amidine salt was observed near the start line.

Data of the *N*-aryl-*N*',*N*'-dimethylformamidinium chlorides obtained in this way are shown in Table I.

The IR spectra were compared with authentic spectra; the samples were prepared from the amide chloride solution described in Section 2 and from the appropriate aromatic amine.

In the IR spectra the amidinium $C{=}\overset{+}{N}$ band appears at 1690—1710 cm^{-1} in all cases.

4. Hydrolysis of carbamoylamidinium chlorides

Compound **3** (0.01 mole) was stirred with water (30 ml) at room temperature for 1 h. A white, fluffy precipitate separated, this was filtered off, washed with water and dried.

***N*-formyl-*N*-phenyl-*N*'-4-chlorophenylurea (6f)** from **3f** M.p. 108—110 °C (about 10% **6'f** isomer). M.p. of the authentic sample; 120 °C.

$C_{14}H_{11}ClN_2O_2$ (274.5). Calcd. C 61.20; H 4.00; N 10.20. Found C 61.25; H 4.05; N 10.22%.
IR (KBr): 3180 (νNH); 1730, 1690, cm^{-1} (νCO).
PMR ($CDCl_3$): δ 7.12—7.54 m (9H,ArH); 8.75 s (1H;CH).

***N*-formyl-*N*-4-tolyl-*N*'-phenylurea (6i)** from **3i**

M.p. 102—103 °C (about 20% **6'i** isomer). M.p. of the authentic sample: 109—110 °C.
$C_{15}H_{14}N_2O_2$ (254.02). Calcd. C 70.86; H 5.51; N 11.02. Found C 70.21; H 5.69; N 11.12%.
IR (KBr): 3320 (νNH); 1690, 1710 cm^{-1} (νCO).
PMR ($CDCl_3$): δ 7.04—7.52 m (9H;ArH); 8.8 s (1H,CH); 2.30 s (20%), 2.40 s (80%) (CH_3).

***N*-formyl-*N*-4-anisyl-*N*'-phenylurea (6j)** from **3j**

M.p. 90 °C (about 19% **6'j** isomer). M.p. of the authentic sample 101—102 °C.
$C_{15}H_{14}N_2O_3$ (270). Calcd. C 66.66; H 5.18; N 10.37. Found C 66.25; H 5.23; N 10.51%.
IR (KBr): 3260 (νNH); 1695, 1710 cm^{-1} (νCO).
PMR ($CDCl_3$): δ 6.9—7.46 m (9H,ArH); 8.86 s (1H,CH); 3.78 s (19%), 3.83 s (81%) (CH_3O.).

***N*-formyl-*N*-phenyl-*N'*-2-tolylurea (6k) from 3k**

M.p. 74—75 °C; m.p. of the authentic sample 76—78 °C.
$C_{15}H_{14}N_2O_2$ (254). Calcd. C 70.86; H 5.51; N 11.02. Found C 70.65; H 5.65; N 10.77%.
IR (KBr): 3220 (νNH); 1730, 1690 cm^{-1} (νCO).
PMR ($CDCl_3$): δ 7.0—7.57 m (9H,ArH); 8.6 s (1H,CH); 2.25 s (3H,CH_3).

Preparation of the authentic *N*-formylurea samples

Formanilide (0.01 mole) and the aryl isocyanate (0.01 mole) were refluxed in anhydrous toluene (20 ml) for 3 h. The solvent was evaporated in vacuum and the residue crystallized from alcohol.

Both possible *N*-formylureas were prepared by this method.

5. Decomposition of carbamoyl amidinium chlorides with triethylamine

Compound **3** (0.01 mole) in anhydrous chloroform (20 ml) and triethylamine (0.015 mole) were allowed to stand at room temperature for 0.5 h. Aniline (0.01 mole) was then added and, after standing for 2 h, the solvent was evaporated in vacuum and the residue crystallized from alcohol. The urea formed was identified on the basis of the m.p. and IR spectrum (Table IV).

REFERENCES

[1] Csürös, Z., Soós, R., Bitter, I., Kárpáti-Ádám, É.: Acta Chim. Acad. Sci. Hung., **73,** 239 (1972)
[2] Mukaiyama, T., Ozaki, S., Hoshino, T.: Bull. Chem. Soc. Japan, **27,** 578 (1954)
[3] Badani, N. V., Cramlyn, R. J. W., Swinbourne, F. J.: Austr. J. Chem., **30,** 1793 (1977)

István Bitter
Éva Kárpáti-Ádám
László Tőke
H-1521 Budapest, Műegyetem

Acta Chimica Academiae Scientiarum Hungaricae, Tomus 102 (3), pp. 247—257 (1979)

PREPARATION AND INVESTIGATION OF THE PHOSPHOROUSORGANIC DERIVATIVES OF TRANSITION METAL CYANO COMPLEXES, VIII

^{1}H-NMR INVESTIGATION OF THE ION ASSOCIATION OF HEXACYANOFERRATE(III) ANION WITH QUATERNARY PHOSPHONIUM CATIONS

S. PAPP and P. KVINTOVICS

(Department of General and Inorganic Chemistry, University of Chemical Industry, Veszprém)

Received May 18, 1978
Accepted for publication December 13, 1978

The derivatives of hexacyanoferrate(III) anion formed with quaternary phosphonium cations have been prepared, and their ^{1}H-NMR spectra have been recorded in $CDCl_3$ and D_6-DMSO. On the basis of the spectra the nature and mechanism of the interactions between the anion and cation in solution have been discussed.

Introduction

In contrast with previous assumptions, paramagnetic compounds, with some exceptions, give rise to acceptable NMR spectra [1, 2, 3]. These spectra and the measured chemical shifts permit conclusions to be drawn on the structure of complexes and the distribution of unpaired electrons.

For the interpretation of the nucleus-electron interactions in transition metal complexes containing unpaired electrons, several mechanisms have been proposed. They can be divided into two main groups, which both may cause signal shifts.

The contact (Fermi) interaction is an interaction between the nucleus and the electron density of the unpaired electrons (spin density) at the site of the nucleus [4]. The spin density at the resonating nucleus, or more generally on the ligand, may change in many ways [5]. Depending on the symmetry of the orbital involved in electron delocalization, the basic types of σ- and π-delocalization mechanisms can be distinguished [6, 7].

The shift due to the pseudo-contact or dipole interaction arises from a direct magnetic dipole-dipole interaction between the spins of the unpaired electrons and the resonating nuclei [5, 3]. The actual form of the relationship which describes the pseudo-contact shift is determined by the magnitudes of the correlation time of the molecular rotation (τ_c), the electron spin — lattice relaxation time (T_{1e}) and the Landé g factor [7, 8]. When $T_{1e} \ll \tau_c$, the equation

can be given [7, 9] as

$$\frac{\Delta\nu_i}{\nu} = -\frac{\beta^2 S(S+1)}{45\,kT}(3g_{\parallel} + 4g_{\perp})(g_{\parallel} - g_{\perp})\frac{3\cos^2\Theta_i - 1}{R_i^3} \qquad (1)$$

where β is the Bohr magneton,

S is the resultant spin,
k is the Boltzmann constant,
T is absolute temperature,
$g_{\parallel}$ and $g_{\perp}$ are the components of the g tensor parallel with or perpendicular to the main axis of the molecule,
R_i is the distance between the paramagnetic central nucleus and the ith proton, and
Θ_i is the angle between the main axis of the molecule and the vector R_i.

A simplified form of the equation is

$$\frac{\Delta\nu_i}{\nu} = F(g_{\parallel}, g_{\perp})\,[\text{G. F.}] \qquad (2)$$

where the "geometric factor", G. F., is

$$[\text{G. F.}] = (3\cos^2\Theta_i - 1)\,R_i^{-3} \qquad (3)$$

The shifts due to the above two mechanisms can be separated by various methods [7, 3], but their application gives satisfactory results in relatively few cases.

Although it has been known for a time that shifts can be observed in the NMR spectra of diamagnetic cations if their solution contains paramagnetic anion [10, 11, 12], this method was utilized only recently for the investigation of ion associations. These investigations had to explain why only one signal (or signal group) can be assigned to the equivalent proton groups, *i.e.* the protons in dia- and paramagnetic environments do not separate [13, 14], and it was also necessary to answer the problem whether the ion pairs are subjected to both types of interaction, or to the pseudo-contact interaction only [13, 5]. The results have shown that a weak covalent interaction also occurs between the cation and anion of the ion pair. The two components of the shift are, however, very complicated to determine for the case of ion pairs [15, 16, 17].

The measured shifts can be used to draw conclusions on the geometry of the ion associate [14, 18, 19, 20, 15, 21], and to determine association constants

[18, 22, 23, 24]. It is to be noted that the calculation of the latter is very complicated, and in many cases, when the association of ions with unequal charges are investigated, the results are unsatisfactory [18, 23, 24].

Results

The preparation and analysis of the complexes were described in one of our previous papers [25]. The present paper deals with the ^{1}H—NMR investigation of the following compounds:

$$[(C_4H_9)_3PCH_3]_3[Fe(CN)_6] \equiv M_3^1[Fe(CN)_6]$$
$$[C_4H_9)_4P]_3[Fe(CN)_6] \equiv M_3^2[Fe(CN)_6]$$
$$[(C_4H_9)_3PCH_2CHCH_2]_3[Fe(CN)_6] \equiv M_3^3[Fe(CN)_6]$$
$$[(C_4H_9)_3PCH_2C_6H_5]_3[Fe(CN)_6] \equiv M_3^4[Fe(CN)_6]$$
$$[(C_6H_5)_3PCH_2C_6H_5]_3[Fe(CN)_6] \equiv M_3^5[Fe(CN)_6]$$
$$[(C_6H_5)_4P]_3[Fe(CN)_6] \equiv M_3^6[Fe(CN)_6]$$

The spectra of the complexes were measured at 32 °C in two solvents ($CDCl_3$ and D_6-DMSO), at various concentrations, on a Varian-T 60 instrument. The concentration range was determined by the evaluability of the spectrum, *i.e.* by the solubility of the complex. The above solvents have substantially different donicities, enabling the association conditions in the solution to be investigated over a wide range.

The chemical shifts of the resonance signals were related to the spectrum of the same cation in the same solvent in diamagnetic environment. (In the presence of diamagnetic anion, *i.e.* halides or $[Co(CN)_6]^{3-}$, the resonance frequencies of the cation protons were found to be concentration independent.) The signals of the various proton groups were assigned on the basis of intensities and literature data. The multiplet line systems were resolved by spectrum analysis using coupling constants.

It is known that unpaired electrons cause line broadening. With the complexes studied, the extent of broadening was relatively small, in accord with the experimental results of other authors [26, 27] obtained on the complexes containing iron(III) central atoms of low spin number. Since for all line groups the shift was calculated from the most prominent, characteristic line, the deviation of shift differences was ± 4 Hz.

For the various solvents and proton types the shift differences ($\Delta\nu_i$) measured in the solutions of the complexes with different concentrations (Raoult) are given in Table I.

Table I

Concentration dependence of shift differences ($\Delta\nu_i$) in $[R_3PR']_3[Fe(CN)_6]$ complexes

Cation	Solvent	Concentration $C_R \cdot 10^2$	$\Delta\nu_i$ (Hz)				
			C_1	C_2-C_3	C_4	C_0	
M_1 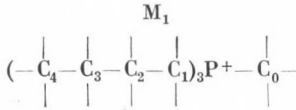	$CDCl_3$	0.65	44	14	12	42	
		6.5	70	28	27	62	
		13.0	84	42	39	74	
	D_6-DMSO	0.82	10	4	2	10	
		8.5	26	16	16	20	
		16.5	42	30	30	32	
			C_1	C_2-C_3	C_4		
M_2 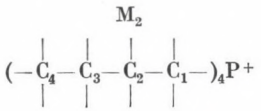	$CDCl_3$	0.65	44	16	12		
		6.4	55	24	20		
		12.7	72	41	38		
	D_6-DMSO	0.82	10	10	7		
		8.1	22	20	17		
		16.2	36	30	29		
			C_1	C_2-C_3	C_4	C_0	H_A
M_3 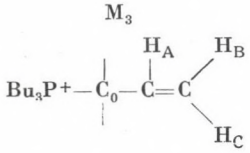	$CDCl_3$	0.65	42	14	9	86	12
		6.5	62	28	24	102	24
		13.0	78	42	38	118	38
	D_6-DMSO	0.82	9	8	6	16	6
		8.2	20	16	15	26	15
		16.4	32	23	23	40	23

Table I (continued)

M^4 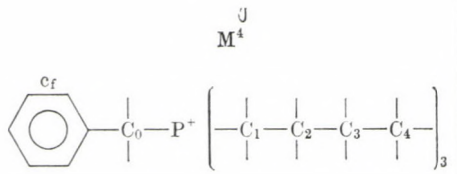	$CDCl_3$	0.65	50	12	12	74	10
		6.5	64	20	20	88	18
		13.0	84	38	38	106	35
	D_6-DMSO	0.81	8	4	4	15	6
		8.2	16	10	10	22	12
		16.4	26	20	20	34	20
			phenyl *p-m*	phenyl *o*	benzyl *m-p*	benzyl *o*	C_0
M^5 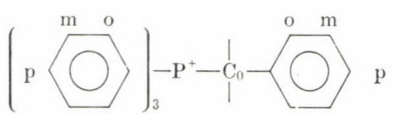	D_6-DMSO	0.4	4	4	1	4	14
		0.8	7	7	2	10	16
		4.0	12	12	6	14	20
			p-m	*o*			
M^6 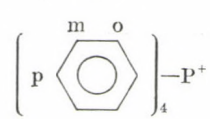	D_6-DMSO	0.79	2	4			
		7.8	14	16			
		15.7	24	26			

Discussion

In interpreting the chemical shifts, it appeared worth studying the changes in the shifts of certain characteristic proton groups upon the effect of different cations. Thus, the conclusions were drawn from the resonance frequencies of the protons for which the shift is large, or the corresponding line can be readily identified in the spectrum. For this purpose, the most appropriate protons were those attached to the C_1 or C_4 atoms of butyl chains, and to the fourth substitutent C_0 of the phosphorous atom. The chemical shift differences of these protons, measured in the two solvents at various concentrations, are shown in Figs 1, 2 and 3.

As the diagrams indicate, the shifts strongly vary with the concentration of the complexes, and they are positive in all cases. This is in agreement with the results of other authors on the same anion [18, 28, 4]. The occurrence of shift in itself already proves the existence of ion pairs, and to a first approximation it can be assumed that the shift is due completely to pseudo-contact interaction.

According to equation (1), the positive shift implies that $g_{\perp} > g_{||}$ for the $[Fe(CN)_6]^{3-}$ anion. The anisotropy of the g factor, which is unexpected on the basis of the symmetry of the anion, can be interpreted only by the arguments given by WALKER [29].

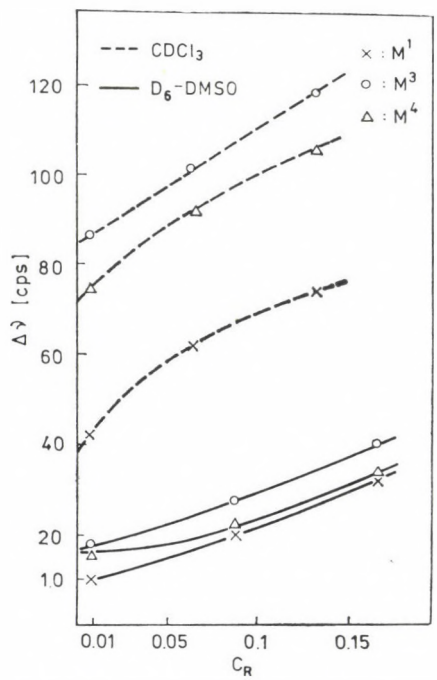

Fig. 1. Chemical shifts for the C_0 protons

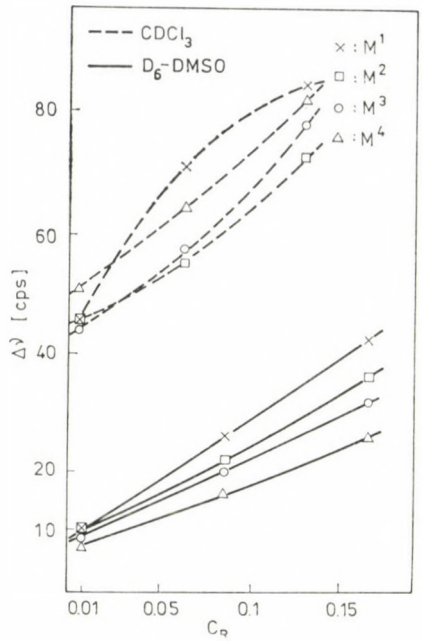

Fig. 2. Chemical shifts for the C_1 protons

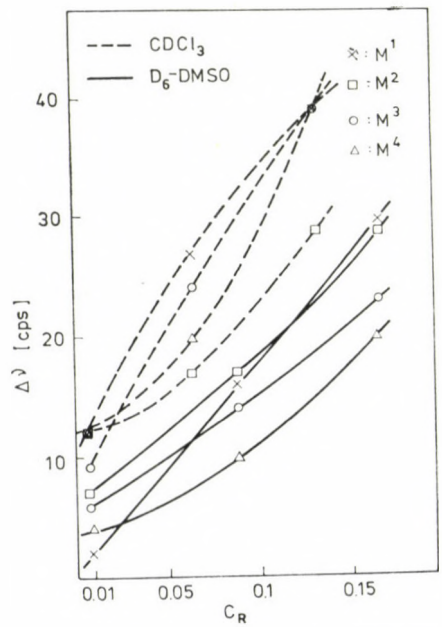

Fig. 3. Chemical shifts for the C_4 protons

Furthermore, it can be seen that the shifts are the largest for the C_0 and C_1 protons (*i.e.* for the protons closest to phosphorous, which have the most acidic character). The shifts of protons C_2—C_3 are about the half of the above, and that of C_4 is approximately the same.

It also surprising that the shifts of all proton groups are higher in $CDCl_3$ than in D_6-DMSO. This is most probably due to the different solvatation abilities of the two solvents. In $CDCl_3$ of low dielectric constant (and low donicity) the formation of ion pairs is much easier than in D_6-DMSO of relatively high dielectric constant (and donicity).

It is known that if only a pseudo-contact interaction occurs in an ion pair, the sequence of shifts *e.g.* on the protons of the butyl chain of quaternary ammonium cation is $\Delta\nu(C_1) > \Delta\nu(C_2) > \Delta\nu(C_3) > \Delta\nu(C_4)$ [13]. As in our case the sequence of shifts is different, another type of interaction can be assumed.

The chemical shift ratios for the four cations (containing butyl groups) studied here were calculated and normalized to the shift of the C_1 protons (Table II). These ratios also give the experimental ratios of the geometric factors [G.F.] for the ion pairs.

Comparison of the above data of tetrabutylphosphonium cation with the literature data obtained for tetrabutylammonium cation [13], taking into account that the C—P bond length is greater than the C—N bond length, indi-

Table II

The experimental [G.F.] *ratios*

Cation	$G_2 = \frac{\Delta\nu(C_2—C_3)}{\Delta\nu(C_1)}$		$G_3 = \frac{\Delta\nu(C_4)}{\Delta\nu(C_1)}$		$G_4 = \frac{\Delta\nu(C_0)}{\Delta\nu(C_1)}$	
	$CDCl_3$	D_6-DMSO	$CDCl_3$	D_6-DMSO	$CDCl_3$	D_6-DMSO
	0.32	0.40	0.27	0.29	0.96	1.00
M[1]	0.40	0.62	0.39	0.62	0.89	0.77
	0.50	0.71	0.46	0.71	0.86	0.75
	0.36	0.80	0.27	0.70		
M[2]	0.44	0.83	0.36	0.77	—	—
	0.57	0.89	0.53	0.81		
	0.33	0.78	0.21	0.67	2.05	1.78
M[3]	0.45	0.80	0.39	0.70	1.65	1.30
	0.54	0.83	0.49	0.73	1.51	1.25
	0.24	0.50	0.24	0.50	1.48	1.88
M[4]	0.31	0.63	0.31	0.63	1.37	1.39
	0.45	0.77	0.45	0.77	1.26	1.31

cated substantial differences between the data obtained in two ways, and no reasonable ion-pair distance could be found that would satisfy the experimental results. This implies that the measured shifts cannot be interpreted on the basis of pseudocontact interaction alone.

Consequently, it can be stated that the observed chemical shifts are caused by the net result of two types of interaction.

On the basis of Figs 1, 2 and 3, certain conclusions can also be drawn on the geometry of the ion pairs. The sequence of shifts for the C_0 protons is the same ($M^3 > M^4 > M^1$) in the two solvents, and it does not change when the differences are taken between the shifts measured in the two solvents. There

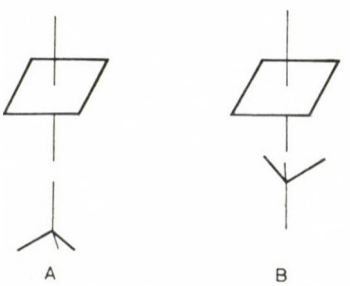

Fig. 4. Two possible "rigid" ion-pair models

may be two types of the relative orientations of the formally octahedral anion and the cation of C_{3v} symmetry, not taking into account that the cation may be attached to a peak, edge or face (Fig. 4).

If geometry "A" is correct then, owing to the pseudo-contact interaction, the shifts of the other protons of the group starting with C_0 should be even greater than that of the C_0 protons themselves. Since this is not the situation even for the allyl or benzyl group, it is probable that the ion pair geometry "B" is closer to the reality. The picture is not modified appreciably if certain contact effect causing opposite shift is taken into account, since *e.g.* in the case of σ delocalization the spin density decreases very rapidly from the central atom along the alkyl chain [16]. Therefore, it can be assumed that there is no spin density on C_4, and thus the shift of the protons attached is caused by the pseudo-contact interaction alone.

The extent of shift is substantially influenced by changes in the structures of ion pairs or aggregates formed in solution [23, 24]. In dilute solutions the formation of mainly 1 : 1 ion pairs and larger aggregates can also be assumed. It is also evident that in aggregates the extent and quality of interaction is not the same as in ion pairs. Investigations [23] have shown that when the magnitudes of chemical shifts of the individual proton groups vary with con-

centration but their ratios remain the same, this proves that the ion pair geometry is essentially concentration invariant.

In contrast, it can be seen from the data of Table II that in our case the ratios of shift change with concentration, which also implies that the extent and nature of interactions has changed. This explains why no method could be found for the separation of the shifts due to the two types of interaction, and why attempts to calculate association constant have also failed.

The mechanism of the electron delocalization causing the contact interaction is very difficult to find. In this respect there are theoretically two possibilities for the systems investigated. It cannot be ruled out that the unpaired electron on the d orbital on the central atom increases with the empty 4s or with an appropriately oriented 3d orbital of phosphorous. This change can be detected by Mössbauer spectroscopic measurements on frozen solutions. (Such investigations are in progress with samples enriched in ^{57}Fe.) The mechanism of delocalization can be detected in a different way if it affects the bonding properties of the CN ligand, and thus observable changes take place in the ν_{CN} vibrational frequencies. If the non-bonding d orbitals of iron(III) take part in the interaction, any change in the metal-cyanide back-coordination involves a change in the ν_{CN} frequency. If, on the other hand, an intermediate interaction takes place between the CN^- ligand and the cation, the CN^- group will occupy a bridge position, which also affects the ν_{CN} vibrational frequency (to an even higher extent).

In the infrared spectra of the $CDCl_3$ and D_6-DMSO solutions with various concentrations the bands of terminal CN groups appear at 2110 cm^{-1}. Other ν_{CN} bands also appear in the spectra at wavenumbers higher by 50—100 cm^{-1}, indicating the presence of bridging CN^- ions. Consequently, the delocalization proceeds very probably through an interaction between the cyanide ligands and the cation protons in the systems investigated. It is known from literature data [15] that an interaction of this type may produce a spin density sufficient to cause the contact interactions observed here.

REFERENCES

[1] Eaton, D. R., Phillips, W. D.: Advances in Magnetic Resonance 1. Academic Press, New York, 1965, p. 103
[2] Keller, H. J., Schwarzhans, K. E.: Angew. Chem., **82,** 227 (1970)
[3] Eaton, D. R., Zaw, K.: Coord. Chem. Rev., **7,** 197 (1971)
[4] Brown, D. G., Drago, R. S.: J. Am. Chem. Soc., **92,** 1871 (1970)
[5] Schwarzhans, K. E.: Angew. Chem., **82,** 975 (1970)
[6] Malrieu, J. P.: J. Chem. Phys., **46,** 1654 (1867)
[7] Webb, G. A.: Annual Reports on NMR Spectroscopy 3, Academic Press, London—New York, 1970, p. 211
[8] de Boer, E., Maclean, C.: J. Chem. Phys., **44,** 1334 (1966)
[9] McConnel, H. M., Robertson, R. E.: J. Chem. Phys., **29,** 1361 (1958)
[10] Kluiber, R. W., Horrocks, W. D.: J. Am. Chem. Soc., **88,** 1399 (1966)

[11] FIGGIS, B. N.: Trans. Faraday Soc., **55,** 1075 (1959)
[12] JARDETZKY, O , WERTZ, J. E.: J. Am. Chem. Soc., **82,** 318 (1960)
[13] LA MAR, G. N.: J. Chem. Phys., **41,** 2992 (1964)
[14] LA MAR, G. N.: J. Chem. Phys., **43,** 235 (1965)
[15] WALKER, I. M., ROSENTHAL, L., QUERESHI, M. S.: Inorg. Chem., **10,** 2463 (1971)
[16] ROSENTHAL, L., WALKER, I. M.: Inorg. Chem., **11,** 2444 (1972)
[17] WALKER, I. M., WEEDEN, D. H.: Inorg. Chem., **12,** 772 (1973)
[18] LARSEN, D. W., WAHL, A. C.: Inorg. Chem., **4,** 1281 (1965)
[19] LARSEN, D. W.: Inorg. Chem., **5,** 1109 (1966)
[20] LARSEN, D. W.: J. Am. Chem. Soc., **91,** 2920 (1969)
[21] QUERESHI, M. S., ROSENTHAL, L., WALKER, I. M.: J. Coord. Chem., **5,** 77 (1976)
[22] HAQUE, R., COSHOW, W. R., JOHNSON, L. F.: J. Am. Chem. Soc., **91,** 3822 (1969)
[23] FANNING, J. C., DRAGO, R. S.: J. Am. Chem. Soc., **80,** 3987 (1968)
[24] TAN, T. C., LIM, Y. Y.: Inorg. Chem., **12,** 2203 (1973)
[25] PAPP, S., KOVÁCS, S., LISZI, I.: J. Inorg. Nucl. Chem., **34,** 3111 (1972)
[26] SHULMAN, R. G.: J. Chem. Phys., **29,** 945 (1958)
[27] LARSEN, D. W., WAHL, A. C.: J. Chem. Phys., **41,** 908 (1964)
[28] RETTIG, M. F., DRAGO, R. S.: J. Am. Chem. Soc., **88,** 2966 (1966)
[29] WALKER, I. N., DRAGO, R. S.: J. Am. Chem. Soc., **90,** 6951 (1968)

Sándor PAPP
Pál KVINTOVICS
H-8201 Veszprém, Schönherz Z. u. 12.

Acta Chimica Academiae Scientiarum Hungaricae, Tomus 102 (3), pp. 259—266 (1979)

PREPARATION AND INVESTIGATION OF THE PHOSPHOROUSORGANIC DERIVATIVES OF TRANSITION METAL CYANO COMPLEXES, IX

^{1}H-NMR INVESTIGATION OF THE ION ASSOCIATIONS OF TRIPHENYLPHOSPHINO-PENTACYANOFERRATE(III) ANION WITH QUATERNARY PHOSPHONIUM CATIONS

S. PAPP and P. KVINTOVICS

(Department of General and Inorganic Chemistry, University of Chemical Industry, Veszprém)

Received May 18, 1978

Accepted for publication December 13, 1978

In the ion associations of $[Fe(CN)_5P(C_6H_5)_3]^{2-}$anion with quaternary phosphonium cations, the extent and nature of the interactions between the anion and cation, and between the protons of the $P(C_6H_5)_3$ ligand and the central atom have been studied.

Introduction

As known, the extent of pseudo-contact interaction in paramagnetic ion pairs is very much influenced by the symmetry of the anion. To determine how the extent of interaction changes with respect to the octahedral hexacyanoferrate(III) anion in the substituted derivatives of this anion, various quaternary phosphonium compounds of $[Fe(CN)_5P(C_6H_5)_3]^{2-}$ ion were studied here by ^{1}H-NMR methods. As in these compounds the anion itself is asymmetric, a larger shift of resonance frequencies could be expected to occur.

Results

The measurements were carried out at 32 °C in $CDCl_3$ and D_6-DMSO solutions of different concentrations, on a Varian T60 instrument. The spectra were evaluated by the method described in our previous paper [1]. The shifts of the resonance signals of $P(C_6H_5)_3$ ligand were related to the resonance signals of the non-complexed ligand measured in the same solvent. For the measurements the following complexes were prepared [2, 3]:

$$[(C_4H_9)_3PCH_3]_2[Fe(CN)_5PPh_3] \equiv M_2^1[Fe(CN)_5PPh_3]$$

$$[(C_4H_9)_4P]_2[Fe(CN)_5PPh_3] \equiv M_2^2[Fe(CN)_5PPh_3]$$

Table I

Chemical shifts of protons in the ion associates of $[R_3PR']_2[Fe(CN)_5P(C_6H_5)_3]$ *complexes*

Cation	Solvent	Concentration $C_R \cdot 10^3$	$\Delta\nu_i$ (Hz) cation				$\Delta\nu_i$ (Hz) anion	
			C_1	C_2-C_3	C_4	C_0	*m*	*o*
M_1 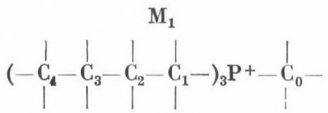	$CDCl_3$	1.4	32	8	8	26	10	136
		7.2	40	16	18	32	22	142
		13.5	48	30	31	42	36	154
	D_6-DMSO	1.8	14	6	6	10	4	140
		9.1	22	12	14	15	14	148
		18.3	30	24	24	26	24	160
			C_1	C_2-C_3	C_4		*m*	*o*
M_2 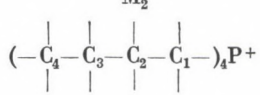	$CDCl_3$	1.0	22	11	15		10	148
		13.0	58	39	43		40	176
		19.9	70	53	56		48	180
	D_6-DMSO	1.3	14	8	10		2	132
		13.2	24	17	18		8	140
		25.9	40	34	36		30	168
			C_1	C_2-C_3	C_4	C_0	*m*	*o*
M_3 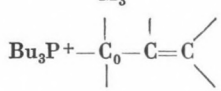	$CDCl_3$	1.3	30	7	6	78	12	144
		6.6	38	18	17	97	25	156
		13.1	44	28	21	106	36	164
	D_6-DMSO	1.5	14	4	3	64	4	136
		7.6	28	16	13	86	14	148
		15.2	41	28	24	102	22	156

Table I (continued)

M^4 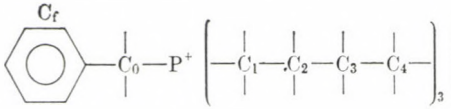			C_1	C_2—C_3	C_4	C_0	C_l .	*m*	*o*
	$CDCl_3$	0.7	20	4	4	38	4	4	138
		3.3	33	10	14	50	14	14	154
		9.8	46	24	28	64	28	28	167
		19.5	60	38	43	82	42	42	182
	D_6-DMSO	0.8	12	2	3	14	4	4	132
		4.1	18	8	10	18	12	10	144
		12.4	30	20	23	30	22	20	156
		24.8	44	34	36	44	35	34	172
M^5 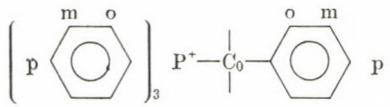			phenyl	benzyl-phenyl		C_0	*m*	*o*	*p*
	$CDCl_3$	0.7	2	2		42	4	150	380
		10.0	20	14		66	30	160	400
		20.1	24	22		76	40	170	408
	D_6-DMSO	0.9	22	14		40	4	148	324
		12.7	34	26		62	22	158	332
		25.5	44	40		72	30	166	338
M^6 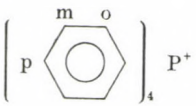			*p-m*			*o*	*m*	*o*	*p*
	$CDCl_3$	0.6	16			20	2	144	350
		9.7	50			60	30	186	352
		19.5	58			66	40	200	354
	D_6-DMSO	0.8	6			8	2	134	305
		12.3	18			20	10	152	312
		24.7	26			28	22	164	316

$$[(C_4H_9)_3PCH_2CHCH_2]_2[Fe(CN)_5PPh_3] \equiv M_2^3[Fe(CN)_5PPh_3]$$
$$[(C_4H_9)_3PCH_2C_6H_5]_2[Fe(CN)_5PPh_3] \equiv M_2^4[Fe(CN)_5PPh_3]$$
$$[(C_6H_5)_3PCH_2C_6H_5]_2[Fe(CN)_5PPh_3] \equiv M_2^5[Fe(CN)_5PPh_3]$$
$$[(C_6H_5)_4P]_2[Fe(CN)_5PPh_3] \equiv M_2^6[Fe(CN)_5PPh_3]$$

The chemical shifts of the various protons of cations are given in Table I.

In the spectra of the ion pairs formed with cations M^1 to M^4, the signals of the *para*-protons of $P(C_6H_5)_3$ ligand could not be identified. It is very probable that this signal appears in the region of aliphatic protons; this is also supported by literature data [4]. In answering this question measurements on phosphonium cations containing no aliphatic chain could also be applied to advantage.

Discussion

The experimental results were interpreted on the basis of the shifts in the signals of the C_0, C_1 and C_4 protons of derivatives formed with cations M^1 to M^4 (Fig. 1, 2 and 3).

Comparing the measured shifts with the corresponding data of hexacyanoferrate(III) anion [1] we have found that the magnitudes of shifts are nearly the same. This apparent contradiction can be resolved if the electronic structure of the $[Fe(CN)_5P(C_6H_5)_3]^{2-}$ anion is investigated from the aspects of the mechanisms causing the shifts, with particular regard to the fact that the magnitude of pseudo-contact interaction depends, in addition to the symmetry of the anion, on other factors, too. To a first approximation it can be stated, of course, that the ion-pair geometries in the ion associates of the two anions are most certainly different, but this does not explain the almost identical shifts. In this respect the unpaired electron of the central metal atom plays a much more important role.

In the $[Fe(CN)_6]^{3-}$ anion the back-coordination effect of the d electrons of the metal is the same toward all cyanide groups. When, however, a CN^- group is substituted by a ligand of stronger π-acceptor character, the electron distribution changes. If there is a strong delocalization in the direction of the new ligand, a relatively low unpaired spin density remains on the central atom. Consequently, the pseudo-contact interaction will be smaller than in the complexes in which the unpaired electron is localized on the metal atom [5].

The shifts of $[Fe(CN)_5P(C_6H_5)_3]^{2-}$ derivatives, regarding the cations, are similar in many respects to those of hexacyanoferrate(III) derivatives. Also in this case, the C_0 and C_1 protons have the largest chemical shifts, but the difference $\Delta\nu(C_0) - \Delta\nu(C_1)$ is higher here. The measured shifts are always larger in $CDCl_3$ than in D_6-DMSO, owing most probably to the different solvatation abilities of the two solvents.

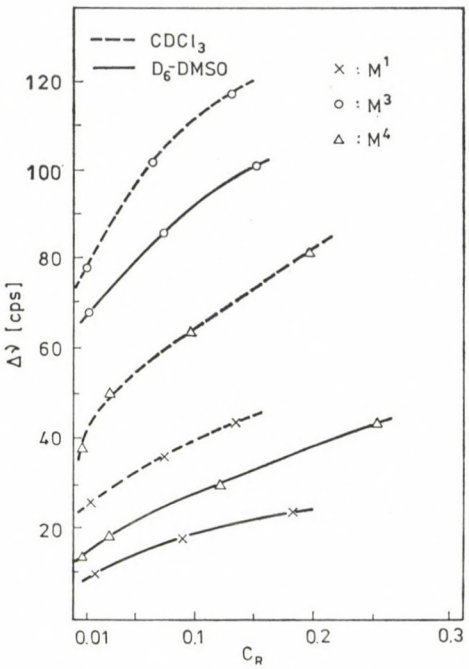

Fig. 1. Chemical shifts of C_0 protons

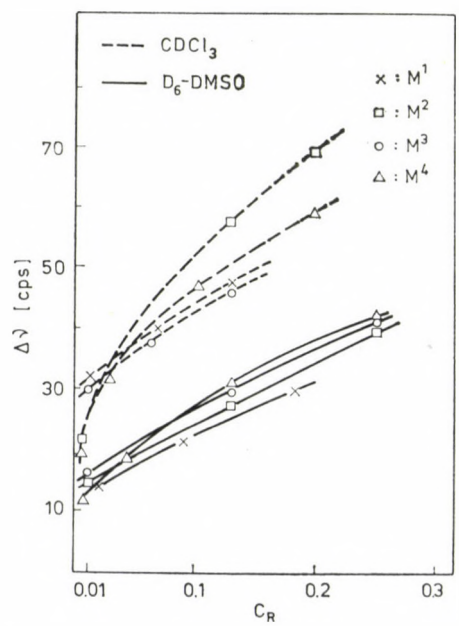

Fig. 2. Chemical shifts of C_1 protons

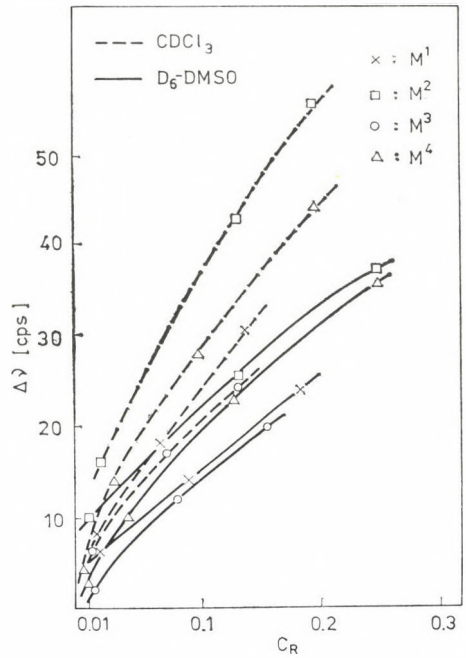

Fig. 3. Chemical shifts of C_4 protons

Regarding the individual lines, there are further differences between the derivatives of the two anions. Although the sequence of the shifts of C_0 protons is the same, the shift of the C_0 proton of the M^3 derivative is extremely high, and the sequences of the shifts of C_1 and C_4 protons are opposite for the two anions. In the complex of cation M^5 the C_0 protons have the largest shift, and the two types of phenyl protons show nearly the same shift, indicating that the latter are equivalent with respect to the geometry of the associate. Consequently, the ion-pair geometry is the same as with the other cations. This also applies to cation M^6.

Taking into account the shifts of C_2, C_3 and C_4 protons, too, it can be derived from the calculated geometric factors that the resonance frequencies are determined by the combined effect of the pseudocontact and contact interactions which cause positive (in the direction of higher fields) and negative shifts, respectively.

The mechanism of contact interaction can be assumed to be the same as with hexacyanoferrate(III) derivatives [1]; the assumption has been proved again by infrared investigations in solution phase. The arguments concerning ion-pair geometry and the concentration dependence of shifts are also the same as in the previous paper [1]. The only difference is that the relative positions

of cation and anion can now be determined with confidence, since the former must approach the anion from the side opposite to the $P(C_6H_5)_3$ ligand (Fig. 4).

The experimental data show a strong interaction between the $P(C_6H_5)_3$ ligand and the iron(III) central atom. According to Table I the shifts are positive for all protons, *i.e.* the signals of *ortho*, *meta* and *para* protons are uniformly shifted towards higher fields. The sequence of shifts can be interpreted on the basis of investigations on model compounds containing $P(C_6H_5)_3$ ligand [6, 7, 8] as follows. If a pseudo-contact interaction is assumed to exist, the sequence of the ligand protons, on the basis of the theoretical geometric

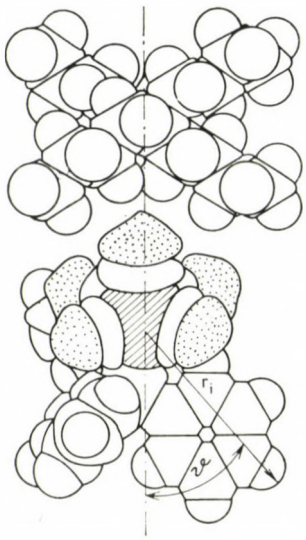

Fig. 4. Suggested structure for the $[(C_4H_9)_4P]^+$ $[Fe(CN)_5P(C_6H_5)_3]^-$ ion pair

factors, will be *ortho* > *meta* > *para*. As the observed sequence *(para* > > *ortho* > *meta)* is different, the phenomenon cannot be attributed to pseudo-contact interaction alone.

On the other hand, if only a contact interaction is present, the sequence of shifts depends on the symmetry of the orbitals involved in delocalization. For σ type delocalization the sequence is *ortho* > *meta* > *para*, *i.e.* the extent of shift decreases with increasing distance from the central atom, which is again different from the observed sequence. Finally, for π delocalization the sequence is *para* > *ortho* > *meta*, but the chemical shift of *meta* protons is negative, *i.e.* the resonance signal appears at lower field than in diamagnetic environment.

The observed sequence of signals agrees with the one caused by π delocalization, the observed shifts of *meta* protons are, however, positive for all

iron(III) complexes studied. It can therefore be assumed that the shifts are influenced by π delocalization, with a simultaneous pseudo-contact interaction, the extent of which is sufficient (small proton — central atom distances) to overcompensate the negative contact shifts of *meta* protons. On the basis of these qualitative considerations the tendencies of the experimental data can be interpreted satisfactorily.

The results of the investigations carried out so far indicate that in these systems, in addition to the dipole interaction between the central atom and the protons of the cation, there is a weak covalent interaction between them, *i.e.* the unpaired electron is delocalized to a certain extent. This may be one of the explanations of the fact generally observed in preparative chemistry that chemically unstable complex anions (*i.e.* sensitive to oxidation or hydrolysis), which do not exist in the form of alkali metal compounds, can be prepared with bulky organic cations.

The quantitative interpretation of experimental data, on the basis of calculations on ion-pair geometry, is in progress.

REFERENCES

[1] PAPP, S., KVINTOVICS, P.: Acta Chim. Acad. Sci. Hung., **102,** 247 (1979)
[2] NAST, R., KRÜGER, K. W.: Z. Anorg. Allg. Chem., **341,** 189 (1965)
[3] KVINTOVICS, P.: Thesis, Veszprém, 1975
[4] LA MAR, G. N.: J. Chem. Phys., **41,** 2992 (1964)
[5] SCHWARZHANS, K. E.: Angew. Chem., **82,** 975 (1970)
[6] HORROCKS, W. D., FISCHER, R. H., HUTCHINSON, J. R., LA MAR, G. N.: J. Am. Chem. Soc., **88,** 2436 (1966)
[7] LA MAR, G. N., FISCHER, R. H., HORROCKS, W. D.: Inorg. Chem., **6,** 1798 (1967)
[8] BROWN, D. G., DRAGO, R. S.: J. Am. Chem. Soc., **92,** 1871 (1970)

Sándor PAPP
Pál KVINTOVICS } H-8201 Veszprém, Schönherz Z. u. 12.

Acta Chimica Academiae Scientiarum Hungaricae, Tomus 102 (3), pp. 267—275 (1979)

INFLUENCE OF PHOTOGRAPHIC AND PHOTOMETRIC EFFECTS ON SPECTROGRAPHIC EVALUATION, II*

MICRODENSITOMETER FOR SPECTROGRAPHIC RESEARCH AND PRACTICE

L. KOZMA

(Research Institute for Technical Physics of the Hungarian Academy of Sciences, Budapest)

Received September 18, 1978

Accepted for publication December 20, 1978

Linear microdensitometer of classical optical arrangement has been designed for wide range measurements. The linearity, reproducibility and range of the optical density measurements and data acquisition has been investigated.

The improved detection system, the direct supply of optical density data and the method of the adjustment of the optics ensure accurate and reproducible measurements. The logics for the search of preselected lines and optical density extreme on them make the analysis quicker and more reliable.

Introduction

The development of the methods of the emission spectroscopy has made the improvement of the radiation detection indispensable. The modern excitation and dispersion techniques cannot be fully exploited because of the limited potentials of the detection.

The photographic method, which has a great information recording capacity, could not become the ultimate one of the detection, because its accuracy and resolution were not attained by those of the optical density (absorbance) measurement. This can be explained by that that the basic design of the majority of the microdensitometers for spectrography is some fifty-year old and therefore they cannot cope with the increased demands.

It has been found, that the characteristic curve of certain spectral plates was linear to the high exposures up to $S = 4$ [1].

However, this wide range cannot be used because of the poor performance of the microdensitometers over $S = 2$ [2]. The study of the problems of optical density measurement, such as range, linearity and reproducibility and the requirement of fast evaluation of spectra in large numbers led to designing of a precise, automatic densitometer of classical arrangement.

* Previous paper: ZIMMER, K., HELTAI, Gy.: Acta Chim. Acad. Sci. Hung., **100,** 319 (1979).

Papers of this series are simultaneously published in Magyar Kémiai Folyóirat in Hungarian.

Some problems of the optical density measurement

The quantitative information recorded on spectral plates and films is in the form of optical density. The useful range of the photographic response to the exposure is $S = 0—4$ [1]. The geometrical resolution attainable with spectral plates is a few micrometers even at perfect exposure and development technique. The performance of the microdensitometer must meet or possibly surpass these data.

The classical microdensitometer, which is based on the optical system and arrangement of the microscope can cope with these demands on the range and resolution, if its parameters are properly chosen. Optical density can be measured up to $S = 4$, if the sensitivity of the light detection and the intensity of the illumination of the object are sufficient and the stray light, which determines the upper limit of the range of the measurement, is reduced to 0.01% of the total flux. The two former factors determine the minimal size of the measuring slit, which for some practical reasons *(e.g.*: linearity of the optical transfer, graininess of the emulsion *etc.)* must be as narrow as 5 micrometers in effective width (projected on the film).

The portion of the stray light in the transmitted flux depends not only upon the quality of the optical system, but upon the structure of the spectrum as well. The finer it is, the harder is its contrast with the background, the more is the portion of the stray light. Two commercial microdensitometers and the microdensitometer described here were tested for stray light. The improved optical system and the introduction of complementary filters resulted in a reduction of the stray light with two orders of magnitude [2].

A very important prerequisite of the quantitative microdensitometry is the linearity, that is the response of the instrument be strictly proportional to the absorbance of the object. The non-linearity of the instrument can be caused by the error in the electronic response [3] or by that in the optical setting. The linearity of the optical transfer is influenced by the partial incoherence of the light source, which is unavoidable, if incandescent lamp is used. In spite of that linearity can be ensured, if the measuring slit in the image plane transmits a homogeneous flux over its whole size [4, 5].

This implies that in order to ensure the linear optical transfer the slit should be chosen the narrowest so that the variations in the structure of the spectrum lines be then relatively large compared to the size of the slit and so the partial incoherence of the light source has no impact on the optical transfer. The minimum attainable measuring slit width, which is equivalent to the impulse response width of the optical system is determined by the imaging optics [5]:

$$W = \frac{\lambda}{\mathrm{NA}}$$

where λ is the wave-length of the illumination and NA is the numerical aperture of the objective. In the case of the generally used $10\times$-magnification objective the minimal slit width is about 2 microns. This value is much smaller than the detail changes within a line and comparable with the resolution of the emulsions. The observation on different spectrum lines have suggested an optimum effective slit width of 5 microns.

Reproducibility is a basic demand on quantitative densitometry. Apart from the instability of the illumination [2], which can be eliminated, the defocus is the greatest problem. It has been shown [4], that reproducibility can be maintained within the focal tolerance. This is relatively small:

$$\delta \text{ (focal tolerance)} = \frac{\lambda}{2 \cdot \text{NA}}$$

It is about 1 micrometer in the case of a $10\times$ imaging objective and considerably smaller than the thickness of a spectral emulsion. Therefore the reproducibility depends upon the precision of the visual focusing.

To study the dependence of reproducibility upon focusing spectrograms with well characterized thin single lines or with continuous spectrum were measured with this microdensitometer. It has been observed that the visual focus tolerance is generally quite great, about ± 20 μm over the whole magnification range ($10\times$—$50\times$).

Figs 1a and 1b show the measured optical density of a single line in dependence on the defocus of the imaging objective. The error due to the visual

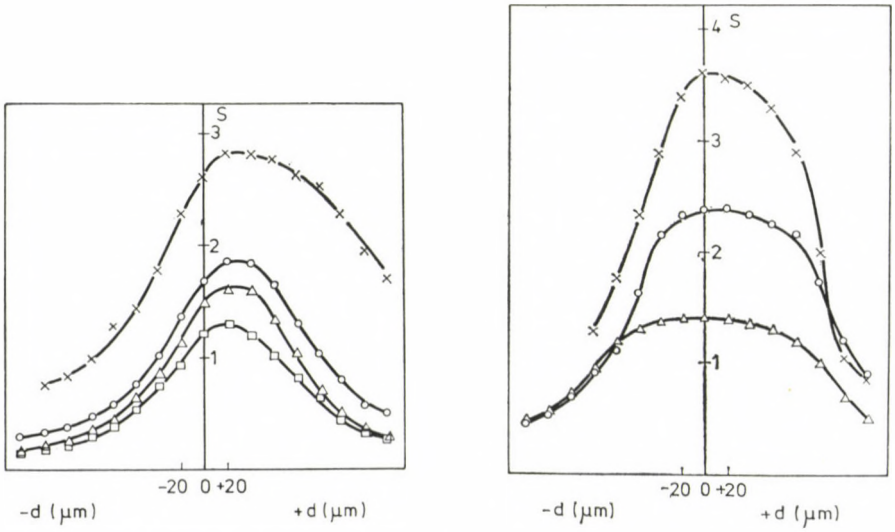

Fig. 1. The effect of the defocus of the objective on the optical density measurement of spectral lines of *a)* 25 μm, *b)* 50 μm width. Objective: $10\times$, measuring slit: 5 μm wide

setting of the objective increases with the optical density. This is more marked in the case of thinner lines. The curves show maximum, which belongs to the optimum focus. If objects of uniform absorbance are measured, the focus at the minimum value is the right one (Fig. 2). The problem of the defocus of the substage condenser is as important as that of the objective. At its best setting the measured optical density is maximum on single lines (Fig. 3), and minimum on background or continuous spectrum. The uncertainties and errors introduced by visual focusing are caused by slight misalignment of the optical system.

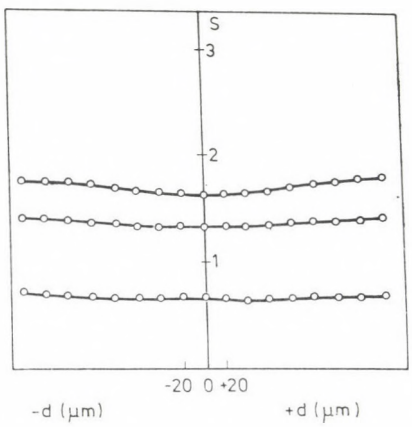

Fig. 2. The effect of the objective defocus on the optical density measurement of continuous spectrum. Objective: 10×, measuring slit: 5 μm wide

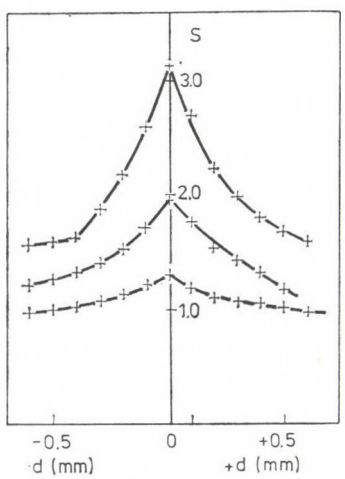

Fig. 3. The dependence of the optical density measurement upon the defocus of the substage condenser. Objective and condenser: 10×, measuring slit: 5 μm wide, width of the spectrum line: 25 μm

However, it is possible to adjust the optics precisely, if the objective is not visually focused but its working distance is set according to the maximum absorbance value measured on a single line. The substage condenser can be similarly set optimum.

Description of the microdensitometer

Taking into consideration the up-to-date requirements on precise and high resolution measurements a reliable, advanced microdensitometer has been built (Fig. 4). The optical system is based on that of the widely spread Zeiss Jena Schnellphotometer, which has been improved and the imaging/measuring optics have been partly redesigned (Fig. 5).

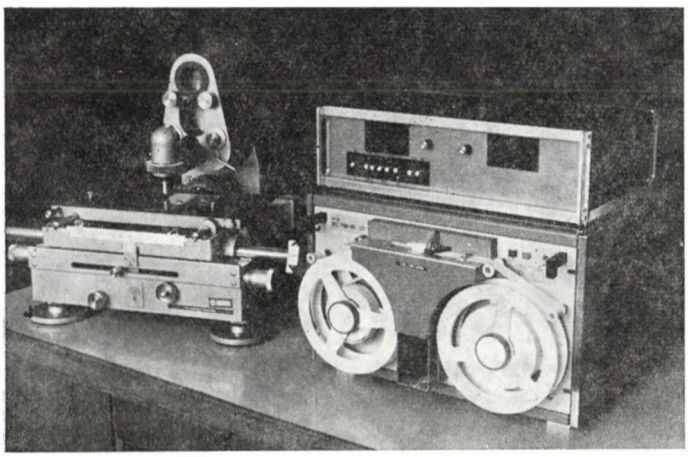

Fig. 4. The microdensitometer with the measuring, control and recording electronics

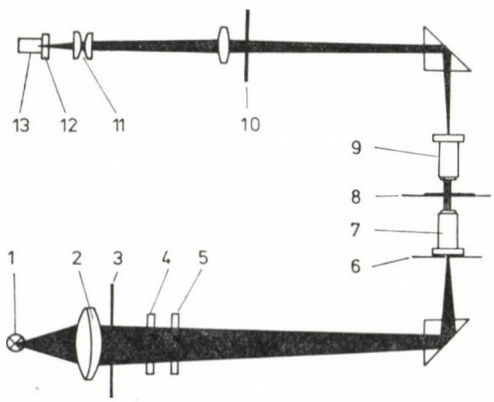

Fig. 5. The optical arrangement of the microdensitometer; 1 halogene lamp, 2 lamp condenser, 3 field diaphragm, 4 heat filter, 5 green filter preslit, 6 aperture diaphragm, 7 substage condenser, 8 object (plate, film), 9 objective, 10 measuring slit, 11 collecting lens system, 12 red filter, 13 light measuring device

The optical arrangement of the instrument

The optical system of the single-beam microdensitometer is based on the Koehler-type illumination and microscope projection system. The light intensity transmitted by the object (8) is measured by a silicon photodiode (13).

In this design the illumination system was devoted so much importance as the image projection part. In order to get sufficient light intensity even at high-resolution measurements, a single filament 100 watt halogen lamp (1) is used, which is operated on a DC power supply with 0.01% stabilization. A poor quality lamp condenser can introduce flare. To avoid this detrimental effect a compound condenser (2) was placed in front of the lamp. In order to ensure the Koehler-type illumination of the object iris diaphragms were fitted both just in front of the lamp condenser (3) and in the rear focal plane (6) of the substage condenser (7). The former controls the size of the image of the light source and that of the object field. The object field is specified by the NA of the objective (9). The greater the magnification, the smaller is the size of the illuminated field. It is very important that the image of the lamp condenser should fill the aperture of the substage condenser to obtain the maximum photometric efficiency. If the diaphragm is not narrowed to the required extent it gives rise to the stray light from the areas directly not used in the image plane.

The iris diaphragm situated in the rear focal plane of the substage condenser is the efficient aperture of both the condenser and objective.

In order to eliminate the heat hazard at the object a heat filter (4) was placed in front of the first iris diaphragm. A green filter preslit of maximum transmittance at $\lambda = 550$ nm (5) was fitted to improve the definition of the objective and as a part of the complementary filter system.

The image of the object is projected on a white screen in the primary plane, in the centre of which is the square measuring slit (10). This can be continuously varied between 1—10 mm in height and between 0.1—2.0 mm in width. The magnification of the sample in the primary image plane is between $10\times$—$15\times$ depending on the objective in use. So the effective size of the measuring slit can be adjusted between 2—200 μm. Just behind the measuring slit a compound lens system (11) was placed to focus all the transmitted flux on the surface of the silicone PIN diode.

A red filter (12) is situated in front of the detector to ensure its maximum spectral sensitivity and to reduce the stray light in combination with the green filter preslit.

All the internal surfaces has been painted matt-black or covered with black paper.

Measurement of optical density

The transmittance of the object is measured by a silicon PIN photodiode. The linearity of the response of this device has been checked over 4 decades of the incident light, the deviation has not exceeded 0.5%. This is superior to that of a photomultiplier tube, which showed acceptable linearity only over two orders of magnitude. Moreover the high speed measurements with photomultiplier are unreliable because of drift, memory-effect and fatigue of the device. The problem of the lower output at the same incident flux in the case of the photodiode has been overcome by using an operational amplifier of very good stability. In this way as small as 100 μm^2 effective measuring slit can be used at the illumination with a 100 watt halogen lamp.

The intensity of the current of the photodiode is proportional to the transmittance of the object. A logarithmic amplifier is used to develop the optical density values from the input signals. This circuit makes use of the relationship between the base-emitter voltage and the collector current of the transistor. It operates over 4 decades of the input signals with a log conformity of 0.5%. The output is displayed in the form of true optical density on a 3 1/2 digit panel meter.

The accuracy of the optical density measurement has proved approx. 0.2% in the range of $S = 0$—1, and 0.3% up to $S = 3$.

The reproducibility is 1% over 2 hours of operation.

Automatic evaluation of spectra

In order to simplify the measurements and improve the reliability of the acquisition of spectrum data the scanning and the resolution of the image of the spectrum are realized in discrete steps, whose length is equal to the width of the slit. For the search of the location of the preselected lines and of the maximum value of their optical density storing and comparing circuits have been developed.

The object stage is driven by a stepper motor through a backlashfree leadscrew. The pitch of the leadscrew and the transmission between it and the motor were so chosen that the distance made by the stage at a single step is 5 microns. So the spectrum lines can be quite finely resolved, generally into 8—10 points, which is the prerequisite for the reliable extreme searching.

The stage is moved with a speed continuously variable between 0.05—1.00 mm $\cdot$ sec^{-1}, the number of the steps taken is added and displayed.

Related to a chosen line the location of 16 different lines can be stored in the memory in the form of step numbers and at following scannings these lines can be automatically searched in the order of the step numbers. It is

imperative that the reference line and the exposure conditions *(e.g.* dispersion) remain unchanged.

The extreme searching logic makes one of the most tiring and time-consuming job in spectrum evaluation obsolete. The principle of its operation is shown on Fig. 6. The electronics have a one step memory, the content of

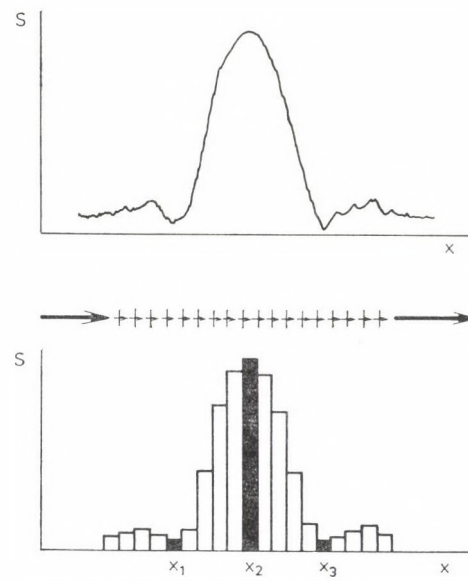

Fig. 6. Scheme of the searching of the optical density maximum on a spectral line

which is continuously compared to the instantaneous measurement value. If the latter exceeds the stored one, the memory is erased and the new, higher signal gets stored. The process goes on until the maximum is reached. This value with the respective coordinate given in step numbers is then ready to be displayed and recorded. The search for background minima is similar, but in this case decreasing signals are processed.

Complete acquisition of the chosen 16 lines with the determination of their optical density maximum and the background lasts about 5 minutes.

Data handling

The optical density data are digitally displayed. The coordinates of the measurement points related to the stage movement are also supplied.

A punch tape recorder and a printer were fitted to the instrument for further data processing.

*

The author wishes to thank dr. L. BARTHA for the generous support of the project. The discussions with Prof. K. ZIMMER and dr. Gy. HELTAI and their counsels for the design of the microdensitometer are very much appreciated.

Mr. T. BORSOS is thanked for his help in the experimental work.

REFERENCES

[1] VECSERNYÉS, L., ZÁRAY, Gy.: Proc. XV. Annual Hung. Symp. on Emission Spectral Analysis, Tatabánya, 1972, 155
[2] ZIMMER, K., HELTAI, Gy.: Acta Chim. Acad. Sci. Hung. **100,** 319 (1979)
[3] HELTAI, Gy., ZIMMER, K., KOZMA, L.: Proc. XX. Annual Hung. Symp. on Spectral Analysis, Gyula, 1977, 19
[4] SWING, R. E.: Opt. Eng., **12,** 185 (1973)
[5] SWING, R. E.: J. Opt. Soc. Am., **62,** 199 (1972)

László KOZMA H-1325 Budapest, Újpest 1. P. O. Box 76.

Acta Chimica Academiae Scientiarum Hungaricae, Tomus 102 (3), pp. 277—288 (1979)

INFLUENCE OF PHOTOGRAPHIC AND PHOTOMETRIC EFFECTS ON SPECTROGRAPHIC EVALUATION, III*

DETERMINATION OF THE PARAMETERS OF BLACKENING CURVE AND *l*-TRANSFORMATION BY MEANS OF GRAPHICAL METHOD AND COMPUTER

K. FLÓRIÁN[1], Gy. HELTAI[2] and K. ZIMMER[3]

([1] *Department of Chemistry of Metallurgical Faculty of Technical University, Košice, Czechoslovakia,* [2] *Department of Chemistry of the University of Agricultural Sciences, Gödöllő,* [3] *Institute for Inorganic and Analytical Chemistry of L. Eötvös University, Budapest)*

Received September 18, 1978
Accepted for publication December 20, 1978

Methods for the determination of the parameters of blackening curve are discussed. For the graphical determination of the γ-value as well as density values S_L and S_{LL} essentially the CHURCHILL preliminary curve method was used. A computer programme has been elaborated for the determination of constants γ and k of the *l*-transformation. The programme is based on the iteration calculation considered to be the most reliable principle by TÖRÖK and ZIMMER. The values of the filter constant usually agree with the average of the value $\overline{\Delta l}$, with an accuracy of 0.001 when applied the γ and k values calculated by the programme. This accuracy is perfectly satisfactory for practical demands.

Introduction

A precondition of spectrographic analysis is to know the so-called intensity-scale blackening curve [1] expressing the relation between logarithm intensity ($\lg I \equiv Y$) of the light illuminating the photographic emulsion and the density S. For the determination of this intensity-scale blackening curve it is, of course, necessary to have the intensity scale well-defined at suitable wavelengths. For this purpose such a light source radiating with stable intensity is needed which produces line spectrum at the wave-lengths of all analysis lines. The stability of the light sources used for analytical chemical purposes usually is not able to fulfil this requirement.

Therefore in the spectrographic practice the methods used are such that radiations of different intensities emitted by the same light source are photographed not successively, but simultaneously. The error deriving from fluctuation of the intensity of the radiation source during the exposure can be eliminated if the light projected with uniform intensity on the slit of the spectrograph is

* Previous paper: KOZMA, L.: Acta Chim. Acad. Sci. Hung., **102,** 267 (1979)
Papers of this series are simultaneously published in Magyar Kémiai Folyóirat in Hungarian language.

produced in different intensity steps along the longitudinal axis of the slit [2—5]. To decrease the radiation intensity multi-step rotating sectors (mainly in America) are generally used, and multi-step light absorbing filters as well (mainly in Europe). In the latter case, light absorption of the single filter step should be calibrated in the function of wave-length. At a given wave-length the necessary intensity scale is provided by a series of numbers expressing the light transmission of the single steps. These numbers are proportional values with the absolute intensity falling to a given spot of the photographic emulsion. For analytical calibration it is sufficient to have a series of numbers expressing the relative intensity values, provided that the conditions of analysis and calibration are similar in other respects.

However, the method based on multi-step intensity decrease involves technical difficulties. On the one hand, intensity scale produced in this way contains relatively few — at most 2—10 — points, on the other hand, the great slit height necessary to this method can hardly be illuminated uniformly. In order to solve this problem processes based on two-step intensity reduction have been elaborated for the determination of blackening curve [2]. For this, a series of spectrograms should be produced by applying a two-step intensity-decreasing device and varying the amount of radiation falling on the photo-emulsion.

Theoretically the proper solution is to vary the light intensity keeping the exposure time at a constant value. It is proved, however, that even the change of exposure time is allowed [6]. The basis of the further calculation is, namely, the logarithm intensity difference of the light transmitted through two steps:

$$\lg I_a - \lg I_b = \Delta Y_m$$

i.e. the filter constant, the value of which is not dependent on the exposure time.

No intensity scale is obtained by using two-step intensity reduction, but only a series of density differences belonging to given intensity ratios. With the help of these data pairs the blackening curve can be plotted and constants of blackening transformations determined.

Graphical determination of blackening curve

The simplest methods of the graphical determination of blackening curve are based upon the application of the so-called preliminary curve [7—12]. From among these methods essentially the CHURCHILL's preliminary curve was used which contains every necessary information on the shape of the blackening curve [7, 13]. This can be obtained on the way that the densities S_b measured on the attenuated step are plotted against the corresponding

densities S_a measured on the unattenuated step of 100% transparency of the step-filter (Fig. 1). The equation describing this curve can be given as follows $S_b = S_a - \Delta S_m$, where ΔS_m represents the density difference belonging to ΔY_m logarithm intensity difference. It is easy to see that the value of ΔS_m depends on the density, at the bent sections of the blackening curve different ΔS_m values belong to a given ΔY_m difference. However, if both densities fall onto the straight section of the blackening curve, the value of ΔS_m is constant. So this section is linear, its slope equals 1, and the intercept of this straight

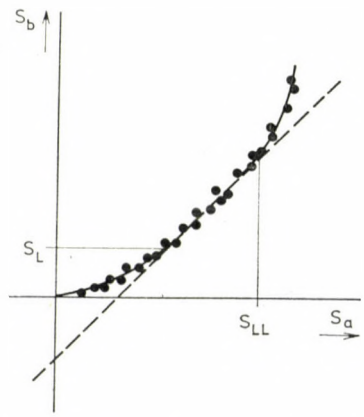

Fig. 1. Churchill's preliminary curve

line gives just the average of ΔS_m values measured on the straight part. This section is achieved on the preliminary curve when the density value belonging to the lower intensity also reaches the linear section of the blackening curve. Till this limit the ΔS_m values and consequently the slope of the preliminary curve increase. So S_L is the ordinate's value belonging to the point where the straight and lower bent part of the curve join. If the density measured on the unattenuated step exceeds the upper S_{LL} point of the linear section, ΔS_m starts to decrease, and the graph deviates from the straight line. The abscissa belonging to this point has just the same value as S_{LL}. Accordingly, with the help of the preliminary curve, the most important parameters of the blackening curve can be directly determined and by the simple plotting methods offered by the above authors even the blackening curve itself can be drawn. The constants of *l*-transformation [14] $\gamma = \dfrac{\Delta S_m}{\Delta Y_m}$ and $k = \dfrac{S_L}{\gamma}$ can similarly determined on the basis of Fig. 1. However, the accuracy of these values is generally not satisfactory for practical purposes. However, the γ value can be fairly well estimated, the accuracy of the end point readings (S_L and S_{LL}) is not sufficient and strongly depends on the standard deviation. The calculation of transfor-

mation constants is required even when the graphical method is applied. However, also in this case it is necessary to plot at least the preliminary curve in order to be able to determine the upper S_{LL} limit of density values to be considered at calculation.

Determination of constants of *l*-transformation by calculation

Constants of *l*-transformation can be determined with relatively simple methods when not many data are available [14]. Although, the accuracy and precision of the methods are strongly depending on the number of data used, the reliable and rapid processing of high number of data can be solved only by the help of computer.

A computer programme based on the above. preliminary curve method is suggested by MATHERNY [15, 16]. This programme was widely applied by us and generally reliable results were obtained. In certain cases, however, the differences between the calculated and true values significantly exceed the standard deviation permitted. This appears if the basic assumptions of the programme are not fulfilled because of the experimental conditions: if the distribution of the points to drawing the preliminary curve is not sufficiently uniform or if the standard deviation is relatively high [17].

Therefore, for the determination of the constants of *l*-transformation a new computer programme based on the iteration method found to be most reliable by TÖRÖK and ZIMMER [18] was elaborated.

Computer programme for the determination of constants of *l*-transformation by iteration method

To the computer programme $S_{a,i}$, $S_{b,i}$ pairs ($S_a > S_b$) of density values obtained with the application of two-step filter were used. It is expedient that the number of density pairs reach at least 30, and they are spread possibly uniformly on the straight and underexposed sections of the blackening curve.

The first step of the calculation is to order the data pairs according to the decreasing value of S_a if these are equal, according to values S_b. Afterwards differences are formed as follows:

$$\Delta S_i = S_{a,i} - S_{b,i}$$

To determine the lower limit of the linear section of blackening curve the ΔS_j limit value must be found following which the further ΔS_i values monotonously decrease. This task is to be solved as follows:

With the help of the first 5 values, the $\overline{\Delta S}_j$ average values and the corresponding $s_{\overline{\Delta S}_j}$ standard deviation are calculated

$$\overline{\Delta S}_j = \sum_{i=1}^{j} \frac{\Delta S_i}{j} \qquad (j = 5) \tag{1}$$

$$s_{\overline{\Delta S}_j} = \sqrt{\frac{1}{j-1} \sum_{i=1}^{j} (\overline{\Delta S}_j - \Delta S_i)^2} \qquad (j = 5) \tag{2}$$

Then it is examined whether the inequality (3) exists or not:

$$\Delta S_{j+1} < \overline{\Delta S}_j - t \cdot s_{\overline{\Delta S}_j} \tag{3}$$

where t is a constant corresponding to the chosen statistical safety. This can arbitrarily be chosen in the programme; according to our experiences $t = 1.55$ is a quite suitable value ($\sim$ 80% statistical safety).

In the case of appropriately chosen S_a, S_b data pairs inequality (3) does not exist, if the $\overline{\Delta S}_j$ average is formed of the first 5 ΔS_i values. For this reason the $\overline{\Delta S}_j$ value on the basis of formula (1) and its standard deviation on the basis of formula (2) are calculated, taking one more value ($j = 5 + 1$) into consideration. This process is continued by gradually rising the j values ($j = 5 + 2, j = 5 + 3, \ldots$) till inequality (3) is reached. If it occurs, one has to investigate whether the value in question is an accidentally outstanding one, or not, therefore the forthcoming ΔS_{j+2} value should be compared to the mean value:

$$\Delta S_{j+2} < \overline{\Delta S}_j - t \cdot s_{\overline{\Delta S}_j} \tag{3.a}$$

(but in this case, it is suggested to take $t = 2.0$).

In the case, if inequality (3.a) does not exist, calculation returns to the first step taking additional ΔS_i value, as described above. When inequality (3.a) is reached, simultaneously the point is obtained where the linear section of the blackening curve approximately comes to an and: $S_{b,j} = S_L$. If some data pairs, or at least one member of them, are corresponding already to the upper bent section, *i.e.* $S_{a,i} > S_{LL}$, the $\overline{\Delta S}_j$ mean value will be wrong. Therefore ΔS_i values significantly differing from the calculated $\overline{\Delta S}_j$ value should be left out from the calculations. In the next step ΔS_i values used for the calculation of mean value are examined, and in the course of the further calculations those values for which inequality

$$|\Delta S_i - \overline{\Delta S}_j| > t \cdot s_{\overline{\Delta S}_j} \tag{4}$$

is valid, are neglected. The value of constant t is taken 1.55. Values omitted this way, are separately presented, and the above process (cycle 2) is repeated without them, as a result of which $\overline{\Delta S}_j$, and $s_{\overline{\Delta S}_j}$, values, respectively, are obtained. By means of $\overline{\Delta S}_j$, of the *initial* γ-value can be calculated:

$$\gamma_1 = \frac{\Delta S_{j'}}{\Delta Y_m} \tag{5}$$

where ΔY_m is the logarithmic filter constant of the applied two-step filter in the examined wave-length range.

At the same time the *initial* k-value can also be calculated with the help of the $S_{b,j}$, value belonging to the ΔS_j, limit value:

$$k_1 = \frac{S_{b,j'}}{\gamma_1} \tag{6}$$

Using the *initial* constants obtained this way

$$s_{a,i} = \frac{S_{a,i}}{\gamma_1} \quad \text{and} \quad s_{b,i} = \frac{S_{b,i}}{\gamma_1} \tag{7}$$

can be calculated from all $S_{a,i} - S_{b,i}$ values. Then $l_{a,i}$ and $l_{b,i}$ values, respectively, are obtained from the equation (7.c) of l-transformation from $s_{a,i}$ and $s_{b,i}$ values for which inequality

$$s_{a,i} < k_1 \quad \text{and} \quad s_{b,i} < k_1 \tag{7.a}$$

is valid. In other cases, according to the definition of l-transformation

$$s_{a,i} = l_{a,i} \quad \text{and} \quad s_{b,i} = l_{b,i} \tag{7.b}$$

$$l = s - (k - s)\, d \tag{7.c}$$

Then

$$\Delta l_i = l_{a,i} - l_{b,i} \tag{7.d}$$

values are calculated and the mean value

$$\overline{\Delta l} = \frac{1}{M} \sum_{i=1}^{M} \Delta l_i \tag{8}$$

is got from all those Δl_i values, for at least one component of which inequality (7.a) is valid. In equation (8) M is the number of Δl_i values.

Mean value $\overline{\Delta l}$ calculated on the basis of equation (8) is compared with the value ΔY_m of the filter constant.
If

$$|\overline{\Delta l} - \Delta Y_m| < P \tag{9}$$

the chosen k-value is suitable with the accuracy required. The value P can be chosen arbitrarily; for practical purposes $P = 0.01$ or $P = 0.005$.

In the case, when inequality (9) is not fulfilled, the k-value is varied as follows:
If

$$\overline{\Delta l} < Y_m \qquad k_{\text{new}} = k_{\text{former}} + 0.005 \tag{9.a}$$

$$\overline{\Delta l} > Y_m \qquad k_{\text{new}} = k_{\text{former}} - 0.005 \tag{9.b}$$

When accuracy defined by formula (9) is reached, iteration is stopped and the *preliminary* k_2 value is obtained. After this the $S_{b,j''}$ and $\overline{\Delta S}_{j''}$ values are calculated corresponding to k_2:

$$S_{b,j''} = \gamma_1 \cdot k_2 \tag{10}$$

Following this, the previous part of calculation (cycle 3) is repeated, *i.e.* the new *initial* γ- and k-value is calculated

$$\gamma_2 = \frac{\overline{\Delta S}_{j''}}{\Delta Y_m} \tag{11.a}$$

$$k_3 = \frac{S_{b,j''}}{\gamma_2} \tag{11.b}$$

Iteration of k-value is repeated as described above with the values of the *second initial* transformation constants applying formulas (7)—(9.b) and finally k_4-value is got.

If the value of γ_1 and γ_2 does not differ more than the error permitted [4, 14], *i.e.*

$$|\gamma_2 - \gamma_1| < 0.02 \tag{12}$$

then γ_2- and k_4-values can be regarded *final*. If this condition is not fulfilled, the calculations given by formulas (10) and (11) are repeated using the values of γ_2 and k_4. With the γ_3 and k_5 *preliminary* values obtained this way the iteration is performed again which results in the final γ_3- and k_6-values.

This step was necessary, because a significant difference between γ_1 and γ_2 values refers to wrong initial γ- and k-values. The cause of this lies in the not sufficiently accurate determination of ΔS_j limit value and $\overline{\Delta S_j}$ mean value, respectively. This occurs, when the standard deviation of the measurements is too high, or the distribution of $S_{a,i} - S_{b,i}$ data pairs is uneven on the linear and under-exposed part of the blackening curve.

Three insoluble cases may arise, in which the calculation automatically ceases. These are the followings:

1. In the course of k-value iteration according to formulas (9.a) and (9.b), respectively, it may occur that k constantly changes between two values without reaching the required iteration accuracy. In this case the calculation can be repeated with lower iteration accuracy.

2. The $S_{b,j'}$ and $\overline{\Delta S}_{j'}$ values got with the help of preliminary γ_1- and k_2-values correspond to less than 5 ΔS_i values of the series. This time the ***precondition*** of the calculation is not fulfilled according to which at least the first 5 ΔS_i values should fall to the linear section of the blackening curve.

3. During iteration the k-value continuously decreases and takes a ***non-defined negative*** value. In this case, however, the calculation can be repeated with a lower iteration accuracy requirement.

The following scheme gives a survey on the calculating process in a simplified from.

In the course of the practical test of the above program first of all the accuracy reachable has been examined. This examination shows simultaneously what precision can reliably be requested during the application of the method.

To characterize the precision of transformation the program gives the following data at the single steps of iteration:

a) The average and standard deviation of Δl values calculated from all data pairs of density:

$$\overline{\Delta l}_{l \leqslant k} = \frac{1}{N} \sum_{i=1}^{N} \Delta l_i \tag{13.a}$$

$$s_{\Delta l_{l \leqslant k}} = \left[\frac{1}{N-1} \sum_{i=1}^{N} (\overline{\Delta l}_{l \leqslant k} - \Delta l_i)^2 \right]^{\frac{1}{2}} \tag{13.b}$$

b) The average and standard deviation of Δl_j-values calculated from data pairs $(l_{a,j}, l_{b,j})$ lower than the k-value:

$$\overline{\Delta l}_{l<k} = \frac{1}{M} \sum_{j=1}^{M} \Delta l_j \qquad M < N \tag{14.a}$$

$$s_{\Delta l_{l<k}} = \left[\frac{1}{M-1} \sum_{j=1}^{M} (\overline{\Delta l}_{l<k} - \Delta l_j)^2 \right]^{\frac{1}{2}} \tag{14.b}$$

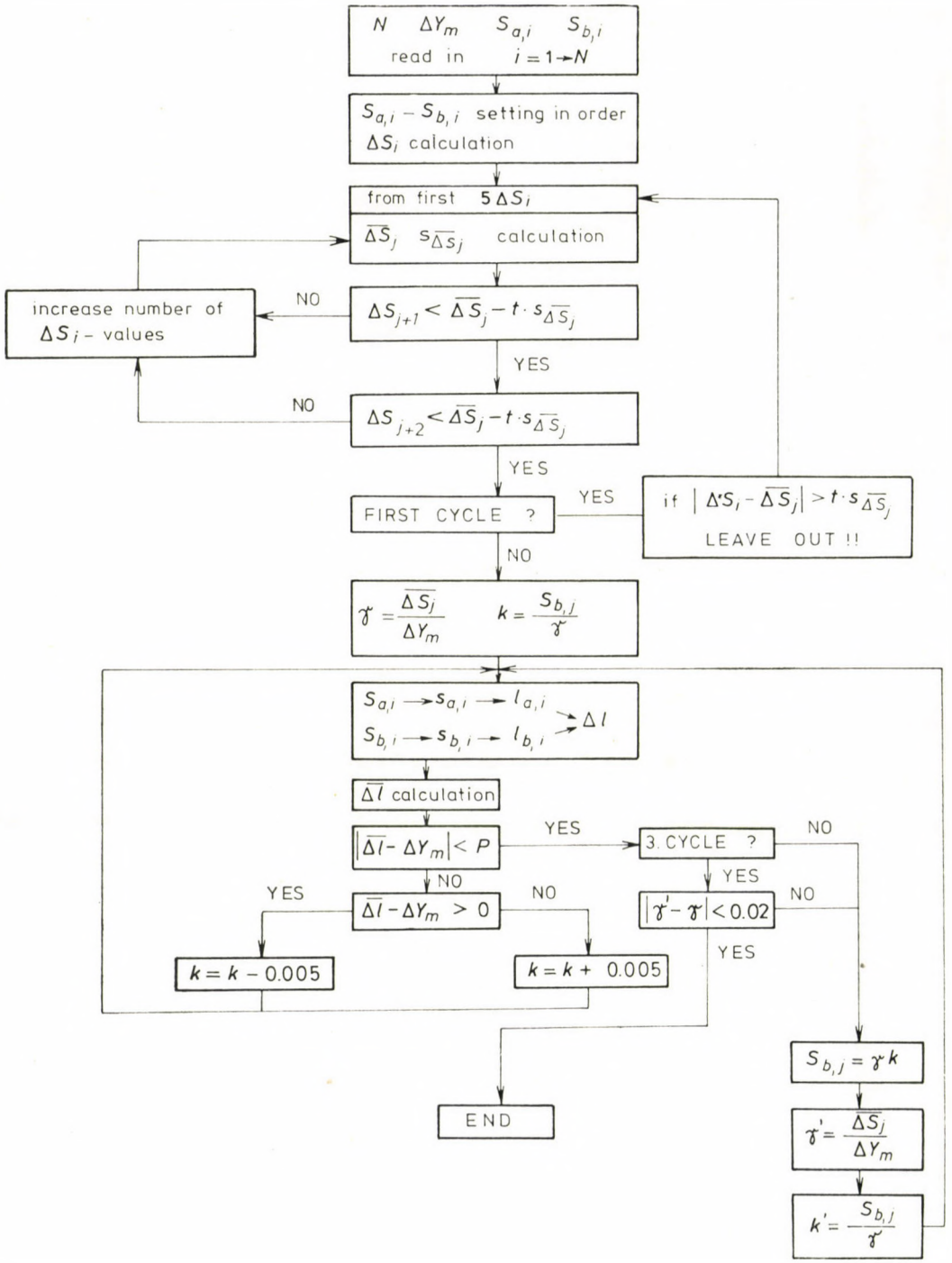
N ΔY_m S_a,i S_b,i
read in i = 1→N
S_a,i − S_b,i setting in order
ΔS_i calculation
from first 5 ΔS_i
ΔS̄_j s_ΔS̄_j calculation
increase number of ΔS_i - values
NO
ΔS_j+1 < ΔS̄_j − t · s_ΔS̄_j
YES
NO
ΔS_j+2 < ΔS̄_j − t · s_ΔS̄_j
YES
FIRST CYCLE ?
YES
if | ΔS_i − ΔS̄_j | > t · s_ΔS̄_j
LEAVE OUT !!
NO
γ = ΔS̄_j / ΔY_m
k = S_b,j / γ
S_a,i → s_a,i → l_a,i
S_b,i → s_b,i → l_b,i
Δl
Δl̄ calculation
|Δl̄ − ΔY_m| < P
YES
3. CYCLE ?
NO
YES
NO
Δl̄ − ΔY_m > 0
YES
NO
|γ' − γ| < 0.02
NO
YES
k = k − 0.005
k = k + 0.005
S_b,j = γ k
γ' = ΔS̄_j / ΔY_m
k' = S_b,j / γ
END

c) The difference of the filter constant and mean value $\overline{\Delta l}_{l<k}$ obtained from the transformed density values, as well as the standard deviation of Δl_j values characteristic for the deviation from the filter constant:

$$P = |\Delta Y_m - \overline{\Delta l}_{l<k}| \tag{15}$$

$$s_{\Delta l_{l<k},\Delta Y m} = \left[\frac{1}{M-1}\sum_{j=1}^{M}(\Delta Y_m - \Delta l_j)^2\right]^{\frac{1}{2}} \tag{16}$$

Accuracy of transformation is characterized primarily by the last two data. On Figures 2.a, b, c, d some practical examples are demonstrated. The variation of $s_{\Delta l_l \lessgtr k}$, $s_{\Delta l_{l<k}}$, $s_{\Delta l_{l<k},\Delta Y_m}$ and that of *P*-value in function of the parameter k is presented in the figures. The most important experimental conditions (spectral plate, spectrograph, wave-length) are shown in the legends to the figures.

On the basis of the figures the followings can be stated:

a) The *P*-value has an extremely sharp minimum in function of parameter k. It can be seen that the step value $k = \pm 0.005$ applied in the course of iteration, ensures the approach of this minimum with 0.001 accuracy in all cases. To demand a better agreement between filter factor and value $\overline{\Delta l}_{l<k}$ would be pointless both theoretically and practically. Namely, the filter constant is a photometrically determined value, and the error of absorbance measurement is ± 0.001 with the usual instruments in favourable case.

b) The standard deviation $s_{\Delta l_{l<k},\Delta Y m}$ passes through a minimum in function of k-value and the k-value belonging to the minimum is equal to the k belonging to the minimum of *P* value. Here

$$s_{\Delta l_{l<k},\Delta Y m} \equiv s_{\Delta l_{l<k}}$$

c) Standard deviation $s_{\Delta l_l \lessgtr k}$ similarly gives a minimum at the above k-value. The degree of its change is, however, not significant, even if k is changed so, as the value of *P* reaches 0.010. The variation of $s_{\Delta l_{l<k}}$ can also be neglected in the above limit of k-values, and does not exhibit unambiguous tendency. These observations well support the rule obtained by the application of *l*-transformation without computer; according to which for practical purposes always sufficiently accurate the k-value at which $P = |\Delta Y_m - \overline{\Delta l}_{l<k}| = 0.005$ has been reached [4, 14]. However, computer calculations offer possibility for gaining better accuracy, too. Naturally, it is important only in that case when for theoretical purposes the k-value itself is intended to be determined as precisely as possible.

The above described graphical and computerized processes have been widely applied in the course of our further investigations. Line and continuous

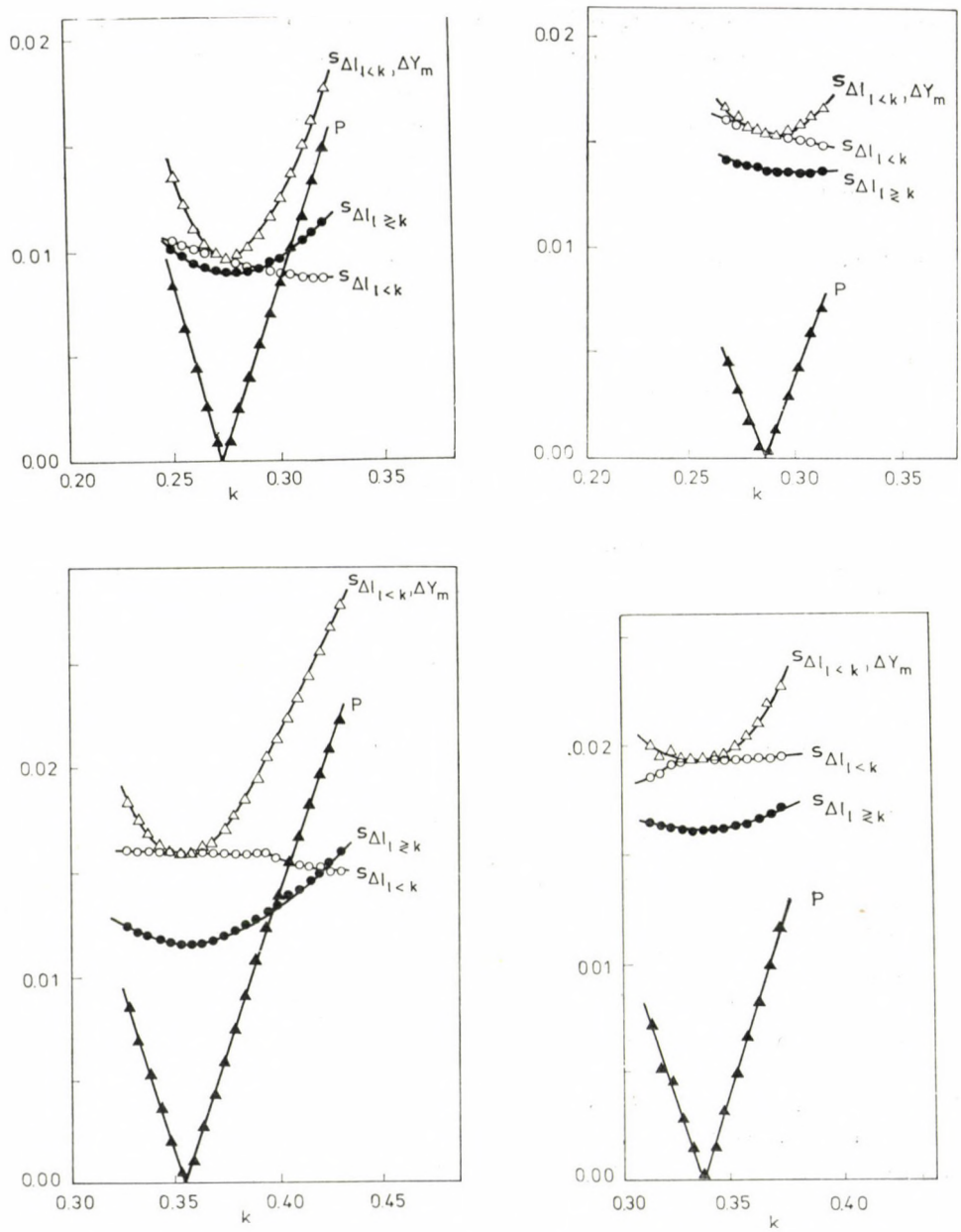

Fig. 2. Variation of different *s*-values and *P*-value characteristic for the accuracy of *l*-transformation in function of *k*-value in the course of iteration, in different cases. *a)* Spectral plate: Agfa-Gevaert 23 D 56. Recording: continuous spectrum of D-lamp with spectrograph type Q 24. Wave-length: 340 nm. *b)* Spectral plate: Agfa-Gevaert 23 D 56. Recording: Fe-spectrum (d.c. arc excitation) with spectrograph type Q 24. Wave-length: 340 nm. *c)* Spectral plate: Agfa-Gevaert 23 D 50. Recording: Fe-spectrum (d.c. arc excitation) with spectrograph type Q 24. Wave-length: 300 nm. *d)* Spectral plate: ORWO WU 3. Recording: Fe-spectrum (d.c. arc excitation) with PGS-2 grating spectrograph. Wave-length: 300 nm

spectra have been investigated, and both prism and grating spectrographs were used. For stepped attenuation of light intensity before the slit of spectrograph either two steps of three-step filter built into the apparatus, or the selective γ-compensating two-step filter constructed by NAGY have been applied [19]. Varying light amount were produced by changing intensity or exposure time depending on the other conditions of experiment. In the case of line spectra determinations were mostly performed with iron spectrum. At single wave-length appropriate number of data pairs were created with close lines falling into a narrow (4—6 nm) range. Effects originating from the change of exposure in function of the time (intermittence, *etc.)* were generally reduced by d.c. excitation. The concrete experimental conditions are briefly described at the corresponding investigations.

REFERENCES

[1] HURTER, F., DRIFFIELD, V. C.: J. Soc. Chem. Ind., **9,** 455 (1890)
[2] KAISER, H.: Spectrochim. Acta, **3,** 518 (1949)
[3] MIKA, J., TÖRÖK, T.: Analytical Emission Spectroscopy, ed. Akadémiai Kiadó, Budapest and Butterworths, London, 1973, p. 419
[4] ZIMMER, K.: D.Sc. Thesis, Budapest, 1970
[5] ZIMMER, K.: Rev. Roum. de Chim., **10,** 707 (1965)
[6] ZIMMER, K.: Magy. Kém. Folyóirat, **72,** 413 (1966)
[7] CHURCHILL, J. R.: Ind. Eng. Chem. Anal. Ed., **16,** 653 (1944)
[8] TÖRÖK, T.: Photography in Quantitative Spectral Analysis without the Use of Reference Samples. Publication of the Institute for Special Engineering Studies, Budapest, V. 59, II (1948)
[9] TÖRÖK, T.: Annales Univ. Sci. Budapest, Sect. Chim., **2,** 415 (1960)
[10] TÖRÖK, T.: Acta Geol. et Geogr. Univ. Comenianae, Bratislava, Geol., **6,** 122 (1959)
[11] van CALKER, J., KASSELMAN, H.: Z. Anal. Chem., **198,** 143 (1963)
[12] KÁNTOR, T.: Dissertation, Budapest, 1965
[13] PLŠKO, E.: Chem. Zvesti, **23,** 150 (1969)
[14] TÖRÖK, T., ZIMMER, K.: Quantitative Evaluation of Spectrograms by Means of *I*-Transformation, ed. Akadémiai Kiadó, Budapest and Heyden and Sons, London (1972)
[15] MATHERNY, M.: Kém. Közlem., **48,** 363 (1977)
[16] MATHERNY, M.: Kém. Közlem., **48,** 365 (1977)
[17] FLÓRIÁN, K., MATHERNY, M.: Spectrochim. Acta, **33 B,** 429 (1978)
[18] TÖRÖK, T., ZIMMER, K.: Acta Chim. Acad. Sci. Hung., **41,** 97 (1964)
[19] NAGY, Z.: Magy. Kém. Folyóirat, **73,** 104 (1967)

Karol FLÓRIÁN Košice, Czechoslovakia 04385, Švermova 9
György HELTAI H-2103 Gödöllő
Károly ZIMMER H-1443 Budapest, P. O. Box 123.

Acta Chimica Academiae Scientiarum Hungaricae, Tomus 102 (3), pp. 289—296 (1979)

A NOVEL AMIDE-PROTECTING GROUP

A. JUHÁSZ and S. BAJUSZ

(Institute for Drug Research, Budapest)

Received January 6, 1978
Accepted for publication January 8, 1979

Application of 2,2',4,4'-tetramethoxybenzhydryl (Tbh), a new amide-protecting group is reported. Protected amides can be prepared by condensing the corresponding carboxyl compounds with Tbh—NH_2, the synthes of which is also described. The acid lability of Tbh is similar to that of *t*-butyloxycarbonyl (Boc), thus it can readily be removed by acidolysis in trifluoroacetic acid at room temperature.

In the synthesis of asparagine and glutamine peptides the ω-amide group can be involved in side reaction [1—3] and can increase the hydrophilic character of certain intermediates, making their isolation and purification difficult [4]. To overcome these difficulties, protection of the amide group has been proposed. Thus the use of xanthyl- [5], 2,4-dimethoxy- or 2,4,6-trimethoxybenzyl- [6] and 4,4'-dimethoxybenzhydryl- [7] groups were described. Methoxybenzyl derivatives can be prepared by condensation of the corresponding carbonyl compound with benzylamine, while xanthyl- and 4,4'-dimethoxybenzhydrylamides are obtained by the acidcatalyzed alkalation of amides with xanthydrol and 4,4'-dimethoxybenzhydrol, respectively. Each group can be cleaved by acidolysis, *e.g.* with HBr in AcOH or TFA in the presence of cation acceptors such as anisol. In respect of the ease of removal, the 4,4'-dimethoxybenzhydryl group appeared to be the most promising.

Even in this case, however, we observed difficulties when larger peptides were deblocked. Complete removal of the 4,4'-dimethoxybenzhydryl group requires either a long reaction time or elevated temperature, and in both cases side reactions can occur in the acid sensitive portion of the peptide.

Obviously a protective group with greater acid lability could be removed under milder conditions. For obtaining such a blocker the simpliest way seemed to be the introduction of further methoxyl groups into the 4,4'-dimethoxybenzhydryl moiety whereby the electron density at the carbon atom between the benzene rings as well as the hydrophobic character would increase. Thus the use of 2,2',4,4'-tetramethoxybenzhydryl group was considered. This paper describes the preparation of the new reagent and some experiences on its applications.*

* Abbreviations are those recommended by IUPAC-IUB Biochem. J., **126**, 773 (1972). In addition, DCC stands for dicyclohexylcarbodiimide, Mbh for 4,4'-dimethoxybenzhydryl, Tbh for 2,2',4,4'-tetramethoxybenzhydryl, TCP for 2,4,5-trichlorophenyl, TFA for trifluoroacetic acid and DMF for dimethylformamide.

Acta Chim. Acad. Sci. Hung. 102, 1979

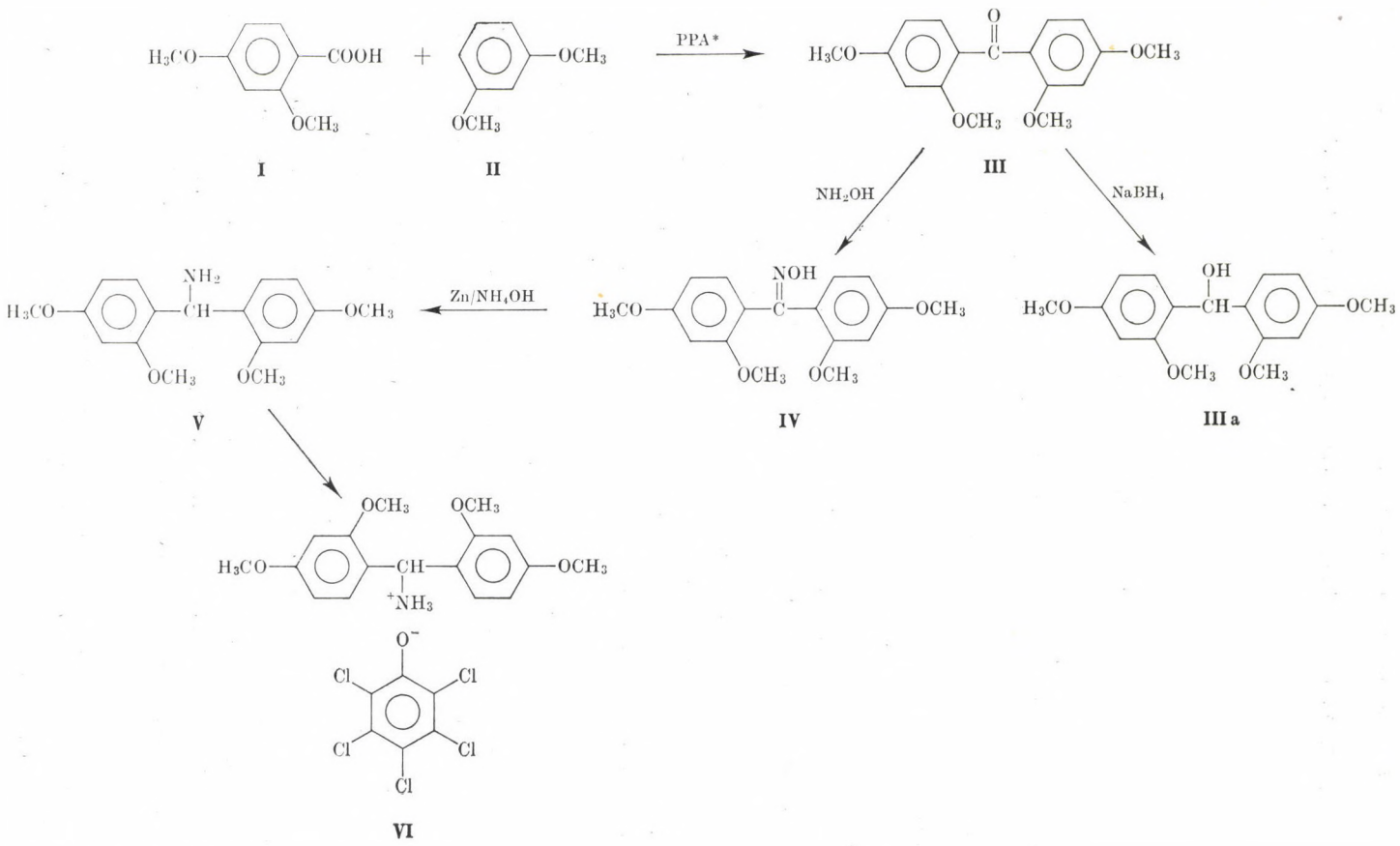

*PPA = polyphosphoric acid

Fig. 1. Synthesis of 2,2',4,4'-tetramethoxybenzhydrylamine

The synthesis of the new reagent started from 2,2',4,4'-tetramethoxybenzophenone which was first prepared by VANALLAN [8]. The original procedure was significantly improved by some modification.

Condensation of 2,4-dimethoxybenzoic acid (**I**) and resorcinol dimethyl ether (**II**) gave in the presence of polyphosphoric acid 2,2',4,4'-tetramethoxybenzophenone (**III**) in an excellent yield. As the corresponding benzhydrol (**IIIa**) prepared by the sodium borohydride reduction of **III** did not react with amides, the benzhydrylamine was prepared.

Treatment of **III** with hydroxylamine in ethanol gave the oxime (**IV**), which was reduced by zinc dust in ammonium hydroxyde [9] to the corresponding amine (**V**).

Although this compound is a solid, its melting point is very low; therefore its pentachlorophenolate salt (**VI**) was used in further experiments (Fig. 1).

The protected amides can be synthesized either from an appropriate activated ester and **V**, or from the corresponding carboxyl compound and **VI** by DDC condensation (Table I).

In spite of its bulkiness, the new group did not hinder the reactions of the protected amino acids and peptides blocked on the amino or carboxyl terminus or on both (Table II).

The Tbh-protected derivatives crystallize readily and, as expected, their solubility in organic solvents is greater than that of Mbh-protected compounds. The Tbh group is stable under the circumstances of peptide synthesis in solution, and resists catalytic hydrogenation. It can be removed much easier than the corresponding Mbh group under similar conditions and it can selectively be split off even in the presence of Boc groups (Table III).

It is a well known fact that Boc and other protecting groups which are split off as cations can alkylate the tryptophane residue(s) in peptides [10].

Table I

Preparation of Tbh derivatives

Derivative	Method	Yield, %	M.p. °C
Z-Gly-NH-Tbh (**VII**)	A	95	124—126
Z-Asn(Tbh)-ONB (**VIII**)	A	83	145—147
Z-Asn(Tbh)-ONB (**VIII**)	B	75	144—146
Z-Gln(Tbh)-OMe (**IX**)	A	88	111—112
Z-Gln(Tbh)-OMe (**IX**)	B	80	111—112
Z-Trp-Asn(Tbh)-Gly-OMe (**XIX**)	C	65	155—158

Methods: activated ester + **V** (A); free carboxylic acid + **VI** + DCC (B); Z-Trp + + Asn(Tbh)-Gly-OMe + DCC (C).

Table II

Transformation of Tbh derivatives

Product	Starting material	Type of reaction*	Yield, %	M.p., °C
H-Gly-NH-Tbh **(X)**	**(VII)**	H	95	119—120
Z-Asn(Tbh)OH **(XI)**	**(VIII)**	S	76	84—85
Z-Asn(Tbh)OTCP **(XIII)**	**(XI)**	DCC	88	—
Z-Gln(Tbh)OH **(XII)**	**(IX)**	S	95	95—97
Z-Gln(Tbh)OPCP **(XIV)**	**(XII)**	DCC	90	—
Z-Asn(Tbh)-Gly-OMe **(XV)**	**(XIII)** + Gly-OMe	AEC	95	126—127
H-Asn(Tbh)-Gly-OMe **(XVa)**	**(XV)**	H	90	92—94
Z-Gln(Tbh)-Leu-NH_2 **(XVI)**	**(XIV)** + Leu-NH_2	AEC	72	152
Z-Gln(Tbh)-Phe-OMe **(XVII)**	**(XII)** + Phe-OMe	DCC	86	134—135
Z-Gln-Phe-OMe **(XVIII)**	**(XVII)**	TFA	94	—
Z-Trp-Asn-Gly-OMe **(XIXa)**	**(XIX)**	TFA	*cca.* 30	—
Z-Trp(Tbh)-Asn-Gly-OMe **(XIX**b)	**(XIX)**	TFA	*cca.* 30	—
Z-Trp(Tbh)-Asn-Gly-OMe **(XIX**c)	**(XIX)**	TFA	*cca.* 30	—

* H = Hydrogenolysis; S = saponification; DCC = DCC coupling; AEC = activated ester coupling; TFA = acidolysis in TFA/CH_2Cl_2

Table III

Acid lability of the Tbh group of peptide amides[a]

Splitting mixture[b]	Time required for complete removal at 20 °C
80% TFA in chloroform	5 min
80% TFA in water	15 min[c]
50% TFA in dichloromethane	30 min[c]
25% TFA in dichloromethane	6 h
10% TFA in chloroform	24 h
2*N* HCl in ethanol	stable for 24 h
3*N* HCl in water	stable for days
2*N* citric acid in aqueous DMF	stable for days
3*N* oxalic acid in aqueous DMF	stable for weeks

[a] Complete cleavage of the Mbh group with the mixture of TFA/anisole (9 : 1) recommended [7] requires 2—3 h at 20 °C or 5 min at 70 °C (*cca.* 1 mmole Mbh-protected amino acid or peptide amide in 7 ml mixture).

[b] 1 ml/0.5 mmole Tbh-protected peptide amide.

[c] Less than 5 min in the case of Tbh-protected amino acid amides.

As Tbh is split off in the form of tetramethoxybenzhydryl cation, it also attacks the indole ring. When trying to cleave Tbh from Trp-containing peptides, the desired product were obtained in about 30% yield only. The alkylated products

appeared in the same yield, and sometimes a ninhydrine-positive compound was also formed in 30% yield. This means that while splitting off the Tbh group, the benzyloxycarbonyl function also was partly cleaved.

Thus the general use of the new protecting group is recommended for the synthesis of amide group containing peptides in the absence of tryptophane residues.

Experimental

2,2',4,4'-Tetramethoxybenzophenone (III)

2,4-Dimethoxybenzoic acid (55 g; 0.3 mole) and 45 g (0.35 mole) of resoricnol dimethyl ether were thoroughly mixed with 210 ml of commercial polyphosphoric acid, and the thick suspension was heated on a steam bath for 10 min. During the reaction a deep purple colour appeared and the mixture became clear. The reaction mixture was poured onto crushed ice and after standing for a few hours the precipitated pink crystals were collected, washed successively with water, 5% aqueous $NaHCO_3$ solution and water until the filtrate became neutral. The wet cake was dissolved in ethanol and water was added just to make the solution cloudy. Almost colourless crystals separated. After filtering and washing with water, the white powder was allowed to stand over P_2O_5 till attaining constant weight. Yield 91%, m.p. 135—136 °C (*lit.* [8] 38%, m.p. 134—136 °C).

$C_{17}H_{18}O_5$ (302.3). Calcd. C 67.53; H 6.00. Found C 67.48; H 6.05%.

2,2',4,4'-Tetramethoxybenzophenone oxime (IV)

A solution of 30.2 g (0.1 mole) of **III**, 19 g (0.264 mole) of hydroxyammonium chloride and 21.4 ml (0.264 mole) of pyridine in 150 ml ethanol was refluxed for 3 h. After evaporating the solvent the syrupy residue was dissolved in 200 ml $CHCl_3$ and 200 ml water. The organic layer was washed with 2% aqueous citric acid solution, water, 5% $NaHCO_3$ solution and again with water, and dried over anhydrous sodium sulfate. $CHCl_3$ was removed in vacuum and the residue triturated with ether. On standing overnight in a refrigerator, the oil crystallized. After filtering and washing with ether the white crystals were dried to yield 27.3 g (86%) of the product, m.p. 144—145 °C.

$C_{17}H_{19}O_5N$ (317.4). Calcd. C 64.34; H 6.03; N 4.41. Found C 64.45; H 6.14; N 4.48%.

2,2',4,4'-Tetramethoxybenzhydrylamine (V) and its pentachlorophenolate salt (VI)

Compound **IV** (21 g; 66.2 mmoles), 20 g (0.306 g-atom) of activated zinc dust, 2.4 g (31 mmoles) of ammonium acetate and 350 ml of concentrated ammonium hydroxide were placed into a round-bottomed flask and 75 ml of ethanol was added. The mixture was refluxed in a well-ventilated hood for 4 h. During this time the suspension became an emulsion of the desired amine. After removal of the ethanol, the suspension of zinc, zinc oxide and solid Tbh—NH_2 was filtered, and the filter cake was extracted twice with ether. The ethereal solution was dried and the solvent evaporated. The yellow oily residue (**V**) was dissolved in 200 ml anhydrous ether and 19 g (71.5 mmoles) of pentachlorophenol was added. A white, amorphous precipitate separated. After filtering and washing with ether the salt (**VI**) was dried over paraffin turnings to yield 28.3 g (75%) of the product, m.p. 88—90 °C.

$C_{23}H_{24}NO_5Cl_5$ (569.7). Calcd. C 48.47; H 4.24; N 2.46. Found C 48.49; H 4.23; N 2.46%.

Z-Gly-NH-Tbh (VII)

Z-Gly-OTCP (0.74 g; 1.9 mmoles) and 1.08 g (1.9 mmoles) of **V** were dissolved in 2 ml of DMF and allowed to react at room temperature for 2 h. After removal of the solvent the oily residue was taken up in 20 ml ether and 20 ml water was added. The protected amide separated, and after filtering and washing with ether it was recrystallized from ethyl acetate – ether to obtain 0.92 g (98%) of **VII**, m.p. 124—126 °C.

$C_{27}H_{30}O_7N_2$ (494.6). Calcd. C 65.58; H 6.11; N 5.66. Found C 65.66; H 6.07; N 5.81%.

Z-Asn (Tbh)-ONB (VIII)

Z-Asp (OTCP)-ONB (1.28 g; 2.2 mmoles) and 1.25 g (2.2 mmoles) of **V** were dissolved in 3 ml of DMF and allowed to react as above. The protected crude ester was crystallized from ethanol – water. Yield 1.25 g (83%), m.p. 145 °C.

$C_{36}H_{37}O_{11}N_3$ (687.7). Calcd. C 62.88; H 5.42; N 6.11. Found C 62.94; H 5.63; N 6.21%.

Z-Gln(Tbh)-OMe (IX)

Z-Glu (OPCP)-OMe (1.28 g; 2.36 mmoles) and 1.35 g (2.4 mmoles) of **V** were allowed to react as described above. The product was obtained as white crystals from $CHCl_3$ – n-hexane in a yield of 1.2 g (88%), m.p. 111—112 °C.

$C_{31}H_{36}O_9N_2$ (580.6). Calcd. C 64.12; H 6.25; N 4.84. Found C 64.26; H 6.44; N 4.83%.

The protected amides **VIII** and **IX** could be prepared by the DCC condensation of the free β- or γ-COOH containing derivatives and **VI**; the yields are somewhat lower than those of the activated ester couplings. The reactons were carried out as follows: 10 mmoles of free acid and 10 mmoles of **VI** were dissolved in 10 ml of $CHCl_3$; the solution was chilled in ice to 5 °C with stirring, and 10 mmoles of DCC was added. The mixture was allowed to react at 5°C for 1 h, and then 1 more at 20 °C. DCU was filtered off, the solvent evaporated and the residue crystallized from $CHCl_3$ – hexane. The yields were 75 and 85% respectively; m.p.'s and analytical data were the same as above.

Gly-NH-Tbh (X)

Compound **VII** (1.3 g; 2.65 mmoles) was dissolved in 10 ml of DMF, Pd-on-charcoal was added, and the solution was hydrogenated at atmospheric pressure. After 2 h the catalyst was filtered off, the solution evaporated in vacuum and the residue was triturated with ether. The product was crystallized from methanol – ether. Yield 0.9 g (95%), m.p. 119—120 °C.

$C_{19}H_{24}O_5N_2$ (360.4). Calcd. C 63.32; H 6.71; N 7.76. Found C 63.27; H 6.98; N 7.84%.

Z-Asn(Tbh)-OH (XI)

Compound **VIII** (1.25 g; 1.8 mmole) was dissolved in 10 ml of methanol and 1 ml of 4*M* NaOH was added. The solution became clear in a few minutes. After 3 h the solution was evaporated to dryness, the residue was triturated with ether, then with 5% aqueous citric acid rolution, filtered, and washed with water to obtain a white amorphous powder. This was recrystallized from methanol – ether to yield 0.75 g (76%) of **XI**, m.p. 84—85 °C.

$C_{29}H_{32}O_9N_2$ (552.6). Calcd. N 4.97. Found N 5.07%.

Z-Gln(Tbh)-OH (XII)

Compound **IX** (0.69 g) was treated as above to yield 0.64 g (95%) of **XII** m.p. 95—97 °C.

$C_{30}H_{34}O_9N_2$ (566.6). Calcd. C 63.59; H 6.05; N 4.94. Found C 63.35; H 6.11; N 5.01%.

Z-Asn(Tbh)-OTCP (XIII)

Compound **XI** (5.52 g; 10 mmoles) was dissolved in 20 ml of DMF, 2.2 g (11 mmoles) of 2,4,5-trichlorophenol was added, and the solution was cooled to 5 °C. DCC (2.3 g; 11 mmoles) was added with stirring in several portions and the reaction mixture was stirred for 1 h at room temperature. DCU was filtered off and the solution concentrated to a small volume. Ether was added and the filtered amorphous activated ester was washed with ether and dried; yield 6.44 g (88%).

$C_{35}H_{33}O_9N_2Cl_3$ (732.0). Calcd. Cl: 14.45; N 3.83. Found Cl 14.47; N 3.87%.

Z-Gln(Tbh)-OPCP (XIV)

DCC (2 g; 9.7 mmoles) was added, in several portions to a cooled solution of 5 g (8.82 mmoles) of **XII** and 2.66 g (10 mmoles) of pentachlorophenol in 20 ml of $CHCl_3$; the mixture was treated then as above to obtain 5.4 g (75%) of **XIV**.

$C_{36}H_{33}O_9N_2Cl_5$ (814.9). C 53.05; H 4.08; N 3.44. Found C 53.33; H 4.04; N 3.38%.

Z-Asn(Tbh)-Gly-OMe (XV)

Compound **XIII** (14 g; 19 mmoles) was added to a solution of 2.51 g (20 mmoles) of methyl glycinate hydrochloride and 2.8 ml (20 mmoles) of NEt_3 in 20 ml of DMF and the solution was allowed to stand 3 h at room temperature. After evaporating the solvent ether was added, and the separated crystals were collected, washed with ether and recrystallized from $CHCl_3$ – ether to yield 11.8 g (95%) of **XV**, m.p. 127 °C.

$C_{32}H_{37}O_{10}N_3$ (623.7). Calcd. N 6.73. Found N 6.69%.

Asn(Tbh)-Gly-OMe (XVa)

XV (3.6 g; 5.6 mmoles) in 20 ml of DMF was hydrogenated in the presence of Pd-on-charcoal. After 2 h the catalyst was filtered off, the solution was evaporated, and the residue crystallized from methanol – ether. Yield 2.54 g (90%), m.p. 92—94 °C.

$C_{25}H_{33}O_8N_3$ (503.5). Calcd. N 8.35. Found N 8.29%.

Z-Gln(Tbh)-Leu-NH_2 (XVI)

To a solution of 0.78 g (6.2 mmoles) of leucine amide in 10 ml of DMF, 4.76 g (5.95 m(moles) of **XIV** was added and the reaction mixture was worked up as usual. Yield 3.03 g 72%), m.p. 152 °C.

$C_{36}H_{46}O_8N_3$ (678.8). Calcd. N 6.19. Found N 6.22%.

Z-Gln(Tbh)-Phe-OMe (XVII)

Phe-OMe. HCl (0.5 g; 2.3 mmoles) in 10 ml of DMF was treated with 0.32 ml (2.3 mmoles) of NEt_3 and 1.14 g (2 mmoles) of **XII** was added. The solution was cooled to 5 °C, 0.6 g (2.3 mmoles) of DCC was added, and the mixture was allowed to stand for 1 h at 5 °C and 1 h more at 20 °C. DCU was filtered off and the solvent evaporated. The residue was taken up in 20 ml of $CHCl_3$ and washed successively with 5% aqueous citric acid solution, water, 5% aqueous $NaHCO_3$ solution and water; the organic layer was then dried and concentrated to a small volume. Ether was added and the substance which precipitated was filtered off, washed with ether and dried to obtain 1.25 g (86%) of the product, m.p. 134—135 °C.

$C_{40}H_{45}O_{10}N_3$ (727.8). Calcd. C 66.02; H 6.23; N 5.77. Found C 66.05; H 6.44; N 5.66%.

Illustrative deprotection

Compound **XVII** (0.72 g; 1 mmole) was dissolved in 0.5 ml of $CHCl_3$ and 1.5 ml of TFA was added. After 15 min the solvents were evaporated in vacuum at 20 °C and the residue was rubbed with ether, filtered and washed. Z-Gln-Phe-NH_2 (**XVIII**) thus obtained could be crystallized from methanol – ether. Yield 0.44 g (94%), m.p. 155—166 °C.

$C_{23}H_{27}O_6N_3$ (441.5). Calcd. C 62.57; H 6.61; N 9.51. Found C 62.44; H 6.21; N 9.48%.

Z-Trp-Asn(Tbh)-Gly-OMe (XIX)

Asn (Tbh)-Gly-OMe (**XVa**) (4.88 g; 10 mmoles) and 3.4 g (10 mmoles) of Z-Trp-OH were dissolved in 20 ml of DMF and 5 g (10 mmoles) of DCC · 3 HOPCP complex was added at 0 °C. After stirring for 4 h, DCU was filtered off, the solvent evaporated and the residue triturated with ether to yield 4.95 g (65%) of **XIX**.

$C_{43}H_{47}O_{11}N_5$ (809.9). Calcd. N 8.64. Found N 8.55%.

Deprotection of Z-Trp-Asn(Tbh)-Gly-OMe (XIX)

100 mg each of **XIX** was dissolved in 1 ml of the following solvent systems:
TFA–water–indole (8 : 1 : 1)
80% TFA in methylene chloride
TFA–water–mercaptoethanol (70 : 15 : 15)

After 30 min the reactions showed identical patterns on TLC (ethyl acetate–pyridine–acetic acid–water 72 : 1.5 : 0.45 : 0.82), *i.e.* the same three spots appeared with R_f values of
0.14—0.26,
0.29—0.31 and
0.49—0.61 respectively.

The lower spot (R_f 0.14—0.26) gave a positive reaction with ninhydrine indicating that the peptide had lost its benzyloxycarbonyl function during deprotection. Elementary analysis of the isolated material (20 mg; about 30%) indicated a structure of Trp(Tbh)-Asn-GlyOMe.

$C_{35}H_{41}O_9N_5$ (675.6). Calcd. C 62.21; H 6.12; N 10.36. Found C 62.28; H 6.21; N 10.31%.

The second spot (R_f 0.29—0.31) was found to be the desired, partially deprotected peptide Z-Trp-Asn-Gly-OMe; yield 20 mg (30%).

$C_{26}H_{29}O_7N_5$ (523.5). Calcd. C 59.64; H 5.58; N 13.37. Found C 59.72; H 5.62; N 13.33%.

The third product (25 mg; 25%) represented by the fastest moving spot (R_f 0.49—0.61) had the same elementary analysis as the starting material Z-Trp-Asn(Tbh)-Gly-OMe, the R_f value of the latter was, however, higher (0.77—0.83). Obviously, the leaving Tbh cation alkylated the tryptophane ring thus the molecular weight and elementary analysis data remained unchanged, but the mobility decreased due to the free amide function.

$C_{43}H_{47}O_{11}N_5$ (809.9). Calcd. C 63.77; H 5.85; N 8.65. Found C 63.70; H 5.88; N 8.64%.

Deprotection of **XIX** with mercaptoethanesulfonic acid (3.5*M* in acetic acid) afforded the desired and the transalkylated products, *i.e.* Z-Trp-Asn-Gly-OMe and Z-Trp(Tbh)-Asn-Gly-OMe, in the same proportion.

REFERENCES

[1] SCHRÖDER, E., LÜBKE, K.: The Peptides, Vol. I, pages 110, 191, 202; Academic Press, New York, London 1965
[2] SCHNABEL, E., KOSTERMEYER, H., DAHLMANS, J., ZAHN, H.: Ann., **707,** 232 (1967)
[3] ZAHN, H., FÖLSCHE, E. Th. J.: Chem. Ber., **102,** 2158 (1969)
[4] BAJUSZ, S., TURÁN, A., FAUSZT, I., JUHÁSZ, A.: In Peptides 1972 (H. HANSON, H-D JAKUBKE, eds.) p. 93., North Holland Publishers, Amsterdam, 1973
[5] AKABORI, S., SAKAKIBARA, S., SHIMONISHI, Y.: Bull. Chem. Soc. Japan, **34,** 739 (1961); **35,** 1966 (1962)
SAKAKIBARA, S., SHIMONISHI, Y., KISHIDA, Y., OKADA, M., SUGIHARA, H.: Bull. Chem. Soc. Japan, **40,** 2164 (1967)
[6] WEYGAND, F., STEGLICH, W., BJARNASON, J., AKHTAR, R., CHYTIL, N.: Chem. Ber., **101,** 3623, 3642 (1968)
WEYGAND, F., STEGLICH, W., BJARNASON, J., AKHTAR, R., KHAN, N. M.: Tetrahedron Letters, **1966,** 3483
[7] KÖNIG, W., GEIGER, R.: Chem. Ber., **103,** 2041 (1970)
[8] VANALLAN, J. A.: J. Org. Chem., **23,** 1679 (1958)
[9] JOCHIMS, J. C.: Monatshefte, **94,** 677 (1963)
[10] ALAKHOV, YU. B., KIRYUSHKIN, A. A., LIPKIN, V. M., MILNE, G. W. A.: Chem. Commun., **1970,** 406

Attila JUHÁSZ
Sándor BAJUSZ
H-1325 Budapest, P. O. Box 82.

Acta Chimica Academiae Scientiarum Hungaricae, Tomus 102 (3), pp. 297—304 (1979)

CONFORMATIONAL AND CONFIGURATIONAL STUDIES ON 3,7-DIAZABICYCLO[3.3.1]NONANE DERIVATIVES, II*

P. SCHEIBER and K. NÁDOR

(Department of Chemistry, Veterinary University, Budapest)

Received October 9, 1978

Accepted for publication January 8, 1979

The conformation and configuration of some *N*-substituted bispid-9-ones and bispidin-9-ols were investigated through analysis of the results obtained from dipole moment and PMR measurements.

The chair-boat form was found to be the predominant conformation of both the 9-keto and 9-hydroxy derivatives. The application of lanthanide shift reagents provided a useful method to assign the relative configuration of the C(9) atom in the case of asymmetrically *N*-substituted bispidin-9-ols.

Introduction

The conformation of compounds having bicyclo-[3.3.1]nonane carbocyclic ring structure has been relatively well established, and their chair-chair form was found experimentally [2] and theoretically [3] to be the most stable one. Conformations of the 3,7-diaza analogues have been, in contrast, less studied, and the results obtained previously by different authors [1, 4—6] are not fully consistent. The main tasks are to find out the probable conformation of the six-membered rings and the steric orientation of the *N*-substituents in the 9-keto compounds, moreover to reveal the C(9)-configuration of the asymmetrically *N*-substituted 9-hydroxy derivatives.

In this paper we describe the results obtained from dipole moment measurements and proton magnetic resonance studies on the 3,7-dimethyl- and 3-methyl-7-ethyl-3,7-diazabicyclo[3.3.1]nonan-9-ones (**I**, **II**) [4] and their 9-hydroxy derivatives (**III**, **IV**, **V**) [7]. For the sake of brevity, the bicyclic skeleton of these compounds will be named bispidine, following MANNICH's nomenclature [8].

Results

The measured dipole moments whose magnitudes depend on the relative steric position of the dipolar chemical bonds, are shown in Table I.

* Part I, see Ref. [1]

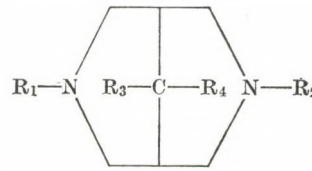

	R_1	R_2	R_3	R_4
I	CH_3	CH_3	=O	
II	CH_3	C_2H_5	=O	
III	CH_3	CH_3	H(OH)	OH(H)
IV	CH_3	C_2H_5	OH	H
V	CH_3	C_2H_5	H	OH

In order to determine the probable conformation of the amino-ketones **I** and **II**, the dipole moments of the possible conformations were also calculated from the moments of the individual dipolar groups. In our calculations the bond moments $\mu_{C=O} = 3.10$ D and $\mu_{NR_3} = 0.80$ D obtained previously [9, 10] were applied. The bond angles were regarded as tetrahedral. Only those conformations were taken into consideration which could be constructed with

Table I

*Experimental results of dipole moment measurements**

Compound	a_ε**	a_n+	μ++
3,7-Dimethylbispid-9-one, **I**	7.26	−0.10	3.38 D
3-Methyl-7-ethylbispid-9-one, **II**	7.20	0.06	3.46 D
3,7-Dimethylbispidin-9-ol, **III**	3.52	0.00	2.35 D
3-Methyl-7-ethylbispidin-9β-ol, **IV**	3.32	0.09	2.34 D
3-Methyl-7-ethylbispidin-9α-ol, **V**	3.22	0.06	2.32 D

* Measured in benzene solution at 25.0 C

** a_ε is defined as the slope of the straight line function of dielectric constant increments of benzene solutions *versus* the concentration expressed in weight fraction of the solute, w_2 ($\Delta\varepsilon = a_\varepsilon \cdot w_2$)

\+ a_n is defined similarly as a_ε for increments in quadratic refractive indices, n^2 ($\Delta n^2 = a_n \cdot w_2$)

\++ Calculated by the equation:

$$\mu^2 = \frac{27kT}{4\pi N} \cdot \frac{M}{(\varepsilon_1 + 2)^2 d_1} \cdot (a_\varepsilon - a_n) \text{ [16]}.$$

Dreiding models. The chair (C) and boat (B) conformation of the six-membered rings and the *axial* (*a*) or *equatorial* (*e*) steric position of the alkyl group attached to the tertiary nitrogen atom were varied when establishing the conformers. The calculated dipole moments agree with those calculated for 1,5-diphenyl-*N*,*N*'-dimethylbispid-9-one [1] and are summarized in Table II.

Table II

*Calculated dipole moments of the N,N'-dimethylbispidone conformers**

Conformation	CC_{ee}	CC_{ea}	CB_{ee}	CB_{ae}	CB_{aa}	CB_{ea}	BB_{ee}	BB_{ea}	BB_{aa}
Dipole moment (D)	2.17	2.53	3.43	3.51	2.17	2.53	4.63	3.51	2.17

* Abbreviations: C = chair, B = boat, *e* = *equatorial*, *a* = *axial*

In the PMR spectrum of **I**, the *N*-methyl groups show only one sharp singlet at room temperature. The methylene and the bridgehead protons have a broad and highly complex multiplet. Similarly, in the spectrum of **II** a singlet and a triplet can be found, due to the N—CH_3 and the N—CH_2CH_3 groups, respectively.

Insertion of the hydroxyl group into the C(9) position influences the chemical shifts of the *N*-alkyl groups differently. The absorption lines of the compounds investigated are assembled in Table III.

Table III

PMR spectral data of N,N'-dialkylbispidines*

Compound	N—CH_3	N—CH_2CH_3	C—CH_2—N, | —CH—	C(9)—H
N,*N*'-Dimethylbispid-9-one, **I**	2.24 s	—	2.35—3.22 m	—
N-Methyl-*N*'-ethylbispid-9-one, **II**	2.24 s	1.00 t	2.30—3.20 m	—
N,*N*'-Dimethylbispidin-9-ol, **III**	2.15 s			
	2.14 s	—	1.85—3.02 m	3.40 t
N-Methyl-*N*'-ethylbispidin-9β-ol, **IV**	2.11 s	0.95 t	1.83—3.20 m	3.35 t
N-Methyl-*N*'-ethylbispidin-9α-ol, **V**	2.15 s	0.97 t	1.80—3.20 m	3.35 t

* Chemical shifts in ppm (δ scale)

In the study of the conformation of **III**, and that of the configurations of **IV** and **V** by NMR spectroscopy, the application of lanthanide shift reagents (LSR) has proved helpful. The magnitudes of the lanthanide-induced shifts

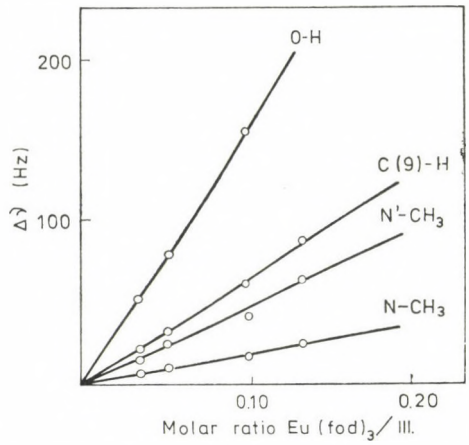

Fig. 1. LIS values *vs.* the molar ratio Eu $(fod)_3$/3,7-dimethylbispidin-9-ol (**III**)

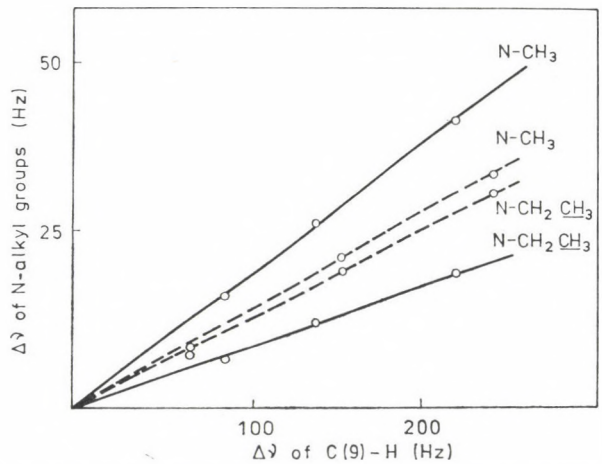

Fig. 2. LIS values of the *N*-alkyl groups *vs.* the LIS of the C(9)—H proton in compounds **IV** (solid lines) and **V** (dotted lines)

(LIS) of the *N*-alkyl groups are distinctly different, permitting conclusions about the stereochemistry of the substrate under examination. Upon adding a known amount of the fluorine containing shift reagent $Eu(fod)_3$, the greatest induced shielding was exhibited by the OH proton. Likewise, the signal of the C(9)—H was also strongly shifted, but somewhat less than that of the former. This proves that complex formation takes place between the LSR and the hydroxyl group of compounds **III**, **IV** and **V**. The plot of the LIS against the ratio LSR/substrate in the case of *N*,*N*'-dimethylbispidin-9-ol (**III**) gave a nearly straight line for the different kinds of protons as illustrated in Fig. 1.

As the effect of LSR is very markedly influenced even by traces of moisture, which might occur in the sample, solvent, NMR tube, *etc.*, in order to obtain comparable LIS data for isomers **IV** and **V**, the induced shifts were plotted in another manner than usually done; the shifts of the *N*-alkyl groups were plotted against the shift of the C(9)—H proton (Fig. 2), having taken into consideration that the site of complexation, *i.e.* the C(9)—OH group, is in the same environment in both molecules and, in consequence, an identical effect of the Eu atom on the C(9)—H proton can be expected.

Discussion

Analysis of the dipole moments. The conformation of bispid-9-ones

Comparison of the measured (Table I) and calculated (Table II) dipole moments makes possible to find the probable conformation(s) among the different possible geometries. In this way the conformations CB_{ee}, CB_{ae} and BB_{ea} (for abbreviations *cf.* Table II) should be taken into consideration. The appearance of the poorly resolved, highly complicated "ethylene envelope" between δ 2.3—3.2 ppm does not preclude unambiguously the possibility of the BB_{ea} form, nevertheless the existence of both six-membered rings in boat conformation, because of their unfavourable steric structure, should be considered slightly probable. Although the more stable chair form of six-membered rings [11] is present in the twin-chair conformation CC, the dipole moment data indicate that to be unlikely.

As a result it can be concluded that *N,N'*-dimethylbispidone (**I**) has a chair-boat conformation. The two kinds of the CB conformations are characterized by dipole moments of essentially the same magnitude, hence differentiation between them, in other words the exact determination of the steric orientation of the lone pair on the tertiary nitrogen atom by an analysis of the dipole moments, cannot be anticipated at all. It is well known that nitrogen inversion readily takes place at room temperature [12], and the *N*-methyl group favours the *equatorial* site at equilibrium [13, 17]. Therefore, by analogy, it can be said that *N,N'*-dimethylbispid-9-one assumes a chair-boat conformation with *equatorial* *N*-methyl substituents. This conclusion is in accordance with our results [1] obtained previously for 1,5-diphenyl-*N,N'*-dimethylbispid-9-one. The phenyl groups have, therefore, no serious influence on the conformation of the diazabicyclic ring system studied.

The simple PMR spectrum of 1,5-diphenyl-*N,N'*-dimethylbispid-9-one described previously [1] was interpreted by a rapid CB $\rightleftharpoons$ BC ring inversion resulting in a time-averaged AB pattern for the CH_2 groups. In the present case the spin system is more complicated and does not allow a first order

analysis of the spectra. The rapid equilibrium between the chair and boat form seems, however, very likely.

The dipole moment of *N*-methyl-*N'*-ethylbispid-9-one (**II**) (3.46 D) is nearly equal to that of *N,N'*-dimethylbispid-9-one (**I**). Obviously, its conformation agrees with the CB conformation of the dimethyl derivative (**I**), bearing in mind the similar slight difference between the dipole moments of *N*-methyl- and *N*-ethylpiperidine (0.80 D and 0.77 D, respectively) [10].

Conformation and configuration of bispidin-9-ols

The methyl groups of *N,N'*-dimethylbispidin-9-ol (**III**) show markedly different behaviour in the PMR study carried out in the presence of $Eu(fod)_3$ (Fig. 2). As the strongest effect of the shift reagent can be observed in the case of the OH proton, it can be inferred that the site of the coordination is the oxygen atom. This suggestion is supported by the fact that the C(9)—H proton displays a greater shift than the protons of any other kind in the molecule. Considering the chair-chair form of *N,N'*-dimethylbispidin-9-ol (**III**), owing to the nearly similar distances between the Eu atom and the CH_3 groups, one would suspect their nearly equal shielding. In fact, one of the *N*-methyl groups shows an approximately 2.5-fold greater induced shielding than the other. This observation might be rationalized with a chair-boat conformation of **III**,

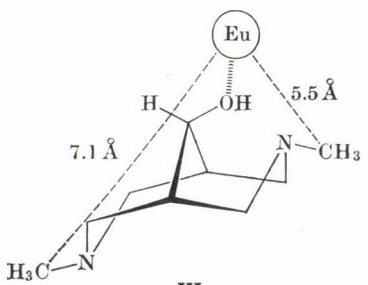

III

in which the methyl group of the boat ring is positioned in the proximity of the OH group.

Assuming that the interaction of lanthanide complexes is predominantly pseudocontact, the magnitude of the LIS is inversely proportional to the cube of the average distance from the metal ion [14]. If the angle term is regarded as constant, the LIS depends on the distance parameter only, which can be expressed in a simplified form as $\Delta\nu = b/r^3$.

If we take for the bond length Eu—O 2.45 Å [15], and the Eu atom is assumed to lie in the bisector of the C(9)—O—H angle in the symmetry plane of the molecule, the resulting distances of the methyl groups measured from the

Eu atom are approximately 5.5 and 7.1 Å (see the perspective figure of **III**). Considering such a geometry, the ratio of the LIS of the *N*-methyl groups calculated by the above equation would be about 2.2. As the observed ratio of the LIS values is somewhat greater, it may be assumed that the nitrogen atom in the ring of the boat form may also assist in complexing with LSR, resulting in a pronounced difference between the effects on the *N*-methyl groups. It should be noted that although such an approach of determining the position of the Eu atom is not precise, the geometry arising from it is suitable for decision between the two alternatives.

The existence of **III** in a chair-boat conformation with a transannular N. . .OH hydrogen bond is supported by infrared spectroscopy. In a 0.1*M* $CHCl_3$ solution the OH absorption appeared at 3270 cm^{-1}, which remained unchanged upon tenfold dilution and no absorption band of the free OH group near to 3620 cm^{-1} was observed. The appreciable decrease in the wavenumber of the OH absorption can be interpreted by the formation of a strong intramolecular hydrogen bond [6].

The relative configuration of epimeric 3-methyl-7-ethylbispidin-9-ols (**IV** and **V**) can also be deduced from the PMR spectra run with $Eu(fod)_3$. The plot in Fig. 2 clearly suggests that the C(9) epimer showing the largest $N—CH_3$ and the least $N—CH_2CH_3$ lanthanide-induced shifts should have β* configuration (**IV**), and the other, having similar measures of LIS values, bears con-

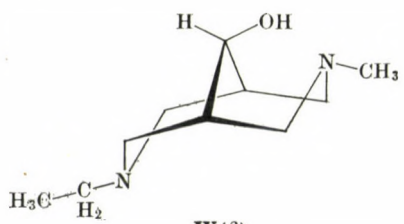

IV (β)

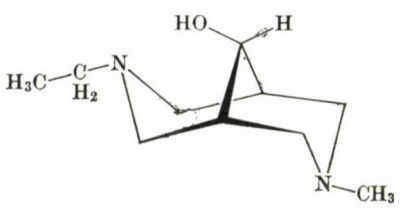

V (α)

sequently the hydroxyl group in α position (**V**). The LIS values of both isomers are in a good agreement with the approximate intramolecular distances obtained by inspection of the Dreiding stereomodels.

Further arguments for the identical conformational behaviour of the diazabicyclic alcohols **III**, **IV** and **V** are provided by the dipole moments (Table I). Although it was not possible to add the individual group moments vectorially due to the formation of intramolecular hydrogen bonds, the very good agreement of the dipole moments measured in benzene solution reveals that these compounds have the same conformation, as outlined above.

* The assignment of the C(9) configuration as α and β is based on the *N*-methyl-OH distance, as generally used in alkaloid chemistry.

Experimental

Synthesis of compunds

Compounds **I** and **II** were prepared by known methods [4]; the procedure was, however, modified and improved in this laboratory [7].

The *N,N'*-dialkylbispidin-9-ols were obtained from **I** and **II** by reduction and in the case of **II** subsequent separation of the C(9) epimeric alcohols. The melting points were 130—31 °C, 98—99 °C and 88—89 °C, for **III**, **IV** and **V**, respectively. A detailed description of the syntheses will be published elsewhere [7].

Measurements

The dipole moments were determined by measurement of the dielectric constants and the refractive indices in dilute benzene solutions at 2 MHz and 589 nm, respectively. The evaluation of the experimental data and the instruments used have been described in detail previously [16]. The a_ε and a_η values, *i.e.* the slopes of the straight line function of the dielectric constants (ε) and quadratic refractive indices (n^2) *versus* the concentration of the benzene solution are summarized in Table I.

All nuclear magnetic resonance spectra were recorded at 80 MHz on a Tesla BS 487 A spectrometer. The samples were dissolved in $CDCl_3$, and hexamethyldisiloxane was used as internal standard.

The shift reagent tris(6,6,7,7,8,8,8-heptafluoro-2,2-dimethyl-3,5-octanedionato) europium $Eu(fod)_3$ was obtained commercially (Aldrich Resolve-Al EuFOD) and stored in a desiccator. During the LIS measurements the concentration of **III** was maintained at 1.60*M* (14.7 *w*/*w*%). The molar ratio LSR/substrate was kept in the range 0.033—0.133. Extrapolation to the unit molar ratio yielded $\Delta\delta$2.13 ppm, 5.50 ppm, 7.75 ppm and 19.38 ppm induced shifts for the N—CH_3, N'—CH_3, C(9)—H and OH protons, respectively. The concentration of the epimeric alcohols **IV** and **V** was about 1.50*M* (*cca.* 15 *w*/*w*%); after adding the LSR, the molar ratio LSR/substrate varied in the range of about 0.1—0.3.

REFERENCES

[1] Scheiber, P., Nádor, K.: Acta Chim. Acad. Sci. Hung., **84,** 193 (1975)
[2] (a) Brown, W. A. G., Martin, J., Sim, G. A.: J. Chem. Soc., **1965,** 1844;
(b) Macrossen, W. D. K., Martin, J., Parker, W.: J. Chem. Soc., **1965,** 2589
[3] Allinger, N. L., Tribble, M. T., Miller, M. A., Wertz, D. H.: J. Am. Chem. Soc., **93,** 1637 (1971)
[4] Douglass, J. E., Ratliff, T. B.: J. Org. Chem., **33,** 355 (1968)
[5] Chakrabarty, M. R., Ellis, R. L., Roberts, J. L.: J. Org. Chem., **35,** 541 (1970)
[6] Smissman, E. E., Ruenitz, P. C.: J. Med. Chem., **19,** 184 (1976)
[7] Sinko, K., Kraiss, G., Nádor, K.: To be published
[8] Mannich, D., Mohs, P.: Ber., **63,** 608 (1930)
[9] Le Févre, C. G., Le Févre, R. J. W., Rao, B. P.: J. Chem. Soc., **1959,** 2340
[10] Bishop, R. J., Deneen, D., Jones, R. A. Y., Katritzky, A. R., Sutton, L. B., Wyatt, R. J.: J. Chem. Soc., **1967,** 493
[11] Eliel, E. L., Allinger, N. L., Angyal, S. J., Morrison, G. A.: Conformational Analysis, p. 36. Interscience Publ., 1965
[12] Lehn, J. M., in Topics in Current Chemistry, Band 15/3, p. 311. Springer-Verlag, 1970
[13] (a) Bishop, R. J., Fodor, G., Katritzky, A. R., Sóti, F., Sutton, L. E., Swinbourne, F. J.: J. Chem. Soc. (C), **1966,** 74;
(b) Scheiber, P., Kraiss, G., Nádor, K.: J. Chem. Soc. (B), **1970,** 1366
[14] Mayo, B. C.: Chem. Soc. Rev., **2,** 49 (1973)
[15] Dyer, D. S., Cunningham, J. A., Brooks, J. J., Sievers, R. E., Rondeau, R. B. in Nuclear Magnetic Resonance Shift Reagents, edited by R. E. Sievers p. 38. Academic Press, 1973
[16] Scheiber, P., Kraiss, G., Nádor, K., Neszmélyi, A.: J. Chem. Soc. (B), **1971,** 2149

Pál Scheiber
Károly Nádor
H-1400 Budapest, P. O. Box 2.

Acta Chimica Academiae Scientiarum Hungaricae, Tomus 102 (3), pp. 305–315 (1979)

AN ANOMALOUS REACTION BETWEEN PYRIDINECARBOXALDEHYDE AND BENZYL CYANIDE IN POLYPHOSPHORIC ACID

THE SYNTHESIS OF 4-PICOLINYL-1-PYRIDYL-3(2*H*)-ISOQUINOLINONE

L. HAZAI[1], Gy. DEÁK[1], G. SZABÓ[1]* and E. KOLTAI[2]

([1]*Institute of Experimental Medicine, Hungarian Academy of Sciences, Budapest, and* [2]*Institute for Drug Research, Budapest)*

Received October 6, 1978
Accepted for publication January 18, 1979

4- and 3-Pyridinecarboxaldehyde and benzyl cyanide were converted into 1-pyridyl-1,4-dihydro-3(2*H*)-isoquinolinones **1** and **8**, respectively, in PPA having a high (84.0 or 82.8%) P_2O_5 equivalence, while in PPA with a 76% P_2O_5 equivalence the 4-picolinyl-1-pyridyl-3(2*H*)-isoquinolinones, **2** and **10**, respectively, were obtained in satisfactory yields. When using a shorter reaction time, 4-pyridinecarboxaldehyde gave the bis-amide **4** too, while in the reaction of 3-pyridinecarboxaldehyde the 4-(3′-picolinylidene) derivative could also be isolated. It has been confirmed by the isotopic technique that arylidene-bis(phenylacetamide) can decompose in PPA to give phenylacetamide and araldehyde in an equilibrium reaction.

Earlier the preparation of 1-aryl-1,4-dihydro-3(2*H*)-isoquinolinones that can be regarded as a new group of anticonvulsive agents [1, 2] was reported; further, the reactions of derivatives, non-substituted in position 4, with aromatic aldehydes in the presence of strong bases yielding 1-aryl-4-benzyl-3(2*H*)-isoquinolinones through a 4-benzylidene intermediate were described [3, 4].

In the course of the preparation of 1,4-dihydro-3(2*H*)-isoquinolinones it has been supposed that the reaction takes place through a bis-amide intermediate [5]; this bis-amide could not be isolated, yet when synthesized in an independent way, it rapidly transformed into the corresponding isoquinolinone in 1 : 1 polyphosphoric acid (prepared from 1 g of 85% phosphoric acid and 1 g of phosphorus pentoxide by heating the mixture at 100 °C for 8 h [6]).

In an extension of the reaction to heterocyclic aldehydes, the aldehyde component used first was 4-pyridinecarboxyldehyde (Scheme 1). When R was a methyl group, the expected 4,4-dimethyl-1-(4-pyridyl)-1,4-dihydro-3(2*H*)-isoquinolinone **3** was obtained.

When, however, the non-substituted benzyl cyanide was employed (R=H), two products were obtained in the reaction. These were separated and identified as the expected 1,4-dihydro-3(2*H*)-isoquinolinone **1**; the other compound was 4-(4-picolinyl)-1-(4-pyridyl)-3(2*H*)-isoquinolinone **2**. The UV spec-

* Present address: Postgraduate Medical School, Central Research Division, Budapest

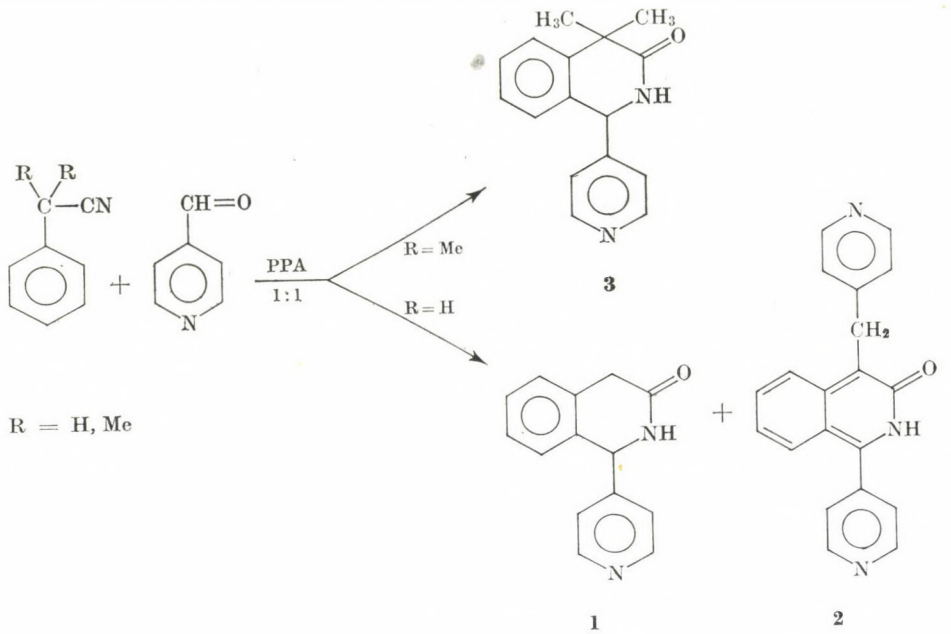

Scheme 1

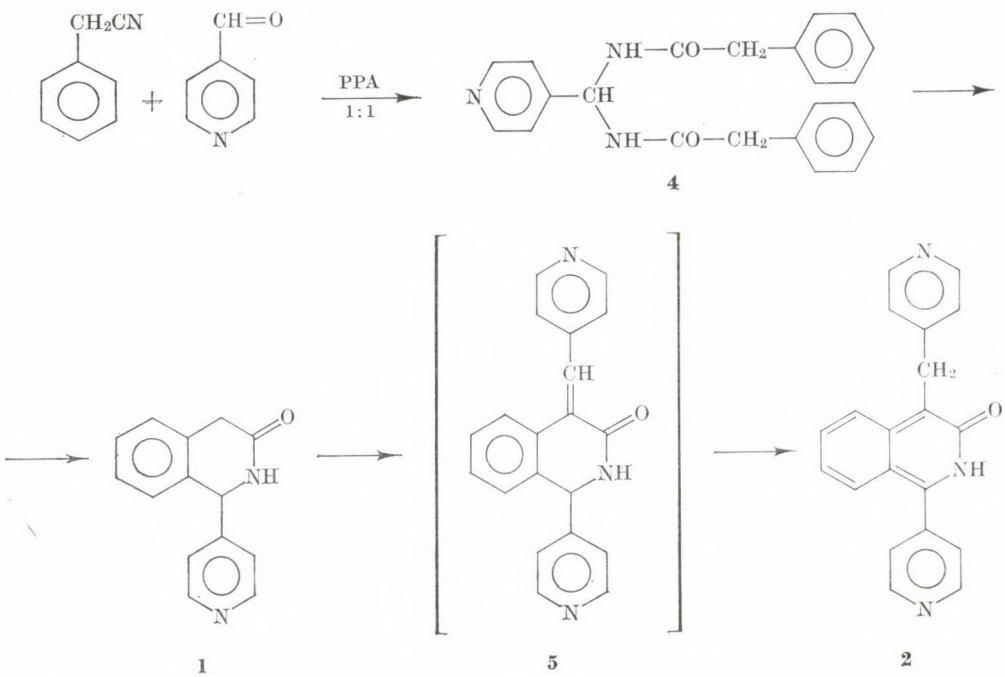

Scheme 2

trum of the latter clearly indicated the lactam-lactim tautomerism characteristic of 3(2*H*)-isoquinolinones.

This result was surprising, since in the earlier experiments with benzaldehydes and aryl-acetonitriles it had never been observed that the produced 1-aryl-1,4-dihydro-3(2*H*)isoquinolinone reacted in PPA with the aromatic aldehyde through its C-4 methylene group; such a conversion took place only in the presence of a strong base.

The reaction effected at 120 °C was monitored by TLC for 10 h. First only the 1-pyridylisoquinolinone **1** could be identified, then the spot characteristic of the 4-picolinyl-1-pyridyl derivative **2** also appeared and became more intense with time. The reaction mixture was processed after a 10-h reaction time, and **2** was isolated in 51% yield. It was also remarkable that at the beginning of the reaction an unknown substance was detected, but this rapidly disappeared, *i.e.* became further transformed.

In the next experiments, the reaction was stopped at a given point of time and the products were isolated. It was found (Scheme 2) that the 3(2*H*)-isoquinolinone **1** could be isolated in 27% yield after 15 min, while traces of an unknown compound were isolated from the reaction mixture processed after a reaction time of 5 min. This proved to be the bis-amide **4**. When a lower temperature was applied (100 °C), this substance was obtained in 45% yield after 30 min reaction time. These facts indicate that in the reaction involving several steps, the bis-amide **4** is formed first; this is rapidly converted into the isoquinolinone derivative **1**, from which the end-product **2** is formed probably in a reaction with another molecule of 4-pyridinecarboxaldehyde. The assumed intermediate **5**, a 4-picolinylidene derivative, could not be isolated.

Now the individual reaction steps were examined separately. First the reaction of the bis-amide **4** was studied and it was found that it partly undergoes cyclization under the above conditions, partly decomposes into aldehyde and acid amide. The aldehyde reacts with some of the cyclized product to give 3(2*H*)-isoquinolinone:

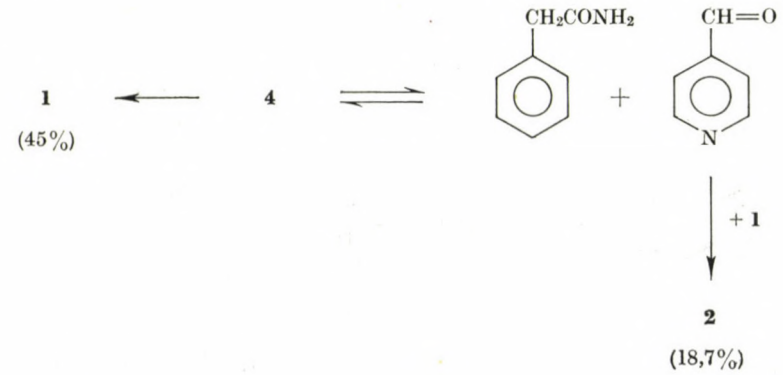

This was the first case in the synthesis of 1,4-dihydro-3(2*H*)-isoquinolinones that a bis-amide could be isolated from the reaction mixture. Earlier, in our studies on the reactions with PPA of arylidene-bis-amides prepared from phenylacetamides carrying substituents of high space requirement at the α-position, it was found that these compounds probably transform into the starting materials (acid amide and aldehyde), instead of undergoing cyclization. In the case of the bis-amide **4** prepared from 4-pyridinecarboxaldehyde this reversibility has been decidedly proved.

In order to confirm the general validity of this two-directional reactivity of bis-amides in PPA, benzylidene-bis(phenylacetamide) has also been tested. When phenylacetamide labelled with ^{14}C was also added to the reaction mixture containing benzylidene-bis(phenylacetamide), both unlabelled and labelled isoquinolinones were isolated (Scheme 3). The labelled isoquinolinone can only be formed from the labelled phenylacetamide with the benzaldehyde produced by the decomposition of the bis-amide; thus the reversibility assumed can be regarded as proved.

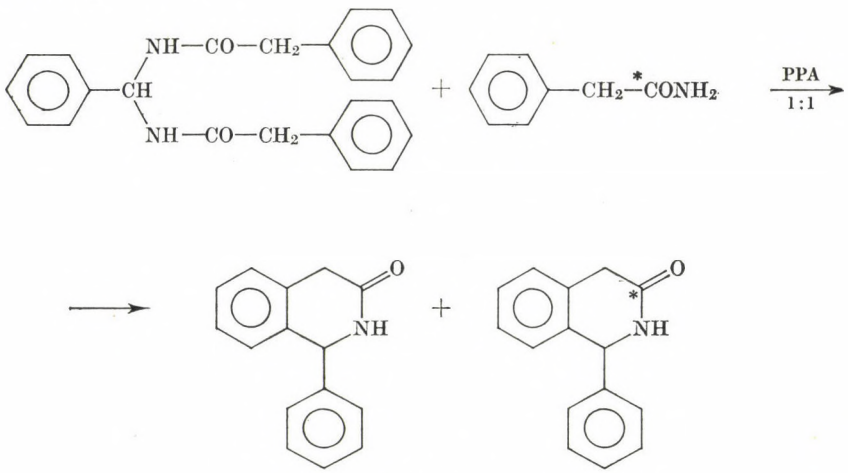

Scheme 3

In the following experiments the reaction of the isoquinolinone and 4-pyridinecarboxaldehyde was examined.

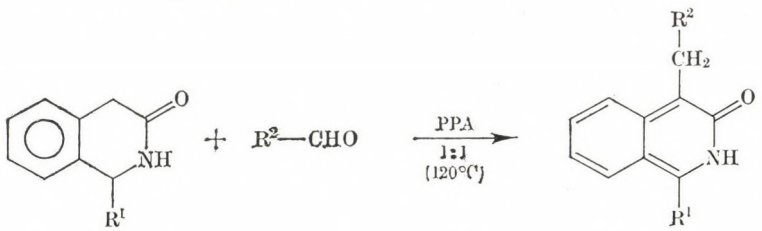

6: R^1=Ph, R^2=4-Py

The pyridylisoquinolinone **1** and 4-pyridinecarboxaldehyde were converted into derivative **2** in 45% yield at 120 °C in a 6-h reaction. It was to be elucidated next, whether in the condensation reaction of the C-4 methylene group, being active to a certain extent in 1,4-dihydro-3(2*H*)-isoquinolinone, with the aldehyde in PPA, the heteroaromatic nature of the aldehyde component or of the C-1 aryl group of the isoquinolinone is required for the accomplishment of the reaction. 1-Pyridyl-1,4-dihydro-3(2*H*)-isoquinolinone **1** did not react with benzaldehyde and 2,4-dinitrobenzaldehyde, and in the reaction of 1-phenyl-1,4-dihydro-3(2*H*)-isoquinolinone with 4-pyridinecarboxaldehyde at 150 °C, 1-phenyl-4-picolinyl-3(2*H*)-isoquinolinone **6** could be isolated only in 11% yield from the strongly tarred and decomposed mixture. In order to enhance the electron-withdrawing nature of the C-1 substituent, 1-(4-nitrophenyl)-1,4-dihydro-3(2*H*)-isoquinolinone was used in a reaction with 4-pyridylcarboxaldehyde, but no product of type **2** was formed from this substance. The conversion yielding the 3(2*H*)-isoquinolinone derivative **2** could be effected neither with sulfuric acid, nor with BF_3 in acetic acid; PPA is thus a specific catalyst of the reaction. Therefore it seemed to be of interest to examine the effect of the composition of PPA on the reaction. In these experiments orthophosphoric acid and two different PPA compositions (1 : 1.5 and 1 : 2) were used, in addition to 1 : 1 PPA, these were prepared in this laboratory. In orthophosphoric acid and in PPA with the lower P_2O_5 equivalence (76% P_2O_5), the protonating capability of the catalyst is predominating, while in PPA of higher P_2O_5 equivalence (80.0 and 82.8% P_2O_5) the anhydride character must be the decisive factor.

In 1 : 1.5 PPA the course of the reaction was significantly altered; no bis-amide could be isolated, but **1** was obtained in 54% yield after 60 min reaction time. The bis-amide **4** was converted exclusively into **1** (49%), and the reaction **1** → **2** also became slower; 20 h were required for this conversion (47%), whereas in 1 : 1 PPA a similar yield was attained in 6 h.

The use of 1 : 2 PPA and orthophosphoric acid does not cause a significant change. In orthophosphoric acid it is probably the low rate of cyclization which makes necessary the longer reaction time in the preparation of **2** (10 h, 26%). When the starting material was **1**, in orthophosphoric acid the reaction yielded again **2**.

4-Picolinyl-1-pyridyl-3(2*H*)-isoquinolinone **2** was also prepared according to the procedure described earlier [3], by the reaction of **1** with 4-pyridinecarboxaldehyde in the presence of NaH. The reaction was very slow in benzene; the products was obtained in 44% yield by refluxing reagents in toluene for 30 h. In this case DMSO did not prove to be a suitable solvent, the maximum yield being 17% at 50 °C in 6 h.

Summarizing the reactions between benzyl cyanide and 4-pyridinecarboxaldehyde in 1 : 1 and 1 : 1.5 PPA, in the series of consecutive reactions,

which can be characterized by four rate constants, the correlation between the composition of the PPA and the ratio of the rate constants is as follows:

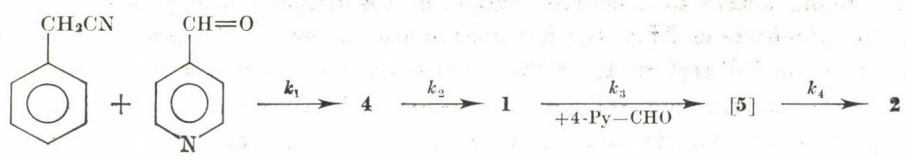

in 1:1 PPA: $k_4 \gg k_3$, $k_1 > k_2$, $k_2 \approx k_3$

in 1:1.5 PPA: $k_4 \gg k_3$, $k_2 \gg k_1$, $k_2 > k_3$

According to our results, k_4 is higher than k_3 in both kinds of PPA: the 4-picolinylidene derivative **5** could not be isolated. In 1 : 1 PPA, $k_1 > k_2$; in our syntheses of 1,4-dihydro-3(2*H*)-isoquinolinones, this was the first case when the supposed intermediate, the bis-amide, could be isolated from the reaction mixture. This ratio of the reaction rates is just reversed in 1 : 1.5 PPA. As regards 1,4-dihydro-3(2*H*)-isoquinolinone and the aromatic 3(2*H*)-isoquinolinone, both compounds could be isolated in 1 : 1 PPA, whereas in 1 : 1.5 PPA $k_2 > k_3$, and consequently the condensation was significantly slower.

It was now examined, whether the reactivity for carbonyl addition observed in 4-pyridinecarboxaldehyde with acid catalysis exists in the other pyridinecarboxaldehydes or not. The C-2 isomer did not yield even the corresponding 3(2*H*)-isoquinolinone, however, the experiments with 3-pyridinecarboxaldehyde were finally successful. This is shown by the reactions in Scheme 4.

In this case, too, the reaction was effected first in 1 : 1 PPA; it was monitored by TLC and the samples that seemed suitable were processed. However, no pure products was obtained; even after 30 h the mixture consisted of three substances which could not be separated. Therefore, a system was chosen which had been prepared by mixing calculated amounts of 85% phosphoric acid and P_2O_5 (1 g of P_2O_5 for 1 ml of phosphoric acid) without heating for 8 h (so-called 'fresh PPA'). These attempts were successful. When benzyl cyanide and 3-pyridinecarboxaldehyde were allowed to react in this system at 140 °C for 40 h, 4-(3-picolinyl)-1-(3-pyridyl)-3(2*H*)-isoquinolinone **10** was obtained in 47% yield. For the preparation of 1-(3-pyridyl)-1,4-dihydro-3(2*H*)-isoquinolinone **8**, the 1 : 1.5 PPA was found to be the most favourable medium, in which the compound could be prepared in 59% yield. In fresh PPA, the conversion **8** → **10** took place in 16 h at 140 °C in 45% yield. When the latter reaction was effected for 3 h and 120 °C instead of 140 °C, the 4-(3-picolinylidene) derivative **9** could

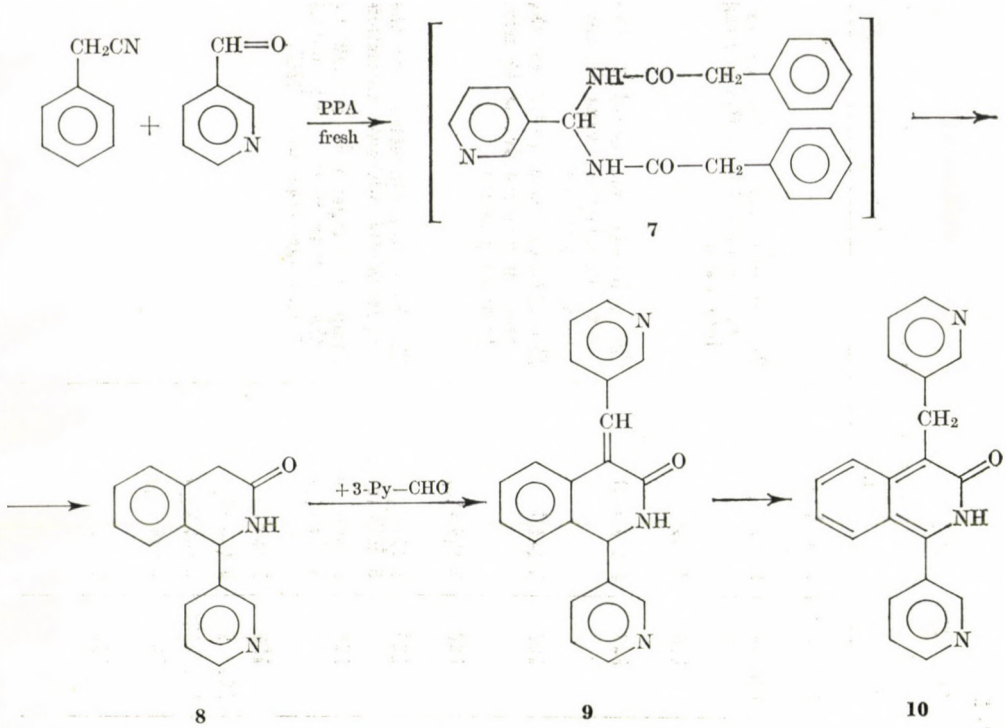

Scheme 4

also be isolated and prepared as a pure compound in 29% yield. However, the attempted isolation of the bis-amide **7** remained unsuccessful in the case of the 3-pyridinecarboxaldehyde. The aromatic derivative **10** was also prepared by the NaH method in a satisfactory yield (49%) from **8** in DMSO.

In summary, in the reaction of benzyl cyanide with 3-pyridinecarboxaldehyde in fresh and 1 : 1.5 PPA, the series of consecutive reactions, characterized by four rate constants, gives the following correlation between the ratio of rate constants and the composition of PPA:

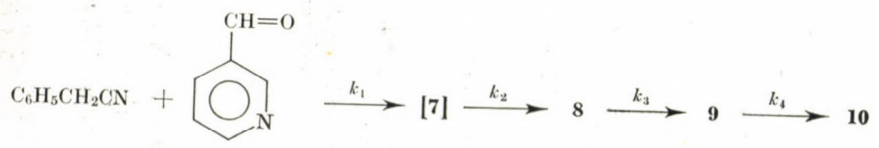

in fresh PPA: $k_2 > k_1$, $k_3 > k_2$, $k_3 \approx k_4$

in 1:1.5 PPA: $k_2 > k_1$, $k_2 > k_3$

Table I

Preparation of the 1-(4-pyridyl)-3(2H)-isoquinolinones

Starting compounds	Molar ratio	PPA	Reaction time, h	Temp., °C	Product (yield)	Comments
Benzyl cyanide + 4-pyridine-carboxaldehyde	1 : 2.2	1 : 1	10	120—125	**2** (51.12%)	
Benzyl cyanide + 4-pyridine-carboxaldehyde	2 : 1	1 : 1	1/4	120—5	**1** (26.8%)	The product was isolated by extraction with $CHCl_3$ after pouring into water
Benzyl cyanide + 4-pyridine-carboxaldehyde	2 : 1	1 : 1	1/2	100	**4** (45%)	
Benzyl cyanide + 4-pyridine-carboxaldehyde	1 : 1	1 : 1.5	1	120	**1** (53.6%)	The aldehyde was added to the reaction mixture during 45 min, in three portions
Benzyl cyanide + 4-pyridine-carboxaldehyde	1 : 1	1 : 2	1	120	**1** (44.7%)	The aldehyde was added to the reaction mixture during 45 min, in three portions
Benzyl cyanide + 4-pyridine-carboxaldehyde	1 : 2	ortophos-phoric acid	10	120	**2** (25.5%)	
α,α-Dimethyl-benzyl cyanide + + 4-Pyridinecarboxaldehyde	1 : 1	1 : 1	3	125	**3** (51%), **3**·HCl (61%)	The base was converted into the hydrochloride without purification
4		1 : 1	3	125	**1** (45%) + **2** (18.7%)	Compound **2** separated when pouring the reaction mixture into water; **1** was extracted with $CHCl_3$
4		1 : 1.5	3	120	**1** (49%)	
1 + 4-Pyridinecarboxaldehyde	1 : 1	1 : 1	6	120—5	**2** (44.8%)	
1 + 4-Pyridinecarboxaldehyde	1 : 1	1 : 1.5	20	120—125	**2** (46.9%)	
1 + 4-Pyridinecarboxaldehyde	1 : 1	orthophos-phoric acid	5	120	**2** (38.5%)	
1-Phenyl-1,4-dihydro-3(2*H*)--isoquinolinone + 4-pyridine-carboxaldehyde	1 : 1	1 : 1	3	150	**6** (11%)	

In fresh PPA, **9** and **10** could also be prepared; in 1 : 1.5 PPA the reaction stopped at **8**.

According to our investigations, the mechanisms of the reactions between 1,4-dihydro-3(2*H*)-isoquinolinones and benzaldehyde in the presence of a strong base, and with pyridine carboxaldehyde reagent in PPA are similar, both involving the 4-arylidene intermediate. In the reaction with pyridinecarboxaldehyde, the nature of the aldehyde component (4- or 3-isomer) and the composition of PPA significantly affect the rates of the individual steps in the four-step reaction, and this renders possible the preparation of the different individual compounds in optimum yield.

Experimental

Polyphosphoric acid was prepared from phosphorus pentoxide and 85% phosphoric acid; the given amounts of the components were stirred under anhydrous conditions until dissolution of the solid, followed by heating at 100 °C for 8 h when necessary.

The reactions in PPA (Tables I and II) and processing of the reaction mixtures were effected as described earlier [1].

Table II

Preparation of the 1-(3-pyridyl)-3(2H)-isoquinolinones

Starting compounds	Molar ratio	PPA	Reaction time, h	Temperature, °C	Product (yield)
Benzyl cyanide + 3-pyridinecarboxaldehyde	1 : 2	'fresh'	40	140	**10** (46.9%)
Benzyl cyanide + 3-pyridinecarboxaldehyde	1 : 1	1 : 1.5	4.5	130	**8** (59%)
8 + 3-pyridine-carboxaldehyde	1 : 1	'fresh'	16	140	**10** (44.6%)
8 + 3-pyridinecarboxaldehyde	1 : 1	'fresh'	3	120	**9** (28.6%)

Condensation in the presence of NaH was carried out as given in Ref. [3].

Physical data of the compounds prepared are given in Table III.

The ^{14}C-labelling experiments were made as follows.

Benzylidene-bis(phenylacetamide) (429.38 mg; 1.198 mmole) [7] and ^{14}C-phenylacetamide (171.22 mg; 1.266 mmole), prepared on the analogy of [8], were allowed to react in 1 : 1 PPA (5 ml) in the usual manner.

The activity of the phenylacetamide was

A_{sp} 13 608.76 Bq/mg

A_m 1 839.36 kBq/mmole

mole number: 3.66 mmoles.

The activity of the product [1-phenyl-1,4-dihydro-3(2*H*)-isoquinolinone] was:

A_{sp} 754.75 Bq/mg

A_m 168.50 kBq/mmole

Activity introduced: 2330.09 kBq.

A_m of phenylacetamide in the mixture was 636.32 kBq/mmole. Incorporation: 26.5%.

Table III

Physical data of the 1-pyridyl-3(2H)-isoquinolinones and of the 4-picolinylidene-bis(phenylacetamide)

Compound	No.	M.p., °C[a] (recrystallizing solvent[b])	IR[c]	UV	Formula[g]
4-Picolinylidene-bis(phenylacetamide)	**4**	235—6 (DMF)	νCO 1660		$C_{22}H_{21}N_3O_2$
1-(4-Pyridyl)-1,4-dihydro-3(2*H*)-isoquinoline	**1**	167—9 (EtOH)	νCO 1665	265 (3150) 258 (3790)	$C_{14}H_{12}N_2O$
4-(4-Picolinyl)-1-(4-pyridyl)-3(2*H*)-isoquinolinone	**2**	231—2 (DMF)	νC=N 1620 νOH 3550	434 (1166)[e] 359 (8270)[f] 293 281	$C_{20}H_{15}N_3O$
1-Phenyl-4-(4-picolinyl)-3(2*H*)-isoquinolinone	**6**	238—40 (EtOAc)	νC=N 1625		$C_{21}H_{16}N_2O$
4,4-Dimethyl-1-(4-pyridyl)-1,4-dihydro-3(2*H*)-isoquinolinone · HCl	**3**	262 (d.)	νCO 1670		$C_{16}H_{17}ClN_2O$
1-(3-Pyridyl)-1,4-dihydro-3(2*H*)-isoquinolinone	**8**	189—91 (EtOH)	νCO 1670	260 (3465) 256 (3371)	$C_{14}H_{12}N_2O$
4-(3-Picolinylidene)-1-(3-pyridyl)-1,4-dihydro-3(2*H*)-isoquinolinone[d]	9	230—2 (EtOH)	νCO 1670 νC=C 1620	308 (15642)	$C_{20}H_{15}N_3O$
4-(3-Picolinyl)-1-(3-pyridyl)-3(2*H*)-isoquinolinone	**10**	229—30 (70% EtOH)	νC=N 1620	430 (899) 350 (7192) 296 (4894) 286 (5410)	$C_{20}H_{15}N_3O$

[a] Uncorrected melting points, capillary tube-method
[b] DMF, dimethylformamide; EtOH, ethanol; EtOAc, ethyl acetate
[c] The IR spectra were determined on a Perkin-Elmer 377 spectrometer (KBr pellets)
[d] NMR ($CDCl_3$): CHNH 5.73d (1, $J_{CH, NH}$ 2.5 Hz) 7.83d (1), ArH 7.0—7.75 m (8), 8.12d (1), 8.35—8.55 m (3), 8.66d (1, 1.5 Hz)
[e] Lactam
[f] Lactim
[g] All compounds were analyzed for C,H,N with results of at least 0.4% accuracy

The authors express their thanks to Mrs. J. HASKÓ-BREUER and to Mr. G. TÓTH for recording the IR and NMR spectra, respectively, and to Miss M. FODOR and Mrs. G. KALÁSZ for the microanalyses. Excellent technical assistance of Miss I. TÉGLÁS is gratefully acknowledged.

REFERENCES

[1] CSÜRÖS, Z., DEÁK, Gy., HOFFMANN, I., TÖRÖK-KALMÁR, A.: Acta Chim. Acad. Sci. Hung., **60,** 177 (1969)
[2] DEÁK, Gy., DÓDA, M., GYÖRGY, L., HAZAI, L., STERK, L.: J. Med. Chem., **20,** 1384 (1977)
[3] DEÁK, Gy., HAZAI, L.: Acta Chim. Acad. Sci. Hung., **79** (1), 113 (1973)
[4] DEÁK, Gy., HAZAI, L., TÓTH, G.: J. Heterocycl. Chem., **14** (4), 583 (1977)
[5] DEÁK, Gy., GÁLL-ISTÓK, K., KÁLMÁN, Zs., HASKÓ-BREUER, J.: Acta Chim. Acad. Sci. Hung., **76** (3), 299 (1973)
[6] DEÁK, Gy., GÁLL-ISTÓK, K., HAZAI, L., STERK, L.: Synthesis, **1975** (6), 393
[7] DEÁK, Gy., GÁLL-ISTÓK, K., HAZAI, L.: Acta Chim. Acad. Sci. Hung., **84,** 477 (1975)
[8] CRAIG, J. T., TINDALL, J. B., SENKUS, M.: Ann. Chem., **23,** 332 (1951)

László HAZAI, Gyula DEÁK } H-1083 Budapest, Szigony u. 43.

Géza SZABÓ H-1135 Budapest, Szabolcs u. 33/35.

Ernő KOLTAI H-1045 Budapest, Szabadságharcosok u. 47—49.

RECENSIONES

Recent Results in Chemistry, Vol. 39 (In Hungarian)

Editor Béla Csákvári

János Holló, László Keviczky, László Kirchknopf, Imre Kurucz, László Nyeste, Béla Sevella, László Szigeti and Attila Veres: *Some Problems in Modern Research on Fermentation*

Budapest, Akadémiai Kiadó, 1978
296 pages, 10 tables, 66 figures

Under the comprehensive title "Some problems in modern research on fermentation", the authors report on their results achieved in the field of a new, progressing interdisciplinary science, bioengineering operations and processes. Two papers in the book deal with the problems of industrial microbiology, a sector of the above field, which has undergone dynamic development during the last decade. This special attention is also due to the fact that the interdisciplinary character of industrial microbiology requires the close cooperation of biologists, chemists, physicists, mathematicians and physicians. The Fermentation Research Team, organised about ten years ago at the Agricultural Chemical Technology Department of the Technical University, Budapest, which began its work with researchers of various basic education, has amalgamated into a uniform team under the direction of Professor Holló. Their work is introduced by the two papers in the book:

1. Some Theoretical and Practical Problems of the Application Possibilities of Computer Technique in Fermentation Research (134 pages, 8 tables, 39 figures; references)
2. Mathematical Modelling of Bacterium Fermentations (144 pages, 2 tables, 27 figures; references)

The papers deal with two logically correlated part-fields of bioengineering operations and processes for microorganisms; they describe automated, computer-coupled fermentation apparatus and its application possibilities in the controlling and automation of fermentation systems, as well as their mathematical modelling methods. Discussion of the authors' own results is subordinated to a treatment of the basic problems in these two fields, and solutions on the laboratory scale are suggested. This serves primarily the intensification of Hungarian microbiological processes, primarily in the pharmaceutical industry; at the same time its importance on the world scale is pointed out.

The first paper is divided into seven chapters. The introductory chapter gives a short survey of the computerized fermentation systems which have been realized up to now, including the logic steps of coupling. The next two chapters give information regarding the fermentation process and the actual parameters, and the fundamental conditions of measurement are described. Chapters 4 and 5 make up more than two-thirds of the paper; these are: "The automated fermentation apparatus" and "Off-line optimum direction of continuous fermentation processes". Here the fermentation apparatus built by them, technical methods of controlling the physical parameters (variables) and the breeding method based on the turbidostat principle (where the concentration of the microorganism cells is measured by measuring optical density and this is used as the control signal) are described. The experimental procedure studied on laboratory scale was the conversion gluxose → gluconic acid → 5-ketogluconic acid, based on a process catalyzed by the enzymes of a species—of *Acetobacter suboxydans* denoted by ATCC 621 in the industry. The continuous fermentation model process was studied at 27 °C, 30 °C and 33 °C temperatures. In the course of the 100-h experimental programs, the reproducibility of the biological state of the microorganism breed and the stability of the value of the propagation rate were determined repeatedly. The rate of the formation of gluconic acid was measured through the measurement of the consumption rate of base added for neutralization. Of the control parameters of the process, the temperature, pH and the concentration of cells were varied, and the specific growth rate, the specific rate of product formation and the actual gluconic acid concentration as the state parameters were examined. It was established experimentally, which parameters are to be regarded as technological limits of the process and which are the starting working points of the optimation experiments. In order to approach

the optimum, an experimental program was constructed and realized to determine the control parameters ensuring the maximum values of the individual state parameters.

These investigations are far from being finished, therefore, in Chapters *6* and *7*, the authors shortly outline the possible methods for off-line optimation of the non-continuous breeding technique and the algorithms required for controlling the on-line static optimation of the continuous operation.

The second part of the book describes the principles of mathematical modelling of fermentation systems, the model types given in the literature. The authors' experiences are illustrated again on the glucose-converting reaction of *Acetobacter suboxydans*, considering two residual enzyme catalysts (glucose dehydrogenase and gluconic acid dehydrogenase), in accordance with the black box approach applied by them.

The second paper deals with the modelling of non-continuous fermentation processes usual in industrial practice. The authors' primary purpose is the illustration of model formation, "one fermentation — one model" on the example chosen by them. When reading the paper, it can be felt that there has been a serious synthesizing work behind the 83 references. Therefore it is not evident, why they limited the subject to "bacterial fermentation", when Hungarian researchers deal extensively with the regularities of propagation and product formation of yeast and mould species. The majority of this work has been published in periodicals of the Hungarian Academy of Sciences (*e.g.* Acta Chimica, Acta Alimentaria).

Both papers in the book reflect the modern concept that the level of development of technological procedures in this special chemical-biological interdisciplinary field of science is ready for the application of system-technical treatment, modelling and computerized methods. The authors were the first who developed and operated a fermenter-computer unit for experimental purposes in Hungary, and in this work one must recognize the significant role of one of the authors deceased since then, Attila VERES.

P. BIACS

chemBUYdirect International Chemical Buyers Directory

edited by Friedrich W. DERZ, dipl. chem.

Walter de Gruyter, Berlin, New York, 1976

This enormous collection work consists of the following parts:

chemPRODUCTindex in two volumes
chemSUPPLIERSdirectory
chemADDRESSbook
chemSYNONYMdictionary

chemPROCUCTindex

The chemPRODUCTindex lists in alphabetical order about 300 000 names (synonyms) of chemicals (organics and inorganics), radioactive-labelled compounds, isotopes, dyes, polymers, active principles of pharmaceuticals, *etc.*, and their molecular formulas.

In order to make the knowledge of chemical nomenclature as far as possible unnecessary for the use of the system, each name in the list is referred to the Chemical Abstracts Service Registry Number (CARNO) or, if such one is not available, to an interim Number (iNo). Knowing the registry number, one can find information in the other volumes of the series.

As the names of chemical compounds rarely change, the usefulness of the chemPRODUCTindex will not diminish with time. For keeping it up to date, supplementary lists are sufficient. The supplements will be embodied in the yearly revised editions of the chemSUPPLIERSdirectory.

chemSUPPLIERSdirectory

The object of this volume is to give information about companies which may be taken into consideration as suppliers of a particular chemical.

The basis of searching is the registry number (CARNO or iNo) which can be found in the chemPRODUCTindex after the name or synonim of a given chemical. This makes it unnecessary always and everywhere to include the often very long chemical name.

Every registry number listed in the chemSUPPLIERSdirectory is accompanied by a number of codes. These identification codes are the abbreviations for suppliers. The code consists of the international identification for automobiles for the country and an individual abbreviation for the respective company. Additional information, as the chemical formula and the molecular mass, ionic couplings, *etc.*, are sometimes indicated under the CARNO. There are included also references from one CARNO to another new CARNO as well as iNo-CARNO and iNo-iNo equivalents.

chemADDRESSbook

The chemADDRESSbook includes approximately 23 000 company addresses from some 40 developed capitalist and socialist countries.

It consists of three parts:

Part 1: company identification code index

The identification code is the abbreviation for a company to be found in the chemSUPPLIERSdirectory or in part 2 of this book. The information under this code contains company name with complete address including post code or postal code number (ZIP-code), telephone number, telex number and telegram address. The codes are arranged according to national identification codes (in alphabetical order) of the countries. Within a country, the identification codes of the companies are listed alphabetically.

Part 2: company name index

In this part all companies included in the chemADDRESSbook are listed alphabetically. Due to alphabetical listing, branch offices (affiliates) of one company in different countries are listed together with the name of the original company (mother company). The identification code is given after the name of the company. Once the identification code is known, the complete address can be found in part 1 of this volume.

Part 3: chemPOSTCODEindex-international

This part is arranged to the alphabetically listed national identification codes of the countries. Within a country, the postal code numbers are listed in alpha-numerical order. Under the post code are listed the name of the city, the district, the company name and the company identification code. For countries without post codes, the city names are listed alphabetically as headings for the respective company. The company names are given in alphabetical order after the city names.

By means of the POSTCODEindex it is possible to find all companies located in the same or directly neighbouring postal districts.

chemSYNONYMdictionary will be issued later.

The publication of a postCODEpostal-international is planned, which includes a comparative description of the postal code systems of the countries.

The chemBUYdirect International Chemical Buyers Directory is one of the most comprehensive registers of the commercially available chemicals and of the manufacturer, supplier or wholesaler companies which may be taken into consideration when ordering a particular chemical. It is very useful in the case of rare chemicals, where it is important to find any entry at all. Its system is clear and well understandable. The use of the Chemical Abstracts Service Registry Numbers makes it easy to handle in every case where the chemical name is unknown or ambiguous. Each volume contains prefaces and explanations in English, German and French which make it suitable for international use.

V. TAKÁCS

M. William RANNEY: *Fertilizer Additives and Soil Conditioners*

Chemical Technology Review No. 116. 301 pp.

Noyes Data Corporation, Park Ridge, New Yersey, U.S.A., 1978

The application of chemicals in agriculture has greatly increased in the past decades and contributes to obtaining high yields and products of good quality. The number of chemicals introduced into practical agriculture has mupltiplied within a short period. A better knowledge of these chemical products, their properties, technology, production and mechanism of their action is very important in up-to-date farming.

The author selected several groups of modern chemicals as the subject of his book, with particular regard to a large variety of additive or complementary products which improve fertilizer production, application and efficiency. The book deals with both liquid and granual products, as well as with chemicals for soil conditioning. The latter are highly important for improving soil structure and, consequently, the water and nutrient status of the soil.

In the first part of the book additives and processing aids for granular products are described with particular regard to modern fertilizer production and application. Granulation aids and processes for several types of fertilizer are described in detail in this part, with indication of methods and patterns of use. In some cases specific examples illustrate the manufacturing of various fertilizers and other products.

The second part of the book deals with additives and processing aids for liquid products.

In the third part micronutrient compositions are described. In the first section the author deals with iron complexes and chelates. In addition to chelates, iron-containing compositions are also described, partly produced from cast iron chips, mine tailing, *etc.* Very interesting and remarkable is the method of producing fertilizers from sea-water by adding bivalent iron ions to the water. The resulting iron hydroxide precipitates after having adsorbed microelements and organic substances present in the water.

In this part zinc- and manganese-containing products are also described as micronutrient compositions. In most cases the new patterns are also described and the methods of manufacturing indicated. Many of the described methods are remarkable for practical utilization, for instance stabilizer for the manganese salt of sulphonited liquid. The micronutrient compositions also include liquid products for different purposes in agricultural practice, such as growth promoters, fertilizers, inhibitors, *etc.*

The fourth part of the book deals with nitrification and urease inhibitors.

The fifth part describes soil conditioners and peat-moss compositions. The aim of application of these materials is mainly to improve the physical properties of the soil. There are compounds of different chemical composition to be used for this purpose. The author lists a broad spectrum of such materials, including synthetic and semisynthetic substances as well as treated and untreated by-products of industry and agriculture.

Polyacrylic compounds, silicon dioxide, waste paper, metallurgical dust from waste gases, chicken manure, liquid products represent several of the materials described in this chapter. Patents and methods of their manufacture are throughly described and recommendations are made for their utilization.

In addition to the above-mentioned products, peat-moss compositions and mulches are described in view of their possible applications as soil conditioners.

In the last section of this part, the author gives a description and the method of preparation of a few patterns of synthetic soils, including foamed polymers, treated clay minerals, *etc.*

In the last part of the book the reader finds detailed descriptions of humus and compost soil conditioners. This part starts with patents for humus processing and methods of recovering different humic acids and humates. Besides the descriptions of methods, equipment, devices and analytical processes of the raw products for obtaining humus lignite, brown coal and other substances are also discussed here.

The book includes a company index listing the manufacturers mentioned in the patterns, an inventor index and a U.S. patent number index.

The author succeeded in giving a good guide to the subject: his book is useful for both manufacturers and users of fertilizers and soil conditioners.

I. SZABOLCS

INDEX

ANALYTICAL CHEMISTRY

PHYSICAL AND INORGANIC CHEMISTRY

ORGANIC CHEMISTRY

Printed in Hungary

A kiadásért felel az Akadémiai Kiadó igazgatója — Műszaki szerkesztő: Zacsik Annamária

A kézirat nyomdába érkezett: 1979. VI. 6. — Terjedelem: 9,45 (A/5) ív, 61 ábra

80.7220 Akadémiai Nyomda, Budapest — Felelős vezető: Bernát György

ACTA CHIMICA

ТОМ 102—ВЫП. 3

РЕЗЮМЕ

Устойчивость комплексов гексакис-ДМСО-хром(III) типа внешней сферы

Ж. АҚОШ-САБО, И. ОРСАГ и ДЬ. БАЖА

Комплексы гексакис-ДМСО-хром(III) типа внешней сферы были исследованы в воде и ДМСО.

На основе измерения растворимости в водном растворе при 25 °C были определены константы устойчивости при величине I-1, которые равны:

$$F^- : \quad \beta_1 < 0.2$$

$$NO_3^- : \ \beta_1 = 5, \ \beta_2 = 19$$

$$SCN^- : \beta_1 = 3, \ \beta_2 = 60.$$

Порядок устойчивости в ДМСО следующий: $NO_3^- < ClO_4^- < SCN^-$.

Кинетика и катализ образования и аквации комплекса $Cr(ДМСО)_{6-n}^{+3}$

ДЬ. РАБАИ, ДЬ. БАЖА и М. Т. БЭК

Была изучена кинетика реакций комплексов $Cr(H_2O)_n(ДМСО)_{6-n}^{3+}$ с водой и диметилсульфоксидом, а также эффект нитрита и двуокиси углерода на скорость этих реакций. Была определена скорость аквации и механизм сольволиза в случае $n = 6$. Было найдено, что в случае $n = 2-6$ замещение воды на ДМСО и обратно катализируется нитритом и CO_2, но если $n = 0$, то ни нитрит, ни CO_2 не проявляют каталитического эффекта на аквацию. Эффект повышения скорости объясняется образованием карбонато- и нитритохром(III) комплексов с высокой реакционной способностью в быстром предварительном равновесии. Константа устойчивости комплекса $Cr(H_2O)_5(OCO_2H)^{2+}$ бала получена из данных скорости.

Реакция амидхлоридов с карбамидами, II

Реакция с асимметрически дизамещенными карбамидами

И. БИТТЕР, Е. КАРПАТИ-АДАМ и Л. ТЁКЕ

Была исследована реакция асимметрически дизамещенных карбамидов с хлористым хлорометилендиметиламмонием. Образующиеся хлориды карбамоиламидиния не удалось изолировать в кристаллической форме. Однако, путем идентификации продуктов разложения под влиянием тепла и третичных оснований, а также продуктов гидролиза, удалось выяснить их структуру и объяснить путь их образования. Согласно экспериментальным результатам, вероятно протекает непосредственное *N*-ацилирование.

Получение и исследование фосфорорганических производных цианокомплексов переходных металлов, VIII

Исследование ионных ассоциатов аниона гексацианоферрата(III) с четвертичными фосфонийными катионами методом ЯМР—H^1

Ш. ПАПП и П. КВИНТОВИЧ

Были получены производные аниона гексацианоферрата(III) с некоторыми четвертичными фосфонийными катионами. На основе спектров ЯМР—H^1, снятых в двух растворителях $CDCl_3$ и ДМСО—D_6, был обсужден характер и механизм взаимодействий аниона с катионом в растворе.

Получение и исследование фосфорорганических производных цианокомплексов переходных металлов, IX

Исследование ионных ассоциатов аниона трифенилфосфино-пентацианоферрата(III) с четвертичными фосфонийными катионами методом ЯМР—H^1

Ш. ПАПП и П. КВИНТОВИЧ

В связи с предыдущими работами были исследованы характер и степень взаимодействий аниона и катиона, а также протонов лиганда $P(C_6H_5)_3$ с центральным атомом в ионных ассоциатах аниона $[Fe(CN)_5P(C_6H_5)_3]^{2-}$ с четвертичными фосфонийными катионами.

Влияние фотографического и фотометрического факторов на спектрографическую оценку, II

Микродензитометр для современных спектрально-аналитических исследований и для практических целей

Л. КОЗМА

Описанный микродензитометр работает линейно в широком интервале оптической плотности ($S = 0 \ldots 4$) и при оптимальных фотометрических и оптических условиях.

Система измерения света, электронное превращение пропускания в поглощение и дигитальное сигнализирование величин оптической плотности соответствует требованиям точности и воспроизводимости. Логическая система накопления данных и поисков граничных значений, а также автоматический контроль приводят к упрощению и значительному повышению скорости измерений.

Влияние фотографического и фотометрического факторов на спектрографическую оценку, III

Определение кривой почернения и параметров *l*-трансформации графическим методом и с помощью ЭВС

К. ФЛОРИАН, ДЬ. ХЕЛТАИ и К. ЦИММЕР

Обсуждаются методы определения параметров кривых почернения. Для графического определения величины γ, а также величин плотности S_L и S_{LL} был использован, по существу, метод предварительной кривой Чёрчиля. Была составлена программа ЭВС для определения констант γ и k *l*-трансформации. Программа основана на итерационном вычислении, являющемся наиболее достоверным принципом, согласно Тёрёку и Циммеру. Величины констант фильтра обычно согласуются со средней величиной Δl и с точностью 0,001 при использовании величин γ и k, рассчитанных программой. Эта точность совершенно достаточна для практических требований.

Новая амидозащищающая группа

А. ЮХАС и Ш. БАЮС

Сообщается применение новой амидозащищающей группы — 2,4,2', 4'-тетраметоксибензгидрила (Tbh). Защищенные амиды могут быть приготовлены конденсацией соответствующего карбоксильного соединения с Tbh—NH_2, синтез которого также описан. Кислотная стабильность Tbh подобна стабильности трет.-бутилоксикарбонила (Boc), т. е. Tbh может быть легко удалена с помощью ацидолиза в трифторуксусной кислоте при комнатной температуре.

Конформационные и конфигурационные исследования производных 3,7-диазабицикло (3.3.1)-нонана, II

П. ШЕЙБЕР и К. НАДОР

Конформация и конфигурация некоторых *N*-замещенных биспид-9-онов и биспидин-9-олов были исследованы через анализ результатов, полученных измерением дипольных моментов и спектров ЯМР—H^1. Было найдено, что форма стулважна является доминирующей конформацией как для 9-кето-, так и 9-гидроксипроизводных. Применение реагентов с лантанидным сдвигом оказалось весьма удобным методом для ассигнации относительной конфигурации атома C(9) в случае асимметрически *N*-замещенных биспидин-9-олов.

Аномальная реакция между пиридинкарбоксальдегидом и бензилцианидом в полифосфорной кислоте

Синтез 4-пиколинил-1-пиридил-3(2*H*)-изохинолинона

Л. ХАЗАИ, ДЬ. ДЕАК, Г. САБО и Э. КОЛТАИ

Из 4- и 3-пиридинкарбоксальдегидов и бензилцианида в полифосфорной кислоте (ПФК), эквивалентной содержанию P_2O_5 84,0 и 82,8%, с хорошим выходом были получены 1-пиридил-1,4-дигидро-3(2*H*)-изохинолиноны *1* и *8*, а в ПФК с содержанием P_2O_5 78% — 4-пиколинил-1-пиридил-3(2*H*)-изохинолиноны *2* и *10*, соответственно. При более коротких временах реакции, в случае 4-пиридинкарбоксальдегида удалось изолировать бис-амид **4**, а в случае 3-пиридинкарбоксальдегида — 4-(3'-пиколинилиденовое) производное *9*. С помощью изотопной техники удалось доказать, что арилиден-бис(фенилацетамид) в ПФК в равновесной реакции распадается на фенилацетамид и аральдегид.

Les Acta Chimica paraissent en français, allemand, anglais et russe et publient des mémoires du domaine des sciences chimiques.

Les Acta Chimica sont publiés sous forme de fascicules. Quatre fascicules seront réunis en un volume (4 volumes par an).

On est prié d'envoyer les manuscrits destinés à la rédaction à l'adresse suivante:

Acta Chimica
Budapest, P.O. Box 67, H-1450, Hongrie

Toute correspondance doit être envoyée à cette même adresse.

La rédaction ne rend pas de manuscript.

Le prix de l'abonnement: $ 36,00 par volume.

Abonnement en Hongrie à l'Akadémiai Kiadó (1363 Budapest, P. O. B. 24, C. C. B. 215 11488), à l'étranger à l'Entreprise du Commerce Extérieur « Kultura » (H-1389 Budapest 62, P. O. B. 149 Compte-courant No. 218 10990) ou chez représentants à l'étranger.

Die Acta Chimica veröffentlichen Abhandlungen aus dem Bereich der chemischen Wissenschaften in deutscher, englischer, französischer und russischer Sprache.

Die Acta Chimica erscheinen in Heften wechselnden Umfanges. Vier Hefte bilden einen Band. Jährlich erscheinen 4 Bände.

Die zur Veröffentlichung bestimmten Manuskripte sind an folgende Adresse zu senden

Acta Chimica
Budapest, Postfach 67, H-1450, Ungarn

An die gleiche Anschrift ist jede für die Redaktion bestimmte Korrespondenz zu richten.

Manuskripte werden nicht zurückerstattet.

Abonnementspreis pro Band: $ 36,00.

Bestellbar für das Inland bei Akadémiai Kiadó (1363 Budapest, Postfach 24, Bankkonto Nr. 215 11488), für das Ausland bei »Kultura« Außenhandelsunternehmen (H-1389 Budapest 62, P. O. B. 149. Bankkonto Nr. 218 10990) oder seinen Auslandsvertretungen.

«Acta Chimica» издают статьи по химии на русском, английском, французском и немецком языках.

«Acta Chimica» выходит отдельными выпусками разного объема, 4 выпуска составляют один том и за год выходят 4 тома.

Предназначенные для публикации рукописи следует направлять по адресу:

Acta Chimica
Budapest, P.O. Box 67, H-1450, ВНР

Всякую корреспонденцию в редакцию направляйте по этому же адресу.

Редакция рукописей не возвращает.

Подписная цена — $ 36,00 за том.

Отечественные подписчики направляйте свои заявки по адресу Издательства Академии Наук (1363 Budapest, P.O.B. 24, Текущий счет 215 11488), а иностранные подписчики через организацию по внешней торговле «Kultura» (H-1389 Budapest 62, P.O.B. 149. Текущий счет 218 10990) или через ее заграничные представительства и уполномоченных.

Reviews of the Hungarian Academy of Sciences are obtainable at the following addresses:

AUSTRALIA
C.B.D. LIBRARY AND SUBSCRIPTION SERVICE, Box 4886, G.P.O. *Sydney N.S.W. 2001*
COSMOS BOOKSHOP, 145 Ackland Street, *St. Kilda (Melbourne), Victoria 3182*

AUSTRIA
GLOBUS, Höchstädtplatz 3, *1200 Wien XX*

BELGIUM
OFFICE INTERNATIONAL DE LIBRAIRIE, 30 Avenue Marnix, *1050 Bruxelles*
LIBRAIRE DU MONDE ENTIER, 162 Rue du Midi, *1000 Bruxelles*

BULGARIA
HEMUS, Bulvar Ruszki 6, *Sofia*

CANADA
PANNONIA BOOKS, P.O. Box 1017, Postal Station "B", *Toronto, Ontario M5T 2T8*

CHINA
CNPICOR, Periodical Department, P.O. Box 50, *Peking*

CZECHOSLOVAKIA
MAD'ARSKÁ KULTURA, Národní třida 22, *115 66 Praha*
PNS DOVOZ TISKU, Vinohradská 46, *Praha 2*
PNS DOVOZ TLAČE, *Bratislava 2*

DENMARK
EJNAR MUNKSGAARD, Norregade 6, *1165 Copenhagen*

FINLAND
AKATEEMINEN KIRJAKAUPPA, P.O. Box 128. *SF-00101 Helsinki 10*

FRANCE
EUROPÉRIODIQUES S. A., 31 Avenue de Versailles, *78170 La Celle St.-Cloud*
LIBRAIRIE LAVOISIER, 11 rue Lavoisier, *75008 Paris*
OFFICE INTERNATIONAL DE DOCUMENTATION ET LIBRAIRIE, 48 rue Gay-Lussac, *75240 Paris Cedex 05*

GERMAN DEMOCRATIC REPUBLIC
HAUS DER UNGARISCHEN KULTUR, Karl-Liebknecht-Strasse 9, *DDR-102 Berlin*
DEUTSCHE POST ZEITUNGSVERTRIEBSAMT, Strasse der Pariser Kommüne 3—4, *DDR-104 Berlin*

GERMAN FEDERAL REPUBLIC
KUNST UND WISSEN ERICH BIEBER, Postfach 46, *7000 Stuttgart 1*

GREAT BRITAIN
BLACKWELL'S PERIODICALS DIVISION, Hythe Bridge Street, *Oxford OX1 2ET*
CUMPUS, HALDANE AND MAXWELL LTD., Cowper Works, *Olney, Bucks MK46 4BN*
COLLET'S HOLDINGS LTD., Denington Estate, *Wellingborough, Northants NN8 2QT*
W.M. DAWSON AND SONS LTD., Cannon House, *Folkes-one Kent CT19 5EE*
H. K. LEWIS AND CO., 136 Gower Street, *London WC1E 6BS*

GREECE
KOSTARAKIS BROTHERS, International Booksellers, 2 Hippokratous Street, *Athens-143*

HOLLAND
MEULENHOFF-BRUNA B.V., Beulingstraat 2, *Amsterdam*
MARTINUS NIJHOFF B.V., Lange Voorhout 9—11, *Den Haag*
SWETS SUBSCRIPTION SERVICE, 347b Heereweg, *Lisse*

INDIA
ALLIED PUBLISHING PRIVATE LTD., 13/14 Asaf Ali Road, *New Delhi 110001*
150 B-6 Mount Road, *Madras 600002*
INTERNATIONAL BOOK HOUSE PVT. LTD., Madame Cama Road, *Bombay 400039*
THE STATE TRADING CORPORATION OF INDIA LTD., Books Import Division, Chandralok, 36 Janpath, *New Delhi 110001*

ITALY
EUGENIO CARLUCCI, P.O. Box 252, *70100 Bari*
INTERSCIENTIA, Via Mazzé 28, *10149 Torino*
LIBERIA COMMISSIONARIA SANSONI, Via Lamarmora 45, *50121 Firenze*
SANTO VANASIA, Via M. Macchi 58, *20124 Milano*
D. E. A., Via Lima 28, *00198 Roma*

JAPAN
KINOKUNIYA BOOK-STORE CO. LTD., 17-7 Shinjuku-ku 3 chome, Shinjuku-ku, *Tokyo 160-91*
MARUZEN COMPANY LTD., Book Department, P.O. Box 5056 Tokyo International, *Tokyo 100-31*
NAUKA LTD. IMPORT DEPARTMENT, 2-30-19 Minami Ikebukuro, Toshima-ku, *Tokyo 171*

KOREA
CHULPANMUL, *Phenjan*

NORWAY
TANUM-CAMMERMEYER, Karl Johansgatan 41—43, *1000 Oslo*

POLAND
WĘGIERSKI INSTYTUT KULTURY, Marszałkowska 80, *Warszawa*
CKP I W ul. Towarowa 28 *00-958 Warsaw*

ROUMANIA
D. E. P., *Bucureşti*
ROMLIBRI, Str. Biserica Amzei 7, *Bucureşti*

SOVIET UNION
SOJUZPETCHATJ — IMPORT, *Moscow*
and the post offices in each town
MEZHDUNARODNAYA KNIGA, *Moscow G-200*

SPAIN
DIAZ DE SANTOS, Lagasca 95, *Madrid 6*

SWEDEN
ALMQVIST AND WIKSELL, Gamla Brogatan 26, *101 20 Stockholm*
GUMPERTS UNIVERSITETSBOKHANDEL AB, Box 346, *401 25 Göteborg 1*

SWITZERLAND
KARGER LIBRI AG, Petersgraben 41, *4011 Basel*

USA
EBSCO SUBSCRIPTION SERVICES, P.O. Box 1943, *Birmingham, Alabama 35201*
F. W. FAXON COMPANY, INC., 15 Southwest Park, *Westwood, Mass, 02090*
THE MOORE-COTTRELL SUBSCRIPTION AGENCIES, *North Cohocton, N. Y. 14868*
READ-MORE PUBLICATIONS, INC., 140 Cedar Street, *New York, N. Y. 10006*
STECHERT-MACMILLAN, INC., 7250 Westfield Avenue, *Pennsauken N. J. 08110*

VIETNAM
XUNHASABA, 32, Hai Ba Trung, *Hanoi*

YUGOSLAVIA
JUGOSLAVENSKA KNJIGA, Terazije 27, *Beograd*
FORUM, Vojvode Mišića 1, *21000 Novi Sad*

28. XII. 1979 HU ISSN 0001—5407 Index: 26.007

ACTA CHIMICA

ACADEMIAE SCIENTIARUM HUNGARICAE

TOMUS 102 FASCICULUS 4

AKADÉMIAI KIADÓ, BUDAPEST

1979

ACTA CHIM. ACAD. SCI. HUNG. ACASA2 102 (4) 321–432 (1979)

ACTA CHIMICA

A MAGYAR TUDOMÁNYOS AKADÉMIA KÉMIAI TUDOMÁNYOK OSZTÁLYÁNAK IDEGEN NYELVŰ KÖZLEMÉNYEI

Acta Chimica is a journal for the publication of papers on all aspects of chemistry in English, German, French and Russian.

Acta Chimica is published in 4 volumes per year. Each volume consists of 4 issues of varying size.

Manuscripts should be sent to

Acta Chimica
Budapest, P.O. Box 67, H-1450, Hungary

Correspondence with the editors should be sent to the same address. Manuscripts are not returned to the authors.

Subscription: $36.00 per volume.

Hungarian subscribers should order from Akadémiai Kiadó, 1363 Budapest, P.O. Box 24. Account No. 215 11488.

Orders from other countries are to be sent to "Kultura" Foreign Trading Company (H-1389 Budapest 62, P.O. Box 149. Account No. 218 10990) or its representatives abroad

Acta Chimica Academiae Scientiarum Hungaricae, Tomus 102 (4), pp. 321—332 (1979)

INFORMATION THEORY ANALYSIS OF THE NODAL PROPERTIES OF π-MOLECULAR ORBITALS

D. BONCHEV, G. LICKOMANNOV and N. TRINAJSTIĆ[1]

(Department of Physical Chemistry, Higher School of Chemical Technology, Burgas, Bulgaria and [1]The Rudjer Bošković Institute, Zagreb, Croatia, Yugoslavia)

Received December 29, 1977

In revised form December 11, 1978

Accepted for publication January 22, 1979

An approach based on information theory which reflects well the main features of the nodal properties of π-molecular orbitals was developed. The frontier orbitals (HOMO and LUMO) are found to have the maximum information content whilst the lowest occupied and the highest unoccupied molecular orbitals (LOMO and HUMO) the minimum one. Equations describing the information on the nodal properties of polyenes and annulenes are derived. A possible prediction of the nodal properties of π-MO's is discussed on this basis.

Introduction

Chemistry of conjugated systems has a long and distinguished history [1] and still is of interest for both experimental and theoretical chemists [2]. One of the prime ways to study conjugated systems theoretically, in order to set rules with the predictive power to guide the efforts of experimentalists, appears to be a simple π-molecular orbital theory proposed years ago by HÜCKEL and further developed by COULSON [4]. Recent interest [5,6] in this simple MO theory has been stimulated by recognizing that many properties of conjugated systems may be obtained solely from the information on the molecular connectivity [7].

Nodal properties of π-molecular orbitals are important in discussions concerning spectroscopic transitions [8], frontier orbitals (highest occupied and lowest empty molecular orbitals: HOMO, LUMO) [9], selection rules for ring closure or ring opening in chemical reactions [10], non-bonding molecular orbitals (NBMO) [11], *etc.* However, there is a very limited systematic work carried out on nodal properties of π-MO's [12] besides some special applications where the nodal surfaces yielded information on the relative ordering of molecular orbitals [13, 14].

The aim of the present work is to investigate the information features of the π-MO nodal properties.

Information theory is already used in chemistry in the study of molecular topology [15—18] and symmetry [19], as well as for some problems of molecular orbital theory like loge-theory of DAUDEL [20], quantum information theory of INGARDEN [21], *etc.* One of the approaches based on information theory most often used introduces the so-called information content of the system under consideration. The equation of SHANNON and WEAVER [22] is usually taken as a basis which defines the average information content of the system, $\bar{I}$, in bits:

$$\bar{I} = -\sum_{i=1}^{k} p_i \cdot \log_2 p_i . \tag{1}$$

A modification of this equation [23] is used to define the total information content of the system, I:

$$I = N \cdot \bar{I} = N \cdot \log_2 N - \sum_{i=1}^{N} N_i \cdot \log_2 N_i \tag{2}$$

where N is the total number of elements of the system, N_i, is the number of elements in the i-th group of elements (all N elements are supposed to be partitioned, according to a certain criterion, into k groups having N_1, N_2, . . ., N_k elements, respectively). p_i (= N_i/N) in Eq. (1) is the probability of a randomly chosen element to be in the i-th group of elements.

Methods

The simplest approach in applying information theory to the analysis of the nodal properties of π-molecular orbitals is concerned with a complete set of coefficients belonging to a given molecular orbital. Dividing this set into subsets according to the coefficients signs only (plus, minus, or zero), a certain quantity of information may be associated with the molecular orbital, following Eqs (1) and (2). This approach reminds that of the simplified molecular orbitals, suggested by HERNDON and SILBER [24], in which the MO coefficients have the values +1, −1 and 0 only. This information measure on nodal properties of molecular orbitals, however, is not sensitive enough, often being the same for different MO's. For instance, five out of eight molecular orbitals describing the π-electron system of the cyclooctatetraene molecule have the same information content.

Another possible approach is to construct the set of molecular spatial regions between every pair of adjacent atoms in the molecule under consideration. These regions may have or may have not a node, manifesting nodal or non-nodal properties (see Fig. 1a).

When the node is not located between two adjacent atoms, but on a given atomic nucleus (Fig. 1b) a question arises how to interpret such a case and to remain within the same definition. One could view the two interatomic regions in Fig. 1b, belonging to a third kind of such region which is neither nodal, nor non-nodal. We prefer another interpretation according to which half of the interatomic regions of this kind is nodal (that which borders the node), and the other half is non-nodal. This will introduce non-integer values

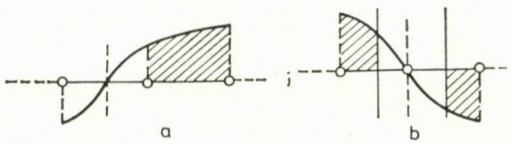

Fig. 1. Partitioning of the π-molecular orbital space into nodal ([ ]) and non-nodal ([////]) regions

for the interatomic regions since such a node always borders two regions. Treating these two regions always together one obtains as a whole one nodal and one non-nodal region. In such a way the whole intramolecular π-molecular orbital space could be divided into nodal and non-nodal regions. The set of π-MO spatial regions thus constructed (their number is denoted by m) has n nodal and $m-n$ non-nodal regions. Applying Eq. (2) an information measure on nodal properties, I^{NP}, can be specified:

$$I^{NP} = m \cdot \log_2 m - n \cdot \log_2 n - (m - n) \cdot \log_2 (m - n) \qquad (3)$$

This approach is applied to π-molecular orbitals of polyenes and annulenes.

Polyenes

Butadiene, C_4H_6, is a convenient example to detail the method. It has four π-molecular orbitals [25]. Their nodal properties are depicted in Fig. 2.

The number of carbon atoms is denoted by $N(=4)$ and the set of the spatial regions has $m = N - 1$ $(= 3)$ elements. By writing the number of the non-nodal and nodal regions as ordered pairs of elements the following sets can be constructed:

$$S_1(3,0); \quad S_2(2,1); \quad S_3(1,2); \quad S_4(0,3)$$

Applying Eq. (3) one can calculate the information on the nodal properties of MO's to be $I^{NP} = 0$ for S_1 and S_4 and $I^{NP} = 3 \cdot \log_2 3 - 2 = 2.75$ bits for S_2 and S_3. Therefore, the paired orbitals (S_1 and S_4; S_2 and S_3) have the same

information content. In addition, the lowest occupied and highest unoccupied molecular orbitals (LOMO, HUMO) have a minimum information content. The information content of the frontier orbitals (HOMO, LUMO) is higher than that of any other orbital.

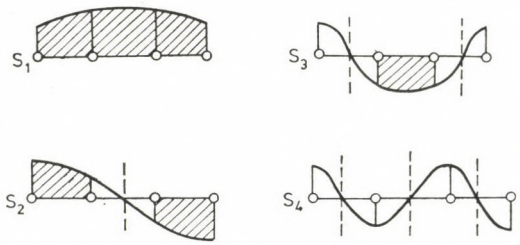

Fig. 2. Nodal and non-nodal regions (and , respectively) of the four π-molecular orbitals of butadiene

The sets of π-molecular orbital spatial regions of polyenes having 2 to 10 carbon atoms are given in Table I. One can see that if the molecular orbitals are labelled by 1,2,3, . . . , k, respectively, the nodal regions are $k-1$ in number. Hence, the information on the nodal properties of the polyene π-molecular orbitals I_k^{NP}, may be expressed as a function of the number of carbon atoms and the MO label only:

$$I_k^{NP} = (N-1)\cdot\log_2(N-1) - (N-k)\cdot\log_2(N-k) - (k-1)\cdot\log_2(k-1) \quad (4)$$

Table I

Number of the non-nodal and nodal regions in π-molecular orbitals of polyenes up to ten carbon atoms

π-MO	2	3	4	5	6	7	8	9	10
S_1	1,0	2,0	3,0	4,0	5,0	6,0	7,0	8,0	9,0
S_2	0,1	1,1	2,1	3,1	4,1	5,1	6,1	7,1	8,1
S_3		0,2	1,2	2,2	3,2	4,2	5,2	6,2	7,2
S_4			0,3	1,3	2,3	3,3	4,3	5,3	6,3
S_5				0,4	1,4	2,4	3,4	4,4	5,4
S_6					0,5	1,5	2,5	3,5	4,5
S_7						0,6	1,6	2,6	3,6
S_8							0,7	1,7	2,7
S_9								0,8	1,8
S_{10}									0,9

This function is expressed in Fig. 3 for even and odd polyenes having from 3 to 10 carbon atoms.

The following conclusions can be reached from the results presented in Fig. 3:

(1) The presence of three types of molecular orbitals: bonding, nonbonding, and antibonding is well reflected in the information theory analysis. (The bonding and antibonding molecular orbitals lie on the left, and, respec-

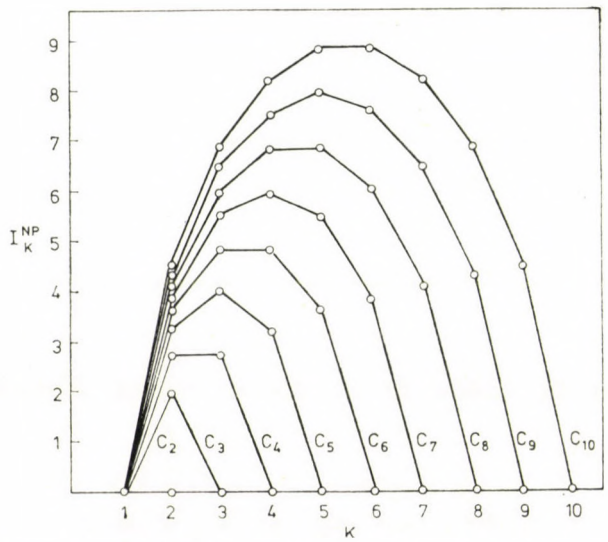

Fig. 3. Information on the nodal properties of π-molecular orbitals of polyenes having from 3 to 10 carbon atoms as a function of the MO label k. The points of each curve express the different π-MO whose number equals the number of carbon atoms in the polyene under consideration. The ethylene molecule is presented by the line 1—2 on the abscissa

tively, right side of the information curve, whilst the nonbonding orbital is given in a single maximum point of this curve.)

(2) Similarly, the symmetry that exists between the bonding and antibonding orbitals of polyenes (the pairing theorem of COULSON and RUSHBROOKE [26] is also reflected.

(3) The frontier orbitals (HOMO and LUMO) have the *maximum* information content. In the case when the number of carbon atoms is odd the information content of the frontier NBMO in bits is equal to this number.

(4) The lowest occupied and the highest unoccupied molecular orbitals (LOMO and HUMO) have the *minimum* information content, equal to zero.

(5) The increase in the information content of frontier orbitals, occurring when the number of carbon atoms increases by one, is greater on going from

even to odd than from odd to even polyenes, and in parallel with some molecular properties becomes smaller at a larger N.

Since the polyene π-electron energy [27] E_k, and information content of each π-molecular orbital of a given polyene are functions of the same quantities (*i.e.*, the total number of carbon atoms and the MO label k) they can be related by the following expression:

$$I_k^{NP} = (\alpha k\pi - 2) \cdot \log_2 (\alpha k\pi - 2) - (\alpha k\pi - k - 1) \cdot \\ \cdot \log_2 (\alpha k\pi - k - 1) - (k - 1) \cdot \log_2 (k - 1) \quad (5)$$

where

$$\alpha = 1/\arccos (-0.5E_k) \quad (6)$$

Equations (5) and (6) reflect (see also page 324, lines 6 to 8) the well-known fact [4, 25] that E_k increases with the increase of the number of nodes in π-molecular orbital.

Annulenes

[N] annulenes represent a family of the monocyclic conjugated hydrocarbons, C_NH_N ($N = 3, 4, 5, \ldots$) [28]. Benzene may be taken as an example to illustrate the application of our procedure to cyclic systems. The nodal properties of the molecular orbitals of benzene are depicted in Fig. 4.

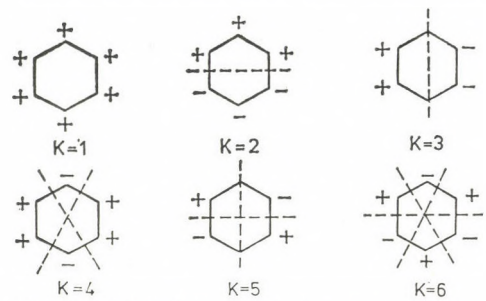

Fig. 4. Nodal planes of the benzene π-MO's

In annulenes the cardinality n of the set constructed from the nodal and non-nodal regions (*i.e.*, the total number of π-MO's) is equal to the number of carbon atoms N: $n = k_{max} = N$. The following sets are formed for the benzene π-MO's, in which the number of the nodal and non-nodal regions are expressed as ordered pairs:

$$S_1(6,0); \quad S_2, S_3(4,2); \quad S_4, S_5(2,4); \quad S_6(0,6)$$

The sets of nodal and non-nodal regions in annulenes having from 3 to 10 carbon atoms are presented in Table II.

Utilizing relations (1) and (2) the following equations were derived which link the information on the nodal properties of π-MO's of annulenes with

Table II

Number of the non-nodal and nodal regions in π-molecular orbitals of annulenes up to ten carbon atoms

π-MO	C_3H_3	C_4H_4	C_5H_5	C_6H_6	C_7H_7	C_8H_8	C_9H_9	$C_{10}H_{10}$
S_1	3,0	4,0	5,0	6,0	7,0	8,0	9,0	10,0
S_2	1,2	2,2	3,2	4,2	5,2	6,2	7,2	8,2
S_3	1,2	2,2	3,2	4,2	5,2	6,2	7,2	8,2
S_4		0,4	1,4	2,4	3,4	4,4	5,4	6,4
S_5			1,4	2,4	3,4	4,4	5,4	6,4
S_6				0,6	1,6	2,6	3,6	4,6
S_7					1,6	2,6	3,6	4,6
S_8						0,8	1,8	2,8
S_9							1,8	2,8
S_{10}								0,10

the number of carbon atoms and the molecular orbitals label k:

$$I_k^{NP} = N \cdot \log_2 N - (N - k) \cdot \log_2 (N - k) - k \cdot \log_2 k; \quad k = \text{even} \tag{7}$$

$$I_k^{NP} = N \cdot \log_2 N - (N - k + 1) \cdot \log_2 (N - k + 1) - \\ - (k - 1) \cdot \log_2 (k - 1); \quad k = \text{odd} \tag{8}$$

Results for annulenes up to $N = 10$ are presented in Fig. 5.

Annulenes with even number of atoms N, as seen from Fig. 5, exhibit all the features of the information function established earlier in this work for π-MO's of polyenes. In addition, the degeneracy of the frontier orbitals is also reflected. In the case of odd annulenes (non-alternant monocycles) the lack of symmetry between the bonding and antibonding orbitals narrows the general conclusions obtained from the information function making them also more complicated:

(1) The presence of two types of molecular orbitals, bonding and antibonding, is again reflected by the left, and, respectively, right side of the information curve. The four kinds of cyclic compounds, having carbon atoms, respectively, $N = 4n$, $4n + 1$, $4n + 2$, and $4n + 3$, differ, however, in the way in which the orbitals with a maximum information content are referred

to the two types of MO's. In the case of $N = 4n + 2$ the four maximum points are symmetrically partitioned into two bonding and two antibonding MO's. In the other cases two maximum points appear which for $N = 4n + 1$ refer to the antibonding MO's, for $N = 4n + 3$ refer to bonding MO's, and only

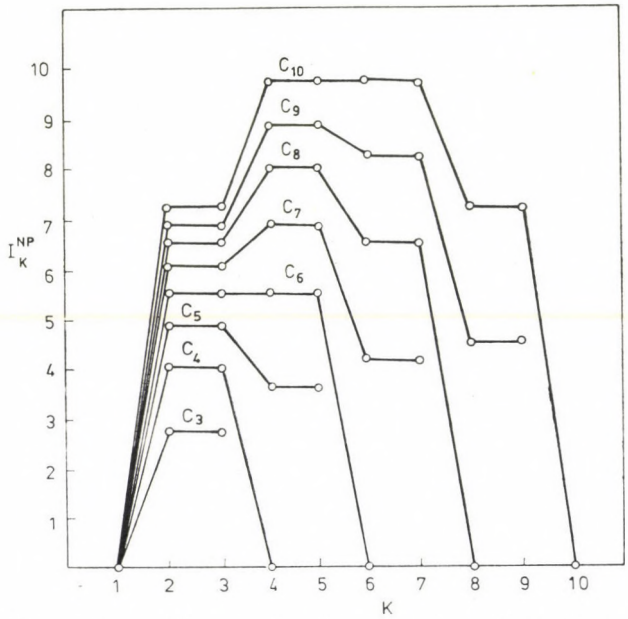

Fig. 5. Information on the nodal properties of π-molecular orbitals of annulenes having 3 to 10 carbon atoms as a function of the MO label k. The points of each curve express the different π-MO's, whose number equals the number of carbon atoms in the annulene under consideration

for $N = 4n$ they refer to the third kind of molecular orbitals — the non-bonding ones.

(2) The frontier orbitals (HOMO and LUMO) have the *maximum* information content. Expressed in bits, the latter is equal to the number of carbon atoms N for $N = 4n$, and less than it for $N \neq 4n$, being relatively the smallest for $N = 4n + 2$.

(3) LOMO and HUMO have the *minimum* information content in comparison with the other orbitals, respectively ($I^{NP}_{LOMO} = 0$; $I^{NP}_{HUMO} = 0$, or $\neq 0$).

(4) The increase in the information content of the frontier orbitals appearing when the number of carbon atoms increases by one, is different for rings having $4n + 2$, $4n + 3$, $4n$, and $4n + 1$ atoms, decreasing regularly in this order.

Making use of Eqs (7) and (8) a one-to-one correspondence between the energy and information on nodal properties of π-molecular orbitals of annulenes is found:

$$I_k^{NP} = 2\alpha k\pi \cdot \log_2 2\alpha k\pi - (2\alpha k\pi - k) \cdot \log_2 (2\alpha k\pi - k) - \\ - k \cdot \log_2 k; \quad k = \text{even} \tag{9}$$

$$I_k^{NP} = 2\alpha k\pi \cdot \log_2 2\alpha k\pi - (2\alpha k\pi - k + 1) \cdot \log_2 (2\alpha k\pi - k + 1) - \\ - (k - 1) \cdot \log_2 (k - 1); \quad k = \text{odd} \tag{10}$$

where

$$\alpha = 1/\arccos (0.5E_k) \tag{11}$$

In addition, the expressions for the total information on the MO nodal properties of polyenes and annulenes are derived:

$$I_{TOTAL}^{NP} \text{ (Polyenes)} = N(N-1) \cdot \log_2 (N-1) - \\ - \sum_{k=1}^{N} (N-k) \log_2 (N-k) + (k-1) \cdot \log_2 (k-1) \tag{12}$$

$$I_{TOTAL}^{NP} \text{ (Annulenes)} = N^2 \cdot \log_2 N - \sum_{k=2a}^{k\text{-HOMO}} (N - k + \Delta) \cdot \\ \cdot \log_2 (N - k + \Delta) + (k - \Delta) \cdot \log_2 (k - \Delta) \tag{13}$$

where for $k =$ even, $\Delta = 0$ and for $k =$ odd, $\Delta = 1$.

On the basis of Eqs (4), (7), and (8) it can be concluded that the information content of the frontier orbitals of polyenes increases upon their cyclization. This increase is maximal for structures having $4n$ — carbon atoms, and minimal for those with $4n + 2$ — carbons. In the case of structures having $4n + 1$ or $4n + 3$ — carbon atoms the increase is of the same order and they have intermediate values between $4n$ and $4n + 2$ rings.

By comparing polyenes and annulenes having $N + 1$, and N carbon atoms, respectively, one can also find a great similarity that exists between the nodal properties of their molecular orbitals (Tables I and II). The distribution of the nodal and non-nodal regions in annulene π-MO's can be deduced from those of the corresponding polyene π-MO's using the following procedure:

1. In the even-annulenes the number of nodal and non-nodal regions in each π-MO should be even, due to the molecular symmetry. Hence, all the distributions of polyene π-MO's having odd number of nodal and non-nodal regions should not be taken into account and all others, except LOMO and HUMO distributions, should be duplicated in the corresponding annulene.

2. In the odd-annulenes, due to symmetry, the total number of interatomic regions is divided always into an odd number of non-nodal and an even number of nodal regions. Then again, that distribution in polyene π-MO's which do not fulfil these conditions should be excluded from consideration for annulenes, and all other distributions, except that corresponding LOMO, should be duplicated.

This procedure could be extended for predicting nodal properties of π-MO's in different series of compounds, which have similar topology, taking polyenes as reference compounds. The reference polyene should be selected as such to reproduce the same total number of nodal and non-nodal regions of a molecule under study. It is known that the monocyclic, bicyclic, tricyclic, *etc.* compounds have respectively 1, 2, 3, *etc.* bonds (or regions between the neighbouring atoms) more than the corresponding polyene having the same number of carbon atoms N. Then the reference polyenes having the same number of bonds with the three structures given below should have 1, 2, 3, *etc.* carbon atoms more than the corresponding cyclic structure, *i.e.* these polyenes should have 19, 20, and respectively 21, instead of 18 carbon atoms:

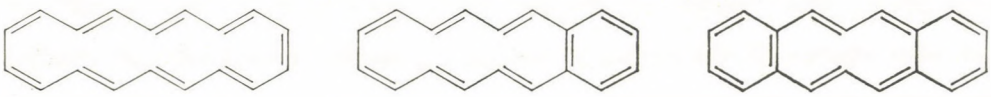

Another interesting result is that the information on nodal properties of the frontier orbitals in most cases is conserved during the transmutation of a certain structure into another one. For instance, in the case of polyenes and annulenes a typical transmutation is given below:

This holds for all N-membered rings except the most stable $4n + 2$-ones:

$$I^{N+1\text{-polyenes}}_{\text{HOMO(LUMO)}} = I^{N\text{-annulenes}}_{\text{HOMO(LUMO)}} \qquad (14)$$

where $N = 4n$, $4n + 1$, and $4n + 3$.

Equality (14) is confirmed from the comparison of Figs 3 and 5. It is easily proved from the equality between equation (8) given for MO's with odd label k in annulenes having N carbon atoms, and Eq. (4) given for MO's with the same label k, but in polyenes having $N + 1$ instead of N atoms. Due to the degeneracy, a frontier MO with an odd label k always exists in annulenes. The comparison of the data from Tables I and II shows that the same odd label k, in polyenes having one carbon atom more than the corresponding annulene, also belongs to a frontier orbital with the same nodal properties. For instance, for C_5H_5 and C_6H_6 this is the label $k = 3$. The same holds for the pair C_4H_4 and C_5H_8, for the pair C_7H_7 and C_8H_{10} it is $k = 5$, *etc.* Only for annulenes having $N = 4n + 2$ carbon atoms (C_6H_6, $C_{10}H_{10}$, *etc.*) the same odd MO-label k in the corresponding polyene does not belong to a frontier orbital. In the latter case the polyene's frontier orbital has a label $k' = k + 1$, and Eqs (4) and (8) are no more identical.

Other reactions in the organic chemistry of conjugated hydrocarbons could be examined in searching for more examples of the conservation of information on nodal properties of frontier orbitals which could be of use for the theory of chemical reactivity.

Conclusion

The most interesting result of the information theory analysis of the nodal properties of π-molecular orbitals is that the frontier orbitals (HOMO, LUMO) have the *maximum* information content due to the equal or almost equal number of their nodal and non-nodal regions. It is well known [9, 10, 29] that the frontier orbitals are of the great importance in the studies of chemical reactivity and are of use in predicting (within the Klopmans' theorem) the first ionization potentials and electron affinities.

On the other hand, the hypothesis of the existence of a general trend toward the maximum information content of matter was recently proposed [30]. The Pauli exclusion principle, the first Hund rule and other known or yet unknown rules may appear as specific cases of a certain general principle of maximum information. The result concerning the maximum information content of frontier orbitals and its preserving in some chemical reactions offers a possibility to investigate whether the WOODWARD—HOFFMAN (DEWAR—EVANS) rules [10, 29, 31, 32] may also be associated with this general information principle. Studies in this direction are in progress[33].

*

We thank Dr. Ante GRAOVAC and Mr. Branko RUŠČIĆ (Zagreb) for useful comments.

REFERENCES

[1] CLAR, E.: Polycyclic Hydrocarbons, Academic Press, London 1974
[2] The recent international meetings on aromatic compounds in San Francisco (August 22—30, 1977) and Columbus (September 28—30, 1977) are supporting this statement rather well
[3] HÜCKEL, E.: Z. Physik, **70,** 204 (1931)
[4] "Coulson's Hückel theory for Organic Chemists" Edited by R. B. MALLION and B. O'LEARY, Academic Press, London, in press
[5] AIHARA, J. I.: J. Am. Chem. Soc., **98,** 2750 (1976)
[6] GUTMAN, I., MILUN, M., TRINAJSTIĆ, N.: J. Am. Chem. Soc., **99,** 1692 (1977)
[7] TRINAJSTIĆ, N., in: "Semiempirical Methods of Electronic Structure Calculations, Part *A:* Techniques", Edited by G. A. SEGAL, Modern Theoretical Chemistry, Vol. **7,** Plenum Press, New York 1977, p. 1
[8] MURREL, J. N.: "The Theory of the Electronic Spectra of Organic Molecules", Methuen, London 1963
[9] FUKUI, K.: Topics Curr. Chemistry, **15,** 1 (1970); "Theory and Stereoselection", Springer-Verlag, Berlin 1975

[10] WOODWARD, R. B., HOFFMAN, R.: J. Am. Chem. Soc., **87,** 395 (1965); "The Conservation of Orbital Symmetry", Verlag-Chemie, Weinheim 1970
[11] WILCOX, C. F., Jr.: Tetrahedron Lett., **1968,** 795; J. Am. Chem. Soc., **91,** 2732 (1969)
[12] RANDIĆ, M.: Theoret. Chim. Acta, (In press)
[13] SCHMIDTKE, H. H.: Int. J. Quantum Chem., **7,** 127 (1973)
[14] WILSON, E. B.: J. Chem. Phys., **63,** 4870 (1975)
[15] RASHEVSKY, N.: Bull. Math. Biophys., **17,** 229 (1955)
[16] TRUCCO, E.: Bull. Math. Biophys., **18,** 129 (1956); *ibid.*, **18,** 237 (1956)
[17] MOWSHOWITZ, A.: Bull. Math. Biophys., **30,** 175, 225, 387, 353 (1968)
[18] BONCHEV, D., TRINAJSTIĆ, N.: J. Chem. Phys., **67,** 4517 (1977)
[19] BONCHEV, D., KAMENSKI, D., KAMENSKA, V.: Bull. Math. Biol., **38,** 119 (1976)
[20] *e.g.:* "Localization and Delocalization in Quantum Chemistry", Edited by CHALVET and DAUDEL Dordrecht, Amsterdam 1975
[21] INGARDEN, R.: Reports on Mathematical Physics, (In press). We thank Professor INGARDEN (Torun) for informing us about his work prior to publication
[22] SHANNON, C., WEAVER, W.: "Mathematical Theory of Communications", University of Illinois Press, Urbana 1949
[23] BRILLOUIN, L.: "Science and Information Theory" Academic Press, New York 1956
[24] HERNDON, W. C., SILBER, E.: J. Chem. Educ., **48,** 502 (1971)
[25] COULSON, C. A., STREITWIESER, A. Jr.: "Dictionary of π-Electron Calculations" Pergamon Press, Oxford 1965
[26] COULSON, C. A., RUSHBROOKE, G. S.: Proc. Comb. Phill. Soc., **36,** 193 (1940)
[27] GUTMAN, I., TRINAJSTIĆ, N., ŽIVKOVIĆ, T.: Chem. Phys. Lett., **14,** 342 (1972)
[28] SONDHEIMER, F., WOLOVSKY, R.: J. Am. Chem. Soc., **84,** 260 (1962)
[29] FLEMING, I.: "Frontier Orbitals and Organic Chemical Reactions", Wiley, London 1976
[30] BONCHEV, D.: J. Math. Phys. (submitted)
[31] DEWAR, M. J. S.: Angew. Chem. Internat. Edition, **10,** 761 (1971)
[32] PEARSON, R. G.: "Symmetry Rules for Chemical Reactions", Wiley, London 1976
[33] BONCHEV, D.: Work in preparation

Danail Georgiev BONCHEV
George Nikolov LICKOMANNOV

Department of Physical Chemistry,
Higher School of Chemical Technology,
8010 Burgas, Bulgaria

Nenad TRINAJSTIĆ

Institute "Rudjet Bošković",
P.O.B. 1016, 41001 Zagreb,
Croatia, Yugoslavia

Acta Chimica Academiae Scientiarum Hungaricae, Tomus 102 (4), pp. 333—339 (1979)

PRESSURE-HYDROTHERMAL PREPARATION OF ScOOD

A. BUREWICZ and S. ZIELIŃSKI

(Institute of Chemistry, Adam Mickiewicz University, Poznań, Poland)

Received November 21, 1978

Accepted for publication January 23, 1979

Pressure-hydrothermal method was developed in order to obtain scandium oxide deuteroxide. The most suitable conditions for the preparation are as follows: 30 atm, 90 °C, conversion time 150 hrs. Isotopically and structurally pure ScOOD was obtained by this method using scandium metal as a starting material and separating the first fraction (about 20%) of scandium orthodeuteroxide.

Calcination of $Sc(OD)_3$ in the temperature range of 20—500 °C did not yield pure ScOOD.

The identification of samples was carried out by chemical analysis, X-ray and spectroscopic measurements.

The structural investigation on transition metal oxide hydroxides by means of IR [1] and the possibility of determining the position of hydrogen ions by means of neutron diffraction [2] for which the deuterated compounds are essential, were the reasons to elaborate a method for the preparation of structurally pure scandium oxide deuteroxide preparation. MILLIGAN's proposition to obtain scandium oxide hydroxide by high-pressure method [3], appeared to be of no use in case of scandium deuteroxide because of technical difficulties. The method of AUER-WELSBACH and SEIFER [4] could not be applied because of unsatisfying purity of the obtained preparation. Preparations obtained by the method which had been used to prepare iron(III)metadeuteroxides [5, 6] were heterogeneous both from chemical and X-ray structural points of view. After many trials we elaborated the pressure-hydrothermal method for the preparation of pure scandium oxide deuteroxide. The method is similar to that which has been proposed by M. FIGLARZ *et al.* [7] for the oxidation of cobalt(II)hydroxide.

Experimental

$Sc(OD)_3$ was obtained by two methods from two different starting materials. Hydrated $ScCl_3$ (Koch Light Laboratorium Ltd., Cotubrook Bucks, England) dried in air at 120 °C for 42 hours was used in the first case. As a result of drying, scandium chloride with a water content of 4.86% was obtained; this was found by determining scandium by complexometric titration [8]. The determination of Cl^- was carried out by precipitating AgCl, dissolving the precipitate in NH_4OH in the presence of $K_2[Ni(CN)_4]$, and determining the liberated Ni^{2+} ions by the method of FLASCHKA and HUTITZ [9]. 5.26 g of the preparation obtained in the above described way, containing 5 g of $ScCl_3$, was dissolved in 33 cm^3 of 99.75% pure D_2O (produced

in the Institute of Nuclear Research, Warsaw, Poland) followed by slow addition of 90 cm^3 of 1.1*M* NaOD solution in D_2O of an isotopic purity of 99.65% in order to precipitate $Sc(OD)_3$. The obtained pD was 6.9.

The negligible amount of H_2O present in D_2O was obtained by adding of *ca* 1*M* solution of NaOD. The $Sc(OD)_3$ precipitate formed was filtered, and dried at 20 °C in dry nitrogen.

In the second case 1.48 g of scandium metal (99.98%) was dissolved in hot DCl solution (40 cm^3 of 10% solution in D_2O) and after evaporating to 33 cm^3, $Sc(OD)_3$ was precipitated as in the first case.

Independently, the samples of $Sc(OD)_3$ were prepared but the first portion (*ca* 20%) was precipitated and removed, whereafter the other part of scandium deuteroxide was precipitated and treated in the same way as described above.

The ScOOD and ScOOH preparations were obtained by pressure-hydrothermal method.

The apparatus consisted of a pressure reactor in which the suspension of scandium orthodeuteroxide (obtained in the above described manner) in 20 cm^3 of heavy water was placed. The suspension was stirred during reaction, the reactor was kept under constant oxygen pressure and the whole reactor was thermally controlled.

Scandium in $Sc(OD)_3$ and ScOOD was determined by EDTA titration, and deuterium by oxydation method on a Perkin—Elmer 240 apparatus. The IR spectra were taken on a Perkin—Elmer 580 apparatus in the range of 4000 — 400 cm^{-1} using KBr pellets. The X-ray diffraction patterns (Co K_α) were obtained on a TUR M-62 diffractometer with horizontal goniometer with GM counter moving at a speed of 1° min^{-1}. In all measurements a voltage of 30 KV and a current of 25 mA were applied.

Results and Discussion

$Sc(OD)_3$ obtained from two different starting materials were of high purity both structurally and isotopically. The commercial $ScCl_3$ after prolonged drying at 120 °C still contained 4.86% of H_2O due to increased $Sc(OH)_3$ content in precipitated $Sc(OD)_3$. In case of scandium metal used as a starting material the presence of OH groups in $Sc(OD)_3$ depends on the amount of H_2O in D_2O and the amount of NaOH in NaOD. Taking into account H_2O and NaOH present in D_2O and NaOD, respectively, and the H_2O content in scandium chloride, theoretically the maximum content of $Sc(OH)_3$ in scandium orthodeuteroxide obtained by the first method is 31.5%, and by the second one 17.0%. The real content of OH groups in $Sc(OD)_3$ is slightly smaller than mentioned above. The results of IR measurements (curve 1 in Fig. 1) confirm that even the application of reagents of high isotopic purity cannot assure the formation of isotopically pure ScOOD independently of the starting material, if the whole amount of precipitated $Sc(OD)_3$ is used for the preparation of scandium oxide deuteroxide. We have found experimentally, that in case of $Sc(OD)_3$ obtained from scandium metal, containing theoretically maximum 17.0% of $Sc(OH)_3$ after removing the first portion of precipitate (*ca* 20%), from the remained part we can obtain isotopically pure ScOOD by pressure hydrothermal method. This can be confirmed by the absorption band at 2700 cm^{-1} corresponding to OD group vibrations (curve 2 in Fig. 1). ScOOD obtained under these new conditions by the first method still contained some OH groups [absorption bands at 3300 cm^{-1} corresponding to stretching vibration of OH group (curve 3 in Fig. 1)]. For comparison, curve 4 in Fig. 1

represents the spectra of pure ScOOH. The presence of OH groups in ScOOD is caused by the water remained in the starting material — scandium chloride, dried at 120 °C. The purity of ScOOD is also influenced by the pD of the solution after the precipitation of the scandium orthodeuteroxide. The proper pH for the precipitation of $Sc(OH)_3$ is between 6.0 and 6.5 [10]. This value was kept when precipitating $Sc(OD)_3$ taking into account that pD = pH + 0.4

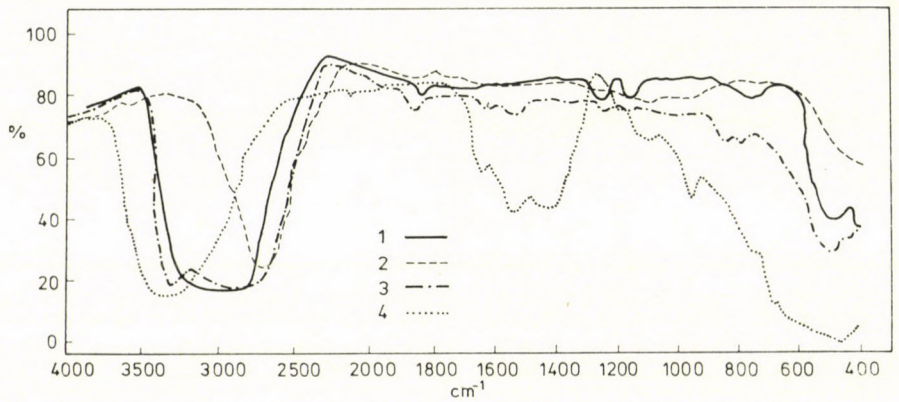

Fig. 1. IR spectra of ScOOD/ScOOH in the range of 4000—400 cm^{-1}; 1. ScOOD obtained from scandium metal without the separation of the first fraction; 2. ScOOD obtained from scandium metal after the separation of the first fraction; 3. ScOOD obtained from $ScCl_3$ dried after the separation of the first fraction; 4. ScOOH

[11]. It was found that an increase of 0.5 in pD caused a decrease in ScOOD yield of 16% and that a decrease of 0.2 in pD caused the product to contain 3.7% of Cl^-. This ion cannot be removed by washing, probably because it is occluded by $Sc(OD)_3$.

At the conversion of scandium orthodeuteroxide to oxide deuteroxide by the pressure-hydrothermal method the time of the procedure determined the formation of particular crystallographic phases in the final product (other parameters remained constant: pressure 30 atm, temperature 90 °C). This was found by means of chemical and X-ray analysis. For example — for the preparation obtained by pressure hydrothermal method lasting for 75 hours — it was found by means of chemical analysis — that the content of scandium in this compound was 51.2%. This value is smaller than the theoretical one for scandium oxide deuteroxide by 5.7%, whereas the X-ray study shows that the only phase which occurs is the phase of scandium oxide deuteroxide (curve 1 in Fig. 2). An increase in the time of preparation up to 150 hours causes the increase of scandium content in the preparation (56.8%) and from X-ray diffraction study it is concluded that the only phase, which is present is scandium oxide deuteroxide. It seems that the decrease of background in

diffractogram (curve 2 in Fig. 2) confirms the presence of X-ray-amorphous scandium orthodeuteroxide. Prolongation of the time of preparation up to 225 hours leads to the formation of a second crystallographic phase (curve 3 in Fig. 2), which was also confirmed by the increase of scandium content up to 62.7%. It can be concluded from these data that together with scandium oxide deuteroxide, scandium oxide was formed under these conditions. This leads

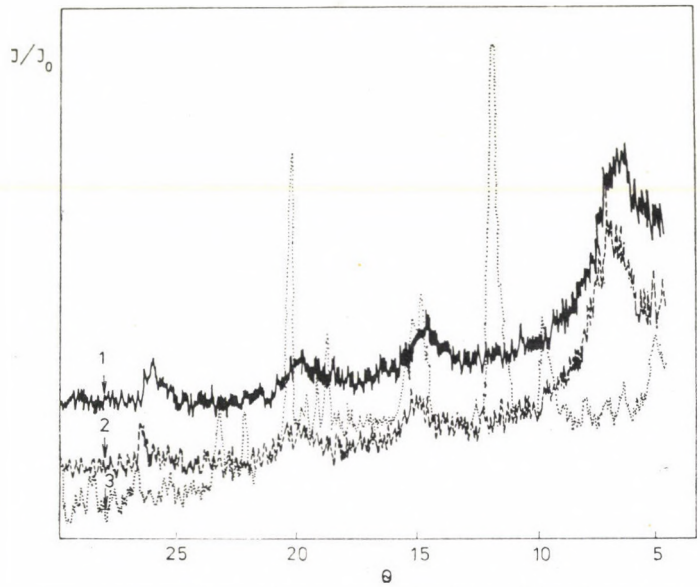

Fig. 2. Diffractograms of scandium oxide deuteroxide obtained by the pressure-hydrothermal method — 1—75 hrs, — 2—150 hrs, — 3—225 hrs

to the conclusion that the most suitable period of time for the preparation is 150 hours. During this period of time scandium orthodeuteroxide is completely converted into scandium oxide deuteroxide, and scandium oxide is not yet formed. The scheme of phase changes shown in Fig. 3 was established by investigating the dehydration of $Sc(OD)_3$ over a wide temperature range and by the X-ray and chemical analyses of the preparations. It has been pointed out that during the scandium oxide hydroxide formation the conversion occurs at a pressure of 15 atm and the product (taking into account X-ray data) corresponds to scandium oxide deuteroxide obtained at 30 atm. Scandium orthodeuteroxide obtained from scandium metal was dried at different temperatures between 20° and 500 °C for two hours at each temperature in order to study the dehydration of $Sc(OD)_3$ during calcination (Table I). After drying at 20 °C the scandium content was 5.4% and at 500 °C 65.1%, and the deuterium content was 10.1% at 20 °C and above 450 °C deuterium

was not present in the sample. At 120 °C scandium and deuterium content are almost identical with the theoretical ones in ScOOD, which suggests the formation of pure phase of this compound. The X-ray study curve in Fig. 4 confirmed the presence of Sc_2O_3 phase and of amorphous $Sc(OD)_3$, thus the

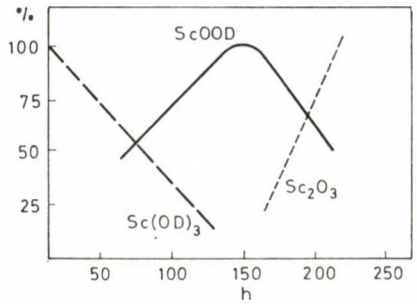

Fig. 3. Phase changes of scandium orthodeuteroxide during the preparation of scandium oxide deuteroxide by the pressure-hydrothermal method

Table I

Percentage of scandium and deuterium content in the preparation after two hours calcination of scandium orthodeuteroxide and oxide deuteroxides in the temperature range of 20—500 °C

°C	$Sc(OD)_3$		ScOOD	
	% SC	% D	% Sc	% D
20	5.4	10.1	19.2	5.1
50	12.4	6.2	27.4	3.9
100	51.2	4.1	56.9	2.6
120	56.9	2.5	56.9	2.6
150	57.2	2.1	57.1	2.5
200	58.4	1.9	57.3	2.5
220	59.1	1.2	57.3	2.5
250	60.1	1.0	57.4	2.5
300	61.2	0.6	57.4	2.5
400	64.1	0.1	64.8	—
450	64.9	—	65.1	—
500	65.1	—	65.1	—

analytical results were the mean of the $Sc(OD)_3$ and Sc_2O_3 phases. Calcination of $Sc(OD)_3$ at higher temperatures does not result in the formation of X-ray pure ScOOD although it was found in calcination products. Obtained by pressure-hydrothermal method isotopically pure ScOOD was calcinated under the same conditions. Up to 100 °C the preparation loses most of its D_2O content,

and in the temperature range of 100—120 °C a preparation of chemical composition close to the theoretical one is obtained.

In temperature range of 150—300 °C slow conversion of ScOOD into Sc_2O_3 is observed whereas above 300 °C this conversion is rapid. The second diffractogram in Fig. 4 confirms the presence of Sc_2O_3 phase in the products of ScOOD calcination at 400 °C.

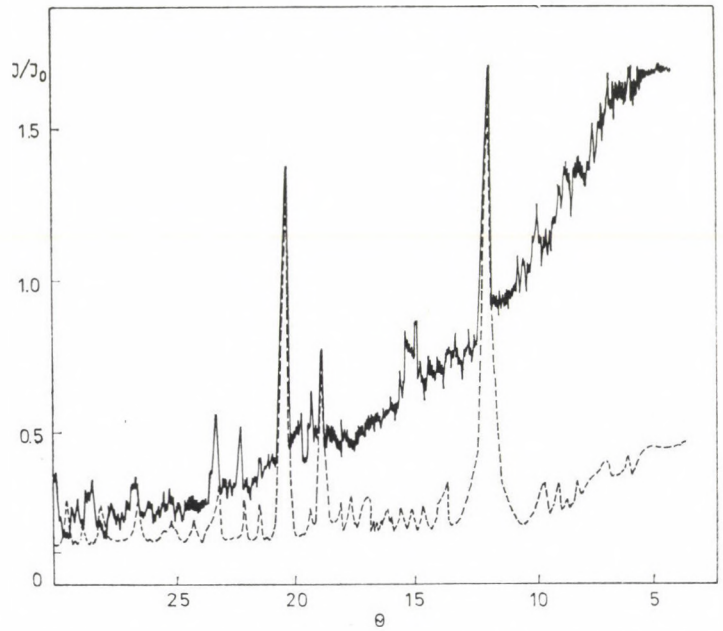

Fig. 4. Diffractograms of calcination products: 1. $Sc(OD)_3$ dried at 120 °C; 2. ScOOD dried at 400 °C

Table II

Percentage of scandium content in scandium oxide deuteroxide dried at 20 °C for 2 to 500 hours

h	% Sc
2	19.1
5	21.9
10	24.5
50	56.8
100	56.9
150	56.9
200	56.9
300	56.9
400	56.9
500	56.9

Pure ScOOD obtained by pressure-hydrothermal method was also dried at 20 °C for 500 hours (Table II). The analysis of products shows that after 50 hrs of drying a stable compound is obtained. The composition of this compound does not change during the time at analysis.

Conclusion

There are two stages of the preparation of ScOOD by pressure-hydrothermal method:

1. $Sc(OD)_3$ formation
2. $Sc(OD)_3$ conversion into ScOOD.

The most favourable conditions of conversion are: 90 °C, 30 atm, and a conversion time of 150 hrs.

Pressure-hydrothermal method, established by us, assures the formation of isotopically and X-ray pure ScOOD provided the first fraction (*ca* 20% of total) of $Sc(OD)_3$ precipitate is removed and scandium metal is used as a starting material. ScOOD obtained by this method is stable at 20 °C in dry air for 500 hrs. The preparations obtained after $Sc(OD)_3$ calcination in the temperature range of 20—500 °C under atmospheric pressure are not pure ScOOD but they contain Sc_2O_3 phases. The pressure-hydrothermal method can also be used to prepare pure ScOOH. The most suitable conditions of $Sc(OH)_3$ conversion into scandium oxide hydroxide are the following 90 °C, a conversion time of 150 hrs, and 15 atm.

REFERENCES

[1] Snycer, R. G., Ibers, J. A.: J. Chem. Phys., **36,** 1356 (1962)
[2] Szytuła, A., Burewicz, A., Dimitrijevic, Z., Kraśnicki, S., Rzany, H., Todorovic, J., Wanic, A., Wolski, W.: Phys. Stat. Sol., **26,** 429 (1968)
[3] Milligan, W. O., McAtee, J. L.: J. Phys. Chem., **60,** 273 (1978)
[4] Auer-Welsbach, H., Seifer, K.: Monatsh., **93,** 111 (1962)
[5] Burewicz, A.: Acta Chim. (Budapest) **91,** 253 (1976)
[6] Burewicz, A.: Z. neorg. Chim., **3,** 598 (1977)
[7] Figlarz, M., Guenot, J., Tournemolle, J. N.: J. Materials Sci., **9,** 772 (1974)
[8] Wünsch, L.: Coll. Czech. Chem. Comm., **20,** 1107 (1955)
[9] Flaschka, H., Hutitz, F.: Z. Anal. Chem., **137,** 104 (1952)
[10] Aphangielski, I. V., Komisarova, L. N., Puszkina, T. J., Tetiekin, E. G.: Z. neorg. Chim., **7,** 1756 (1967)
[11] Mikkelson, E., Nielson, S. O.: J. Phys. Chem., **64,** 632 (1966)

Andrzej Burewicz
Stanislaw Zieliński
Institute of Chemistry, Adam Mickiewicz University, Grunwaldzka 6, 60—780 Poznań, Poland

Acta Chimica Academiae Scientiarum Hungaricae, Tomus 102 (4), pp. 341—350 (1979)

HYDROGEN-BONDED POLY(VINYL ALCOHOL) GELS*, II

MECHANICAL STUDIES

J. GYÖRGYI-EDELÉNYI and M. NAGY

(Department of Colloid Science, Eötvös L. University, Budapest)

Received September 22, 1978

Accepted for publication January 25, 1979

Thermolabile hydrogels of poly(vinyl alcohol) (PVA) have been prepared and investigated in order to get information on the structural differences of the gels using solubility and mechanical measurements. In this work unilateral compression measurements were carried out on physically bonded PVA gels. The experimental results proved the validity of the theory for rubber-elastic polymer networks taking into account the slow-slippage of the junction points under mechanical stress.

The influence of gelation conditions and the solvent exchange upon the gel structure is apparent from the constant C, which is proportional to the elastic modulus.

The comparison of the results of solubility and mechanical measurements permits the conclusion that for thermally treated gels the initial decrease of the elasticity is a result of a structural rearrangement. The observed plateau and the subsequent decrease of the modulus can be explained by stepwise breakdown of the structure which causes the decrease of the number of elastically effective chains only if the temperature is higher than 335 K.

The results mentioned above are in agreement with our previous findings about the approximate bond-energy spectrum in these gels.

Introduction

An account was given by us earlier [1] on the solubility of hydrogen-bonded PVA gels. The mechanism of the transition of gel → polymer solution seemed to be more complicated than it was found on the basis of rheological measurements. Through changes in the solubility of thermolabile hydrogels with increasing temperature allowed to get information on the energy values of the different junction sites in the physically bonded hydrogels. With the help of the H-bond disrupting effect of *n*-propanol the supermolecular structural differences could be established.

The main purpose of the present work was to study the mechanical–rheological behaviour of these thermolabile gels getting further information on the gel structure and the thermal stability of the junction sites.

Few reports are dealing with the mechanical–rheological investigations of physically bonded hydrogels, the interest is mainly focused so far on the

* Presented before the Committee on Physics of Plastics, Hungarian Academy of Sciences, October 1977

rubber elasticity of chemically cross-linked gels. Among several basic problems it seems very important that how the mechanical behaviour of these physically bonded networks can reflect their structural characteristics, and whether the theory of rubber elastic chemical networks could be applied in the case of these gels.

It seems to be evident that, if the junction sites do not break down on mechanical deformation, and no volume changes are taken place, the physically bonded gels can be treated as the chemically cross-linked ones.

Among others it has been found [2] that the time dependent stress can be factored into a function of time and function of strain. The time dependent and equilibrium mechanical behaviour of gelatine, agar-agar and PVA—ethylene glycol hydrogels were studied by PINES and PRINS [3]. The stress relaxation data indicated that only in the case of gelatine gels fulfilled the abovementioned conditions, the separability of the time and deformation dependences of the stress. So the theory of rubber-like chemical networks could be applied and the modulus of elasticity could be calculated only for the gelatine hydrogels.

SHIBATANI [4] studied the changes of gel rigidity as a function of gelling time at different temperatures on lightly cross-linked PVA hydrogels by stress-strain measurements and calculated the numbers of junctions in the gel using the theory of rubber elasticity.

OGASAWARA *et al.* [5] studying the syneresis of PVA hydrogels pointed out that the logarithmic relationship, found by HIRAI, between the elastic moduli of the gel and the polymer concentration was valid in the case when the PVA concentration in the gel varied due to syneresis.

OGASAWARA *et al.* [6] have studied the effect of syndiotacticity on the rigidity of the gel by determining the blending modulus of a rod-like gel. According to the rubber elastic theory of FLORY the number of moles of chains in the network (ν) was calculated from the elastic moduli (10^4—10^5 Nm^{-2}).

In our previous work [1] thermolabile PVA hydrogels with different supermolecular structure have been prepared by using dioxane as a precipitant which has been changed against water after gelation had taken place. It was found that these hydrogels behaved as soft rubber elastic materials, the junction sites of the network were stable enough, and no volume change took place on unilateral compression. Thus we have made an attempt by the help of mechanical measurements to get further information on gel structure.

Experimental

Materials. The gels were prepared from a commercial PVA, Rhodoviol 16/20 (Rhone-Poulenc, Paris). The acetate content of the sample was reduced by alkaline hydrolysis to $\sim$0.3 mol%. The homogeneity with respect to molecular weight was increased by fractionation

($\overline{M}_w = 80{,}000$). The syndiotactic triad content determined from the IR spectrum data by means of the KENNY–WILLCOCKSON equation [7] was 36%.

The PVA gels were prepared using dioxane as a precipitant, which has been exchanged against water after gelation had taken place [1].

The characteristics of the hydrogels studied by mechanical measurements are listed in Table I. These characteristics are the composition of the system under gelation (w_{PVA}, $w_{dioxane}$), the volume fraction of the polymer in the gel (v_2), and the constant (C) from mechanical measurements, which is proportional to the number of elastically effective network chains and the modulus of elasticity.

Table I

Some characteristic parameters of the PVA hydrogels

Gelling system		PVA hydrogel	
PVA content, w_{PVA}	Dioxane content, $w_{dioxane}$	v_2	C (kN m^{-2})
0.08	0.46	0.047	12.6
0.04	0.48	0.029	4.0
0.06	0.48	0.048	17.3
0.08	0.48	0.072	40.3
0.04	0.50	0.030	3.2
0.06	0.50	0.047	11.5
0.08	0.50	0.060	19.2
0.04	0.52	0.029	3.1
0.06	0.52	0.044	8.3
0.08	0.52	0.057	12.4
0.04	0.54	0.030	2.8

Methods

Unilateral compression measurements were carried out by means of a modified analytical balance [8]. The apparatus allowed us to measure both the applied force and deformation with high accuracy *i.e.* $\pm 10^{-4}$ N and ± 0.02 mm, respectively. The compression measurements were undertaken on $10 \times 10 \times 10$ mm gel cubes and on isodimensional cylindrical specimens. Within the applied deformation ratios ($\Lambda = 1.0 - 0.7$), the cross-sectional changes due to the deformation did not cause greater deviations than the systematic error of the method. The dimensions of the gel samples before compression were determined with 0.02 mm accuracy by means of a cathetometer. The measurements were carried out at 298 K, and the reproducibility of the method was within $\pm 5\%$.

Results and Discussion

As it has been mentioned earlier, the investigated PVA hydrogels had a rubber-like elasticity, they were deformed isotropically and did not change their volume under compression at the applied deformation ratios.

For evaluation of the results it was important to decide whether these physically-bonded hydrogels can be interpreted by the theory of chemically

cross-linked rubber-like gels, *i.e.* whether the unidirectional time-dependent stress (σ_{11}) can be factored into a function of time and function of strain [2]:

$$\sigma_{11}(\Lambda_1,t) = \Gamma(\Lambda_1)\, E(t) \tag{1}$$

where

$$E(t) = E_e\left[1 + \left(\frac{t}{t_m}\right)^{-m}\right] \tag{2}$$

i.e. the logarithmic plots of σ_{11} against time at different tensile strains are closely parallel.

The stress relaxation of two PVA hydrogels with different polymer content at constant unilateral compression ratios are shown in Fig. 1. The logarithmic plots of the force (F), needed to maintain constant deformation against time (t) are closely parallel with a slope of -0.02. It is nearly by one order smaller than the -0.28 value, found for gelatine hydrogels by PINES and PRINS [3].

It was also investigated whether the theoretical relationships, referring to the rubber-like behaviour of chemically cross-linked networks was applicable to these physically bonded PVA hydrogels. According to the statistical theory of rubber-like elasticity

$$\sigma_d = ARTv^* q_i^{\frac{1}{3}} q_0^{-\frac{2}{3}}\left(\Lambda - \frac{q}{q_i \Lambda^2}\right) = \sigma q^{\frac{2}{3}} \tag{3}$$

where σ_d is the force per unit area of the unswollen, unstretched sample, and σ referred to the swollen unstretched cross-section. A is a theory dependent factor, its value in general equals to 1, v^* is the concentration of network chains per unit dry volume, q and q_i are the volume degree of swelling of the stretched and unstretched sample, respectively, q_0 is the reference degree of swelling (memory parameter), Λ is the deformation ratio, the ratio of actual and initial length of the swollen gel sample, R the gas constant and T the temperature [9].

Since at the applied deformation ratios no volume change has taken place on the studied PVA hydrogels,

$$q = q_i \quad \text{and} \quad \frac{q}{q_i} = 1,$$

thus Eq. (3) can be written as follows

$$\frac{\sigma q^{\frac{1}{3}}}{(\Lambda - \Lambda^{-2})} = \frac{\sigma_d q^{-\frac{1}{3}}}{(\Lambda - \Lambda^{-2})} = RTv^* q_0^{-\frac{2}{3}} = C\,(\text{const}). \tag{4}$$

So the constant C is proportional to the number of elastically effective network chains and to the modulus of elasticity.

Yet another important question from the viewpoint of experimental technique awaited an answer namely whether the shape of the gel samples affects the results. (It may be noted that PVA hydrogel cubes could be prepared much easier than cylindrical samples.)

The validity of Eq. (4) is illustrated in Fig. 2 for cubic and cylindrical gel samples, prepared with different PVA content. The good agreement of the data

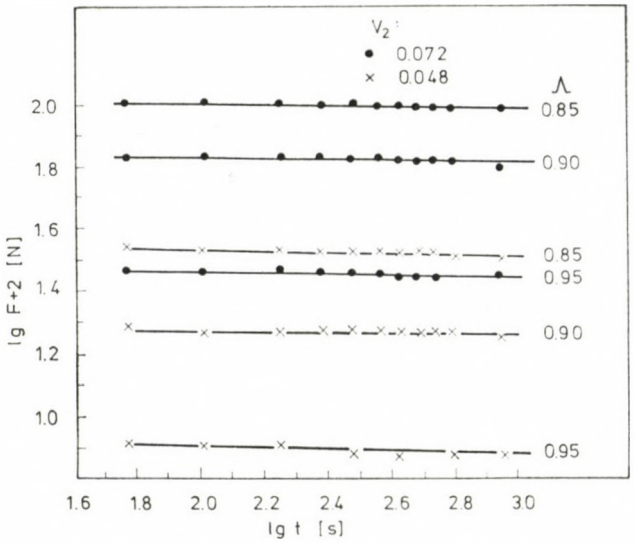

Fig. 1. The logarithmic plot of force, (F) needed to maintain constant deformation ($\lambda = 0.95-0.85$) as a function of time

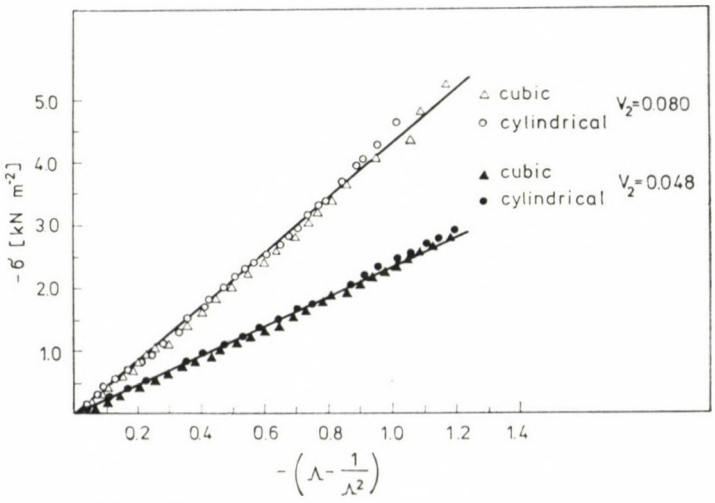

Fig. 2. Verification of the validity of Eq. (3) for gel samples with cubic and cylindrical shape

shows, that the shape of the gel samples does not affect the results, and that Eq. (4) is satisfactorily applicable for these physically bonded PVA hydrogels.

Mechanical studies rendered possible to demonstrate the influence of gelation conditions, polymer and dioxane content of the system upon the gel elasticity. In Fig. 3 the C values are plotted against the weight fraction of PVA (w_{PVA}) under gelation at given dioxane concentration. From the shape

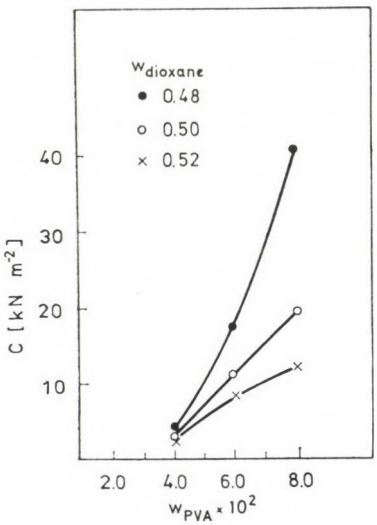

Fig. 3. Effect of the polymer content (w_{PVA}) of the gelling system on the C values of PVA hydrogels, at constant precipitant concentrations

of the curves it can be concluded, that with increasing polymer content the number of elastically effective network chains increases most significantly at $w_{dioxane} = 0.48$.

The optimum effect of the precipitant will be more obvious when plotting the C values against the precipitant concentration at constant PVA content (Fig. 4). (In the mixture of $w_{dioxane} = 0.46$ gel formation took place only at $w_{PVA} = 0.08$, and in the mixture of $w_{dioxane} = 0.54$ only 0.04 weight fraction of PVA could be solved. So the elasticity maximum could be measured only at $w_{PVA} = 0.08$).

Increasing the dioxane content in the gelling system the conformation of PVA molecules will be altered and the intermolecular interactions become conspicuous. In such systems a preformed structure will be stabilized under gelation, *i.e.* a gel with globular structure will be formed and so the modulus of elasticity will be decreased. This is the explanation of formation of gels with globular structure in a mixture with $w_{dioxane} = 0.52$. For these gels the increase in the modulus of elasticity with the polymer content was much smaller.

During the preparation of PVA hydrogels [1] the precipitant dioxane was exchanged against water. This solvent exchange causes a 10—20% increase in the degree of swelling of the gels depending on the gel structure. This must be the consequence of the disruption and rearrangement of the junction sites.

Latter has suggested the possibility to find connection between the stability of gel structure and the increase of the degree of swelling due to solvent

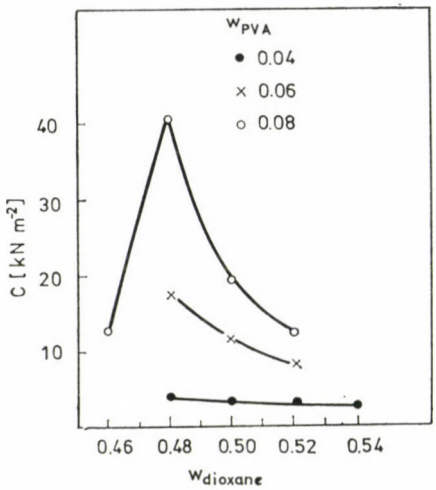

Fig. 4. Effect of the precipitant content ($w_{dioxane}$) of the gelling system on the C values of the PVA hydrogels at constant polymer concentration

exchange. With this possibility in mind a further solvent exchange was made on the gels of various polymer content but prepared at the optimum ($w_{dioxane}$ = = 0.48) dioxane concentration. The swelling medium of the hydrogel was exchanged against pyridine then back to water. Pyridine was chosen because of its perfect miscibility with water and suitable interaction with the polymer. Figures 5, 6, and 7 show the results of mechanical measurements at the different steps of solvent exchange. The exchange of water against pyridine caused a significant increase in the elasticity of the gel samples. This meant a ninefold increase of C in the case of gel with lowest polymer content, and nearly sixfold increase for the two other gels (*cf.* Table II).

The subsequent exchange of pyridine against water made the structural differences due to the polymer content still more conspicuous (*cf.* Table II, $\Delta C/C$ %) comparing the values of C for the aqueous gel after solvent exchange with the C for the original hydrogel. Thus, under optimum gelation conditions the increase of polymer content considerably stabilizes the structure of these PVA hydrogels.

The mechanical investigations furnished further information on changes of the gel structure due to temperature treatment. The solubility measurements, described in our previous report [1], were combined with stress-strain measurements. The temperature of the gel sample in contact with an excess of swelling medium (water) was raised in 2.5 K increments between 298 and 353 K. At

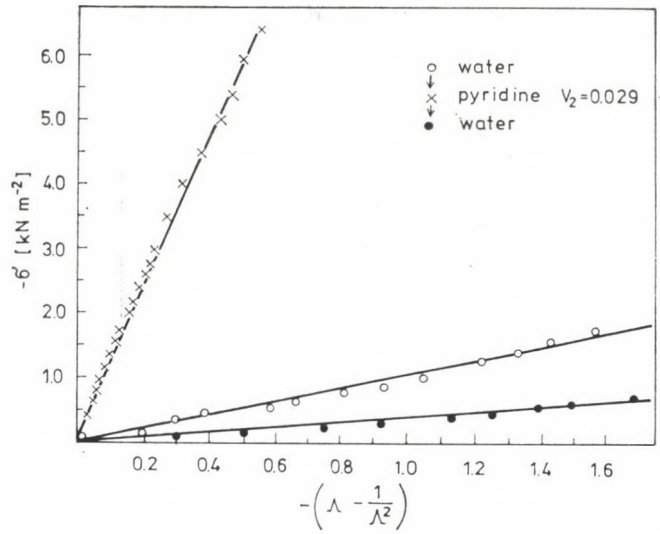

Fig. 5. Effect of the solvent exchange on the stress-strain curves in the case of gel with $v_2 = 0.029$

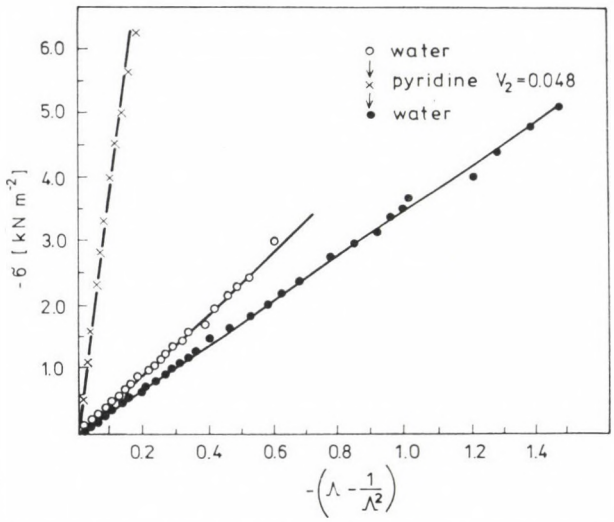

Fig. 6. Effect of the solvent exchange on the stress-strain curves in the case of gel with $v_2 = 0.048$

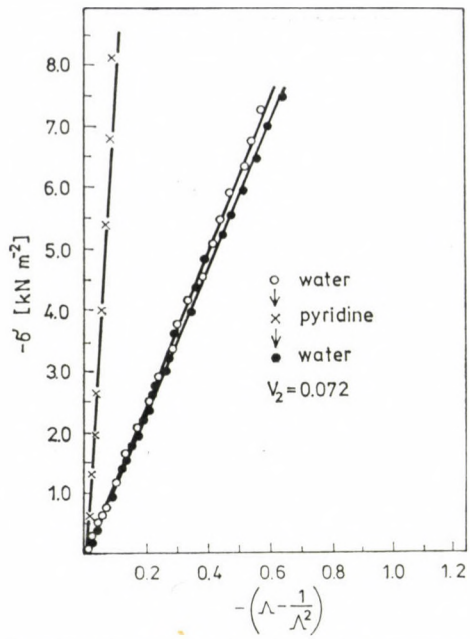

Fig. 7. Effect of the solvent exchange on the stress-strain curves in the case of gel with $v_2 = 0.072$

Table II

Effect of the solvent exchange on the C values

Volume fraction of PVA (v_2) in the original gel	C (kN m^{-2}) water → pyridine → water			$\Delta C/C$ %
0.029	3.5	31.4	1.5	52.2
0.048	14.4	88.9	9.7	32.7
0.072	30.1	198.0	28.1	6.6

each temperature, after attainment of solubility equilibrium, compression measurements were carried out on gel samples at the treating temperature and cooled back to room temperature. The calculated C values plotting against the treating temperature gave curves with similar shape for these two series of measurements. However, the results on gel samples cooled back to room temperature were more reproducible, so only these data are illustrated in Fig. 8, where the C values for gel prepared at $v_2 = 0.048$ and with optimum dioxane content are plotted against the treating temperature. The decrease of the gel elasticity between 298 and 318 K cannot be ascribed to the dissolved amount of PVA (~3% *cf.* Fig. 1 in [1]) thus the decrease of the number of

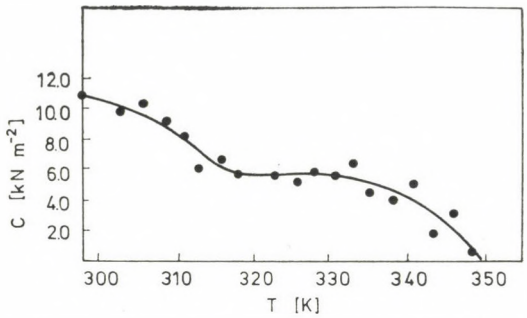

Fig. 8. Dependence of the C values on the treating temperature for gel with $v_2 = 0.048$

elastically active network chains will be the consequence of a rearrangement process. Then, in an interval of nearly 20 K, the C values are practically unaffected by T, the stability of the junction sites prevent the change in ν^* with increasing temperature. Then the significant decrease of elasticity at $T > 335$ K is due to the increase of solubility, this being a result of the final breaking down of the junction sites.

So these mechanical studies are in good agreement with the results of solubility measurements [1] and support our assumption that the bond-energy spectrum of the studied PVA hydrogels is nearly bimodal.

*

The authors wish to express their thanks to Dr. F. HORKAY for the determination of the syndiotactic triad content of the PVA sample by means of IR spectroscopy.

REFERENCES

[1] GYÖRGYI-EDELÉNYI, J., BOGNÁR, J., NAGY, M.: Acta Chim. Acad. Sci. Hung. **102,** 73 (1979)
[2] FERRY, J. D.: Viscoelastic Properties of Polymers, John Wiley and Sons Inc., New York, 1970, p. 439
[3] PINES, E., PRINS, W.: Macromolecules, **6,** 888 (1973)
[4] SHIBATANI, K.: Polymer J., **1,** 348 (1970)
[5] OGASAWARA, K., NAKAJIMA, T., YAMAURA, K., MATSUZAWA, S.: Colloid and Polymer Sci., **254,** 456 (1976)
[6] OGASAWARA, K., NAKAJIMA, T., YAMAURA, K., MATSUZAWA, S.: Colloid and Polymer Sci., **254,** 553 (1976)
[7] KENNY, J. F., WILLCOCKSON, G. W.: J. Polymer Sci., A-1, **4,** 690 (1966)
[8] HORKAY, F.: Thesis, Budapest 1977
[9] DUSEK, K., PRINS, W.: Adv. Polymer Sci., **6,** 1 (1969)

Judit GYÖRGYI-EDELÉNYI
Miklós NAGY
H-1445 Budapest, P.O.Box 328.

Acta Chimica Academiae Scientiarum Hungaricae, Tomus 102 (4), pp. 351—359 (1979)

ERROR ESTIMATION ON THE BASIS OF THE GOVERNING PRINCIPLE OF DISSIPATIVE PROCESSES IN SOME CASES OF STATIONARY HEAT CONDUCTION

A. DANCSÓ

(Institute for Physics, Technical University of Budapest, Budapest)

Received October 2, 1978

Accepted for publication January 25, 1979

In this paper we consider unconditional variational problems of stationary sourceless heat conduction with error bound in case of spherical and cylindrical symmetry on the basis of GYARMATI's Governing Principle of Dissipative Processes.

Introduction

It is well known that for the linear, quasi-linear and certain types of non-linear theory of the thermodynamics of irreversible processes [1, 2], GYARMATI in 1965, proposed a general variational principle by means of which the evolution of dissipative transport processes in space-time can be described [3, 4]. The various applications of this principle frequently called as "The Governing Principle of Dissipative Processes", have already proved its utility for the complete regime of transport phenomena [5—11]. This principle tells us in total generality that the functional

$$L[\Gamma, J] = \int_0^t \int_V (\sigma - \Psi - \Phi)\, \mathrm{d}V\, \mathrm{d}t = \text{maximum} \tag{1}$$

under constraints that the balance equations

$$\varrho a_i + \nabla \cdot J_i = \sigma_i \qquad (i = 1, 2, \ldots) \tag{2}$$

are satisfied [1].

Applying the variational principle (1) to the stationary heat conduction problem, it reads in the so-called Fourier picture [1, 14]:

$$L[T, J] = \int_V \left(J \cdot \nabla T + \frac{1}{2} \lambda \nabla T \cdot \nabla T + \frac{1}{2\lambda} J \cdot J \right) \mathrm{d}V =$$

$$= \int_V \frac{1}{2\lambda} (\lambda \cdot \nabla T + J)^2\, \mathrm{d}V = \text{minimum} \tag{3}$$

where T is the temperature and λ is the heat conductivity. In the stationary case we can omit the time integration in Eq. (1), furthermore, in the sourceless case the heat current density J satisfies the stationary form

$$\nabla \cdot J = 0 \tag{4}$$

of the balance equation of the internal energy, which belongs to (3) as a subsidiary condition. Let us consider now the simplest case of the one-dimensional problem. Let heat conduction occur along the x axis, the system be the closed interval $[0, l]$ and the boundary conditions be

$$T(0) = T_1, \quad T(l) = T_2 = T_1 + \Delta T > T_1 \tag{5}$$

In this case the variational problem of Eq. (3) reduces to

$$H_l = \int_0^l \frac{\lambda(x, T)}{2} \left(\frac{\mathrm{d}T}{\mathrm{d}x}\right)^2 \mathrm{d}x - \frac{(\Delta T)^2}{2 \int_0^l \frac{1}{\lambda(x, T)} \mathrm{d}x} = \text{minimum} \tag{6}$$

derived by FARKAS and NOSZTICZIUS [12]. In this paper Δ is used in the meaning of differences. For this variational problem an error estimate can also be obtained (FARKAS [13]):

$$\varepsilon \leq \sqrt{\frac{l \cdot H_l}{2 \lambda_{\min}} \cdot \frac{1}{1 - K \Delta T \cdot \lambda_{\max}/\lambda_{\min}^2}} \tag{7}$$

where ε is the maximum deviation between the approximate solution $T(x)$ obeying boundary conditions (5) and the correct solution $T_0(x)$; further

$$K = \max_{\substack{x \in [0, l] \\ T \in [T_1, T_2]}} \left\{ \left| \frac{\partial \lambda(x, T)}{\partial T} \right| \right\}, \tag{8}$$

$\lambda_{\max}$ and $\lambda_{\min}$ are the extreme values of λ in the region $x \in [0, l]$; $T \in [T_1, T_2]$. In the following we apply the variational principle (3) cases of cylindrical and spherical symmetry. We derive formulas analogous to (6) and (7).

Heat conduction in a hollow cylinder

In this section we use cylindrical coordinates z, ϱ, φ. The inner radius of the ring is R_1, the outer radius is R_2, and the height is h. The system is heat-isolated at the planes $z = 0$ and $z = h$. The system has the boundary conditions

$$T(R_1) = T_1, \quad T(R_2) = T_2, \quad \Delta T = |T_2 - T_1| \tag{9}$$

We consider the stationary sourceless case. Let λ be a continuous function of ϱ and T:

$$\lambda = \lambda(\varrho, T) \tag{10}$$

$$0 < \lambda_{\min} \leq \lambda(\varrho, T) \leq \lambda_{\max} \tag{11}$$

in the region $\varrho \in [R_1, R_2]$; $T \in [T_1, T_2]$. Since our heat conduction problem has cylindrical symmetry, its correct solution must have the same symmetry, *i.e.* the real temperature distribution T_0 depends only on ϱ:

$$T_0 = T_0(\varrho) \tag{12}$$

Let T be an approximate solution satisfying boundary conditions (9) and depending on ϱ:

$$T = T(\varrho) \tag{13}$$

Since the heat current density J has only one non-zero component, J_ϱ, balance equation (4) reads:

$$\frac{1}{\varrho}\frac{\mathrm{d}}{\mathrm{d}\varrho}(\varrho \cdot J_\varrho) = 0 \tag{14}$$

consequently,

$$\varrho \cdot J_\varrho = C = \text{constant} \tag{15}$$

The form of variational principle (3) in this case is

$$\int_{R_1}^{R_2} \frac{1}{2\lambda}\left(\lambda\frac{\mathrm{d}T}{\mathrm{d}\varrho} + J_\varrho\right)^2 \cdot 2\pi h\varrho\,\mathrm{d}\varrho =$$

$$= \left[\int_{R_1}^{R_2} \frac{\lambda}{2}\left(\frac{\mathrm{d}T}{\mathrm{d}\varrho}\right)^2 \cdot \lambda\pi h\varrho\,\mathrm{d}\varrho + \int_{R_1}^{R_2} \frac{\mathrm{d}T}{\mathrm{d}\varrho} \cdot J_\varrho \cdot 2\pi h\varrho\,\mathrm{d}\varrho + \int_{R_1}^{R_2} \frac{1}{2\lambda} \cdot J_\varrho^2 \cdot 2\pi h\varrho\,\mathrm{d}\varrho\right] =$$

$$= \text{minimum} \tag{16}$$

Now, substituting Eqs (9) and (15) into (16), we find in the physically only significant case of $T_1 > T_2$ that

$$\left[\int_{R_1}^{R_2} \frac{\lambda}{2}\left(\frac{\mathrm{d}T}{\mathrm{d}\varrho}\right)^2 \cdot 2\pi h\varrho\,\mathrm{d}\varrho - C \cdot \Delta T \cdot 2\pi h + C^2 \int_{R_1}^{R_2} \frac{2\pi h}{2\lambda\varrho}\,\mathrm{d}\varrho\right] = \text{minimum}. \tag{17}$$

Hence the following C value minimizes the functional (17) for a fixed $T(\varrho)$ function:

$$C = \frac{\Delta T}{\int_{R_1}^{R_2} \frac{1}{\varrho \cdot \lambda(\varrho, T)} \mathrm{d}\varrho} . \tag{18}$$

Thus we obtain the following unconditional variational problem:

$$4H_c \equiv \left[\int_{R_1}^{R_2} \lambda \left(\frac{\mathrm{d}T}{\mathrm{d}\varrho} \right)^2 \varrho \, \mathrm{d}\varrho - \frac{(\Delta T)^2}{\int_{R_1}^{R_2} \frac{\mathrm{d}\varrho}{\varrho \cdot \lambda}} \right] = \text{minimum} . \tag{19}$$

It is clear from the preceding that H_c is of the total quadratic form:

$$4H_c \equiv \int_{R_1}^{R_2} \frac{1}{\lambda} \left(\lambda \cdot \frac{\mathrm{d}T}{\mathrm{d}\varrho} + \frac{\Delta T}{\varrho \int_{R_1}^{R_2} \frac{\mathrm{d}\varrho}{\lambda \cdot \varrho}} \right)^2 \varrho \, \mathrm{d}\varrho \tag{20}$$

according to the general character of the GYARMATI principle [4]. On the other hand, it is obvious that H_c is a positive definite quantity, and it is zero if and only if $T(\varrho) \equiv T_0(\varrho)$.

Therefore, variational problem (19) uniquely determines the correct solution T_0. Now we establish an error estimate for this problem. Denoting the error by ε:

$$\varepsilon = \max_{\substack{\varrho \in [R_1, R_2] \\ T \in [T_1, T_2]}} \{ | T(\varrho) - T_0(\varrho) | \} \tag{21}$$

we can define the sets M_1 and M_2 so that

$$\frac{\mathrm{d}T}{\mathrm{d}\varrho} - \frac{\mathrm{d}T_0}{\mathrm{d}\varrho} \begin{cases} \geq 0 & \text{if} \quad \varrho \in M_1 \end{cases} \tag{22}$$

$$\begin{cases} < 0 & \text{if} \quad \varrho \in M_2 \end{cases} \tag{23}$$

If the measures of M_1 and M_2 are r_1 and r_2, then

$$r_1 + r_2 = R_2 - R_1 \tag{24}$$

is valid. Now, it follows from Eqs (22, 23) that

$$\int_{M_1} \left(\frac{\mathrm{d}T}{\mathrm{d}\varrho} - \frac{\mathrm{d}T_0}{\mathrm{d}\varrho} \right) \mathrm{d}\varrho = e \geq \varepsilon \tag{25}$$

and

$$\int_{M_2} \left(\frac{\mathrm{d}T}{\mathrm{d}\varrho} - \frac{\mathrm{d}T_0}{\mathrm{d}\varrho} \right) \mathrm{d}\varrho = -e \leqq -\varepsilon \tag{26}$$

where $2e$ is the total variation of the $T - T_0$ function [15]. Let us assume that λ has a continuous partial derivative with respect to T, so it satisfies the Lipschitz condition

$$|\lambda(\varrho, T) - \lambda(\varrho, T_0)| \leqq K \cdot |T - T_0| \tag{27}$$

where

$$K = \max_{\substack{\varrho \in [R_1, R_2] \\ T \in [T_1, T_2]}} \left\{ \left| \frac{\partial \lambda(\varrho, T)}{\partial T} \right| \right\}. \tag{28}$$

Using Eq. (21), we can write that

$$\int_{R_1}^{R_2} \frac{1}{\lambda(\varrho, T)} \left[\left(\lambda(\varrho, T) \cdot \frac{\mathrm{d}T}{\mathrm{d}\varrho} - \lambda(\varrho, T) \frac{\mathrm{d}T_0}{\mathrm{d}\varrho} \right) + \left(\lambda(\varrho, T) \frac{\mathrm{d}T_0}{\mathrm{d}\varrho} + \frac{\Delta T}{\varrho \int_{R_1}^{R_2} \frac{\mathrm{d}\varrho}{\varrho \cdot \lambda(\varrho, T)}} \right) \right]^2 \varrho \, \mathrm{d}\varrho \geqq$$

$$\geqq \int_{R_1}^{R_2} \lambda(\varrho, T) \left(\frac{\mathrm{d}T}{\mathrm{d}\varrho} - \frac{\mathrm{d}T_0}{\mathrm{d}\varrho} \right)^2 \varrho \, \mathrm{d}\varrho + \tag{29}$$

$$+ 2 \int_{R_1}^{R_2} \left(\frac{\mathrm{d}T}{\mathrm{d}\varrho} - \frac{\mathrm{d}T_0}{\mathrm{d}\varrho} \right) \left(\lambda(\varrho, T) \frac{\mathrm{d}T_0}{\mathrm{d}\varrho} + \frac{\Delta T}{\varrho \int_{R_1}^{R_2} \frac{\mathrm{d}\varrho}{\varrho \cdot \lambda(\varrho, T)}} \right) \varrho \, \mathrm{d}\varrho$$

because the omitted term cannot be negative. From the first term of the right-hand side we obtain

$$\int_{R_1}^{R_2} \lambda(\varrho, T) \left(\frac{\mathrm{d}T}{\mathrm{d}\varrho} - \frac{\mathrm{d}T_0}{\mathrm{d}\varrho} \right)^2 \varrho \, \mathrm{d}\varrho \geqq$$

$$\geqq \lambda_{\min} \cdot R_1 \left[\int_{M_1} \left(\frac{\mathrm{d}T}{\mathrm{d}\varrho} - \frac{\mathrm{d}T_0}{\mathrm{d}\varrho} \right)^2 \mathrm{d}\varrho + \int_{M_2} \left(\frac{\mathrm{d}T}{\mathrm{d}\varrho} - \frac{\mathrm{d}T_0}{\mathrm{d}\varrho} \right)^2 \mathrm{d}\varrho \right] \geqq \tag{30}$$

$$\geqq \lambda_{\min} \cdot R_1 \cdot \left(\frac{e^2}{r_1} + \frac{e^2}{r_2} \right) \geqq \frac{4 \lambda_{\min} R_1}{R_2 - R_1} \cdot e^2$$

where formulas (25) and (26) were used. Of course, the second term of the right-hand side of (29) is also transformable. Indeed, by using Eqs (18), (25), (26) and (27) one has

$$2\int_{R_1}^{R_2}\left(\frac{\mathrm{d}T}{\mathrm{d}\varrho}-\frac{\mathrm{d}T_0}{\mathrm{d}\varrho}\right)\cdot\left(\lambda(\varrho,T)\frac{\mathrm{d}T_0}{\mathrm{d}\varrho}+\frac{\Delta T}{\varrho\int_{R_1}^{R_2}\frac{\mathrm{d}\varrho}{\varrho\cdot\lambda(\varrho,T)}}\right)\varrho\,\mathrm{d}\varrho=$$

$$=\frac{-2\Delta T}{\int_{R_1}^{R_2}\frac{\mathrm{d}\varrho}{\varrho\cdot\lambda(\varrho,T_0)}}\cdot\int_{R_1}^{R_2}\frac{\lambda(\varrho,T)}{\lambda(\varrho,T_0)}\left(\frac{\mathrm{d}T}{\mathrm{d}\varrho}-\frac{\mathrm{d}T_0}{\mathrm{d}\varrho}\right)\mathrm{d}\varrho\geq$$

$$\geq\frac{-2\Delta T\,\lambda_{\max}}{\ln\frac{R_2}{R_1}}\left[\max_{\varrho\in[R_1,R_2]}\left\{\frac{\lambda(\varrho,T)}{\lambda(\varrho,T_0)}\right\}\int_{M_1}\left(\frac{\mathrm{d}T}{\mathrm{d}\varrho}-\frac{\mathrm{d}T_0}{\mathrm{d}\varrho}\right)\mathrm{d}\varrho+\right.$$

$$\left.+\min_{\varrho\in[R_1,R_2]}\left\{\frac{\lambda(\varrho,T)}{\lambda(\varrho,T_0)}\right\}\int_{M_2}\left(\frac{\mathrm{d}T}{\mathrm{d}\varrho}-\frac{\mathrm{d}T_0}{\mathrm{d}\varrho}\right)\mathrm{d}\varrho\right]= \tag{31}$$

$$=\frac{2\Delta T\,\lambda_{\max}\cdot e}{\ln\frac{R_2}{R_1}}\left[\min_{\varrho\in[R_1,R_2]}\left\{\frac{\lambda(\varrho,T)}{\lambda(\varrho,T_0)}\right\}-\max_{\varrho\in[R_1,R_2]}\left\{\frac{\lambda(\varrho,T)}{\lambda(\varrho,T_0)}\right\}\right]=$$

$$=\frac{2\Delta T\,\lambda_{\max}\cdot e}{\ln\frac{R_2}{R_1}}\left[\min_{\varrho\in[R_1,R_2]}\left\{\frac{\lambda(\varrho,T)-\lambda(\varrho,T_0)}{\lambda(\varrho,T_0)}\right\}-\max_{\varrho\in[R_1,R_2]}\left\{\frac{\lambda(\varrho,T)-\lambda(\varrho,T_0)}{\lambda(\varrho,T_0)}\right\}\right]\geq$$

$$\geq\frac{2\Delta T\,\lambda_{\max}\cdot e}{\ln\frac{R_2}{R_1}}\left(-2\frac{K\varepsilon}{\lambda_{\min}}\right)\geq-\frac{4K\Delta T}{\ln\frac{R_2}{R_1}}\cdot\frac{\lambda_{\max}}{\lambda_{\min}}\cdot e^2.$$

Inserting Eqs (19), (30), (31) into (29), we find the inequality

$$4H_c\geq\frac{4\lambda_{\min}R_1}{R_2-R_1}\cdot e^2-\frac{4K\Delta T\,\lambda_{\max}}{\lambda_{\min}\cdot\ln\frac{R_2}{R_1}}\cdot e^2. \tag{32}$$

If

$$1>\frac{R_2-R_1}{R_1\ln\frac{R_2}{R_1}}\cdot K\Delta T\frac{\lambda_{\max}}{\lambda_{\min}^2} \tag{33}$$

we obtain the formula

$$\varepsilon \leq \sqrt{\frac{H_c}{\lambda_{min}} \cdot \frac{R_2 - R_1}{R_1} \cdot \frac{1}{1 - K\Delta T(\lambda_{max}/\lambda_{min}^2)\left[(R_2 - R_1)\Big/\left(R_1 \ln \frac{R_2}{R_1}\right)\right]}}. \quad (34)$$

In the case of

$$R_2 - R_1 \ll R_1 \quad (35)$$

relation (34) reduces to

$$\varepsilon \leq \sqrt{\frac{H_c}{\lambda_{min}} \cdot \frac{R_2 - R_1}{R_1} \cdot \frac{1}{1 - K\Delta T(\lambda_{max}/\lambda_{min}^2)}} \quad (36)$$

which is equivalent to (7). With $T_2 > T_1$, we would obtain in just the same way formulas (19) and (34), but this case is hardly of much physical significance.

Heat conduction in a spherical shell

In this section we use spherical coordinates r, ϑ, φ. The inner radius of the system is R_1, the outer radius is R_2. The boundary conditions are given in Eq. (9). Again we consider the stationary and sourceless case. The proof is analogous to the above one. One finds here only the differences.

Let λ be a continuous function of r and T:

$$\lambda = \lambda(r, T), \quad (37)$$

$$0 < \lambda_{min} \leq \lambda(r, T) \leq \lambda_{max} \quad (38)$$

in the region $r \in [R_1, R_2]$; $T \in [T_1, T_2]$. Let T be an approximate solution obeying (9) and depending only on r:

$$T = T(r) \quad (39)$$

Since J has only one non-zero component, J_r, Eq. (4) reads

$$\frac{1}{r^2} \cdot \frac{d}{dr}(r^2 J_r) = 0, \quad (40)$$

consequently,

$$r^2 \cdot J_r = C_1 = \text{constant}. \quad (41)$$

From the adequate form of the variational principle (3) in the case of $T_1 > T_2$, with the value

$$C_1 = \frac{\Delta T}{\int\limits_{R_1}^{R_2} \frac{1}{r^2 \lambda(r, T)} \mathrm{d}r} \tag{42}$$

we obtain the unconditional variational problem

$$4H_s \equiv \int\limits_{R_1}^{R_2} \lambda \left(\frac{\mathrm{d}T}{\mathrm{d}r}\right)^2 r^2 \mathrm{d}r - \frac{(\Delta T)^2}{\int\limits_{R_1}^{R_2} \frac{\mathrm{d}r}{r^2 \lambda}} = \text{minimum} \tag{43}$$

where H_s is again of the total quadratic form

$$4H_s \equiv \int\limits_{R_1}^{R_2} \frac{1}{\lambda} \left(\lambda \frac{\mathrm{d}T}{\mathrm{d}r} + \frac{\Delta T}{r^2 \cdot \int\limits_{R_1}^{R_2} \frac{\mathrm{d}r}{r^2 \lambda}} \right)^2 r^2 \mathrm{d}r . \tag{44}$$

It is obvious that H_s is positive definite and vanishes if and only if $T(r) \equiv \equiv T_0(r)$. Therefore, variational problem (43) uniquely determines the exact temperature distribution.

Now we consider the possible error:

$$\varepsilon = \max_{\substack{r \in [R_1, R_2] \\ T \in [T_1, T_2]}} \{ | T(r) - T_0(r) | \}. \tag{45}$$

Similarly as in the previous section, from the inequality

$$4H_s \geq \frac{4\lambda_{\min} \cdot R_1^2 \cdot e^2}{R_2 - R_1} - \frac{4K \Delta T R_1 R_2}{R_2 - R_1} \cdot \frac{\lambda_{\max}}{\lambda_{\min}} \cdot e^2 \tag{46}$$

if

$$1 > K \Delta T \cdot \frac{R_2}{R_1} \cdot \frac{\lambda_{\max}}{\lambda_{\min}^2} \tag{47}$$

we obtain the error limit

$$\varepsilon \leq \sqrt{\frac{H_s}{\lambda_{\min}} \cdot \frac{R_2 - R_1}{R_1^2} \cdot \frac{1}{1 - K \Delta T \cdot (\lambda_{\max}/\lambda_{\min}^2) \cdot (R_2/R_1)}} . \tag{48}$$

The limit of (48) is equivalent to (7) if $[(R_2 - R_1)/R_1] \to 0$. Formulas (43) and (48) are valid also if $T_2 > T_1$, though this case has only a very little physical reality, because the sphere had to contain a medium of infinite heat capacity, for example a mixture of ice and water.

Conditions (33) and (47) require ΔT to be small enough, the ring or shell to be thin or λ to be a slowly varying function of T. For example, if $\Delta T = 100$ K, λ is a linear function of T and $R_2 = 2R_1$, λ must vary more slowly than 0.7%/K in the spherical shell, or 0.6%/K in the hollow cylinder. If $R_2 = 1.1R_1$, these limits are 0.95%/K and 0.98%/K, respectively.

*

The author wishes to express his thanks to Dr. H. FARKAS for his valuable suggestions.

REFERENCES

[1] GYARMATI, I.: Non-Equilibrium Thermodynamics, Field Theory and Variational Principles. Springer, Berlin—Heidelberg—New York 1970
[2] DE GROOT, S. R., MAZUR, P.: Non-Equilibrium Thermodynamics. North-Holland Publishing Co., Amsterdam 1962
[3] GYARMATI, I.: Zh. Fiz. Khim., **39**, 1489 (1965)
[4] GYARMATI, I.: Ann. Phys., **7**, 23, 353 (1969)
[5] SÁNDOR, J.: Zh. Fiz. Khim., **44**, 2727 (1970)
[6] SÁNDOR, J.: Acta Chim. (Budapest), **67**, 303 (1971)
[7] SÁNDOR, J.: Electrochim. Acta, **17**, 673 (1972)
[8] VERHÁS, J.: Z. Phys. Chem., **249**, 119 (1972)
[9] VINCZE, Gy.: Ann. Phys., **7**, 225 (1971)
[10] VINCZE, Gy.: Acta Chim. (Budapest), **75**, 33 (1972)
[11] VINCZE, Gy.: Ann. Phys., **7**, 30, 55 (1973)
[12] FARKAS, H., NOSZTICZIUS, Z.: Ann. Phys., **7**, 341 (1971)
[13] FARKAS, H.: Int. J. Engng. Sci., **13**, 1029 (1975)
[14] FARKAS, H.: Int. J. Engng. Sci., **13**, 1035 (1975)
[15] SZŐKEFALVI-NAGY, B.: Introduction to Real Functions and Orthogonal Expansions, Akadémiai Kiadó, Budapest 1964

András DANCSÓ H-1521 Budapest, Műegyetem

Acta Chimica Academiae Scientiarum Hungaricae, Tomus 102 (4), pp. 361—370 (1979)

POLYMERIZATION IN LIQUID CRYSTALS, V*

SYNTHESIS OF POLYMERIZABLE COMPOUNDS WITH A LIQUID CRYSTALLINE STATE**

K. NYITRAI, F. CSER and G. HARDY

(Research Institute for Plastics, Budapest)

Received November 21, 1978

In revised form January 18, 1979

Accepted for publication February 6, 1979

Some *p*-alkyl and *p*-alkoxy substituted *p*'-acryloyloxyazo and azoxybenzenes and cholesteryl vinyl mixed esters of dicarboxylic acids were prepared. A few among these have a liquid crystalline state. The unit cells of these compounds, determined by indexing powder diffractograms, indicated that some of the azo and azoxy monomers and all cholesterol derivatives form layer-like lattices. All monomers can be converted into polymers with marked clearing points, *via* initiation by appropriate peroxides in both isotropic and mesomorphic bulk.

Experimental

Several thousand compounds having liquid crystalline states are described in the literature [1], but there are only a few liquid crystalline monomers containing polymerizable active groups [2—25].

To extend the range of monomers, systematic experiments were performed for preparing novel monomers with a liquid crystalline phase. The present report covers the synthesis of some *p*-*n*-alkoxy-*p*'-acryloyloxyazobenzenes and -azoxybenzenes, as well as that of mixed cholesteryl vinyl esters of a few dicarboxylic acids and certain X-ray characteristics of these monomers are described.

The monomers were prepared according to the scheme:

I. Azo-compounds [26]

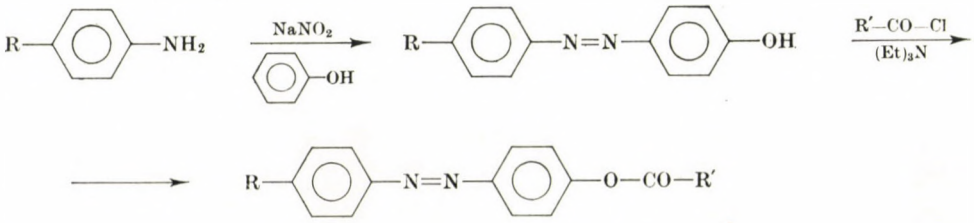

* Part IV of the series: NYITRAI, K., CSER, F., CSERMELY, G., BUI DUC NGOC, FÜZES, L., SAMAY, G., HARDY, Gy.: Europ. Polym. J., **14**, 467 (1978)

** On the same subject, a paper was presented at the "1st Liquid Crystal Conference of Socialist Countries", Halle, GDR, January 1976

where R = H, alkyl or alkoxy (CH_3—, C_2H_5—, n-C_4H_9— or CH_3—O—, C_2H_5O—, n-C_4H_9O—); R' = —CH=CH_2, $(Et)_3N$ = triethylamine.

II. Azoxy compounds[1] [27]

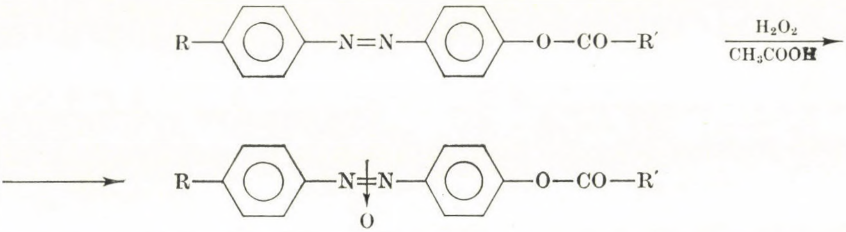

(R has the same meaning as above)

III. Cholesteryl vinylesters of dicarboxyl acids

a)

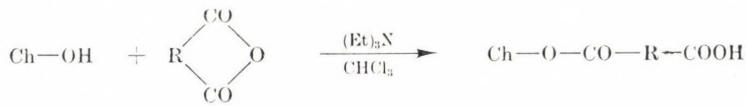

where Ch =

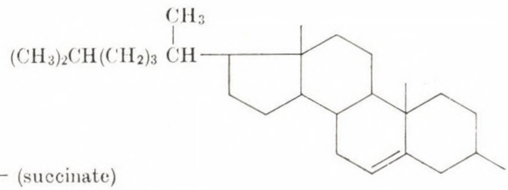

R = —CH_2—CH_2— (succinate)

—CH_2—CH_2—CH_2— (glutarate)

—CH_2—O—CH_2— (diglycolate)

—CH_2—CH— (α,β-methyl-succinic acid mixture)
　　　　|
　　　CH_3

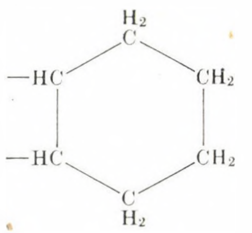

(hexahydrophthalate)

[1] It has to be noted that, in the case of azoxy compounds a mixture of *cis* and *trans* isomers is present. In spite of the initiator character of hydrogen peroxide in radical processes, not even traces of a polymer are formed in the oxidation step.

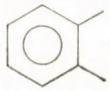

(phthalate)

(maleate)

(fumarate)*

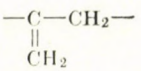

(β-monoithaconate)

b) Ch—O—CO—(R)—CO—OH + $CH_3COOCH=CH_2$ $\xrightarrow{Hg(Ac)_2}$ Ch—OCO—

—(R)—COOCH=CH_2

Preparation of monomers

p-n-Alkylazo and p-n-alkoxyazo derivatives

The starting *p*-substituted aniline derivatives were Aldrich products. They were made by diazotization according to the procedure given in Ref. [26] and coupled with phenol. Their acrylates were prepared from acrylic chloride in ether as solvent, in the presence of triethylamine.

The azoxy derivatives were prepared as in Ref. [27] in acetic acid as solvent, from the corresponding azoacrylates by oxidation with hydrogen peroxide. Ethanol was used for the recrystallization of azoacrylates and azoxyacrylates. The melting points and meso-phase ranges were determined by hot-plate equipped Polmi-A polarizing microscope. The results of C, H, N analyses for each compound and other data of the monomers are summarized in Tables I and II.

Cholesteryl vinyl esters of dicarboxylic acids

0.1 mol of cholesterol (Reanal, Budapest; m.p. 148.5°, $[\alpha]_D^{20} = -39.5$ in 2 g/100 ml chloroform solution) and 0.2 mol of the corresponding dicarboxylic anhydride were dissolved in 50 ml chloroform. The solution was boiled while 1 ml of triethylamine was introduced. After boiling for 6 hrs, the solution was diluted with 150 ml of acetone. At room temperature, the monocholesteryl ester of the corresponding dicarboxylic acid is precipitated in nearly quantitative yield. The monocholesteryl esters of the corresponding dicarboxylix acids were prepared by transvinylation according to ADELMANN [28]. The cholesteryl vinyl esters were recrystallized from ethanol, while cholesteryl vinyl fumarate was crystallized from acetone. The results of C, H analyses for each compound together with other data of the monomers are collected in Table III.

* For preparing monocholesteryl fumarate, acylation was catalyzed by a 40% acetic acid solution of HBr instead of triethylamine. Therefore, monocholesteryl maleate isomerized to fumarate in one step.

Table I

Characteristic data of p-n-alkylazo (a) and p-n-alkylazoxy acrylates (b)

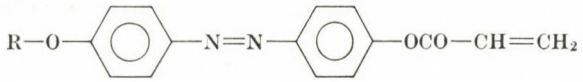

(a)

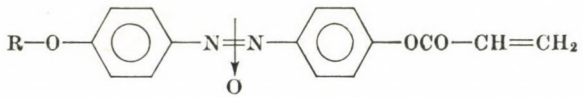

(b)

No.	R	Crystalline m.p. (°C)	Nematic m.p. (°C)	Analysis					
				Calcd. (%)			Found (%)		
				C	H	N	C	H	N
1/a	H	69	—	71.40	4.76	11.12	71.15	4.70	11.01
2/a	CH_3	90	—	72.20	5.27	10.51	72.02	5.07	10.48
3/a	C_2H_5	54	—	72.90	5.72	10.00	73.00	5.80	10.06
4/a	C_4H_9	66	—	74.00	6.49	9.08	74.20	6.53	9.03
1/b	H	69	—	67.20	4.48	10.45	66.84	4.76	10.37
2/b	CH_3	83	89	68.06	4.92	9.92	68.01	5.00	9.60
3/b	C_2H_5	55	73	68.90	5.41	9.46	68.96	5.68	9.50
4/b	C_4H_9	63	84	70.04	6.17	8.64	70.90	6.29	8.68

Table II

Characteristic data of p-n-alkoxyazo (a) and p-n-alkoxyazoxy acrylates (b)

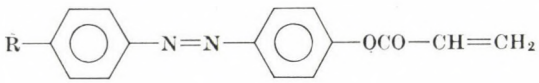

(a)

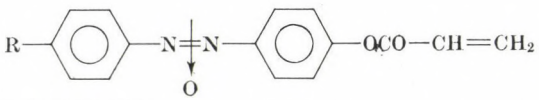

(b)

No.	R	Crystalline m.p. (°C)	Nematic m.p. (°C)	Analysis					
				Calcd. (%)			Found (%)		
				C	H	N	C	H	N
5/a	CH_3	98	118	68.06	4.96	9.92	68.01	5.00	9.60
6/a	C_2H_5	105	142	68.90	5.41	9.46	68.73	5.78	9.59
7/a	C_4H_9	87	123	70.04	6.17	8.64	69.65	6.60	8.51
5/b	CH_3	92	147	64.40	4.69	9.49	64.34	4.68	9.54
6/b	C_2H_5	90	140	65.00	5.09	8.99	65.25	5.25	9.30
7/b	C_4H_9	72	145	67.14	5.87	8.24	67.13	6.06	8.36

Table III

Characteristic data of mixed cholesteryl vinyl esters of dicarboxylic acids

No.	R	Crystalline m.p. (°C)	Smectic m.p. (°C)	Clearing point (°C)	Analysis			
					Calcd.		Found	
					C	H	C	H
8	$-CH_2-CH_2$	82	—	89	77.34	10.31	77.55	10.58
9	$-CH_2-CH_2-CH_2-$	83+	—	(72)	77.70	10.16	77.81	10.59
10	$-CH_2-O-CH_2-$	117	—	—	74.90	9.65	74.81	9.81
11	$-CH_2-CH(CH_3)-$ *	−7	47	57	77.70	10.26	77.87	10.82
12	$-CH=CH-$	105	—	—	77.60	9.60	77.81	10.00
13	$-C(H)=C(H)-$	96		176	77.60	9.82	77.65	10.17
14	$-C(=CH_2)-CH_2-$	—	65	—	77.95	9.92	77.43	10.38
15	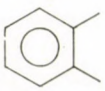	110	—	—	80.06	9.46	80.15	9.85
16	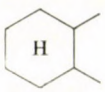	—	50	—	78.40	10.24	78.14	10.47

+ monotropic
* mixture of α, β-methylsuccinic acid

X-ray diffraction investigations

A common characteristic of the above monomers is their quite anisotropic molecular size. The length of the molecule is for each monomer greater than 2.0 nm, while the smallest dimension of the molecules — assuming a planar geometry — may be about 0.38 and 0.45 nm for the series of azo and azoxy compounds and for the cholesteryl derivatives, respectively. The arrangement of the molecules in the crystal lattice was studied by X-ray powder diffraction technique, which permitted to determine the thickness of the possible molecular layers on the basis of the longest identity period and within this layer the arrangement of the molecules with estimated length. The X-ray diffractograms obtained on a Philips wide-angle powder diffractograph are shown schematically in Figs 1 and 2. The reflection angles corresponding to the

diffraction peaks are on the abscissa and the peak heights, measured from the baseline as fractions of the peaks with maximum intensity, are on the ordinate. The identity periods calculated on the basis of powder diffractograms are collected in Table IV. The data shown in Table IV are those periodicities that permit to obtain three identical indices for each line of the diffractogram. The density values indicated in column 8 of Table IV were calculated on the basis of these periodicities. Monoclinic or orthorhombic crystal classes have been presumed for indexing. The low number of investigated reflections was not sufficient to permit a search for their systematic absence. The observed periodicities were not transformed to the possibly correct cell dimensions.

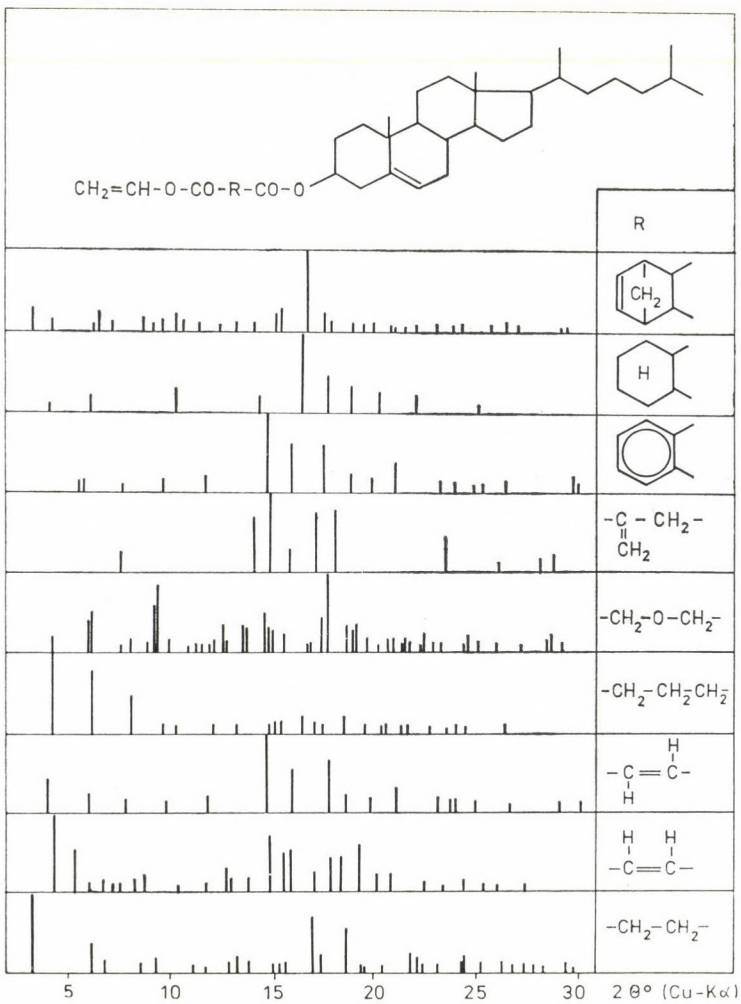

Fig. 1. Schematic representation of the diffractograms of mixed cholesteryl vinyl esters of dicarboxylic acids

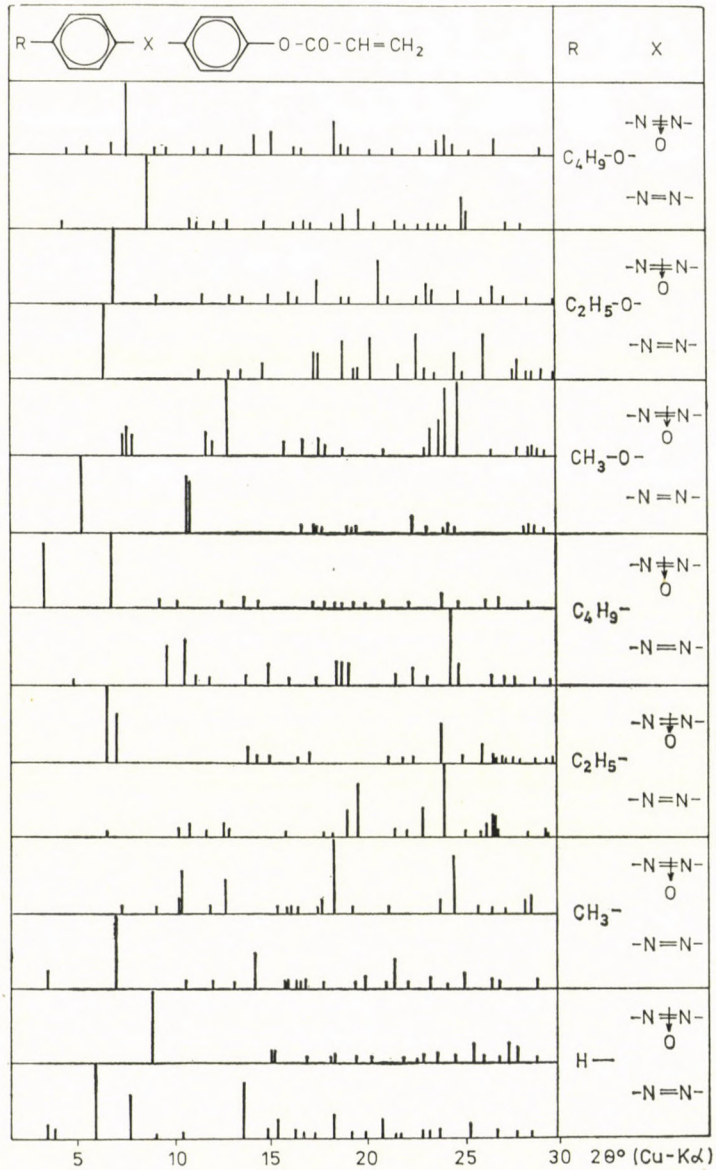

Fig. 2. Schematic graph of the diffractograms of *p*-substituted *p*'-acryloyloxyazo and azoxybenzenes

Table IV

Crystallographic data of the monomers investigated and the melting points of the polymers
(Translation period in nm)

No. of compound	$1/a^*$	$1/b^*$	$1/c^*$	β°	Z	ϱ(g cm^{-3})	Polymer m.p. (°C)
1a	1.005	2.30	2.56	90	16	1.126	300 (b)
1b	1.000	1.028	1.464	90	4	1.182	300 (b)
2a	1.122	1.050	2.480	92.6	8	1.204	270 (b)
2b	1.191	1.460	1.680	90	8	1.293	280
3a	0.750	1.294	1.688	90	4	1.086	290
3b	1.174	1.68	1.887	90	8	1.055	300
4a	0.819	1.094	1.790	92.4	4	1.281	310
4b	0.931	1.372	2.524	90	8	1.338	320 (b)
5a	0.926	1.006	1.595	90	4	1.259	320 (b)
5b	1.166	1.476	1.683	90	8	1.378	340 (b)
6a	1.356	0.787	1.512	96.8	4	1.151	280—290
6b	0.926	1.338	2.543	90	8	1.246	310
7a	1.180	1.320	1.947	90.6	8	1.418	310 (b)
7b	1.544	1.902	2.264	90	16	1.357	320—330
8	1.24	0.79	2.85	90	4	1.165	190
9	0.619	0.996	4.69	93.4	4	1.198	210
10	1.065	1.84	2.08	90	4	1.026	215
12	1.196	1.636	1.98	90	4	1.140	205
13	0.765	0.994	4.43	92.7	4	1.005	280
14	0.751	1.031	4.48	92.9*(a)	4	0.996	216
15	0.753	1.004	4.49	90	4	1.111	165
16	0.934	0.934	2.49	120*(a)	4	0.898	145
17	1.96	1.319	2.51	93.4	8	1.176	?

* (a) = ab angle is γ, $\beta = 90^\circ$
b = melting with simultaneous decomposition

Monomers of cholesteric basis have layer structures. Monomers, numbered 9, 13, 14 and 15 are double-layered, the others mono-layered. Except CVS all layers are tilted, *i.e.* the longitudinal axis of the monomer molecules and the normal of the layer are not parallel. Two monomers — in accordance with the results of polar microscopy — are smectic (16 : S_B, 14 : S_G). The diffractogram of 13 is somewhat deficient in lines.

Within the azo and azoxy series, regularities and similarities cannot be recognized. In general, the cell volume of the azoxy compounds is greater than that of the azo compounds. This is not valid for the unsubstituted monomers.

The longest period is usually much smaller than the estimated length of the molecule, except in the case of **1a**, **4b**, **6b** and **7b**. It can be assumed only for the latter that the acryloyl groups are arranged in one plane. For the other azo and azoxy monomers, the longitudinal axis of the molecules and the longest periods are not parallel. Hence, it is probable that the acryloyl groups do not form a topochemically favourable plane.

Polymerization experiments

The polymerization activity of each monomer has been tested qualitatively. Their 10 wt. % solutions in dioxane were heated at 70 °C in the presence of 0.5 wt. % benzoyl peroxide for 30 min. During the heat treatment, the viscosity of the solutions increased. The polymers formed were precipitated with methanol, afterwards the cholesterol derivatives were dissolved in benzene, the azo and azoxy derivatives in chloroform and all were precipitated again with methanol. The melting points of the precipitated and dried polymers are listed in Table IV.

All polymeric products were optically birefringent. The birefringency ceases at a definite temperature. The clearing point of the polymers is also indicated in the last column of Table IV. The detailed investigation of poly(cholesterylvinyl succinate) and poly(*p*-alkyl-*p*'-acryloyloxy-azoxybenzene) derivatives has already been reported [3, 4].

REFERENCES

[1] Demus, G., Demus, H., Saschke, H.: Flüssige Kristalle in Tabellen. VEB Deutscher Verlag für Grundstoffindustrie, Leipzig 1974
[2] Amerik, Yu. B., Krentsel, B. A., Konstantinov, I. I.: Dokl. Akad. Nauk. SSSR, **165,** 1097 (1965)
[3] Amerik, Yu. B., Krentsel, B. A.: J. Polymer Sci., **C16,** 1383 (1967)
[4] Hardy, Gy., Fedorova, N., Kovács, G., Boros-Gyevi, J.: J. Polymer Sci., **C16,** 2675 (1967)
[5] Hardy, Gy., Nyitrai, K., Cser, F., Cselik, Gy., Nagy, I.: Europ. Polym. J., **5,** 135 (1969)
[6] Amerik, Yu. B., Konstantinov, I. I., Krentsel, B. A.: J. Polymer Sci., **C23,** 231 (1968)
[7] Hardy, Gy., Nyitrai, K., Cser, F.: Kinetics and Mechanism of Polyreactions. Vol. **IV,** p. 121, Akadémiai Kiadó, Budapest 1969
[8] Hardy, Gy., Cser, F., Kalló, A., Nyitrai, K., Bodor, G., Lengyel, B.: Acta Chim. (Budapest), **65,** 287 (1970)
[9] Paleos, C. M., Labes, M. M.: Mol. Cryst. Liqu. Cryst., **11,** 385 (1970)
[10] de Visser, A. C., Feyen, J., de Groot, K.: J. Polymer Sci., **B8,** 805 (1970)
[11] Blumstein, A., Kitagawa, N., Blumstein, R.: Mol. Cryst. Liqu. Cryst., **12,** 215 (1971)
[12] Strzelecki, L., Liébert, L.: Bull. Soc. Chim. France, **1973,** 597
[13] Liébert, L., Strzelecki, L.: Bull. Soc. Chim. France, **1973,** 603
[14] Strzelecky, L., Liébert, L.: Bull. Soc. Chim. France, **1973,** 605
[15] Perplies, E., Ringsdorf, H., Wendorff, H.: Makromol. Chem., **175,** 553 (1974)
[16] Perplies, E., Ringsdorf, H., Wendorff, H.: Ber. Bunsenges. phys. Chem., **78,** 921 (1974)

[17] LECOIN, D., HOCHAPFEL, A., VIOVY, R.: J. Chim. phys., **72,** 1029 (1975)
[18] HARDY, Gy., NYITRAI, K., CSER, F.: Eur. Polym. J., **12,** 785 (1976)
[19] HARDY, Gy., CSER, F., FEDOROVA, N., BÁTKY, M.: Acta Chim. (Budapest), **94,** 275 (1977)
[20] NYITRAI, K., CSER, F., SEYFRIED, É., LENGYEL, M., HARDY, Gy.: Eur. Polym. J., **13,** 673 (1977)
[21] HSU, E. C., LIM, L. K., BLUMSTEIN, R. B., BLUMSTEIN, A.: Mol. Cryst. Liqu. Cryst., **33,** 35 (1976)
[22] STRZELECKI, L., KELLER, F., LIÉBERT, L., GUYOT, H.: C. R. Acad. Sci. Paris, **283C,** 219 (1976)
[23] TANAKA, Y., HITOTSUYANAGI, M., SHIMURA, Y., OKADA, A., SAKURATA, H., SAKATA, T.: Makromol. Chem., **77,** 3035 (1976)
[24] SHIBAEV, V. P., FREIDZON, Ya. S., PLATE, N. A.: Vysokomol. Soed., **A20,** 82 (1978)
[25] FINKELMANN, H., RINGSDORF, H., WENDORFF, J. H.: Makromol. Chem., **79,** 273 (1978)
[26] DIETRICH, H. J., STEIBER, E. Z.: Mol. Cryst., **11,** 385 (1970)
[27] STEINSTRÄSSER, R., POHL, L.: Tetrahedron Lett., **22,** 1921 (1971)
[28] ADELMANN, R. L.: J. Org. Chem., **14,** 1057 (1949)

NYITRAI Károly
CSER Ferenc
HARDY Gyula

H-1950 Budapest, Hungária körút 114.

Acta Chimica Academiae Scientiarum Hungaricae, Tomus 102 (4), pp. 371—381 (1979)

SOME CHEMICAL REACTIONS OF THE ELECTRODE GAP AND THEIR ROLE IN SPECTROCHEMICAL ANALYSIS, XXXIII

BEHAVIOUR OF METAL OXIDES IN THE ARC. THE EFFECT OF O_2 IMPURITIES OF Ar, THE CARRIER ELECTRODE AS REACTION PARTNER AND THE DECOMPOSITION OF METAL OXIDES BY THE ARC

Z. L. SZABÓ and É. BERTALAN

(Department of Inorganic and Analytical Chemistry, Eötvös L. University, Budapest)

Received October 10, 1978

Accepted for publication February 7, 1979

The O_2 contamination of the Ar atmosphere influences in plasma sheath reaction the ratio of carbon oxides formed in reactions within the substance of the electrode. However, in view of their small quantity they scarcely change the intensity of the spectral lines, as compared to other processes and effects of major importance. Carbon used as a carrier electrode reacts also with the metal oxides filled into its boring. In the burning spot of the arc, formed at the electrode and the substance filled into it, and in the environment of the burning spot metal oxides undergo a spontaneous thermal decomposition besides their direct reduction by carbon. In this decomposition oxygen is liberated, which is able to participate in further reactions.

The last parts of our series of publications dealt with the reactions of mixtures of various metal oxides with carbon powder, produced by arc discharge [1—10]. Steady and flowing Ar atmospheres were used to exclude interfering parallel electrode surface reactions. The quantities of CO and CO_2, produced in the polarized a.c. arc ignited at maximum voltage were measured by our gas analytical methods [11], and the change in intensity of the atom line of the main component of the sample, considered as proportional to the evaporation of the sample, was followed. Our results were evaluated by the comparison of data obtained by the two methods. Several questions were left open in these investigations. Thus, a problem to be settled was how far the O_2 impurity of the Ar discharge gas atmosphere affects the results of the measurements, particularly when flowing and thus relatively much more gas is used. Moreover, the suspicion arose in the investigation of carbon powder mixtures that metal oxides might react with the substance of the RW II carbon electrode used as carrier electrode besides with the diluting carbon powder. Similarly it remained an open question whether the spontaneous thermal decomposition of metal oxides may also produce oxygen, giving rise to further reactions. In the following, results in conjunction with the investigation of these problems are reported.

1. Effect of the O_2 contamination of the Ar atmosphere

It seemed in some of our earlier experiments in which flowing Ar atmosphere was used, for which gas was replaced from a balloon gasometer, that O_2 contamination may have got into the Ar gas by diffusion through the walls of the thinner gasometer balloons. This might have influenced the data measured, the quantities of CO and CO_2 and the intensities of the spectral lines. This has been indicated already in the communication [5] reporting on the study of the effect of gas flow rate. With increasing gas flow more oxygen may get into the cell, which might have changed the results of the measurements. The oxygen content of Ar sucked off from the cell and replaced from the balloon gasometer has been measured, and actually, depending on the waiting time, a few tenth percentage of oxygen was found. Therefore, our experimental system has been modified. Gas was taken directly from the Ar cylinder, and a paraffin oil liquid seal was inserted between the steel cylinder and the gas cell, to equalize thereby the difference between suction and gas introduction. The excess of Ar bubbled through the liquid seal into the air, and oxygen could not get into the system. In this case the gas atmosphere was actually free of oxygen contamination.

Next, measurements under changing of the gas flow rate were repeated, now already in certainly oxygen free atmosphere. The carrier electrode was RW II carbon, a carbon powder (SU-601) mixture of a mole fraction of 0.6 CuO was filled into its boring, and the system was investigated against a counter electrode, made similarly of RW II carbon, by polarized a.c. arc excitation, ignited at maximum voltage. The average current of the arc was 7 A, the burning time 10 s. Figure 1 shows the CO production, while Fig. 2 the CO_2 production of the arc. (The markings *a* and *c* indicate the anodic or cathodic excitation of the sample.) As contrary to our earlier results [5], it can be seen from the figures plotted as a function of the flow rate of Ar gas that the quantity of both carbon oxides first increases with increasing flow rate and then decreases. With increasing gas flow the partial pressure of the gaseous reaction products decreases in the vicinity of the electrode, and the possibility of the reaction increases. Later, this is counterbalanced by the electrode cooling effect of the larger gas stream and consequent slowing down of reaction. The ratio of the two carbon oxides, the CO_2/CO ratio, decreases throughout (Fig. 3). The larger gas stream primarily cools the superficies of the elctrode, reducing thus the temperature of the site of CO_2 formation. Therefore, as contrary to our earlier opinion, the freezing-in of the reaction $CO_2 + C = 2\,CO$ by the higher flow rate is of minor importance. According to our results obtained in Ar atmosphere contaminated by oxygen the quantity of CO_2 increased while that of CO decreased with increasing gas flow rate. At that time there seemed to be two possible explanations. One of these was the afore-mentioned freezing-in of the

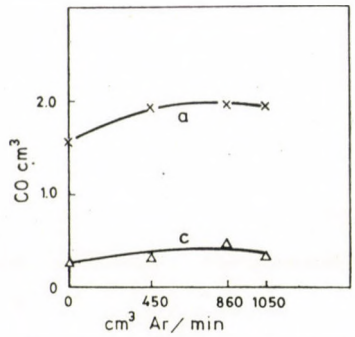

Fig. 1. CO production as a function of the flow rate of Ar gas; RW II carbon electrode; *a:* anodic, *c:* cathodic excitation

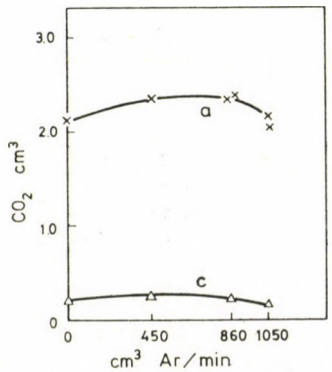

Fig. 2. CO_2 production as a function of the flow rate of Ar gas; RW II carbon electrode; *a:* anodic, *c:* cathodic excitation

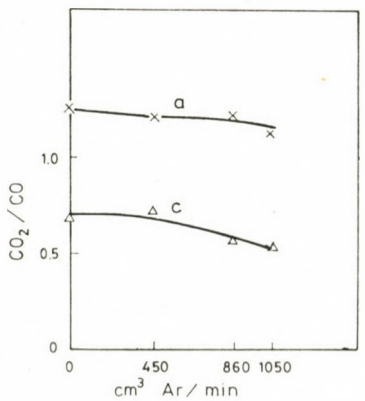

Fig. 3. CO_2/CO ratio as a function of the flow rate of Ar gas; RW II carbon electrode; *a:* anodic, *c:* cathodic excitation

reaction, the other the effect of oxygen contamination. Our present experiments verified this latter assumption.

The intensity of the Cu I 282.4 nm atom line follows also the curves of formation of the carbon oxides (Fig. 4). Thus, the temperature of the ignition spot of the arc and the extent of chemical reactions change to a certain degree parallel.

It seemed then worth-while to investigate the behaviour of gas analytical and spectral values as a function of carbon powder ratio, and compare them

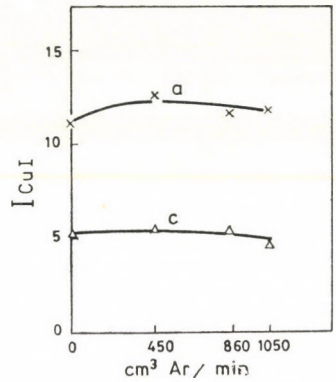

Fig. 4. Change in intensity of the Cu I 282.4 line as a function of the flow rate of Ar gas; RW II carbon electrode; *a:* anodic, *c:* cathodic excitation

with values obtained in an atmosphere contamined by oxygen. Figures 5 and 6 show the quantities of CO and CO_2 measured in Ar atmosphere contamined by oxygen, while Figs 7 and 8 those obtained in oxygen-free atmosphere. Numeration on the horizontal axis of the figures is bidirectional, because, as described earlier [6, 7, 10], reactions are determined from one of the sides by the quantity of CuO introduced with the powder mixture into the boring of the electrode, and from the other side by the smaller quantity of C powder. The shape of the curves and the location of maxima remained unchanged in the two cases, the oxygen contamination in the gas space has no effect on the reaction proceeding in the boring of the electrode, within the substance of the same. Thus, this can not cause that the production of carbon oxides falls between the 1 : 1 and 2 : 1 CuO : C mole ratios optimal for CO and CO_2 formation, and our earlier considerations concerning the parallel course of the two reactions hold true [4, 7]. However, the magnitude of the maxima changes. It can be clearly seen from the figures that under oxygen-free conditions, in spite of the fact that the new carrier electrodes held by about 20% more powder mixture, the quantity of CO_2 has been reduced and that of CO has increased because of the absence of the

$$2\,CO + O_2 = 2\,CO_2$$

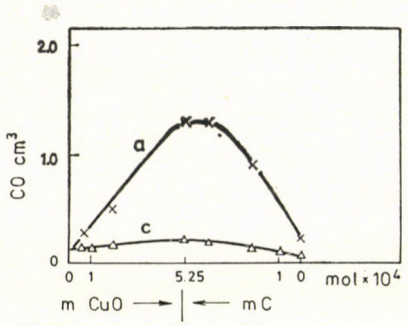

Fig. 5. CO production as a function of carbon powder ratio; RW II carbon electrode; *a:* anodic, *c:* cathodic excitation; Ar atmosphere contaminated with oxygen

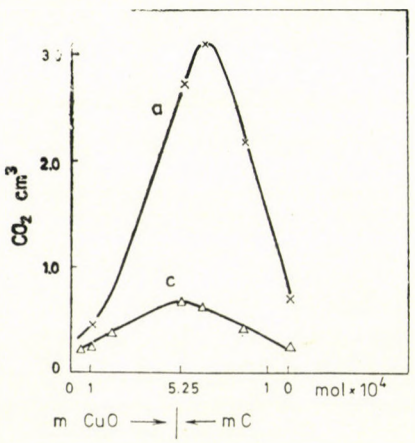

Fig. 6. CO_2 production as a function of carbon powder ratio; RW II carbon electrode; *a:* anodic, *c:* cathodic excitation; Ar atmosphere contaminated with oxygen

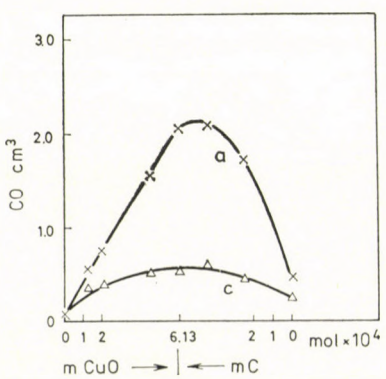

Fig. 7. CO production as a function of carbon powder ratio; RW II carbon electrode; *a:* anodic, *c:* cathodic excitation; oxygen-free atmosphere

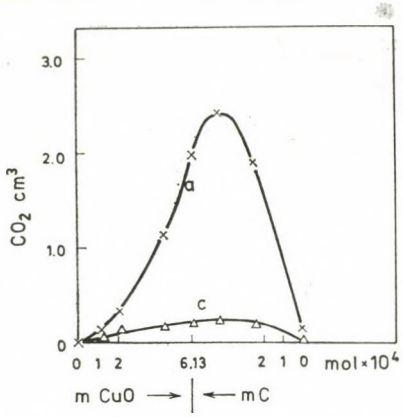

Fig. 8. CO_2 production as a function of carbon powder ratio; RW II carbon electrode; *a:* anodic, *c:* cathodic excitation; oxygen-free atmosphere

reaction. This is therefore the effect of O_2 contamination in the Ar atmosphere, which changes in the plasma sheath reaction values measurable by gas analytical methods. At the same time, carbon oxide may be formed in a smaller amount also in electrode surface reaction.

The change in intensity of the Cu I 282.4 nm atom line with carbon powder ratio, characteristic of the evaporation of the sample, reveals the same characteristics in Ar atmosphere contaminated by oxygen (Fig. 9) as in pure Ar atmosphere (Fig. 10). Numerical data of the curves are also in fairly good agreement. Thus, in a gas containing only a few tenth per cents of oxygen the excitation of metal vapours can be considered as virtually equal beside the dominant properties of Ar atmosphere and the relatively more pronounced reactions within the substance in the electrode. Thus an unambiguous effect could not be detected in the spectra with our not too sensitive experimental method, though according to data in the literature [11, 12] the effect of oxygen impurities is revealed already, particularly in the case of metal electrodes, where electrode surface reactions are decisive. Spectral character data as a function of carbon powder ratio gave also results of identical character and nearly identical numerical value for contaminated and pure atmosphere. This again is indicative of a plasma sheath reaction, which scarcely affects the hotter parts of the plasma and the evaporation of the sample.

2. Carbon carrier electrode as a reaction partner

It could be seen already from the figures of the preceding chapter that the production of the two carbon oxides as a function of carbon powder ratio falls between CuO : C mole ratios separately optimal for each. This was explained

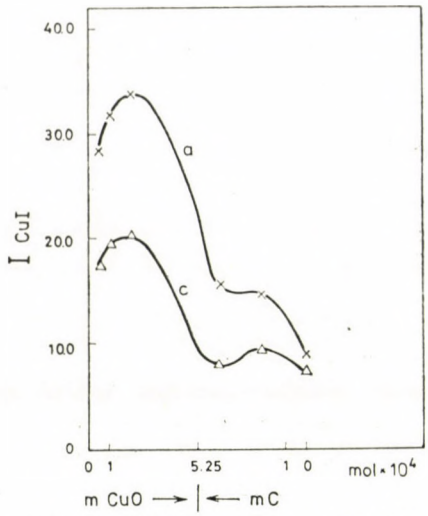

Fig. 9. Change in intensity of the Cu I 282.4 nm line as a function of carbon powder ratio in the mixture RW II carbon electrode; *a:* anodic, *c:* cathodic excitation; Ar atmosphere contaminated with oxygen

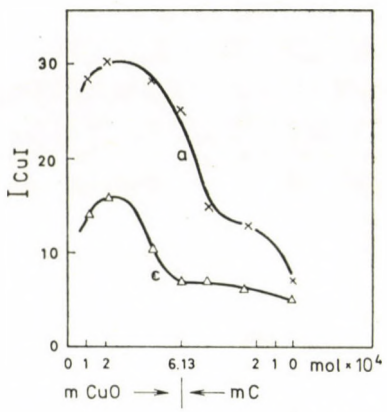

Fig. 10. Change in intensity of the Cu I 282.4 nm line as a function of carbon powder ratio in the mixture RW II carbon electrode; *a:* anodic, *c:* cathodic excitation, oxygen-free atmosphere

by the parallel course of the two reactions. It was thought possible, however, that other factors also play a part. The possible effect of oxygen contamination in the gas space can be excluded on the basis of the preceding chapter, but the shift of the maxima from the mole ratio of 1 : 1 towards higher values can have a further reason. The carbon carrier electrode may also react with the copper oxide filled into its boring. Thus, the precise weighing in of the metal

oxide and carbon powder mixtures will be of no use, if possibly more carbon than calculated participate in the reaction. In order to eliminate the reaction of the carrier electrode, measurements have been repeated with copper auxiliary electrodes at an average current of 16 A and a burning time of 10 s. According to Fig. 11, the maximal CO_2 production of the arc falls also in this case between the values optimal for the formation of the two carbon oxides. This proves that the parallel formation of the two carbon oxides determined the location of the maxima on the CO_2 curves. Figure 12 shows the CO production of the arc under identical conditions, this time only for the case of anodic excitation. This curve actually shows a maximum at a CuO : C mole ratio of 1 : 1. The different behaviour of the two carbon oxides indicates a certain separation of the reaction sites [3, 4, 8]. This is proved also by the fact that CO_2 production decreased more pronouncedly (in the interior of the sample) by copper of better heat conduction. The production reactions of the two carbon oxides are connected with one another, consuming competitively the reaction partners. This could be graphically modelled by the addition of the calculated quantities of the two carbon oxides (Fig. 13). The possibilities of the two reactions as a function of the metal oxide (MeO) and carbon powder ratio were calculated and plotted for the quantity of the powder mixture held by the boring of the electrode for the case if the two reactions were independent from one another and only one at a time would proceed. Decreasing CO_2 was plotted at identical CO production, and the two curves of the respective parallel reactions were added. It can be seen that the maximum of the resultant curve (broken line in the Figure) is shifted with decreasing CO_2 content towards the mixture ratio of 1 : 1, optimal for CO formation. This resultant curve features break points, while the top of the directly measured curves is rounded off. This, too, indicates a linkage of the two reactions.

It follows from the above-mentioned that the carbon electrode plays as a reaction partner only a minor role. That its substance nevertheless reacts with the metal oxide filled into it becomes clear also from the curves of Figs 5—8, the end points of which, the values relevant to pure CuO, show a gas production higher than zero. In this case carbon oxides can react only with the wall of the electrode, a reaction to be taken less and less into consideration with higher carbon content of the powder mixture. Two modes of reactions are now conceivable. One possible mode is the direct contact and reaction of the filled in metal oxide with the wall of the carrier electrode, the other the thermal decomposition of the metal oxides by the arc, and the reaction of the oxygen formed with the carbon vapours, simultaneously evaporated in the zones of appropriate temperature of the plasma. It seemed therefore essential to investigate the thermal decomposition of metal oxides, *i.e.* whether a measurable quantity of free oxygen is present in the arc.

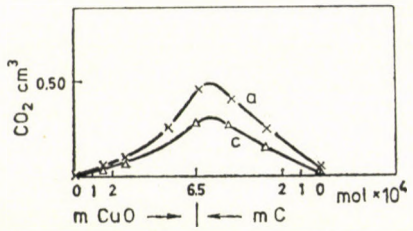

Fig. 11. CO production as a function of carbon powder ratio Cu auxiliary electrode; *a:* anodic, *c:* cathodic excitation

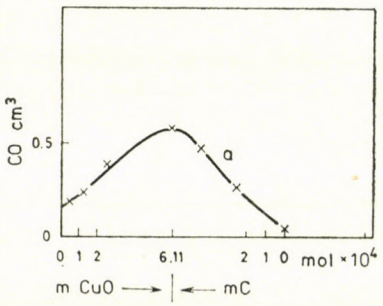

Fig. 12. CO production as a function of carbon powder ratio Cu auxiliary electrode; anodic excitation

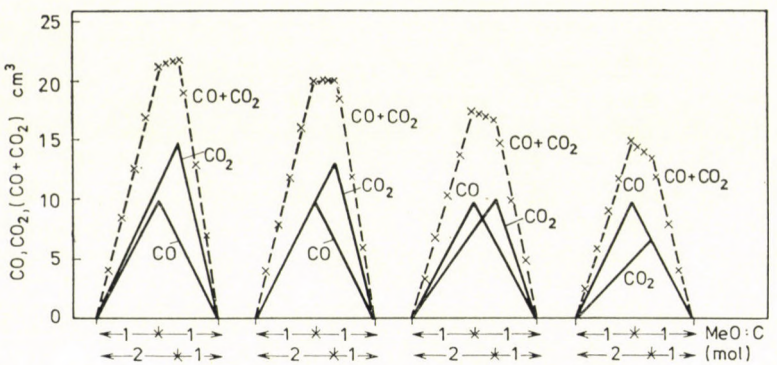

Fig. 13. Joint formation of CO and CO_2 (scheme)

3. Thermal decomposition of metal oxides

It has been mentioned already that two reaction zones are to be found in the packing of the electrode. One of these is the interior of the filling, where mainly CO_2 is formed, the other the burning spot of the arc and its immediate environment, where CO is produced independently of the properties of the metal oxides [3]. This latter site is thought to be also the decomposition zone

of the metal oxides [8]. For the verification of this assumption CuO was mixed in various ratios instead of diluting carbon powder with Al_2O_3 and filled into the boring of a copper carrier electrode. The arc burned at 16 A for 10 s. The quantity of oxygen appearing in the gas space was measured with our titrimetric gas analytical method [13]. Our assumption of thermal decomposition could be actually proved (Fig. 14), oxygen is present in the gas space.

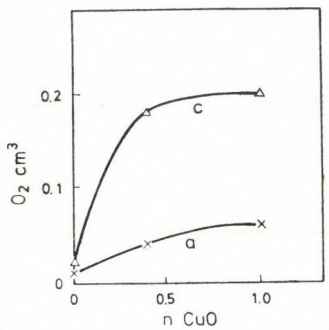

Fig. 14. Change in O_2 quantity with Al_2O_3 powder ratio measured in the decomposition of CuO; Cu auxiliary electrode; *a:* anodic, *c:* cathodic excitation

The figure permits two conclusions. One of these is that the quantity of measurable O_2 increases with the increasing of the less stable copper oxide content of the mixture, but not linearly. This is due to the fact that the temperature of the burning spot of the arc does not remain constant with changing the composition of the mixture. The quantity of metallic copper formed in the decomposition increases too, and exerts a cooling effect because of its good thermal conductivity [3, 4, 6]. Therefore, the curve is bending back though the active oxygen content of the powder mixture increases. Another observation is that in accordance with data in the literature [14, 15] and our earlier assumptions [16] the temperature of the cathode spot is higher than that of the anode spot, so that the decomposition of the metal oxide is also higher there. This indirectly proves at the same time the different temperatures of the burning spots of the arc on the electrodes of two kinds of polarities.

The question arose whether a decomposition of this character exists or can be detected also in the presence of carbon powder and in the carbon carrier electrode. This has been investigated by anodic excitation, using RW II carbon auxiliary electrodes and CuO + C mixtures (Fig. 15). Oxygen was measurable also in this case, though here not only the metal vapours but also carbon attempted to bind it. The curves pass through a maximum, with a higher value of the maximum than in the case of the copper carrier electrode. The reason for this is not only the stronger warming up of the carbon electrode, but also the heating up of carbon powder to a higher temperature than the diluting Al_2O_3

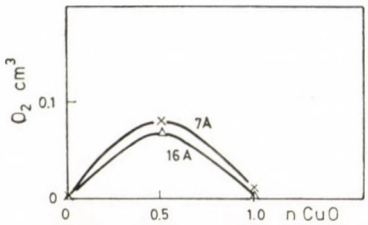

Fig. 15. Change in O_2 quantity with carbon powder ratio measured in the decomposition of CuO; RW II carbon electrode; anodic excitation

additive. The drop-down of the second half of the curves is due again to the cooling effect of metallic copper formed in the reaction. The quantity of metallic copper formed is larger for excitation at 16 A than at 7 A. More carbon is evaporated at higher current, and the volume of the plasma is also larger (see part XXXV of the communication series), so that the possibility for recombination to oxide is also higher. Oxygen will be present in the gas space only if the oxygen atoms formed during decomposition are recombined in the outer colder zones of the plasma besides with the evaporated metal and carbon also in a parallel reaction with one another, to give oxygen molecules. A relatively small amount of free oxygen is present in the gas space, because the metal vapours are strong reducing agents even with relatively inactive substances as copper, and moreover, carbon vapours are also present. Thus, the decomposition of metal oxides proceeds in the burning spot of the arc and in its immediate environment. At the same time, this zone coincides with the metal evaporating zone of the arc, so that, depending on the thermal stability of the metal oxides, the reaction must affect also the intensities of the spectral lines.

REFERENCES

[1] Szabó, Z. L., Dobolyi-Fejérdy, H.: Acta Chim. Acad. Sci. Hung., **96,** 189 (1978)
[2] Szabó, Z. L., Dobolyi-Fejérdy, H.: Acta Chim. Acad. Sci. Hung., **96,** 201 (1978)
[3] Szabó, Z. L., Dobolyi-Fejérdy, H.: Acta Chim. Acad. Sci. Hung., **97,** 1 (1978)
[4] Szabó, Z. L., Dobolyi-Fejérdy, H.: Acta Chim. Acad. Sci. Hung., **97,** 13 (1978)
[5] Szabó, Z. L., Dobolyi-Fejérdy, H.: Acta Chim. Acad. Sci. Hung., **97,** 27 (1978)
[6] Szabó, Z. L., Dobolyi-Fejérdy, H.: Acta Chim. Acad. Sci. Hung., **97,** 111 (1978)
[7] Szabó, Z. L., Dobolyi-Fejérdy, H.: Acta Chim. Acad. Sci. Hung., **97,** 125 (1978)
[8] Szabó, Z. L., Dobolyi-Fejérdy, H.: Acta Chim. Acad. Sci. Hung., **97,** 137 (1978)
[9] Szabó, Z. L., Dobolyi-Fejérdy, H.: Acta Chim. Acad. Sci. Hung., **98,** 147 (1978)
[10] Szabó, Z. L., Dobolyi-Fejérdy, H.: Acta Chim. Acad. Sci. Hung., **98,** 157 (1978)
[11] Boyd, B. R., Goldblatt, A.: Appl. Spectroscopy, **19,** 22 (1965)
[12] Slickers, K.: Spectrochim. Acta, **28/M,** 441 (1973)
[13] Szabó, Z. L., Tóth, I.: Acta Chim. (Budapest), **73,** 363 (1972)
[14] Anderman, G., Kemp, J. W.: ASTM Tech. Publ. (Philadelphia) 259 (1959)
[15] Zalesszkij, A. M.: A villamos ív (The electric arc). Műszaki Könyvkiadó, Budapest 1968
[16] Szabó, Z. L., Pöppl, L.: Acta Chim. (Budapest), **77,** 125 (1973)

Zoltán László Szabó
Éva Bertalan
H-1088 Budapest, Múzeum krt. 4/b.

Acta Chimica Academiae Scientiarum Hungaricae, Tomus 102 (4), pp. 383—390 (1979)

SOME CHEMICAL REACTIONS OF THE ELECTRODE GAP AND THEIR ROLE IN SPECTROCHEMICAL ANALYSIS, XXXIV

BEHAVIOUR OF THE METAL OXIDES IN THE ARC. AVERAGE TEMPERATURE OF THE ELECTRODES AND THE CHEMICAL REACTIONS

Z. L. SZABÓ and É. BERTALAN

(Department of Inorganic and Analytical Chemistry, Eötvös L. University, Budapest)

Received October 10, 1978

Accepted for publication February 7, 1979

It has been proved by electrode temperature measurements and their comparison with gas analytical data that there is a correlation between the temperature of the electrode and the chemical reactions. In the case of CuO + C powder mixtures at anodic excitation of the sample the temperature of the electrode increases proportional to the reaction of greater extent. It became evident from experiments on the effect of current that the temperature of the electrode is controlled decisively by the current of the arc, but heat evolved in the reaction of the substance filled in the boring of the electrode modifies this temperature, and affects thereby also the evaporation of the sample.

Two effects of the reactions between the components of the powder mixtures within the substance of the electrode have been demonstrated [1—5]. One of these is the energetical effect, known also from the literature, according to which heat evolved in the reaction heats up the sample, enhancing thereby its evaporation. The other effect involves the gas production of the reactions, which changes the composition of the plasma gases and consequently the excitation of the metal vapours. The aim of our present communication was a more detailed investigation of the first, the energetical effect, at an excitation of 7 A as a function of the composition of the metal oxide — carbon powder mixture, and on a mixture of 0.6 mole fraction of metal oxide as a function of the current of the arc. As earlier, a polarized a.c. arc excitation ignited at maximum voltage (essentially a pulsating direct current) of a burning time of 10 s, and auxiliary electrodes made of RW II and RW O carbon have been used. The average temperature of the electrode was measured with an iron-constantan thermocouple, the sensor being fitted into a 2 mm deep boring at the side of the electrode, located 1 mm below the 4 mm boring, holding the powder sample. Evidently, this yields only comparative data, as the measurement is not carried out in the reacting powder mixture filling itself. To produce possible reactions of different extent, mixtures of different ratio of CuO with carbon

powder and with Al_2O_3 and mixtures of Al_2O_3 with carbon powder were used as model substances. The reactions were followed by the measurement of the CO and CO_2 production of the arc with the titrimetric gas analytical methods described earlier [6].

1. Investigations as a function of the composition of the powder mixture

Figure 1 shows temperature values measured for CuO + C powder mixtures of various ratios at anodic (*a*) and cathodic (*c*) excitation of the RW II carrier electrode. The horizontal axis of the diagram carries bidirectional numeration, in accordance with the fact that chemical reactions in the mixture are determined from the two sides by the quantity, or more exactly by the mole number of CuO and C powder, respectively, which the boring of the electrode can hold [2, 3]. For comparison, the figure published in one of our previous communications [3], showing the simultaneously measured and now more characteristic CO_2 production of the arc, is shown again (Fig. 2). It has been found earlier that the temperature of the test sample depends in addition to the current of the arc primarily on the CO_2 producing reaction in the substance filled in the boring of the carrier electrode. Figure 2 clearly shows that the reaction of the powder mixture is rather insignificant at the cathodic excitation of the sample. This scarcely changes the temperature of the electrode (curve *c*, Fig. 1), which gradually decreases with increasing CuO content of the powder mixture. As mentioned already several times [7], and as could be proved now, the heating up of the electrode is controlled by the temperature of the burning spot of the arc. This depends in the case of a larger excess of carbon powder on the temperature of sublimation (3500—4000 °C) of carbon, while it becomes lower at higher CuO content, because the boiling point of copper (2336 °C) reduces the temperature of the burning spot, and thereby, that of the whole electrode. In anodic excitation of the carrier electrode a maximum curve is obtained for the temperature of the electrode. The location of the maximum is exactly the same as that of the maximum of the reaction proceeding in the filling, obtained for a mixture of about 0.6 mole fraction of CuO. This convincingly proves that heat liberated in the carbon oxide producing reaction increases the temperature of the whole mass of the electrode.

To check the above-said, CuO was diluted instead of carbon powder in different ratios with Al_2O_3, which does not react with CuO. Chemical reactions and the average temperature of the carrier electrode were measured again with an arc of 7 A and RW II auxiliary electrodes. In this case only a very weak reaction was obtained as a function of the CuO content of the mixture both for CO (Fig. 3) and for CO_2 (Fig. 4) production. The quantity of CO formed by the action of the arc, slightly increases at both polarities with increasing CuO

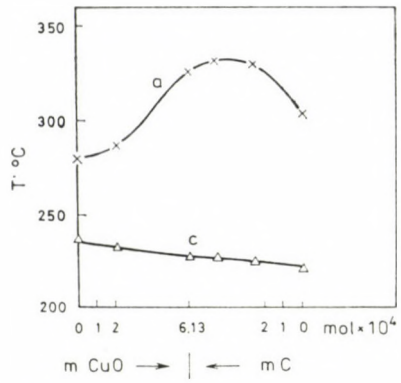

Fig. 1. Temperature of the RW II carrier electrode and the ratio of CuO + C powder; 7 A; *a:* anodic, *c:* cathodic excitation

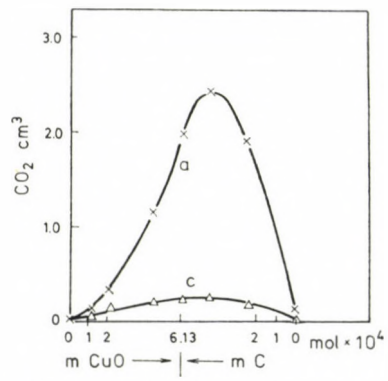

Fig. 2. The CO_2 production of the arc as a function of the composition of the CuO + C mixture; 7 A; *a:* anodic, *c:* cathodic excitation

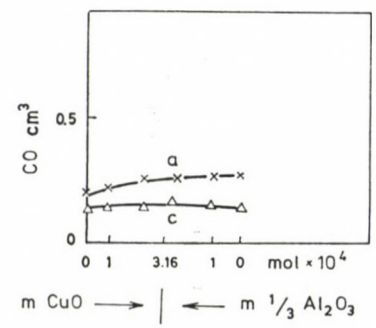

Fig. 3. CO production as a function of the metal oxide ratio; *a:* anodic, *c:* cathodic excitation

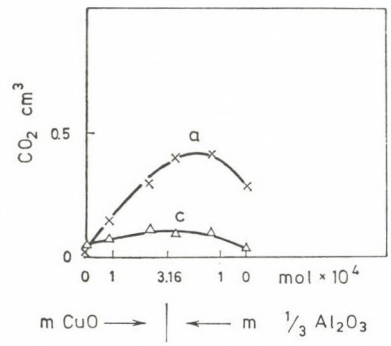

Fig. 4. CO_2 production as a function of the metal oxide ratio; *a:* anodic, *c:* cathodic excitation

content of the mixture. The decomposition of CuO yields increasing amounts of oxygen, which can react with the substance of the carbon carrier electrode [8]. At the same time, in the CO_2 production of the arc low values give as a function of the composition of the powder mixture maximum curves. Here the heat conductions of the powder mixture and of metallic copper formed from CuO by decomposition play already a more important role. Owing to the small extent of the reaction, the average temperature of the carrier electrode (Fig. 5) does not show a maximum, temperature values slightly decrease because of the cooling effect of the composition of the mixture and of metallic copper formed in the reaction, though there was a higher scatter of values measured, than in the case of CuO + C mixtures.

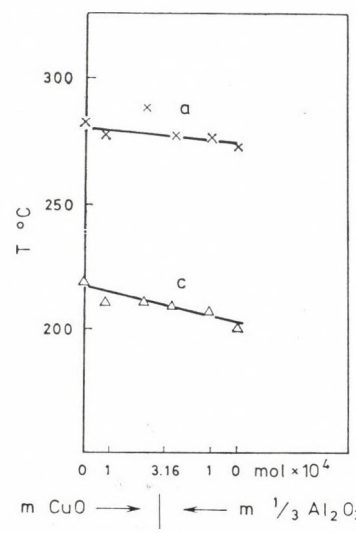

Fig. 5. Temperature of the RW II carrier electrode and the metal oxide ratio; *a:* anodic, *c:* cathodic excitation

It has been proved thereby that in the absence of a reaction of higher extent the temperature of the electrode can be changed only by the physical characteristics of the powder mixture. These are decisively determined by the current of the arc, as will be clearly seen from the next chapter.

2. Investigations as a function of the current of the arc

Our further aim was to study the effect of heat evolved during the chemical reactions on the temperature of the RW II carbon carrier electrode and of the substance filled in it as a function of the average current of the arc. The carbon powder mixture of 0.6 CuO mole fraction, yielding maximal gas production was used for the experiments. For comparison measurements were carried out also with Al_2O_3 + C powder mixtures, in which the oxygen content bound in the metal oxide was the same as that in the CuO + C mixture. As earlier [1—3], this was attained by dividing the formula weight of Al_2O_3 by three, the number of oxygen atoms contained, and calculating with this "equivalent weight" as molecular weight, we prepared also from Al_2O_3 a mixture of 0.6 mole fraction.

Figure 6 shows electrode temperatures obtained for CuO + C mixtures as a function of the average current of the arc at anodic (*a*) and cathodic (*c*) excitation of the sample. Naturally, the curves ascend with increasing current, anodic excitation resulting higher temperatures, in the same way as it did give higher gas production [9]. The temperature curves obtained for Al_2O_3 + C

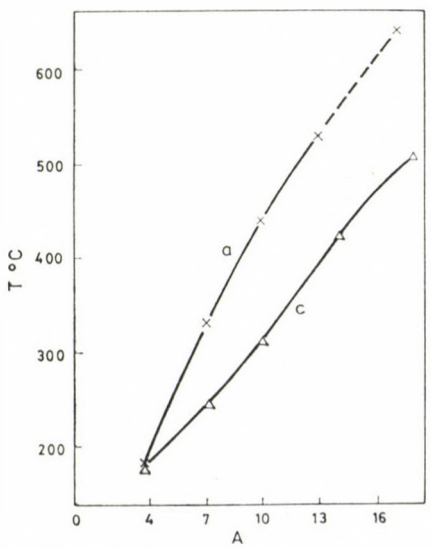

Fig. 6. Temperature of the RW carrier electrode and the current; CuO + C filling; *a:* anodic, *c:* cathodic excitation

mixtures (Fig. 7) are flatter. This decrease is particularly noticeable in the more intensive anodic excitation, because here, due to the very small extent of reaction, the temperature of the electrode is determined by the current of the arc alone, and is scarcely influenced by the small reaction occurring here.

The relationship between the temperature of the electrode and chemical reactions becomes still more evident from results obtained with graphitic carrier

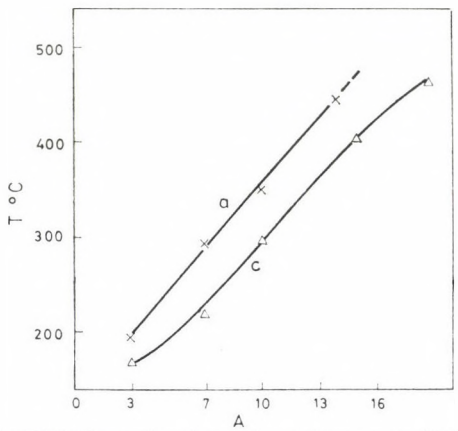

Fig. 7. Temperature of the RW II carrier electrode and current; Al_2O_3 + C filling; *a:* anodic, *c:* cathodic excitation

electrodes of type RW O, being better heat conductors, and therefore cooler. The average temperature of the electrode (Fig. 8) reveals within rather wide current limits at cathodic excitation higher values, similarly to the gas production of the reactions, of which again only data relevant to CO_2 are shown in Fig. 9. (The CO production of the arc, too, gave curves of similar character [10]). The relative magnitude of temperature and gas analytical data obtained for excitation with the two kinds of polarity changes only at higher current, each pair of curves intersecting above 10 A.

Thus, the course of all the experimental electrode temperature curves in conjunction with the changing of current follows well the curves of chemical reactions obtained by gas analytical measurements. It follows from this that chemical reactions are determined besides the reactivity of the reactants primarily by the temperature conditions of the electrode and the sample, depending on the current. There may be random fluctuations, but the two values, electrode temperature and gas production, are strictly correlated. This could be further supported by experiments in which the trend of fluctuation of CO_2 quantities, measured by gas analytical methods, and of the electrode temperature, measured simultaneously, was compared. Owing namely to the relatively large scatter of the values, each measured point of the curves re-

presents the mean value of several parallel measurements. Thus, with a mixture of 0.6 CuO mole fraction in the RW II carbon auxiliary electrode the behaviour of the two kinds of each 10 parallel values could be compared. In the fluctuation of the data of measurement, the volumetric values of CO_2 formed plotted a-

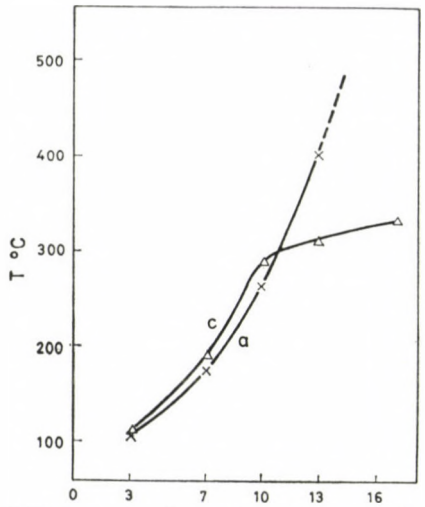

Fig. 8. Temperature of the RW O carrier electrode and current; CuO + C filling; *a:* anodic, *c:* cathodic excitation

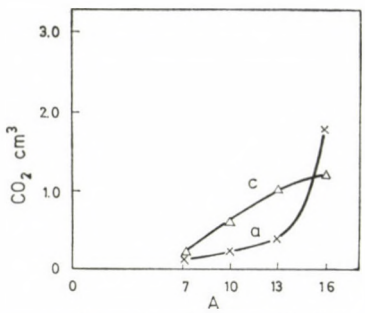

Fig. 9. CO_2 production of the arc as a function of current; RW O auxiliary electrode; CuO + C packing; *a:* anodic, *c:* cathodic excitation

gainst the simultaneously established average electrode temperature actually give a linear relationship except for some minor scatter (Fig. 10), which proved the dependence of the reactions on the temperature of the electrodes and also the reverse relationship.

It has been shown in our earlier experiments [2, 3] that a similar relationship exists also between the chemical reactions and the intensities of the spectral

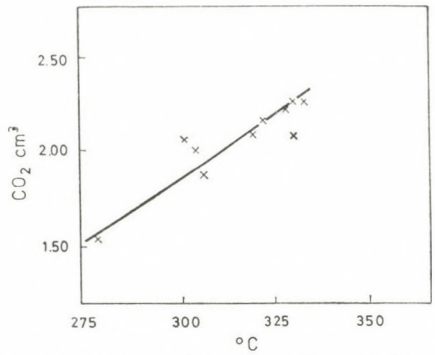

Fig. 10. Temperature of the RW II carbon electrode and the quantity of CO_2 produced; CuO + C filling; 7 A

lines obtained. It can be established thus on the basis of the triple relationship that chemical reactions, as well as their effect and the intensities of the spectral lines are controlled by the temperature conditions of the sample, which depend on the instantaneous electric parameters (current *etc.*).

REFERENCES

[1] Szabó, Z. L., Dobolyi-Fejérdy, H.: Acta Chim. Acad. Sci. Hung., **97,** 1 (1978)
[2] Szabó, Z. L., Dobolyi-Fejérdy, H.: Acta Chim. Acad. Sci. Hung., **97,** 13 (1978)
[3] Szabó, Z. L., DSbolyi-Fejérdy, H.: Acta Chim. Acad. Sci. Hung., **97,** 125 (1978)
[4] Szabó, Z. L., Dobolyi-Fejérdy, H.: Acta Chim. Acad. Sci. Hung., **97,** 137 (1978)
[5] Szabó, Z. L., Dobolyi-Fejérdy, H.: Acta Chim. Acad. Sci. Hung., **98,** 157 (1978)
[6] Szabó, Z. L., Tóth, I.: Acta Chim. (Budapest), **73,** 363 (1972)
[7] Szabó, Z. L., Dobolyi-Fejérdy, H.: Acta Chim. Acad. Sci. Hung., **96,** 201 (1978)
[8] Szabó, Z. L., Bertalan, É.: Acta Chim. Acad. Sci. Hung. (In the press)
[9] Szabó, Z. L., Dobolyi-Fejérdy, H.: Acta Chim. Acad. Sci. Hung., **97,** 111 (1978)
[10] Szabó, Z. L., Dobolyi-Fejérdy, H.: Acta Chim. Acad. Sci. Hung., **98,** 147 (1978)

Zoltán László Szabó
Éva Bertalan
H-1088 Budapest, Múzeum krt. 4/b.

Acta Chimica Academiae Scientiarum Hungaricae, Tomus 102 (4), pp. 391—400 (1979)

SOME CHEMICAL REACTIONS OF THE ELECTRODE GAP AND THEIR ROLE IN SPECTROCHEMICAL ANALYSIS, XXXV

BEHAVIOUR OF METAL OXIDES IN THE ARC. CHEMICAL REACTIONS, AVERAGE TEMPERATURE OF THE PLASMA AND ARC VOLTAGE

Z. L. SZABÓ and É. BERTALAN

(Department of Inorganic and Analytical Chemistry, Eötvös L. University, Budapest)

Received October 10, 1978

Accepted for publication February 7, 1979

Gaseous products formed in reactions within the substance of the electrode change the average temperature of the plasma and the arc voltage. Thereby, the energy conditions of the plasma are changed, and this has an effect on the intensity of the spectral lines.

It has been found in the study of the mixtures of various metal oxides with carbon powder that carbon oxides produced in the reaction with carbon powder change the composition of plasma gases [1—5], and this influences also the excitation of the spectral lines. Our aim was a further study of this effect by measuring the changes occurring in the state of the plasma. Up to now namely, our relevant conclusions were drawn only from the behaviour of the intensities of the spectral lines and of the spectral character curves. In our present work, the temperature of the plasma was measured with 1% ZnO temperature measuring additive to metal oxide and carbon powder mixtures by the usual two-line method, with the aid of the intensity ratio of the Zn I 307.6 and 307.2 nm spectral lines, and the formula

$$T = \frac{20\,510}{2.654 + \Delta Y_{307.6,\,307.2}}$$

was used for calculation. The slit of the spectrograph was directly illuminated from a distance of 330 mm. Thus, disregarding temperature distribution in the plasma, some kind of average value was obtained, the change of which was investigated as a function of the current of the arc and of the composition of the powder mixture. These values were then compared with spectral character and spectral line intensity data obtained earlier. In our other series of experiments the arc voltage has been measured with a large-screen oscilloscope, featuring a measuring net, calibrating the magnitude of the oscilloscope signals

with voltages of known magnitude. From these two kinds of measuring results conclusions were drawn on the changes in the state of the plasma produced by the chemical reactions.

1. Average temperature of the plasma

First it has been investigated whether phenomena to be studied do not change by the action of the ZnO temperature measuring additive. ZnO is namely rather volatile and might act as a carrier in the auxiliary electrode, while metallic zinc evaporating into the plasma may change the temperature of the same because of its relatively larger quantity. Table I shows for RW II

Table I

Effect of ZnO, the temperature measuring additive, on the spectrum RW II carbon carrier electrode; *a:* anodic, *c:* cathodic excitation

		Without ZnO	Whit 1% ZnO
$I_{Cu\ 282.4}$	*a*	20.6	19.3
	c	14.3	16.5
$\Delta Y_{Cu\ 237.0,\ 282.4}$	*a*	−44	−45
	c	−39	−40

carbon auxiliary electrode and a CuO and C mixture of 1 : 1 weight ratio the intensity of the Cu I 282.4 nm line and spectral characters ($\Delta Y_{Cu\ 237.0,\ 282.4}$) with and without ZnO additive. It can be seen from the results that while there is virtually no change in spectral character data, the intensity of the copper atom line is slightly decreased by the ZnO additive in anodic excitation (*a*) and slightly increased in cathodic excitation (*c*). The same was found for RW O auxiliary electrode when changing the CuO and C powder ratio. (Fig. 1; see also Fig. 3 of part XXXII [5]). However, the character of the curves and the relationship between the two kinds of excitation did not change essentially, so that the effect of the ZnO additive was not considered as essentially interfering at the given concentration.

On changing the current of the arc, the intensity values shown in Fig. 2 were obtained for the said atom line of copper with a CuO + C powder mixture of 0.6 mole fraction of metal oxide in the boring of an RW O auxiliary electrode. The spectral character data for the same cases are shown in Fig. 3. It can be seen that, similarly as earlier [5], with the better heat-conductor and therefore colder RW O auxiliary electrode of graphite basis, line intensities are higher at

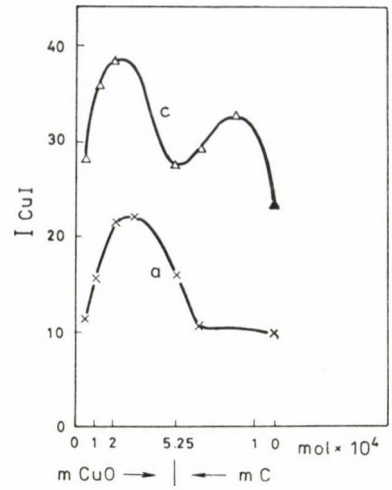

Fig. 1. Change in intensity of the Cu I 282.4 nm line as a function of the carbon powder mixture; RW O carbon carrier electrode; *a:* anodic, *c:* cathodic excitation

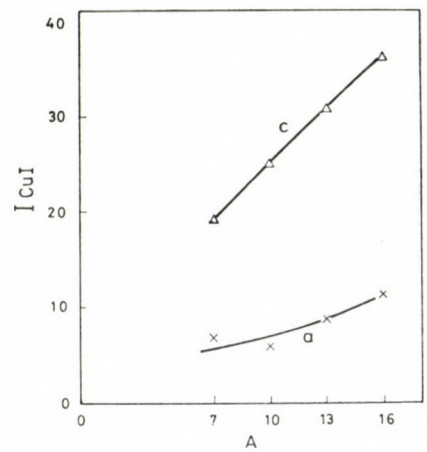

Fig. 2. Change in intensity of the Cu I 282.4 nm line with current strength; RW O carbon auxiliary electrode, *a:* anodic, *c:* cathodic excitation

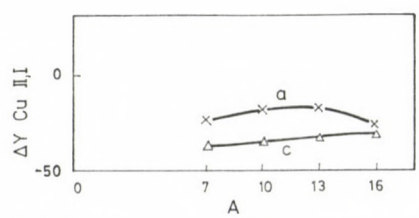

Fig. 3. Change of the spectral character data ($Y_{Cu\ 237.0,\ 282.4}$) with current; RW O carbon auxiliary electrode; *a:* anodic, *c:* cathodic excitation

cathodic excitation, because evaporation of the sample is stronger now from the burning spot of higher temperature of the arc at the cathode. Spectral character data are more diminished by the larger quantity of metal vapour evaporating into the plasma, so that in this case the spectral character curve lying higher is obtained at anodic excitation. These spectral character data scarcely change as a function of the current. At the same time, the average temperature of the plasma increases (Fig. 4), though the slope of the curves decreases. Cathodic excitation gives higher values, which is in apparent contradiction with spectral character data. To elucidate this inconsistency, the change of the relative volume of the plasma, considered of the shape of an ellipsoid body of rotation, as a function of the average current of the arc has been measured photographically and calculated from cross section and diameter data (Fig. 5). These values increase too, but result curves of steadily increasing slope, and in each case values obtained at anodic excitation are higher. It seems therefore that the effects of the changes in the two kinds of values counterbalance each other, and because of this virtually constant spectral character data are obtained. However, a problem is raised by the fact that the average

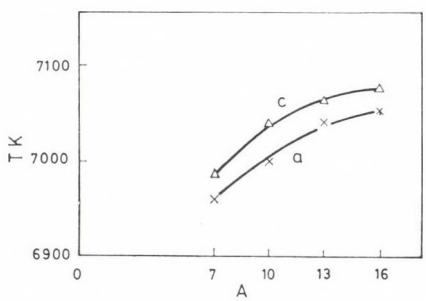

Fig. 4. Average temperature of the plasma and current; RW O carbon carrier electrode; *a:* anodic, *c:* cathodic excitation

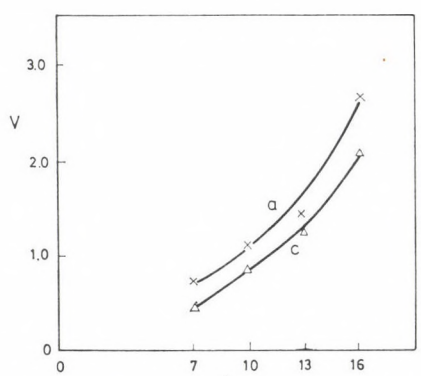

Fig. 5. Average volume of the plasma and current; RW O carbon carrier electrode; *a:* anodic, *c:* cathodic excitation

temperature of the plasma, without the consideration of its radial and axial distribution, characterizes only in a limited extent the state of the plasma, particularly in the present case, where the electron pressure of the plasma is unknown. Presumably, measurement at the zinc line gives information only on a definite zone of the plasma, and this zone is not necessarily the same in which the two lines of very different energy, measured as the spectral lines of the main component of the sample are excited. Indeed, it is well known that with other temperature measuring elements (Mg, Cd) temperature values different from those measured with zinc are obtained [6, 7]. Thus, when temperature distribution in the plasma is not taken into consideration, spectral character data may give more realistic information on plasma processes affecting the spectral lines investigated, than the average temperature of the plasma. Nevertheless, data of the latter are suitable for the characterization of changes caused by chemical reactions. This becomes evident from the pattern of temperature data measured with reactive CuO + C and slightly reacting Al_2O_3 mixtures. In the case of Al_2O_3 + C mixtures of changing ratio, values (in the RW O auxiliary electrode) change along a maximum curve (Fig. 6), starting from relatively low values, characteristic of pure carbon powder filling. Curves

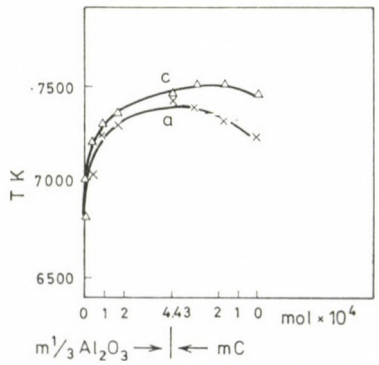

Fig. 6. Average temperature of the plasma as a function of the Al_2O_3 + C powder ratio; RW O carbon carrier electrode; *a:* anodic, *c:* cathodic excitation

obtained for excitation at the two kinds of polarities show also here with respect to each other the very opposite location and changes as compared to spectral character data (Fig. 7, $\Delta Y_{Al\,281.6,\,305.0}$). At the same time, in the case of the CuO + C mixtures, resulting a stronger reaction, the middle part of the curves is flattened (Fig. 8), the curve reveals a broad minimum. This is to be attributed in addition to an increased evaporation because of the reaction also to changes occurring in the composition of the gas atmosphere. The spectral character data of copper give similar minimum curves as the Al_2O_3 + C powder mixtures, so that these curves are not shown here.

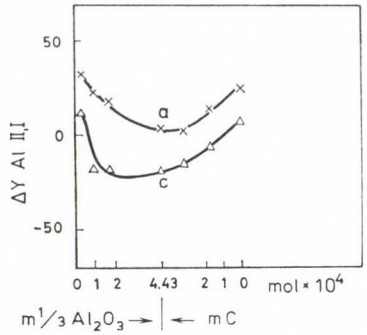

Fig. 7. Spectral character data ($\Delta Y_{\text{Al } 281.6,\ 305.0}$) and the carbon powder ratio; RW O carbon carrier electrode; *a:* anodic, *c:* cathodic excitation

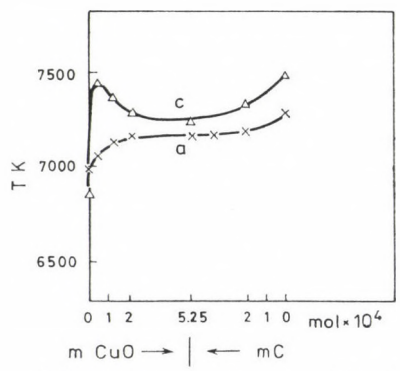

Fig. 8. Average temperature of the plasma as a function of the CuO + C powder ratio; RW O carbon carrier electrode; *a:* anodic, *c:* cathodic excitation

It has been decided to continue the investigation of these phenomena by the measurement of the arc voltage the results of which were thought to be more reliable.

2. Arc voltage and chemical reactions

As a basis of comparison, the behaviour of the arc voltage has been studied with combinations of electrode pairs made of four kinds of pure substances (C, Fe, Cu, Al) in four kinds of pure gas atmospheres (Ar, N_2, O_2 and CO_2), changing also the polarity of the electrodes. These results showed that arc voltage depends decisively and primarily on the nature of the gas atmosphere. Independent of the composition and the polarity of the electrode couple, in increasing order the following average data were obtained for arc voltage:

$$Ar < N_2 < O_2 \leqq CO_2 = 39.6,\ 42.6,\ 44.5 \text{ and } 44.4 \text{ V}$$

Measurements in conjunction with Ar + O_2 mixtures of various ratios have been reported already [8] and show that arc voltage gradually increases on passing over from the monoatomic argon to the diatomic oxygen, because the dissociation of increasing amounts of oxygen consumes increasing quantities of energy in the plasma. Thus, less energy is left for ionization, the number of conducting particles decreases in the plasma. The resistance of the arc increases, and voltage drop across the arc will be larger. This is proved also by the above data in consideration of the decreasing order of the dissociation energies of nitrogen, oxygen and carbon dioxide (9.76, 5.11 and 4.07 eV), owing to which more energy is consumed in the arc for dissociation in the above order of the gases. The arc voltage value of 44.5 V for oxygen is somewhat high, coming close to that obtained for carbon dioxide atmosphere. This can be partly attributed to the fact that the carbon electrode produces in the arc carbon dioxide, the effect of which increases the average values obtained by computation of the mean. If the carbon electrode is not included in the above averaging, 44.0 V is obtained for oxygen as the average of measurements with the other three electrodes, which fits well into the series. At the same time, for carbon dioxide only the energy of decomposition to carbon monoxide was taken into consideration in the above value. However, it is essential from the aspect of the following that in CO_2 atmosphere the arc voltage is higher by about 5 V than in pure Ar.

In Ar atmosphere, with CuO + C powder mixtures in the boring of the RW II carbon electrode, arc voltage increases with the extent of the chemical reactions. At anodic excitation (Table II), measured in the first second, when the reaction did not yet start, low arc voltage, characteristic of pure Ar was obtained. According to the curves obtained by gas analytical measurements [9], the reaction accelerates in the 4th second in anodic excitation. Values of arc voltage are also the highest at this point, particularly in the case of the mixture of 0.6 CuO mole fraction, producing the largest quantity of CO_2.

Table II

Arc voltage values in volts with changing CuO + C mixture ratios at various moments of the burning time of the arc

Ar atmosphere, anodic excitation

CuO content in mole fraction	Time of measurement, s			
	1	4	10	15
0.03	37.2	38.7	38.7	38.7
0.07	38.7	38.7	38.7	38.7
0.13	40.1	40.1	38.7	38.7
0.50	40.1	41.5	41.5	38.7
0.60	41.5	43.0	41.5	41.5
0.75	40.1	41.5	40.1	40.1
1.00	40.1	40.1	40.1	40.1

Later, when the main part of the reaction is already terminated, arc voltage values become again smaller. In cathodic excitation the electrode is colder, produces less carbon dioxide and it is heated up more slowly. The curves of gas production begin to bend upwards later, and arc voltage attains even with the mixture of 0.6 CuO mole fraction, producing the largest quantity of CO_2, only in the 10–15th second the highest value. However, this value does not attain the magnitude of the maximum value obtained with anodic excitation and more carbon oxide production (Table III).

Table III

Arc voltage values in volts with changing CuO + C ratios at various moments of the burning time of the arc

Argon atmosphere, cathodic excitation

CuO content in mole fraction	Time of measurement, s			
	1	4	10	15
0.03	38.7	38.7	38.7	38.7
0.07	38.7	40.1	40.1	38.7
0.13	38.7	38.7	38.7	38.7
0.50	38.7	38.7	40.1	40.1
0.60	38.7	40.1	**41.5**	**41.5**
0.75	40.1	40.1	40.1	40.1
1.00	38.7	38.7	38.7	38.7

The role of CO_2 produced in the reaction in the establishement of arc voltage was proved by two further series of experiments. Owing to the absence of reaction, with the carbon powder mixtures of scarcely reacting Al_2O_3, the small values characteristic of Ar atmosphere are reflected in the arc voltage values, independently of the composition of the mixture (Table IV). The situa-

Table IV

Arc voltage values in volts with changing Al_2O_3 + C mixture ratios at various moments of the burning of the arc

Argon atmosphere, anodic excitation

Al_2O_3 content in mole fraction	Time of measurements, s			
	1	4	10	15
0.03	37.2	37.2	37.2	37.2
0.07	38.7	37.2	37.2	37.2
0.10	38.7	38.7	37.2	37.2
0.50	38.7	38.7	38.7	38.7
0.60	38.7	38.7	38.7	38.7
0.75	37.2	37.2	37.2	37.2
1.00	37.2	38.7	38.7	38.7

tion is the same in cathodic excitation, so that these data are omitted here. At the same time, in CO_2 atmosphere CuO + C powder mixtures gave at anodic excitation (Table V) high arc voltage, characteristic of CO_2, which was even larger than values shown above obtained with compact, pure electrodes. This

Table V

Arc voltage values in volts with changing CuO + C mixture ratios at various moments of the burning of the arc
CO_2 atmosphere, anodic excitation

CuO content in mole fraction	Time of measurements, s			
	1	4	10	15
0.03	50.1	50.1	50.1	50.1
0.07	47.3	47.3	48.7	48.7
0.13	47.3	48.7	50.1	50.1
0.50	47.3	48.7	50.1	48.7
0.60	47.3	50.1	50.8	48.7
0.75	47.3	48.7	50.1	47.3
1.00	47.3	50.1	50.1	48.7

arc voltage scarcely depends on the composition of the mixture, because of whatever extent the CO_2 producing reaction, this does not change anymore the composition of the gas atmosphere. This is supported also by arc voltage values measured on Al_2O_3 + C powder mixtures in CO_2 atmosphere, similarly at anodic excitation (Table VI), the data agreeing well with those obtained for CuO + C powder mixtures. At cathodic excitation, too, identical values were measured with the two kinds of powder mixtures.

Table VI

Arc voltage values in volts with changing Al_2O_3 + C mixture ratios at various moments of the burning of the arc
CO_2 atmosphere, anodic excitation

Al_2O_3 content in mole fraction	Time of measurement, s			
	1	4	10	15
0.03	48.7	50.1	50.1	50.1
0.07	48.7	50.1	50.1	50.1
0.10	48.7	51.5	51.5	53.0
0.50	45.8	50.5	48.7	48.7
0.60	45.8	50.5	50.1	48.7
0.75	47.3	50.5	51.5	48.7
1.00	45.8	48.7	48.7	48.7

Thus, the above finding prove well that when the extent of the reaction is higher, gaseous reaction products formed in the reaction change the composition of the plasma gases and also the arc voltage. The energy conditions of the plasma are changed thereby, and this affects the intensity of the spectral lines. Moreover, it follows from these results that if a carbon oxide producing reaction of higher extent is to be expected, it is worth-while to use *a priori* for the equalization of the state of the plasma a CO_2 discharge gas atmosphere, or to apply pre-arcing time and wait until the major part of the reaction has taken place.

REFERENCES

[1] SZABÓ, Z. L., DOBOLYI-FEJÉRDY, H.: Acta Chim. Acad. Sci. Hung., **97**, 1 (1978)
[2] SZABÓ, Z. L., DOBOLYI-FEJÉRDY, H.: Acta Chim. Acad. Sci. Hung., **97**, 13 (1978)
[3] SZABÓ, Z. L., DOBOLYI-FEJÉRDY, H.: Acta Chim. Acad. Sci. Hung., **97**, 125 (1978)
[4] SZABÓ, Z. L., DOBOLYI-FEJÉRDY, H.: Acta Chim. Acad. Sci. Hung., **97**, 134 (1978)
[5] SZABÓ, Z. L., DOBOLYI-FEJÉRDY, H.: Acta Chim. Acad. Sci. Hung., **98**, 157 (1978)
[6] KRASKOVSKÁ, E.: Zbornyik ved prác VST. Kosice (in print)
[7] URHEGYI-VANYEK, M.: C. Sc. Thesis, Budapest 1975
[8] SZABÓ, Z. L., PÖPPL, L.: Acta Chim. (Budapest), **79**, 237 (1973)
[9] SZABÓ, Z. L., DOBOLYI-FEJÉRDY, H.: Acta Chim. Acad. Sci. Hung., **97**, 111 (1978)

Zoltán László SZABÓ
Éva BERTALAN
H-1088 Budapest, Múzeum krt. 4/b.

Acta Chimica Academiae Scientiarum Hungaricae, Tomus 102 (4), pp. 401—412 (1979)

CONDUCTIVITY OF RATHER CONCENTRATED ELECTROLYTE SOLUTIONS AT CONSTANT CATION (ANION) CONCENTRATION — THE APPLICABILITY OF CONDUCTOMETRY IN COORDINATION CHEMISTRY

M. PÁLFALVI-RÓZSAHEGYI, Á. BUVÁRI, L. BARCZA and Z. G. SZABÓ

(Institute of Inorganic and Analytical Chemistry, Eötvös L. University, Budapest)

Received October 16, 1978

Accepted for publication February 7, 1979

Conductivity of many (more or less simple) electrolyte mixtures has been investigated, where the concentration of one of the ions (in most cases that of the cation) and the temperature have been kept constant.

It could be pointed out that deviations exist from an assumed additivity nearly in every case, but their maxima are rather low: *e.g.* the average of differences in 5*M* solutions amounts only 2.8%. The deviations depend on temperature and total concentration, but they are not a function of ionic strength. In simplest cases these differences are not significant, which allow to draw conclusions for the stability of new species in other system when the difference is high enough.

It seems that the deviations from additivity in solutions of constant cation (anion) concentration can be explained neither by electrostatic principles nor by ion pair formation alone, but special interactions must also be taken into account. As a working hypothesis, hydrogen bridged association of hydrated anions was supposed.

Conductometry is one of the oldest methods in coordination chemistry but its use for quantitative purposes gives some problems [1]. In spite of this, as the conductivity is influenced by the whole structure of the solution, conductometry is one of the most important methods for studying the structure of electrolyte solutions [2, 7—9].

For interpreting the observed phenomena, for the possible structures of diluted and concentrated electrolyte solutions, several theoretical, semi-empirical and fully empirical relations are known [2—6 and references therein] but it becomes evident that the problems to be solved increase with increasing concentration in more and more complex and individual ways.

It follows that no conclusion can be drawn for the conductivity of a mixture of two solutions (even if they contain the same electrolyte) from the individual conductivities of the base solutions. The reason that the conductivity measurements are less important for the investigation of equilibria in coordination chemistry lies first of all in this fact. There are problems also with stable complexes (where the conductivities could be measured in very diluted solutions) as no neutral salt can be added to achieve a constant ionic strength, because the conductivity change due to the complex formation would be in-

significant in this case. But the possibility is open for the investigation of complexes with low stability, only we ought to know the conductivity behaviour of rather concentrated simple electrolyte mixtures, where no interactions can be supposed.

Our following discussion will be limited to conductivities of electrolyte mixtures at constant ionic strength, that is where:

$$c_M = \Sigma c_i = \text{const.} \tag{1}$$

(dealing only with 1 : 1 electrolytes at the beginning); or even the condition can be postulated that one of the ions in all electrolytes (the anion or the cation) must be common.

At constant total concentration, taking some neglections and conditions into consideration, the following additivity of conductivities can be supposed:

$$\varkappa_M = \Sigma \lambda_i c_i \tag{2}$$

that is, in the simplest (and to a certain extent: idealized) cases, the additivity problem of conductivities arises as a question of constancy of equivalent conductivities.

There are known some examples indicating the additivity of the conductivities at constant total concentration and with one common ion, and in several other mixtures (but without common ion) the maxima of the deviations from Eq. (2) ($\Delta\varkappa_{1/2}$, measured at $c_1 = c_2 = c_M/2 = 0.5M$) can be characterized with good approximation by the following empirical relationship [8]:

$$\Delta\varkappa_{1/2} = |0.021(\lambda_A - \lambda_B)| \tag{3}$$

This also means that even in relatively concentrated $1M$ solutions the estimated error caused by the deviation from the law of additivity is about 1% or less (except some extreme cases).

Our aim was to investigate the conductivities of several simple (or supposedly simple) electrolyte mixtures and to answer the following questions:

a) how large are the deviations from the additivities;

b) in what degree are they influenced by the total concentration;

c) what is the effect of changes in ionic strength or in temperature;

d) what is the direction of deviations;

e) can anomalies be detected in conductivities when the interaction between the components is a well-known fact;

f) are deviations shown by changes of other parameters similar to those of conductivity changes?

Change of the conductivity of mixtures as a function of the changes in ions

Solutions of 5.000*M* concentration have been prepared at 25.00 °C from the following substances of analytical grade (and controlled) purity: $NaClO_4$, $NaNO_3$, NaOH, NaCl, NaBr and NaI. The conductivities of the solutions and their mixtures have been measured using a Radiometer CDM2 Conductometer and Radiometer CDC 104 electrode in a vessel thermostated to 25.00 $\pm$ 0.02 °C.

As typical results, the conductivity changes of sodium perchlorate — sodium halide mixtures are shown in Fig. 1. In Fig. 2, the enlarged percental deviations from Eq. (2) are presented. The results indicate obvious (although not significant) deviations and suggest the possibility of an empirical approxima-

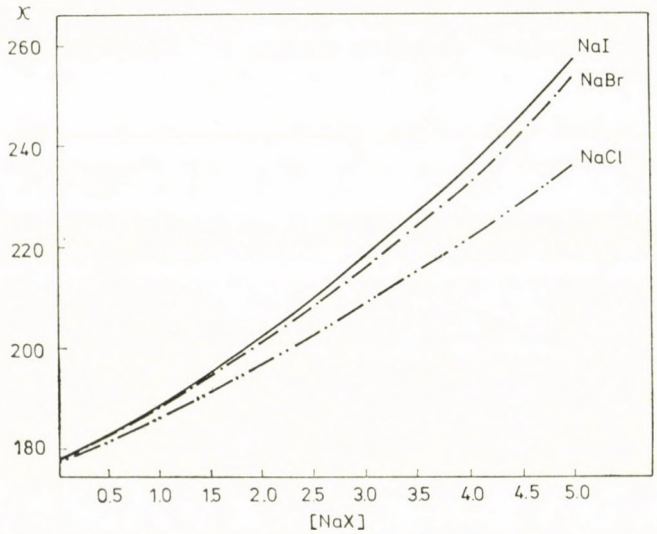

Fig. 1. Conductivities of 5 *M* sodium perchlorate — sodium halide mixtures in function of halide concentration ($\varkappa$ in 1000 $ohm^{-1}cm^{-1}$)

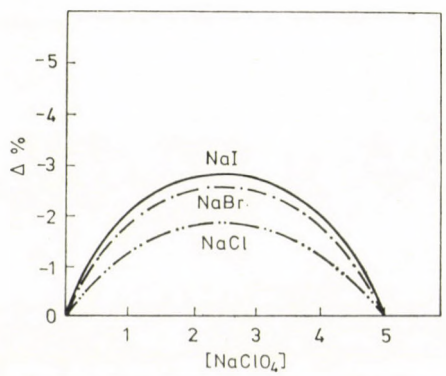

Fig. 2. Deviations from the supposed additivity in 5 *M* $Na(ClO_4, X)$ solutions

tion according to Eq. (3)(but with a larger constant). Except the solutions containing sodium hydroxide, negative deviations of similar type and direction have been found in all cases.

The sequence of effects is reversed when the conductivities of sodium hydroxide — sodium halide mixtures are investigated (see Figs 3 and 4). The highest difference exists between the equivalent conductivities of 5*M* NaOH and NaCl and the lowest between those of NaOH and NaI, but the deviation from additivity is considerably higher in the latter case.

Figures 3 and 4 show the conductivity changes of $NaOH—NaNO_3$ mixtures, too, as a single case observed by us where the conductivity deviated in positive direction from additivity.

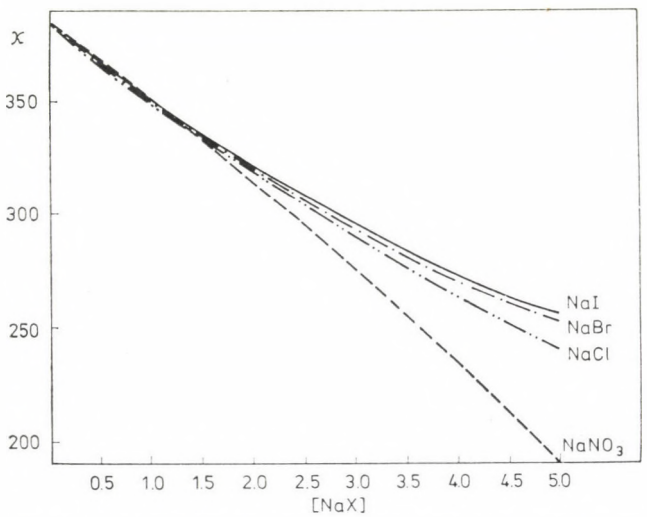

Fig. 3. Conductivities of 5 *M* sodium hydroxide — sodium halide (and nitrate) solutions at 25.00 °C (in 1000 $ohm^{-1}cm^{-1}$)

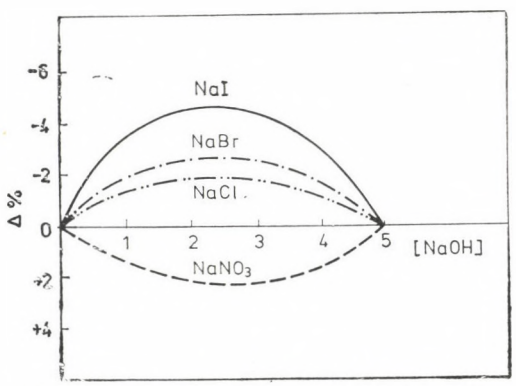

Fig. 4. Deviation of conductivities (in %) from additivity in 5 *M* Na(OH, I), Na(OH, Br), Na(OH, Cl) and Na(OH, NO_3) solutions

Figure 5 presents the phenomena observed in 5*M* NaI—KI solutions, the expectable deviation according to Eq. (3) is shown by dotted line. (A constant of 0.084 was used as an average of all differences from additivities excepting the data of system containing sodium hydroxide.)

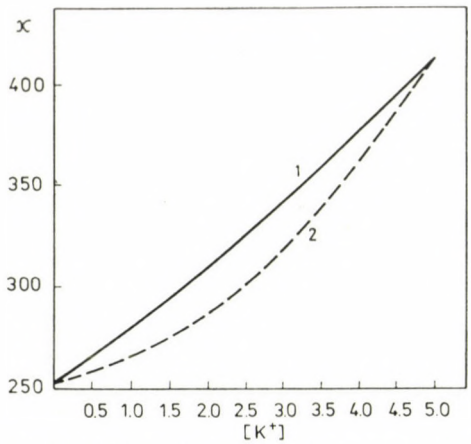

Fig. 5. The conductivity of 5 *M* (Na, K)I solutions (1: measured; 2: calculated using Eq. 5 with a constant of 0.084)

Our investigations carried out so far clearly indicate that in concentrated 5*M* solutions

a) deviations from additivity can always be observed;

b) the differences are not too significant: the mean value of the studied 17 systems is 2.86%;

c) there are, however, typical deviations from this average referring to special interactions;

d) a relationship of type 3 is at best of an informative character;

e) most of the deviations (16 out of 17) point to negative direction;

f) the differences at the simplest systems are not too significant: a conclusion can be allowed for the stability of new species in the case of high(er) deviations.

Effect of the total concentration and the temperature

As a model, the $NaClO_4$—NaOH system was employed: 2.000, 4.000 and 6.000*M* solutions were prepared at 25.00 °C (in some cases at 15 and 35 °C) and the conductivities of the mixtures were measured at the given temperature and at constant sodium ion concentrations.

As before, the highest deviations were observed in 1 : 1 mixtures: at 25.00 °C −4.1% in 6*M*; −1.6% in 4*M* and −0.6% in 2*M* solutions. In solutions of 2 and 4*M* sodium ion concentrations and at 35.00 ± 0.02 °C, the conductivities were additive within the error of the measurement according to Eq. (2) and even in 6*M* solution the deviation was only −1.8% at the same temperature.

At 15.00 ± 0.02 °C the deviations from additivities increase to a significant extent: in case of 2*M* total concentration it was −1.4%, at 4 *M* about 3.0%.

Without drawing final conclusions from the results, the followings can be summarized (supported also by some further measurements):

a) the deviation from additivity is significantly affected by the total concentration. (This was already indicated by the lower 0.021 coefficient in Eq. (3) relating to more diluted 1*M* solutions and by the 0.084 average for 5*M* solutions);

b) the effect of the temperature is very explicit and refers to special interactions depending primarily on temperature.

Effect of changes in ionic strength

All of the mentioned investigations have been performed with 1 : 1 electrolytes and their mixtures, that is the constant total concentration meant constant ionic strength, too. It might be assumed that the observed phenomena at different total concentrations are caused by the change of ionic strength and the consequence thereof. However, systems, where a monovalent anion is continuously substituted by a bivalent or even trivalent anion (but the concentration of the cation is kept constant), seem to be better for studying the effect of ionic strength.

The first system investigated at 25.00 ± 0.02 °C was 2.000*M* NaOH and 1.000*M* Na_2SO_4. When these solutions were mixed, the concentration of sodium ions was 2.000*M* but the ionic strength changed by 50%. In addition, a rather big difference exists between the equivalent conductivities of the two electrolytes, therefore (according to Eq. (3) a significant deviation from additivity could be expected.

In spite of this, the measurements have shown that even the maximum of the deviations lies at the limit of measurement errors: in this system the conductivities are practically additive.

Next we investigated the following systems (in solutions at constant 5*M* potassium ion concentrations) at 25.00 °C: KI—K_2CO_3; KOH—K_2CO_3; KI—K_3PO_4 and KOH—K_3PO_4. (In the first cases the ionic strengths changed by 50%, in the second ones by 100%.) Although significant negative deviations

could be observed in conductivities from the additivities, their sizes were below those calculated on the basis of (modified) Eq. (3), and their sequence was reversed in mixtures containing potassium hydroxide (similar to the mentioned systems contained sodium hydroxide).

The surprising results can be summarized as follows:

a) not the ionic strength but the constant cation concentration plays the main role* (if there is an anion–anion exchange),

b) both the earlier conclusions and these experimental facts point to the importance of special interactions.

Both conclusions are supported also by the following experiment: a series of solutions was prepared at 25 °C, where the sodium hydroxide concentration was 3.000*M*, while the ionic strength was continuously varied from 5.000 to 6.000 using sodium perchlorate. The change in ionic strength was only 20% (like to the concentration of the cation) but the conductivity decreased by 15.3%. (In other words: the conductivities of solutions with higher total concentrations and higher ion contents are lower than those of lower total concentrations but with the same sodium hydroxide content.)

The effect of mercury(II) chloride on the conductivity of sodium chloride solution

It is well known that mercury(II) ions form stable complexes with chloride ions. The stability of $HgCl_2$ is big enough [11] that in the presence of chloride excess the dissociation of mercury(II) chloride can be neglected. In this case, even the formation of mixed hydroxo complexes, *i.e.* the hydrolysis of mercury(II) ions may also be neglected [11]. In spite of these, the formation constants of trichloro-mercurate(II) and tetrachloro-mercurate(II) species are in the order of magnitude that their influence on conductivity can be expected just in more concentrated solutions. The formation of these species has been studied by many authors and by several methods [11], and the results obtained at 25 °C are in good agreement with each other: the log K_3 values vary from 0.75 to 0.95; the lg K_3K_4 values from 1.85 to 2.13.

Independently from these well-known facts, the conductivities of sodium chloride-mercury(II) chloride solutions might previously be assumed in different ways:

a) Assuming that $HgCl_2$ is a regular electrolyte, higher conductivities migth be expected in mixtures containing mercury(II) chloride than in solutions with the same sodium chloride concentration.

* Similar to the Olson—Simonson effect, which can be noticed in the case of some reactions [10]

b) Knowing the fact that $HgCl_2$ practically does not dissociate and disregarding other interactions, it might be expected that the conductivities of sodium chloride solutions are unaffected by mercury(II) chloride.

c) Considering further associations and assuming that the equivalent conductivities of mercury(II) chloro complexes differ from that of chloride (they have lower values), a decrease in conductivities of sodium chloride solutions might be expected in function of the mercury(II) chloride concentration.

The measured data (Fig. 6) (at 25.00 °C and at constant, 1.000*M* sodium chloride concentration) prove the expected assumption *c*, as the conductivity

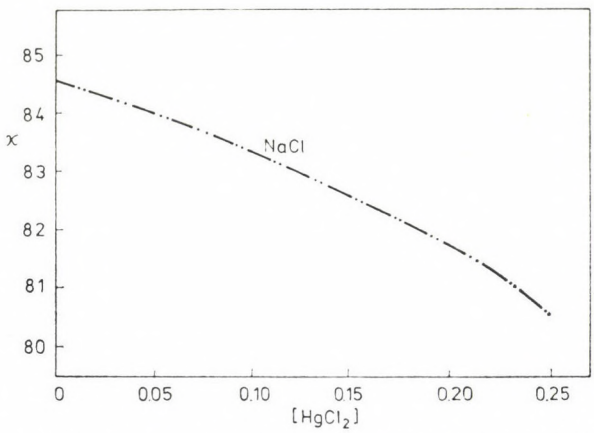

Fig. 6. The influence of mercuric chloride on the conductivity of 1.000 *M* NaCl solution

decreases continuously with increasing mercury(II) chloride concentration but not linearly. It can be understood if we assume the validity of Eq. (2) in a concrete form:

$$\varkappa = \lambda_{Na^+}[Na^+] + \lambda_{Cl^-}[Cl^-] + \lambda_{HgCl_3^-}[HgCl_3^-] + \lambda_{HgCl_4^{2-}}[HgCl_4^{2-}] \qquad (4)$$

and consider the expressions of total concentrations:

$$[Cl^-]_T = [Cl^-] + [HgCl_3^-] + 2\,[HgCl_4^{2-}] \qquad (5)$$

$$[HgCl_2]_T = [HgCl_2] + [HgCl_3^-] + [HgCl_4^{2-}] \qquad (6)$$

Equation 4 can be rewritten using the formation constants

$$K_3 = \frac{[HgCl_3^-]}{[HgCl_2][Cl^-]} \text{ and } K_3K_4 = \frac{[HgCl_4^{2-}]}{[HgCl_2][Cl^-]^2}$$

as

$$\varkappa = \lambda_{Na^+}[Na^+] + \lambda_{Cl^-}[Cl^-] + \lambda_{HgCl_3^-}K_3[HgCl_2][Cl^-] + \\ + \lambda_{HgCl_4^{2-}}K_3K_4[HgCl_2][Cl^-]^2 \quad (7)$$

If the assumptions (first of all that the equivalent conductivities are constant at constant cation concentration) are valid, curve 6 can unambiguously described using Eqs (5—7) and some constants defined in them. In other words, the equilibrium constants (together with the mentioned λ values) can be calculated directly. As a result of (rather simple) computer calculations, we obtained the following constants: $\lg K_3 = 0.90 \pm 0.06$ and $\lg K_3K_4 = 1.99 \pm 0.08$. These constants are suitable for the clear description of the measured conductivities and fit well to those given in literature.

The good agreement of measured and calculated data (see Fig. 6) proves the validity of additivity and constancy of equivalent conductivities [(Eqs 2, 7)] in solutions at constant ionic concentrations and gives a precise interpretation for the "negative" equivalent conductivities obtained by the rough approximation of *a* and *b*.

Relations between viscosity (and density) and conductivity

To characterize the relationship between conductivities and viscosities of solutions containing a given substance in different solvents, WALDEN's rule [12] can be employed:

$$\lambda^0\eta^0 = \text{const.} \quad (8)$$

This equation is often used for comparing the viscosities and conductivities of the given substance at different concentrations but in the same solvent (of course in a sense dissimilar to Eq. (8)).

For studying this relation, again the $NaClO_4$—NaOH model was chosen and both the changes in viscosities and conductivities have been investigated (in addition to those in densities) in solutions of constant cation concentration. The densities were measured by pycnometer method, the viscosities in an Ostwald viscosimeter made of resistant glass and having a capillary diameter of 0.8 mm. (The flowtime of solutions varied from 60 to 150 second. The temperature was kept constant with an accuracy of ± 0.02 °C.)

As a typical result we present the conductivity, viscosity and density data of 6*M* $NaClO_4$—NaOH system at 25 °C in Fig. 7. The highest regularity can be observed in density changes: the density depends linearly on the concentration of one of the anions within the limits of measuring errors, *i.e.* the additivity of the densities seems to be valid at constant cation concentration in this system. It can also mean that the hydrations which affect mainly the

densities do not change or change only slightly during mixing: or the quality of possible interactions is not significantly different from those existing in base electrolytes.

Since the direction of changes is the same in the values of conductivities and viscosities, it is obvious that Eq.(8)is unsuitable even for the approximate description of the phenomena. It is more interesting that a deviation from additivity can be observed on the viscosity curve, which has the same character and magnitude as that of the conductivity curve. Thus the product of viscosities and conductivities is not only unsteady but also fails to be in direct

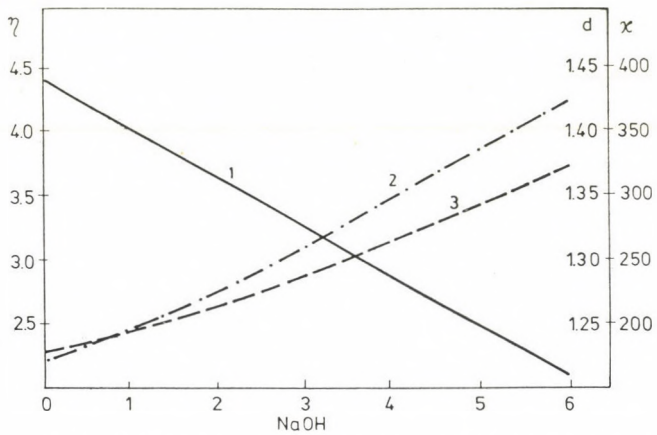

Fig. 7. The change of conductivity, viscosity and density in 6 *M* Na(OH, ClO_4) mixtures at 25.00 °C (1: density, in g cm^{-3}; 2: conductivity, in 1000 $ohm^{-1}cm^{-1}$; 3: viscosity, in cP)

proportion to one of the anion concentrations: in 1 : 1 mixture a definite maximum deviation can be seen.

The change of viscosity can not be attributed to the individual species, it reflects in every case the structure of the solution: the distortion of water polymers, the competing hydrations of ions [13] and the formation of heteroconjugates, too. A relationship like Eq.(2)is possible only formally and only with the approximation that each component contributes to the build-up of the structure linearly with its concentration.

As it had to be expected the structure and also the viscosity of the solutions are more expressively affected by sodium hydroxide than by sodium perchlorate. This is indicated by the well-known fact, too, that the viscosity of sodium hydroxide solutions increases faster with increasing concentrations than that of solutions containing sodium perchlorate.

Comparing these facts with the measured results the assumption that deviations are caused by the change in degree of ion-pair formation becomes

very doubtful. If the phenomena would indeed be caused by this, the deviations ought to have different signs. (If the decreased "dissociation" of sodium hydroxi dewould be coordinated to the apparent minimum of conductivity it would lead to the deduction that an apparent viscosity maximum has to appear at the same place.)

All these suggest (comparing them with data proving the monotonous change of densities and assumptions made them probable) that an interaction of other type than cation–anion pairing is responsible for the deviations. In our opinion all anomalies can be solved if we assume that less stable hydrogen bridged anion–anion complexes might be formed between the hydrated anions. As a very rough approximation, we may assume *e.g.* the formation of a complex between the slightly hydrated perchlorate and the strongly hydrated hydroxide ions in a following or a similar form:

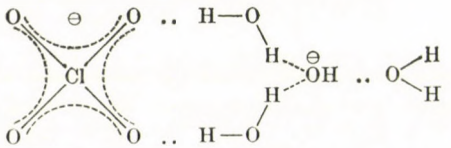

(9)

This picture is well supported by our results discussed earlier about the effect of changes in total concentration and temperature. When the total concentration is lower, (relatively) more water molecules are available for the hydrogen bridged hydrations of anions, thus the formation of the assumed complex is hindered by competing reactions, that is no anomalous behavior exists. The increase of temperature has a similar effect: the apparent minima of conductivities observed at lower temperature disappear because of the breaking of hydrogen bonds.

(It is to be mentioned here that viscosities have been studied at several total concentrations and at various temperatures. In all cases the relation shown in Fig. 7 was determined, and viscosity minima have been measured in such $NaClO_4$—NaOH systems where the conductivities already seemed to be additive within the limits of measurement errors.)

Based on the developed model and using equations like (5—7), we tried to evaluate the conductivity data of solutions with constant $6M$ sodium ion concentration at 25.00 °C. We found that Curve 7 can exactly be described when the formation constant of perchlorate — hydroxide complex is given as

$$K = 0.038 \pm 0.004$$

We must be fully aware of the fact that this is merely an apparent constant since it comprises all hitherto unknown constants referring to the structure (hydration, ion-pair formation, *etc.*) of $6M$ solutions.

REFERENCES

[1] BECK, M. T.: Chemistry of Complex Equilibria, Akadémiai Kiadó, Budapest — Van Nostrand Reinhold Co., London 1970
[2] ERDEY-GRÚZ, T.: Transport Phenomena in Aqueous Solutions, Akadémiai Kiadó, Budapest 1974
[3] ROBINSON, P. A., STOKES, R. H.: Electrolyte Solutions, Butterworths, London 1970
[4] HARNED, H. S., ROBINSON, R. A.: Multicomponent Electrolyte Solutions, Pergamon Press, London 1968
[5] FUOSS, R. M., ACCASCINA, F.: Electrolytic Conductance, Interscience, New York 1959
[6] FUOSS, R. M.: J. Phys. Chem., **79,** 525, 1983 (1975); **80,** 2091 (1976)
[7] BERECZ, E.: Acta Chim. (Budapest), **79,** 81 (1973); **87,** 353, 371 (1975)
[8] DAVIES, C. W.: Ion Association, Butterworths, London 1962
[9] SCHIAVO, S., MARROSU, G.: Z. phys. Chem. N. F., **105,** 157 (1977)
[10] SCHWETLICK, K.: Kinetische Methoden zur Untersuchung von Reaktionsmechanismen, Deutsche Verl. der Wissenschaften, Berlin 1971
[11] SILLÉN, L. G., MARTELL, A. E. (eds): Stability Constants, The Chemical Society, London 1964 and 1971
[12] WALDEN, P., ULRICH, H., BUSCH, C.: Z. phys. Chem., **123,** 429 (1926)
[13] WANG, J. H.: J. Phys. Chem., **58,** 686 (1954)

Márta PÁLFALVI-RÓZSAHEGYI
Ágnes BUVÁRI
Lajos BARCZA
Zoltán G. SZABÓ

H-1443 Budapest, B. O. Box 123.

Acta Chimica Academiae Scientiarum Hungaricae, Tomus 102 (4), pp. 413—421 (1979)

CARBON-13 DYNAMIC NMR STUDY OF ROTATIONAL BARRIERS OF THE AMIDE BOND IN GLYCINE ESTER DERIVATIVES*

G. SZALONTAI and A. VASS

(Research Institute for Heavy Chemical Industries, Veszprém)

Received December 13, 1978

Accepted for publication February 13, 1979

The rotational barriers of the amide bond between the two rotamers present in liquid phase were studied in 16 glycine ester derivatives. The steric, electron-withdrawing and conjugative effects of substituents on the amide bond rotation were investigated. Rate constants of the dynamic exchange between rotameric forms A and B were calculated from the complete line-shape analysis of NMR spectra. The free energies of activation, ΔG^{+}_{AB}, obtained by means of the Eyring equation are also given.

Introduction

The partial double bond character of the amide carbon—nitrogen bond was one of the first problems studied by dynamic NMR spectroscopy. Although the majority of temperature dependent NMR studies carried out so far used the proton, this nucleus suffers from deficiencies [1]. The use of the carbon-13 nucleus in studying the rotational behaviour of the amide bond was first reported by GANSOW and his co-workers [2].

In previous papers [3—7] the effect of substituents R_1, R_2 and R_3 on the stability of the ground and transition states (see below) were reported.

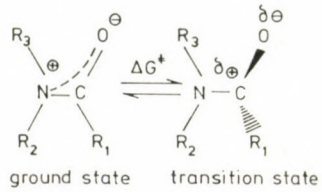

The effects of substituent electronegativity and bulk, conjugation ability and steric properties on rotational barriers have been studied.

In this work we present results concerned with substituent effects and their relative importance in the case of monochloro- and dichloroacetyl glycine ethyl ester derivatives **I—XVI.**

* Presented in part at EUROANALYSIS III, Dublin, August 20—26, 1978

Compounds **I—X** (monochloroacetyl derivatives) and **XI—XVI** (dichloroacetyl derivatives) can be characterized with the following formulas:

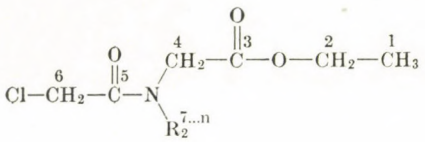

I—X

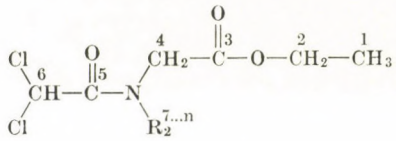

XI—XVI

(for R_2, see Table I)

Experimental

The ^{13}C spectra were obtained at 20 MHz on a Varian CFT-20 spectrometer, pulsing was carried out by locking on the deuterium signal of the solvents, 8 mm spinning tubes were used and all spectra were proton broad-band decoupled. Normally 8192 data points were used in the interferogram and spectral widths of 4000 Hz were employed, therefore, the digital resolution limit was 0.98 Hz.

Spectra were recorded for solutions in $CDCl_3$, CD_3COCD_3 or in dioxane-d_6, depending on the solubility and probe temperature. The probe temperatures were controlled by a Varian Variable Temperature Controller Accessory with an accuracy of ± 1.5 °C.

Samples. Compounds **I—XVI** are chemically new, biologically active materials. They were synthesized according to known procedures for preparing *N*-alkyl and *N*-acylamino esters [8]. The raw materials obtained were purified on alumina columns with an activity grade IV according Brockman.

Results and Discussion

Analysis of conformers

The NMR spectral data of compounds **I—XVI** are presented in Table I. The assignments of spectral lines are based mainly on chemical shift data but in a few cases the off-resonance spectra were also recorded. In order to permit unambiguous assignment of C-3 and C-5 carbons, we compared the chemical shifts of the two carbonyl groups in the derivatives with $R_1 = CH_2Cl$, $R_1 = CHCl_2$, and $R_1 = CCl_3$ [9]. A diamagnetic shielding was expected for the carbonyl which has adjacent chlorine atoms as the number of the latter increases, the higher field carbonyl line showed this behaviour, indicating that this line belongs to C-5.

In the liquid phase at ambient temperatures two rotamers of compounds **I—VIII** and **XI—XV** were observed according to their spectra. The structures of rotamers A and B were assumed to be the following.

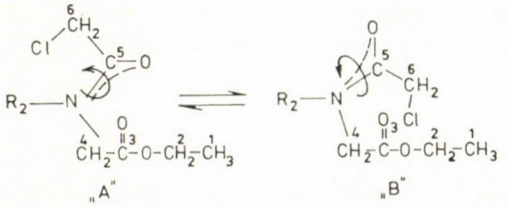

Fig. 1. Assumed conformations of rotamers A and B

At ambient temperature most of the lines split according to the different magnetic environments existing in conformers A and B, but the C-1 methyl carbons remain unaffected, showing a sharp singlet. A straightforward explanation of this phenomenon may be that these are far from the amide bond and rotate freely.

At the same time an irregular behaviour of C-3 carbonyl lines has been observed (see Table I). In compounds **I**, **III**, **V**, **VI**, **VII**, **XI**, **XIII** and **XV** they appeared as single, sharp lines but in compounds **II**, **IV**, **XII** and **XIV**, where R_2 was a *sec*-butyl or isopropyl group, they showed the same splitting as most of the remaining carbons of the molecules. One possible explanation of this unexpected behaviour is that the C-3 carbonyl groups are normally out of the rotation space of the amide bond (2a), thereby their magnetic environment remains unaffected, but this situation changes in the presence of sterically crowded groups such as *sec*-butyl or isopropyl groups. In these cases, probably the carbony groups are forced into the rotation space (Fig. 2b).

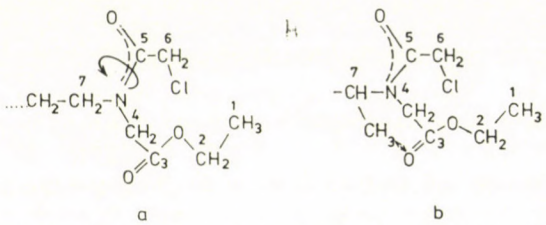

Fig. 2. Steric effects of substituents R_2 on the C-3 carbonyl group: (a) with no steric interaction, (b) with steric interaction

In accordance with the above observation, an increased rotational barrier was expected in the *sec*-butyl and isopropyl derivatives.

A few other carbons of R_2 substituents show a similar behaviour to the C-1 methyl carbons but they are also far enough from the amide group to remain unaffected.

The assignment of conformers A and B is based on the observed diamagnetic shielding caused by the sterically close groups. According to the chemical

Table I

Chemical shift data of compounds **I**—**XVI** *at ambient temperature*

Compound	$R_x(7...n)$		C-1	C-2	C-3
I	$-{}^{7}CH_2-{}^{8}CH_2-{}^{9}CH_2-{}^{10}CH_3$	A B	14.4	61.1 61.9	169.3 170.0
II	$-{}^{7}CH(-{}^{10}CH_3)-{}^{8}CH_2-{}^{9}CH_3$	A B	14.3	60.9* 61.9	169.4 170.7
III	$-{}^{7}CH_2-{}^{8}CH_2-{}^{9}CH_3$	A B	14.4	60.2* 61.9	169.4 170.6
IV	$-{}^{7}CH({}^{8}CH_3)_2$	A B	14.4	61.0 61.9	169.6 170.0
V	$-{}^{7}CH_2-{}^{8}CH_2-{}^{9}CH_2-O-{}^{10}CH_3$	A B	14.3	61.2* 61.9	169.4 170.0
VI	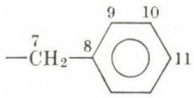	A B	14.2	61.2* 61.8	169.0 169.4
VII	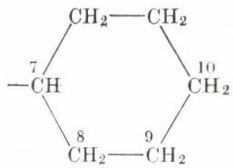	A B	14.4	61.0* 62.0	169.5 170.8
VIII	$-{}^{7}C({}^{8}CH_3)_3$**	A B	14.3	61.8	170.9
IX	$-{}^{7}C({}^{8}CH_3)_2-{}^{9}CO-{}^{10}CH_3$**	A B	14.4	61.8	171.1
X	2.6** diethyl phenyl	A B	14.3	61.2	168.0
					Dichloroacetyl derivatives
XI	$-{}^{7}CH_2-{}^{8}CH_2-{}^{9}CH_2-{}^{10}CH_3$	A B	14.2	61.2 61.9	168.0 169.2
XII	$-{}^{7}CH(-{}^{8}CH_3)-{}^{9}CH_2-{}^{10}CH_3$	A B	14.2	61.0 62.1	168.6 169.9
XIII	$-{}^{7}CH_2-{}^{8}CH_2-{}^{9}CH_3$	A B	14.3	61.2* 61.1	168.6 169.2
XIV	$-{}^{7}CH({}^{8}CH_3)_2$	A B	14.2	61.1 62.0	166.8 170.0
XV	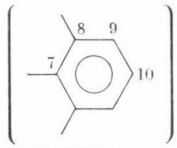	A B	14.0	61.2* 61.7	168.2 168.4
XVI	$-{}^{7}C({}^{8}CH_3)_3$**	A B	14.2	60.8	169.5

* Lines used for the line-shape analysis
** Only one rotamer present

(relative to TMS ppm) Monochloroacetyl derivatives ($R_1 = CH_2Cl$)

C-4	C-5	C-6	C-7	C-8	C-9	C-10	C-11
49.7 50.1	166.9	41.8 42.3	48.5 47.9	31.3 29.8	20.4	14.0	—
43.4 44.9	166.2 167.3	42.1 42.9	55.6 52.3	29.8 27.3	11.2	19.0 17.6	—
48.4 49.9	167.0	41.8 42.4	51.4 50.1	22.3 20.9	11.2 11.3	—	—
43.1 44.8	166.4 166.6	42.1 43.1	49.6 46.7	20.9* 19.6	—	—	—
48.5 50.5	167.3	41.5 42.2	46.7 46.1	28.8 27.8	69.3 70.3	58.5	—
48.1 49.3	167.5	42.0 42.2	52.8 50.7	136.8 137.2	128.9 129.4	128.5 128.3	128.3
44.1 45.7	166.6	42.2 43.2	57.9 54.8	31.8	26.2	25.7	—
47.9	167.5	44.5	58.7	28.2	—	—	—
51.2	167.5	42.5	59.4	27.0	44.6	207.1	31.0
52.8	167.0	41.6	137.0	130.0	127.8	142.8	

($R_2 = CHCl_2$)

49.8	164.2	65.2 65.9	49.0	31.0* 29.3	20.1	13.7	
44.0 45.0	163.9 164.8	65.8 66.3	55.5 53.7	18.5* 17.4	28.0 27.1	10.9	
49.1 50.0	164.4	65.2 65.9	51.5 50.8	22.1 20.6	11.1		
43.9 45.0	164.3 164.9	66.1	49.6 48.2	19.4* 19.8	—	—	—
48.4 48.9	164.6	65.2 65.6	52.7 51.3	135.5 136.0	128.2 128.0	129.0	
47.0	163.2	66.7	58.9	27.6	—	—	

shift data for conformers A (which represents the more stable form) the monochloroacetyl group is close to the R_1 chain as carbons C-1. . . C-6 are diamagnetically shielded and carbons C-7. . .C-*n* have small paramagnetic shielding compared to the same carbons of conformers B (for details, see Table I). Consequently, in conformers B the mono- or dichloroacetyl group is close to the R_2 substituent. The population of the more stable conformer A varies between 55 and 75% in compounds **I**—**VII** and **XI**—**XV** (see the ΔG°_{AB} values in Table II).

In compounds **VIII**—**X** and **XVI**, where R_2 is a *t*-butyl or a 2,6-diethylphenyl or a $C(CH_3)_2CH_2COCH_3$ group, only one conformer can be observed. Spectra obtained from high temperature experiments ($T = 135$ °C) show similar features, therefore, we assume that, due to strong steric hindrance, the carbon—nitrogen bond does not rotate, and only one conformer formed in the chemical reaction exists. In compounds **VIII**—**IX** the similarity of chemical shifts to those compounds **I**—**VII** suggests that in these cases the conformation is probably of the B form. In compounds **X** and **XVI** the chemical shifts do not confirm this assumption.

Calculation of the rate constants, k'_{AB}, and activation parameters (ΔG^{+}_{AB} and ΔG°_{AB}) of exchange processes

We used the classical line shape theory [10] in the interpretation of exchange processes. In all the cases studied, the dynamic process can be considered as a classical two-side exchange. The spectra were recorded in the low exchange region, *i.e.* at temperatures below the coalescence point, T_c. The rate constants, k'_{AB}, were obtained from the complete line-shape analysis of the spectra. The absorption line-shape, $S(w)$, was calculated from the following Eq. (10):

$$S(w) = I_m \left\{ \frac{-iC\tau\, 2p_A p_B - \tau(p_A \alpha_B + p_B \alpha_A)}{p_A p_B - \tau^2 \alpha_A \alpha_B} \right\}$$

where I_m stands for the imaginary part

$$\alpha_A = -\left[i(w_A - w) + \frac{1}{T_{2A}} + \frac{p_B}{\tau} \right]$$

$$\alpha_B = -\left[i(w_B - w) + \frac{1}{T_{2B}} + \frac{p_A}{\tau} \right]$$

$$\tau = \frac{p_A}{k_{BA}} = \frac{p_B}{k_{AB}}$$

p_A and p_B are the observed populations of A and B forms,
w_A and w_B are the resonance frequencies, of lines A and B, respectively,

Table II

Calculated activation free energy values of compounds **I**—**VII** *and* **XI**—**XV**

Compound	R_2	T(K)	$\Delta G^{\ddagger}_{AB}$ kcal/mol	ΔG°_{AB} kcal/mol
	Monochloroacetyl derivatives ($R_1 = CH_2Cl$)			
I	*n*-butyl	324	18.7 $\pm$ 0.15**	0.40
II	*sec*-butyl	323	18.1 $\pm$ 0.15	0.40
III	*n*-propyl	335	18.6 $\pm$ 0.15	0.45
IV	isopropyl	335	18.15 $\pm$ 0.15	0.45
V	methoxy-*n*-propyl	333	18.6 $\pm$ 0.15	0.45
VI	benzyl	333	18.5 $\pm$ 0.15	0.15
VII	c.hexyl	334	17.85 $\pm$ 0.15	0.15
	Dichloroacetyl derivatives ($R_1 = CHCl_2$)			
XI	*n*-butyl	316	18.5 $\pm$ 0.15	0.45
XII	*sec*-butyl	317	18.3 $\pm$ 0.15	0.40
XIII	*n*-propyl	331	18.4 $\pm$ 0.15	0.60
XIV	isopropyl	332	18.1 $\pm$ 0.15	0.60
XV	benzyl	316	18.2 $\pm$ 0.15	0.30

* Calculated from the following equation:

$$\Delta G^{\circ}_{AB} = -RT \ln \frac{p_B}{p_A} \qquad [11]$$

** Accuracy obtained by taking into account the error of temperature measurement ($\pm$1.5 °C) and a $\pm$10% standard deviation of the k'_{AB} values [11]

T_{2A} and T_{2B} are the transverse relaxation times of the selected A and B lines, contributions from field-inhomogeneity are also included in these terms.

The relaxation times were calculated from the widths at half height, $W_{1/2}$, of the not exchange broadened NMR lines. The C-1 carbons usually meet this requirement. In the absence of exchange, the line widths are usually dominated by the Lorentzian field-inhomogeneity broadening.

For calculation of the theoretical line-shape, we used the computer program of BINCH [10a], completed with an iteration process to optimize the τ values in a more accurate way. The following formula was employed to calculate the difference, $D_{eff.}$, between the theoretical and experimental line shapes

$$\sqrt{\frac{\sum_{i=1}^{N} (y_{calc.} - y_{exp.})^2}{N}} = D_{eff.}$$

where $y_{\text{cacl.}}$ and $y_{\text{exp.}}$ are the ordinates of the theoretical and experimental $S(w)$ functions, respectively,

N is the number of data points.

In the iteration process, different τ values were selected to obtain τ_{optimal}, *i.e.* the τ value that affords the smallest $D_{\text{eff.}}$. Considering the final $S(w)_{\text{calc.}}$ function resulting from the τ optimal value, the $y_{\text{calc.}} - y_{\text{exp.}}$ differences were less than 5% of the total line height in the region studied.

With the help of rate constants obtained from $\tau_{\text{opt.}}$ values, the activation free energies of the exchange process $A \rightleftharpoons B$ were calculated by means of the Eyring equation [11]. The ΔG^{+}_{AB} and ΔG°_{AB} values obtained, are given in Table II.

The data of Table II permit the following conclusions.

— No remarkable substituent effect has been observed on the carbonyl side between the monochloro- and the dichloroacetyl derivatives, indicating that the inductive destabilization of the transition state is not significant.

— An expected substituent effect on the nitrogen atom was that caused by the different electronic properties of substituents R_2. The alkylation of the nitrogen atom must exert an effect similar to that of the carbonyl atom [11a]. Therefore, a decrease of barriers was expected in the order of CH_3CH_2-, $(CH_3)_2CH$-, $(CH_3)_3C$. However, the observed decrease of barriers in the case of isopropyl and *sec*-butyl derivatives varied between 0.2—0.6 kcal/mol, *i.e.* they were considerably smaller than the values estimated on the basis of literature data [11a].

However, keeping in mind the unusual behaviour of the C-3 carbonyl lines of these derivatives, it is reasonable to assume that the increased steric hindrance partly compensates the ground state destabilization effect of these substituents.

— The above steric hindrance became predominant in compounds **VIII**—**X** and **XVI**, therefore, only one isomer could be observed in these molecules.

*

We wish to thank L. PARRAGH for preparing the modified version of the Binch computer program and for his helpful assistance.

REFERENCES

[1] WERHLI, F. W., WIRTHLIN, T.: Interpretation of Carbon-13 NMR Spectra, pp. 197—199. Heyden, London 1976
[2] GANSOW, O. A., KILLOUGH, J., BURKE, A. R.: J. Am. Chem. Soc., **93,** 4297 (1971)
[3] ISAKSSON, G., SANDSTRÖM, J.: Acta Chem. Scand., **21,** 1605 (1967)
[4] WALTER, V., SCHAUMANN, E., ROSE, H.: Org. Magn. Resonance, **5,** 191 (1973)
[5] HOBSON, R. F., REEVES, L. W.: J. Magn. Res., **10,** 243 (1973)

[6] ALLAN, E. A., HOBSON, R. F., REEVES, L. W., SHAW, K. N.: J. Am. Chem. Soc., **94**, 6604 (1972)
[7] PENDLEBURY, M. H., PHILIPS, L.: Org. Magn. Resonance, **4**, 529 (1972)
[8] VASS, A.: unpublished data
[9] SZALONTAI, G.: unpublished data; The carbonyl lines of these derivatives appear between 158 and 161 ppm
[10] Topics in Stereochemistry, (eds) E. L. ELIEL and N. L. ALLIGER, Vol. **3**, G. BINCH: The study of Intramolecular Rate Processes by DNMR, pp. 98—151. Interscience, 1968
[10a] *Ibid.* Appendix p. 152
[11] Dynamic Nuclear Magnetic Resonance Spectroscopy, L. M. JACKMAN, F. A. COTTON, (eds), Chapter **3**, G. BINCH, pp. 45—78. Academic Press, New York 1975
[11a] *Ibid.* L. M. JACKMAN, p. 208

Gábor SZALONTAI
András VASS
H-8201 Veszprém, P. O. Box 39.

Acta Chimica Academiae Scientiarum Hungaricae, Tomus 102 (4), pp. 423—427 (1979)

SOME ASPECTS OF THE UPTAKE OF MAGNESIUM BY CALCIUM HYDROXYLAPATITE AND EFFECT OF SUCH INCORPORATION ON THE SOLUBILITY OF THE BONE MINERAL

S. PANDEY[1], B. NANDA[2] and P. PATEL*[1]

([1]P. G. Department of Chemistry, G. M. College, Sambalpur, India, [2]P. G. Department of Zoology, G. M. College, Sambalpur, India)

Received October 13, 1978

In revised form January 18, 1979

Accepted for publication February 20, 1979

The uptake of magnesium by synthetic and natural calcium hydroxylapatite is found to (*i*) increase with increasing Mg^{2+} ion concentration (*ii*) decrease with increasing particle size of calcium hydroxylapatite, (*iii*) decrease with increasing pH in the range 5.0 to 8.0 of the medium of exchange, and (*iv*) increase with increasing period of equilibration. Adsorption of Mg^{2+} and its accompanying diffusion into the interior of the crystals explain the mechanism of exchange. The solubilities of solid solutions of calcium—magnesium hydroxylapatites determined in the pH range 5.0—8.0 decrease with increase in pH of the dissolving medium. This is due to dissolved phosphate ions, functioning as proton acceptors and undergoing hydrolysis in aqueous media.

Calcium hydroxylapatite (CaHA), $Ca_{10}(PO_4)_6(OH)_2$ is the primary crystalline inorganic component of the human skeletal system [1, 2] amounting to about 40 wt.%. It is isomorphous with the naturally occurring mineral known as fluorapatite, $Ca_{10}(PO_4)_6(F)_2$(Fap). It undergoes a series of cationic and anionic exchange reactions which are of biological and physicochemical significance. The $OH^- \rightarrow F^-$ substitution is the basis for the prophylactic action of fluorine against dental caries. Environmental pollution due to some poisonous divalent cations is increasing in recent times. Divalent cations from the environments are incorporated into the human skeletal system leading to poisoning and the consequent metabolic effect. The problem of incorporation of Ca^{2+}, Mn^{2+}, Mg^{2+}, Zn^{2+}, Fe^{+2} or Cu^{2+} (cations whose ionic radii are smaller than that of calcium) into the human skeletal system has not been thoroughly investigated as is evident from the literature and hence the present work has been undertaken. The replacement of Ca^{2+} for Mg^{2+} results in the formation of solid solutions of calcium magnesium hydroxylapatite and magnesium hydroxylapatite,

* To whom correspondence is to be addressed

$Mg_{10}(PO_4)_6(OH)_2$, which is a product obtained by complete replacement of calcium by magnesium according to the following equation

$$Ca_{10-n}(PO_4)_6(OH)_2 + n\,Mg^{2+} \rightarrow Ca_{10-n}Mg_n(PO_4)_6(OH)_2 + n\,Ca^{2+}$$

The ionic radii [3] of Ca^{2+} (0.99 Å) and Mg^{2+} (0.65 Å) are close enough to one another so that it would not be surprising if solid solutions could be formed between isomorphous substances containing these ions.

The present communication deals with investigations on the dependence of magnesium uptake by CaHA and the effect of incorporation on the solubility of the bone mineral. In addition, the studies were extended to natural hydroxylapatite obtained from human bone and teeth.

Experimental

The details of preparation and identification of CaHA, MgHA and a series of their solid solutions were reported elsewhere [4, 5]. The natural sample was obtained by heating adult human bone and teeth to 900 °C in a Mufile Furnace for ~24 hrs to remove volatile constituents. The resulting brittle lumps were powdered and sieved to the required particle size. Chemical compositions (calcium and phosphorus) of these samples were determined by a complexometric procedure.

The dependence of magnesium uptake by calcium hydroxylapatite (synthetic and natural) on factors like

(*i*) pH in the physiologically important range of 5.0 to 8.0,
(*ii*) concentration of Mg^{2+} ions in the range between 0.01*M* to 0.1*M* $Mg(NO_3)_2$,
(*iii*) particle size between 60 mesh to 35 mesh (BSS), were thoroughly investigated and
(*iv*) the period of euilibration required for the attainment of saturation of exchange was determined through kinetic studies.

Glass containers were found to be unsuitable for the samples due to interference by the dissolution of their ingredients. Potassium hydrogen phthalate — sodium hydroxide and sodium diethyl barbiturate — hydrochloric acid were used as buffer combinations for the medium of equilibration. The pH was measured with a line operated Beckman Zeromatic pH meter before and after equilibration to ascertain its constancy.

The buffer solutions were prepared in a 0.165*M* solution of sodium chloride as solvent to simulate the biological conditions and to maintain the activity coefficients of the dissolving species of apatites effectively constant. 0.2 g of 200 mesh (BSS) CaHA (synthetic and natural) was equilibrated at the physiologically important temperature of 37 ± 0.5 °C with a solution of 100 cm^3 of $Mg(NO_3)_2$ (AR) by shaking mechanically in air-tight polyethylene containers, changing the factors effecting the uptake under investigation each time, while the other factors were kept constant. In another experiment carried out to differentiate the steps of the exchange process, the reaction mixture was refluxed at 100 °C under a given set of experimental conditions. At the end of the desired period of equilibration, the contents were filtered through an IG_4 crucible. The residue was washed thoroughly with redistilled water until it was free of adsorbed Mg^{2+} and the calcium and magnesium content of the residue was determined.

The knowledge of the solubility of hydroxylapatite is of extensive importance for the physiology of bone from the point of view of calcification and resorption. In addition, considerations of the occurrence of dental caries and the protective action of fluorine are based on information about the solubility of hydroxylapatites. Such solubility studies have additional utility in soil chemistry to account for the action of phosphate containing fertilizers. The solubility studies were based exclusively on the microanalytical determination of phosphate [6, 7] in solutions of the samples. The apatites are colloidally dispersed in their aqueous solutions due to their low solubilities and minute particle size. To test for efficient separation of the colloidal component, suspensions of a series of saturated CaHA systems were filtered through an IG_4 sintered glass crucible (particle size retention, 5—10 μ) and phosphorus contents of the

filtrates compared with those of the corresponding filtrates obtained through a millipore filter (Pore size $\sim$10 mμ) fitted to a filter holder attached to a hypodermic syringe. The phosphorus contents of the two filtrates were equal within the limits of experimental error ($\pm$0.02 wt.%). Extraneous ions dissolved due to the momentary contact of colloidal suspensions with the glass crucibles were found to be too low to affect the accuracy of subsequent analyses. Each system shaken mechanically at a regulated speed was set up by adding 0.2 g of 200 mesh (BSS) solute to 100 cm^3 of the buffer solution prepared in CO_2-free redistilled water. The systems were placed in air-tight polyethylene containers to exclude the presence of carbon dioxide to avoid changes in the pH of the dissolving medium and to prevent the formation of carbonate-apatite. The assembly was kept in a thermally insulated cabin maintained at 37 $\pm$ 0.5 °C to simulate biological conditions. The period of equilibration required for the attainment of saturation was determined through dissolution kinetics as described earlier [8] and maintained at 3 hrs for all the systems. A few ml each of chloroform and toluene were added to the stock solution as well as to the systems to eliminate bacterial growth. The systems were separately filtered through an IG_4 crucible and the phosphate content in the filtrate was determined complexometrically [7].

Results and Discussion

The results on magnesium uptake by CaHA (synthetic and natural) are represented in Fig. 1. The uptake of Mg^{2+} by CaHA was found to (*i*) decrease with increasing pH of the medium of equilibration in the physiologically important range of 5.0 to 8.0, (*ii*) increase with increasing particle size of CaHA. The uptake of Mg^{2+} was found to be very rapid within the first 60 min (7.2 wt.% for synthetic and 4.9 wt.% for natural) and remained almost constant (Fig. 1a). The uptake was found to decrease from 15.16 wt.% to 12.30 wt.% with synthetic and from 12.24 wt.% to 10.16 wt.% with natural CaHA when the pH was decreased from 8.0 to 5.0 (Fig. 1b). It was also a linear function from 6.0 wt.% to 15.4 wt.% for synthetic and from 3.6 wt.% to 11.4 wt.% for natural as the concentration of $Mg(NO_3)_2$ medium increased from 0.01*M* to 0.1*M* (Fig. 1c). Figure 1d shows that the uptake under a given set of experimental conditions increases from 16.4 wt.% to 23.2 wt.% with synthetic and from 11.4 wt.% to 16.6 wt.% with natural CaHA, when the mean radius of the particle decreases from 350 μm to 60 μm. The results of two experiments, one at 35 °C and another at 100 °C, are represented in (Fig. 1a); it was found that the uptake of Mg^{2+} increases and reaches a maximum of 7.2 wt.% at 60 min and thereafter remains constant probably due to the adsorption of Mg^{2+} on the surface of CaHA crystals in the first case and in second case it reaches up to 10.5 wt.% of CaHA at 100 °C within 60 min and thereafter remains constant. This can be due to the subsequent diffusion of adsorbed Mg^{2+} into the interior of the crystal lattice. Thus the uptake of Mg^{2+} by CaHA at lower temperatures is governed by adsorption, while at higher temperatures the process is adsorption-diffusion controlled.

The effect of incorporation of magnesium on the solubility of the bone mineral is represented in Fig. 2. The dependence of solubility on (*i*) the pH of the medium of equilibration in the physiologically important range of 5.0 to

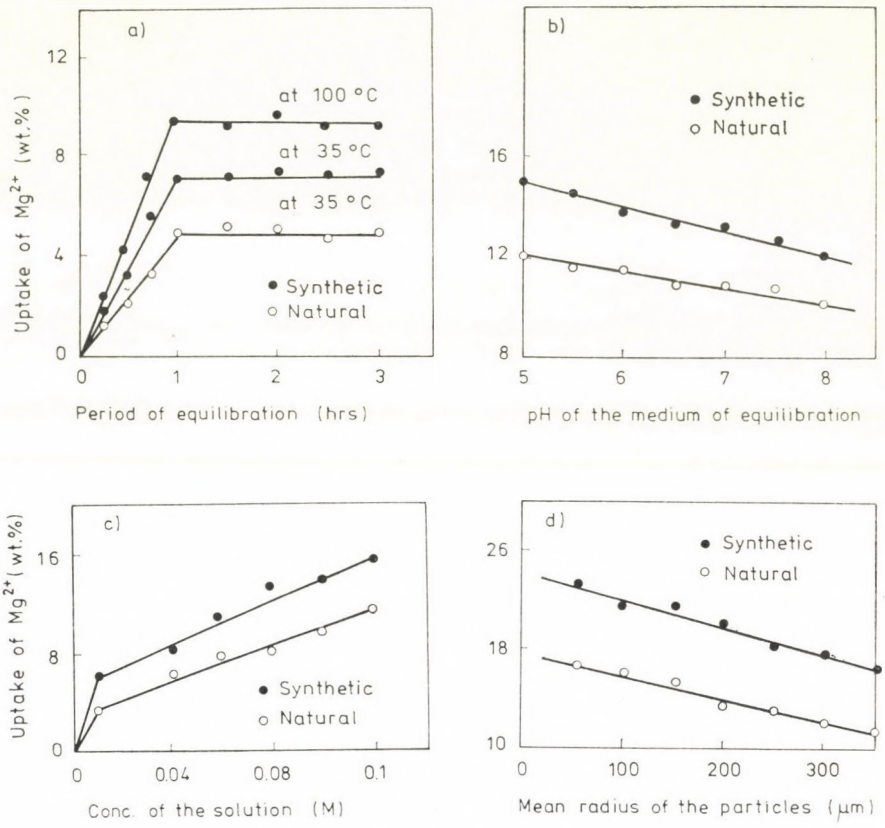

Fig. 1. Uptake of magnesium by CaHA

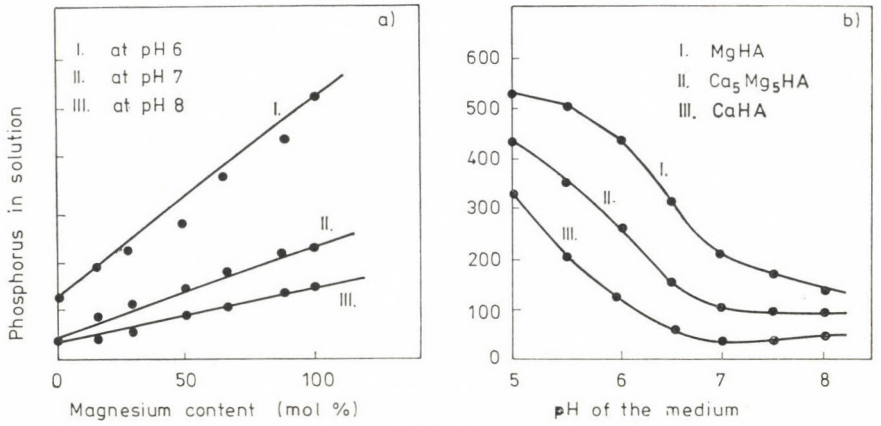

Fig. 2. pH dependence of the solubility of Ca—MgHA

8.0 and (*ii*) the magnesium content in the sample at a given pH was investigated. It was observed that (*i*) the solubility of a given sample decreases with increasing pH of the dissolving medium (Fig. 2b), which is due to the protonation of PO_4^{3-} in the dissolving medium [7], and (*ii*) at a given pH the solubility increases with the magnesium content in the solid solution (Fig. 2a). This observation can be explained on the basis of (*i*) the common ion effect applied to solubility products of the solid solutions according to MILHOFER [9], and (*ii*) due to the formation of covalent bonds on the introduction of Mg^{2+} in CaHA [10]. This explains the role of incorporation of Mg^{2+} in the solubility of the bone mineral.

*

One of the authors (PNP) thanks University Grants Commission for a research grant.

REFERENCES

[1] ROBINSON, R. A.: J. Bone and Joint Surg., **34,** 389 (1952)
[2] NEWMAN, W. F., NEUMAN, M. W.: Chem. Rev., **53,** 1 (1953)
[3] WELLS, A. F.: Structural Inorganic Chemistry, p. 70, Oxford University Press, London 1950
[4] COLLIN, R. L.: J. Amer. Chem. Soc., **81,** 5275 (1969)
[5] PATEL, P. N.: J. Solid State Chem. (Communicated), 1978
[6] SCHEEL, K. C.: Z. Analt. Chem., **105,** 256 (1936)
[7] NARASARAJU, T. S. B., CHICKERUR, N. S., SINGH, R. P.: J. Inorg. Nucl. Chem., **33,** 3194 (1971)
[8] PATEL, P. N.: J. Ind. Chem. Soc. (In press, 1978)
[9] MILHOFER, H. F.: Sci. Monogr. on Particle Growth in Suspension, Symposium Brunel University, London 1973
[10] PHILLIPS, V. S. G., WILLIAM, R. S. P.: Inorganic Chemistry, Vol. I, p. 527, Oxford University Press, London 1965

Shanty PANDEY, Prema N. PATEL — P. G. Department of Chemistry, G. M. College, Sambalpur, India

Baiaram NANDA — P. G. Department of Zoology, G. M. College, Sambalpur, India

RECENSIONES

C. P. SLICHTER: *Principles of Magnetic Resonance*

Springer Verlag, Berlin, 1978

Springer Verlag have started a new series, edited by M. CARDONA, P. FULDE and J. H. QUEISSER, on the topic of "Solid-state Sciences". The first volume of this series, Principles of Magnetic Resonance, was written by C. P. SLICHTER, Professor of Physics of Urbana University. The book is a second edition of the original work; extended, revised and enriched in contents. The publishers released this volume with the following remarks:

"A handbook for physicists, chemists and applied scientists wishing to learn nuclear magnetic or electron spin resonance; its aim being to elucidate the physics of magnetic resonance and to provide skill in all basic theoretical methods necessary for reading scientific papers; the emphasis is laid upon the depth of understanding in the most important topics, not covering all phenomena connected to magnetic resonance."

The new edition realizes the above aims in 11 chapters on 397 pages, with 115 figures. The volume is completed with 7 appendices, references, author and subject indexes. The readers are guided by selected references which also cover areas beyond the scope of the volume. In a separate chapter of Problems readers may check if they studied the book of C. P. SLICHTER with appropriate attention.

In comparison with the previous edition, the volume has been supplemented with three new chapters on spin temperature, double resonance methods and spin–flip narrowing, well illustrating the topics developed after the publication of the first edition and being of key importance in the investigation of solids by means of magnetic resonance methods.

In the first chapter (elements of resonance) the fundamental principles of energy absorption and spin–lattice relaxation are explained. The second chapter contains the classical and quantum mechanical description of the motion of non-interacting spins in constant and alternating magnetic fields, the Bloch equations and their solutions, the interpretation of spin-echo, and finally the relationships between the response functions of spin systems on continuous and pulsed excitation.

The topic of the third chapter is the Van Vleck theory of dipole–dipole interaction of magnetic moments arranged in rigid lattice, whereas chapter 4 deals with the magnetic interaction of electrons and nuclei along with its consequences on the shift and broadening of the resonance lines.

Chapter 5 is concerned with spin–lattice relaxation, the narrowing of resonance signals due to molecular motions, the Bloch–Wangsness–Redfied theory of relaxation and with the nucleus-spin relaxation of metals.

The part of Chapter *6* dealing with spin temperatures covers an area relatively unknown in Hungarian literature. It proves the validity of the Redfied hypothesis in detail and describes some application possibilities of the concept of spin temperature.

"Why to apply double resonance?" — begins the author in Chapter 7, then introducing the reader into the ENDOR (Electron Nuclear Double Resonance) method, the Overhauser effect, the Hahn condition and the three-level maser of Bloembergen.

The subject of Chapter *8* can be regarded as a methodological revolution, since the pulse combinations discussed here opened the way towards the high-resolution nuclear magnetic resonance spectroscopy of solids.

Chapter *9* deals with the interaction of the electric quadrupole moment of nuclei with the gradient of electric field, and with its consequences. Unfortunately the latter subject is discussed cursorily only, like in the first edition.

As to electron spin resonance, some mention has so far been made of it in the discussion of electron–nucleus interactions. Chapter *10* is devoted to this topic; the spin–orbit interaction,

crystal fields and hyperfine structure are briefly discussed, and the chapter is closed by the discussion of V_k centre.

Chapter *11* is a single Hamiltonian, with all terms necessary for understanding magnetic resonance, this colourful class of phenomena.

The merits of this volume can be described in superlatives only. For the reviewer the most attractive feature was the demanding physicists's attitude, also supported by precise methodology, which stems from the direct research experience and education carreer of the author.

After the perusal of the book, the reader may well feel that he has become acquainted not only with a technique, with the method of magnetic resonance, but also with the classical and quantum mechanical description of the behaviour of a set of elementary magnetic moments.

The attractive appearance of the book is in full harmony with its contents.

K. TOMPA

Advances in Polymer Science (Fortschritte der Hochpolymeren-Forschung) Vol. 28

Springer Verlag, Berlin—Heidelberg—New York, 1978, 157 pages

The volume contains the following review articles: Y. YAMASITA: ***Random and block copolymers by ring-opening polymerization*** (46 pages, in English, with 6 figures, 3 tables and 412 (!) references).

The preparation of block and graft copolymers by ring-opening polymerization is a very interesting method for the synthesis of tailor-made polymers. In addition to the anionic living polymerization of vinyl monomers, various types of new block and graft copolymers could be synthesized by ring-opening polymerization. Especially useful are the specific properties of heterochain polymers, which are not found in vinyl polymers.

Owing to the great differences in the properties of vinyl and heterochain polymers, copolymerization of a vinyl and a cyclic monomer is very interesting. However, relatively little success has been achieved in the preparation of such random copolymers, because the reactivities of vinyl and cyclic monomers are very different.

Studies on the mechanism of ring-opening polymerization have led to suitable control of the process, resulting in desirable products; yet many problems have remained unsolved and extensive studies on ring-opening copolymerization are still required. It is worht mentioning that two works of Hungarian authors, KELEN and TÜDŐS, are also cited in the paper.

H. SUMITOMO and M. OKADA: ***Ring-opening polymerization of bicyclic acetals, bicyclic lactones and bicyclic lactams***
(36 pages, in English, with 11 figures, 12 tables and 70 references).

Ring-opening homopolymerization is playing an important part in the synthesis of polysaccharides and in the elucidation of their biomedial characteristics in relation to their molecular structures.

The reaction mechanism of polymerization, the structures and properties of 6,8-dioxabicyclo[3.2.1]octane (DBO); 6,8-dioxa-bicyclo[3.2.1]oct-3-ene (DBOE); 6,8-dioxabicyclo-[3.2.1]-octan-7-one (DBOO); 8-oxa-6-azabicyclo[3.2.1]octan-7-one (BOL) and similar heterobicyclic compounds are described. Cyclic acetals can be polymerized only by cationic initiators; lactones undergo polymerization both on cationic and anionic initiation.

Polysaccharide analogues can be prepared from DBO and DBOE. New type of macrocyclic oligoesters are obtainable from DBOO in high yields. BOL yields a new hygroscopic polyamide membrane of high molecular weight.

J. P. KENNEDY and P. D. TRIVEDI: *Cationic olefin polymerization using alkyl halide alkylaluminium initiator systems* (68 pages, in English)

1. *Reactivity studies* (with 4 figures, 8 tables, and 41 references)
2. *Molecular weight studies* (with 17 figures, 8 tables and 45 references)

Isobutylene polymerization is described which has been carried out using *t*-BuX initiators, Me_3AlX and $EtAlCl_2$ co-initiators, MeX (X = Cl, Br, I) and *n*-pentane solvents at different temperatures from $-25°$ to -100 °C. The effect of these on the polymerization rate, polyisobutylene yield, molecular weight and molecular weight distribution (MWD) have been determined. The reactivity series of initiators have been established and the effects of solvents evaluated. It has been found that the initiation consists of four steps: complexation, displacement, ionization and actual initiation. The initiator reactivity order is shown to change depending on whether displacement or ionization is the rate controlling step.

The molecular weights were determined by GPC and viscosimetry. The influence of monomer concentration on $\overline{M}_n$ and $\overline{M}_v$ of the resulting polymer was analyzed by Mayo plots and the relative rate constants were calculated. A large amount of data on $\overline{M}_n$, $\overline{M}_w$, MWD as well as $\overline{M}_v$ and ΔE_{M_v} (activation energy of viscosity average molecular weight: $\overline{M}_v$) have been established. Examination of the ΔE_{M_v} data has shown that their values fall into three groups and these reflect three different mechanisms governing the molecular weight: transfer to monomer, a combination of this and termination and finally only. Furthermore the effect of counteranions and solvents on the molecular weight in isobutylene polymerization is explained.

Of the reviewed articles, the paper by SUMITOMO and OKADA is by far the best. This paper discusses the topic in a light yet exact style. This cannot be always experienced when reading the two other articles. In particular, the two compilations of KENNEDY and TRIVEDI are full of contradictions, arbitrary statements and reiterations, not to mention the misprints which could have been eliminated by more careful proof reading.

To facilitate better use of the series, a cumulative author index to the volumes published so far (1—28) has been included in the present volume. In sum, the 28th volume of "Advances in Polymer Science" contains three reviews from the field of polymer chemistry, which offer useful information on the present state of knowledge concerning the topics discussed.

I. GÉCZY

H. H. KAUSCH: *Polymer Fracture*
Vol. 2 of the series: *Polymers/Properties and Applications*

Springer Verlag. Berlin—Heidelberg—New York, 1978, 332 pages, 180 figures, 29 tables, 867 references

The second volume of the series "Polymers/Properties and Applications" deals with the "kinetic theory" of fracturing processes, *i.e.* with those physical and chemical changes on the molecular level, which lead to the macroscopic deformation and fracture of polymeric systems of various supermolecular structures, when exposed to mechanical load.

The volume contains 9 chapters.

After Chapter *1*, setting forth the subject of the problem and its mode of discussion, Chapter *2* deals with the elements constituting the supermolecular structure of solid polymers, and their pattern of arrangement, to discuss then the deformation of the complex forms and the approximate models of the deformations.

Chapter *3* gives a survey on three conceptionally different fracture theories, based on statistical, continuum-mechanical and process rate principles.

According to the molecular theories, the macroscopic fracturing process can often be traced back to the rupture of the weakest primary bond of the polymer chain, therefore, Chapter *4* gives a brief survey on quantummechanical fundamentals for the interpretation of the strength of the primary chemical bond.

Chapter *5* discusses molecular changes in the polymer chain and macroscopic changes of the polymeric system, caused by the action of various (punctiform, dynamic, thermic, *etc.*) loads.

Greatest attention is given in the book to the sphere of problems connected with the rupture of the polymer molecule by mechanical force, and with the relationships between macroscopic deformation and fracture (Chapters *6—8*).

A brief summary with several data and examples of application is given of the ESR technique, used for the detection and identification of free radicals formed on chain rupture, of the most important reactions of the mechanically excited radicals, and of theories interpreting the relationships of chain rupture and the homogeneous deformation and fracture of variously ordered high polymers. The author attempts to give a full survey of the literature on this topic (220 references up to 1978).

The last Chapter discusses the behaviour of the polymer chains in heterogeneous fracturing processes.

The book surveys all theories which aim at explaining the behaviour of polymeric systems under extreme mechanical excitation. Within this scope, it deals preferentially with molecular theories approaching the problem non-mechanistically. It presents in this respect a complete, critical discussion of the subject. Several practical examples and experiments, serving as the basis or the confirmation of fracture theories, are given.

M. IRING

INDEX

ANALYTICAL CHEMISTRY

PHYSICAL AND INORGANIC CHEMISTRY

ORGANIC CHEMISTRY

Printed in Hungary

A kiadásért felel az Akadémiai Kiadó igazgatója. Műszaki szerkesztő: Zacsik Annamária

A kézirat nyomdába érkezett: 1979. VI. 12. — Terjedelem: 10,15 (A/5) ív, 78 ábra

80.7244 Akadémiai Nyomda, Budapest — Felelős vezető: Bernát György

Application of Zeolites in Catalysis

EDITED BY G. K. BORESKOV AND KH. M. MINACHEV

The increasingly wide-spread use of zeolites in petrochemical manufacturing processes motivates the great topical interest in the USSR All-Union Conference on Zeolite Catalysis, which dealt with the most recent results in the theory and applications of zeolites.

This book contains the material of eight lectures delivered by Soviet scientists on topics such as the acidity of zeolite catalysts, the transport of cations within them, factors affecting the activity and selectivity of zeolites in cracking processes, the role of transition metals present in zeolite catalysts, and the spectroscopic investigation of such zeolites. Further topics are the diffusion processes in zeolite catalysts, and also the use of these materials in organic syntheses.

The book is an interesting survey of advanced Soviet research in this field.

In English — 179 pages — 78 figures — 25 tables — 17 × 25 cm — Cloth — ISBN 963 05 1848 1

AKADÉMIAI KIADÓ, Budapest
Publishing House of the Hungarian Academy of Sciences

ACTA CHIMICA

ТОМ 102 – ВЫП. 4

РЕЗЮМЕ

Информационно-теоретический анализ нодальных свойств π-молекулярных орбиталей

Д. БОНЧЕВ, Г. ЛИКОМАНОВ и Н. ТРИНАЙСТИЧ

Был разработан подход, основанный на информационной теории, отражающий основные особенности нодальных свойств π-молекулярных орбиталей. Было найдено, что в то время как фронтальные орбитали (**HOMO** и **LUMO**) обладают максимальным информационным содержанием, наинизшие заполненные и наивысшие незаполненные молекулярные орбитали (**LOMO** и **HUMO**) обладают минимальным содержанием. Были выведены уравнения, описывающие информацию относительно нодальных свойств полиенов и циклоенов. Исходя из этого, обсуждается возможное предсказание нодальных свойств π-**MO**.

Получение ScOOD с помощью гидротермического метода под давлением

А. БУРЕВИЧ и С. ЗЕЛИНСКИ

Был разработан гидротермический метод под давлением с целью приготовления дейтеропероксиси скандия. Наиболее благоприятными параметрами оказались следующие: давление 30 атм., температура 90°С и время 150 часов. Изотопно и структурно чистый **ScOOD** был послучен с помощью данного метода, исходя из металлического скандия и отделяя первую фракцию ортодейтероокиси скандия в количестве 20% веса.

Кальцинирование $Sc(OD)_3$ в интервале температур 20 – 500°С, однако, не приводит к образованию чистого **ScOOD**.

Идентификация образцов производилась с помощью химического анализа, рентгенографического и спектроскопического исследований.

Исследование гелей поливинилового спирта с водородными мостиками, II

Механические свойства гелей

Й. ДЬЁРДИ-ЭДЕЛЕНИ и М. НАДЬ

Термически нестабильные гидрогели поливинилового спирта (ПВС) были приготовлены и исследованы с целью получения сведений относительно структурных различий гелей, используя измерения растворимости и механических свойств. Были произведены измерения однонаправленной компрессии на физических гелях ПВС. Экспериментальные результаты подтверждают справедливость теории резиноэластичной сшивки полимеров, принимающей во внимание медленное скольжение узлов под влиянием механического нажима.

Влияние условий гелеобразования и обмена растворителя на структуру геля является очевидным из констант C, пропорциональных модулю эластичности.

Сравнение результатов растворимости и механических измерений позволяет заключить, что начальное уменьшение модуля термически обработанных гелей является результатом структурных перегруппировок. Наблюдаемое плато и последующее уменьшение модуля объясняется ступенчатым разрывом структуры, что вызывает уменьшение числа элластично эффективных цепей лишь при температурах выше 335°К.

Эти результаты находятся в согласии с нашими первичными заключениями относительно приблизительного спектра энергий связи в этих гелях.

Определение погрешности на основе общего принципа процессов рассеивания в некоторых случаях стационарной теплопроводности

А. ДАНЧО

Рассматриваются неопределенные вариационные проблемы стацинарной теплопроводности без источника и погрешности в случае сферической и цилиндрической симметрии на основе общего принципа процессов рассеивания, предложенного Дьярмати.

Полимеризация в жидких кристаллах, V

Синтез материалов в жидком кристаллическом состоянии, способных к полимеризации

К. НИТРАИ, Ф. ЧЕР и ДЬ. ХАРДИ

Были получены некоторые *п*-алкильные и *п*-алкоксильные замещенные *п'*-акрилилокси азо- или азоксибензолов и холестерил-виниловые смешанные эфиры дикарбоксильных кислот. Немногие из них обладают жидким кристаллическим состоянием также. Единичные ячейки этих соединений, определенные с помощью дифрактограмм порошков, указывают на то, что некоторые из азо- и азоксимономеров, а также все производные холестерина образуют слоистоподобную решетку. Все мономеры могут быть превращены в полимеры с заметными осветлительными точками с помощью инициирования соответствующих пероксидов как в изотропной, так и в мезоморфной массе.

Некоторые химические реакции в электродной щели и их роль в спектрохимическом анализе, XXXIII

Поведение окислов металлов в дуге. Влияние примеси кислорода в аргоне, носитель электрода как реакционный партнер и разложение окислов металло в под влиянием дуги

З. Л. САБО и Е. БЕРТАЛАН

Экспериментально было установлено, что примесь кислорода в газовой атмосфере аргона, реагируя в оболочке плазмы, влияет на отношение окисей углерода, образующихся в реакциях внутри материала электрода. Небольшие количества примеси, однако, едва влияют на интенсивность полос спектра, несмотря на значительные эффекты и процессы. Углерод, используемый в качестве носителя электрода, вступает в реакцию с окислами металлов, заполняющими каналы. На электроде дуги и на пятне горения, образующемся на материале, заполняющем электрод, а также в его окрестностях наряду с непосредственным углеродным восстановлением протекает спонтанное термическое разложение окислов металлов. В таком случае выделяется кислород, который способен к дальнейшим реакциям.

Некоторые химические реакции в электродной щели и их роль в спектрохимическом анализе, XXXIV

Поведение окислов металлов в дуге. Средняя температура электродов и химические реакции

З. Л. САБО и Е. БЕРТАЛАН

Иемерения температуры дуги, сравненные с газовоаналитическими измерениями, свидетельствует о том, что температура электрода и протекающие химические реакции связаны друг с другом. В случае порошковых смесей **CuO + C** при анодном возбуждении образца температура электрода увеличивается пропорционально интенсивности реакции. Из исследований, проведенных в зависимости от силы тока, вытекает, что температуру электрода, в основном, определяет сила тока дуги. Тепловая энергия, освобождающаяся при реакции вещества, заполняющего каналы электрода, модифицирует эту температуру и, таким образом, оказывает влияние и на испарение образца.

Некоторые химические реакции в электродной щели и их роль в спектрохимическом анализе, XXXV

Поведение окислов металлов в дуге. Химические реакции, средняя температура плазмы и напряжение дуги

З. Л. САБО и Е. БЕРТАЛАН

Газовые продукты, образующиеся в реакции внутри материала электрода, изменяют среднюю температуру и напряжение возбуждения дуги. Т. о., изменяются энергетические условия плазмы, что оказывает влияние на интенсивность спектров.

Проводимость концентрированных электролитных растворов при простоянной концентрации катиона (аниона) — применимость кондуктометрии в координационной химии

М. ПАЛФАЛВИ-РОЖАХЕДИ, А. БУВАРИ, Л. БАРЦА и З. Г. САБО

Была исследована проводимость многих (более или менее простых) смесей электролитов, поддерживая постоянной концентрацию одного из ионов (в большинстве случаев катиона) и температуру.

Было показано, что отклонения от аддитивности существуют почти в каждом случае, однако, их максимум достаточно низок: так напр., средние различия в 5*M* растворах достигают лишь 2,8%. Отклонения зависят от температуры и суммарной концентрации, но не зависят от ионной силы. В простейших случаях эти отклонения незначительны, что позволяет делать заключения относительно стабильности новых частиц в других системах с достаточно большими различиями.

Оказалось, что отклонения от аддитивности в растворах с постоянной концентрацией катиона (аниона) не могут быть объяснены ни на основе электростатических принципов, ни на основе одного образования ионных пар, т. к. следует принимать в учет специальные взаимодействия. В качестве рабочей гипотезы полагается существование ассоциатов гидратированных анионов с водородными мостиками.

Исследование вращательных барьеров амидной связи в производных глицина с помощью динамического ЯМР—C^{13}

Г. САЛОНТАИ и А. ВАШ

Вращательные барьеры амидной связи между двумя ротамерами, присутствующими в жидкой фазе, были исследованы на 16 производных глицина. Были исследованы стерический и электроноакцепторный эффекты, а также влияние, сопряжения заместителей на вращение амидной связи. Константа скорости динамического обмена между двумя ротамерными формами A и B была рассчитана, исходя из полного анализа формы линии спектра ЯМР. Приводятся также величины энергии активации ΔG^{+}_{AB}, полученные с помощью уравнения Айринга.

Некоторые вопросы поглощения магния с помощью гидроксилапатита кальция и эффект такого встраивания на растворимость скелетального минерала

Ш. ПАНДИ, Б. НАНДА и П. ПАТЕЛ

Было найдено, что встраивание магния в синтетические и природные гидроксилапатиты кальция 1) увеличивается с увеличением концентрации иона Mg^{+2}, 2) уменьшается с увеличением размера частиц гидроксилапатита кальция, 3) уменьшается с повышенем pH в интервале pH обменной среды от 5,0 до 8,0 и 4) увеличивается с увеличением периода равновесия. Адсорбция Mg^{+2} и сопровождающая ее диффузия во внутренний объем кристаллов объясняется с помощью механизма обмена. Растворимость твердых растворов гидроксилапатитов кальция-магния, определенная в интервале pH 5,0—8,0, уменьшается с повышением pH растворяющей среды. Это происходит благодаря растворенным ионам фосфата, функционирующим как протон-акцепторы, и гидролизу в водных средах.

Les Acta Chimica paraissent en français, allemand, anglais et russe et publient des mémoires du domaine des sciences chimiques.

Les Acta Chimica sont publiés sous forme de fascicules. Quatre fascicules seront réunis en un volume (4 volumes par an).

On est prié d'envoyer les manuscrits destinés à la rédaction à l'adresse suivante:

Acta Chimica
Budapest, P.O.B. 67, H-1450, Hongrie

Toute correspondance doit être envoyée à cette même adresse.

La rédaction ne rend pas de manuscript.

Le prix de l'abonnement: $36,00 par volume.

Abonnement en Hongrie à l'Akadémiai Kiadó (1363 Budapest, P.O.B. 24, C. C. B. 215 11488), à l'étranger à l'Entreprise du Commerce Extérieur « Kultura » (H-1389 Budapest 62, P.O.B. 149 Compte-courant No. 218 10990) ou chez représentants à l'étranger.

Die Acta Chimica veröffentlichen Abhandlungen aus dem Bereich der chemischen Wissenschaften in deutscher, englischer, französischer und russischer Sprache.

Die Acta Chimica erscheinen in Heften wechselnden Umfanges. Vier Hefte bilden einen Band. Jährlich erscheinen 4 Bände.

Die zur Veröffentlichung bestimmten Manuskripte sind an folgende Adresse zu senden:

Acta Chimica
Budapest, Postfach 67, H-1450, Ungarn

An die gleiche Anschrift ist jede für die Redaktion bestimmte Korrespondenz zu richten:

Manuskripte werden nicht zurückerstattet.

Abonnementspreis pro Band: $36,00.

Bestellbar für das Inland bei Akadémiai Kiadó (1363 Budapest, Postfach 24, Bankkonto Nr. 215 11488), für das Ausland bei »Kultura« Außenhandelsunternehmen (H-1389 Budapest 62, P.O.B. 149. Bankkonto Nr. 218 10990) oder seinen Auslandsvertretungen.

«Acta Chimica» издают статихи по химии на русском, английском, французском и немецком языках.

«Acta Chimica» выходит отдельными выпусками разного объекта, 4 выпуска составхяют один том и за год выподят 4 тока.

Предназначенные для публикации рукописи следует направлять по адресу:

Acta Chimica
Budapest, P.O.B. 67, H-1450, ВНР

Всякую корреспонденцию в редакцию направляйте по этому же адресу.

Редакция рукописей не возвращает.

Подписная цена — $ 36,00 за том.

Отечественные подписчики направляйте свои заявки по адресу Издательства Академии Наук (1363 Budapest, P.O.B. 24, Текущий счет 215 11488), а иностранные подписчики через организацию по внешней торговие «Kultura» (H-1389 Budapest 62, P.O.B. 149. Текущий счет 218 10990) или через ее заграничные представительства и уполномеченных.

Reviews of the Hungarian Academy of Sciences are obtainable at the following addresses:

AUSTRALIA
C.B.D. LIBRARY AND SUBSCRIPTION SERVICE, Box 4886, G.P.O., *Sydney N.S.W. 2001*
COSMOS BOOKSHOP, 145 Ackland Street, *St. Kilda (Melbourne), Victoria 3182*

AUSTRIA
GLOBUS, Höchstädtplatz 3, *1200 Wien XX*

BELGIUM
OFFICE INTERNATIONAL DE LIBRAIRIE, 30 Avenue Marnix, *1050 Bruxelles*
LIBRAIRIE DU MONDE ENTIER, 162 Rue du Midi, *1000 Bruxelles*

BULGARIA
HEMUS, Bulvar Ruski 6, *Sofia*

CANADA
PANNONIA BOOKS, P.O. Box 1017, Postal Station "B", *Toronto, Ontario M5T 2T*

CHINA
CNPICOR, Periodical Department, P.O. Box 50, *Peking*

CZECHOSLOVAKIA
MAD'ARSKÁ KULTURA, Národni třida 22, *115 33 Praha*
PNS DOVOZ TISKU, Vinohradská 46, *Praha 2*
PNS DOVOZ TLAČE, *Bratislava 2*

DENMARK
EJNAR MUNKSGAARD, Norregade 6, *1165 Copenhagen*

FINLAND
AKATEEMINEN KIRJAKAUPPA, P.O. Box 128, *SF-00101 Helsinki 10*

FRANCE
EUROPERIODIQUES S. A., 31 Avenue de Versailles, *78170 La Celle St.-Cloud*
LIBRAIRIE LAVOISIER, 11 rue Lavoisier, *75008 Pari*
OFFICE INTEHNATIONAL DE DOCUMENTATION ET LIBRAIRIE, 48 rue Gay-Lussac, *75240 Paris Cedex 05*

GERMAN DEMOCRATIC REPUBLIC
HAUS DER UNGARISCHEN KULTUR, Karl-Liebknecht-Strasse 9, *DDR-102 Berlin*
DEUTSCHE POST ZEITUNGSVERTRIEBSAMT, Strasse der Pariser Kommüne 3—4, *DDR-104 Berlin*

GERMAN FEDERAL REPUBLIC
KUNST UND WISSEN ERICH BIEBER, Postfach 46, *7000 Stuttgart 1*

GREAT BRITAIN
BLACKWELL'S PERIODICALS DIVISION, Hythe Bridge Street, *Oxford OX1 2ET*
BUMPUS, HALDANE AND MAXWELL LTD., Cowper Works, *Olney, Bucks MK46 4BN*
COLLET'S HOLDINGS LTD., Denington Estate. *Wellingborough, Northant NN8 2QT*
WM. DAWSON AND SONS LTD., Cannon House, *Folke tone, Kent CT19 5EE*
H. K. LEWIS AND CO., 136 Gower Street, *London WC1E 3BS*

GREECE
KOSTARAKIS BROTHERS, International Booksellers, 2 Hippokratous Street, *Athens-143*

HOLLAND
MEULENHOFF-BRUNA B.V., Beulingstraat 2, *Amsterdam*
MARTINUS NIJHOFF B.V., Lange Voorhout 9—11, *Den Haag*
SWETS SUBSCRIPTION SERVICE, 347b Heereweg, *Lisse*

INDIA
ALLIED PUBLISHING PRIVATE LTD., 13/14 Asaf Ali Road, *New Delhi 110001*
150 B-6 Mount Road, *Madras 600002*
INTERNATIONAL BOOK HOUSE PVT. LTD., Madame Cama Road, *Bombay 400039*
THE STATE TRADING CORPORATION OF INDIA LTD., Books Import Division, Chandralok, 36 Janpath, *New Delhi 110001*

ITALY
EUGENIO CARLUCCI, P.O. Box 252, *70100 Bari*
INTERSCIENTIA, Via Mazzé 28, *10149 Torino*
LIBRERIA COMMISSIONARIA SANSONI, Via Lamarmora 45, *50121 Firenze*
SANTO VANASIA, Via M. Macchi 58, *20124 Milano*
D. E. A., Via Lima 28, *00198 Roma*

JAPAN
KINOKUNIYA BOOK-STORE CO. LTD., 17-7 Shinjuku-ku 3 chome, Shinjuku-ku, *Tokyo 160-91*
MARUZEN COMPANY LTD., Book Department, P.O. Box 5050 Tokyo International, *Tokyo 100-31*
NAUKA LTD. IMPORT DEPARTMENT, 2-30-19 Minami Ikebukuro, Toshima-ku, *Tokyo 171*

KOREA
CHULPANMUL, *Phenjan*

NORWAY
TANUM-CAMMERMEYER, Karl Johansgatan 41—43, *1000 Oslo*

POLAND
WĘGIERSKI INSTYTUT KULTURY, Marszałkowska 80, *Warszawa*
CKP 1 W ul. Towarowa 28 *00-95 Warsawa*

ROUMANIA
D. E. P., *Bucureşti*
ROMLIBRI, Str. Biserica Amzei 7, *Bucureşti*

SOVIET UNION
SOJUZPETCHATJ — IMPORT, *Moscow*
and the post offices in each town
MEZHDUNARODNAYA KNIGA, *Moscow G-200*

SPAIN
DIAZ DE SANTOS, Lagasca 95, *Madrid 6*

SWEDEN
ALMQVIST AND WIKSELL, Gamla Brogatan 26, *101-20 Stockholm*
GUMPERTS UNIVERSITETSBOKHANDEL AB, Box 346, *401 25 Göteborg 1*

SWITZERLAND
KARGER LIBRI AG, Petersgraben 31, *4071 Basel*

USA
EBSCO SUBSCRIPTION SERVICES, P.O. Box 1943, *Birmingham, Alabama 35201*
F. W. FAXON COMPANY, INC., 15 Southwest Park, *Westwood, Mass. 02090*
THE MOORE-COTTRELL SUBSCRIPTION AGENCIES, *North Cohocton, N.Y. 14868*
READ-MORE PUBLICATIONS, INC., 140 Cedar Street, *New York, N. Y. 10006*
STECHERT-MACMILLAN, INC., 7250 Westfield Avenue, *Pennsauken N.J. 08110*

VIETNAM
XUNHASABA, 32, Hai Ba Trung, *Hanoi*

YUGOSLAVIA
JUGOSLAVENSKA KNJIGA, Terazije 27, *Beograd*
FORUM, Vojvode Mišića 1, *21000 Novi Sad*

11. II. 1980 HU ISSN 0001—5407 Index: 26 007